



6th INTERNATIONAL CONFERENCE ON RENEWABLE FUELS COMBUSTION AND FIRE

CONFERENCE PROCEEDINGS

May 18–21, 2017

Cappadocia, TURKEY



6th INTERNATIONAL CONFERENCE ON RENEWABLE FUELS COMBUSTION AND FIRE



Conference Proceedings

May 18-21, 2017

Cappadocia, TURKEY

Editor in Chief

Assoc. Prof. Dr. Bilge Albayrak Çeper

Editors

Prof. Dr. Sebahattin Ünal

Prof. Dr. Nafiz Kahraman

Prof. Dr. Hakan Serhad Soyhan

Prof. Dr. Selahaddin Orhan Akansu





ORGANISED BY

Erciyes University, Engineering Faculty, Kayseri, Turkey

Sakarya University, Engineering Faculty, Sakarya, Turkey

The Conference Organizing Committee is not responsible for the views expressed or any errors contained in the papers as these are the responsibility of the individual authors. Only minor corrections to the text may have been carried out by the Conference Organizing Committee.

All rights reserved.

**INTERNATIONAL Conference On Renewable Fuels Combustion And Fire
(6 ; 2017 ; Cappadocia) FCE 2017, 6th International Conference on
conference proceedings, 18 -21 of May, Kayseri, Turkey**

The organizing committee gratefully would like to acknowledge Erciyes University, for the Scientific Research Projects Unit of Erciyes University, Turkey, for the financial support under the grant number FBS-2017-7471.

INTERNATIONAL FCE CONFERENCE - 2017

The Organizing Committee

Prof. Dr. Muhammet Güven (Rector of Erciyes University)

Prof. Dr. Cem Soruşbay

Prof. Dr. Roger Cracknell

Prof. Dr. Hakan Serhad Soyhan

Prof. Dr. Sebahattin Ünal

Assoc. Prof. Dr. Bilge Albayrak Çeper

Prof. Dr. Nafiz Kahraman

Prof. Dr. Selahaddin Orhan Akansu

The Local Organizing Committee

Ms. Evrim Ozrahat

Mr. Melih Yıldız

Mr. H. Enes Fil

Mr. Selçuk Sarikoc

Ms. Esenay Arslan

International Advisory Committee

Prof. Dr. Ahmet Erdil Kocaeli Uni.

Prof. Dr. Alı Sürmen Bursa Tec. Uni.

Dr. Ali Türkcan Kocaeli Uni.

Dr. Alper Calık Istanbul Tec. Uni.

Dr. Bart Somers Tu Eindhoven

Doç. Dr. Bilge A. Çeper Erciyes Uni.

Prof. Dr. Can Haşimoğlu Sakarya Uni.

Prof. Dr. Cem Soruşbay Istanbul Tec. Uni.

Doç. Dr. Ekrem Büyükkaya Sakarya Uni.

Dr. Ertan Alptekin Kocaeli Uni.

Dr. George Skevis Cperı/Crerth

Prof. Dr. Filiz Karaosmanoğlu Istanbul Tec. Uni.

Doç. Dr. Halit Yaşar Sakarya Uni.

Prof. Dr. Hakan Serhad Soyhan Sakarya Uni., Teamsan Co.

Prof. Dr. İmdat Taymaz Sakarya Uni.

Dr. Hüseyin Karadeniz Bosch

Prof. Dr. Hüseyin Serdar Yücesu Gazı Uni.

Dr. İsmail Altın Karadeniz Tec. Uni.

Prof. Dr. İskender Gokalp Cnrs

Dr. Julian Dızy Cmel

Prof. Dr. İsmet Çevik Sakarya Uni.

Dr. Amit Bhawe Cmel

Prof. Dr. Mario Costa Instituto Superior Tecnico

Prof. Dr. Mehmet İhsan Karamangil Uludag Uni.

Prof. Dr. Mehmet Tekin Gaziosmanpasa Uni.

Prof. Dr. Mohy Mansour Cairo Uni.

Dr. Mustafa Yılmaz Marmara Uni.

Prof. Dr. Mustafa Acaroğlu Selcuk Uni.

Prof. Dr. Nafiz Kahraman Erciyes Uni.

Prof. Dr. Oğuz Borat Istanbul Com. Uni.

Prof. Dr. Osman Eldoğan Sakarya Uni.

Dr. Philippe Dagautt Cnrs

Prof. Dr. Rafiq Mehdiyev Gebze Tec. Uni.

Prof. Dr. Roger Cracknell Shell Global Solutions

Doç. Dr. Tarkan Sandalcı Yıldız Tec. Uni.

Prof. Dr. Veli Çelik Ankara Yıldırım Beyazıt Uni.

Doç. Dr. Yakup Erhan Böke Istanbul Tec. Uni.

Prof. Dr. Zehra Şahin Karadeniz Tec. Uni.

CONTENTS

CHAPTER 1 - ALTERNATIVE FUELS

Comparison of the performance, combustion and the emissions of crambe abyssinica biodiesel	5
The performance, emissions and combustion investigation on mixing of crambe and waste frying biodiesels blended with diesel	18
The effect of pressure on the biogas flame characteristics: a numerical study	32
The investigate of effects on performance and emission parameters of safflower biodiesel-bioethanol-diesel fuel blends at different injection pressures	39
Using in a CI engine of biodiesel production from waste cooking oil	45
Theoretical determination of optimum ethanol fuel blends rate within gasoline	51
Experimental study on a spark ignition engine fuelled by methane-oxygen enriched air	59
Biomethane recovery from anaerobic co-digestion of sewage sludge and waste coffee	66
Experimental investigation of effects of hydrogen addition to gasoline engine	73
The effect on performance and emission parameters of diesel- biodiesel-butanol blend	80
An experimental study on performance and emissions of an SI engine fueled by acetylene-hydrogen and acetylene-methane blends.....	87
Comparision of engine performance and exhaust emission values of sunflower biodiesels with diesel fuel	101
The effect of sunflower biodiesel on cyclic variation using wavelet analysis method	112

CHAPTER 2 - FIRE

Comparison of the design fire load methodologies and calorific values of the combustible materials in the light of various design guidelines and handbooks	122
Yangın ve patlama potansiyeli olan tehlikeli ekipmanların belirlenmesi: dow indeksi	131
İş güvenliği uygulamalarının yaygınlaştırılmasının yangından korunmaya katkıları	139
Yangın önlemede istatistiksel verilerin kullanımı	145

CHAPTER 3 – COMBUSTION

Evaluation of mathematical models of devolatilization for numerical simulations of pulverized coal combustion	151
The numerical and experimental investigation of a monoblock natural gas burner for reducing NO _x emissions	162
Simulational energy analyses of hybrid vehicle's electric engine	171
Kinetics study of Adiyaman-Golbasi lignite during oxygen enriched combustion	177
Effects of using different electric motors on hybrid engine's performance	185
Oxy-fuel combustion of low calorific value coal gases: burner modifications and flame characteristics	193
Evaluation of combustion and NO _x formation in a gas turbine combustor by changing primary zone length.....	207
Numerical investigation on combustion behavior of premixed hydrogen/air flames in a micro combustor with varying geometric properties: part - I effect of backward facing step and cavity	212
Numerical investigation on combustion behavior of premixed hydrogen/air flames in a micro combustor with varying geometric properties: part - II effect of multi-channel arrangement	225
Experimental analysis of turbulent premixed coal gas combustion	237

Diffuser combustor to study the influence of turbulence on turbulent lean premixed flame	249
Numerical investigation on oxy enriched air combustion with methane fuel in combustion chamber of a boiler	255

CHAPTER 4 – CORPORATE PRESENTATIONS

Wind turbine fires	266
Yangın yayılımı etkileri düzleminde tünel yangınları - tunnel fire with HRR	278
Securitas itfaiye hizmetleri kurumsal sunum	292
Endüstride yangın güvenliği ve uygulamaları	297
Firepro aerosol söndürme sistemleri	309

CHAPTER 5 - ABSTRACTS

Atrium binalarda duman emiş fanı seçiminin hesaplamalı akışkanlar dinamiği yöntemi ile belirlenmesi	314
Canola based biodiesel production using microwave technology	315
Effect of side ports on the flow field of a rotary engine	316
CFD investigation of twin swirl application to diesel engine	318
Investigation of air flow simulation for a single cylinder spark ignition engine	320
Developing emergency escape scenarios by using fire simulation softwares.....	322
Spherical flame front propagation model and its validation in simplified pent-roof combustion chamber	323
Mühendislikte yanıcı ve patlayıcı gazların iş sağlığı ve güvenliği açısından yarattığı sorunlar	324
Baca gazı atık ısı geri kazanımı için endüstriyel pişirme fırınında enerji verimliliği sağlayan inovatif sistem geliştirilmesi	325



Chapter – 1

Alternative Fuels

Comparison of the performance, combustion and the emissions of *crambe abyssinica* biodiesel

Dr. Ayhan UYAROĞLU¹, Doç. Dr. Hamit SOLMAZ²

¹ Selçuklu Vocational and Technical Anatolian High School

ayhanuyaroglu@hotmail.com

² Gazi University Faculty of Technology, Department of Automotive Engineering
hsolmaz@gazi.edu.tr

Abstract: *Crambe abyssinica* is an annual herb that is an inedible oil due to erucic acid content. *Crambe* is drought and cold tolerant plant that grows under extreme conditions. Other available characters are such as short growing season, potentiality of high yield and good resistance to diseases. The interest of *crambe* is increasing progressively by means of the promising oil crop. The aim of this paper was to assess the performance, combustion and emissions when *crambe* biodiesel and diesel oil are used in a single-cylinder, four-stroke, direct injected diesel engine with air cooling system at 2200 1/min fixed engine speed and with four different engine loads. The used fuels were *crambe* biodiesel (B20, B40, B60) and diesel oil (D0). The results obtained from the experimental study were compared with No. 2 diesel fuel. The effects of blends on CO, CO₂, THC, NO_x and smoke were investigated by emission tests. Additionally brake specific fuel consumption, heat release rate and the in-cylinder pressure of test fuels were examined. In respect to environmental effects and increasing interest of inedible oils, *crambe* biodiesel will become more important in the near future.

Keywords: Biodiesel, combustion, *crambe* oil, diesel fuel, emissions

1. Introduction

In recent years, studies on alternative fuels have been increased due to environmental effects and scarcity of petrol. Alternative fuel studies have been evolved in itself such as first generation biofuels and second generation biofuels. While the first generation biofuels are produced directly from food crops, second generation biofuels are generally not food crops. First generation biofuels threatens the food supplies and causes increasing the price of food supplies. For these reason second generation biofuels become important all over the world and increase the investigation of crops that are inedible oil. Among these crops, *crambe abyssinica* can be preferred by means of its some advantages; drought and cold tolerant plant that grows under extreme conditions, short growing season, potentiality of high yield and good resistance to diseases, flea beetle resistant, moderately tolerant to salinity and herbicides [1-5]. *Crambe abyssinica*, classified under the genus *Crambe* and the family Cruciferae which oil content of its whole seed 34.48%, of which 62.50% is erucic acid [5]. *Crambe* has a wide range of applications in the industry. *Crambe* and derivatives are used as polyamides, copolyamides, plasticizers and polyurethane elastomers [6], mold-release agent [2, 5, 7-9], textile [8-11], shipping industry, metal-forming [10], cutting oil [10, 11], machine oil [3, 5, 10], inhibitor of the corrosion [3, 5], nylon [3, 12], electrical isolation [3], pharmaceuticals detergents and cosmetics [5], paints and coatings [5, 13], high temperature hydraulic fluids [5, 11],

engine oil [8], automatic transmission fluid additives, power steering fluids [11], printing inks [13, 14], slip agent [10, 13, 14]. The erucic acid can be converted by ozonolysis into brassylic and pelargonic acids. Pelargonic acid is used for making modern jet aircraft engine lubricants [9, 15]. Despite its wide use of *crambe* and its derivatives, evaluation of *crambe* oil as a biodiesel source is limited so a few studies have been conducted. Table 1. shows the physical and chemical properties of *crambe abyssinica* oil. The most obvious feature of *crambe abyssinica* oil is erucic acid content that's why *crambe* is non edible oil and its iodine value meets the standard of EN14214 that of upper limit of 120.

Table 1. Physical and chemical properties of *crambe abyssinica* oil.

Typical fatty acid profile	
Palmitic acid (C16:0)	1.0-4.0%
Palmitoleic acid (C16:1)	0.1-0.5%
Stearic acid (C18:0)	0.5-2.0%
Oleic (C18:1)	10.0-25.0%
Linoleic (C18:2)	7.0-15.0%
Linolenic (C18:3)	2.0-5.0%
Arachidic (C20:0)	0.5-2.0%
Eicosenoic (C20:1)	2.0-6.0%
Eicosadienoic (C20:2)	0.0-4%
Behenic (C22:0)	1.0-3.0%
Erucic (C22:1)	50.0-65.0%
Lignoceric (C24:0)	0.0-1.0%
Chemical and physical data	
Apperance (20 °C)	Clear Yellow Liquid
Specific Gravity (20 °C)	0.906-0.911
Acid Value (mg KOH/g)	0.5 max.
Saponification Value	160-175
Iodine Value	85-105
Refractive Index (20 °C)	1.465-1.475
Viscosity (cSt)	53.0 [16]
Flash Point (°C)	284 [16]
Higher Heating Value (MJ/kg)	39.83 [16]

The purpose of the study is to perform experimentally parametric tests of a single cylinder diesel injection engine performance, combustion and emissions fueled with biodiesel obtained from *crambe abyssinica* oil with 2200 1/min fixed engine speed and at four different engine loads.

2. Materials and methods

2.1. Fuel description

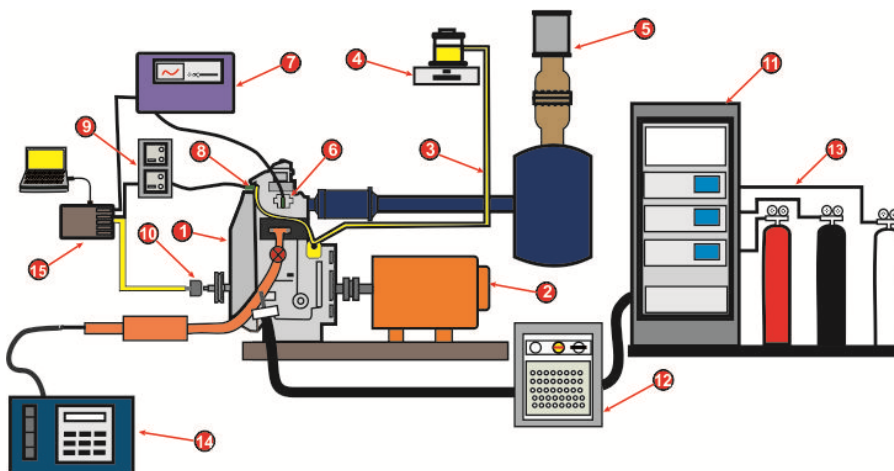
Crambe abyssinica oil was purchased from Elementis Specialities Company by the name of Fancor Abyssinian Oil. Methanol 99.9%, potassium hydroxide pellets for analysis were provided by Merck, Germany. A flat-bottom flask was used as a laboratory scale reactor with a reflux condenser for the experimental studies in this work, and Daihan MSH-20D Digital Precise Hotplate with temperature probe arrangements was used for heating the mixture in the flask. Shimadzu UW620H accuracy 0.001g electronic balance was used for scaling chemicals. The *crambe* oil was

transesterified using methanol in the presence of KOH. The transesterification parameters of *crambe abyssinica* oil was applied as 6:1 Methanol to oil molar ratio with KOH catalyst 0.8 g (w/w), 57°C reaction temperature, and 60 minutes reaction time and transesterification yield 96.5%. After the alkali transesterification reaction was completed, the mixture was left in separating funnel for 8-10 hours for gravity separation of the methyl esters and glycerol. The heavier glycerin settled at the bottom and was removed; the remaining sample was washed with hot distilled water (about 85°C) several times until the wash water became clear. After washing, the biodiesel was heated up 110°C for 20 minutes to remove any remaining water. Biodiesel blends were prepared in different proportions by volume basis like B20-B40-B60. Chemical properties were determined for both of used fuels according to European Fatty Acids Methyl Ester (FAME) standard draft (EN 14214), as shown in Table 2.

Table 2. Fuel properties used in tests.

Properties	<i>Crambe</i> methyl ester	Diesel fuel
Viscosity (cSt)	6.492	3.354
Flash Point (°C)	190 [16]	102 [17]
Higher Heating Value (MJ/kg)	41.98 [16]	42.3 [17]
Density (g/L)	879.7	841.75
Sulfur (mg/kg)	1.3	-
Water content (mg/kg)	378.49	-
Cetane index	-	53.1

2.2. Engine test facility



- 1- Test engine 2- DC dynamometer 3- Diesel fuel line 4- Sensitive scale 5- Laminar flow meter 6- In-cylinder pressure sensor 7- Combustion analyzer 8- Diesel fuel line pressure sensor 9- Diesel fuel line pressure sensor amplifier 10- Encoder 11- Emission gas analyzer 12- Emission sampling system 13- Function gases (N₂, O₂, H₂/He) and span gases (C₃H₈, CO₂, CO, O₂) 14- Smoke meter 15- Data acquisition card

Figure 1. Test rig

The test rig used in this study is shown in Fig. 1 and the specifications of the single cylinder diesel engine are given in Table 3. The engine was loaded with Cussons brand P8160 model DC type dynamometer measuring up to 10 kW at 4000 rpm. The inlet air flow rates were measured with Merriam brand Z50MC2-4F model laminar flow meter. The inlet air, the lubrication oil and the exhaust gas temperatures were measured using NiCr–Ni type thermocouples. The fuel consumption

values were measured using an electronic balance with high precision. The engine torque was calculated from the force values acquired with a strain gauge type load cell and the engine speeds were obtained with a magnetic collector type sensor. In order to minimize the variations of the inlet air temperature, PID (ENDA ETC. 9420) controlled air heater (Farnam Flow Torch 400) was used. The in-cylinder gas pressures were acquired with AVL-8QP500c water cooled pressure transducer and Cussons P4110 combustion analysis device with NIUSB-6259 data acquisition (DAQ). In order to determine injection characteristics, the fuel line pressures were measured using AVL SL-31D 2000 model pressure sensor and AVL 3009 A04 model amplifier. The encoder with 1000 pulses was placed on crankshaft axis in order to record crank angle and Top Dead Centre (TDC) values.

Table 3. General specifications of the Antor diesel engine.

Make/model	Antor/6LD400
Engine type	DI-diesel engine, natural aspirated, air cooled
Cylinder number	1
Bore x stroke (mm)	86 × 68
Displacement (cm³)	395
Compression ratio	18:1
Maximum power (kW)	5.4 @ 3000 rpm
Maximum torque (Nm)	19.6 @ 2200 rpm
Combustion chamber geometry	ω type
Fuel injection system	PF jerk-type fuel pump
Injection nozzle	0.24 mm × 4 holes × 160°
Nozzle opening pressure (bar)	180
Fuel delivery advance angle (°CA)	28 BTDC
Valve timings IVO/IVC (°CA)	7.5 BTDC/25.5 ABDC
EVO/EVC (°CA)	21 BBDC/3 ATDC

2.3. Measurements of exhaust gas emissions

Exhaust gas emissions were measured using Environnement SA-EGAS 2M gas analyzer that specifications were given in the Table 4. The EGAS 2M gas analyzer measures THC emissions with Heated Flame Ionization Detection (HFID) analyzer, NO_x with heated chemiluminescence (CLA) analyzer and CO/CO₂ with a Non-Dispersive Infrared Sensor (NDIR).

Table 4. Technical specifications of exhaust gas analyzers.

Analyzer	GRAPHITE 52M	TOPAZA 32M	MIR 2M
Measuring compound	THC (wet)	NO-NO _x (wet)	CO-CO ₂ -O ₂ (dry)
Measurement principle	HFID	HCLD	NDIR Paramagnetic
Linearity	<1%	<1%	<1%
Measurement rate	0-10/30000 ppm	0-10/10000 ppm	0-500/10000 ppm (CO) 0-1/20% (CO ₂) 0-5/25% (O ₂)
Lower detectable limit	0.05 ppm (0-10 ppm range)	0.1 ppm (0-10 ppm range)	<2% (FSO)
Response time (T90 s)	<1.5 s	<2 s	<2 s

AVL 4000 DiSmoke opacity meter specifications were shown in Table 5. AVL 4000 DiSmoke opacity meter is partial flow meter, which have 0.1 m⁻¹ sensibility and range of 0–99.99 m⁻¹.

Table 5. Technical specifications of opacimeter.

Analyzer	AVL DiSmoke 4000	
Measurement principle	Partial flow opacimeter	
Measurement range	Opacity	K value
Accuracy	0-100% 0-99.99 m ⁻¹	Accuracy 0.1% 0.01 m ⁻¹

2.4. Heat Release calculation

Heat release analysis was calculated from Eq. (1) according to single-zone combustion model based on the first law of the thermodynamics. The heat loss from the wall is neglected. In this study, cylinder pressure and heat emission analysis were carried out and $\gamma = 1.35$ was taken for all fuels [18]. In each cycle 2000 raw in-cylinder pressure data are received at intervals of 0.36 °C. For the purpose of negating the effect of cyclic differences, corrections were made on 50 consecutive cycles and their average was calculated for analyses. Noise is generated as a result of the numeric operations performed with cylinder pressure data in heat dissipation analysis. With the aim of to reduce these noises, the filtering operation presented in Eq. (2) was implemented.

$$\frac{dQ_n}{d\theta} = \frac{\gamma}{\gamma-1} p \frac{dv}{d\theta} + \frac{1}{\gamma-1} v \frac{dp}{d\theta} \quad (1)$$

$$(du/dx)_i = (u_i + 2u_{i+1} + 3u_{i+2} + 4u_{i+3} + 3u_{i+4} + 2u_{i+5} + u_{i+6})/16 \quad (2)$$

2.5. Testing procedure

The experiments were conducted at four different engine loads (BMEP, 0.12 MPa, 0.24 MPa, 0.36 MPa and 0.48 MPa) and 2200 rpm engine speed. At the beginning of the tests, the engine was warmed with No. 2 diesel fuel. The oil and inlet air temperatures were kept at 85 ± 2 °C and 25 ± 1 °C, respectively, Biodiesel blends containing 20%, 40% and 60% proportions by volume were tested in the experiments and the results were compared with conventional No. 2 diesel fuel operation. The accuracy of all devices and uncertainties are given in Table 6.

Table 6. Measurement accuracy and uncertainties of calculated results.

	Accuracy	Uncertainty
Time (s)	±0.5%	
Temperature (°C)	±1	
Fuel (g)	±0.1	
Engine speed (1/min)	±1%	
Load (N)	±0.25%	
Cylinder pressure	11.96 (pC/bar)	
Torque (Nm)		±0.25%
Fuel flow rate (g/min)		±0.72%
Specific fuel consumption (g/kW-h)		±1.26%

3. Results and discussion

3.1. Brake specific fuel consumption (BSFC)

The changings of brake specific fuel consumption of tested fuels under the four engine loads (BMEP, 0.12 MPa, 0.24 MPa, 0.36 MPa and 0.48 MPa) and 2200 rpm engine speed are shown in Figure 2. Biodiesel blends have higher brake specific fuel consumption values at all engine loads. BSFC increases as biodiesel blend ratio increases. Researchers indicated that this could contribute to the lower calorific value of biodiesel as compared to diesel [19-21]. In addition, the density of biodiesel is higher than that of diesel fuel, it causes increasing in mass than the volumetrically sprayed fuel amount [22]. As it can be noticed in Fig.2. the maximum BSFC increase of 12.47% in B60 biodiesel occurs at 0.48 MPa engine load.

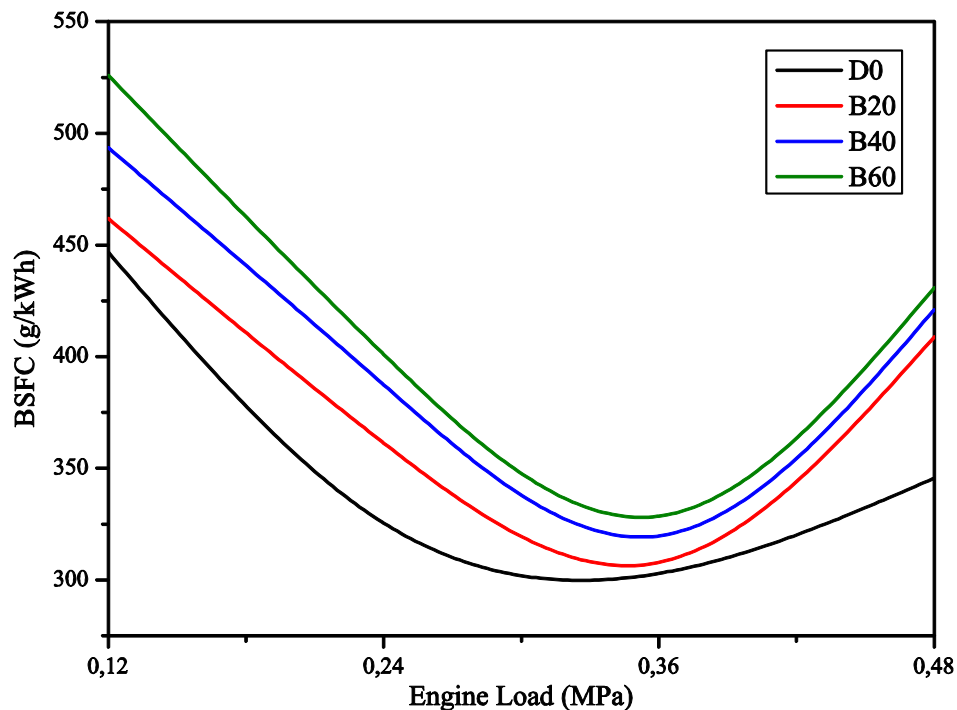


Figure 2. Effects of biodiesel addition and engine load on brake specific fuel consumption at 2200 rpm engine speed.

3.2. Combustion characteristics

Fig. 3 shows the variations in combustion (in-cylinder pressure, heat release rate) and fuel injection (fuel line pressure) parameters for No. 2 diesel fuel and biodiesel fuel blends (B20, B40 and B60) at four engine loads (BMEP, 0.12 MPa, 0.24 MPa, 0.36 MPa and 0.48 MPa) and 2200 rpm engine speed. According to the figures, fuel line pressure of tested fuels has increased by the engine load by reason of the increased fuel amount. As seen in the figures, maximum cylinder gas pressure increased with increasing engine load for the all fuels. According the graph, with the use of biodiesel, the peak cylinder pressure slightly decreases as compared to diesel, due to the lower calorific value [19, 23] and higher viscosity of biodiesel [23]. When it comes to burning biodiesel, the combustion of biodiesel fuel blends started earlier than that of No 2 diesel fuel at all engine loads due to higher density, viscosity, cetane number and bulk modulus of the biodiesel blends [24–26]. Biodiesel injection pressure rise higher than diesel fuel due to the lower compressibility (higher bulk modulus) of biodiesel, and also propagates faster towards the injectors as a consequence of its higher sound velocity. Additionally greater viscosity of biodiesel reduces pump leakage, resulting in increased injection line pressure. Consequently, with the use of biodiesel, faster and earlier needle opening occurs compared to diesel fuel [27].

As the engine load increase heat release rate of tested fuels increases owing to increment in fuel amounts. Heat release rate of biodiesel is lower than diesel at all engine loads attributing to the lower calorific value of biodiesel as compared to diesel [19]. When the biodiesel fraction increased in the blends the premixed phase peak decreased, while an increased mixing–controlled phase peak occurred because of the presence of additional oxygen molecules in biodiesel fuel. This may have led to a more complete combustion and consequently higher peak of heat release [28].

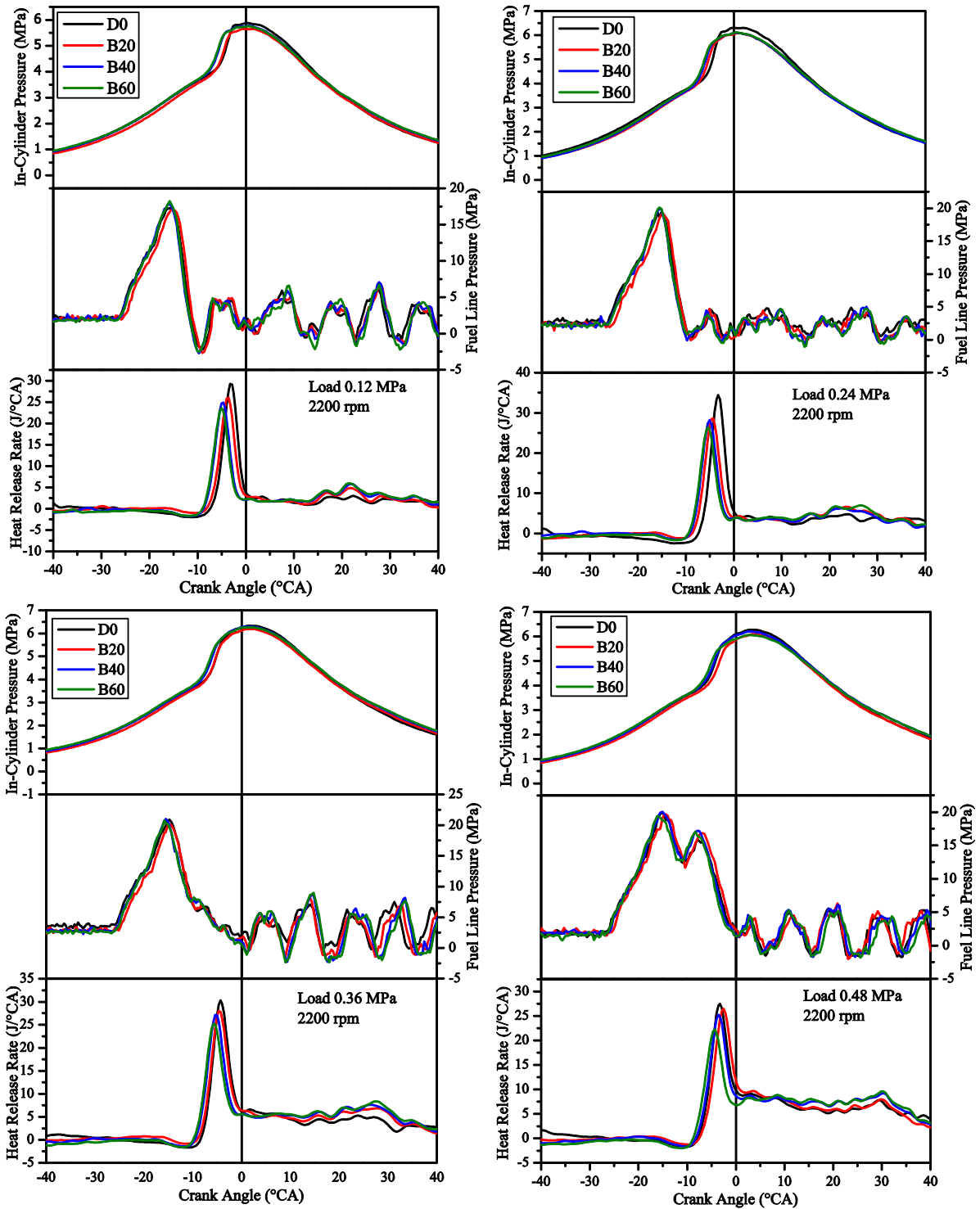


Figure 3. Effects of biodiesel addition on in-cylinder pressure, heat release rate and fuel line pressure at 0.12 MPa, 0.24 MPa, 0.36 MPa and 0.48 MPa engine loads and 2200 rpm engine speed.

3.3. Exhaust gas emissions

The variations of exhaust gas emissions of smoke, THC, CO, CO₂ and NO_x at four engine loads (BMEP, 0.12 MPa, 0.24 MPa, 0.36 MPa and 0.48 MPa) and 2200 rpm engine speed are shown in Figure 4. The main reason of CO emission among combustion products is lower air fuel ratio [22]. As the engine load increases, CO emissions of all tested fuels also increase because of increasing fuel amount. Increment in fuel amount both lead to the air-fuel mixture as rich and so increasing CO emission. CO emission level decreases by means of the 11% biodiesel oxygen content that helps for the complete combustion [29]. In addition, CO emissions reduce when using biodiesel due lower carbon to hydrogen ratio in biodiesel compared to diesel [26, 30]. With regard to CO emission, B60 *crambe* biodiesel has lower emission of 33.8% compared to diesel at 0.48 engine load. Rosa et al. CO emission of *crambe* biodiesel stated that 43.42% less emission than diesel [31].

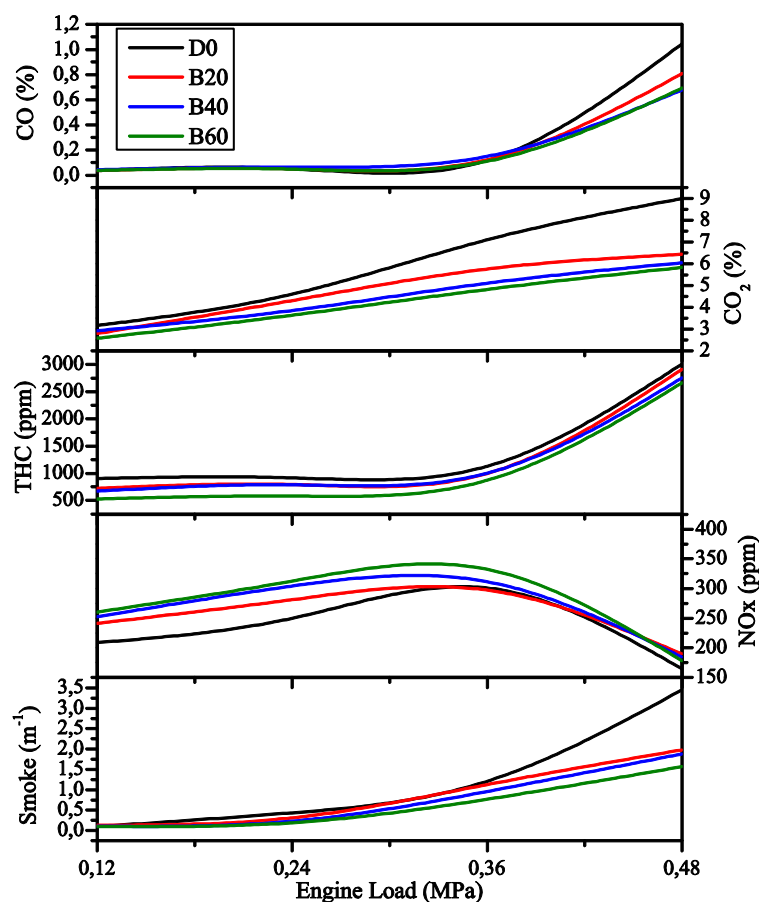


Figure 4. Effects of biodiesel addition and engine load on exhaust emissions (Smoke, THC, CO, CO₂, NO_x) at 2200 rpm engine speed.

Lower CO₂ emissions of biodiesel may be because (1) biodiesel is a lower carbon fuel due to the presence of oxygen atoms and (2) biodiesel has lower carbon to hydrogen ratio [19]. Depending on the increasing in the engine load, CO₂ emissions increase since more fuel injected into the engine. The other effects are increasing in combustion temperature and oxidization rates [32]. Figure 4 shows the CO₂ emission. The lowest CO₂ emissions propagate B60 *crambe* biodiesel of 35.2% compared to diesel at 0.48 engine load.

The variations of HC emissions shows in Fig. 4. The unburned HC emissions are caused by two major phenomena: the first one is the over-mixing leading to overlean regions and the second one

is the under-mixing leading to over-rich regions [33]. HC emissions of tested fuels increase with increasing engine load because of the more fuel injected into the engine. The use of biodiesel improves the combustion process due to oxygen content in biodiesel and the lower carbon content in biodiesel causes reducing the HC emissions [19, 34]. Additionally the higher cetane number and less aromatic content of biodiesel reduces the combustion delay which results in the THC emissions reduction [24-25, 30]. Furthermore, the feedstock of biodiesel and its properties like the different chain length or saturation level of biodiesels have an effect on HC emissions. The advance in injection and combustion of biodiesel promotes the lower HC emissions [35].

Fig. 4 shows that biodiesel addition leads to an increase in NO_x emissions. The NO_x emission is related to the engine combustion temperature which increases with the increasing engine speed and load. It is thought that higher cylinder temperature causes higher the NO_x emissions [19]. Furthermore, the higher cetane number promotes NO_x formation because of the higher cycle temperature and higher residence time [33]. Additionally, complete combustion causes higher combustion temperature, which results in higher NO_x formation [36]. The other reasons that higher NO_x are; increased iodine number and fatty acids with two double bond, fatty acids with one double bond have less NO_x emissions than that of fatty acids with two double bond [30], biodiesel has an advance of injection timing due to the lower compressibility [26, 37, 38], and another different physical properties such as density, viscosity, speed of sound and higher cetane number which lead to early start of combustion timing and longer combustion period [26]. Rosa et al. found that NO_x emission 9.06% decreased while in this study NO_x emission of biodiesel blends found that slightly increased. The reasons of higher NO_x emission explained above [31].

Smoke is mainly produced in the diffusive combustion phase; the oxygenated fuel blends lead to an improvement in diffusive combustion [36]. As it can be noticed in Fig. 4, at low loads, the evolution of PM with respect to BMEP is slow but at high loads, the PM emissions increase rapidly due to rich air-fuel mixture. Because a higher fuel fraction burns lately at the expansion stroke where the oxidation ability is very low, and the chamber temperature is not high enough [33]. The smoke emission of biodiesel is lower than diesel fuel due to more oxygen molecules present in the biodiesel [39], decrease in the carbon content, lower aromatic and sulfur compounds, higher cetane number, and the increase of oxygen content for biodiesel [26, 30, 35, 38].

4. Conclusion

In this study, the performance, combustion and emission characteristics of diesel fuel and biodiesel derived from *crambe abyssinica* oil and its blends of B20, B40 and B60 were compared under 0.12 MPa, 0.24 MPa, 0.36 MPa and 0.48 MPa engine loads and 2200 rpm engine speed. Based on the experimental results, the following major conclusions have been drawn. BSFC of biodiesel blends were slightly higher than diesel fuel due to lower heating value. In respect to engine emissions, Smoke, CO, CO₂ and THC emissions decreased, whereas there was slightly increase in NO_x emission. The presence of oxygen in the biodiesel molecule causes an increase of NO_x emissions while it reduces the smoke emissions. When biodiesel blends is used, fuel line pressure has risen before the diesel fuel due to the less compressibility of biodiesel. The peak cylinder gas pressure of *crambe* biodiesel blends are slightly higher than that of the No 2 diesel fuel. Biodiesel blends have an earlier premixed combustion phase with regard to diesel fuel, by the reason of their earlier start of combustion and higher cetane number and biodiesel blends have shown lower heat release by means of the lower calorific value. Biodiesel production from *crambe* oil can take part in alternative fuel research from non edible oils by virtue of its the advantages in near future.

References

- [1] Köybaşı, Ö., *Çukurova koşullarında bazı crambe türlerinin verim ve yağ oranlarının saptanması*, Yüksek Lisans Tezi, Çukurova Üniversitesi Fen Bilimleri Enstitüsü, Adana (2008) 3–15, 47.
- [2] Çömlekçioğlu, N., *Ülkemizde doğal yayılış gösteren crambe spp.'nin kimyasal içeriğinin ve endüstriyel kullanım alanlarının incelenmesi*, Yüksek Lisans Tezi, Kahramanmaraş Sütçü İmam Üniversitesi Fen Bilimleri Enstitüsü, Kahramanmaraş (2005) 1-2, 4, 14, 17, 30, 33.
- [3] Falasca, S.L., Flores, N., Lamas, M.C., Carballo, S.M., Anschau, A., *Crambe Abyssinica: An Almost Unknown Crop With A Promissory Future To Produce Biodiesel In Argentina*, International Journal Of Hydrogen Energy 35 (2010) 5808–5812.
- [4] Vollmann, J., Ruckebauer, P., *Agronomic performance and oil quality of crambe as affected by genotype and environment*, Die Bodenkultur 44 (1993) 335–343.
- [5] Wang, Y.P., Tang, J.S., Chu, C.Q., Tian, J., *A preliminary study on the introduction and cultivation of crambe abyssinica in China, an oil plant for industrial uses*, Industrial Crops and Products 12 (2000) 47–52.
- [6] Pryde, E.H., *Vegetable oil raw materials*, J. Am. Oil Chemists' soc, 56 (1979) 719–725.
- [7] Mustakas, G.C., Kirk, L.D., Griffin, E.L., JR., *Crambe seed processing. Improved feed meal by soda ash treatment*, The Journal of the American Oil Chemists' Society 45 (1968) 53–57.
- [8] Grewal, V.S., Ramamurthi, S., McCurdy, A.R., *Synthesis and properties of erucic acid triacylglycerols*, JAOCS 70(10) (1993) 955–959.
- [9] Nieschlag, H.J., Wolff, I.A., *Industrial uses of high erucic oils*, JAOCS 48 (1971) 723–727.
- [10] Vargas-Lopez, J.M., Wiesenborn, D., Tostenson, K., Cihacek, L., *Processing of crambe for oil and isolation of erucic acid*, JAOCS 76(7) (1999) 801–809.
- [11] Anonymos, *Crambe, Industrial Rapeseed, and Tung Provide Valuable Oils*. Economic Research Service, USDA Industrial Uses/IUS-6/September (1996) 17–23.
- [12] Reuber, M.A., Johson, L.A., Watkins, L.R., *Dehulling crambe seed for improved oil extraction and meal quality*, JAOCS 78(6) (2001) 661–664.
- [13] Derksen, J.T.P., Cuperus, F.P., Kolster, P., *Renewable resources in coatings technology: a review*, Progress in Organic Coatings 27 (1996) 45–53.
- [14] Molnar, N.M., *Erucamide*, The Journal of the American Oil Chemists' Society 51 (1974) 84–87.
- [15] Bruun, J.H., Matchett, J.R., *Utilization potential of crambe abssinica*, JAOCS 40 (1963) 1–5.
- [16] Demirbaş, A., *Relationships derived from physical properties of vegetable oil and biodiesel fuels*, Fuel 87 (2008) 1743–1748.

-
- [17] Özçelik, A.E., Aydoğan, H., Acaroğlu, M., *Determining the performance, emission and combustion properties of camelina biodiesel blends*, Energy Conversion and Management 96 (2015) 47–57.
- [18] Gogoi, T.K., Sarma A.K., Misra P.S., Haque S.T., *Combustion analysis of jatropha methyl ester and its ethanol and acetone blends in a diesel engine*, International Journal of Emerging Technology and Advanced Engineering 3(3) (2013) 51–57.
- [19] An, H., Yang, W.M., Chou, S.K., Chua, K.J., *Combustion and emissions characteristics of diesel engine fueled by biodiesel at partial load conditions*, Applied Energy 99 (2012) 363–371.
- [20] Raheman, H., Phadatare, A.G., *Diesel engine emissions and performance from blends of karanja methyl ester and diesel*, Biomass and Bioenergy 27 (2004) 393–397.
- [21] Vedaraman, N., Puhan, S., Nagarajan, G., Velappan, K.C., *Preparation of palm oil biodiesel and effect of various additives on NO_x emission reduction in B20: an experimental study*, International Journal of Green Energy 8 (2011) 383–397.
- [22] Özsezen, A.N., Çanakçı, M., *Biyodizel ve Karışımlarının Kullanıldığı bir Dizel Motorda Performans ve Emisyon Analizi*, Pamukkale Üniversitesi Mühendislik Bilimleri Dergisi 15(2) (2009) 173–180.
- [23] How, H.G., Masjuki, H.H., Kalam, M.A., Teoh, Y.H., *An investigation of the engine performance, emissions and combustion characteristics of coconut biodiesel in a high-pressure common-rail diesel engine*, Energy 69 (2014) 749–759.
- [24] Can, Ö., *Combustion characteristics, performance and exhaust emissions of a diesel engine fueled with a waste cooking oil biodiesel mixture*, Energy Conversion and Management 87 (2014) 676–686.
- [25] Lapuerta, M., Armas, O., Fernandez, J.R., *Effect of biodiesel fuels on diesel engine emissions*, Progress in Energy and Combustion Science 34 (2008) 198–223.
- [26] Gürü, M., Koca, A., Can, Ö., Çınar, C., Şahin, F., *Biodiesel production from waste chicken fat based sources and evaluation with Mg based additive in a diesel engine*, Renewable Energy 35 (2010) 637–643.
- [27] Caresana, F., *Impact of biodiesel bulk modulus on injection pressure and injection timing. The effect of residual pressure*, Fuel 90 (2011) 477–485.
- [28] Martins, M.E.S., Zientarski, R.R., Machado, P.R.M., Dornelles, H.M., Antolini, J.B.V., Nora, M.D., *Analysis of Engine Performance and Combustion Characteristics of Diesel and Biodiesel Blends in a Compression Ignition Engine*, SAE TECHNICAL PAPER SERIES (2016) 36-0391.
- [29] Ramadhas, A.S., Muraleedharan, C., Jayaraj, S., *Performance and emission evaluation of a diesel engine fueled with methyl esters of rubber seed oil*, Renewable Energy 30 (2005) 1789–1800.
- [30] Xue, J., *Combustion characteristics, engine performances and emissions of waste edible oil biodiesel in diesel engine*, Renewable and Sustainable Energy Reviews 23 (2013) 350–365.

-
- [31] Rosa, H.A., Wazilewski, W.T., Secco, D., Chaves, L.I., Veloso, G., Souza, S.N.M., Silva, M.J., Santos, R.F., *Biodiesel produced from crambe oil in Brazil-A study of performance and emissions in a diesel cycle engine generator*, Renewable and Sustainable Energy Reviews 38 (2014) 651–655.
- [32] Gümüş, M., Sayın, C., Çanakçı, M., *The impact of fuel injection pressure on the exhaust emissions of a direct injection diesel engine fueled with biodiesel–diesel fuel blends*, Fuel 95 (2012) 486–494.
- [33] Awad, S., Loubar, K., Tazerout, M., *Experimental investigation on the combustion, performance and pollutant emissions of biodiesel from animal fat residues on a direct injection diesel engine*, Energy 69 (2014) 826–836.
- [34] Man, X.J., Cheung, C.S., Ning, Z., Wei, L., Huang, Z.H., *Influence of engine load and speed on regulated and unregulated emissions of a diesel engine fueled with diesel fuel blended with waste cooking oil biodiesel*, Fuel 180 (2016) 41–49.
- [35] Xue, J., Grift, T.E., Hansen, A.C., *Effect of biodiesel on engine performances and emissions*, Renewable and Sustainable Energy Reviews 15 (2011) 1098–1116.
- [36] Devan, P.K., Mahalakshmi, N.V., *A study of the performance, emission and combustion characteristics of a compression ignition engine using methyl ester of paradise oil–eucalyptus oil blends*, Applied Energy 86 (2009) 675–680.
- [37] Çanakçı, M., *Combustion characteristics of a turbocharged DI compression ignition engine fueled with petroleum diesel fuels and biodiesel*, Bioresource Technology 98 (2007) 1167–1175.
- [38] Dia, Y., Cheung, C.S., Huang, Z., *Experimental investigation on regulated and unregulated emissions of a diesel engine fueled with ultra-low sulfur diesel fuel blended with biodiesel from waste cooking oil*, SCIENCE OF THE TOTAL ENVIRONMENT 407 (2009) 835–846.
- [39] Sivasami, K., Selladurai, V., Devadasan, S.R., Rajan, K., *Reduction of NO_x and Smoke Emission with the effect of Biodiesel-Water Emulsion Mixture Fuel in a Diesel Engine*, International Journal of Engineering and Technology (IJET) 5(5) Oct-Nov (2013) 4378–4387.

The performance, emissions and combustion investigation on mixing of *crambe* and waste frying biodiesels blended with diesel

Dr. Ayhan UYAROĞLU¹, Doç. Dr. Fatih AKSOY²

¹ Selçuklu Vocational and Technical Anatolian High School,

ayhanuyaroglu@hotmail.com

² Afyon Kocatepe University Faculty of Technology, Department of Automotive Engineering,

faksoy@aku.edu.tr

Abstract: Biodiesel production from inedible oils is gaining importance all over the world with regard to the economically. Inedible oils can help to prevent the increase in edible oil prices by diminishing the demand to producing biodiesel from the edible oils. On the other hand increasing environmental concerns have induced the researchers to produce alternative fuel from renewable sources. With the aim of this study, the impacts of biodiesel/diesel blend fuels were examined the performance, emissions and combustion on a single-cylinder, four-stroke, direct injected diesel engine with air cooling system were evaluated with the reference fuel of No. 2 diesel fuel. The tests have been performed at 2200 1/min fixed speed and four different engine loads. The dual biodiesel blends that produced from inedible oils were prepared in different proportions by volume basis. Used blended fuels were (25Cr75WFO) B20-B40-B60, (50Cr50WFO) B20-B40-B60, (75Cr25WFO) B20-B40-B60 mixed with *crambe* (Cr) and waste frying (WFO) biodiesel and diesel oil (B0). Numbers in parentheses show the mixing ratio of *Crambe* and Waste frying oil by volume. Both the effects of blends on CO, CO₂, THC, NO_x and smoke emissions and the brake specific fuel consumption, heat release rate and the in-cylinder pressure were investigated. As a result biodiesel can be considered eco-friendly.

Keywords: Biodiesel, combustion, *crambe abyssinica*, emissions, waste frying oil.

1. Introduction

Biodiesel has desirable attributes such as biodegradable, renewable, sustainable and carbon neutral so it can be accepted as an alternative to conventional diesel [1]. The advantages of biodiesels as an alternative diesel fuel are the minimal sulfur and aromatic content, and the higher flash point, lubricity and cetane number. The disadvantages of biodiesel are the higher viscosity, the higher pour point, the lower calorific value and volatility, the hygroscopic tendency, and the lower oxidation stability [2]. There are many researches about biodiesel fuels that are widely considered as alternative fuel source. These researches are mostly related to the native crops due to obtained easily. For example soybean oil in the USA and Brazil, rapeseed and sunflower oil in Europe, palm oil in Malaysia and Indonesia, coconut oil in Philippines and waste oil in Japan [3-5]. On the other hand, importance of biodiesel production from inedible oil is growing rapidly. From this point of view, both inedible oils and waste frying oils become prominent in biodiesel production. While biodiesel production from inedible oil has an advantage due to of its lower prices, biodiesel

production from waste frying oil has an advantage to solve of its disposal problems. *Crambe abyssinica* is an inedible oil because of its erucic acid content. *Crambe abyssinica* is winter crop, has a short cycle (between 90 and 100 days) and acts in crop rotation [6]. While in literature, very few experiments have been conducted with the combination of dual biodiesel and diesel as a fuel, most of the literatures focused on single biodiesel and its blends. Dual biodiesel can enable to adjust fuel properties of biodiesel such as pour point, cetane number, flash point, viscosity, density.

The objective of the present study is to perform experimentally parametric tests of a single cylinder diesel injection engine performance, combustion and emissions fueled with biodiesel obtained from mixing *crambe abyssinica* and waste frying oil with 2200 1/min fixed engine speed and at four different engine loads.

2. Materials and methods

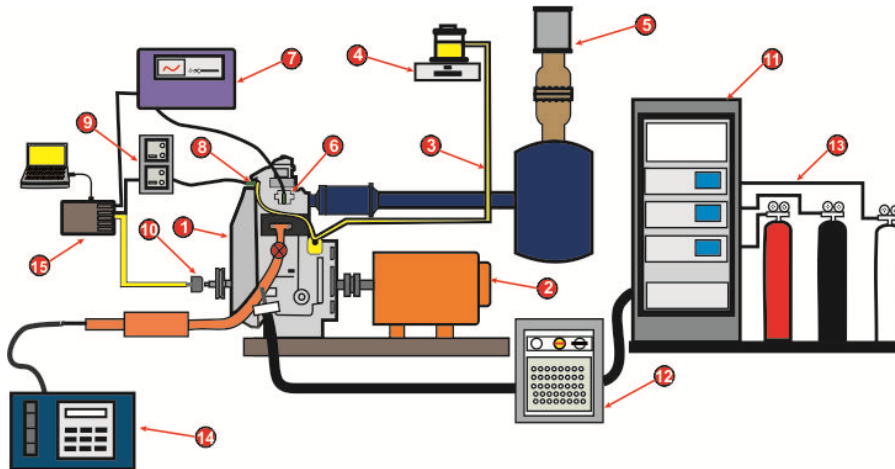
2.1. Fuel description

Waste frying oil was collected from a Turkish restaurant and filtered from solid impurities. Only one restaurant was used as a source for uniformity reasons. The origin of the waste frying oil is sunflower oil. *Crambe abyssinica* oil was purchased from Elementis Specialities Company by the name of Fancor Abyssinian Oil. The used oil was transesterified using methanol in the presence of NaOH. The transesterification parameters of mixing *crambe* oil and waste frying oil was applied as 6:1 Methanol to oil molar ratio with NaOH catalyst 0.42 g (w/w), 57°C reaction temperature, and 60 minutes reaction time and transesterification yield for blends was found as 25Cr75WFO 97.1%, 50Cr50WFO 97.3% and 75Cr25WFO 96.8%. The numbers next to the abbreviations show the mixing ratio of *Crambe* and Waste frying oil by volume. After the alkali transesterification reaction was completed, the mixture was left in separating funnel for 8-10 hours for gravity separation of the methyl esters and glycerol. The heavier glycerin settled at the bottom and was removed; the remaining sample was washed with hot distilled water (about 85°C) several times until the wash water became clear. After washing, the biodiesel was heated up 110°C for 20 minutes to remove any remaining water. Biodiesel blends were prepared in different proportions by volume basis like B20-B40-B60. Chemical properties were determined for both of used fuels according to European Fatty Acids Methyl Ester (FAME) standard draft (EN 14214), as shown in Table 1.

Table 1. Fuel properties used in tests

	25Cr75WFO	50Cr50WFO	75Cr25WFO	Diesel fuel
Density 15 °C (kg/m ³)	887.49	884.30	883.31	841.75
Kinematic viscosity 40 °C (mm ² /s)	5,314	5,592	6,138	3.354
Flash point °C	-	-	-	-
Lower heating value (MJ/kg)	-	-	-	-
Sulfur (mg/kg)	1,3	1,1	1,1	-
Water content (mg/kg)	481,67	463,97	431,04	-
Cetane index	-	-	-	53,1

2.2. Engine test facility



1- Test engine 2- DC dynamometer 3- Diesel fuel line 4- Sensitive scale 5- Laminar flow meter 6- In-cylinder pressure sensor 7- Combustion analyzer 8- Diesel fuel line pressure sensor 9- Diesel fuel line pressure sensor amplifier 10- Encoder 11- Emission gas analyzer 12- Emission sampling system 13- Function gases (N_2 , O_2 , H_2/He) and span gases (C_3H_8 , CO_2 , CO , O_2) 14- Smoke meter 15- Data acquisition card

Figure 1. Test rig

The test rig used in this study is shown in Fig. 1 and the specifications of the single cylinder diesel engine are given in Table 2. The engine was loaded with Cussons brand P8160 model DC type dynamometer measuring up to 10 kW at 4000 rpm. The inlet air flow rates were measured with Merriam brand Z50MC2-4F model laminar flow meter. The inlet air, the lubrication oil and the exhaust gas temperatures were measured using NiCr–Ni type thermocouples. The fuel consumption values were measured using an electronic balance with high precision. The engine torque was calculated from the force values acquired with a strain gauge type load cell and the engine speeds were obtained with a magnetic collector type sensor. In order to minimize the variations of the inlet air temperature, PID (ENDA ETC. 9420) controlled air heater (Farnam Flow Torch 400) was used. The in-cylinder gas pressures were acquired with AVL-8QP500c water cooled pressure transducer and Cussons P4110 combustion analysis device with NIUSB-6259 data acquisition (DAQ). In order to determine injection characteristics, the fuel line pressures were measured using AVL SL-31D 2000 model pressure sensor and AVL 3009 A04 model amplifier. The encoder with 1000 pulses was placed on crankshaft axis in order to record crank angle and Top Dead Centre (TDC) values.

Table 2. General specifications of the Antor diesel engine.

Make/model	Antor/6LD400
Engine type	DI-diesel engine, natural aspirated, air cooled
Cylinder number	1
Bore x stroke (mm)	86 × 68
Displacement (cm³)	395
Compression ratio	18:1
Maximum power (kW)	5.4 @ 3000 rpm
Maximum torque (Nm)	19.6 @ 2200 rpm
Combustion chamber geometry	ω type
Fuel injection system	PF jerk-type fuel pump
Injection nozzle	0.24 mm × 4 holes × 160°
Nozzle opening pressure (bar)	180
Fuel delivery advance angle (°CA)	28 BTDC
Valve timings IVO/IVC (°CA)	7.5 BTDC/25.5 ABDC
EVO/EVC (°CA)	21 BBDC/3 ATDC

2.3. Measurements of exhaust gas emissions

Exhaust gas emissions were measured using Environnement SA-EGAS 2M gas analyzer that specifications were given in the Table 3. The EGAS 2M gas analyzer measures THC emissions with Heated Flame Ionization Detection (HFID) analyzer, NO_x with heated chemiluminescence (CLA) analyzer and CO/CO₂ with a Non-Dispersive Infrared Sensor (NDIR).

Table 3. Technical specifications of exhaust gas analyzers.

Analyzer	GRAPHITE 52M	TOPAZA 32M	MIR 2M
Measuring compound	THC (wet)	NO-NO _x (wet)	CO-CO ₂ -O ₂ (dry)
Measurement principle	HFID	HCLD	NDIR Paramagnetic
Linearity	<1%	<1%	<1%
Measurement rate	0-10/30000 ppm	0-10/10000 ppm	0-500/10000 ppm (CO) 0-1/20% (CO ₂) 0-5/25% (O ₂)
Lower detectable limit	0.05 ppm (0-10 ppm range)	0.1 ppm (0-10 ppm range)	<2% (FSO)
Response time (T₉₀ s)	<1.5 s	<2 s	<2 s

AVL 4000 DiSmoke opacity meter specifications were shown in Table 4. AVL 4000 DiSmoke opacity meter is partial flow meter, which have 0.1 m⁻¹ sensibility and range of 0–99.99 m⁻¹.

Table 4. Technical specifications of opacimeter.

Analyzer	AVL DiSmoke 4000	
Measurement principle	Partial flow opacimeter	
Measurement range	Opacity	K value
Accuracy	0-100% 0-99.99 m ⁻¹	Accuracy 0.1% 0.01 m ⁻¹

2.4. Heat Release calculation

Heat release analysis was calculated from Eq. (1) according to single-zone combustion model based on the first law of the thermodynamics. The heat loss from the wall is neglected. In this study, cylinder pressure and heat emission analysis were carried out and $\gamma = 1.35$ was taken for all fuels [7]. In each cycle 2000 raw in-cylinder pressure data are received at intervals of 0.36 °CA. For the purpose of negating the effect of cyclic differences, corrections were made on 50 consecutive cycles and their average was calculated for analyses. Noise is generated as a result of the numeric operations performed with cylinder pressure data in heat dissipation analysis. With the aim of to reduce these noises, the filtering operation presented in Eq. (2) was implemented.

$$\frac{dQ_n}{d\theta} = \frac{\gamma}{\gamma-1} p \frac{dv}{d\theta} + \frac{1}{\gamma-1} v \frac{dp}{d\theta} \quad (1)$$

$$(du/dx)_i = (u_i + 2u_{i+1} + 3u_{i+2} + 4u_{i+3} + 3u_{i+4} + 2u_{i+5} + u_{i+6})/16 \quad (2)$$

2.5. Testing procedure

The experiments were conducted at four different engine loads (BMEP, 0.12 MPa, 0.24 MPa, 0.36 MPa and 0.48 MPa) and 2200 rpm engine speed. At the beginning of the tests, the engine was warmed with No. 2 diesel fuel. The oil and inlet air temperatures were kept at 85 ± 2 °C and 25 ± 1 °C, respectively, Biodiesel blends containing 20%, 40% and 60% proportions by volume were tested in the experiments and the results were compared with conventional No. 2 diesel fuel operation. The accuracy of all devices and uncertainties are given in Table 5.

Table 5. Measurement accuracy and uncertainties of calculated results.

	Accuracy	Uncertainty
Time (s)	±0.5%	
Temperature (°C)	±1	
Fuel (g)	±0.1	
Engine speed (1/min)	±1%	
Load (N)	±0.25%	
Cylinder pressure	11.96 (pC/bar)	
Torque (Nm)		±0.25%
Fuel flow rate (g/min)		±0.72%
Specific fuel consumption (g/kW-h)		±1.26%

3. Results and discussion

3.1. Brake specific fuel consumption (BSFC)

Figure 2. shows the variations of brake specific fuel consumption of tested fuels under the four engine loads (BMEP, 0.12 MPa, 0.24 MPa, 0.36 MPa and 0.48 MPa) and 2200 rpm engine speed. The higher specific fuel consumption for the dual biodiesel fuel consumption is due to the lower calorific value of the blends [8]. As specific fuel consumption was calculated on weight basis, higher densities lead to higher values for BSFC [9]. The higher viscosity of biodiesel fuel results in poor mixing with air and leads to poor atomization which consumes more fuel [10]. The BSFC increased with the increase of biodiesel blends [11].

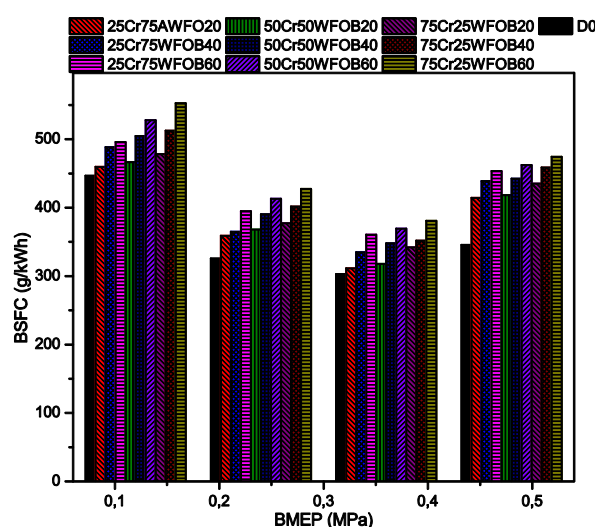


Figure 2. Effects of biodiesel addition and engine load on brake specific fuel consumption at 2200 rpm engine speed.

3.2. Combustion characteristics

The variations in combustion (in-cylinder pressure, heat release rate) and fuel injection (fuel line pressure) parameters for No. 2 diesel fuel and biodiesel fuel blends (B20, B40 and B60) at four engine loads (BMEP, 0.12 MPa, 0.24 MPa, 0.36 MPa and 0.48 MPa) and 2200 rpm engine speed was shown in Fig. 3. Peak pressure increased with increasing engine load for the all fuels. However the decreasing in peak pressure with the addition of biodiesel concentration in the blends may be by the reason of the combined effects of higher viscosity and lower calorific values of the biodiesel fuel [12]. Biodiesel fuel injection is earlier than No 2 diesel fuel due to less compressible. Also, ignition delay is short because of the higher cetane number of biodiesel [13]. Therefore the combustion of biodiesel fuel blends started earlier than that of No 2 diesel fuel at all engine loads by virtue of viscosity, higher density, cetane number and bulk modulus of the biodiesel blends [13-15].

Heat release rate of tested fuels increases depending on the increasing the engine load and increasing engine load resulted in more fuel injected to the cylinder. Heat release rate of biodiesel is lower than diesel fuel at all engine loads attributing to the lower calorific value of biodiesel as compared to diesel [16]. Due to earlier start of combustion and having a less premixed combustible mixture of biodiesel and its blends, premixed combustion phase

occurs earlier with regard to diesel fuel. As well, the biodiesel has the less premixed combustion as the result of the slower vaporization of biodiesel and smaller accumulation of fuel during the shorten ignition delay time. Additionally the lower calorific value and higher cetane number of used cooking oil biodiesel and its blends may contribute to lower heat release [13, 17-19]. As the biodiesel fraction increased in the blends the premixed phase peak decreased, while an increased mixing-controlled phase peak occurred because of the presence of additional oxygen molecules in biodiesel fuel. This may have led to a more complete combustion and consequently higher peak of heat release and higher in-cylinder temperatures [13, 19-20].

According to the figures, fuel line pressure of tested fuels has increased by the engine load by reason of the increased fuel amount. Thanks to the lower compressibility (higher bulk modulus) of biodiesel, biodiesel injection pressure rise higher than diesel fuel and also propagates faster towards the injectors as a consequence of its higher sound velocity. Moreover higher viscosity of biodiesel reduces pump leakage, resulting in increased injection line pressure. Consequently, with the use of biodiesel, faster and earlier needle opening occurs compared to diesel fuel [21].

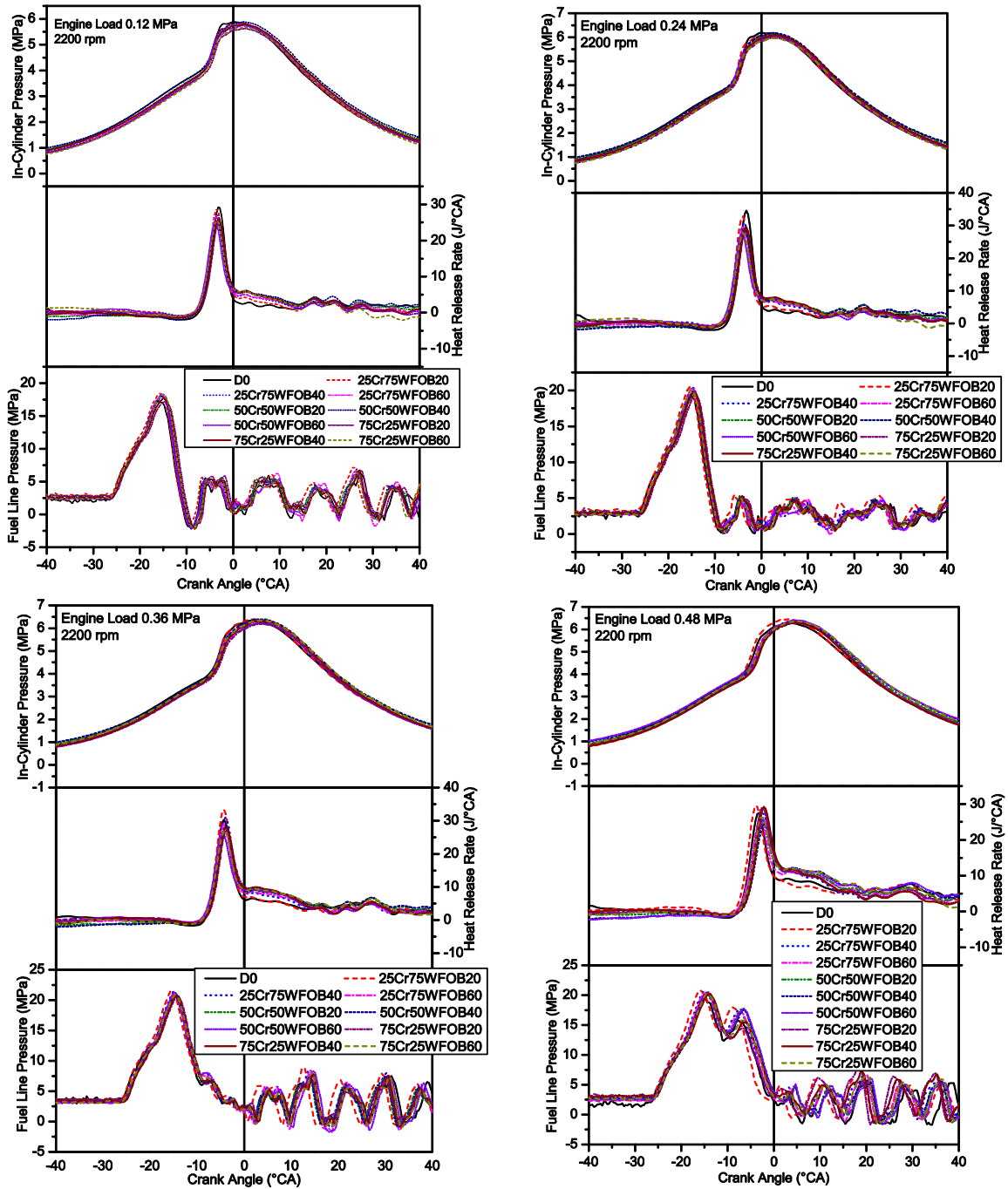


Figure 3. Effects of biodiesel addition on in-cylinder pressure, heat release rate and fuel line pressure at 0.12 MPa, 0.24 MPa, 0.36 MPa and 0.48 MPa engine loads and 2200 rpm engine speed.

3.3. Exhaust gas emissions

3.3.1. CO emissions

The variations of Carbon monoxide are shown in Fig. 4. The higher percentages of CO can be attributed to local rich regions and poor mixture formation in some locations of the

combustion chamber [22]. Carbon monoxide's (CO) content is also increasing with engine load. Lower CO at maximum load is by way of the oxygen contents in the biodiesel which makes easy burning at higher temperature in the cylinder [8]. The higher the CN in biodiesel blends, the shorter the ignition delay. It prolongs combustion period and therefore results in lower possibility of formation of rich fuel zone and reduced CO emission [11]. 75Cr25WFO blends have lower CO emission values.

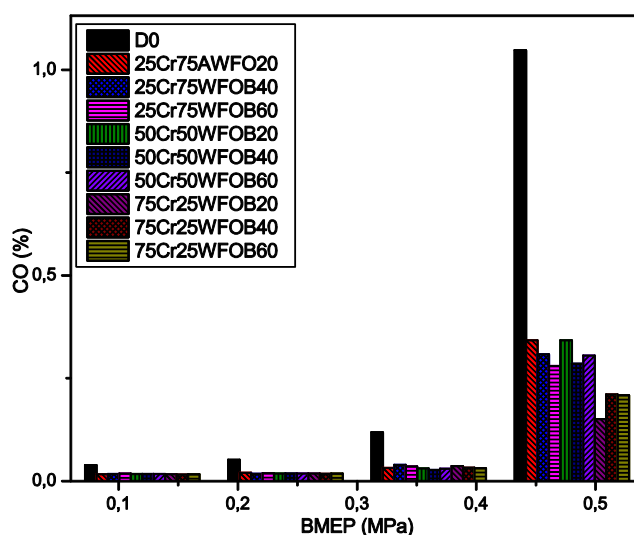


Figure 4. Variation in CO emissions with the engine load.

3.3.2. CO₂ emissions

The amount of CO₂ is an indication of complete combustion of fuel test inside the engine cylinder [11]. From the Figure 5, it is observed that, Increasing engine load causes more fuel injected into the cylinder so CO₂ emissions increases. While diesel fuel CO₂ emissions increased gradually, CO₂ emissions of biodiesel blends increased slowly. Higher oxygen content in biodiesel is the reason for lesser CO₂ emissions [10]. Lower CO₂ emissions of biodiesel than diesel fuel is resulted from the lower carbon to hydrogen ratio [17].

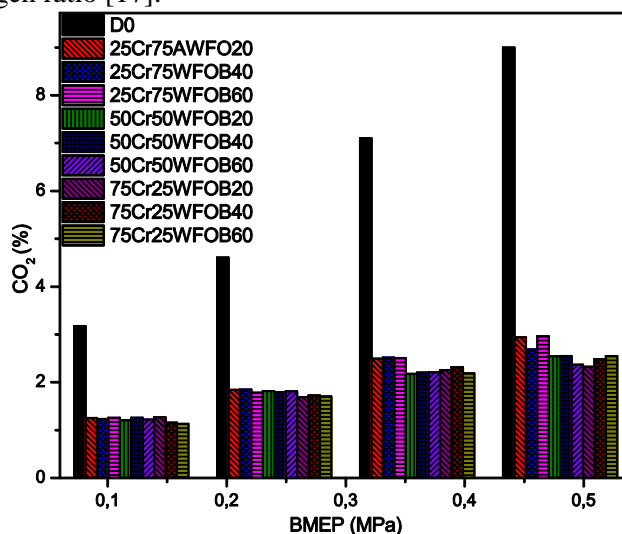


Figure 5. Variation in CO₂ emissions with the engine load.

3.3.3. THC emissions

From the Fig. 6. it can be seen that, as the engine load increases HC emissions of tested fuels increase. HC formation results from incomplete/partial combustion of fuel inside the engine cylinder [10] and also a small portion of these hydrocarbons originates from the lubricating oil [23]. The biodiesel have more oxygen content and the lower carbon content compared to diesel and hence it is expected that the HC emissions for biodiesel should be less than neat diesel. This is because higher oxygen content may lead to better combustion [10, 24]. Additionally the higher cetane number and less aromatic content of biodiesel reduces the combustion delay which results in the THC emissions reduction [14-15, 17].

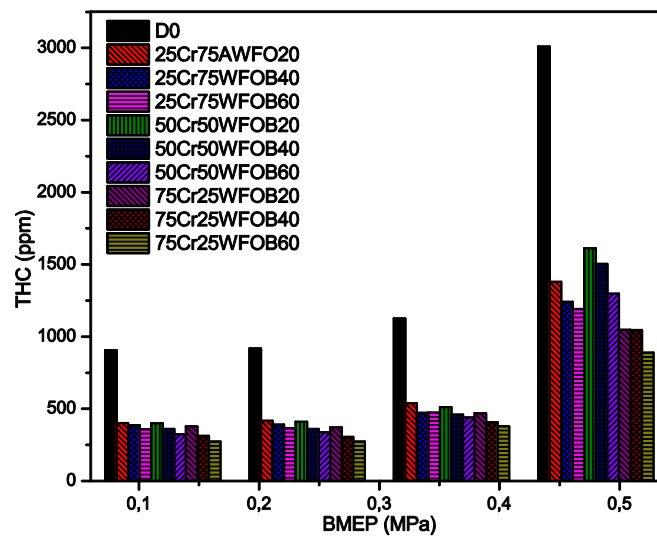


Figure 6. Variation in THC emissions with the engine load.

3.3.4. Smoke emissions

Smoke originates from the incomplete combustion of the hydrocarbon fuel and the partial reaction of the carbon content in the liquid fuel [12]. Fig. 7. depicts the variations of smoke emissions of tested fuels with the engine load. The amount of smoke increases at all tested fuels depending on the increase in engine load. Smoke emissions reduces as the blending ratio of biodiesel in the fuel blend increases. This reduction is due to oxygen content of the biodiesel molecule, enables more complete combustion even in regions of the fuel-rich diffusion flames in combustion chamber [25]. In addition, the lack of aromatic hydrocarbons and sulphur compounds further contribute to particulate emissions reduction since these compounds increase the soot nucleation rate [26]. According to Fig. 7. maximum decrease results from the 0.48 MPa engine load.

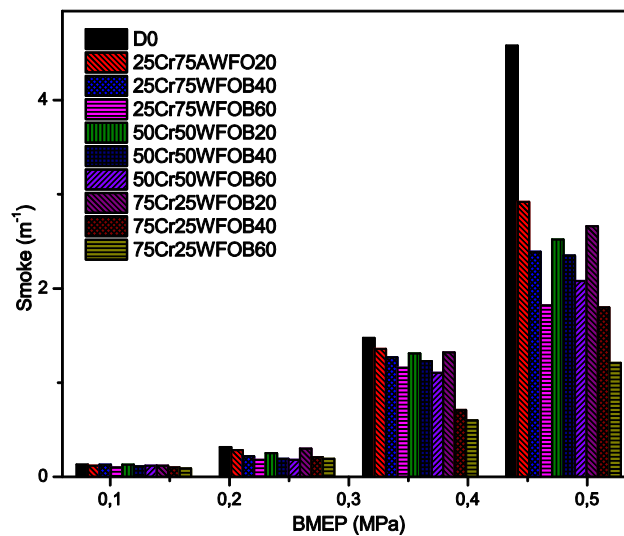


Figure 7. Variation in smoke emissions with the engine load.

3.3.5. NOx emissions

Fig. 8. illustrates the variation in NOx emission with the engine load. The formation of NOx depends on the fuel type, fuel properties and engine operating conditions [12]. In a diesel engine, NOx propagation is very sensitive to the engine combustion temperature which increases with the increasing engine speed and load. It is generally agreed that the higher the cylinder temperature, the higher the NOx emissions [16]. NOx formation is not only affected by the combustion temperature but also the local oxygen concentration and the residence time [8, 24]. Furthermore, an increase in fuel density results in higher NOx emissions [27] and presence of small amount of nitrogen in vegetable oil based biodiesel results in higher NOx emissions [8, 27]. On the other hand, because of the higher bulk modulus of biodiesel which leads to earlier fuel injection, favors NOx formation [24]. Besides, it can explain in increasing NOx emissions that the reduction in the heat dissipation by radiation, as a consequence of the lower amount of soot emitted with the use of biodiesel [12]. When we examine the Fig. 8. NOx emissions increase as the engine load increases except 0.48 MPa engine load in all tested fuels.

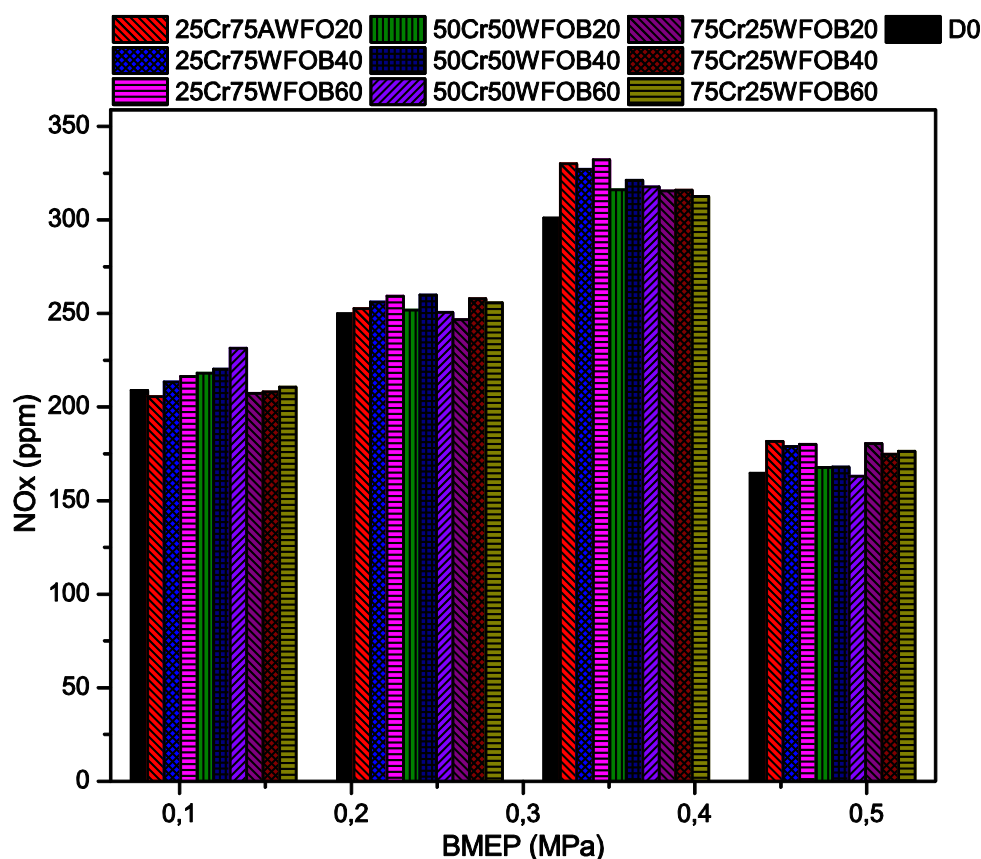


Figure 8. Variation in NOx emissions with the engine load.

4. Conclusion

In this study, the experiments were conducted using diesel and biodiesel blend fuels under 0,12 MPa, 0,24 MPa, 0,36 MPa, and 0,48 MPa loads to investigate the impact of biodiesel on the performance, combustion, and emission characteristics of diesel engine at 2200 rpm engine speed. Based on the experimental results, the following major conclusions have been concluded. Due to the lower calorific value of biodiesel, the BSFC increases with the increasing biodiesel blend ratio at all engine loads. For the combustion characteristics, it is found that the cylinder pressure decreases slightly with the use of biodiesel at all engine loads. Furthermore, it is observed the heat release rate of biodiesel blends are lower compared to diesel due to lower calorific value of biodiesel. When biodiesel blends is used, fuel line pressure has risen before the diesel fuel due to the less compressibility of biodiesel. The engine load is found to have significant influences on the emissions. Increasing engine load contributed to the increment in emissions. As the biodiesel ratio increases, Smoke, CO, CO₂ and THC emissions decreased, whereas there was significant increase in NOx emission. Generally, 75CR25WFO blends gave better results in terms of the emissions. Using dual biodiesel can enable to adjust fuel properties of biodiesel such as pour point, cetane number, flash point, viscosity, density. Biodiesel fuels with different physical and chemical characteristics can be blended to obtain the fuel with the desired characteristics.

References

- [1] Maghbouli, A. Yang, W., An, H., Li, J., Shafee, S., *Effects of injection strategies and fuel injector configuration on combustion and emission characteristics of a D.I. diesel engine fueled by bio-diesel*, Renewable Energy 76 (2015) 687–698.
- [2] Rakopoulos, D.C., Rakopoulos, C.D., Giakoumis, E.G., Papagiannakis, R.G., Kyritsis, D.C., *Influence of properties of various common bio-fuels on the combustion and emission characteristics of high-speed DI (direct injection) diesel engine: Vegetable oil, bio-diesel, ethanol, n-butanol, diethyl ether*, Energy 73 (2014) 354–366.
- [3] Agarwal, A.K., *Biofuels (alcohols and biodiesel) applications as fuels for internal combustion engines*, Progress in Energy and Combustion Science 33 (2007) 233–71.
- [4] Oo, C.W., Shioji, M., Nakao, S., Dung, N.N., Reksowardojo, I., Roces, S.S., Dugos, N.P., *Ignition and combustion characteristics of various biodiesel fuels*, Fuel 158 (2015) 279–287.
- [5] Pinto, A.C., Guarieiro, L.L.N., Rezende, M.J.C., Ribeiro, N.M., Torres, E.A., Lopes, W.A., Pereira, P.A. deP., Andrade, J.B., *Biodiesel: An Overview*, J. Braz. Chem. Soc., 16 (6B) (2005) 1313–1330.
- [6] Rosa, H.A., Wazilewski, W.T., Secco, D., Chaves, L.I., Veloso, G., Souza, S.N.M., daSilva, M.J., Santos, R.F., *Biodiesel produced from crambe oil in Brazil—A study of performance and emissions in a diesel cycle engine generator*, Renewable and Sustainable Energy Reviews 38 (2014) 651–655.
- [7] Gogoi, T.K., Sarma, A.K., Misra, P.S., Haque, S.T., *Combustion analysis of jatropha methyl ester and its ethanol and acetone blends in a diesel engine*, International Journal of Emerging Technology and Advanced Engineering 3(3) (2013) 51–57.
- [8] Srithar, K., Balasubramanian, K.A., Pavendan, V., Kumar, B.A., *Experimental investigations on mixing of two biodiesels blended with diesel as alternative fuel for diesel engines*, Journal of King Saud University—Engineering Sciences 29 (2017) 50–56.
- [9] Prabhakar, S., Annalai, K., Lalvani, I.J.R., *Experimental study of using hybrid vegetable oil blends in diesel engine*, Journal of Scientific&Industrial Research September 71 (2012) 612–615.
- [10] Samuel, K.J., Raj, R.T.K., Sreenivasulu, N., Rajasekhar, Y., Edison, G., Saco, S.A., *An Experimental Study on Performance and Emissions of a Direct Ignition Diesel Engine with Crude Pongamia, Pongamia Methyl Ester and Diethyl Ether Blended with Diesel*, INTERNATIONAL JOURNAL of RENEWABLE ENERGY RESEARCH 6(4) (2016) 1506–1515.
- [11] Chuah, L.F., Abd Aziz, A.R., Yusup, S., Bokhari, A., Klemes, J.J., Abdullah, M.Z., *Performance and emission of diesel engine fuelled by waste cooking oil methyl ester derived from palm olein using hydrodynamic cavitation*, Clean Techn Environ Policy, 09 April 2015.
- [12] How, H.G., Masjuki, H.H., Kalam, M.A., Teoh, Y.H., *An investigation of the engine performance, emissions and combustion characteristics of coconut biodiesel in a high-pressure common-rail diesel engine*, Energy 69 (2014) 749–759.
- [13] Gürü, M., Koca, A., Can, Ö., Çınar, C., Şahin, F., *Biodiesel production from waste chicken fat based sources and evaluation with Mg based additive in a diesel engine*, Renewable Energy 35 (2010) 637–643.
- [14] Lapuerta, M., Armas, O., Fernandez, J.R., *Effect of biodiesel fuels on diesel engine emissions*, Progress in Energy and Combustion Science 34 (2008) 198–223.

-
- [15] Can, Ö., *Combustion characteristics, performance and exhaust emissions of a diesel engine fueled with a waste cooking oil biodiesel mixture*, Energy Conversion and Management 87 (2014) 676–686.
- [16] An, H., Yang, W.M., Chou, S.K., Chua, K.J., *Combustion and emissions characteristics of diesel engine fueled by biodiesel at partial load conditions*, Applied Energy 99 (2012) 363–371.
- [17] Xue, J., *Combustion characteristics, engine performances and emissions of waste edible oil biodiesel in diesel engine*, Renewable and Sustainable Energy Reviews 23 (2013) 350–365.
- [18] Enweremadu, C.C., Rutto, H.L., *Combustion, emission and engine performance characteristics of used cooking oil biodiesel—A review*, Renewable and Sustainable Energy Reviews 14 (2010) 2863–2873.
- [19] Ryu, K., Oh, Y., *Combustion Characteristics of an Agricultural Diesel Engine using Biodiesel Fuel*, KSME International Journal 18 (4) (2004) 709–717.
- [20] Martins, M.E.S., Zientarski, R.R., Machado, P.R.M., Dornelles, H.M., Antolini, J.B.V., Nora, M.D., *Analysis of Engine Performance and Combustion Characteristics of Diesel and Biodiesel Blends in a Compression Ignition Engine*, SAE TECHNICAL PAPER SERIES (2016) 36–0391.
- [21] Caresana, F., *Impact of biodiesel bulk modulus on injection pressure and injection timing. The effect of residual pressure*, Fuel 90 (2011) 477–485.
- [22] Pavani, A., Hebale, A., Poojary, V., Parulekar, S., Kiran, C., Neeta, K., *Waste Sunflower Oil as an Alternative Fuel for Diesel Engines*, 2015 International Conference on Nascent Technologies in the Engineering Field (ICNTE-2015).
- [23] Puhan, S., Saravanan, N., Nagarajan, G., Vedaraman, N., *Effect of biodiesel unsaturated fatty acid on combustion characteristics of a DI compression ignition engine*, Biomass and Bioenergy 34 (2010) 1079–1088.
- [24] Man, X.J., Cheung, C.S., Ning, Z., Wei, L., Huang, Z.H., *Influence of engine load and speed on regulated and unregulated emissions of a diesel engine fueled with diesel fuel blended with waste cooking oil biodiesel*, Fuel 180 (2016) 41–49.
- [25] Lahane, S., Subramanian, K.A., *Effect of different percentages of biodiesel–diesel blends on injection, spray, combustion, performance, and emission characteristics of a diesel engine*, Fuel 139 (2015) 537–545.
- [26] Adaileh, W.M., AlQdah, K.S., *Performance of Diesel Engine Fuelled by a Biodiesel Extracted From A Waste Cooking Oil*, Energy Procedia 18 (2012) 1317–1334.
- [27] Nalgundwar, A., Paul, B., Sharma, S.K., *Comparison of performance and emissions characteristics of DI CI engine fueled with dual biodiesel blends of palm and jatropha*, Fuel 173 (2016) 172–179.

The effect of pressure on the biogas flame characteristics: a numerical study

Murat ŞAHİN¹ and Mustafa İLBAŞ^{2,*}

¹ Gazi University, Technology Transfer Implementation and Research Center, 06500
Teknikokullar, Ankara, Turkey

² Gazi University, Technology Faculty, Department of Energy Systems Engineering,
06500 Teknikokullar, Ankara, Turkey

Abstract: The present study focuses on the effects of air and fuel inlet pressure changes on combustion characteristics of a biogas turbulent flame. The modellings were performed using a CFD code. The inlet pressure values were varied between 21 mbars and 1000 mbars. It is predicted that when the air pressure is increased, the flame length of the biogas stretches in the combustion chamber. When the fuel pressure is increased, the flame length of the biogas also stretches in the combustion chamber due to velocity changes. Therefore, it has been found that the axial velocity of the biogas increases as the inlet pressure is increased. In the gradual increase of the air and fuel pressures, On the other hand it has been observed that the flame has moved away because of increasing turbulence intensity. It is predicted that the flame structure of the biogas changes significantly with changing inlet pressures. It has been found that the temperature values of the biogas increase as the inlet pressures are increased. The longest flame structure emerges when the air and fuel pressures are 1000 mbar.

Keywords: Biogas, high pressure combustion, high velocity, non-premixed combustion.

1. Introduction

Combustion is a process in which a reaction between fuel and oxidant takes place. Heat and electricity are normally generated after the reaction takes place. Fuel is also defined as energy-containing substance. If it reacts with any oxidant, heat can release. Coal, crude-oil and natural gas are well-known fuels all over the World. However, the scientist estimate that their resources will run out of in the near future. For this reason, alternative fuels such as biomass or biogas are very attractive. Biogas can be defined as an alternative fuel. It contains high amount of methane and carbondioxide depending on its gasification process. The more the methane is, the greater the thermal value in biogases as expected [1].

There are a lot of studies related to biogas combustion under different combustion conditions in the literature. Adouane et al. [2], for example, carried out an experimental study regarding decrement of NO_x emissions that arise from fuel NO_x mechanism. Hosseini et al. [3] investigated a biogas combustion under flameless combustion conditions. Lafay et al. [4] compared methane and biogas flames in terms of their stability combustion domains, flame structures and dynamics. Somehsaraei et al. [5] examined the fuel flexibility and performance analysis of biogas in micro gas turbines. Bhoi and Channiwala [6] have experimentally investigated combustion of producer gas that includes high amount of nitrogen.

Combustion brings about under different conditions such as thermal power, equivalence ratio, inlet pressure and temperature etc. These conditions affect combustion behaviours of any fuel considerably. Therefore, to investigate effects of these conditions are crucial for better comprehending combustion behaviours of fuels. So, this study concentrates on effects of the air and the biogas inlet pressures on combustion behaviours of the biogas in a combustor.

2. Cfd Modelling

3D CFD modelling has been performed by using the existing burner in order to determine the effects of the air and the biogas inlet pressures on the combustion characteristics of the biogas such as temperature and velocity distributions in the present study. This burner is shown in Figure 1a and 1b. It has turbulators with 15° angles in the side of air stream in order to provide tangential air velocity. Besides, the fuel inlet of this burner has radial inlets to achieve better mixing of air and fuel can be seen in Figure 1b. The combustor used in this study is shown in Figure 2. This combustor is sudden expansion type It has a length of 100 cm and a diameter of 40 cm.

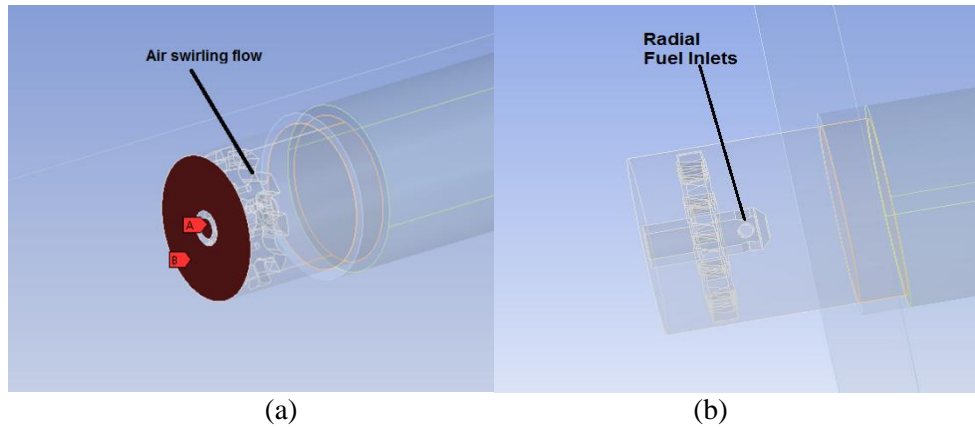


Figure 1a. Fuel and air inlets in the burner; **Figure 1b.** Radial fuel inlets

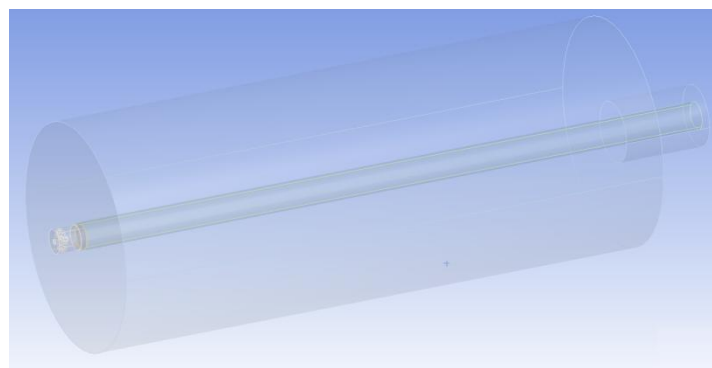


Figure 2. The Combustor

2.1. Governing Equations

The mathematical modelling described for the gas mixture fuel combustion is based on the steady-state condition, 3D continuity, momentum, energy and species equations. The general form of transport equation is below [7]:

$$\frac{\partial(\rho\Phi)}{\partial x} + \text{div}(\rho\Phi u) = \text{div}(\Gamma \text{grad}\Phi) + S_\Phi \quad (1)$$

where Φ represents the dependent variables. Γ shows the transport coefficient for variable Φ and S_Φ states the source term of the transport equation for Φ .

The Mixture Fraction/PDF Model has been used as combustion model in this study. This combustion model consists of the solution of transport equations for a single conserved scalar (the mixture fraction). In this model transport equations for individual species are not solved. Instead, individual component concentrations for species of interest are derived from the predicted mixture fraction distribution. The interaction of turbulence and chemistry are accounted for with the help of a probability density function (PDF) [8].

The PDF modelling approach was specifically developed for the simulation of turbulent diffusion flames. For a fuel/oxidant system, the mixture fraction, f can be expressed in terms of the local fuel mass fraction as:

$$f = \frac{m_F}{m_F + m_O} \quad (2)$$

Where m_F and m_O are mass fraction of fuel and oxidant respectively.

The mixture fraction, f is a conserved quantity whose value at each point in the flow domain is computed by the solution of the following conservation equation for the time averaged value of in the turbulent flow field [8].

$$\frac{\partial(\rho \bar{f})}{\partial t} + \frac{\partial(\rho u_i \bar{f})}{\partial x_i} = \frac{\partial}{\partial t} \left(\frac{\mu_t}{\sigma_t} \frac{\partial \bar{f}}{\partial x_i} \right) + S_m \quad (3)$$

where S_m is the source term which is due solely to transfer of mass into the gas phase from liquid fuel droplets.

In addition to solving for the mean mixture fraction, a conservation equation is solved for the mixture fraction variance, $\overline{f'^2}$ which is used in the closure model describing turbulence-chemistry interactions [8]:

$$\frac{\partial(\rho \overline{f'^2})}{\partial t} + \frac{\partial(\rho u_i \overline{f'^2})}{\partial x_i} = \frac{\partial}{\partial x_i} \left(\frac{\mu_t}{\sigma_t} \frac{\partial \overline{f'^2}}{\partial x_i} \right) + C_g \mu_t \left(\frac{\partial \overline{f'^2}}{\partial x_i} \right)^2 - C_d \rho \frac{\epsilon}{k} \overline{f'^2} \quad (4)$$

where σ_t , C_g and C_d are constants used in the mixture fraction/PDF model.

The radiation heat transfer happens at high temperatures. In combustors, the flame temperature is generally high (1000-1600°C) especially at near stoichiometric combustion conditions. Therefore, the heat transfer from swirl combustors is significant. Thus, It is essential to include the radiation model for a more accurate prediction of the temperature distribution in combustors [8].

Table 1. Components of the biogas [1]

	CH_4 (%)	CO_2 (%)	N_2 (%)	H_2S (ppm)	LHV (kcal/m ³)	$Density$ (kg/m ³)
Biogas	55	43,15	1,56	10	4124	1,070

2.2. Operating Conditions

All modellings were carried out under thermal power of 10 kW and an equivalence ratio of $\phi = 0.83$. Fuel and air inlet temperatures are also fixed at 283 K. Fuel and air inlet pressures were changed from 21 mbar to 1000 mbar (1 bar). The combustor outlet is open to atmosphere.

3. Results and Discussions

The effects of the air and fuel inlet pressures on combustion characteristics of the biogas have been numerically investigated in the present study. The predicted temperature distributions are shown in Figure 3. According to the Figure 3, it can be readily said that the maximum temperature values for all cases emerge in the flame region as reaction takes place in this region. Then, the predicted temperature values decrease gradually towards the combustor outlet. The predicted temperature values are nearly the same throughout the combustor even if the inlet pressures are changed. However, temperature values are slight different in some regions inside the combustor. In particular, at the combustor outlet, the predicted temperature values are almost the same although the temperature values predicted for air inlet pressures of 500 mbar and 1000 mbar are virtually different. These values have been predicted as of almost 750 K at the combustor outlet. It can be consequently said that change in inlet pressures affects the temperature distributions of the biogas flame slightly in the combustor.

Figure 4 shows the effects of the inlet pressure changes on the velocity distributions of the turbulent biogas flame. It can be said that the maximum velocity values for all combustion conditions show up in the flame zone. Then, the predicted velocity values descend rapidly due to expansion of the combustion products towards to the combustor as can be seen in Figure 4. However, the predicted velocity values increase as the air inlet pressure is increased. In particular, for the air inlet pressure of 1000 mbar, the predicted velocity value is higher than those of other combustion conditions. But, this value change rapidly towards the combustor outlet and it has been predicted as of almost 1 m/s at the combustor outlet while the predicted velocity value for the air and the fuel inlet pressures of 21 mbar is 1,4 m/s at the combustor outlet. Therefore, it may be said that change in the air and the fuel inlet pressures affects the velocity distributions of the biogas relatively.

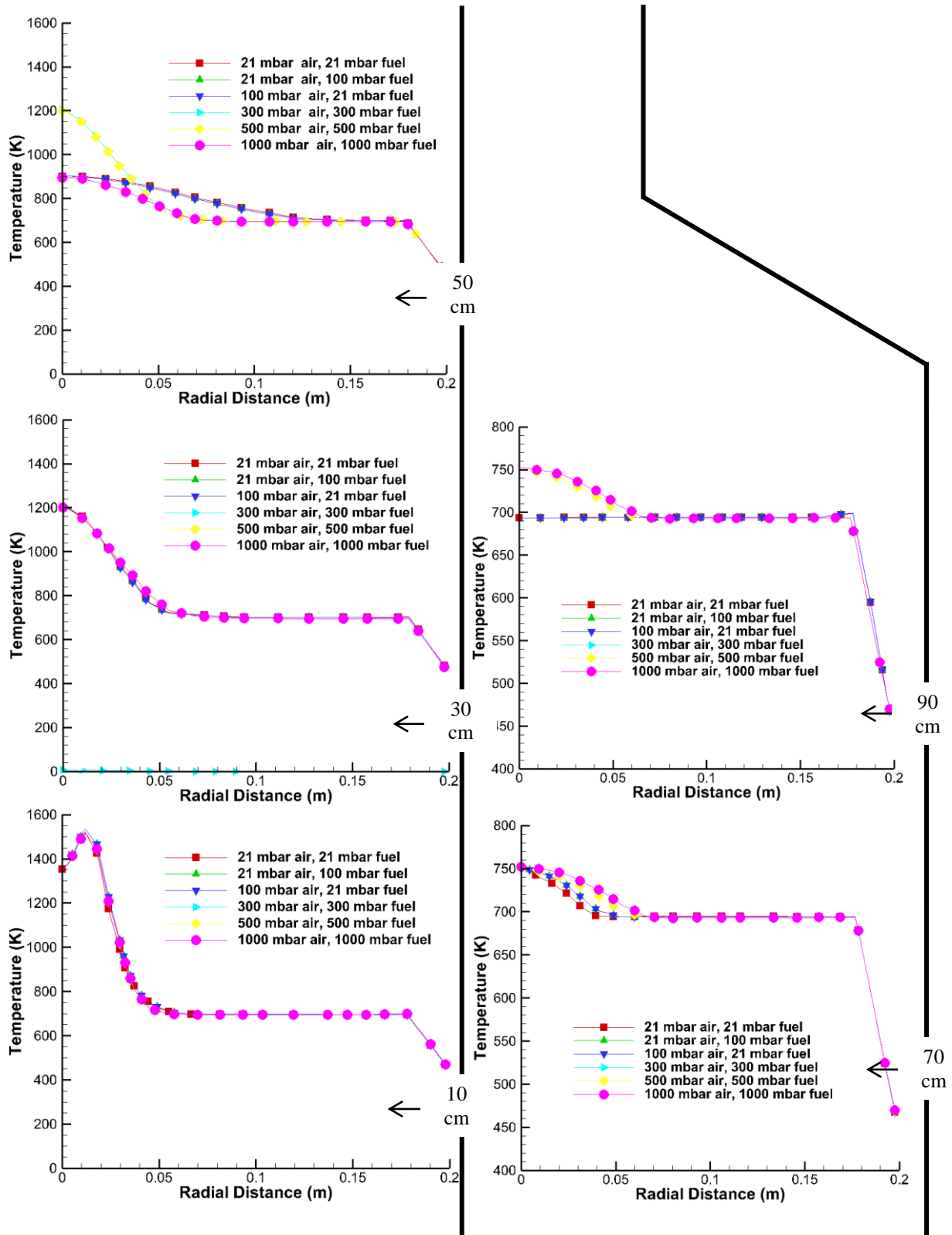


Figure 3. The predicted temperature distributions throughout the combustor

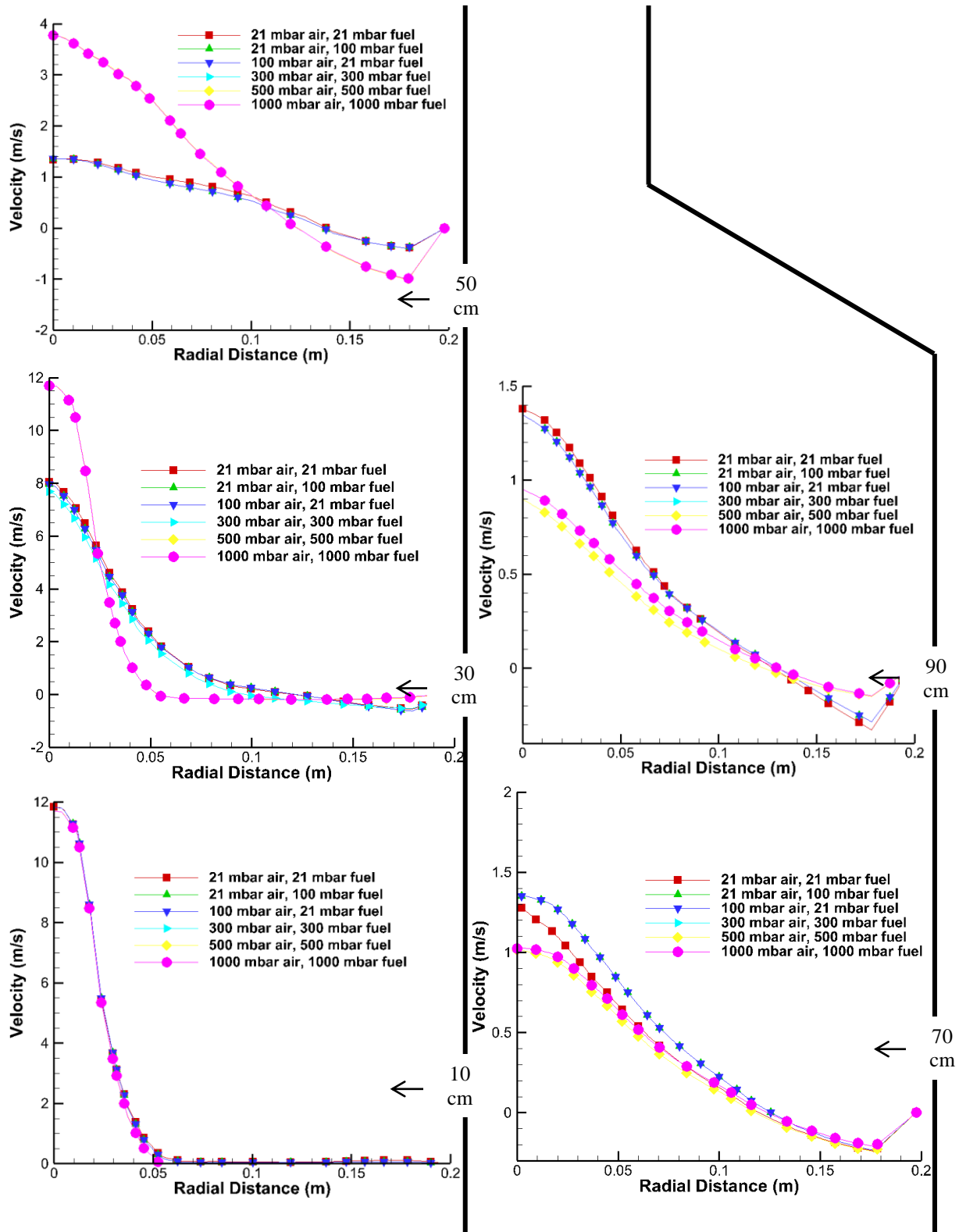


Figure 4. The predicted axial velocity distributions throughout the combustor



5. Conclusions

A numerical study has been carried out in order to investigate the combustion behaviours of the biogas for varying air and fuel inlet pressures. The numerical results bring about the following conclusions:

- The temperature values have been predicted as nearly the same throughout the combustor for all conditions even if the inlet pressures have been changed.
- The predicted temperature values for air inlet pressures of 500 mbar and 1000 mbar are somewhat different from temperature values for 21mbar inlet pressure.
- The predicted velocity values increase as the air inlet pressure is increased. It can be concluded that the velocity distributions of the biogas change relatively as the air and the fuel inlet pressures are changed.

References

- [1] M. Ilbas, M. Sahin, S. Karyeyen, 3D numerical modelling of turbulent biogas combustion in a newly generated 10 KW burner, Journal of the Energy Institute, Article in Press.
- [2] B. Adouane, W. de Jong, J.P. van Buijtenen, G. Vitteveen, Fuel-NO_x emissions reduction during the combustion of LCV gas in an air staged Winnox-TUD combustor, Applied Thermal Engineering, 30 (2010) 1034-1038.
- [3] S.E. Hosseini, G. Bagheri, M.A. Wahid, Numerical investigation of biogas flameless combustion, Energy Conversion and Management 81 (2014) 41-50.
- [4] Y. Lafay, B. Taupin, G. Martins, G. Cabot, B. Renou, A. Boukhalfa, Experimental study of biogas combustion using a gas turbine configuration, Experiments in Fluids, 43 (2007) 395-410.
- [5] H.N. Somehsaraei, M.M. Majoumerda, P. Breuhausb, M. Assadia, Performance analysis of a biogas-fueled micro gas turbine using a validated thermodynamic model, Applied Thermal Engineering 66 (2014) 181-190.
- [6] P.R. Bhoi, S.A. Channiwala, Emission characteristics and axial flame temperature distribution of producer gas fired premixed burner, Biomass and Bioenergy 33 (2009) 469-477.
- [7] H. K. Versteeg, W. Malalasekera, An introduction to computational fluid Dynamics, Second Edition, PEARSON Prentice Hall, 1995.
- [8] M. Ilbas, Studies of ultra low NO_x burner. PhD Thesis: University of Wales, College of Cardiff, UK, 1997.

The investigate of effects on performance and emission parameters of safflower biodiesel-bioethanol-diesel fuel blends at different injection pressures

Ilker Ors ^{1,*}, Murat Ciniviz ^{2,*}, Ali Kahraman ³, Bahar Sayin Kul ²

¹*Department of Motor Vehicles and Transportation Technology, Vocational School of Technical Sciences, Aksaray University, Aksaray, Turkey.*

ilkerors@hotmail.com

²*Mechanical Engineering Department, Selcuk University, Technolgy Faculty, Turkey.*

mciniviz@selcuk.edu.tr

³*Energy Systems Engineering Department, Necmettin Erbakan University, Faculty of Engineering, Turkey.*

Abstract: Nowadays, biofuels are widely used in internal combustion engines. In this study, biodiesel from safflower oil and bioethanol from sugar beet were blended with diesel fuel at certain rates. The effects on performance and emission parameters of obtained ternary fuel blends were investigated at the different injection pressure in a single cylinder and direct injection diesel engine. 10% biodiesel and 5%, 10% bioethanol were added into diesel fuel as volumetric. Bioethanol improved especially cold flow properties. Besides, density and kinematic viscosity values of blend fuels were decreased by added bioethanol. The engine performance values decreased due to both biodiesel and bioethanol have lower LHV (lower heating value) than diesel fuel. However, CO, HC and smoke opacity emissions decreased compare to diesel fuel due to both biofuels content oxygen. Although biodiesel increased NO emissions slightly, they were decreased by added bioethanol. While the increasing injection pressure improved performance and emission values of biodiesel, it caused decrease at performance of bioethanol blends. An improve detected at performance and emission values of bioethanol blends with decreasing injection pressure..

Keywords: Safflower biodiesel, bioethanol, different injection pressure, engine performance, exhaust emissions.

1. Introduction

Internal combustion engines, particularly diesel engines play an important role in automotive, industrial and agricultural sectors [1]. Diesel engines have been received a great attention due to their high power performance, thermal efficiency and low emissions in comparison with gasoline engines [2]. The stringent emission norms imposed by different regulating authorities throughout the world and the anxiety over the upcoming energy crisis generate a need to find out an alternative fuel to diesel [3]. The twin crisis of fossil fuel depletion and environmental degradations has led to the search for an alternative fuel which should be sustainable and also environment friendly without sacrificing the performance [4].

The role biofuels can play within these economies becomes clearer when their relatively developed agricultural sector is taken into account [5-6]. As an alternative fuel, biodiesel has many similar or better properties than diesel fuel, such as cetane number, non-toxic, biodegradable and good

inherent lubricity, which make it more suitable for diesel engines. Biodiesel fuels can be produced from various feedstocks [7]. Some of them are Soybean oil, Rapeseed oil, mustard oil, canola oil, Palm oil, Sunflower oil, Jatropha oil, Rice bran oil, Pongamia oil, waste used cooking oil etc., besides, animal fats and algae [8].

Alcohols (ethanol and methanol) have been considered as alternative fuels for Diesel engines. Ethanol is a biomass based renewable fuel, which can be produced from vegetable materials, such as corn, sugar cane, sugar beets, sorghum, barley and cassava, and it has higher miscibility with Diesel fuel. Besides ethanol reduce emissions in Diesel engines, and it has the advantages of being a renewable fuel and of having higher miscibility [9].

Gumus et al. investigated the effects on exhaust emissions of diesel-biodiesel blends at different injection pressure. They shown that, as results, brake specific fuel consumption (BSFC) of higher percentage biodiesel–diesel blends decreased with the increased injection pressure. Besides, increased injection pressure caused to decrease insmoke opacity, UHC, and CO, and it caused to increase in the emissions of CO₂, O₂ and NO_x [10].

Sastry et al. studied effect of fuel injection pressure, ethanol addition on performance of diesel-biodiesel fueled. They presented that BSFC increases by using blends with ethanol as additive which however decreases with increase in injection pressure. CO and smoke density found to decrease with increase in injection pressure. Also, NO_x emission found to increase with injection pressure [11].

Sharanappa et al. investigated performance and combustion characteristics of diesel-biodiesel-ethanol blends at different injection pressure. According to results of their study, brake thermal efficiency (BTE) of blend fuels increased with increase in injection pressure. Exhaust gas temperature reduced with increase in injection pressure. Peak cylinder pressure reduced as injection pressure increases. Net heat release rate increased with increase in injection pressure [12].

In this study, we investigated performance and exhaust emissions of a DI diesel engine fuelled with ternary fuel blend at different injection pressure. Feedstocks of used biofuels are safflower seed oil for biodiesel, and sugar beet for bioethanol.

2. Material and Methods

Test fuels were prepared: %100 diesel fuel, %90 diesel, %10 biodiesel (DB10), and %85 diesel fuel, %10 biodiesel and 5% bioethanol (DBE5) and %80 diesel fuel, %10 biodiesel and 10% bioethanol (DBE10). Some properties of test fuels were given in Table 1. Test engine which technical features given in Table 2 is used at experiments. The features of Bosch-BEA350 model gas analyzer used in experiments are given Table 3.

Table 1. Properties of test fuels.

Fuels	Density at 15°C	Viscosity at 40 °C	LHV MJ/kg	Cetane Number
DF	834.5	2.794	43.14	55.2
B10	837	2.855	42.54	55.3
DBE5	836.4	2.776	41.8	53.8
BDE10	833.9	2.701	41.06	51.1

The engine was run with different injection pressure (IP) 170 bar, 190 bar (original) and 220 bar; IP was set by adjusting the spring pressure and was calibrated in the lab. Exhaust gas emissions were measured as CO (% vol), HC (ppm), NO (ppm) and smoke opacity. These emission values were converted to the units of g/kWh as the study of Pilusa et al.[13].

Table 2. Technical features of test engine.

Model	Antor 3 LD 510
Engine type	Four stroke, direct injection
Cylinder number	1
Cylinder volume, cm ³	510
Bore - Stroke, mm - mm	85 - 90
Compression ratio	17.5:1
Max. engine speed, rpm	3300
Max. engine torque, Nm	32.8
Max. engine power, kW	9
Injector pressure	190 bar

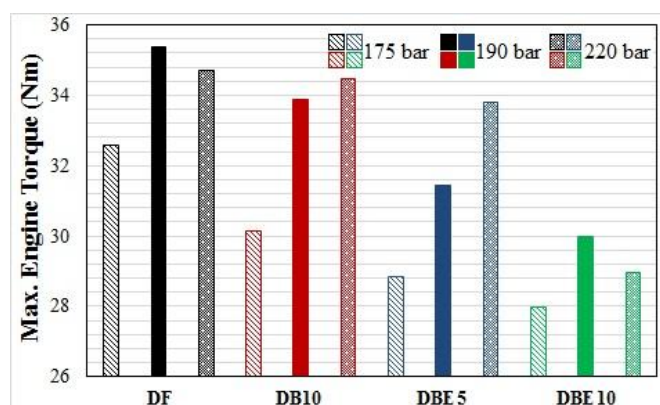
Table 3. The features of measurement equipment

Bosch BEA 350	Accuracy
CO (vol. %)	±0.001
NO (ppm)	±1
HC (ppm)	±1
Smoke opacity (vol. %)	±0.01

3. Results and Discussions

3.1. Motor Performance

Torque, power and BSFC values were investigated as engine performance parameters. Figure 1, 2 and 3 shows their changes depending on IP. Maximum torque and power values were obtained 1400 and 2800 rpm respectively during tests.


Figure 1. Changes of max. engine torque depend on IP.

The engine performance values effected negatively due to both biodiesel and bioethanol have lower LHV (lower heating value) than diesel fuel. Torque and power decreased for all test fuels with

decreasing IP. But, increasing IP improved performance parameters except BSFC values of DB10 fuel. The better atomized fuel depending on increasing IP was caused this improve.

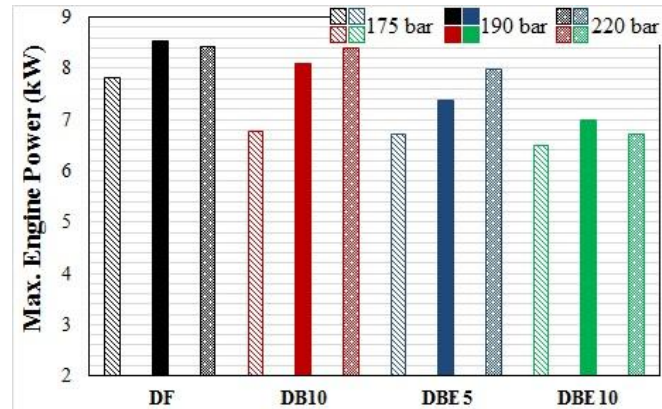


Figure 2. Changes of max. engine power depend on IP.

BSFC values of DBE10 increased due to values of density and viscosity were quite decreased. When ternary fuels are evaluated in terms of engine performance, the best fuel is DBE5 due to increasing IP. Max. torque and power of DBE5 fuel at 220 bar IP are lower approximately 4.44% and 6.52% respectively than that of DF at original IP. Also, BSFC values of DBE5 at 2800 rpm are higher 1.93% than that DF at 190 bar.

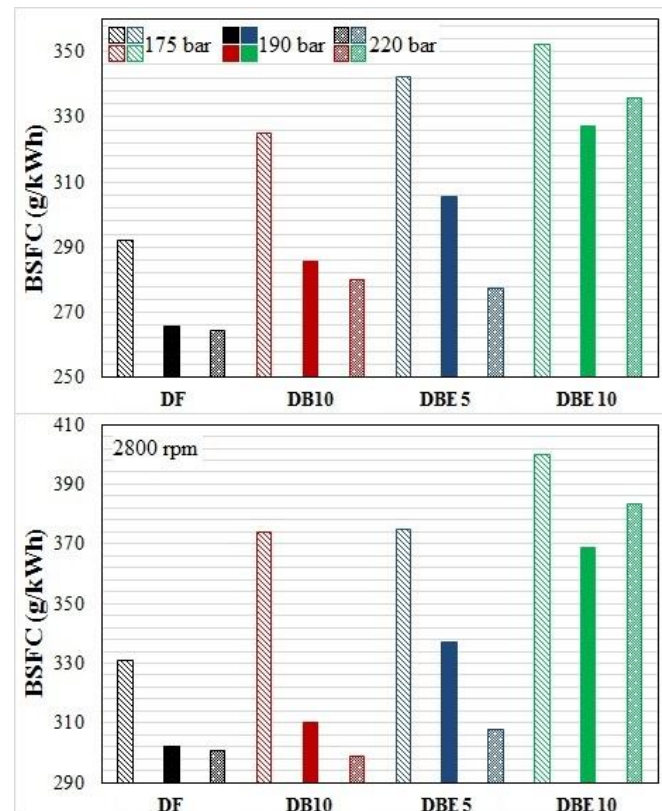


Figure 3. BSFC values depend on IP at 1400 rpm and 2800 rpm.

3.2. Exhaust Emissions

Figure 4 is shown changes of average CO emission values at different IP. It show that CO emissions decreased by change of IP. CO emissions decreased due to increasing heat release rate with high IP [12]. Besides, it is also decrease due to the good fuel–air mixing and easy and complete combustion of the smaller droplets. CO emission of DBE5 fuel at 220 bar IP is lower average 37.38% than that DF at original IP.

Figure 5 show that the increasing injection pressure caused the fuel air mixing in the combustion chamber was more excellent, so the HC emissions was obtained less than that of the low injection pressure. DBE5 at 220 bar IP released lower HC emission average 76%, according to DF at 190 bar IP.

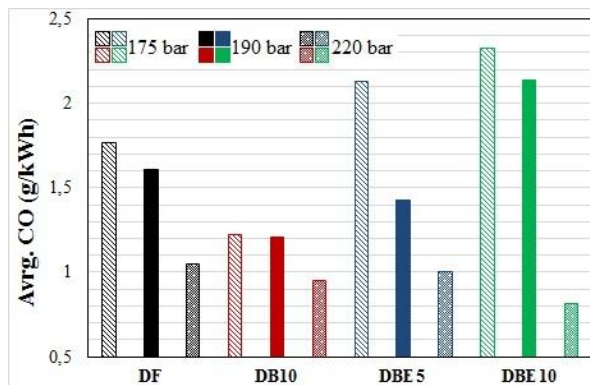


Figure 4. Changes of CO emission at different IP.

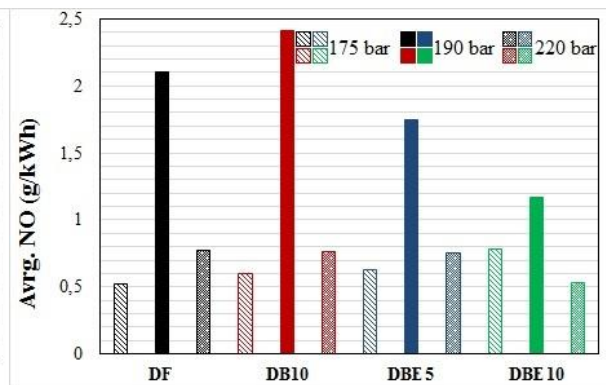


Figure 6. Changes of NO emission at different IP.

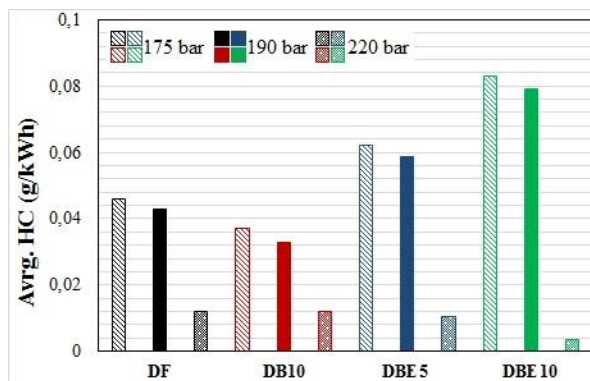


Figure 5. Changes of HC emission at different IP.

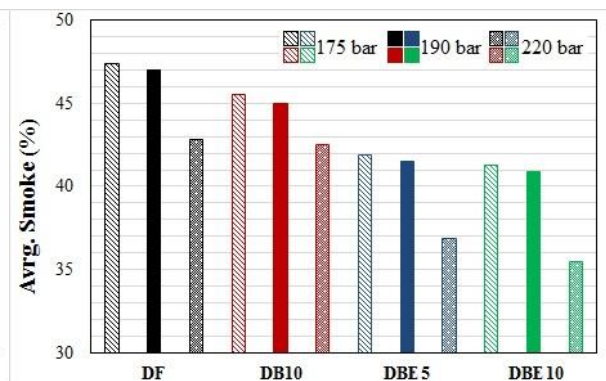


Figure 7. Changes of smoke opacity at different IP.

The variation of NO emission values presented at Figure 6. The most important reason formation of NO emissions is high temperature. Both increased and decreased of IP caused reduction exhaust gas temperature, and therefore changes of IP decreased NO emission [9]. 5% bioethanol added to DB10 at 220 bar IP decreased NO emission as average 64.36% compare to DF at original IP.

The results of smoke opacity were depicted in Figure 7. When injection pressure is increased, fuel particle diameters will become smaller. Because formation of mixing fuel to air becomes better through injection period, smoke opacity will be less [10]. Smoke opacity of DBE5 fuel at 220 bar IP is lower average 21.45% than that of DF at original IP.

4. Conclusions

Test results shown that if a ternary blend fuel will use, it should be DBE5 at 220 bar IP according to experimental study. Because its engine performance results are similar with results of DF. Besides, for all emission parameters, values of DBE5 are better than that of DF at original IP. The added bioethanol into diesel-biodiesel blend not only is improved exhaust emissions, but also is likened its fuel properties to that of DF.

References

- [1] Jaichandar, S., Annamalai, K., 2013. "Combined impact of injection pressure and combustion chamber geometry on the performance of a biodiesel fueled diesel engine", **Energy**, 55: 330-339.
- [2] Shehata, M.S., Attia, A.M.A., Abdel Razek, S.M., 2015. "Corn and soybean biodiesel blends as alternative fuels for diesel engine at different injection pressures", **Fuel**, 161: 49-58.
- [3] Datta, A., Mandal, B.K., 2015. "Engine Performance, Combustion and Emission Characteristics of a Compression Ignition Engine Operating on Different Biodiesel-Alcohol Blends", **Energy**, 125: 470-483.
- [4] Channapattana, S.V., Pawar, A.A., Kamble, P.G., 2015. "Effect of Injection Pressure on the Performance and Emission Characteristics of VCR engine using Honne Biodiesel as a Fuel", *Materials Today: Proceedings*, 2: 1316-1325.
- [5] Subbaiah, G.V., Gopal, K.R., Hussain, S.A., 2010. "The Effect of Biodiesel and Bioethanol Blended Diesel Fuel on the Performance and Emission Characteristics of a Direct Injection Diesel Engine", **Iranica Journal of Energy & Environment**, 1(3): 211-221.
- [6] Gligorijevic, R., Jevtic, J., Borak, D., Petrovic, V., 2009. "Potentials and limitations of alternative fuels for diesel engine", **Thermal Science**, 13(3): 175-183.
- [7] Mo, J., Tang, C., Li, J., Guan, L., Huang, Z., 2016. "Experimental investigation on the effect of n-butanol blending on spray characteristics of soybean biodiesel in a common-rail fuel injection system", **Fuel**, 182: 391-401.
- [8] Lalvani, J.I.J.R., Parthasarathy, M., Dhinesh, B., Annamalai, K., 2016. "Pooled effect of injection pressure and turbulence inducer piston on performance, combustion, and emission characteristics of a DI diesel engine powered with biodiesel blend", **Ecotoxicology and Environmental Safety**, 134: 336-343.
- [9] Özer, C., Çelikten, İ., Usta, N., 2004. "Effects of ethanol addition on performance and emissions of a turbocharged indirect injection Diesel engine running at different injection pressures", *Energy Conversion and Management*, 45: 2429-2440.
- [10] Gumus, M., Sayin, C., Canakci, M., 2012. "The impact of fuel injection pressure on the exhaust emissions of a direct injection diesel engine fueled with biodiesel–diesel fuel blends", **Fuel**, 95: 486-494.
- [11] Sastry, G.R.K., Deb, M., Panda, J.K., 2015. "Effect of Fuel Injection Pressure, Isobutanol and Ethanol Addition on Performance of Diesel-Biodiesel Fuelled D.I. Diesel Engine", **Energy Procedia**, 66: 81-84.
- [12] Sharanappa, P., Navindgi, M.C., 2017. "Investigation of Performance and Combustion Characteristics of DI Diesel Engine Fuelled with Ternary Fuel Blend at Different Injection Pressure", *World Journal of Engineering and Technology*, 5: 125-138.
- [13] Pilusa, T.J., Mollagee, M.M., Muzenda, E., 2012. "Reduction of vehicle exhaust emissions from diesel engines using the whale concept filter", **Aerosol and Air Quality Research**, 12: 994-1006.

Using in a CI engine of Biodiesel Production from Waste Cooking Oil

İlker Örs^{1*}, S. Sarikoc^{2*}, A.E. Atabani², S. Unalan²

¹*Department of Motor Vehicles and Transportation Technology, Vocational School of Technical Sciences, Aksaray University, Aksaray, Turkey.*

**ilkerors@hotmail.com*

²*Department of Mechanical Engineering, Faculty of Engineering, Erciyes University, 38039 Kayseri, Turkey*

**sarikocselcuk@gmail.com*

Abstract: In this study, the effects on engine performance, exhaust emission and combustion characteristics of using in a CI engine of biodiesel obtained from waste cooking oil were investigated. Besides, fuel properties were also presented. In the experiments, a single-cylinder, water-cooled and direct-injection diesel engine was used. Although biodiesel has higher density, viscosity and cetane number according to diesel fuel, its heating value is lower than diesel fuel. In performed study, it also showed that performance, emission and combustion parameters were effected by fuel properties especially such as density, kinematic viscosity, cetane number, heating value. According to performed test results, biodiesel negative effected engine performance due to especially low heating value compere to diesel fuel. Although oxygen content of biodiesel improved exhaust emission parameters in generally, it caused increase of NO emission. It showed that combustion characteristics of biodiesel are near values of diesel fuel. But, as the most important difference, it may say that high cetane number of biodiesel was increasing ignition delay.

Keywords: Waste cooking oil, biodiesel, diesel engine, engine performance, exhaust emissions.

1. Introduction

Due to the depletion of world oil reserves and the impact of increased exhaust emissions on environmental pollution, there is a need for alternative fuels suitable for operating diesel engines [1],[2]. Biofuels are the most suitable alternative engine fuels that can be used in place of current petroleum based fuels. However, in order for biofuels to be used effectively, engines may require some change or modification [3]. In recent years, many researchers have made studies to demonstrate the suitability of vegetable and animal oils as fuels [4]-[5]-[6]-[7]. The most important engine fuels that can be used for diesel engines are biodiesel, which can be produced from both vegetable and animal oils.

Biodiesel can be obtained from many vegetable oils such as sunflower, canola, safflower, palm, jatropha, corn, soybean and etc., as well as from oils of land and sea animals and from waste oils [8]-[9]-[10]-[11]. Today, biodiesel production from different waste oils has become much more popular. Some studies on the use of biodiesel produced from waste oil as fuel are presented below.

Nautiyal et al. have examined the performance and the emission parameters in their studies, using the biodiesel which they obtained as a fuel from waste tallow, in single-cylinder, and four-stroke engine. According to their results, they have shown that biodiesel lowers the thermal efficiency

values and increases the heat release rate at the beginning of the combustion. Nevertheless, they have shown that biodiesel significantly reduces CO, HC and smoke emissions, whereas it increases NOx emissions, especially at high engine loads [12].

Sodhi et al. in their work, mixed the biodiesel that they had obtained from waste cooking oil, with diesel fuel in different ratios, and examined their effects on the emission parameters. As a result, they have shown that the addition of biodiesel to diesel fuel decreases CO emissions, whereas it increases NO emissions to a significant extent [13].

Yadav et al. in their study, mixed the biodiesel that they had obtained from kusum oil with diesel fuel at low ratios and used these mixtures in a 4-cylinder diesel engine as fuel. As a result, they have shown that biodiesel, which was mixed in diesel fuel at a low ratio, negatively affected engine performance parameters to certain extent, and noticeably increases NOx emissions [14], although it significantly reduced CO, HC and smoke emissions.

Borugadda et al. in their study, mixed biodiesel that they had obtained from waste frying oil, with diesel fuel at 10% and 15% and used as fuel. According to the results of the engine performance parameters, while the power and thermal efficiency values of the diesel fuel-biodiesel mixtures are lower than those of the diesel fuel, the specific fuel consumption values are higher than those of diesel fuel. They have shown that biodiesel reduces the exhaust gas temperature. When exhaust emission parameters are examined, they have revealed that biodiesel reduces CO, CO₂ and HC emissions, whereas it increases NOx emissions at medium and high engine loads [15].

Bereczky et al. in their study, have examined the use of biodiesel obtained from waste cooking oil and waste palm oil as fuel in a diesel engine. As a result, they have shown that both biodiesel adversely affect performance values, biodiesel produced from waste cooking oil has better performance values at low engine speeds, whereas biodiesel produced from waste palm oil has better performance values at higher engine speeds [16].

In this study, the fuel properties of biodiesel obtained from waste cooking oil by transesterification, were examined and the its effects on performance, emission and combustion parameters were investigated.

2. Materials and Methods

The biodiesel used in the experiments was obtained by exposing the collected waste cooking oils to the transesterification method and was used as pure fuel. The characteristics of the test fuels are shown in Table 1. The characteristics of the test motor used in the experiments are presented in Table 2. The characteristics of the combustion analysis measurement system and emission devices that make up the experimental setup are shown in Table 3.

Table 1. Properties of test fuels.

Property	D100	B100
Kinematic viscosity at 40 °C (mm ² /s)	2.3255	4.6557
Cloud point (°C)	-7	11
Pour point (°C)	-26	10
Cold Filter Plugging Point (°C)	-25	9.7
Flash Point (°C)	65	157
Density at 20 °C (g/cm ³)	0.8295	0.8766
Cetane number	50-55	56.948

Table 2. Technical features of test engine.

Model	3 LD 510
Engine type	Four stroke, direct injection
Cylinder number	1
Cylinder volume, cm ³	510
Bore - Stroke, mm - mm	85 - 90
Compression ratio	17.5:1
Max. engine speed, rpm	3300
Max. engine torque, Nm	35
Max. engine power, kW	9
Cooling type	Water cooler

The tests were carried out at full throttle opening and at different engine speeds. During the tests, engine torque, fuel consumption, CO, HC, NO and smoke emissions were measured for each engine speed. The cylinder pressure values were measured at the maximum engine speeds where the maximum motor torque and motor power were obtained.

Table 3. The features of measurement equipment

Pressure sensor		Bosch BEA 350		
Mark –	Kistler –	Gas	Range	Sensitivity
Model	6052C			
Measure	0 – 250	CO, %	0-10	0.001
range, bar				
Amplifier				
Mark –	Kistler –	HC,	0-9999	1
Model	5018A	ppm		
Measure	2 –			
range, pC	2200000			
Encoder				
Mark –	Kübler –	NO,	0-5000	1
Model	Sendix	ppm		
	5000			
Measure	0 – 12000	Smoke,	0-100	0.1
range, rpm		%		

3. Results and Discussion

The parameters obtained as a result of the experiments were examined as engine performance, combustion analysis and exhaust emissions.

3.1. Engine Performance

Figures 1 and 2 show changes in engine power and thermal efficiency values obtained from test fuels depending on engine speed. As can be understood from the graphs, the use of biodiesel has affected motor performance negatively. Compared to those of diesel fuel, motor power values obtained with biodiesel decreased 15.16% on average, and thermal efficiency value decreased about 3.78% on average. Since the heating value of biodiesel is lower than that of diesel fuel, the energy that will produced at the end of combustion will also be reduced. And this causes the engine performance of biodiesel to decrease.

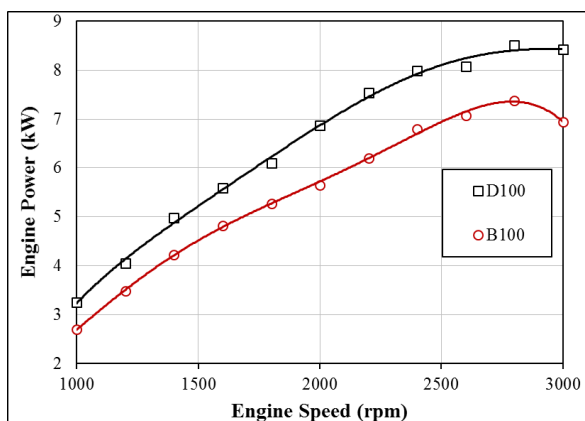


Figure 1. Engine power values at different engine speeds.

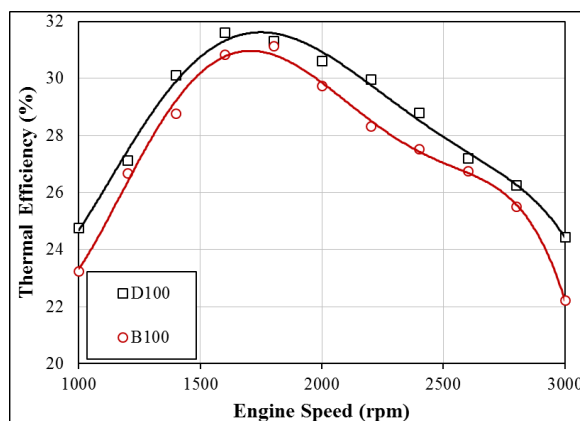


Figure 2. Thermal efficiency values at different engine speeds.

3.2. Combustion Analysis

The pressure and the heat release rate in the cylinder at the end of combustion, determine the combustion characteristics of the fuel. Figures 3 and 4 show the changes in cylinder pressures and heat release rate values of test fuels at engine speeds at which maximum torque and power values were obtained. It can be seen that biodiesel was burned earlier than diesel fuel at both engine speed. The reason for this is the high cetane number of biodiesel. The oxygen in the biodiesel has caused the maximum cylinder pressure to be higher than that of diesel. Whereas it has caused the heat release rate at the beginning and at the end of the combustion to increase.

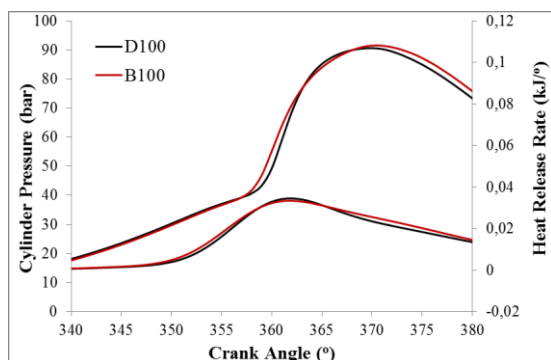


Figure 3. Combustion analyses results at 1400 rpm

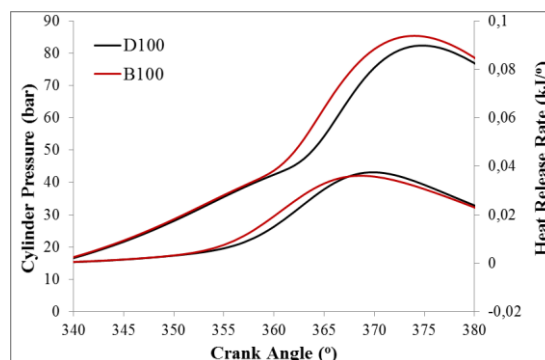


Figure 4. Combustion analyses results at 2800 rpm

3.3. Exhaust Emissions

Figures 5, 6, 7 and 8 show the changes in exhaust gases obtained from test fuels. Biodiesel has caused CO, HC, and smoke darkness emissions to decrease. These emissions are usually due to the incomplete combustion of the fuel. The oxygen content of the biodiesel has enabled this fuel to have a combustion process close to the complete combustion. According to the test results, the average CO emissions of biodiesel are 65.4%, the HC emissions are 61.1% and the smoke darkness is 55% lower. Since the oxygen content of biodiesel increased the reacting ratios of N and O atoms, the NO emissions of biodiesel increased by 24% on average.

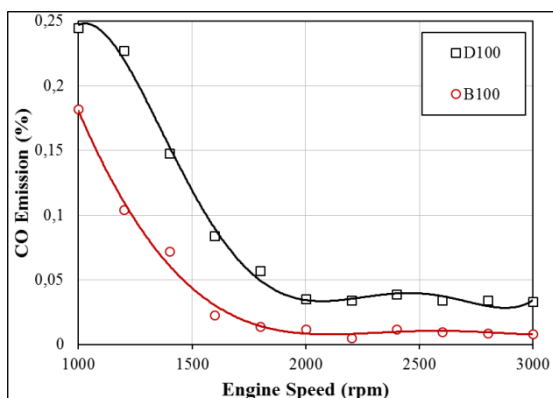


Figure 5. CO emission values at different engine speeds.

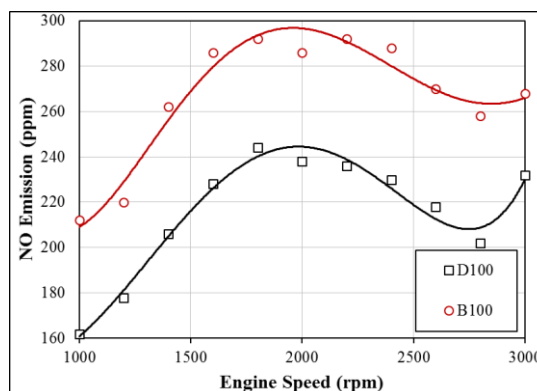


Figure 7. NO emission values at different engine speeds.

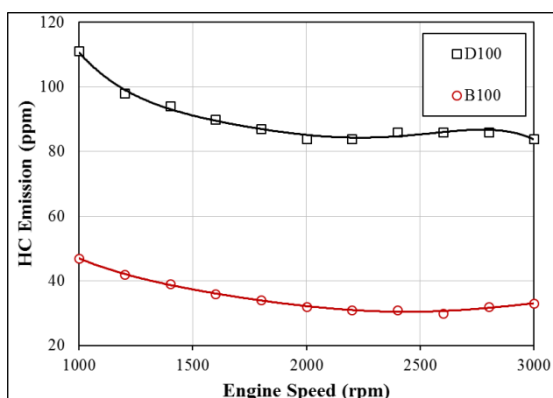


Figure 6. HC emission values at different engine speeds.

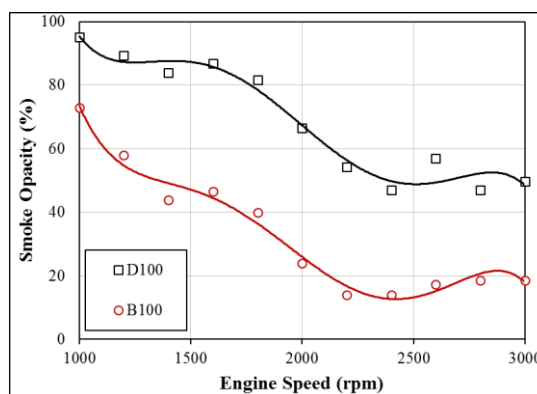


Figure 8. Smoke opacity values at different engine speeds.

4. Conclusions

Fuel characteristics of biodiesel such as density, viscosity, and heating value are disadvantage compared to diesel fuel, and although these properties adversely affect the engine performance parameters, the oxygen content and the high cetane number cause the combustion characteristics and the emission parameters of the biodiesel to be better than those of the diesel fuel. Biodiesel can be used as a fuel in diesel engines having conventional fuel systems, without the need for any modification at the engine. Although it adversely affect the engine performance, biodiesel produced from waste cooking oil is an alternative fuel that must be subjected to extensive research because of being an economical raw material and having environmental sensitivity.

Acknowledgement: The authors gratefully would like to acknowledge Erciyes University and Bayburt University, for the Scientific Research Projects Unit of Erciyes University, Turkey, for the financial support under the grant number FOA-2015-5817 and FOA-2015-5790.

References

- [1] Muralidharan, K., Vasudevan, D., 2014. "Applications of artificial neural networks in prediction of performance, emission and combustion characteristics of variable compression ratio engine fuelled with waste cooking oil biodiesel", **Journal of the Brazilian Society of Mechanical Sciences and Engineering**, **37** (3): 915-928.
- [2] Pramanik, K., 2003. "Properties and use of jatropha curcas oil and diesel fuel blends in compression ignition engine", **Renewable Energy**, **28**: 239-248.
- [3] Karthikeyan, R., Mahalakshmi, N., 2007. "Performance and emission characteristics of a turpentine–diesel dual fuel engine", **Energy**, **32** (7): 1202-1209.
- [4] Murat Karabektas, G.E., Can Hasimoglu, Ahmet Murcak 2016. "Performance and Emission Characteristics of a Diesel Engine Fuelled with Emulsified Biodiesel-Diesel Fuel Blends ", **International Journal of Automotive Engineering and Technologies**, **5** (4): 176-185.
- [5] Shahir, V.K., Jawahar, C.P., Suresh, P.R., 2015. "Comparative study of diesel and biodiesel on CI engine with emphasis to emissions—A review", **Renewable and Sustainable Energy Reviews**, **45**: 686-697.
- [6] Laesecke, J., Ellis, N., Kirchen, P., 2017. "Production, analysis and combustion characterization of biomass fast pyrolysis oil – Biodiesel blends for use in diesel engines", **Fuel**, **199**: 346-357.
- [7] Marchetti, J.M., Miguel, V.U., Errazu, A.F., 2008. "Techno-economic study of different alternatives for biodiesel production", **Fuel Processing Technology**, **89** (8): 740-748.
- [8] Türkcan, A., 2016. "Comparison of the Effects of Animal and Vegetable Based Biodiesel in the Bioethanol-Diesel Blend on the Combustion and Emission Characteristics of a Common Rail Diesel Engine ", **International Journal of Automotive Engineering and Technologies**, **5** (4): 155-167.
- [9] İlker Örs, V.B., 2016. "An Experimental and ANNs Study of the Effects of Safflower Oil Biodiesel on Engine Performance and Exhaust Emissions in a CI Engine ", **International Journal of Automotive Engineering and Technologies**, **5** (3): 125.
- [10] Alptekin, E., Canakci, M., Ozsezen, A.N., Turkcan, A., Sanli, H., 2015. "Using waste animal fat based biodiesels–bioethanol–diesel fuel blends in a DI diesel engine", **Fuel**, **157**: 245-254.
- [11] Wei, L., Cheung, C.S., Ning, Z., 2017. "Influence of waste cooking oil biodiesel on combustion, unregulated gaseous emissions and particulate emissions of a direct-injection diesel engine", **Energy**, **127**: 175-185.
- [12] Nautiyal, P., Subramanian, K.A., Dastidar, M.G., 2017. "Experimental investigation on performance and emission characteristics of a compression ignition engine fueled with biodiesel from waste tallow", **Clean Technologies and Environmental Policy**.
- [13] Sodhi, A.K., Tripathi, S., Kundu, K., 2017. "Biodiesel production using waste cooking oil: a waste to energy conversion strategy", **Clean Technologies and Environmental Policy**.
- [14] Yadav, A.K., Khan, M.E., Pal, A., Dubey, A.M., 2016. "Experimental Investigations of Performance and Emissions Characteristics of Kusum (Schleichera Oleosa) Biodiesel in a Multi-Cylinder Transportation Diesel Engine", **Waste and Biomass Valorization**, **8** (4): 1331-1341.
- [15] Borugadda, V.B., Paul, A.K., Chaudhari, A.J., Kulkarni, V., Sahoo, N., Goud, V.V., 2016. "Influence of Waste Cooking Oil Methyl Ester Biodiesel Blends on the Performance and Emissions of a Diesel Engine", **Waste and Biomass Valorization**.
- [16] Bereczky, A., 2017. "Effect of the use of waste vegetable oil based biodiesel on the landscape in diesel engines", **Thermal Science**, **21** (1 Part B): 567-579.

Theoretical determination of optimum ethanol fuel blends rate within gasoline

Raif Kenanoğlu¹, Mustafa Kaan Baltacıoğlu^{1,*}, Ertuğrul Baltacıoğlu¹, Kadir Aydın²

¹ Faculty of Engineering and Natural Sciences, Iskenderun Technical University

mkaan.baltacioglu@iste.edu.tr

² The Faculty of Engineering and Architecture, Cukurova University

Abstract: Alternative fuels can be described as clean fuels that provide a more livable world for the future generations. There is a wide variety of alternative fuel types such as; compressed natural gas, propane, hydrogen, biomass, biodiesel and alcohol fuels (ethanol and methanol). Ethanol represents one of the most promising alternative fuels, exhibiting several advantages, such as high octane number, low cetane number, high heat of vaporization and, most importantly, reduction of greenhouse gas emissions. In this study, gasoline with ethanol addition was used as fuel in SI engine by different ratios; E0, E15, E50 and E85. The effects of ethanol addition on performance characteristics were investigated theoretically by AVL-BOOST software program and results showed that E50 gives the best improvements among the ethanol gasoline blends used. As a general result showed that, the using of ethanol was reduced the emission values in each case. It is seen that the volumetric rate of ethanol used in the fuel mixture is inverse proportion with emission gas output values. Therefore, the best reductions of emission values were obtained with E85 fuel blend.

Keywords: AVL-Boost, Alternative Fuels, Ethanol, Performance & Emission

1. Introduction

Nowadays, alternative fuels are widely used in internal combustion engines, due to their positive effects on environment and the engine performance. These fuels can be used to solve problems related to fossil fuels. The automobiles, which are used both gasoline and diesel fuels, are the major sources of greenhouse gases (GHG) emission [1–3]. Alcohols (methanol, ethanol) have some advantages when they are used alone as a fuel in spark ignitions engines, compared to gasoline. But alcohols are not used as a fuel directly because their high prices. With the developing technologies in the next decades, the production cost of alcohol-based fuels will be competitive with fossil fuels, thus, it will be possible to increase alcohol ratio in the fuel mixture. This will be a useful method both in terms of environment and engine efficiency. Additionally, when fuels are used as mixtures, they can cause positive effects on the engine performance and combustion end products by volumetric ratios of fuels. Due to methyl alcohols are obtained from wood or natural gas, ethanol-gasoline fuel blends are more preferred in SI engines because of its renewability and less harmful effects.

Ethanol is a hydrocarbon which is oxygenated, colorless, transparent, volatile and flammable; it has also a pungent odor and a naturally liquid form [4]. Some of the crucial physical and fuel properties of ethanol, gasoline and also their blends with various ratios are represented in Table 1 below.

These properties are very important for understanding of the SI engines performance characteristics with these fuels.

Table 1. Properties of used fuels.

Properties	Gasoline	Ethanol	E15	E50	E85
Chemical Formula	C ₈ H ₁₅	C ₂ H ₅ OH	-	-	-
Molecular Weight	111,21	46,07	101,44	78,64	55,84
Oxygen Content, wt. %	-	34,73	5,21	17,37	29,52
Carbon Content, wt. %	86,3	52,2	81,19	69,25	57,32
Hydrogen Content, wt. %	24,8	13,1	23,05	18,95	14,86
Stoichiometric AFR	14,5	8,94	13,67	11,72	9,77
Lower Heating Value	44,3	27	41,71	35,65	29,6
Heat of Evaporation, Mj/kg	305	840	385,25	572,5	759,75
Research Octane Number	96,5	111	98,68	103,75	108,83
Motor Octane Number	87,2	92	87,9	89,6	91,28
Vapor Pressure (kPa)	61,4	19,3	55,1	40,35	25,615

Ethanol-gasoline blends have been used with different ratios on spark ignition engine for many years. Renzi et al., studied with three blends of ethanol and gasoline fuels (E0, E50 and E80) and effects of these fuel mixtures on performance were investigated. The investigation showed that the best improvement about brake specific fuel consumption and the highest brake thermal efficiency were obtained with E50, in spite of minor torque and power reductions [5].

Celik M. B. at al., investigated the performance effects of different ethanol gasoline blends (E0, E25, E50, E75, E100) and the results had shown that, E25, E50 and E75 fuel blends were increased power output 3%, 6% and 2%, respectively when compared to E0 fuel at the same compression ratio [6]. Badwan conducted with E10 to E70 fuel mixtures in his study, as a result that E50 was shown the highest antiknock capability among these fuels [7].

Clement et al., studied with hydrous ethanol (water concentration 7%) or E22 (22% ethanol and 78% gasoline) fuel blend in his experiments. When the results were examined, using hydrous ethanol was provided 9% and 14% improvement about peak torque and peak power, respectively, compared to the E22 fuel. On the other hand, specific fuel consumption of ethanol-gasoline blend was better than hydrous ethanol by 35%, because of water content of hydrous ethanol [8].

In addition, there are many studies in the literature. Some of them were conducted by Yücesu et al.[9], Hsieh et al.[10], Palmer [11], Al Hasan [12], Topgül et al.[13], Gorse et al.[14], Salih at.al.[15], Chandler et al.[16]. When studies were examined in detail, it was observed that when ethanol content is increased, the performance outputs are increased to a certain point. Furthermore, it appears that all of the ethanol increases have resulted in a reduction in exhaust emissions.

In another study, Najafi et al. investigated the effects of different ethanol-gasoline mixtures (E0, E5, E10, E15, E20) on performance using artificial neural networks method. In the study, the connection among brake torque, power and specific fuel consumption, brake thermal efficiency and volumetric efficiency was tried to be predicted in the ANN model, which was created by using different ethanol-gasoline mixtures and speed data. When the results obtained by using the artificial neural network method were examined, it is seen that the R value was very close to 1, though root mean square errors (RMSE) value was low [17].

As the seen above, many researchers were conducted lots of studies by using wide variety ratios of ethanol-gasoline blends. These studies had given in a useful table by Amit Kumar et al. [18]. However, there aren't enough studies which were simulation based or comparison between theoretical and practical studies. Present study was conducted with AVL BOOST simulation program with different ethanol-gasoline blends. The most related studies were compared with this study in the next sections with all details.

2. Description of Simulation

Simulations are performed to analyze of the system behaviors and to investigate of effects of the different parameters on the modelled system. There are two main step of the simulations, design modeling and experiments. Model design is the creation of a model that represents all important aspects of the system. It is the most important step of the simulation studies. AVL BOOST is the powerful simulation program which has ability to model of precise design and to calculate of the complex system as well as actual system. The engine which is 2.0 L, four-stroke and spark ignition, was modelled by using AVL BOOST simulation program [19].

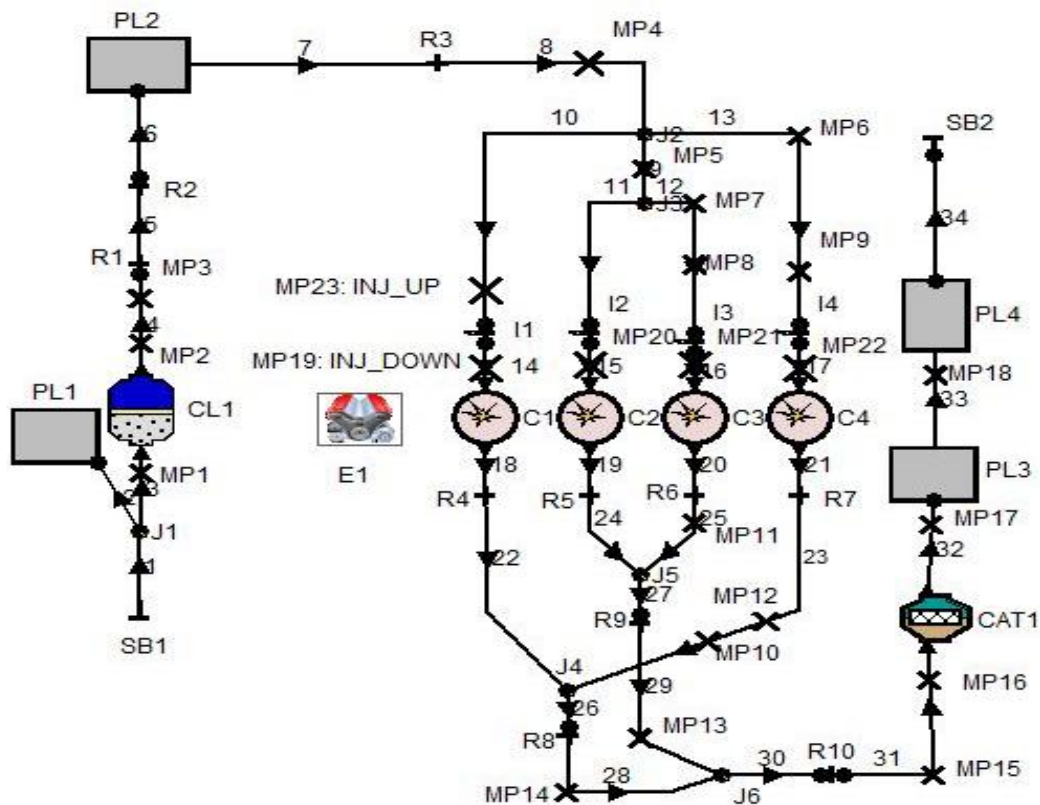


Figure 1. AVL BOOST System Model

This simulation study was performed to examine performance outputs of three different ethanol-gasoline blends which are E15, E50 and E85 with respect to pure gasoline (E0). The simulations were repeated 500 times to reduce mistakes related with computation of simulation. All fuels and elements of modelled engine were given by Tables 2 and 3, respectively.

Table 2. Variation of fuels

Fuel	Ethanol vol. (%)	Gasoline vol. (%)
E0	-	100
E15	15	85
E50	50	50
E85	85	15

Table 3. Elements of Modelled Engine

No	Element	Quantity	Abbreviations	Definition
1	Cylinder	4	C	Engine cylinders which are designed for perfect mixing scavenging model.
2	Engine	1	E	1998 cm ³ , four-stroke S.I. engine
3	Air Cleaner	1	CL	Intake air cleaner is used to model the gas dynamic of air depending on the actual flow
4	Catalyst	1	CAT	The catalyst model is only used for monitoring exhaust gas dynamics.
5	Injector	4	I	The fuel supply which is specified by the A/F ratio of each cylinders.
6	System Boundary	2	SB	The system boundaries provides to define ambient properties for all calculations.
7	Plenum	4	PL	The plenums are used to collect or deliver input air or exhaust gas.
8	Junction	6	J	Junctions are used to determine actual flow conditions of air or exhaust gases in pipes.
9	Restriction	10	R	The flow coefficients of restrictions are related to the minimum attached pipe cross-section.
10	Measuring Point	18	MP	Measuring points are provide to control every each step of the simulation.
11	Pipe	34	-	One dimensional flow pipes.

3. Results and Discussion

The simulation results are given in this section by graphs. The aim of this study was determination of optimum ethanol-gasoline mixture ratio by comparison performance outputs of different blends. All performance outputs were examined and explained in detail.

According to overall torque results, E50 fuel blend gives the best performance outputs. The Engine Torque – Engine Speed graph is shown in figure 2. It is clearly seen that, improvement of torque values were provided by all ethanol gasoline blends (E15, E50 and E85) with respect to only gasoline (E0) usage. The engine torque improvement of E50 blend usage was 3.62% while the improvements with E15 and E85 are 1.29% and 1.86%, respectively.

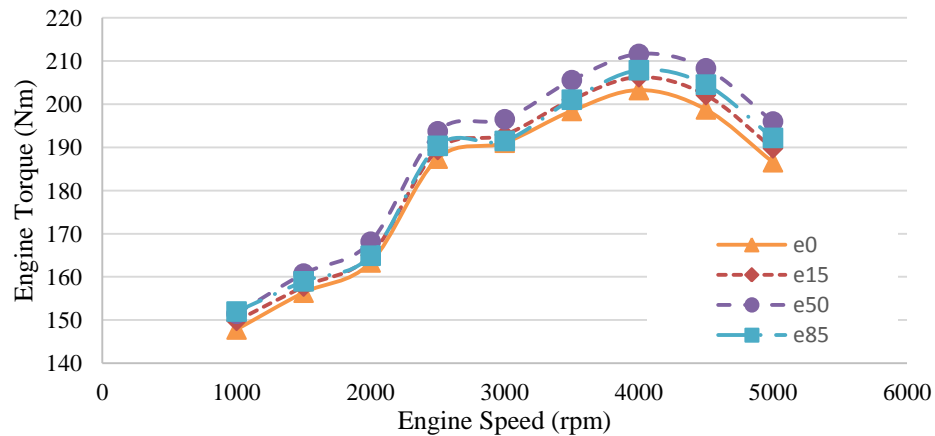


Figure 2. Torque vs. Engine Speed

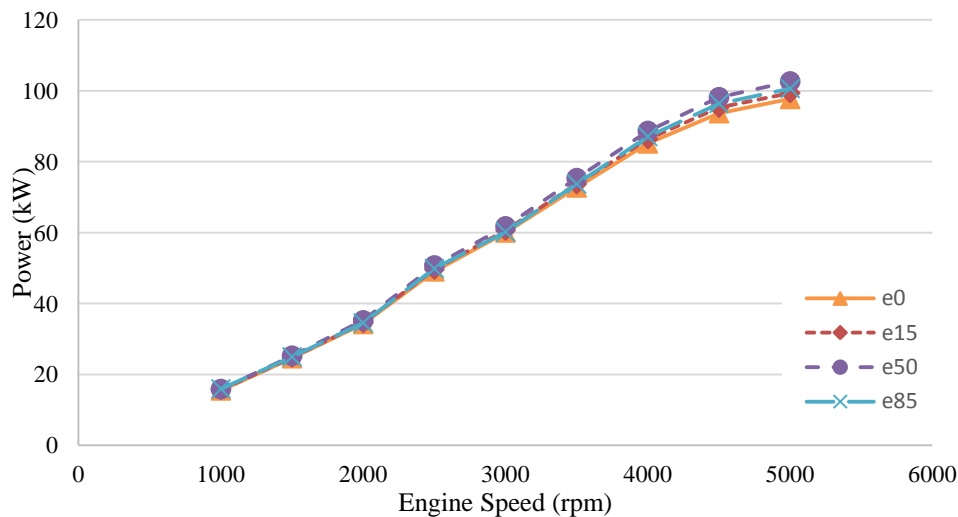


Figure 3. Power vs. Engine Speed

The Power – Engine Speed graph is presented in figure 3. When compared the power outputs of all fuel blends with respect to gasoline, it is observed that the outputs were shown the same characteristics of torque values. It is obviously seen from figure 3, the power difference obtained at high engine speed is increasing gradually. The maximum increase in the engine power was obtained with E50 by 3.94% and the engine power improvement of E15 and E85 were recorded 1.38% and 2.01% in overall.

The Brake Specific Fuel Consumption (BSFC) – Engine Speed graph is shown in figure 4. It is clearly observed that, the BSFC values decrease as the ethanol ratio increases of the blend to a certain point. The maximum reduction of BSFC was obtained with E50 fuel blends. These results are matching with related and similar studies in literature. Najafi G. et al.(2008) conducted that the specific fuel consumption decreased as the ethanol ratio increased [17]. The overall mean reduction of BSFC values were 2.26%, 6.76% and 5.74% for E15, E50 and E85, respectively.

The Volumetric Efficiency - Engine Speed graph is illustrated below in figure 5. As it is seen from the figure, the volumetric efficiency has decreased depending on concentration of ethanol in the

fuel blends. On the other hand, this reduction was observed with engine speed. When engine speed was increased, the volumetric efficiency has decreased depending on it.

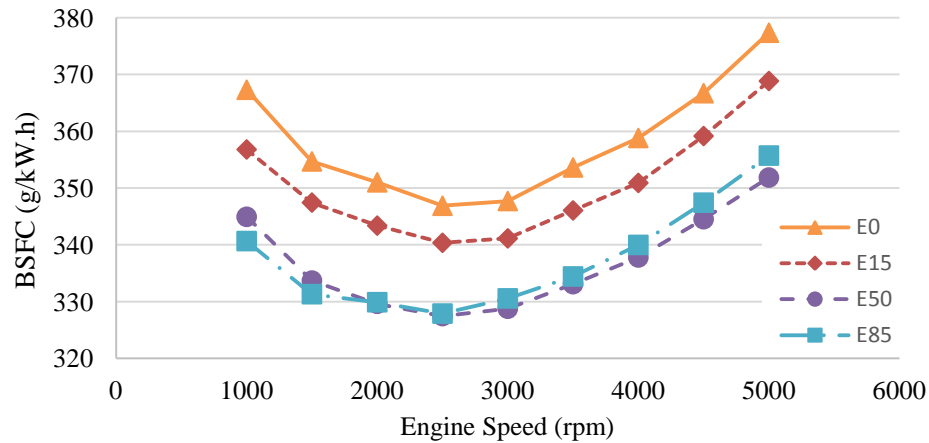


Figure 4. BSFC vs. Engine Speed

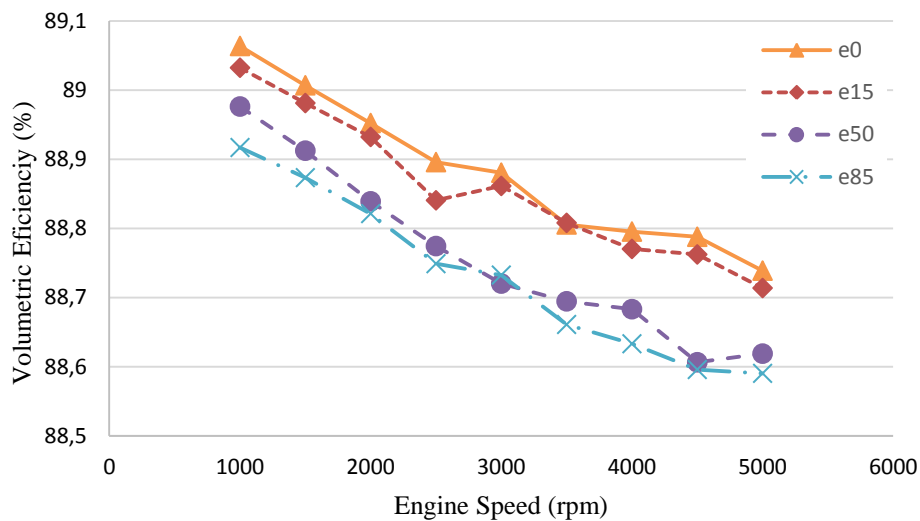


Figure 5. Volumetric Efficiency vs. Engine Speed

Indicated Mean Effective Pressure (IMEP) – Engine Speed graph is presented in figure 6. This term is generally defined as the function of indicated work. As the combustion improves, the pressure inside the cylinder increases and produces more power output. So, the overall results of power and torque outputs provide to understand IMEP characteristics of engines. It is clearly seen that in figure 6, the IMEP results have the same characteristics with the torque and power results. The overall mean improvement values were obtained 1.16%, 3.25% and 1.67% for E15, E50 and E85, respectively.

4. Conclusions

This study was simulation based analysis of ethanol blend usage with gasoline fuel. Additionally, comparisons of most related experimental studies were discussed. AVL-BOOST simulation software was used for this theoretical study. Overall results of this study indicate that ethanol will be promising fuel blend if production cost can be decreased in next decades. All the performance outputs were improved until a certain point of ethanol blend up to 50% and especially lower heating value of ethanol decreased the performance outputs after this point. On the other hand, exhaust gas emissions could be improved as much as the blend ratio of ethanol increases in the gasoline fuel. This can be the subject for future studies.

Optimum blend ratio has determined as E50 and overall improvements were 3.62%, 3.94%, 6.76%, for brake torque, power and specific fuel consumption, respectively. From the view of volumetric efficiency, E50 and E85 results were lower than E0 and E15 as expected.

Acknowledgement: This study was conducted with AVL BOOST simulation program. We are grateful to AVL-AST, Graz, Austria to provide us this program within the scope of UPP (University Partnership Program)

References

- [1] Kessel, Dagobert G. "Global warming—facts, assessment, countermeasures." **Journal of Petroleum Science and Engineering** 26.1 (2000): 157-168.
- [2] Cao, Xia. "Climate change and energy development: implications for developing countries." *Resources policy* 29.1 (2003): 61-67.
- [3] Johansson, Thomas, and S. McCarthy. "Global warming post-Kyoto: continuing impasse or prospects for progress." **Energy Dev Rep Energy** (1999): 69-71.
- [4] Ganguly, A., P. K. Chatterjee, and A. Dey. "Studies on ethanol production from water hyacinth—A review." **Renewable and Sustainable Energy Reviews** 16.1 (2012): 966-972.
- [5] Renzi, Massimiliano, Marco Bietresato, and Fabrizio Mazzetto. "An experimental evaluation of the performance of a SI internal combustion engine for agricultural purposes fuelled with different bioethanol blends." **Energy** 115 (2016): 1069-1080.
- [6] Celik, M. Bahattin. "Experimental determination of suitable ethanol–gasoline blend rate at high compression ratio for gasoline engine." **Applied Thermal Engineering** 28.5 (2008): 396-404.
- [7] Radwan, M. S. Performance and knock limits of ethanol-gasoline blends in spark-ignited engines. No. 850213. **SAE Technical Paper**, 1985.
- [8] Clemente, Rafael C., et al. Development of an internal combustion alcohol fueled engine. No. 2001-01-3917. **SAE Technical Paper**, 2001.
- [9] Yücesu, H. S., Topgül, T., Cinar, C., & Okur, M." Effect of ethanol–gasoline blends on engine performance and exhaust emissions in different compression ratios." **Applied thermal engineering**, 26.17 (2006): 2272-2278.
- [10] Hsieh, W. D., Chen, R. H., Wu, T. L., & Lin, T. H. "Engine performance and pollutant emission of an SI engine using ethanol–gasoline blended fuels." **Atmospheric Environment**, 36.3 (2002): 403-410.

-
- [11] Palmer, F. H. "Vehicle performance of gasoline containing oxygenates." *International Conference On Petroleum Based Fuels And Automotive Applications*. Imeché Conference Publications 1986-11. PAPER NO C319/86. 1986.
- [12] Al-Hasan, M. "Effect of ethanol–unleaded gasoline blends on engine performance and exhaust emission." **Energy Conversion and Management** 44.9 (2003): 1547-1561.
- [13] Topgül, T., Yücesu, H. S., Cinar, C., & Koca, A. "The effects of ethanol–unleaded gasoline blends and ignition timing on engine performance and exhaust emissions." **Renewable energy**, 31.15 (2006): 2534-2542.
- [14] Gorse, R. A., Benson, J. D., Burns, V. R., Hochhauser, A. M., Koehl, W. J., Painter, L. J., ... & Rutherford, J. A. The effects of methanol/gasoline blends on automobile emissions. No. 920327. **SAE Technical Paper**, 1992.
- [15] Salih, F. M., and G. E. Andrews. The Influence of Gasoline/Ethanol Blends on Emissions and Fuel Economy. No. 922378. **SAE Technical Paper**, 1992.
- [16] Chandler, Kevin, Margaret Whalen, and Jeffrey Westhoven. Final results from the state of ohio ethanol-fueled light-duty fleet deployment project. No. 982531. **SAE Technical Paper**, 1998..
- [17] Najafi, G., Ghobadian, B., Tavakoli, T., Buttsworth, D. R., Yusaf, T. F., & Faizollahnejad, M. "Performance and exhaust emissions of a gasoline engine with ethanol blended gasoline fuels using artificial neural network." **Applied Energy**, 86.5 (2009): 630-639.
- [18] Thakur, A. K., Kaviti, A. K., Mehra, R., & Mer, K. K. S. "Progress in performance analysis of ethanol-gasoline blends on SI engine". **Renewable and Sustainable Energy Reviews**, 69, (2017): 324-340.
- [19] AVL, AVL. "BOOST software version 2013–Theory." Graz, Austria (2013).

Experimental study on a spark ignition engine fuelled by methane-oxygen enriched air

Mehmet İlhan İlhak, Selahaddin Orhan Akansu, H. Enes Fil, Nafiz Kahraman

*Department of Mechanical Engineering, Faculty of Engineering, Erciyes University, 38039
Kayseri, Turkey*

Abstract: Oxy-fuel combustion is the process of burning a fuel using pure oxygen instead of air as the primary oxidant. Since the nitrogen component of air is not heated, fuel consumption is reduced, and higher flame temperatures are possible. In this study, four-cylinder four-stroke SI engine was operated with methane fuel. Spark timing was fixed to 11 CA° BTDC under a constant load of 30 Nm at 1500 rpm.

Firstly, engine was tested at Stoichiometric conditions. The gas throttle fixed for air inlet. Then, oxygen was sent from the intake manifold. While the oxygen amount was increased, CO, HC emissions decreased and the maximum peak pressures increased.

1. Introduction

Oxy-enriched combustion is the burning process using pure oxygen or enriched-oxygen instead of air as the primary oxidant. When the oxygen content in combustion air exceeded about 21 %, the air is said to be oxygen-enriched. This combustion process is particularly known to be applied to power plants, industrial furnaces, boilers because of providing CO₂ capture and high efficiency potential. The general characteristics of oxy-fuel or oxy-enriched combustion are less exhaust gas production and less heat lost in the exhaust than air fuel combustion. The subject of Oxy-enriched combustion technology application to internal combustion engines to achieve higher efficiency and low emission is important for reasons decrease of amount of fossil fuel consumption and getting low level emission in the world [1-3].

Wu et al. studied on combining water injection process with an oxy-fuel in internal combustion engine cycle to enhance thermal efficiency. They stated that the thermal efficiency improves with the increase of both engine load and water injection mass, and indicated thermal efficiency increases from 32.1% to 41.5% under appropriate test condition [4]. Asdrubali et al. investigated in a Life Cycle Assessment methodology, in order to evaluate the environmental impacts of these new oxy-fuels; from glycol-ether mixtures production to using them as an additive for diesel fuel [5]. Karagöz et al., experimentally studied on Effect of hydrogen and oxygen addition as a mixture on emissions

and performance characteristics of a gasoline engine. They explained that the brake thermal efficiency values improved by 3.3% and 10.4% with H₂/O₂ addition at all engine operating gaps compared to only gasoline fuel operating condition [6]. Wang et al. investigated performance of a spark-ignited gasoline engine operating with hydrogen and hydrogen–oxygen mixtures. They emphasized that both the additions of hydrogen and hydroxygen helped to increase flame development and propagation periods of the gasoline engine, also reduced HC emissions while raised NO_x emissions with the increase of hydrogen and hydroxygen addition levels [7]. Rajkumar and Govindarajan studied on diesel engine single cylinder to investigate effects of oxygen-enriched combustion on exhaust emission. This study performed at three oxygen-enriched ratio showed that emission of CO and HC decreased, but emission of CO₂ and NO_x increased, when oxygen-enriched ratio increased [8]. Mormani investigated effects of oxygen-enriched combustion on exhaust emissions in a gasoline engine. He stated that the amount of CO and HC emission decreased also, by increasing engine speed, CO emission increased, while HC emission decreased, under oxygen-enriched combustion [9].

In this study, performance and emissions characteristics have been studied fueled by methane at different oxygen-enriched ratio in a four-stroke SI engine.

2. Experimental apparatus and test procedure

This present work was carried out on a Ford engine. This is a four-stroke cycle, four-cylinder spark ignition engine with a bore × stroke of 80.6 x 88 mm. and a compression ratio of 10:1. The engine details are given in [Table 1](#). The view of experimental system has been given in Fig.1.

Table 1. Engine specifications

Ignition line	1-3-4-2
Bore	80.6 mm
Stroke	88 mm
Engine volume	1796 cc
Compression ratio	10:1
Maximum engine cycle	5500 rpm
Power (DIN)	75 kW, 102 PS
Tork (DIN)	150 Nm, (4000 rpm)

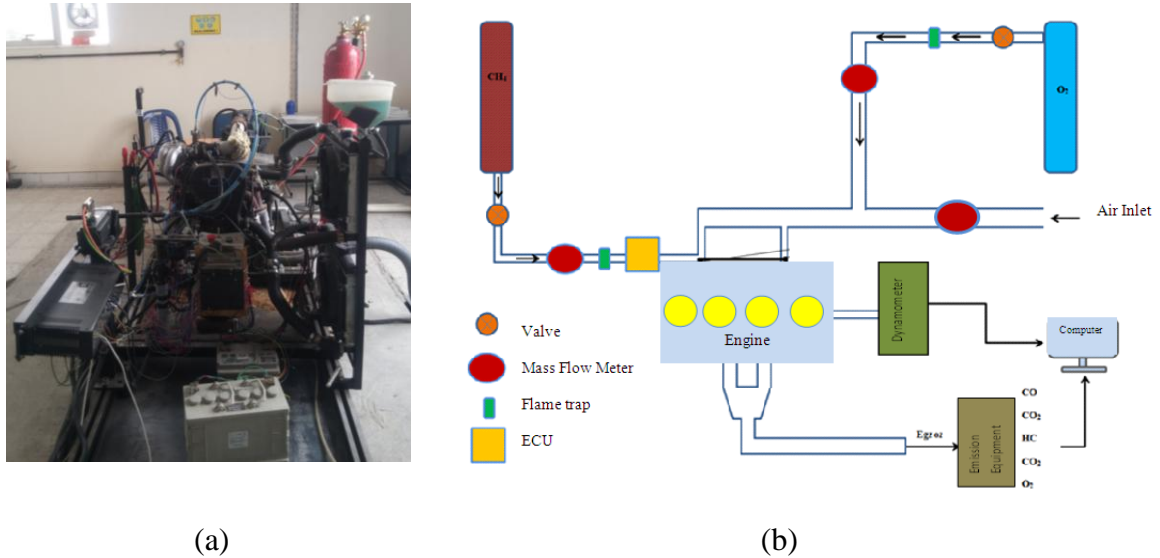


Figure 1. Experimental rig (a) A view in test room (b) Schematically test system.

All work was conducted in the Engine Laboratory in the department of Mechanical Engineering at the University of Erciyes. Methane fuel was used in the SI engine. Firstly, fuel –air blends were prepared for different oxygen fractions. Fuel is supplied to engine intake port through gas mixer, and the amount of fuel and air ratios are controlled by a manual valve. The ignition timing of the engine has been adjusted as constant for all tests (as 11° BTDC). The measurements were fixed half throttle as 50 Nm. Bosch BEA-60 gas analyzer was used to measure CO, NO, CO_2 , HC. All test measurements were analyzed in the constant load and 1500 rpm.

3. Results and discussions

3.1 Cylinder Pressure and Brake Thermal Efficiency

Figure 2 shows the cylinder pressure versus crank angle for different excess oxygen percentage in the exhaust. Figure 2 depicts that moment of combustion duration shortened with the increase of excess oxygen percentage. With the increase of oxygen percentage, the maximum cylinder pressure rises, and the position of maximum cylinder pressure gradually approach the top dead center (360 CA). After the maximum pressure point, with the increase of oxygen percentage, cylinder pressure values have been sharply decreased. The maximum pressure values are 18.21, 19.76, 21.14, 25.97, 29.81 and 30.05 bar and the pressure rise rate ($dP/d\theta$) values are 0.55, 0.61, 1.05, 2.13, 2.94 and 3.07 bar/CA for without oxygen (EAR=1.034), 2%, 4%, 7%, 9% and 15 % oxygen percentage in the exhaust, respectively.

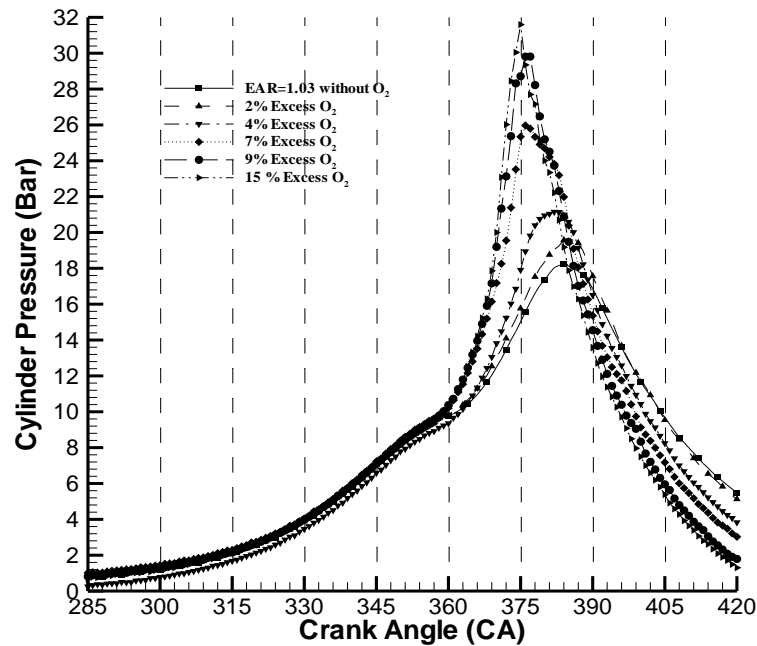


Figure 2. Cylinder Pressure versus the crank angle

Brake thermal efficiency values have been given in Figure 3. As seen this figure, brake thermal efficiency values increase up to 4% O₂ percentage and then the brake thermal efficiency values decrease. As the concentration of oxygen is increased, combustion is accelerated and the burning of the fuel is completed faster.

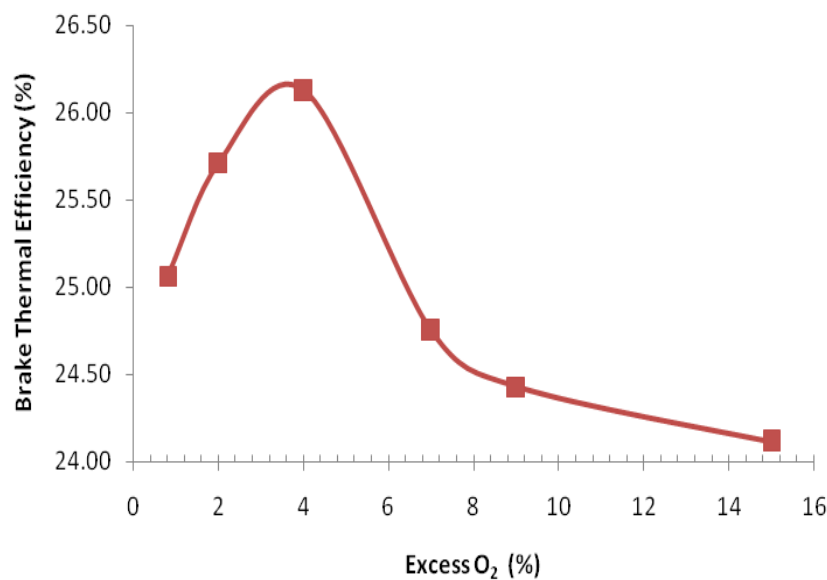


Figure 3. Brake thermal efficiency versus excess O₂

3.2 Emissions

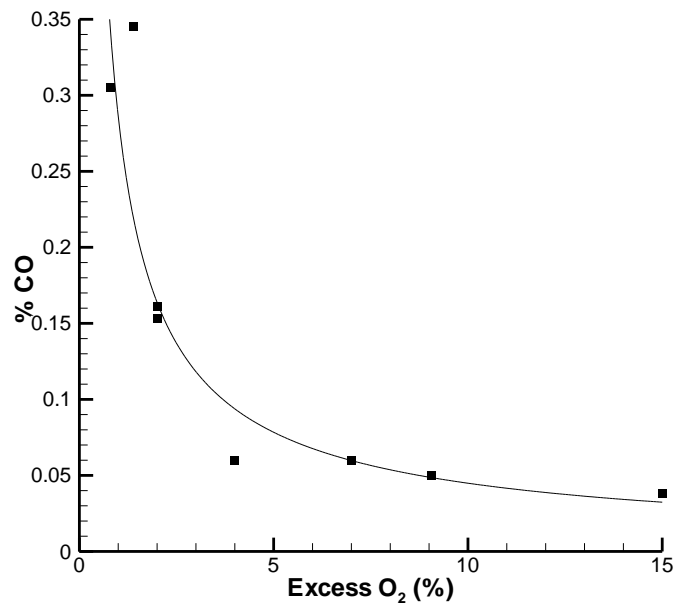


Figure 4. CO% values versus excess O₂

The CO% emissions are plotted versus excess O₂ in exhaust in figure 4. While the O₂ percentage values are increasing, CO values decrease. As seen in this figure, CO% values linearly decrease excess 4% O₂ but CO% values are nearly constant after 4% excess O₂. So, we can say that when about 4% excess O₂ amount is in the exhaust, CO% amount is adequate.

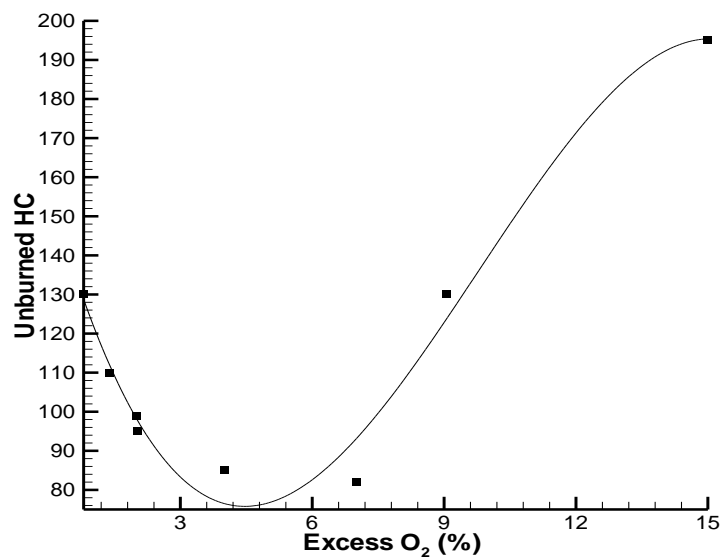


Figure 5. Unburned HC versus excess O₂

Figure 5. shows the unburned hydrocarbon values (ppm) versus the excess $O_2\%$ in the exhaust. UHC values reach its lowest point value at about 4-7% excess O_2 values. UHC concentration increases when O_2 excess ratio higher than 7%.

NO values versus excess $O_2\%$ in the exhaust have been illustrated in Fig. 6. As the oxygen percentage increases up to 4% excess oxygen, after than NO values are almost constant. Increasing with oxygen percentage, combustion speed are increased and temperature values in cylinder also NO values are increased.

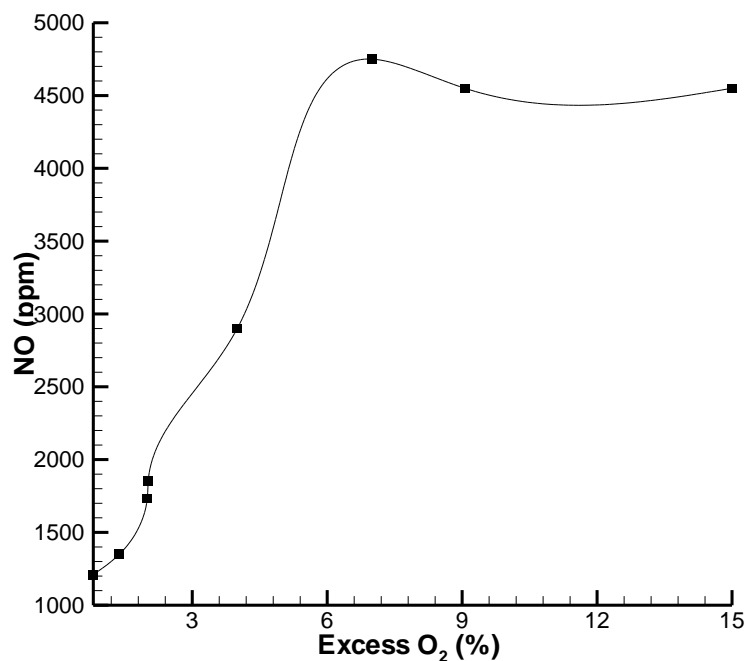


Figure 6. NO values versus excess % O_2

4. Conclusions

The results of this study can be summarized as follows:

- NO emission values increase with increasing O_2 percentage.
- HC and CO emissions values decrease with increasing O_2 percentage up to 4% than rising in HC emissions and nearly constant values in CO emissions have been observed.
- BTE values are between 24% and 26%. The maximum thermal efficiency has been obtained in the 4% excess oxygen in exhaust.

- This study would give forth ideas to help in designing and operating internal combustion engines fuelled by natural gas (NG)–enriched in air.

Consequently, If NG (methane) of the cleanest fossil fuels has been used with oxygen enriched air in an SI engine, more clean combustion and more performance can be obtained. In future studies, experiments can be made with different loads, different ignition timings and rpm.

References

- [1] Wu Z., Kang Z., Deng J., Hu Z., Li L., “Effect of oxygen content on n-heptane auto-ignition characteristics in a HCCI engine”, *Appl Energy*, 184 (2016), 594–604
- [2] Li, SY, Xu, MX, Jia, LF, Tan, L, Lu, QG “ Influence of operating parameters on N₂O emission in O₂/CO₂ combustion with high oxygen concentration in circulating fluidized bed” *Appl Energy*, 173 (2016), pp. 197–209
- [3] Liu, CY, Chen, G, Sipocz, N, Assadi, M, Bai, XS, “Characteristics of oxy-fuel combustion in gas turbines” *Appl Energy*, 89 (2012), pp. 387–394
- [4] Wu, ZJ; Yu X., Fu LZ, Deng J., Hu ZJ., Li LG., “A high efficiency oxyfuel internal combustion engine cycle with water direct injection for waste heat recovery “ 70 (2014), pp 110-120.
- [5] Asdrubali F., Cotana F., Rossi F., Presciutti A., Rotili A., Guattari C., “Life Cycle Assessment of New Oxy-Fuels from Biodiesel-Derived Glycerol”, *Energies* 2015, 8(3), 1628-1643.
- [6] Karagöz Y., Yuca N., Sandalcı T., Dalkılıç A.S., “Effect of hydrogen and oxygen addition as a mixture on emissions and performance characteristics of a gasoline engine”, *Int. J. Hydrogen Energy* 2015(40), pp8750-8760.
- [7] Wang S., Ji C., Zhang J, Zhang B, “Comparison of the performance of a spark-ignited gasoline engine blended with hydrogen and hydrogen–oxygen mixtures”, *Energy* 2011 (36), 5832-5837.
- [8] Rajkumar K, P. Govindarajan P. “Impact of Oxygen Enriched Air Intake on the Exhaust of a Single Cylinder Diesel Engine”, *American Journal of Environmental Sciences* Vol. 7 (2), 2011 136-140
- [9] Momani W., “The Effects of Excess Oxygen to Mixture on the Gases Emissions of a Gasoline Engine”, *American Journal of Applied Sciences* Vol 6 (6), 2009, 1122-1125

Biomethane recovery from anaerobic co-digestion of sewage sludge and waste coffee

M.R. Atelge^{1, 2*}, A.E. Atabani¹, Gopalakrishnan Kumar³, S. Unalan¹

¹Energy Division, Department of Mechanical Engineering, Faculty of Engineering, Erciyes University, 38039 Kayseri, Turkey

²Energy Division, Department of Mechanical Engineering, Faculty of Engineering, Siirt University, 56100 Siirt, Turkey

³Department of Environmental Engineering, Daegu University, South Korea
rasitatelge@gmail.com

Abstract: In this study, anaerobic co-digestion of waste coffee and sewage sludge was used for the production of biogas in a batch scale digester at mesophilic condition (~37 °C). Three experimental conditions were prepared including; sewage sludge (sample 1) which had 2% of solid waste, sewage sludge with waste coffee before oil extraction (sample 2), and sewage sludge with waste coffee after oil extraction (sample 3). 5 grams of waste coffee (before and after oil extraction) were mixed with 100 ml of sewage sludge, the experiments were monitored for 45 days. The results showed that sewage sludge gave the lowest methane yield (0.003 m³/kg VS initial) while the highest was obtained from sample 2 (0.02 m³/kg VS initial) compared to (0.007 m³/kg VS initial) of sample 3. As a conclusion, co-digestion of waste coffee as potential co-substrate is an effective method to enhance biogas yield from sewage sludge. Therefore, more research shall be directed towards the recycling of waste coffee into biogas.

Keywords: Waste cooking oil, biodiesel, diesel engine, butanol, exhaust emissions.

1. Introduction

The widespread use of fossil fuels is responsible for the long-term environmental risks such as global warming. The key contributor to global warming is the emission of carbon dioxide (CO₂) that comes from many combustion sources. Man-made CO₂ is one of the main reasons for greenhouses effect. Kyoto protocol has been established to decrease greenhouse gases emissions. According to the Inventory of the United States Greenhouse Gas (GHG) Emissions and Sinks 1990–2013 report published by the United States Environmental Protection Agency (EPA), GHG emissions from transportation represented 27% of the total amount of US GHG emissions from end-use fossil fuel combustion in 2013 [1]. Recently, alternative fuels have been heavily investigated.

Biogas is a promising renewable fuel, which can be produced from a number of various organic substrates [2]. Biogas makes a contribution towards reduction of GHG owing to less fossil fuel combustion [3]. Biogas is one of cleanest fuel because it produces energy without soot and particulate matter [4]. It is lighter in term of carbon chain length; therefore, less carbon dioxide is

emitted to the atmosphere when it is burnt [4]. In some European countries, buses, trucks, and passenger cars that use biogas as a fuel, are already in use. Besides reduction of GHG, biogas helps to decrease air pollution and increase recycling of waste. It has positive effect not only on energy policies but also agricultural policies [2].

Organic waste management is another concern due to increasing population. Sewage sludge is created during biological wastewater treatment. Sludge includes toxic materials such as pathogens, heavy metals and some organic contaminants [5]. Currently, there have been various sewage sludge treatment systems such as anaerobic digestion, landfill, compost, drying-incineration, and land application. Anaerobic digestion (AD) is the most promising method for sewage sludge treatment owing to elimination of odors, stabilization of sludge and production of alternative fuels such as biogas [5]. Biogas production using AD has become a key role to reduce GHG and organic waste problem.

Once organic materials, such as sewage sludge, animal manure, and waste food, are biologically decomposed under anaerobic condition, biogas is produced. It is composed of 40-70% of methane (CH₄), 25-50% of carbon dioxide, small amount moisture (H₂O), and traces of hydrogen sulfide (H₂S) and hydrogen (H₂) [6]. Recently, biogas has been considered as an important renewable energy resource. In anaerobic co-digestion process some organic feedstocks such as fats, greases or waste food, are mixed with other feedstocks such as sewage sludge and animal manure to increase the yield of methane production [7]. Waste coffee as a feedstock is a strong candidate for biodiesel and biogas production owing to its availability all over the world and its rich components.

More than 9 million tons of coffee was produced in 2016 [8]. The significant quantity of spent coffee ground remains after producing beverage creates waste disposal problem. This waste has high oxygen demand during decay process and releases residual caffeine, tannin, and polyphenol to the environment [9]. Machado [10] reported that one of the possible ways to reduce environmental impact of waste coffee is the biological treatment using fungi [11]. This biological treatment releases phenolic components in waste coffee and reduces its toxicity [11]. Secondly, valorization of spent coffee grounds is a useful method to produce biodiesel and bio-oil because it has lipid content of around 15% of dry weight [12]. Lane [13] and Raetz [14] reported that spent coffee ground was used as a feedstock for anaerobic digestion under mesophilic condition. Kida [15] and Kostenberg [16] studied waste coffee at thermophilic condition. These studies reported that biogas production decreased after a while due to pH problems or inhibition. Under thermophilic condition, 70% of CH₄ production was achieved even if there were some experimental problems such as the high percentage of solids and fiber [17].

Spent coffee ground has been investigated in literature as a feedstock for biofuels production. Obtaining biodiesel from waste coffee was successfully achieved. Anaerobic digestion and anaerobic co-digestion of waste coffee has gained much attention recently. The main problem associated with waste coffee is the long-term stability due to higher lipid content. As far as authors' knowledge, waste coffee after oil extraction has not been considered as a substrate for anaerobic co-digestion. This paper aims to study the effect on biogas yield using waste coffee before and after oil extraction in anaerobic co-digestion under the mesophilic condition in batch scale.

2. Materials And Methods

Spent coffee ground was gathered from local coffee shops in Kayseri. It was prepared to extract the oil and produce biodiesel. Therefore, waste coffee before and after oil extraction were kept for further analysis. Activated sewage sludge was collected from a local wastewater treatment plant in Kayseri. The sewage sludge consists of human wastes such as night soil, washroom waste and

sinks waste and 2% of the sludge was solid waste. The sludge sample has been stored at 4 °C in a refrigerator.

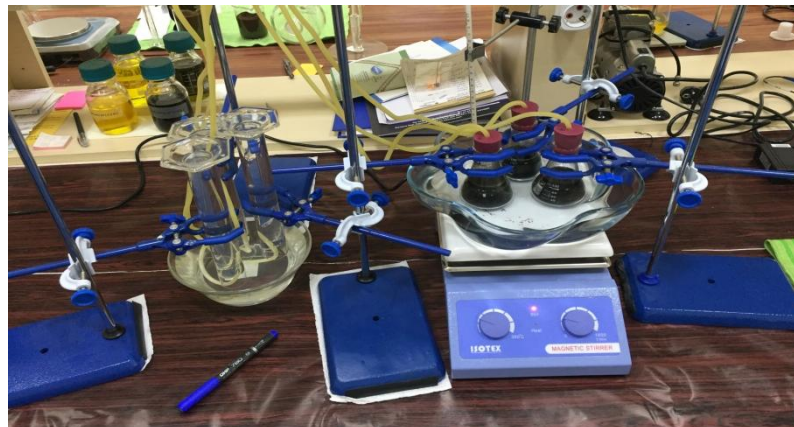


Fig 1. Experimental set-up

For experimental setup, three 100 ml conical flasks have been used. The flasks have been sealed with stoppers to obtain anaerobic environment and N₂ treatment was applied for 7 minutes for each sample. PH was measured using Neomet pH meter pH-200L. To store biogas, the displacement of water method was used as shown in Fig 1. 100 ml of sewage sludge, 5 ml (5.78 g) of sodium bicarbonate (NaHCO₃), 5 grams of waste coffee before oil extraction, and 5 grams of waste coffee after oil extraction have been mixed with sludge.

A bowl has been used as a hot water bed to obtain homogeneous temperature distribution for all samples. For mixing the samples, a magnetic stirrer was placed in each flask and it was fixed at 160 rpm during the entire test. The water temperature in the bowl has been measured 37 °C ± 1 °C.

For the first sample, sewage sludge and NaHCO₃ were mixed and marked as sample 1. PH was measured 7.28 after N₂ treatment. The second sample contained 100 ml of sewage sludge, 5 ml (5.78 g) of sodium bicarbonate (NaHCO₃) and 5 grams of waste coffee after oil extraction is marked as sample 2. The last sample with 100 ml of sewage sludge, 5 ml (5.78 g) of sodium bicarbonate (NaHCO₃) and 5 grams of waste coffee before oil extraction is marked as sample 3. For C/N ratio, night solid in sewage sludge is around 10:1 [18], coffee waste is around 20:1 [19]. The average mixed of C/N ratio was calculated approximately as 18.3:1.

To calculate total solid (TS) and volatile solid (VS), all samples were dried at 105 oC for 24 hours for TS and at 550 oC for 2 hours for VS according to EPA standard [20].

Biogas has been stored in 3 different measuring cylinders. The measurement has been made daily around 5 pm. Table 1 shows the details of each sample.

Table 1. Initial Parameters for Each Sample

		TS initial (g)	VS initial (g)	CH4 Content (%)
Sample 1		1.84	1.76	17.3
Sample 2		2.91	1.94	76
Sample 3		3.33	2.1	33

		Sample No		
		Sample 1	Sample 2	Sample 3
mixing materials	Sludge	100 ml	100 ml	100 ml
	NAHCO ₃	5 ml (5.78 g)	5 ml (5.78 g)	5 ml (5.78 g)
	Coffee waste after extraction	-	5 grams	-
	Coffee waste before extraction	-	-	5 grams
N ₂ treatment		7 mins	7 mins	7 mins
Temperature		37 oC	37 oC	37 oC
Stirring		160 rpm	160 rpm	160 rpm
pH		7.28	6.88	6.88

Shimadzu GC-2010 Plus Gas Chromatography System (Environmental Engineering Department, Erciyes University) was used to analyze biogas content. The measurement was done twice for each sample.

3. Results And Discussion

Table 2 shows the values of TS (total solid) and VS (volatile solid) for each sample. As expected, blank sample 1 had the lowest values of TS and VS which are 1.84 g and 1.74 g respectively. For samples 2 and 3, TS was measured 2.91 g and 3.33 g. VS values for sample 2 and 3 were 1.94 g and 2.1 g. Methane content of biogas is represented in Table 2.

Table 2. TS ,VS and CH₄ content for each sample

	TS _{initial} (g)	VS _{initial} (g)	CH ₄ Content (%)
Sample 1	1.84	1.76	17.3
Sample 2	2.91	1.94	76
Sample 3	3.33	2.1	33

Daily cumulative biogas and methane production in 45 days is shown in Fig. 2.

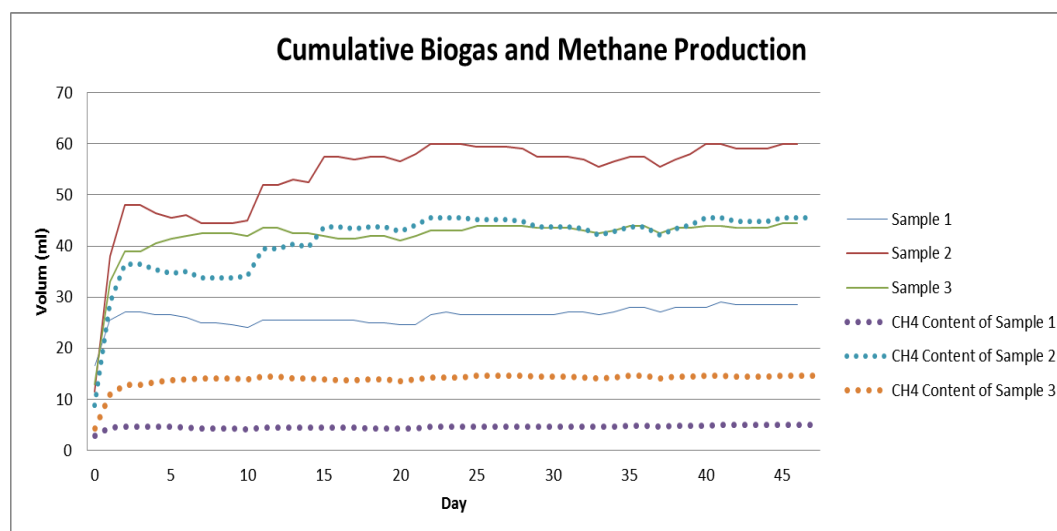


Fig 2. Cumulative biogas and methane production during 45 days

For each sample, specific methane yield was obtained as 0.003, 0.02 and 0.007 m³/kg VS initial respectively. The results indicate that addition of waste coffee as substrate has a positive effect on the overall methane yield. Results show that waste coffee after oil extraction has the highest methane yield (76%) which is 6.6 times more than sample 1. Neves [17] reported that the specific methane yield ranged from 0.25 to 0.28 m³/kg VS initial by mutable co-digestion substrates such as coffee, barley, and rye were used in that study. Vitez [11] indicated that specific methane yield ranged from 0.271 to 0.325 m³/kg dry organic matter. It is obvious that adding waste coffee after oil extraction as a substrate has positive effect on CH₄ yield.

4. Conclusion

Coffee industry creates enormous amount of waste. Therefore, biogas production from this waste is a great opportunity to reduce its environmental impact and produce bio-methane with anaerobic co-digestion. Our results indicate that methane production yield is the highest with waste coffee after oil extraction. The blending ratio shall be further investigation. Moreover, different inoculums should be investigated to obtain higher specific methane yield.

Acknowledgement: The authors would like to thank Erciyes University, Kayseri, Turkey for the financial support under university project FOA-2015-5817. The authors would like also to thank Prof. Dr. Yalcin Sevki YILDIZ and Ars. Gor. Dr. Hamdi MURAT COBANOGU for their supports.

References

- [1] Inventory of U.S. Greenhouse Gas Emissions and Sinks: 1990 - 2013, U.S. Environmental Protection Agency, Washington, EPA 430-R-15-004, 2015. <http://www.epa.gov/climatechange/Downloads/ghgemissions/US-GHG-Inventory-2015-Main-Text.pdf>.
- [2] M. Lantz, M. Svensson, L. Björnsson, P. Börjesson, The prospects for an expansion of biogas systems in Sweden - Incentives, barriers and potentials, *Energy Policy*. 35 (2007) 1819–1829. doi:10.1016/j.enpol.2006.05.018.
- [3] M. Poeschl, S. Ward, P. Owende, Prospects for expanded utilization of biogas in Germany, *Renew. Sustain. Energy Rev.* 14 (2010) 1782–1797. doi:10.1016/j.rser.2010.04.010.
- [4] R. Arthur, M.F. Baidoo, E. Antwi, Biogas as a potential renewable energy source: A Ghanaian case study, *Renew. Energy*. 36 (2011) 1510–1516. doi:10.1016/j.renene.2010.11.012.
- [5] G. Zhen, X. Lu, H. Kato, Y. Zhao, Y. Li, Overview of pretreatment strategies for enhancing sewage sludge disintegration and subsequent anaerobic digestion : Current advances , full- scale application and future perspectives, *Renew. Sustain. Energy Rev.* 69 (2017) 559–577. doi:10.1016/j.rser.2016.11.187.
- [6] J. Zhou, X. Cao, X. Yong, S. Wang, X. Liu, Y. Chen, T. Zheng, P. Ouyang, Effects of Various Factors on Biogas Purification and Nano-CaCO₃ Synthesis in a Membrane Reactor, *Ind. Eng. Chem. Res.* (2014) 1702–1706.
- [7] S.M. Mitchell, N. Kennedy, J. Ma, G. Yorgey, C. Kruger, J.L. Ullman, Craig Frear, Anaerobic Digestion Effluents and Processes : the Basics, Fs171E. (2015) 16. ext.wsu.edu.
- [8] International Coffee Organization - The Current State of the Global Coffee Trade | #CoffeeTradeStats, (n.d.). http://www.ico.org/monthly_coffee_trade_stats.asp (accessed April 19, 2017).
- [9] M.A. Silva, S.A. Nebra, M.J. Machado Silva, C.G. Sanchez, The use of biomass residues in the Brazilian soluble coffee industry, *Biomass and Bioenergy*. 14 (1998) 457–467. doi:10.1016/S0961-9534(97)10034-4.
- [10] E. Machado, Reaproveitamento de resíduos da indústria do café como matéria-prima para a produção de etanol, (2009). https://scholar.google.ca/scholar?hl=en&q=Reaproveitamento+de+resíduos+da+indústriado+café+comomatéria-prima+para+a+produção&btnG=&as_sdt=1%2C5&as_sdt= (accessed April 20, 2017).
- [11] T. Vítěz, T. Koutný, M. Šotnar, J. Chovanec, On the Spent Coffee Grounds Biogas Production, *Acta Univ. Agric. Silvic. Mendelianae Brun.* 64 (2016) 1279–1282. doi:10.11118/actaun201664041279.
- [12] D.R. Vardon, B.R. Moser, W. Zheng, K. Witkin, R.L. Evangelista, T.J. Strathmann, K. Rajagopalan, B.K. Sharma, Complete utilization of spent coffee grounds to produce biodiesel, bio-oil, and biochar, *ACS Sustain. Chem. Eng.* 1 (2013) 1286–1294. doi:10.1021/sc400145w.

-
- [13] A.G. Lane, Anaerobic digestion of spent coffee grounds, *Biomass*. 3 (1983) 247–268. doi:10.1016/0144-4565(83)90017-3.
- [14] E. Raetz, Anaerobic Digestion of wastes; spent coffee grounds, Nestlé Res. Cent. (1990). https://scholar.google.ca/scholar?q=Anaerobic+Digestion+of+wastes+spent+coffee+grounds+&btnG=&hl=en&as_sdt=0%2C5 (accessed April 11, 2017).
- [15] K. Kida, Y. Sonoda, Treatment of coffee waste by slurry-state anaerobic digestion, *J. Ferment. Bioeng.* (1992). <http://www.sciencedirect.com/science/article/pii/0922338X92902853> (accessed April 11, 2017).
- [16] D. Kostenberg, U. Marchaim, Solid waste from the instant coffee industry as a substrate for anaerobic thermophilic digestion, *Water Sci. Technol.* (1993). <http://wst.iwaponline.com/content/27/2/97.abstract> (accessed April 12, 2017).
- [17] L. Neves, R. Oliveira, M.M. Alves, Anaerobic co-digestion of coffee waste and sewage sludge, *Waste Manag.* 26 (2006) 176–181. doi:10.1016/j.wasman.2004.12.022.
- [18] I.J. Dioha, C. Ikeme, T. Nafi, N.I. Soba, Y. Mbs, Effect of Carbon To Nitrogen Ratio on Biogas Production, *Int. Res. J. Nat. Sci.* 1 (2013) 1–10.
- [19] Compost Chemistry - Cornell Composting, (n.d.). <http://compost.css.cornell.edu/chemistry.html> (accessed April 12, 2017).
- [20] U.S. EPA, METHOD 1683 Total, Fixed and Volatile, Solids and Biosolids, *Sci. Technol. EPA-821-R-* (2001) 13.

Experimental investigation of effects of hydrogen addition to gasoline engine

¹Salih Açıkgöz, ¹Mehmet İlhan İlhak, ¹Selahaddin Orhan Akansu

¹Energy Division, Department of Mechanical Engineering, Faculty of Engineering, Erciyes University, 38039 Kayseri, Turkey

Abstract: In this study, an experimental study on the performance and exhaust emissions of a spark-ignition engine fuelled with gasoline–hydrogen mixtures (100% Gasoline, 0.6% H₂ + 94% Gasoline, 1.24% H₂ + 98.76% Gasoline, 2.13% H₂ + 97.87% Gasoline and 3.37% H₂ + 96.63% Gasoline by mass) were performed at 1500 rpm and 50 N.m. The fuel-air mixtures were kept at the stoichiometric.

The results showed that the addition of hydrogen in the gasoline improved the combustion process and improved the combustion efficiency, expanded the range of combustibility of the gasoline, reduced the specific fuel combustion, and reduced emissions. But, nitrogen oxide emissions increased with the adding of hydrogen.

1. Introduction

Energy independence and security, and the adverse impact of fossil fuels on our planet's ecosystem are burning topics of the day. In general, it is understood that in order to maintain the present standard of living and to establish an environmentally sustainable energy future, these challenges have to be solved in conjunction with the development and implementation of carbon-neutral energy systems (i.e., systems that do not increase atmospheric CO₂ concentration) [1]. Hydrogen is thought to be one of the best fuel candidate for spark-ignition engines [2] and [3]. There are many studies about hydrogen enrichment to fuel. The addition of hydrogen can be seen as a simple and feasible way for the gasoline engine to gain the improved operating stability at idle and lean conditions [4]. When excess air ratio was approaching stoichiometric conditions, CO emission tended to increase with the addition of hydrogen. However, when the engine was gradually leaned out, CO emission from the hydrogen-enriched engine was lower than the original one. NO_x emissions increased with the increase of hydrogen addition due to the raised cylinder temperature [5]. Amrouche et al., investigated on hydrogen-enriched gasoline in a Wankel rotary engine. They used 0%, 2%, 4%, 5%, 7%, and 10% hydrogen energy fractions at the intake manifold. They stated that adding hydrogen to gasoline in the engine improved the thermal efficiency and the power output, hydrocarbon and carbon monoxide emissions were reduced while nitrogen oxide emissions increased with the increase of hydrogen fraction [6]. The use of hydrogen as enrichment technique is shown to improve the engine emissions and performance for many fuels [4-16].

The experimental results showed that hydrogen enrichment reduced the value of spark advance for best torque and decreased power due to a reduction in volumetric lower heating value. Kahraman et al. [15] studied on combustion characteristics and emissions in a spark-ignition engine fuelled with Natural Gas-Hydrogen blends.

In this study, performance and emissions characteristics have been studied fuelled by gasoline-hydrogen at different 1500 rpm, 50 N.m constant load and the stoichiometric condition.

2. Experimental Apparatus and Test Procedure

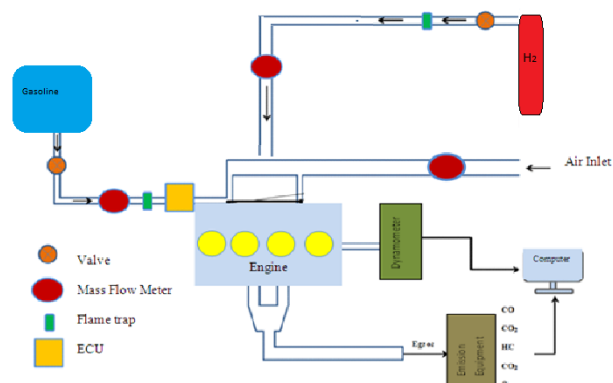
This present work was carried out on a Ford engine. This is a four-stroke cycle four-cylinder spark ignition engine with a bore \times stroke of 80.6 x 88 mm. and a compression ratio of 10:1. The engine details are given in Table 1. The view of experimental system has been given in Fig.1.

Table 1. Engine specifications

Ignition line	1-3-4-2
Bore	80.6 mm
Stroke	88 mm
Engine volume	1796 cc
Compression ratio	10:1
Maximum engine cycle	5500 rpm
Power (DIN)	75 kW, 102 PS
Tork (DIN)	150 Nm, (4000 rpm)



(a)



(b)

Figure.1 Experimental rig (a) A view in test room (b) Schematically test system.

All work was conducted in the Engine Laboratory in the department of Mechanical Engineering at the University of Erciyes. Gasoline fuel was used in the SI engine. Firstly, the all experiments were performed at stoichiometric conditions, 1500 rpm and 50 N.m. Hydrogen was added 0.6% H_2 , 1.24% H_2 , 2.13% H_2 and 3.37% H_2 by mass rate. The ignition timing of the engine has been adjusted as constant for all tests (as 13° BTDC). The measurements were fixed half throttle as 50 Nm. Bosh BEA-60 gas analyzer was used to measure CO, NO, CO_2 , HC.

3. Results And Discussion

The exhaust emissions from the test engine operating with the test fuels at a variety of conditions that span the practical operating range of normal automotive engines were measured.

3.1 Results And Discussion

Figure 2 shows the cylinder pressure versus crank angle for different hydrogen mass fraction in intake manifold. With the increase of hydrogen mass fraction, the maximum cylinder pressure rises, and the position of maximum cylinder pressure gradually approach the top dead center (360 CA). While the maximum cylinder pressure is 18.5 bar at pure gasoline, maximum pressure of 3.37% H_2 addition fuel by mass is obtained as 35.08 bar. However, the maximum decreasing of trend in maximum pressure is at 3.37% H_2 + 96.63% gasoline fuel mixture.

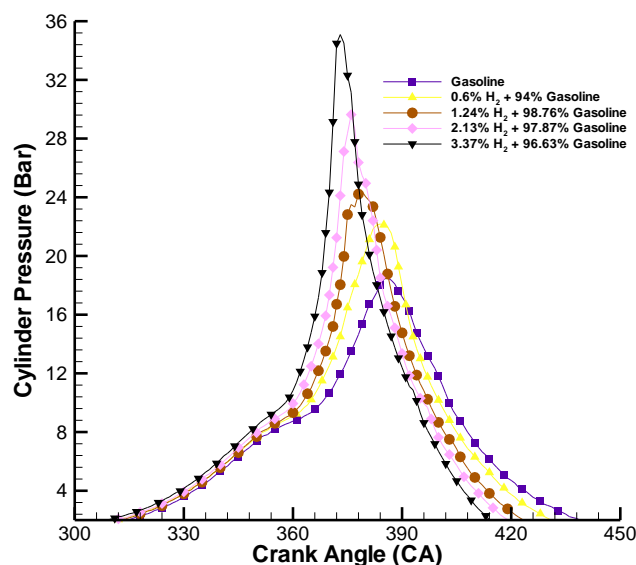


Figure.2 Cylinder Pressure versus the crank angle for various mass fraction of H_2 .

Brake thermal efficiency values have been given in Figure 3. As seen this figure, with increasing hydrogen mass fraction, brake thermal efficiency values increase. Hydrogen has been accelerated the combustion. When hydrogen mass fraction ratios increase than 3.5 % H_2 , back fire and knock was found out.

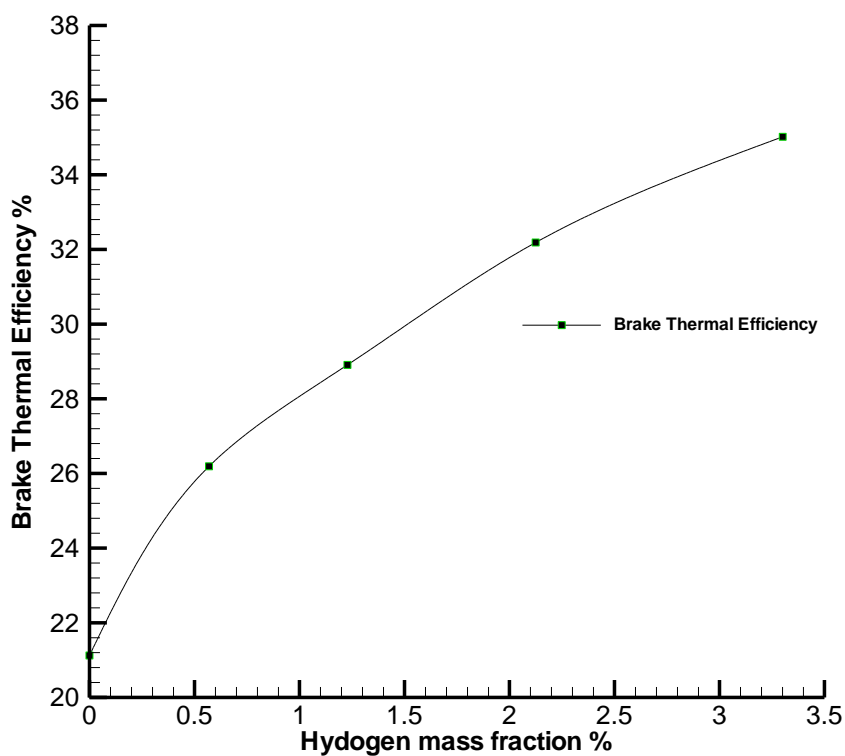


Figure.3 Brake thermal efficiency versus hydrogen mass fraction in intake manifold

3.2 Emissions

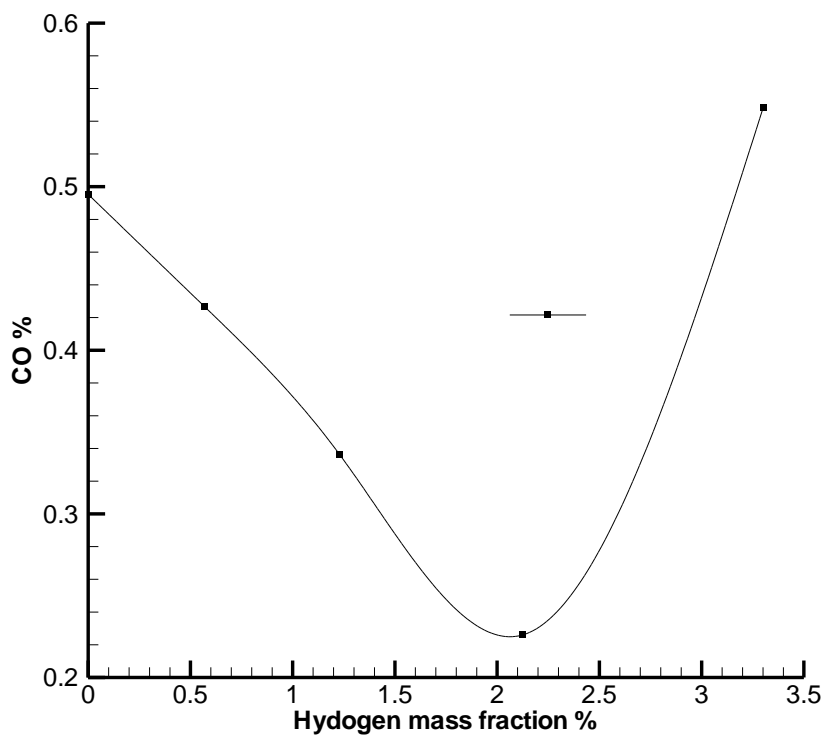


Figure.4 %CO values versus excess O₂

The CO% emissions versus hydrogen mass fraction are given in figure 4. The CO values have been obtained as 0.495, 0.426, 0.336, 0.226 and 0.548 CO % for 0 %, 0.6%, 1.24%, 2.13%, 3.37% H₂ percentage, respectively.

Figure 5 depicts the unburned hydrocarbon values (ppm) versus the hydrogen mass fraction.

UHC values reach its lowest point value at 3.37 % H₂ mass percentage. UHC values are decreased. Reduced HC emission by hydrogen enrichment was also observed in our study which could be explained by the fact that hydrogen could speed up flame propagation and reduces quenching distance, thus depressing the possibilities of incomplete combustion [15,16]

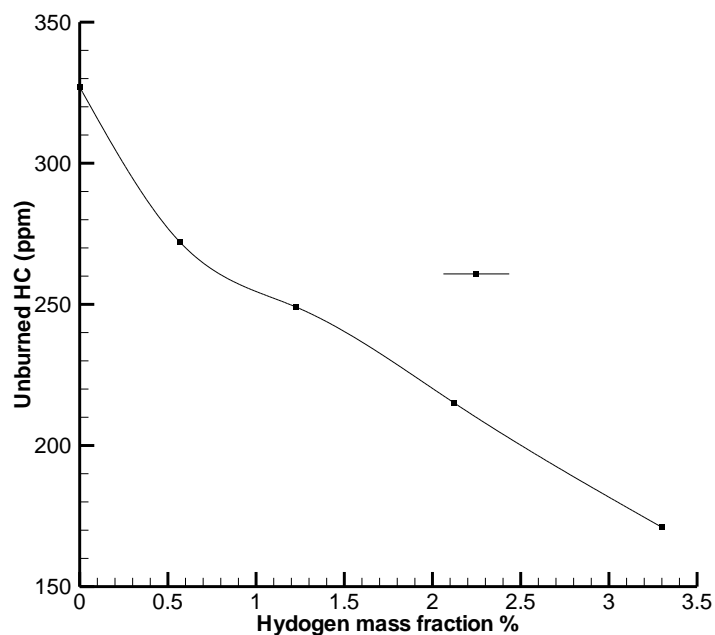
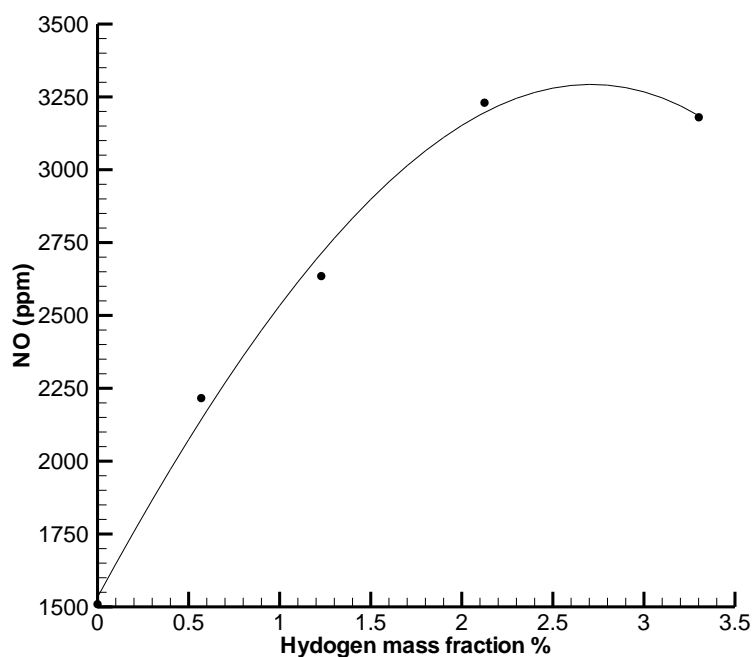


Figure.5 Unburned HC versus hydrogen mass fraction



The nitrogen oxide values (ppm) versus hydrogen mass fraction are illustrated in figure 6.

As NO values increase up to 2.13 hydrogen mass fraction, after than NO values are almost constant. NO concentration increases with the increase of hydrogen fraction, and this is due to the increase of peak combustion temperature by hydrogen addition

4. Conclusions

An experimental study aiming at investigating the effect of hydrogen addition on improving gasoline engine performance under constant speed and constant load was introduced in this article. The main conclusions are listed below:

1. The addition of hydrogen helps in improving cylinder pressure. The maximum cylinder pressure values were obtained at 3.37 %H₂+ 96.63% Gasoline.
2. The addition of hydrogen is effective on improving engine brake thermal efficiency.
3. HC emission values reduces with the increase in percentage of hydrogen mainly due to increase in the cylinder.
4. CO emissions decrease up to 2.13 % H₂ percentage. If hydrogen mass fraction are increased, combustion conditions are closing knocked limits.

Consequently, from the environmental, economic and technical perspectives, blending fuel (gasoline, methane, etc.) with relatively small amounts of hydrogen can significantly improve the emission characteristics of internal combustion engines. In future studies, experiments can be made with different loads, different ignition timings and rpm.

Acknowledgement : The authors are grateful for the financial support of the Unit of the Scientific Research Projects of Erciyes University (project no: FYL-2014-4933).

References

- [1] Muradov N.Z., Veziroglu T.N., Green path from fossil-based to hydrogen economy: an overview of carbon-neutral technologies, *Int J Hydrogen Energy*, 33 (23) 2008, pp. 6804–6839
- [2] Maghbouli A., Yang W., Hui A., Shafee S., Li J., Mohammadi S., “Modeling knocking combustion in hydrogen assisted compression ignition diesel engines”, *Energy*, 76 (2014), pp. 768–779
- [3] Wu H., Wu Z. “Combustion characteristics and optimal factors determination with Taguchi method for diesel engines port-injecting hydrogen”, *Energy*, 47 (2012), pp. 411–420
- [4] Wang S., Ji C., “Cyclic variation in a hydrogen-enriched spark-ignition gasoline engine under various operating conditions”, *Int J Hydrogen Energy*, 37 (1),(2012), pp.1112-1119.

- [5] Ji C., Wang S., Effect of hydrogen addition on combustion and emissions performance of a spark ignition gasoline engine at lean conditions, *Int J Hydrogen Energy*, 34 (18), (2009), pp.7823-7834
- [6] Amrouche F., Ercison P., Park J., Varnhagen S.,” An experimental investigation of hydrogen-enriched gasoline in a Wankel rotary engine”, *Int J Hydrogen Energy*, 39 (16),2014, pp.8825-8535.
- [7] Shrestha S.O.B., NarayananG. , Landfill gas with hydrogen addition – a fuel for SI engines,*Fuel*, 87 (2008), pp. 3616–3626
- [8] Mariani A., Prati M.V., Unich A., Morrone B., “Combustion analysis of a spark ignition i c. engine fuelled alternatively with natural gas and hydrogen-natural gas blends” *Int J Hydrogen Energy*, 38 (2013), pp. 1616–1623
- [9] Moreno F., Munoz M., Arroyo J., Magen O., Monne C., Suelves I.,”Efficiency and emissions in a vehicle spark ignition engine fueled with hydrogen and methane blends” *Int J Hydrogen Energy*, 37 (2012), pp. 11495–11503
- [10] D'Andrea T., Henshaw P.F., Ting D.S.-K., “The addition of hydrogen to a gasoline-fuelled SI engine” *Int J Hydrogen Energy*, 29 (2004), pp. 1541–1552
- [11] Wang S.,Ji C., Zhang M., Zhang B.,”Reducing the idle speed of a spark-ignited gasoline engine with hydrogen addition” *Int J Hydrogen Energy*, 35 (2010), pp. 10580–10588
- [12] Ji C., Wang S., “Experimental study on combustion and emissions performance of a hybrid hydrogen–gasoline engine at lean burn limits”, *Int J Hydrogen Energy*, 35 (2010), pp. 1453–1462
- [13] Wang S., Ji C., Zhang B., “Effect of hydrogen addition on combustion and emissions performance of a spark-ignited ethanol engine at idle and stoichiometric conditions” *Int J Hydrogen Energy*, 35 (2010), pp. 9205–9213
- [14] Akansu SO, Bayrak M., “Experimental study on a spark ignition engine fueled by CH₄/H₂ (70/30) and LPG”, *Int J Hydrogen Energy*, 36 (15) (2011), pp. 9260-9266.
- [15] Kahraman N, Ceper B.A., Akansu S.O., Aydin K., “Investigation of combustion characteristics and emissions in a spark-ignition engine fuelled with natural gas–hydrogen blends”,*Int J Hydrogen Energy*, 34 (2) (2009), pp. 1026–1034
- [16] Wang J., Huang Z., Fang Y., Liu B., Zeng K., Miao H., et al.” Combustion behaviors of a direct-injection engine operating on various fractions of natural gas hydrogen blends”, *Int J Hydrogen Energy*, 32 (15) (2007), pp. 3555–3564
- [17] Lindner B., Sjostrom K.,” Operation of an internal combustion engine: lean conditions with hydrogen produced in an on-board methanol reforming unit” *Fuel* (1984), pp. 1485–1490

The effect on performance and emission parameters of diesel- biodiesel-butanol blend

S. Sarikoc^{1*}, İlker Örs^{2*}, A.E. Atabani¹, S. Unalan¹

¹*Department of Mechanical Engineering, Faculty of Engineering, Erciyes University, 38039 Kayseri, Turkey*
sarikocselcuk@gmail.com

²*Department of Motor Vehicles and Transportation Technology, Vocational School of Technical Sciences, Aksaray University, Aksaray, Turkey.*
ilkerors@hotmail.com

Abstract: In this study, effects on fuel properties, performance and emission parameters of blend fuel obtained by mixing of biodiesel from waste cooking oil and industrial butanol with diesel fuel were investigated. The blend fuel was prepared by 20% waste cooking oil biodiesel + 5% butanol + 75% diesel fuel. According to test results; minimum values of specific fuel consumption were obtained with diesel fuel. The specific fuel consumption values of blend increased average 6.25% due to heating value both biodiesel and butanol is lower than diesel fuel. According to results of exhaust emission parameters; CO, HC and smoke opacity emissions were decreased respectively 29.53%, 22.77% and 18.61% by using of butanol compared to diesel fuel. When NO emissions investigated; although 20% biodiesel added into diesel fuel increased NO emissions, it showed that NO emissions were decreased average 4.23% by adding 5% butanol into binary blend compared to diesel-biodiesel blend. Besides, butanol decreased important fuel properties such as density, viscosity and heating values.

Keywords: Waste cooking oil, biodiesel, diesel engine, butanol, exhaust emissions.

1. Introduction

Increasing carbon chain length in alcohols usually increases the ignition quality of alcohol. For this reason, the use of higher alcohols (> C4) as biofuel compared to lower alcohols (C1-C4) draws more interest [1]. Among the alcohols, butanol stands out as a promising fuel for alternative fuels [2]. The most important advantage of the butanol compared to other alcohols is that it has a higher cetane number. Butanol causes less corrosion compared to ethanol and methanol. Butanol burns easier when mixed with diesel fuel [3]. Butanol is a good solution in decreasing the density and viscosity of diesel-biodiesel fuel mixtures [4].

Kumar et al. found in their studies where they investigated the use of higher alcohols as biofuels in diesel engines that n-butanol is 4-carbon and straight-chain fuel, which can be produced from biomass and fossil-based fuels, butanol having approximately 25 cetane provides better ignition compared to lower alcohols, and it has 25% higher calorific value compared to ethanol. They also stated that the stoichiometric air/fuel ratio of butanol is closer to that of diesel fuel. Besides, they also showed that the butane can be stored for longer periods in normal tanks due to its less corrosion effect. As one of the most important features, they revealed that butanol can be mixed more homogeneously with diesel fuel than ethanol and methanol, and form a more stable mixture [5].

Han et al., in their work, examined the combustion parameters using butanol instead of diesel fuel as a next-generation biofuel for diesel engines. As a result, they also showed that the butanol extends the ignition delay, shortens the combustion duration, significantly reduces NO_x and smoke emissions, increases CO and HC emissions, and reduces combustion efficiency for diesel engines [6].

Atmanlı blended the biodiesel that he had produced from the waste oil with equal amount of diesel fuel, and added 20% butanol into this mixture to get a new fuel, then he made performance and emission analyses using this fuel in a diesel engine. In general, it has been shown that butanol addition reduces the specific fuel consumption to a certain amount and increases the thermal efficiency value. It has been also revealed that butanol increases exhaust gas temperature, lowers HC and NO_x emissions, and increases CO emissions [7].

Ileri et al., examined the performance and emission parameters of a fuel mixture that consists of 70% diesel fuel, 20% rapeseed oil biodiesel and 10% butanol, compared to those of diesel and biodiesel fuels. As a result, they indicated that the addition of biodiesel into a diesel fuel reduces the torque and power values by a small amount, even increases at certain engine speeds, increases specific fuel consumption values, decreases CO, CO₂ and HC emissions, increases NO_x emissions, reduces CO emissions at low engine speeds, and increases CO emissions at high engine speeds. They showed that with butanol addition, the performance values are adversely affected, NO_x and CO emissions are increased, and CO₂ and HC emissions are decreased [8].

Ibrahim added 10% and 20% butanol to the mixture fuels obtained by mixing equal amount of diesel fuel, and biodiesel that it had been produced from waste cooking oil. He indicated that with butanol addition, the specific fuel consumption increases slightly, whereas the thermal efficiency decreases. He noted that NO emission that increases with biodiesel use, decreases with butanol. He revealed that butanol reduces the maximum cylinder pressure, extends the combustion duration, and also reduces the maximum heat release rate [9].

Prabu et al., in their work, used the mixture they had obtained by adding 20% butanol to the diesel-biodiesel mixture containing 30% by volume of biodiesel obtained from waste cooking oil, as fuel in a direct injection diesel engine. They found that butanol adversely influences the engine performance, increases the maximum heat release rate, and reduces the maximum cylinder pressure. While emissions of CO, NO_x, and smoke opacity are significantly reduced by butanol, HC emissions are highly varied dependent on engine load and operating conditions [10].

In this study, the effects of butanol addition into the mixture composed of biodiesel produced from waste cooking oil and diesel fuel, on the fuel properties of mixture fuels, engine performance and exhaust emission parameters were investigated.

2. Materials And Methods

The biodiesel blended to the diesel engine was produced by transesterification method from collected waste cooking oil. Whereas butanol is the industrially produced n-butanol type alcohol. Biodiesel production, mixing of fuels and determination of test fuels characteristics were carried

out at Erciyes University Department of Mechanical Engineering Alternative Fuels Laboratory. Some physico-chemical properties of test fuels are presented in Table 1. In the experiments, a single-cylinder, four-stroke and direct-injection diesel engine, the characteristics of which are given in Table 2, were used.

Table 1. The some fuel properties of test fuels

Property	D100	D80B20	D75B20 But5
Kinematic viscosity at 40 °C (mm ² /s)	2.3255	2.9712	2.7638
Cloud point (°C)	-7	-7	-7
Pour point (°C)	-26	-10	-12
Cold Filter Plugging Point (°C)	-25	-15	-14
Flash Point (°C)	65	67	41
Density at 20 °C (g/cm ³)	0.8295	0.8477	0.8447
Cetane number	50-55	ND	ND

Table 2. Technical features of test engine.

Model	3 LD 510
Cylinder volume, cm ³	510
Bore - Stroke, mm - mm	85 - 90
Compression ratio	17.5:1
Max. engine speed, rpm	3300
Max. engine torque, Nm	35
Max. engine power, kW	9
Cooling type	Water cooler
Injector mark – injection pressure, bar	STANADYNE 41445190 – 190

In the experiments, a hydraulic dynamometer capable of measuring up to 450 Nm was used to brake the engine. The braking torque resulting from engine loading was measured by a load-cell with a sensitivity of 1 gr. Fuel consumption measurement was carried out with another load-cell with a sensitivity of 0.01 gr. During the tests, in order to measure exhaust emission values, a Bosch BEA-350 model gas analyzer that can measure CO with a sensitivity of 0.001%, HC with a sensitivity of 1 ppm, NO with a sensitivity of 1 ppm, and smoke opacity with a sensitivity of 0.1%, was used.

The test data were measured simultaneously (performance and emission) when the gas throttle was opened, as the engine was at full load, at each 200 rpm engine speed.

3. Results And Discussion

Figure 1 shows the changes in specific fuel consumption (SFC) values of test fuels depending on the engine speed. The SFC values of the biodiesel mixed fuel increased by an average of 3.56 % over diesel fuel. On the other hand, the SFC values of butanol blended fuel increased by an average of 2.59 % and 6.25 % over biodiesel blended fuel and diesel fuel, respectively. This increase can be explained by the fact that the heating values of both biodiesel and n-butanol are lower than that of diesel fuel.

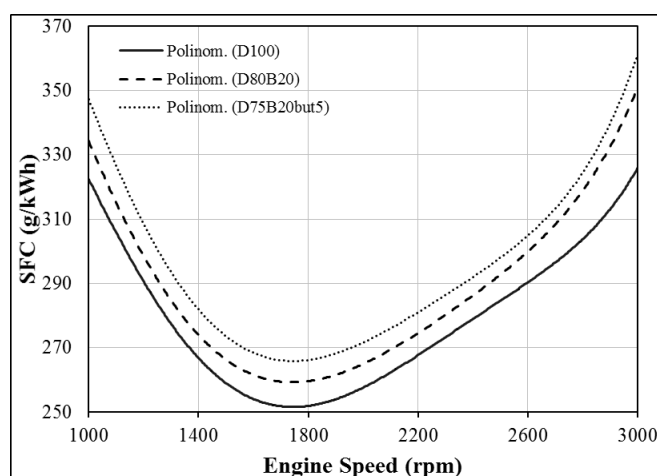


Figure 1. The SFC values according to engine speed.

Exhaust gas temperature is one of the most important parameters in the formation and interpretation of exhaust emissions. As can be seen in Figure 2, the oxygen in the biodiesel content improves the combustion to a certain extent and thus 20% biodiesel addition into diesel fuel increased by an average of 1.31%. Addition of butanol into biodiesel blended fuel increased the amount of oxygen in the mixture and caused the combustion rate to be increased, thus decreased the exhaust gas temperature values by an average of 1.47% and 0.18% over biodiesel blended fuel and diesel fuel, respectively.

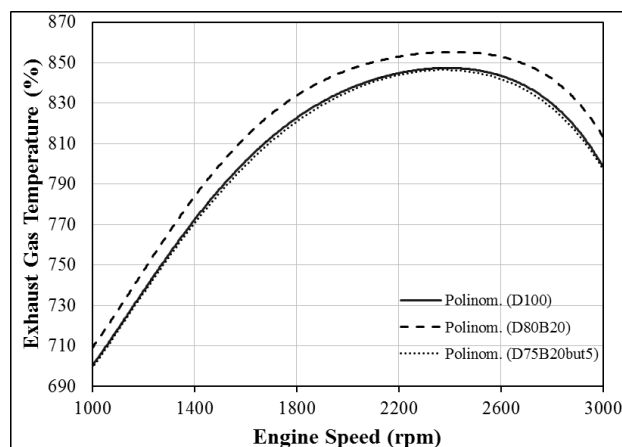


Figure 2. The exhaust gas temperature values according to engine speed.

Because of the oxygen in the mixture fuels, the carbon atoms that are released as a result of combustion were converted to CO₂ gas by finding sufficient oxygen, and thus the formation of CO emissions were reduced. The CO emission value of biodiesel blended fuel is 22.47% lower than diesel fuel and 29.53% lower than that of butanol blended fuel. Figure 3 shows changes in CO emission of test fuels. Figures 4 and 5 show changes in HC emissions and smoke opacity values depending on engine speed. While HC and smoke emission values for the same reasons were lower by an average of 17.95% and 11.24% for biodiesel blended fuels, respectively, those decreases for butanol blended fuels were on average 22.77% and 18.61%, respectively.

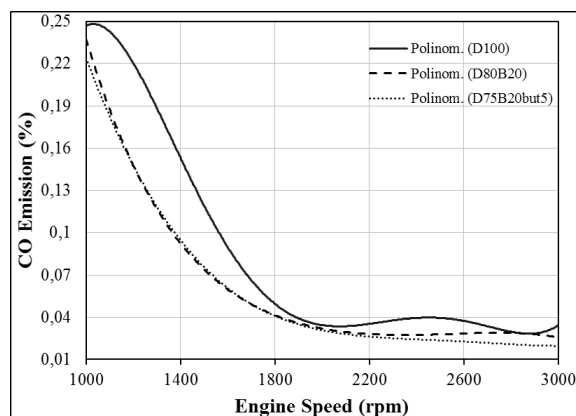


Figure 3. The CO emission values according to engine speed.

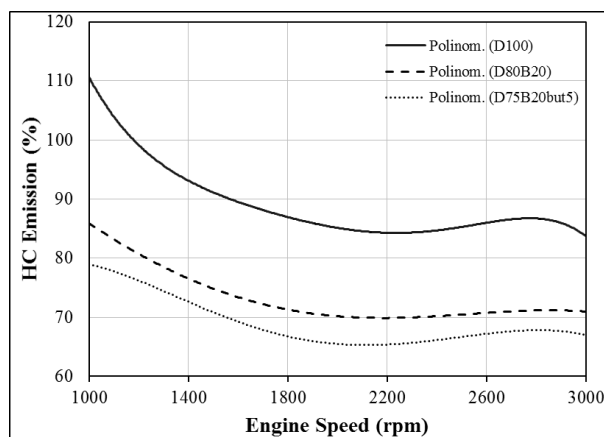


Figure 4. The HC emission values according to engine speed.

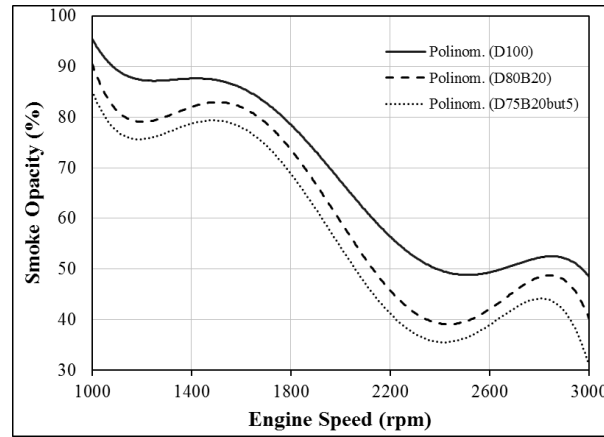


Figure 5. The smoke opacity values according to engine speed.

Figure 6 demonstrates that the addition of 20% biodiesel to diesel fuel increases NO emissions by 7.68% on average, whereas with the addition of butanol to the mixture, NO emissions are decreased by an average of 4.23% compared to biodiesel blended fuel. Increasing the exhaust gas temperature of biodiesel has caused NO emissions to increase. Because the nitrogen and oxygen atoms react at high temperatures. Decreasing the exhaust gas temperature by butanol additions reduced NO emissions.

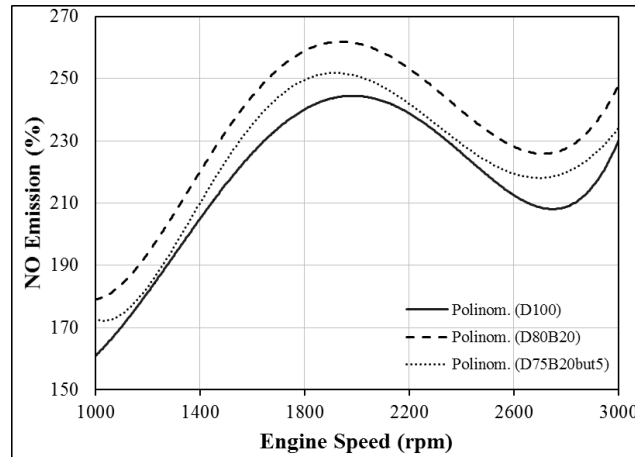


Figure 6. The NO emission values according to engine speed.

4. Conclusion

The results of this experimental work can be summarized as follows;

- A diesel engine with a classic pump-injector fuel system can run smoothly with fuel produced by the addition of biodiesel and butanol into diesel fuel.
- Since biodiesel and butanol reduced the heat energy resulting from the combustion of the fuel in the cylinder, they both adversely affected the performance parameters.
- Thanks to the oxygen contents of biodiesel and butanol, emissions of CO, HC and smoke are better than that of diesel fuel.

- Even if the high exhaust gas temperature values of the biodiesel blended fuel increase the NO emissions, the butanol with lower exhaust gas temperature values decreased NO emissions.

Acknowledgement: The authors gratefully would like to acknowledge Erciyes University and Bayburt University, for the Scientific Research Projects Unit of Erciyes University, Turkey, for the financial support under the grant number FOA-2015-5817 and FOA-2015-5790.

References

- [1] Zhu, L., Xiao, Y., Cheung, C.S., Guan, C., Huang, Z., 2016. "Combustion, gaseous and particulate emission of a diesel engine fueled with n-pentanol (C5 alcohol) blended with waste cooking oil biodiesel", *Applied Thermal Engineering*, 102: 73-79.
- [2] Li, Y., Meng, L., Nithyanandan, K., Lee, T.H., Lin, Y., Lee, C.-f.F., Liao, S., 2016. "Combustion, performance and emissions characteristics of a spark-ignition engine fueled with isopropanol- n -butanol-ethanol and gasoline blends", *Fuel*, 184: 864-872.
- [3] Fayyazbakhsh, A., Pirouzfard, V., 2017. "Comprehensive overview on diesel additives to reduce emissions, enhance fuel properties and improve engine performance", *Renewable and Sustainable Energy Reviews*, 74: 891-901.
- [4] Işık, M.Z., Bayındır, H., İscan, B., Aydın, H., 2017. "The effect of n-butanol additive on low load combustion, performance and emissions of biodiesel-diesel blend in a heavy duty diesel power generator", *Journal of the Energy Institute*, 90 (2): 174-184.
- [5] Rajesh Kumar, B., Saravanan, S., 2016. "Use of higher alcohol biofuels in diesel engines: A review", *Renewable and Sustainable Energy Reviews*, 60: 84-115.
- [6] Han, X., Yang, Z., Wang, M., Tjong, J., Zheng, M., 2016. "Clean combustion of n-butanol as a next generation biofuel for diesel engines", *Applied Energy*.
- [7] Atmanli, A., 2016. "Comparative analyses of diesel-waste oil biodiesel and propanol, n-butanol or 1-pentanol blends in a diesel engine", *Fuel*, 176: 209-215.
- [8] İleri, E., Atmanli, A., Yilmaz, N., 2016. "Comparative analyses of n-butanol–rapeseed oil–diesel blend with biodiesel, diesel and biodiesel–diesel fuels in a turbocharged direct injection diesel engine", *Journal of the Energy Institute*, 89 (4): 586-593.
- [9] Ibrahim, A., 2016. "Performance and combustion characteristics of a diesel engine fuelled by butanol–biodiesel–diesel blends", *Applied Thermal Engineering*, 103: 651-659.
- [10] Senthur Prabu, S., Asokan, M.A., Roy, R., Francis, S., Sreelekh, M.K., 2017. "Performance, combustion and emission characteristics of diesel engine fuelled with waste cooking oil bio-diesel/diesel blends with additives", *Energy*, 122: 638-648.

An Experimental Study on Performance and Emissions of an SI Engine Fueled by Acetylene-Hydrogen and Acetylene-Methane Blends

¹Selim Tangöz, ²Mehmet İlhan İlhak, ²Selahaddin Orhan Akansu

¹ *Erciyes University, Fac. of Aeronautics and Astronautics, Airframe - Powerplant Dept., Kayseri, 38039, Turkey*

² *Erciyes University, Engineering Faculty, Dept. of Mechanical Engineering, Kayseri, 38039, Turkey*

stangoz@erciyes.edu.tr

Abstract: The aim of this paper is analyzing of performance parameters and emission values of an SI engine fueled by acetylene-hydrogen and acetylene-methane blends. The experiments were carried out at a fixed bmep (brake mean effective pressure) of 2.095 bar, a load of 30 Nm and an engine speed of 1500 rpm under lean mixture conditions ($\lambda=1.3-2.8$). Moreover, the air flow ratio was held steady as 83 kg/h and 90 kg/h, while the flow rates of the blends were changed as volumetrically. The parameters of brake thermal efficiency, cylinder pressure, heat release rate and emissions were analyzed for each fuel blends.

The experimental results showed that the values of brake thermal efficiency are declined between 6.2% and 3.3% with the addition of hydrogen and are decreased about 10% by the addition of methane in the blend. The curves of cylinder pressure and heat release rate are advanced to top dead center by the adding of hydrogen to acetylene. But the curves are retarded with methane addition. The adding of hydrogen in acetylene leads to a decrease in CO and HC emissions and an increase in NOX values for fixed lambda. But the increasing of methane fraction causes a rise in CO and HC emissions and a drop in NOX values for fixed lambda.

Keywords: SI engine, Acetylene, Hydrogen, Methane, Alternative Fuel

1. Introduction

Because of the rising oil prices and increased air pollution, many researchers or many producers of engine have been focused the using of gas fuels in engine as an alternative fuel for improving of engine performance and emissions values. One of the most important of these fuels is methane gas or natural gas because it is cheap, partially clean and easily accessible. For these reason, methane have been used as alternative fuel in commercial engine application for a long time.

Another alternative gas fuel is hydrogen. Hydrogen is clean and has a wider limits of flammability [1,2]. Moreover, hydrogen has high flame speed and it has high self-ignition temperature [3]. In addition, hydrogen allows the combustion of ultra-lean mixtures [4]. Because of these properties, many studies have been carried out on the use of hydrogen in internal combustion engines [5,6,7]. Furthermore, since hydrogen has properties promoting of engine performance and emissions value, it can be used as a mixture with other fuels.

Especially hydrogen-natural gas mixtures have been investigated in terms of engine performance and emissions. In one of the studies, Xu et al. [8] have been tested the effect of hydrogen adding on the engine performance and emission values of an SI engine fueled by compressed natural gas. They instrumented that a relatively higher thermal efficiency can be achieved under certain engine conditions when hydrogen was added more than 20% by volume to CNG. In a similar study, Kahraman et al. [9] have been displayed that the highest brake thermal efficiency was measured fueled by hydrogen-natural gas blend compounding 30% hydrogen. In addition, some experiments carried out by Taggart-Cowan et al. [10], Mohammed et al. [11] and Akansu et al. [12] have been showed that the adding of hydrogen to CNG increased thermal efficiency and reduced emissions values.

Acetylene is highly combustible with high flame speed and fast energy release. Moreover, it has a very wide flammability range and minimum ignition energy required for ignition [13, 14]. So, acetylene can be used as alternative fuel in internal combustion engines. But acetylene is a fuel having a high knocking tendency and this tendency should be removed with a mixture of other gases [13]. For this reason, literature has little studies on acetylene as fuel. Most of the studies were carried out especially in diesel engine. In one of the studies, Lakshmanan and Nagarajan [14] have been analyzed the effect acetylene on values of engine performance and emissions in diesel engine. They stated that NO_x, HC and CO emission values decreased when compared to diesel mode. In addition, smoke emissions showed as marginal rise and thermal efficiency was nearer to diesel mode. In the other study carried out by Lakshmanan and Nagarajan [15] have been investigated the effect of injection timing of acetylene in the diesel engine. The tests indicated that optimum injection timing was 10 after top dead center with injection duration of 90 crank angles. The brake thermal efficiency increased for all the gas flow. NO_x decreased by 9% at 110 g/h of fuel flow rate, 6% at 180 g/h of fuel flow rate and 4% at 240 g/h of fuel flow rate when compared with diesel fuel mode at full load. When compared with baseline diesel mode, smoke levels raised and HC, CO and CO₂ emissions declined for the all the gas flow rates at full load. In the other studies, Swami Nathan et al. [16] have been investigated performance and emission parameters of homogeneous charge compression ignition engine at different power outputs fueled by sole acetylene. The experiments showed that NO_x and smoke levels decreased with using acetylene. However, HC levels were high at between 1700–2700 ppm. Moreover, thermal efficiencies were better than according to the compression ignition mode of operation. Some similar studies [17,18,19] have been carried out in diesel engine.

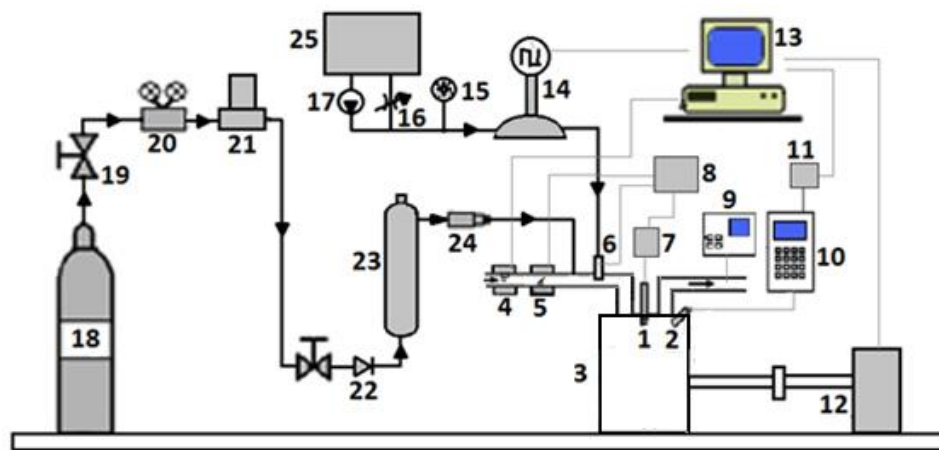
In one of the rare studies in SI engine, Brusca et al. [20] have been investigated engine performance and emission parameters of an SI engine fueled by acetylene and alcohol blends. The studies were carried out 8 kW spark ignition engine having one cylinder with carburetor. The engine was modified with electronic injection control system and two different injectors for the acetylene and the alcohol. Moreover, an optimization method base on Genetic Algorithms and Neural Networks was used to obtain engine parameters map. The results displayed that the new engine configuration based on acetylene-alcohol represents a good alternative to gasoline and diesel engines in terms of pollutant emissions and engine performance parameters. In the other study, Sampath Kumar et al. [21] have been analyzed the emission and performance characteristics of conventional SI engine with minor modifications fueled by hydrogen-acetylene fuel. The experimental results with hydrogen-acetylene mixture indicated that brake thermal efficiency raised

and emissions values descended when compare to gasoline. In the other study carried out using acetylene in SI engine, Jadhav and Mitkari [22] have been compared to the performances of gasoline and acetylene fuels. The experiments tested at 800 rpm and different load and different fuel flow in a four stroke single cylinder engine. The experimental results showed that the brake specific fuel consumption for gasoline was greater than acetylene and the brake thermal efficiency of acetylene was more than gasoline.

It can be seen in literature, the studies carried out on the using acetylene as fuel in SI engine is very little for understanding of acetylene characteristic in SI engine. Moreover, literature does not any study using of the blends formed to acetylene-methane and acetylene-hydrogen. For this reason, the present study will be first study in literature about the using of acetylene-methane and acetylene-hydrogen as alternative fuel in SI engine.

2. Experimental Setup And Test Procedure

The experimental studies were tested in the Engine Laboratory in the department of Mechanical Engineering at the University of Erciyes. The experiments were conducted in a Ford MVH418 1.8L SI engine. The features of the experimental engine are given in Table 1. Moreover, the experimental setup is indicated in Figure 1. Engine torque and engine speed values were measured using a eddy current dynamometer. Acetylene, hydrogen and methane gases were stored in pressured gas tanks. The pressure values of gases were regulated by pressure regulators. Alicat M 1000 SLPM and Alicat M 100 SLPM gas flow meters were used for the measurement of the gas flow. The gases were injected into the intake manifold by gas injectors and one pilot duct. Engine intake air was measured by Bosch air flow meter.



1-Spark plug 2-Pressure transducer 3-Engine 4-Air flowmeter 5-Throttle valve and position sensor 6-Fuel injector 7-Ignition module 8-Engine control unit 9-Exhaust gas analyzer 10-Charge amplifier 11-Data logger 12-Dynamometer 13-Computer 14-Liquid flowmeter 15-Pressure gauge 16-Throttle valve 17-Fuel pump 18-Gas tank 19-Valve 20-Gas regulator 21-Mass flowmeter 22-Check valve 23-Flame trap 24-Flame arrestor 25-Fuel tank

Figure 1. Experimental setup

Table 1. Features of the experimental engine.

Engine	Ford MVH418
Cylinders	4 in line
Engine stroke volume (L)	1.796 L
Bore / stroke (mm)	80.6 / 88
Compression ratio	10
Max. power (kW)	77
Max. torque (Nm)	153 (4000
Idle / max. speed	750 / 5950

Table 2. Specifications and error range of the experimental equipment and sensors.

Instrument	Values	Accuracies
Cylinder pressure transducer (PCB	0 – 5000 PSI	±1 %
Gas flow meter (Alicat M100 SLPM)	9 – 100 SLPM	±0.4%
Gas flow meter (Alicat M1000 SLPM)	9 – 1000 SLPM	±0.4%
Hot film air mass meter(Bosch HFM 5)	10 – 480 kg/h	≤ 3 %
Eddy Current Dynamometer (SAJ SE	150 kW/8000	±1 rpm
Exhaust gas analyzer (Bosch BEA 060)		
CO	0 – 10 % Vol	0.001 %
CO ₂	0 – 18 % Vol	0.010 %
O ₂	0 – 22 % Vol	0.010 %
NO _x	0 – 5000 ppm	1.0 ppm
HC	0 – 9999 ppm	1.0 ppm
Lambda	0.5 – 9.999	0.001

Cylinder pressure values were measured by PCB 111A22 piezoelectric pressure transducer. The cylinder pressure values were digitized at each crank angle and indicated by averaging 80 continuous cycles. The emission values (CO, CO₂, HC and NO_x) were metered with a Bosch BEA 060 gas analyzer. Specifications and error range of the test equipment and sensors are given in Table 2.

In the experimental studies, the engine performance and the emission values were analyzed fueled by acetylene-hydrogen and acetylene-methane blends. The tests were carried out at 2.095 bar bmep value, 30 Nm engine load and 1500 rpm engine speed under lean mixture conditions. In the experiments, the air flow ratio was selected a steady value as 83 kg/h and 90 kg/h. The fuel flow ratios of blends were changed volumetrically. Firstly, the engine was fueled by acetylene. And then, the flow values of hydrogen and methane gases were increased in the blends, from 0% to 100% for methane and from 0% to 78.5% for hydrogen, respectively. The properties of the acetylene, hydrogen and methane are outlined in Table 3. In addition, the tests were performed at different excess air ratios of from $\lambda=1.3$ to $\lambda=2.8$. For this reason, the values of the air flow ratio,

the fractions of the gas, the flow rate of the gas, the flow rate of the blend, the lower heating value of the blend and the lambda for each test are given in Table 4 for methane-acetylene blends. Moreover the same values are given in Table 5 for hydrogen-acetylene blends. The summary of the experimental procedures are given in Table 6.

Table 3. The properties of the acetylene, hydrogen and methane

Properties	Acetylene	Hydrogen	Methane
Formula	C ₂ H ₂	H ₂	CH ₄
Density [kg/m ³]	1.092	0.08	0.65
Adiabatic flame temperature [K]	2500	2400	2200
Lower calorific value [MJ/kg]	48.23	120.0	50.02
Lower calorific value [MJ/m ³]	50.64	9.6	39.84
Flame speed [m/s]	1.5	3.5	0.27
Stoichiometric air fuel ratio	13.2	34.3	17.25
Auto-ignition temperature [K]	578	572	813
Flammability limits [vol. %]	2.5–81	4–74.5	5.0-15.0
Ignition energy [mJ]	0.019	0.02	0.3

Table 4. The values of air flow ratio, fractions of the gas, flow rates of the gas, lower heating value of the blend and lambda for methane-acetylene blends.

Gas	Air flow rate [kg/h]	Exp. no [case]	CH ₄ [Vol. %]	Flow rate of CH ₄ [m ³ /h]	Flow rate of blend [m ³ /h]	Flow rate of blend [kg/h]	LHV of blend [kJ/m ³]	λ
83		1	0	0	0.9984	1.3556	50640	1.96
		2	22.03	0.230	1.0417	1.4846	48260	1.84
		3*	31.00	0.323	1.0433	1.5125	47292	1.72
		4*	43.01	0.439	1.0204	1.5862	45995	1.70
		5	52.46	0.567	1.0801	1.7059	44974	1.58
		6	61.71	0.662	1.0736	1.7538	43976	1.54
		7	70.10	0.779	1.1106	1.8413	43069	1.48
		8*	78.91	0.922	1.1685	1.9432	42118	1.40
		9*	82.08	0.979	1.1927	1.9630	41775	1.39
		10	100	1.198	1.1982	2.1400	39841	1.30
C ₂ H ₂ +CH ₄		11	0	0	0.8419	1.3621	50640	2.24

90	12*	21.37	0.198	0.9281	1.4277	48332	1.99
	13*	46.91	0.641	1.3660	1.5771	45574	1.98
	14	57.40	0.877	1.5286	1.6715	44441	1.90
	15	56.76	0.744	1.3107	1.7584	44510	1.80
	16	64.10	0.874	1.3629	1.8334	43717	1.71
	17*	72.21	1.027	1.4226	1.9134	42841	1.64
	18*	78.79	1.189	1.5089	2.0276	42131	1.64
	19	84.06	1.319	1.5688	2.0926	41562	1.55
	20	100	1.564	1.5653	2.1880	39846	1.44

* used to compare at steady lambda values

Table 5. The values of air flow ratio, fractions of the gas, flow rates of the gas, lower heating value of the blend and lambda for hydrogen-acetylene blends.

Gas	Air flow rate [kg/h]	Exp. no [case]	H2 [Vol. %]	Flow rate of H2 [m3/h]	Flow rate of blend [m3/h]	Flow rate of blend [kg/h]	LHV of blend [kJ/m3]	λ
C ₂ H ₂ +H ₂	83	21*	0	0	0.9024	1.2252	50640	2.13
		22*	27.69	0.313	1.1302	1.1292	39275	2.14
		23	45.79	0.647	1.4126	1.1250	31850	2.18
		24*	61.27	0.988	1.6119	1.0752	25497	2.37
		25*	70.09	1.308	1.8655	1.0317	21873	2.40
		26	78.50	1.656	2.1098	0.9955	18424	2.65
	90	27	0	0	0.8217	1.3295	50640	2.15
		28*	27.02	0.297	1.1012	1.2077	39553	2.38
		29*	45.02	0.629	1.3976	1.1849	32164	2.42
		30	59.96	0.990	1.6503	1.1144	26033	2.60
		31	76.36	1.815	2.3772	1.0630	19301	2.77

* used to compare at steady lambda values

Table 6. The experimental procedures.

Item	Value
Engine speed	1500 rpm
Load	30 Nm
Hydrogen in acetylene (vol.)	From 0 to 78.5 %
Methane in acetylene (vol.)	From 0 to 100 %
Air flow ratio	83 and 90 kg/h
Excess air ratio	1.3-2.8

3. Results And Discussion

In this section, the result values of brake thermal efficiency (BTE), cylinder pressure, heat release rate and emissions (CO, HC and NO_x) are given and discussed.

3.1 Brake Thermal Efficiency

Figure 2 shows the results of the brake thermal efficiency versus different fractions of hydrogen (a) and methane (b) for air flow ratios of 83 kg/h and 90 kg/h. As can be seen from these figures, the maximum BTE (brake thermal efficiency) value as 29.25% is obtained using acetylene at air flow ratio of 83 kg/h. As can be seen from the figures, the BTE values are generally declined by rising of the fractions of the hydrogen and the methane in the acetylene. The adding of hydrogen and methane leads to a decrease in volumetrically heating value (as can be seen in Table 4 and Table 5). For instance, the BTE values are measured as 29.25%, 28.9%, 25.45% and 23.1% with hydrogen fraction of 0%, 27.7%, 61.3% and 78.5% in the blend for 83 kg/h air flow ratio, respectively. The values are measured as 26.4%, 23.4%, 19.9% and 17.9% at methane fraction of 0%, 31%, 61.7% and 78.9% in acetylene mixture for the same air flow ratio, respectively.

Moreover, it can be seen from these figures, the BTE values obtained by the using of hydrogen-acetylene blend are higher than the BTE values at methane-acetylene blend. When the air flow ratio is 90 kg/h, the BTE values are measured as 26.95% and 26.3% fueled by pure acetylene for hydrogen blends and methane blends, respectively. And, the values are obtained as 25.6% and 23.66% fueled by the blend having hydrogen fractions of 45.02% (case 29) and 76.4% (case 31) and the values are obtained as 22.41% and 17.2% fueled by the blend having methane fractions of 46.91% (case 16) and 78.8% (case 18), respectively. In there, as can be seen in Table 4 and Table 5, although the lambda value are decreased by adding of methane to acetylene, the energy values in the cylinder for the cases using hydrogen are lower than the cases using methane for a fixed bmep value. In addition, when the BTE values for fixed lambda values are examined, it is seen that the BTE values are generally declined by ascending of the fractions of the hydrogen and the methane in the acetylene. When the fraction of methane is increased from 31% to 43%, the BTE values decrease from 23.35% to 22.18% at around $\lambda=1.7$ (case 3 and case 4) for 83 kg/h air flow ratio, respectively. Similarly, when the fraction of methane is raised from 21.37% to 46.91%, the BTE values decrease from 24.84% to 22.41% at $\lambda=1.99$ (case 12 and case 13) for 90 kg/h air flow ratio, respectively. For the acetylene-hydrogen blends, when the fraction of hydrogen is increased from

61.27% to 70.09%, the BTE values decrease from 25.45% to 24.29% at around $\lambda=2.38$ (case 24 and case 25) for 83 kg/h air flow ratio, respectively. Similarly, when the fraction of hydrogen is increased from 27.02% to 45.02%, the BTE values decrease from 27.16% to 25.61% at around $\lambda=2.40$ (case 28 and case 29) for 90 kg/h air flow ratio, respectively.

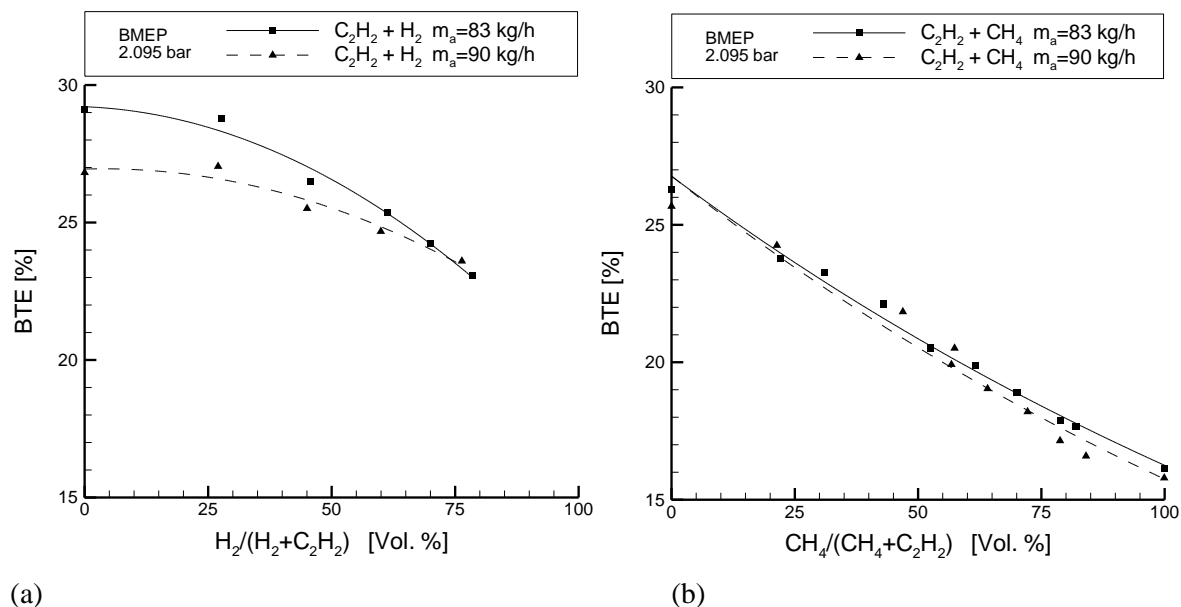


Figure 2. Brake thermal efficiency versus different fractions of hydrogen (a) and methane (b) for air flow ratios of 83 kg/h and 90 kg/h.

Finally, when the air ratio is raised from 83 kg/h to 90 kg/h, it can be seen that the BTE values decline for the blends. In there, the increasing of air flow ratio leads to a rise in the lambda value. So, the rising of the lambda values causes in a decrease of the temperature in the cylinder. For instance, the lambda values are measured as 1.4 and 1.64 fueled by the blend having the methane fractions of around 78.9% (case 8 and case 18) at 83 kg/h and 90 kg/h air flow ratio, respectively. The BTE values are obtained as 17.9% and 17.1% for methane-acetylene blend in the same conditions.

3.2 Cylinder Pressure And Rate Of Heat Release

The results of cylinder pressure and rate of heat release values versus crank angle at different fractions of hydrogen and methane for air flow ratios of 83 kg/h are displayed in Figure 3. The peak pressure values are produced as 12.2, 13.5, 15.4, 16.5 and 18.1 bar at 382, 381, 380, 379 and 378 deg. CA ATDC for 83 kg/h air flow ratio with hydrogen fraction of 0%, 27.69%, 45.78%, 61.26% and 78.5% in the blend, respectively. It can be pointed that the peak pressure values are raised by the addition of hydrogen to acetylene. Moreover, the peak values are generally obtained at a lower crank angle by the adding of hydrogen. The adding of hydrogen leads to an increase in the flame speed of blends.

When the results of methane-acetylene blends are analyzed, it can be said that the adding of methane to acetylene causes a decline in the values of peak pressure. In addition, the curves of pressure are retarded with the adding of methane because of the flame speed of methane is lower than the one's. Moreover, the adding of methane leads to drop in cylinder gas energy. The peak pressure values are produced as 15.7, 13.9, 13.7, 12.9, 12.85 and 11.0 bar at 382, 384, 385, 386, 386 and 390 deg. CA ATDC for 83 kg/h air flow ratio at methane fraction of 0%, 22.03%, 43.01%, 61.71%, 78.91% and 100% in the blend, respectively.

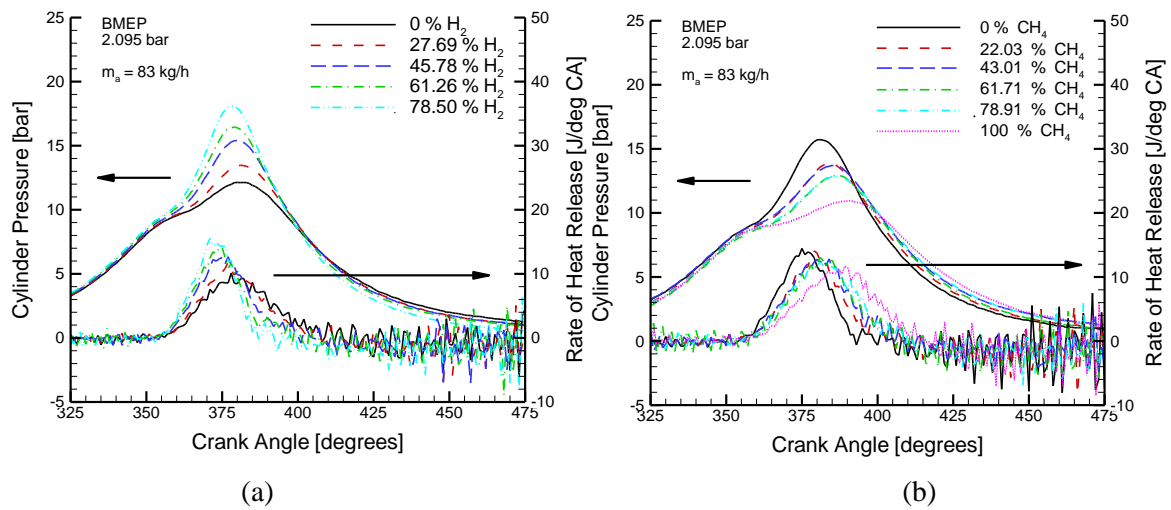


Figure 3. Cylinder pressure and rate of heat release values versus crank angle at different fractions of hydrogen (a) and methane (b) for air flow ratios of 83 kg/h.

The rate of heat release (ROHR) is defined as the rate at which the chemical energy of the fuel is released by the combustion process [23]. The ROHR is an important parameter to analyze the combustion phenomena in the engine cylinder. The combustion parameters such as the start of combustion, combustion duration and combustion intensity can be easily estimated from the heat release rate diagram [24]. It can be clearly seen from the figures that the curves of ROHR are generally advanced by the increase of hydrogen fraction in the blends for the each air flow. This is because the adding of hydrogen to acetylene results in a rise burning velocity of the blend and this made the curves of ROHR close to the top dead center. Opposite to hydrogen, the adding of methane to acetylene leads to generally retarding of the ROHR curves to the top dead center.

The peak values of ROHR are calculated as 10, 11.8, 12.6, 14.1 and 15.5 J/deg. CA at 378, 377, 375, 374 and 371 deg. CA ATDC for 83 kg/h air flow ratio with hydrogen fractions of 0%, 27.69%, 45.78%, 61.26% and 78.5% in the blend, respectively. For the methane-acetylene blends, the peak values are obtained as 14.5, 14.1, 12.8, 13.1, 12.5 and 11.7 J/deg. CA at 375, 379, 380, 381, 384 and 389 deg. CA ATDC for 83 kg/h air flow ratio with methane fractions of 0%, 22.03%, 43.01%, 61.71%, 78.91% and 100% in the blend, respectively.

3.3 Emissions

The emission values are important parameters for analyzing of alternative fuels. The results of CO emission versus different fractions of hydrogen (a) and methane (b) for air flow ratios of 83 kg/h and 90 kg/h are shown in Figure 4. As can be seen from the figure, although the lambda values and the BTE values are decreased by the adding of hydrogen to blend, the CO emission values are dramatically decreased by the increasing of the adding hydrogen to acetylene due to the chemical content of hydrogen not having carbon. But, the addition of methane to acetylene leads to ascend the CO values. In there, the addition of methane to acetylene causes a decrease in the values of lambda and the values of BTE. The CO emission values are metered as 0.037%, 0.031% and 0.02% by the adding of hydrogen to acetylene as 0%, 45.02% and 76.36% for 90 kg/h air flow ratio, respectively. The values are measured as 0.031%, 0.038% and 0.04% at methane fractions of 0%, 46.91% and 78.79% in the blend for the same air flow ratio, respectively.

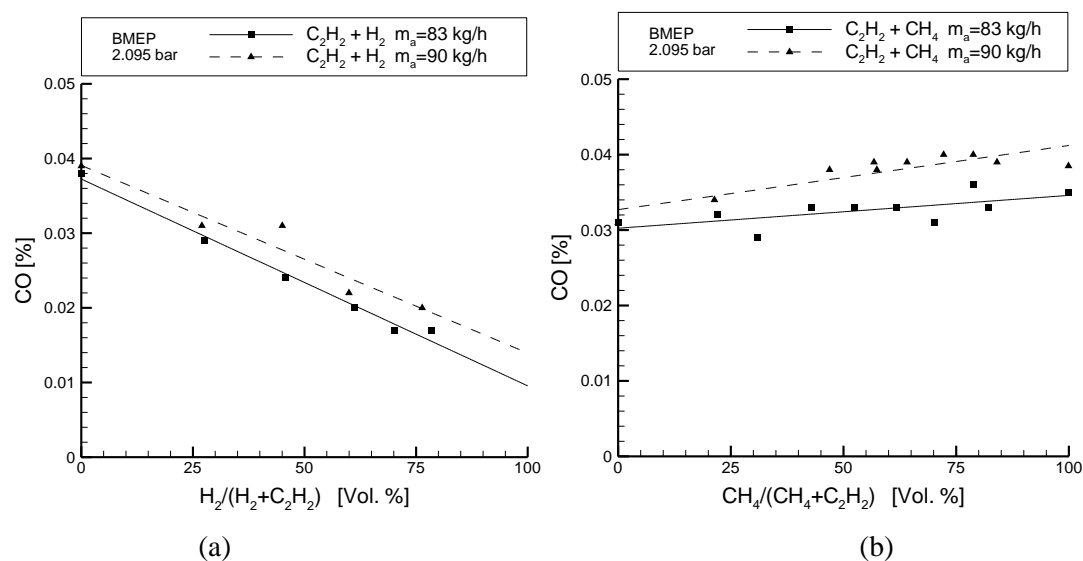


Figure 4. CO emission values versus different fractions of hydrogen (a) and methane (b) for air flow ratios of 83 kg/h and 90 kg/h.

Furthermore, as the air ratio is increased from 83 kg/h to 90 kg/h, the CO values ascend for the each blend. In there, the rising of air flow causes to an increase in the lambda value and causes in a decrease of the gas temperature in the cylinder. The CO values are measured as 0.032% and 0.034% when the methane fractions of 22.03% and 21.37% at 83 kg/h and 90 kg/h air flow ratio, respectively. The values are tested as 0.036% and 0.04% for the blends having volumetrically methane percent of 78.91% and 78.79%, respectively.

Figure 5 shows the values of HC emission versus different fractions of hydrogen (a) and methane (b) for air flow ratios of 83 kg/h and 90 kg/h. As can be seen from the figure, the HC emission values are dramatically increased by the adding of the methane to acetylene and are slightly decreased by addition of hydrogen. In there, the addition of methane leads to the rising of carbon content of the blend and causes the declining of the BTE values and the lambda values. Opposite to the adding of methane, the adding of hydrogen in the blend leads to drop the carbon content of the blend. The HC emission values are obtained as 16 ppm and 17 ppm fueled by pure acetylene at 83 kg/h and 90 kg/h air flow ratio, respectively. The values are obtained as 14 ppm and 12 ppm fueled by the blend having hydrogen fractions of 61.26% and 59.96% at the same air flow ratios, respectively. For the methane-acetylene blends, the HC emission values are metered as 7 ppm and 10 ppm fueled by pure acetylene at 83 kg/h and 90 kg/h air flow ratio, respectively. The values are metered as 37 ppm and 50 ppm fueled by the blend having methane fractions of 61.71% and 64.1% and the values are metered as 66 ppm and 105 ppm for the blend having fully methane at the same air flow ratios, respectively. In additions, the HC emission values are ascended dramatically at the higher methane ratio due to the reasons stated before in the emission section.

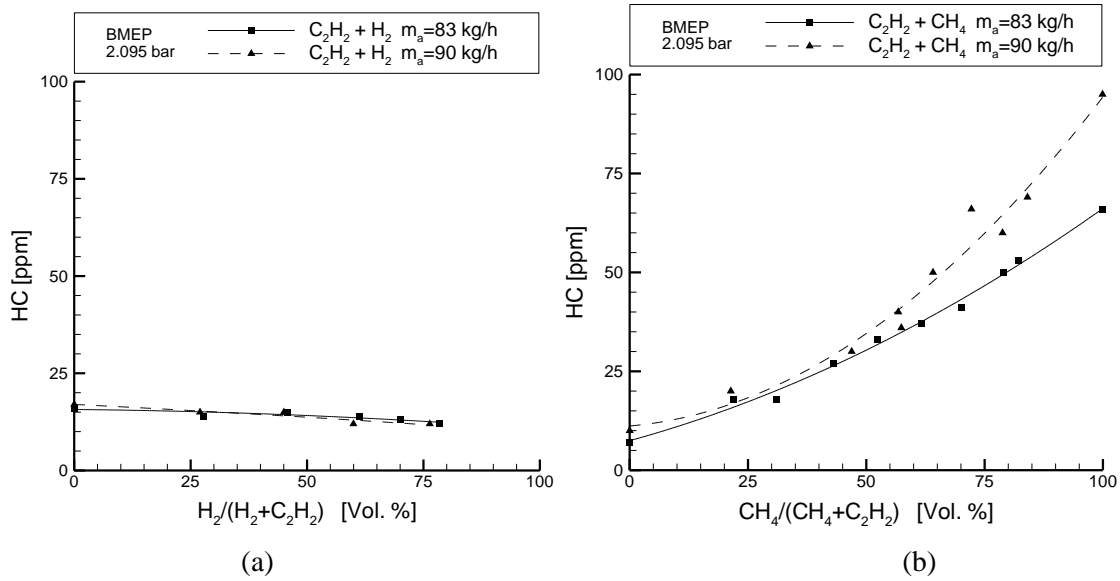


Figure 5. HC emission values versus different fractions of hydrogen (a) and methane (b) for air flow ratios of 83 kg/h and 90 kg/h.

The values of NO_x emission versus different fractions of hydrogen (a) and methane (b) for air flow ratios of 83 kg/h and 90 kg/h are shown in Figure 6. Although it is seen that the increase of hydrogen leads to a decrease in NO_x values, it is stated that this decrease is caused by the increase of the lambda values. Because, when the NO_x emission values are examined for fixed lambda values, it is seen that the increasing of hydrogen increases the NO_x values. Due to high flame temperature and high flame speed of the hydrogen, the increase of the hydrogen fraction in the blend this causes an increase in the temperature of the cylinder and the residual time of air in the heated zone. So, the NO_x values are raised by the addition of hydrogen [10] and [25]. When the fraction of hydrogen is increased from 0% to 27.69%, the NO_x values rise from 250 ppm to 280 ppm at around $\lambda=2.135$ (case 21 and case 22) for 83 kg/h air flow ratio, respectively. Similarly, when the fraction of hydrogen is raised from 61.27% to 70.09%, the NO_x values increase from 175 ppm to 215 ppm at $\lambda=2.37$ and $\lambda=2.40$ (case 24 and case 25) for the air flow ratio, respectively. For 90 kg/h air flow ratio, the fraction of hydrogen is increased from 27.02% to 45.02% leads to increase in the NO_x values from 65 ppm to 75 ppm at $\lambda=2.38$ and $\lambda=2.42$ (case 28 and case 29), respectively.

Though it is seen that the increasing of methane causes a rise in NO_x values, it is stated that the drop is caused by the decreased of the lambda values carried out with the adding of methane to acetylene. It is seen from these figures that the increasing of methane drops generally the NO_x values for fixed lambda. Due to low flame temperature and low flame speed of the methane, the increase of the methane fraction in the blend this causes a decrease in the temperature of the cylinder and the residual time of air in the heated zone. So, the NO_x values are dropped by the addition of methane. When the fraction of methane in the blends is increased from 31% to 43.01%, the NO_x values drop from 65 ppm to 59 ppm at $\lambda=1.72$ and $\lambda=1.70$ (case 3 and case 4) for 83 kg/h air flow ratio, respectively. Similarly, when the fraction of methane is raised from 72.21% to 78.79%, the NO_x values decline from 17 ppm to 14 ppm at $\lambda=1.64$ (case 17 and case 18) for 90 kg/h air flow ratio, respectively. Moreover, when the air ratio is increased from 83 kg/h to 90 kg/h, the NO_x values descend for the blend having a fixed volumetrically fuel content. The rising of air flow causes to a decrease in the lambda value and causes in a decrease of the gas temperature in the cylinder. The NO_x values are measured as 134 ppm and 14 ppm when the methane fractions are 78.91% and 78.79% at 83 kg/h and 90 kg/h air flow ratio, respectively. The values are tested as 260

ppm and 75 ppm for the blends having volumetrically hydrogen percent of 45.79% and 45.02% at 83 kg/h and 90 kg/h air flow ratio, respectively.

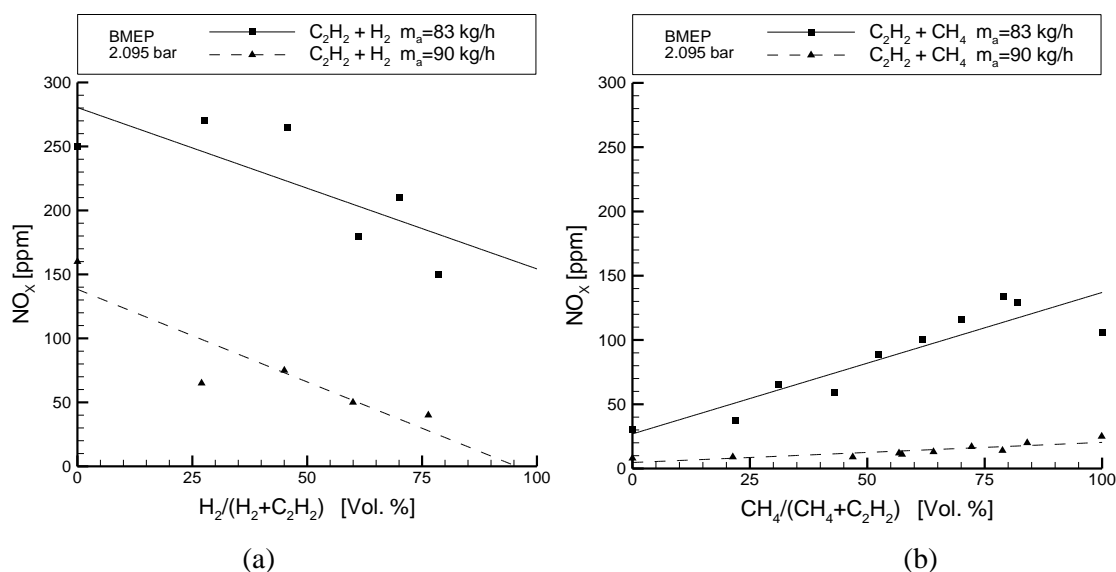


Figure 6. NO_x emission values versus different fractions of hydrogen (a) and methane (b) for air flow ratios of 83 kg/h and 90 kg/h.

Lastly, it can be seen that the values of CO, HC and NO_x emissions obtained in the experiments carried out by using hydrogen-acetylene and methane-acetylene blends are quite low for an SI engine.

4. Conclusion

The following main results are obtained in the present study used the blends of hydrogen-acetylene and methane-acetylene as alternative fuel in the SI engine.

- The BTE values were declined with addition of hydrogen and methane in the blend. The BTE values were decreased between 6.2% and 3.3% with the increasing of hydrogen fraction from 0% to 78.5% for 83 kg/h and from 0% to 76.4% for 90 kg/h air flow ratio, respectively. The BTE values were decreased between 10.2% and 10.5% by the increasing of methane fraction in the blend from 0% to 100% for the 83 kg/h and 90 kg/h air flow ratio, respectively.
- The BTE values for hydrogen-acetylene mixtures were measured higher than the BTE values at methane-acetylene blend. These increases ranged from 2.8% to 5.2% for 83 kg/h and from 0.65% to 6.5% for 90 kg/h.
- The BTE values were declined with the air ratio was raised from 83 kg/h to 90 kg/h for the blend.
- The peak pressure values were increased and were generally obtained at a lower crank angle by the adding of hydrogen.
- The curves closed top dead center by up to 4 degrees. But the adding of methane to acetylene generally made caused a decline in the values of peak pressure. Moreover it made retarded the curves of pressure to top dead center by up to 8 degrees because of the lower flame speed and the lower gas energy of methane. In addition, the curves of heat release rate showed a similarly characteristics.
- The CO emission values were dramatically decreased from nearly 0.04% to 0.01% with the increasing of the adding hydrogen to acetylene. But the addition of methane to acetylene led to

ascend the CO values. In addition, when the air ratio was increased from 83 kg/h to 90 kg/h the CO values increased for the each blend.

- The HC emission values were dramatically increased by the adding of the methane to acetylene and were slightly decreased by the addition of hydrogen.

- Due to the increase of the lambda values, the increase of hydrogen led to a decrease in NOX values from 250 ppm to 130 ppm for 83 kg/h air flow ratio and a decrease in NOX values from 160 ppm to 40 ppm for 90 kg/h air flow ratio. But the increasing of hydrogen increased NOX emission values for fixed lambda values.

- Due to the drop of the lambda values, the increasing of methane caused a rise in NOX values. But the increasing of methane dropped generally the NOX values for fixed lambda.

References

- [1] C. Satheeshkumar, T. Mohammed Shekooor, Evaluation of emission characteristics of hydrogen as a boosting fuel in a four stroke single cylinder gasoline engine, *International Journal of Engineering Research & Technology (IJERT)* 3:10 (2014) 151-154.
- [2] R. Gandhi, Use of hydrogen in internal combustion engine, *International Journal of Engineering and Technical Research (IJETR)* 3:2 (2015) 207-216.
- [3] S. Yousufuddin, S.N. Mehdi, M. Mohammad, Performance and combustion characteristics of a hydrogen-ethanol fuelled engine, *Energy & Fuels* 22 (2008) 3355–62.
- [4] T. Petkov, T.N. Veziroglu, J.W. Sheffield, An outlook of hydrogen as an automotive fuel, *International Journal of Hydrogen Energy* 14 (1989) 449–474.
- [5] F. Ma, Y. He, J. Deng, L. Jiang, N. Naeve, M. Wang, R. Chen, Idle characteristics of a hydrogen fueled SI engine, *International Journal of Hydrogen Energy* 36:7 (2011) 4454–4460.
- [6] A.A. Yamin Jehan, H.N. Gupta, B.B. Bansal, O.N. Srivastava, Effect of combustion duration on the performance and emission characteristics of a spark ignition engine using hydrogen as a fuel, *International Journal of Hydrogen Energy* 25: 6 (2000) 581-590.
- [7] P.C.T. De Boer, W.J. McLean, H.S. Homan, Performance and emissions of hydrogen fueled internal combustion engines, *International Journal of Hydrogen Energy* 1:2 (1976) 153-172.
- [8] J. Xu, X. Zhang, J. Liu, L. Fan, Experimental study of a single-cylinder engine fueled with natural gas-hydrogen mixtures, *International Journal of Hydrogen Energy* 35 (2010) 2909-2914.
- [9] N. Kahraman, B. Çeper, S.O. Akansu, K. Aydın, Investigation of combustion characteristics and emissions in a spark-ignition engine fuelled with natural gas-hydrogen blends, *International Journal of Hydrogen Energy* 34 (2009) 1026-1034.
- [10] G.P. Taggart-Cowan, S.N. Rogak, S.R. Munshi, P.G. Hill, W.K. Bushe, Combustion in a heavy-duty direct-injection engine using hydrogen-methane blend fuels, *International Journal Engine Research* 10 (2009) 1-13.
- [11] S.E.L. Mohammed, M.B. Baharom, A.R.A Azia, Analysis of engine characteristics and emissions fueled by in-situ mixing of small amount of hydrogen in CNG, *International Journal of Hydrogen Energy* 36 (2011) 4029-37.

-
- [12] S.O. Akansu, Z. Dulger, N. Kahraman, T.N. Veziroğlu, Internal combustion engines fueled by natural gas—hydrogen mixtures, *International Journal of Hydrogen Energy* 29 (2004) 1527–1539.
- [13] P.K. Sharma, H. Kuinkel, P. Shrestha, S. Poudel, Use of Acetylene as an Alternative Fuel in IC Engine, *Rentech Symposium Compendium 1* (2012) 19–22.
- [14] T. Lakshmanan, G. Nagarajan, Experimental investigation of port injection of acetylene in DI diesel engine in dual fuel mode, *Fuel* 90 (2011) 2571–77.
- [15] T. Lakshmanan, G. Nagarajan, Experimental investigation of timed manifold injection of acetylene in direct injection diesel engine in dual fuel mode, *Energy* 35 (2010) 3172–78.
- [16] S.S. Nathan, J.M. Mallikarjuna, A. Ramesh, Effects of charge temperature and exhaust gas re-circulation on combustion and emission characteristics of an acetylene fuelled HCCI engine, *Fuel* 89 (2010) 515–521.
- [17] S.K. Basha, P.S. Rao, K. Rajagopal, K.R. Kumar, Experimental study on the performance of an acetylene aspirated diesel engine using EGR, *International Journal of Applied Engineering Research* 11:7 (2016) 5346–51.
- [18] D. Tanwar, R. Tanwar, N. Aggarwal, Analysis of engine performance by using acetylene in CI engine operated on dual fuel mode, *International Journal of All Research Education and Scientific Methods (IJARESM)* 3:7 (2015) 35–45.
- [19] P. Behera, S. Murugan, G. Nagarajan, Dual fuel operation of used transformer oil with acetylene in a DI diesel engine, *Energy Convers Management* 87 (2014) 840–847.
- [20] S. Brusca, R. Lanzafame, A. Marino Cugno Garrano, M. Messina, On the possibility to run an internal combustion engine on acetylene and alcohol, *Energy Procedia* 45 (2014) 889 – 898.
- [21] N.S. Kumar, B.G. Prabhu, K.K. Selvan, R.M. Kumar, K.M. Kumar, Emission and performance characteristics of hydrogen-acetylene fuel in IC engine, *International Journal of Innovative Research in Science, Engineering and Technology* 6:3 (2017) 4620–27.
- [22] R.D. Jadhav, V.U. Mitkari, Experimental analysis of acetylene gas as an alternative fuel for S.I. engine, *International Engineering Research Journal (IERJ)*; Special Issue (2016) Pager 208–215.
- [23] J. Zareei, F.W. Mahmood, S. Abdullah, Y. Ali, T.I. Mohamad, Prediction of performance a direct injection engine fueled with natural gas–hydrogen blends, *International Journal of Mechanical & Mechatronics Engineering* 14:03 (2014) 149–156.
- [24] R. Kumar, A.K. Dixit, Combustion and emission characteristics of variable compression ignition engine fueled with *Jatropha curcas* ethyl ester blends at different compression ratio, *Journal of Renewable Energy* 14 (2014) 1–12.
- [25] F. Ma, S. Li, J. Zhao, Z. Qi, J. Deng, N. Naeve, Y. He, S. Zhao, Effect of compression ratio and spark timing on the power performance and combustion characteristics of an HCNG engine, *International Journal of Hydrogen Energy* 37 (2012) 18486–91.

Comparision of engine performance and exhaust emission values of sunflower biodiesels with diesel fuel

Şükran Efe*, Hakan Temur**

*Electricity Department, Tortum Vocational High School, Ataturk University, Erzurum/Turkey

**Chemical Engineering Department, Engineering Faculty, Ataturk University, Erzurum/Turkey

sukran.ef@atauni.edu.tr; htemur@atauni.edu.tr

Summary: Increasing demand on diesel fuel causes negative environmental effects and decreasing of reserves amount. Today, many studies have been carried out on alternative energy sources that can be used as a substitute for the diesel fuel. Biodiesel has come into prominence in these studies. Biodiesel has many superior properties over the diesel fuel despite some disadvantages. Therefore, there are so many studies in the literature in order to determine the most suitable vegetable oil for biodiesel production. In this study, motor performance and exhaust emissions of sunflower biodiesel produced from sunflower oil by transesterification method were examined and compared with diesel fuel. In the engine test, biodiesel is used in pure form, and as a mixture with diesel fuel (20% and 50%). The effective power, effective fuel consumption, effective efficiency and exhaust emissions values (CO, CO₂, NO, HC, and smoke) were measured in the study. All results are compared with diesel fuel. The engine performance parameters have similar results with literature. However, emission results were different from most literature results. The decrease in NO, CO₂ emission values and increasing of CO, HC emission values are determined in the study.

Keywords: Sunflower biodiesel, engine performance, exhaust emission

Introduction

Energy demand is rapidly increased due to growth of the world population, rising living standards and development of new technologies. Today, both the decreasing reserve amount of energy sources and the increasing negative environmental effects of intensive consumption are forefront because fossil fuels are used heating, transportation, carrying and energy generation areas. Specially, diesel fuel consumption among fossil fuels is very high due to the high power performance of diesel engines.

In the diesel engines, fuel is burnt at high temperatures due to the high compression ratio and thus high energy is obtained. The diesel engines have some harmful effect on the environment. Because NO_x emissions occurs at high combustion heat, it is most important negative impact of diesel fuels on the environment. The NO_x emissions produce photochemical smog and react with hydrocarbons under ultraviolet sunlight. The photochemical smog damages the ozone layer and the respiratory system of living. The main source of acid rain is NO_x emissions [1,2].

Therefore, any alternative technology that will reduce diesel fuel consumption or any alternative fuel that could take the place of diesel fuel is carried out in many studies. The first alternative fuel study was carried out by Dr. Rudolf Diesel who is the inventor of the diesel engine. He used 100% nut oil on the diesel engine at the World Exhibition in 1900. The importance of Dr. Diesel's study was not fully understood in those years. After year, his study come into prominence in alternative energy sector.

Therefore first researches were started on vegetable oils. Researchers determined that long duration use of vegetable oil in diesel engines was not suitable due to high viscosity of it. However, vegetable oils had used some emergency situations as war in the past years [3, 4].

The best solution is to convert vegetable oils to biodiesel so that it can be used as fuel for a diesel engine. Biodiesel is defined by American Society for Testing and Materials (ASTM) as “biodiesel fuel as mono alkyl esters of long-chain fatty acids derived from renewable lipid feed stocks, such as vegetable oils or animal fats, for use in diesel engines” [5].

Biodiesel is very similar to diesel fuel. Biodiesel does not contain any oil product. When it mix with diesel, it creates a stable diesel biodiesel blends. The mixture define as BX. The X value indicates the of the percentage amount of biodiesel in the blend. For example, there are 20% biodiesel 80% diesel at B20, 50% biodiesel 50% diesel at B50 and 100% biodiesel 0% diesel at B100 [4].

Biodiesel has some advantages as lubrication, non-toxic, more reliable for transport and storage, independence world energy resources. On the other hand, high NO_x emissions [6] and poor cold start performance are the disadvantages of biodiesel [7,8].

The amount of NO_x emissions are effected two parameters that high temperature of combustion and high oxygen ration in combustion weather. So NO_x amount is very low during engine start and NO_x emissions change according to the engine load (at low loads less). NO_x emission occurs in diesel or gasoline engines has different reasons [9].

The aim of this study promote to use of biodiesel that has increasing importance day by day. Therefore, the biodiesel performance of sunflower vegetable oil that has common cultivation in Turkey have been examined in this study. At first, sunflower biodiesel are produced by transesterification method from sunflower vegetable oil. Last, the biodiesel is used as fuel that is mixture form with diesel engine different rate (20% or 50%) or pure form (100%) in a diesel engine. The engine performance and exhaust emission values of all kind fuels and diesel fuel are determined in engine tests. Finally, all values are compared with each other.

Experiments

The experimental part of this study consists biodiesel production and engine tests

1. Biodiesel Production

Biodiesel production is performed by transesterification method (alcoholysis). It is a reaction between alcohol and triglycerides (main component of the oils) with the presence of a catalyst. Sunflower oil purchased from a grocery store was used as oil feedstock. Methyl alcohol (CH₃OH) was used as alcohol and potassium hydroxide (KOH) as the catalyst in the reaction. Alcohol is used 20% by volume and catalyst is used 1% by mass at the temperature of 56°C in 60 minutes in a glass reactor (Fig. 1). A mixture of two phases was obtained at the end of the reaction. The mixture contains biodiesel, glycerol, catalyst, alcohol and other substances (tri-di-mono glyceride etc.). Therefore, purification procedure was needed to obtain pure biodiesel from the mixture. During the purification steps glycerol, catalyst, water and excess methyl alcohol were removed the biodiesel (Fig. 2a, 2b and 2c).

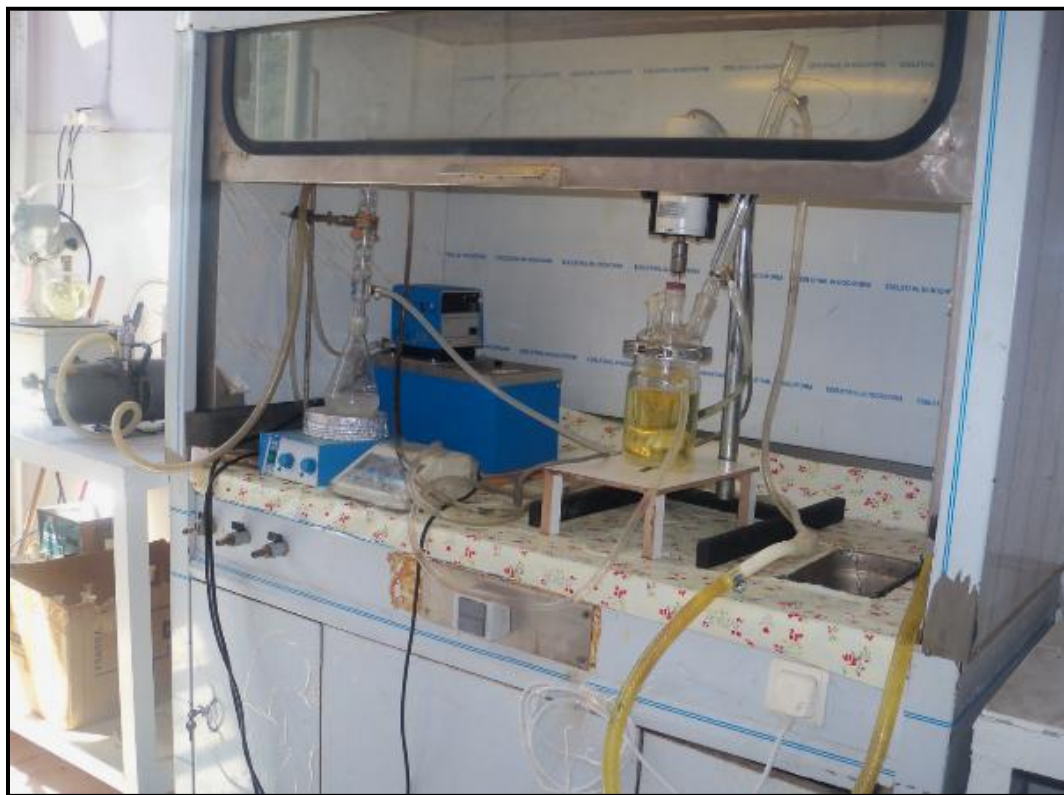


Figure 1. Biodiesel production

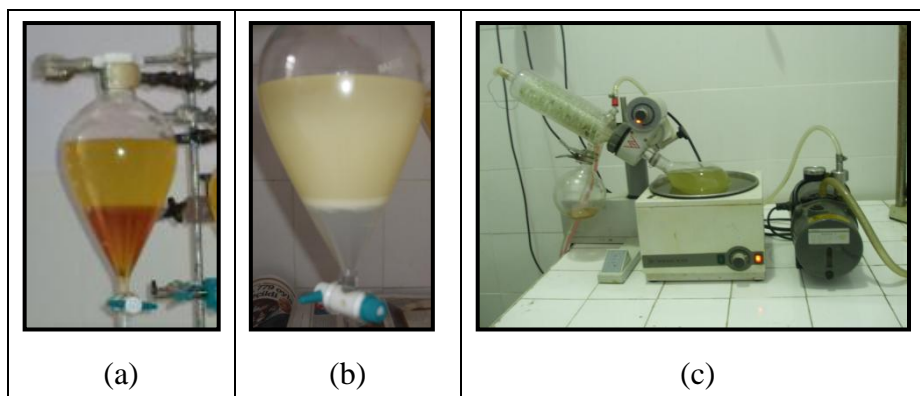


Figure 2. Purification procedure

2. Engine Test

Engine tests are carried out with a 4-stroke 2 cylinders direct injection diesel engine (SuperStar, Motosan Motor Sanayi ve Ticaret A.Ş., Istanbul/Turkey), with 1/17 compression ratio, 1,54 dm³ cylinder volume, and power of 28 HP. A quartz pressure transducer (Kistler 6117BDF17) is placed combustion chamber of only one cylinder. The crank shaft angle is measured with an optical devices. The pressure data and crank shaft angle data are stored in a personal computer with the help of a data acquisition card (National Instruments, M series, 6250 model, 1.25 MS/s DAQ). Torque and speed data in dynamometer were stored in the computer by LabVIEW (National Instruments, Austin, Texas, USA). The fuel consumption was

measured by a gravimetric fuel mass flow meter. The measured data from the fuel mass flow meter were transferred to the computer with the LabVIEW program.

DF (diesel fuel), B100 (100% biodiesel), B50 (50% biodiesel and 50% diesel), and B20 (20% biodiesel and 80% diesel) as fuel are used in the engine test. All experiments are repeated three times in the same conditions. Results are compared with each other. The schematic experimental setup for engine tests is shown in Figure 3.

During engine test both engine performance and exhaust emission values are determined. The brake power (P_b), brake specific fuel consumption (sfc), and thermal efficiency (η_{th}) for effective characteristics and CO, CO₂, NO, HC emissions and smoke amounts for exhaust emissions were measured in the study. Then, all obtained results are compared with diesel fuel.

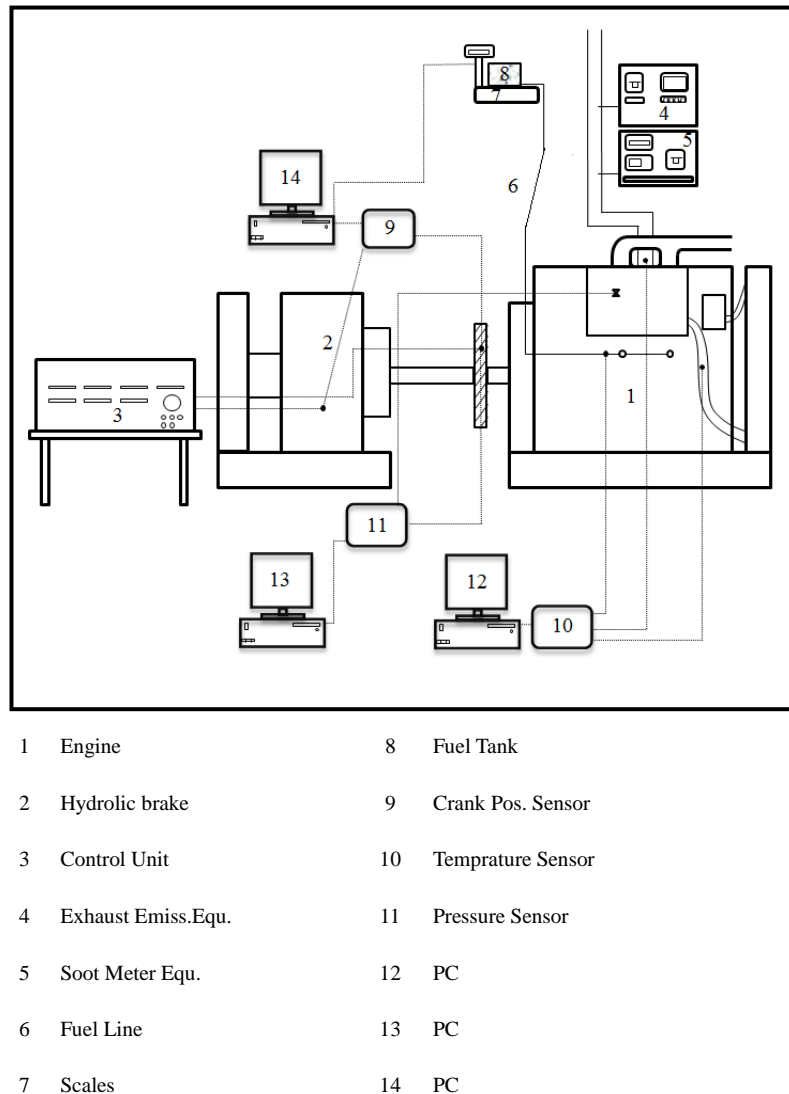


Figure 3. Schema of the engine system

3. Calculations

The cetan number of biodiesel was determined by a formula that is developed with Multi-Linear Regression (MLR) with $R^2=0.9191$. The equation used to determine cetane numbers of the samples is given at Eq.1. [10].

$$CN = 56.16 + 0.07.La + 0.1.M + 0.15.P - 0.05.Pt + 0.23.S - 0.03.O - 0.19.Li - 0.31.Ln + 0.08.Ei + 0.18.Er - 0.1.Ot \quad (1)$$

The independent variables are the fatty acid methyl esters compositions in weight percent found in biodiesel: La is the % of lauric, M is myristic, P is palmitic, Pt is palmitoleic, S is stearic, O is oleic, Li is linoleic, Ln is linolenic, Ei is eicosanoic, Er is erucic and Ot is the sum (trace or rest) of the other fatty acid methyl esters. Fatty acid rate of sunflower biodiesel was shown Table 2.

Table 1. Physical and chemical properties

Fatty Acid	Myristic acid,	Palmitic acid,	Palmitoleic acid,	Margaric acid,	Stearic acid,	Oleic acid,	Elaidic acid,	Linoleic acid,	Linoelaidic acid,	Linolenic acid,	Eicosanoic acid,	Eicosenoic acid,	Behenic acid,	Lignoceric acid,
Rate	0,1	7,6	0,1	–	4,7	29,2	0,7	55,2	0,5	0,1	0,3	0,2	0,9	0,3

The engine performance characteristics were calculated as follows:

- The brake power (P_b) delivered by the engine and absorbed by the dynamometer is [11]

$$P_b = 2 \pi n T 10^{-3} \quad [2]$$

Where, T is the torque (N m) and n is the crankshaft rotational speed (rev s^{-1}).

- The thermal efficiency η_{th} of the engine is,

$$\eta_{th} = P_b / Q \quad [3]$$

Q is the total heat of fuel was calculated from equation [11].

$$Q = CV \dot{m}_f \quad [4]$$

Where CV is the calorific value of the fuel ($kJ kg^{-1}$) and \dot{m}_f is the fuel consumption ($kg sn^{-1}$).

- The specific fuel consumption (sfc) is the fuel flow rate per unit power output and calculated from equation [11].

$$sfc = \dot{m}_f / P_b \quad [5]$$

Results

The physical and chemical properties of the sunflower oil and the sunflower methyl esters are determined in Malaya University (Kuala Lumpur/Malaysia). Euro-diesel fuel sold Petrol Ofisi Company was used in the engine test. The euro-diesel fuel properties was provided by the same Company. The physical and chemical properties of the sunflower oil, the sunflower biodiesel, and the euro-diesel are given in Tab.2.

Table 2. Physical and chemical properties

Properties	Sunflower Oil	Sunflower Biodiesel	Diesel*
Heat Value(kJ/kg)	39583	39913.5	45951
Dyn. Visc. (40°C) (mpa.s)	28.954	3.6596	2.4257
Kin. Visc. (40°C) (mm ² /s)	31.945	4.2162	2.9542
SFTN (°C)	11	-2	-6
Flash Point (°C)	238	162	56
Density (g/cm ³)	0.9064	0.8862	0.8211
Cetane Number	-	46.8	51

* Obtained from Petrol Ofisi Company

Engine tests were carried out at 7 different speeds, 800 (idle speed)-1000-1200-1400-1600-1800-2000 rev/min. All experiments were repeated three times in the same conditions. The values for BMEP, BSFC and BTE are shown in Figure 3(a-c) and the values for CO, CO₂, NO, HC and smoke amount are shown in Figure 4(a-e) respectively.

The BMEP takes the following values 0.5, 1.0, 1.6, 2.7, 3.4, 4.0, 4.7 kW at the engine speeds given above when the diesel fuel is used. Figure-3a where the difference BMEP values are decreased when biodiesel/biodiesel mixtures are used. The amount of reduction was increased with the engine speed. This situation can explain with the high viscosity of the biodiesel. Because the high viscosity of biodiesel causes both delaying of fuel move from the fuel tank to the combustion chamber and decreasing fuel atomization due to the reduced compression stroke duration in the combustion chamber. Less atomized fuel will cause incomplete combustion and therefore the BMEP will be reduced.

The BSFC for diesel fuel are obtained as 923.8, 623.8, 498.7, 420.6, 376.9, 370.1, 373.7 g/kWh for the engine speeds given above, respectively. It can be seen in Figure 3b clearly that the BSFC is higher for biodiesel/biodiesel mixtures than the diesel BSFC. Increase in the BSFC decreases with the increasing speed.

Figure 3c indicates that the BTE decreases when the biodiesel/biodiesel mixtures are used. It is interesting to note that the BTE increases, not decreases, when B100 is used despite the BSFC increases. These results clearly indicate that increasing the BSFC does not affect directly the BTE. The probable reason for this situation is that the amount of oxygen component in the fuel. Also, the low heat value and the high density of the fuel increases the BTE.

Figure 4a shows CO emissions. The values are increased in the use of biodiesel. Inclement increase with increasing of biodiesel percentage and decreases with increasing speed. This situation can be explained as follows. If the number of cycles increases, the piston speed increase in the engine. Because air movement inside of cylinder increases in the circumstances, the injected fuel is dispersed in the air faster. If the percentage of biodiesel increases, the viscosity of the mixture increases in the cylinder. Performance of combustion reduction.

Figure 4b shows change amount of CO₂ emissions. CO₂ emissions are generally decreased in the use of biodiesel. Decrement is increased with biodiesel rate of in the fuel. Less CO₂ emission was shown better quality of combustion. This situation can be explained by the high combustion rate of biodiesel and the O₂ amount in the structure of biodiesel.

Figure 4c shows NO emissions. NO emissions are prominently decreased in the use of biodiesel. The values of reduction are increased with increasing of biodiesel percentage in the fuel as CO₂. NO_x emission is sensitive to adiabatic flame temperature, oxygen content and spray properties. It is well known that biodiesel fuel does not contain any sulphur component. Therefore nitrogen content is very

small. The spray characteristics depend on droplet momentum, droplet size, degree of mixing with air, penetration rate, heat transfer rate and evaporation rate. A change in any of these properties may change the NO_x production [12].

Figure 4d shows HC emissions. HC emissions are increased in the use of biodiesel. In particular, the increase seems more prominent in the mixture B100. The most obvious reasons of increase in HC emissions are the high viscosity and low volatility of fuels, poor atomization in combustion and inconvenient combustion.

Figure 4e shows smoke values. Smoke values are increased from B20 to B100. It is explained by similar reasons as HC and CO emissions.

In literature there are excessive studies that analyzed the engine performance and exhaust emissions of any biodiesel sample. The obtained results from those studies demonstrate to be interesting differences. The differences was analyzed in the two review study. They compared results of some studies in the literature in Table 3.

Table 3. The compared engine characteristics and exhaust emissions in the review studies

Author/Year	Properties	Increases	Decreases	Same	Synergies	Total (number* or %)
Xue et al. 2011 [13]	Eff.Power	2	19	6	-	27
	Eff.Fuel.Cons.	54	6	2	-	62
	Eff.Efficiency	-	-	-	-	-
	NO _x	45 (65,2)	20 (29)	4 (5,8)	-	69 (100)
	CO	7 (10,6)	57 (84,4)	2(5)	-	66 (100)
	CO ₂	6 (46,2)	5 (38,5)	2 (15,4)	-	13 (100)
	HC	3 (5,3)	51 (89,5)	3 (5,3)	-	57 (100)
	PM	7 (9,6)	64 (87,7)	2 (2,7)	-	73 (100)
Lapuerta et al. 2008 [14]	Eff.Power	-	(96)	(2)	(2)	(100)
	Eff.Fuel.Cons.	(98)	-	-	(2)	(100)
	Eff.Efficiency	(8)	(4)	(8)	(80)	(100)
	NO _x	(85)	(5)	-	(10)	(100)
	CO	(2)	(90)	(1)	(7)	(100)
	CO ₂	-	-	-	-	-
	HC	(1)	(95)	(1)	(3)	(100)
	PM	(3)	(95)	-	(2)	(100)

The motor performance values obtained from this study are similar to the literature (Table 3). However, although exhaust emission results are different from many studies in the literature, Table 2 show to us that there are some studies with similar results in the literature.

Conclusion

In this study, which examines the biodiesel quality of sunflower vegetable oil, which is widely cultivated in Turkey, motor performance and exhaust emission values are analyzed. The sunflower biodiesel produced by the transesterification method from sunflower vegetable oil was used as fuel at different ratios on a diesel motor that has with a 4-stroke 2 cylinders direct injection diesel engine, with 1/17

compression ratio and power of 28 HP. The values of engine performance and exhaust emission are compared with diesel fuel. The obtained are also controlled by the literature. As a results, the motor performance values are similar to the literature and exhaust emission results are different from many studies in the literature. The decrease in NO, CO₂ emission values and increasing of CO, HC emission values are determined in the study.

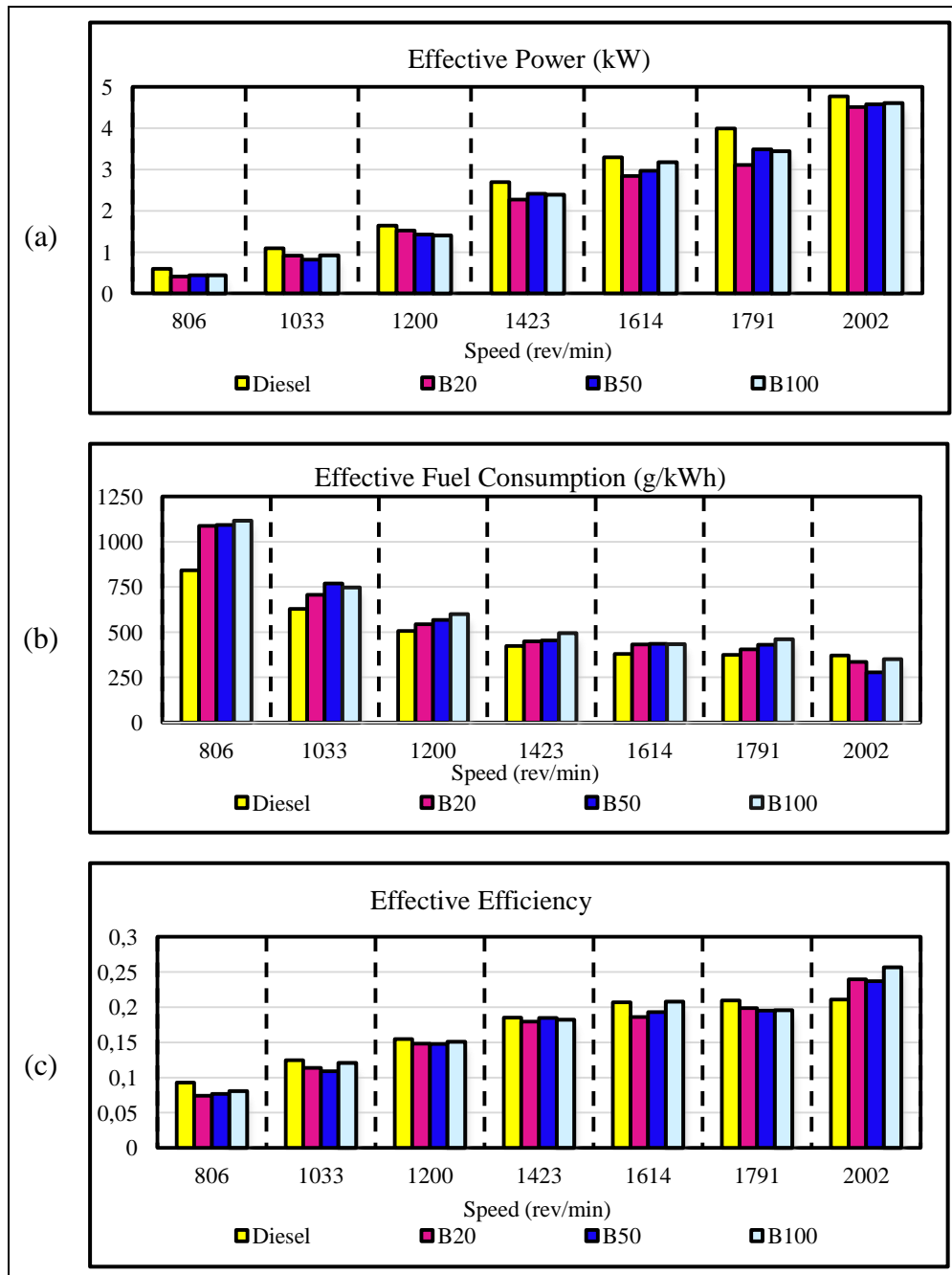


Figure 4. Engine Performance (a) effective power, (b) effective fuel consumption, (c) effective efficiency

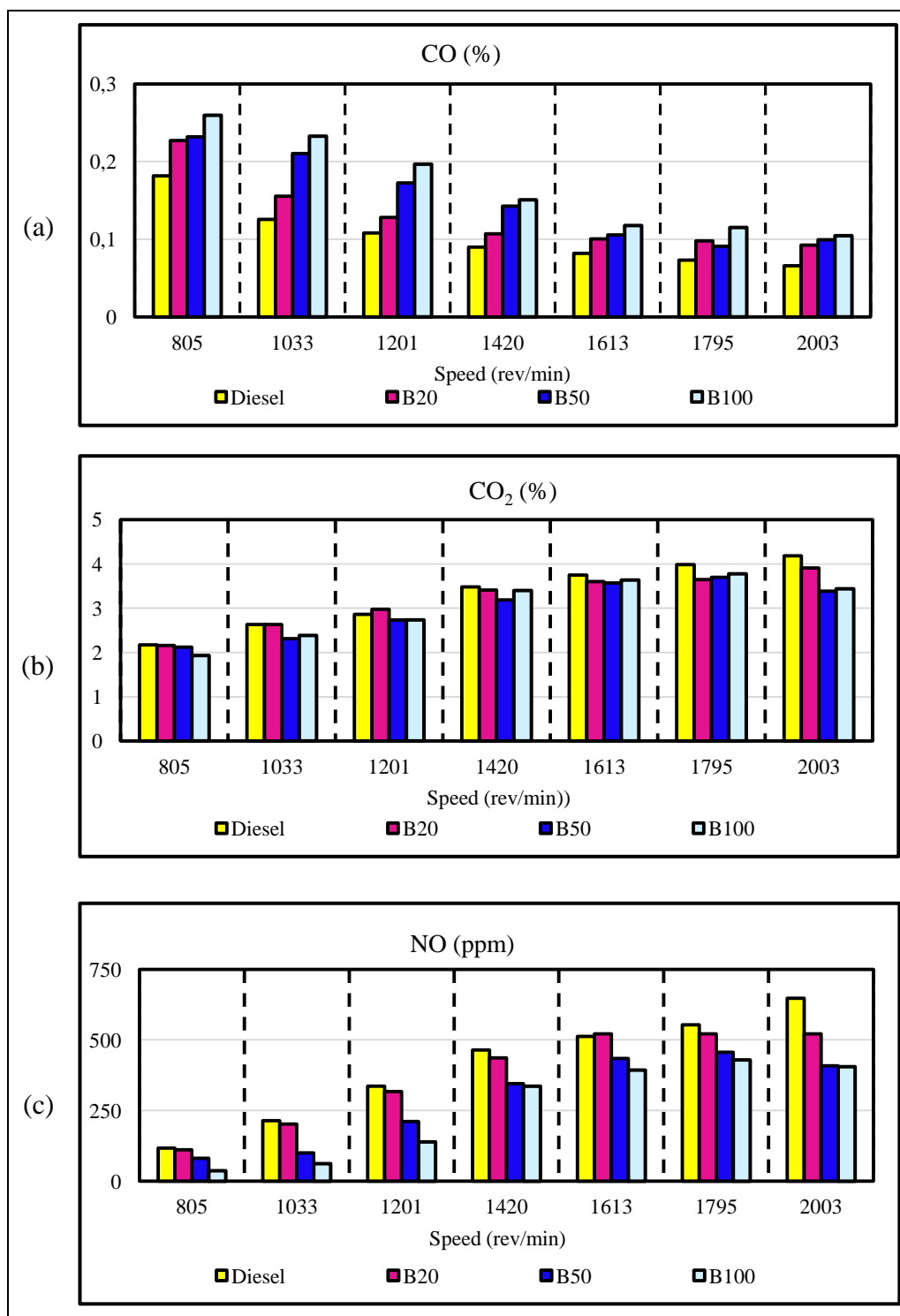


Figure 4. Continued

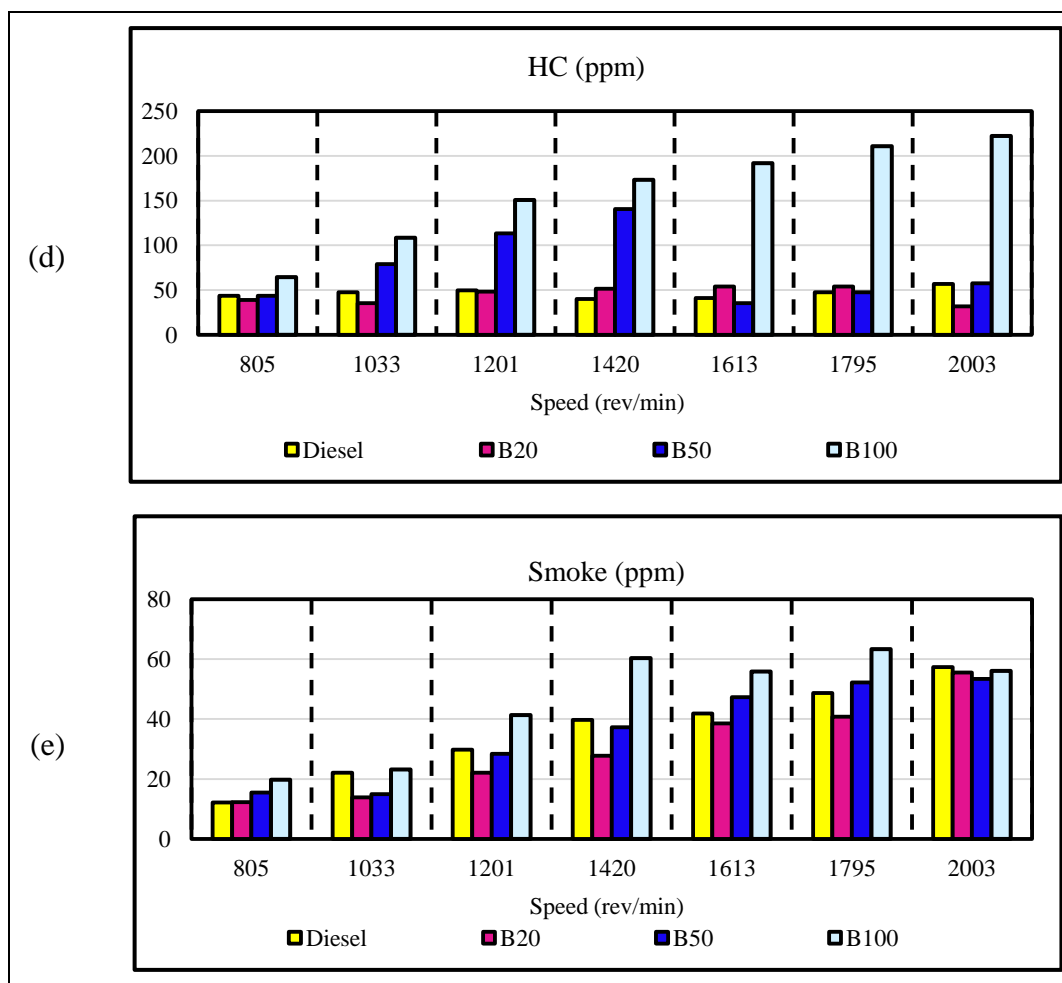


Figure 4. Exhaust Values (a) CO, (b) CO₂, (c) NO, (d) HC, (e) smoke

References

- [1] International Energy Agency. (2015). 2014 Key World Energy Statisc.
- [2] Dincer, I. (1999). Environmental impacts of energy. *Energy Policy*(27), 845-854.
- [3] Kalam, M., Masjuki, H., Jayed, M., & Liaquat, A. (2011). Emission and performance characteristics of an indirect ignition diesel engine fuelled with waste cooking oil. *Energy* (36), 397-402.
- [4] Agarwal, A. K. (2007). Biofuels (alcohols and biodiesel) applications as fuels for internal combustion engines. *Progress in Energy and Combustion Science*, 33, 233-271.
- [5] Rajasekar, E., A. Murugesan, R. Subramanian, and N. Nedunchezian. "Review of NO_x reduction technologies in CI engines fuelled with oxygenated biomass fuels." *Renewable and Sustainable Energy Reviews*, 2010: 2113-2121.
- [6] Roy, M. M., Calder, J., Wang, W., Mangad, A., & Diniz, F. C. (2016). Cold start idle emissions from a modern Tier-4 turbo-charged diesel engine fueled with diesel-biodiesel, diesel-biodiesel-ethanol, and diesel-biodiesel-diethyl ether blends. *Applied Energy*(180), pp. 52-65.
- [7] Broatch, A., Tormos, B., Olmeda, P., & Novella, R. (2014). Impact of biodiesel fuel on cold starting of automotive direct injection diesel engines. *Energy*(73), 653-660.

- [8] Xue, Y., Zhao, Z., Xu, G., Lian, X., Yang, C., Zhao, W., . . . Han, S. (2016). Effect of poly-alpha-olefin pour point depressant on cold flow properties of waste cooking oil biodiesel blends. *Fuel*(184), pp. 110-117.
- [9] Ferguson, Colin R., and Allan T Kirkpatrick. Internal combustion engines: applied thermosciences. New York: John Wiley & Sons, 2001.
- [10] Piloto-Rodríguez, Ramón, Yisel Sánchez-Borroto, Magin Lapuerta, Leonardo Goyos-Pérez, and Sebastian Verhelst. "Prediction of the cetane number of biodiesel using artificial neural networks and multiple linear regression." *Energy Conversion and Management*, no. 6 (2013): 255-261.
- [11] Heywood, J. B. (1988). Internal Combustion Engine Fundamentals. Singapore: McGraw-Hill.
- [12] Enweremadu, C., & Rutto, H. (2010). Combustion, emission and engine performance characteristics of used cooking oil biodiesel; A review. *Renewable and Sustainable Energy Reviews*(14), 2863–2873
- [13] Xue, J., Grift, T. E., & Hansen, A. C. (2011). Effect of biodiesel on engine performances and emissions. *Renewable and Sustainable Energy Reviews* (15), 1098–1116.
- [14] Lapuerta, M., Armas, O., & Rodriguez-Fernandez, J. (2008). Effect of biodiesel fuels on diesel engine emissions. *Progress in Energy and Combustion Science*(34), 198–223.

The effect of sunflower biodiesel on cyclic variation using wavelet analysis method

Şükran Efe*, Hakan Temur**

*Electricity Department, Tortum Vocational High School, Ataturk University, Erzurum/Turkey

**Chemical Engineering Department, Engineering Faculty, Ataturk University, Erzurum/Turkey

sukran.ef@atauni.edu.tr; htemur@atauni.edu.tr

Abstract: Biodiesel that has many superior properties became forefront among the alternative biofuels today. Therefore, many studies were carried out on properties of biodiesel in the literature along with its engine performance. Cyclic variation is a very important parameter in the engine performance. This study focused on cyclic variation of sunflower biodiesel produced from sunflower oil. Sunflower biodiesel was produced from sunflower oil by transesterification method and used in a diesel engine. Three different biodiesel ratios, 20%, 50% and 100% and diesel fuel were used in the tests. In-cylinder pressure signal values for every kind of fuel were observed. All results were compared each other and with diesel fuel. Wavelet analysis method was used for analysis. When they are compared, it is observed that use of biodiesel in the diesel engine has a negative effect on the cyclic variation. Specially, the negative effect is prominent value for pure biodiesel.

Keywords: Wavelet Analysis Method, sunflower biodiesel, cyclic variations

Introduction

When today's energy sources is examined, use of fossil fuel is clearly more common. Day by day use of fossil fuels increases as a result of growing energy demand. This increase in consumption rate reduces existing reserves and increases harmful effects of the fossil fuel on the environment.

Diesel fuel is burnt at high temperatures in the diesel engines due to the high compression ratio and, therefore, high energy is obtained. As a result, diesel engines have greater harmful effect on the environment [1,3]. In order to reduce the harmful effects, use of alternative fuels in diesel engines is at the forefront. Also, geopolitical concerns on the fossil fuels are one of the important reasons why alternative fuel research is needed.

First alternative fuel studies inspired study of Dr. Rudolf Diesel in 1900 were carried out on vegetable oils. The studies was shown that high viscosity of vegetable oils prevents them from becoming alternative fuels. The high viscosity of vegetable oils was an obstacle for them to take up diesel fuel. Therefore, in the result of stuides, the high viscosity of the vegetable oils was reduced and new alternative fuel with lower viscosity was obtained. The new low-viscosity alternative fuel is known as biodiesel [4-5].

Biodiesel is defined as mono alkyl esters of long-chain fatty acids from renewable lipid nutrients as vegetable oils or animal fats by the American Society for Testing and Materials (ASTM) [6]. The higher combustion efficiency than vegetable oil, and contribution to country's energy independence, better lubrication for engine, non-toxic, more reliability in transportation and in storage are advantages of biodiesel. On the other hand, high NO_x emissions, excess fuel consumption and bad cold start performance are disadvantages of it. There are four method to produce biodiesel: pyrolysis, micro-emulsion, dilution and transesterification. Transesterification method has the most common use among of these methods [7-9].

Engine power is associated with the maximum pressure in the cylinder of an ICE. In-cylinder pressure values vary from cycle-to-cycle or from cylinder-to-cylinder. This event is known as cyclic variation. Cyclic variation occur both diesel and gasoline engines. It causes to reduce the engine output power, vibration, noise and unstable operation. Therefore, the cyclic variation is not desired by the engine designers [10]. The change in the movement of the mixture in the cylinder during ignition time, the change in the quantity of the air-fuel mixture during the intake of each cylinder, and the differences between the exhaust gas and charge mixtures inside each cylinder are reasons of cyclic variation [11].

In this study, the biodiesel performance of sunflower vegetable oil has been examined in terms of cyclical variations. In the study, biodiesel was produced from sunflower oil that purchased from a local grocery store. Sunflower biodiesel was used in diesel engine as fuel. Sunflower biodiesel was used both as a mixture at different ratios (20% biodiesel+80% diesel (B20) and 50% biodiesel+50% diesel (B50)) and pure (100% biodiesel (B100)). In-cylinder pressure values were determined for each fuel type. Finally, these values were analyzed by Wavelet analysis method and the effect of biodiesel on cyclic variations was investigated.

Wavelet Analysis Method

It is difficult to analyze of any situation by examining a time series is difficult because of many periodic components. The data must be moved to the frequency domain from the time domain. Frequency domain provides information about the signal and the physical forces. Many mathematical methods such as Wigner distribution, Fourier transform, Hilbert transform, Radon Transform translate a signal from the time domain to the frequency domain. Fourier Transform is the most commonly used all among them. [12-14].

Fourier Transform calculate the different frequency of a signal. Fourier Transform converts the signal from the time domain to the frequency domain. If the signal is converted to the frequency domain, much characteristic information in the time domain is lost. That is, the moment of a special event cannot be detected in the Fourier Transform. If the time domain characteristics of a signal don't change over time, this disadvantage is not important. But, many signals have important critical irregularities that can be the central focus of the analysis. Wavelet Analysis Method (WAM) is used to eliminate this drawback of the Fourier transform. The WAM determines the time of sudden changes in the signal such as broken time, edge detection, space, etc. [15]. The WAM carries a signal from time-frequency domain to time-scales domain different from Fourier Transform. The domain is defined with windows and cannot used signal lines [16].

The start of WAM was introduced in 1805 by Joseph Baptiste Fourier. Alfred Haar used first wavelet word in his doctoral thesis in 1909. The main principle of this theory was first determined by a study group of Marseille Theoretical Physics Centre that was directed by Alex Grossmann and Jean Morlet in 1985 [17].

The most important property of the WAM can be analyzed of signal locally. The basis of WAM is wavelet functions. They are are used to analysis orthogonal or non-orthogonal functions [18].

A wavelet function ($\psi(t)$) should have zero mean and finite energy in equation 1 [19].

$$(\int_{-\infty}^{+\infty} \psi(t)dt = 0), (\int_{-\infty}^{+\infty} \psi^2(t)dt < \infty) \quad (1)$$

The wavelet functions in the WAM process is a effective wave in the limited time. A wavelet function is obtained via changing of translation parameter (τ) and scale parameter (s) from a mother wavelet (ψ). There are 15 different kinds of mother wavelet functions. Some of commonly used are Morlet, Meyer, Haar, Mexican Hat, and Gaussian. Each function has different properties [18].

Energy of signal at certain scale and certain time interval was determined Wavelet Power Spectrum (WPS). WPS represents the temporal variations and fluctuations at various scale and frequency. The additional information about the spectral properties of a time series is obtained Global Wavelet Spectrum (GWS). GWS is average of WPS on a signal. Otherwise, Cone Effect is used to eliminate the error in the time series. Therefore, values outside of cone effect is unreliable.

Experiments

This study has been carried out in three stages including biodiesel production, motor testing and analysis of the obtained results in the wavelet analysis method.

1. Biodiesel Production

Biodiesel production is performed by transesterification method (alcoholysis). It is a reaction between alcohol and triglycerides (main component of the oils) with the presence of a catalyst. Sunflower oil purchased from a grocery store was used as oil feedstock. Methyl alcohol (CH_3OH) was used as alcohol and potassium hydroxide (KOH) as the catalyst in the reaction. Alcohol is used 20% by volume and catalyst is used 1% by mass at the temperature of 56°C in 60 minutes in a glass reactor (Fig. 1). A mixture of two phases was obtained at the end of the reaction. The mixture contains biodiesel, glycerol, catalyst, alcohol and other substances (tri-di-mono glyceride etc.). Therefore, purification procedure was needed to obtain pure biodiesel from the mixture. During the purification steps glycerol, catalyst, water and excess methyl alcohol were removed the biodiesel (Fig. 2a, 2b and 2c).



Figure 1. Experimental setup for biodiesel production

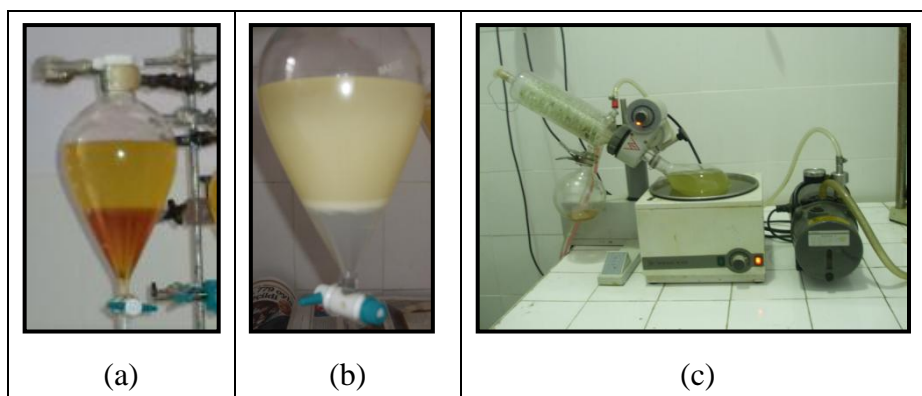


Figure 2. Purification procedure

2. Engine Test

Engine tests are carried out with a 4-stroke 2 cylinders direct injection diesel engine (SuperStar, Motosan Motor Sanayi ve Ticaret A.Ş., Istanbul/Turkey), with 1/17 compression ratio, 1.54 dm³ cylinder volume, and power of 28 hp. A quartz pressure transducer (Kistler 6117BDF17) was placed combustion chamber of only one cylinder. The crank shaft angle was measured with an optical devices. The pressure data and crank shaft angle data were stored in a personal computer with the help of a data acquisition card (National Instruments, M series, 6250 model, 1.25 MS/s DAQ). The cyclic variations were analysed with WAM via the data. Pressure data were obtained at 1400 rev/min engine speed.

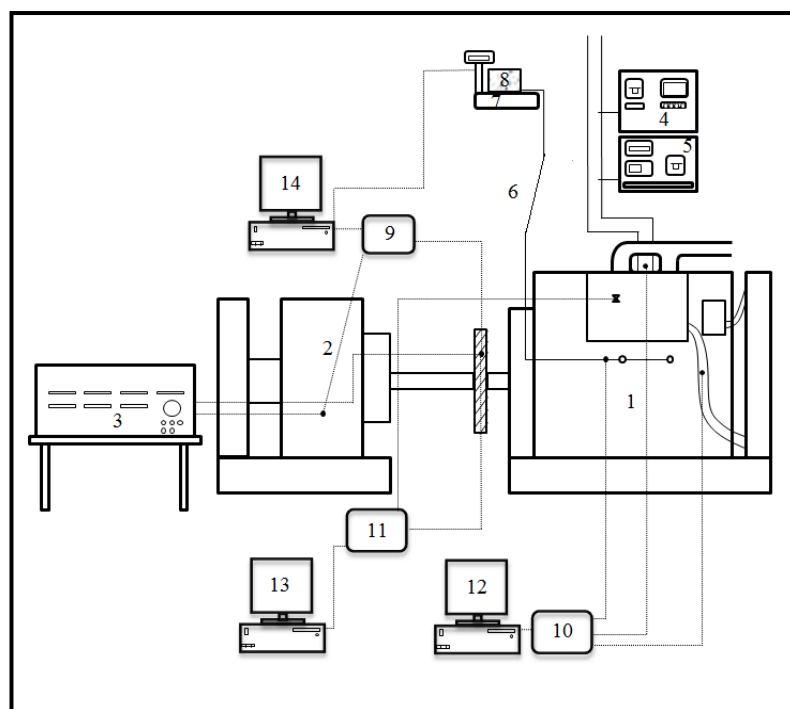
DF (diesel fuel), B100 (100% biodiesel), B50 (50% biodiesel and 50% diesel), and B20 (20% biodiesel and 80% diesel) as fuel were used in the engine test. All experiments were repeated three times at the same conditions. Results were compared with each other. The schematic experimental setup for engine tests is shown in Figure 3.

3. Wavelet Analysis Method

In this section, the in-cylinder pressure signals (P_{mi}) obtained from engine tests were analyzed via WAM and the effect of sunflower biodiesel on cyclic variations was examined. Morlet wavelet, a good compatibility between frequency and time, with central frequency of $\omega_0=6$ was preferred in the WAM. All results were compared.

Results

The physical and chemical properties of the sunflower oil and the sunflower methyl esters are determined in Malaya University (Kuala Lumpur/Malaysia). Euro-diesel fuel sold Petrol Ofisi Company was used in the engine test. The euro-diesel fuel properties was provided by the same Company. The physical and chemical properties of the sunflower oil, the sunflower biodiesel, and the euro-diesel are given in Table 1.



- | | |
|----------------------|----------------------|
| 1 Engine | 8 Fuel Tank |
| 2 Hydrolic brake | 9 Crank Pos. Sensor |
| 3 Control Unit | 10 Temprature Sensor |
| 4 Exhaust Emiss.Equ. | 11 Pressure Sensor |
| 5 Soot Meter Equ. | 12 PC |
| 6 Fuel Line | 13 PC |
| 7 Scales | 14 PC |

Figure 3. Schema of the engine system

Table 1. Physical and chemical properties

Properties	Sunflower Oil	Sunflower Biodiesel	Diesel*
Heat Value(kJ/kg)	39583	39913.5	45951
Dyn. Visc. (40°C) (mpa.s)	28.954	3.6596	2.4257
Kin. Visc. (40°C) (mm ² /s)	31.945	4.2162	2.9542
SFTN (°C)	11	-2	-6
Flash Point (°C)	238	162	56
Density (g/cm ³)	0.9064	0.8862	0.8211
Cetane Number	-	46.8	51

* Obtained from Petrol Ofisi Company

The cetan number of biodiesel was determined by a formula that is developed with Multi-Linear Regression (MLR) with $R^2=0.9191$ [20].

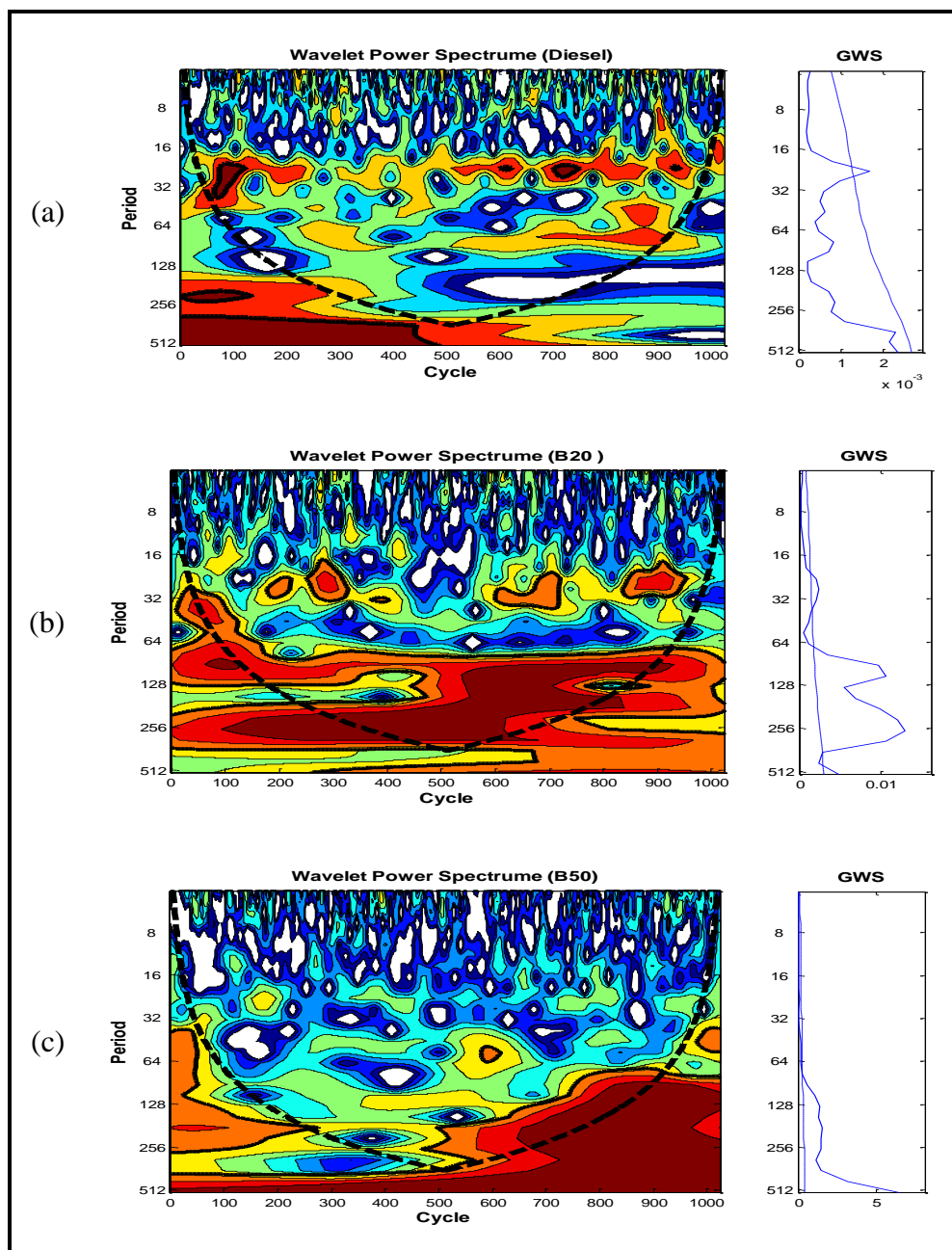
$$\text{CN} = 56.16 + 0.07.La + 0.1.M + 0.15.P - 0.05.Pt + 0.23.S - 0.03.O - 0.19.Li - 0.31.Ln + 0.08.Ei + 0.18.Er - 0.1.Ot \quad (2)$$

The pressure analysis results in the WAM are shown in Figure 4 for diesel, B20, B50, and B100 respectively. There is a periodicity in a narrow region between 16-34 periods for diesel fuel. There is periodicity in band 32 for B20 fuel but there is no significant periodicity in the B50 fuel. B100 fuel has significant periodicity both in the 32 period and in the between 64-128 period band.

It is shown in Figure 4 that cyclic variations is increased with using of sunflower biodiesel in the diesel engine. Specially, When pure biodiesel (B100) used in the diesel engine, adverse effect of cyclic variation was increased prominently.

Conclusion

In this study, the effect of sunflower biodiesel on cyclic variation was investigated. Therefore, it was analysed engine performance of sunflower biodiesel that produced from sunflower vegetable oil. Obtained biodiesel was used pure form (B100) and mixture form with diesel (B20, B50) on the diesel engine. In-cylinder pressure values were saved for all fuels and diesel fuel. The values were analysed Wavelet Analysis Method to describe cyclic variations. All results were shown as graphical and were compared each other. As a results, it was found that the effect of sunflower biodiesel on cyclical differences was poor. Specially, cyclic variations were increased in B100 fuel prominently.



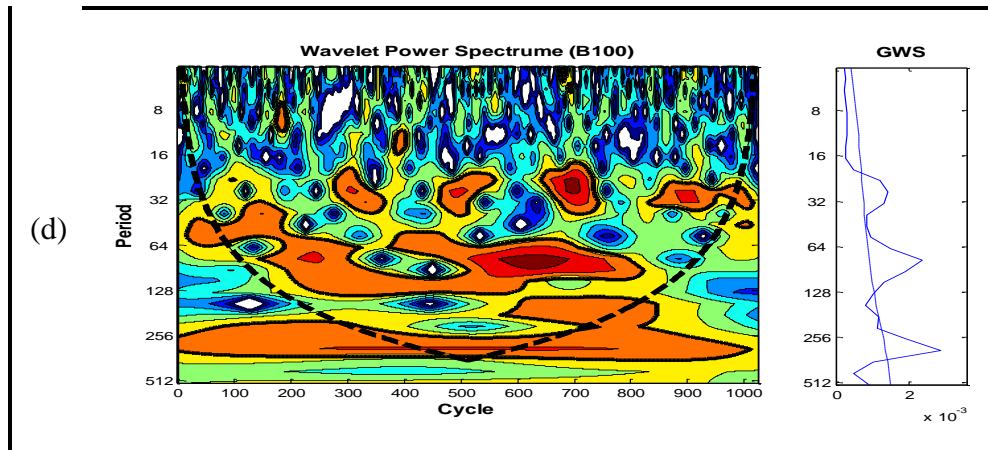


Figure 4. Wavelet Analysis of Pmi (a)euro diesel, (b)B20, (c)b50, (d)B100

References

- [1] International Energy Agency. (2015). 2014 Key World Energy Statistics.
- [2] Lin, Cherng Yuan, and Hsiu An Lin. "Engine performance and emission characteristics of a three-phase emulsion of biodiesel produced by peroxidation." *Fuel Processing Technology*, no. 88 (2007): 35-41.
- [3] Lin, Cherng-Yuan, and Hsiu-An Lin. "Effects of NO_x-inhibitor agent on fuel properties of three-phase biodiesel emulsions." *Fuel Processing Technology*, no. 89 (2008): 1237-1242.
- [4] Agarwal, A. K. (2007). Biofuels (alcohols and biodiesel) applications as fuels for internal combustion engines. *Progress in Energy and Combustion Science*, 33, 233-271.
- [5] Lin, L., Cunshan, Z., Vittayapadung, S., Xiangqian, S., & Mingdong, D. (2011). Opportunities and challenges for biodiesel fuel. *Applied Energy* (88), 1020-1031.
- [6] Hoekmana, S. K., Broch, A., Robbins, C., Cenicerros, E., & Natarajan, M. (2012). Review of biodiesel composition, properties, and specifications. *Renewable and Sustainable Energy Reviews* (16), 143-169.
- [7] Balat, M., & Balat, H. (2010). Progress in biodiesel processing. *Applied Energy* (87), 1815–1835.
- [8] Mwangi, J. K., Lee, W.-J., Chang, Y.-C., Chen, C.-Y., & Wang, L.-C. (2015). An overview: Energy saving and pollution reduction by using green fuel blends in diesel engines. *Applied Energy* (159), 214–236.
- [9] Rasimoglu, N., & Temur, H. (2014). Cold flow properties of biodiesel obtained from corn oil. *Energy*(68), 57-60.
- [10] Ceviz, M. Akif, Asok K. Sen, Alp K. Küleri, and İ. Volkan Öner. "Engine performance, exhaust emissions, and cyclic variations in a lean-burn SI engine fueled by gasoline/hydrogen blends." *Applied Thermal Engineering*, no. 36 (2012): 314-324.
- [11] Heywood, J. B. (1988). "Internal Combustion Engine Fundamentals." Singapore: McGraw-Hill.
- [12] Şükran Efe, M.A. Ceviz "Investigation of the Effect of Canola Methyl Ester on Cyclic Variation Using Wavelet Analysis Method" *Sustainable Aviation Energy and Environmental Issues*. Chapter-3. (2016): 17-25
- [13] Oppenheim, Alan V., Alan S. Willsky, and S. Hamid Nawab. *Signals & Systems*. 2. Prentice Hall, 1997.

-
- [14] Proakis, John G., ve Dimitris G. Manolakis. Sayısal sinyal işleme ilkeler, algoritmalar ve uygulamalar. Çeviren Özgül Salor, Abdurrahman Karamancıoğlu, Nurhan Karabğa, Halis Altun, & Remzi Yıldırım. Nobel, 2010.
- [15] Valens, C. "A really friendly guide to wavelets." 1999.
- [16] Graps, Amara, 2006
http://www.google.com.tr/url?sa=t&rct=j&q=&esrc=s&source=web&cd=1&ved=0CCAQFjAA&url=http%3A%2F%2Fwww.cis.udel.edu%2F~amer%2FCISC651%2FIEEEwavelet.pdf&ei=YmcxVY61A9PcaPPrgagG&usg=AFQjCNHyw_eZctNUgpEi5ScvTq7N3-py8A&bvm=bv.91071109,d.bGg&cad=rja
- [17] Abbak, R. Alpay. Jeodezide Zaman Dizilerinin Dalgacık (Wavelet) Analizi. PhD Semposium, Konya/Turkey. http://193.255.101.90/~aabbak/pubs/Phd_seminar.pdf, 2007.
- [18] Torrence, Christopher, and Gilbert P. Compo. "A practical guide to wavelet analysis." Bulletin of the American Meteorological Society 1 (January 1998).
- [19] Sen, Asok K., Grzegorz Litak, Rodolfo Taccani, and Robert Radu. "Wavelet analysis of cycle-to-cycle pressure variations in an internal combustion engine." Chaos, Solitons and Fractals, no. 38 (2008a): 886–893.
- [20] Piloto-Rodríguez, Ramón, Yisel Sánchez-Borroto, Magin Lapuerta, Leonardo Goyos-Pérez, and Sebastian Verhelst. "Prediction of the cetane number of biodiesel using artificial neural networks and multiple linear regression." Energy Conversion and Management, no. 6 (2013): 255-261.



Chapter – 2

Fire

Tasarım yangın yükü hesaplarının ve yanıcılara ait kalorifik değerlerin yapı yönetmelikleri ve tasarım kılavuzları ışığında kıyaslanması

Comparison of the design fire load methodologies and calorific values of the combustible materials in the light of various design guidelines and handbooks

Erkan AKPINAR¹, Erdem YILDIRIMLAR¹, Necmi C. ÖZDEMİR²

¹ Kocaeli Üniversitesi, İnşaat Mühendisliği Bölümü, Kocaeli

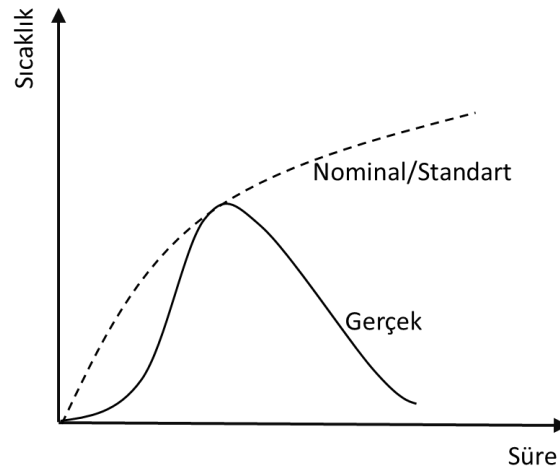
² Kocaeli Üniversitesi, Elektrik Mühendisliği Bölümü, Kocaeli

Özet: Yangın, hayatın doğal seyrini büyük ölçüde olumsuz etkileyen önemli felaketler arasında yer almaktadır. Yangın durumu ve yüklemesi, ülkemizde maalesef ki yapılar ve inşaat mühendisliği açısından birincil sırada göz önüne alınan etki ve yük grupları arasında gerekli yeri henüz bulamamıştır. Yangın durumu ve etkisi çeşitli ülkelerde yapı yönetmelikleri ve tasarım kılavuzlarında, başlıca bir bölüm olarak değerlendirilmekte ve göz önüne alınmaktadır. Bu çalışmada, olası yangın durumunda yapılara etkileyen ilgili yüke ilişkin hesap esasları ve bu yüke neden olan yanıcıların kalorifik değerleri, farklı yapı yönetmelikleri ve tasarım kılavuzları ışığında karşılaştırılmalı olarak incelenmiş ve yapılan değerlendirme ile farklılıklar ortaya konulmuştur.

Abstract: Fire is one of the catastrophic disasters which could alter the daily life severely. Fire condition as a limit state for the design process of the structures and fire load as a loading condition, unfortunately, does not consider one of the leading design condition and parameter among the other primary limit states in Turkey. Incident of fire and design for such condition are taken into account as one of the main titles, even considered as a separate chapter in modern design codes and manuals those are in charge in almost all developed countries. In this paper, the calculation steps of fire load that effects the structures and the calorific values of combustible materials of which role is major for the fire load were investigated according to several design codes and manuals as well as the variations among such expressions and parameters were evaluated.

Giriş

Yangın, gündelik yaşamı olumsuz etkileyen önemli felaketlerden biridir. Kontrol altına alınamadığı durumlarda, önemli ölçüde mal ve hatta can kayıpları yaşanabilmektedir. Günümüz dünyasında modern şehirlerin getirmiş olduğu toplu halde barınma ve yaşama olgusu, aynı çatı altında büyük hacimlerin, orta ve yüksek katlı yapıların inşasını ve kullanımını beraberinde getirmiştir. Genel olarak yapıların yangın güvenliği, olası bir yangın durumunda yapının belirli ve yeterli bir süre ayakta kalabilmesini sağlamak üzerine kurgulanmaktadır. Bu durum, yapıyı oluşturan taşıyıcı elemanların temel olarak süre açısından yangın dayanımını hesaplamak ve olası yangın durumunda yeterli güvenlik süresini doğrulamak yoluyla sağlanmaktadır. Bunun dışında, daha karmaşık ve zahmetli olan, sürecin başından sonuna hesaplandığı, hesaplamalı akışkanlar mekaniğini temel alan ve ortaya çıkan ısı akışının detaylı olarak yapı modeli üzerinde değerlendirildiği daha sofistike bir yöntem de bulunmaktadır. Yapının tümü düşünüldüğünde bu yöntem, zorluğu, zaman ve kaynak açısından ağır külfeti nedenleriyle tercih edilmemekte ve ilk sırada bahsedilen basit yöntem tercih edilmektedir. Yöntemlerin her ikisinde de incelemenin temelini oluşturan yangın büyüklüğünün ve dolayısıyla yangın yükünün ortaya konulması gerekmektedir. Sonrasında, konuya ilişkin yapısal elemanlar üzerinde gerçekleştirilecek tüm hesaplar, olası yangın yükünün başlangıçtaki seçimine ve parametrelerinin belirlenmesine bağlıdır (1, 2).



Şekil 1. Gerçek ve nominal/standart yangınlara ait tipik sıcaklık-süre ilişkisi

Genel olarak, yapıdaki olası gerçek bir yangının gelişim süreci şu şekilde açıklanabilir. İlk olarak yangının gelişim süreci gerçekleşmektedir. Bu aşamada yangın yükünü oluşturan yanıcıların tutuşması gerçekleşmektedir ve kompartıman olarak tanımlanmakta olan yangının geliştiği duvar vb. bölümleyicilerle sınırlı ve göreceli olarak kapalı alanda, bir noktadan diğer bir noktaya sıcaklık önemli farklılıklar göstermektedir. Gelişme aşamasında yangının yayılımı kademeli olmaktadır ve kompartıman içerisinde farklı sıcaklık bölgeleri meydana gelmektedir. Gelişim sürecindeki yangın için merkez bölgede yeteri kadar yanıcı madde bulunması durumunda, kompartıman sıcaklığı giderek artar. Bu süreçte yükselen sıcak dumanın kompartımanın üst bölümünü kaplaması yanan kısımdaki sıcaklığının belirli bir değere erişmesi durumunda (yaklaşık olarak 300°C-500°C arası), kompartımanda bulunan tüm yanıcıların bir anda tutuşması olayı gerçekleşir. Kompartıman bütününe yansıyan bu birden alevlenme ve yanmanın ani olarak genele yayılma noktası (flashover), yapıdaki yangın için kritik bir eşiiktir. Alevlenmenin ani olarak genele yayılması sonrasında kompartımandaki yangının sıcaklığı, içerideki tüm yanıcı maddelerin tutuşması nedeniyle, çok hızlı bir biçimde ulaşabileceği en

büyük değere çıkar ve kompartımanın genelinde yaklaşık eşit olacak bir duruma gelir (Bu değer, müdahale olmadığı durumlarda çoğunlukla 1000°C'yi aşmaktadır). Kompartımanda tüm yanıcı maddelerin tutuşmasının ardından, ortamdaki yanıcı maddelerin tümünün yanmaya başlamasıyla birlikte, bu noktadan itibaren yangın yükünü oluşturan yanıcı maddelerin miktarının giderek azalması sonucunda kompartıman sıcaklığı azalma eğilimine girer. Bu aşama kompartıman yangını için soğuma safhasıdır. Ortamdaki mevcut yanıcı maddelerin yanma özellikleri, dağılımı, kompartımanın büyüklüğü, şekli, sınır elemanlarının termal özellikleri ve havalandırma durumu, olası yangının sıcaklık gelişimini ve belirtilen safhaların sürelerini etkileyen faktörlerdir (1, 2).

Yangın ile ilgili hesapların başlangıç noktasını, yangının kendisine ilişkin parametrelerin belirlenmesi ve olası sıcaklık-süre ilişkisinin tespiti oluşturmaktadır (Şekil 1). Olası yangının, önceki paragrafta açıklanan tüm aşamalarını kapsayacak şekilde, süre sıcaklık ilişkisinin belirlenmesi birçok parametreye bağlıdır. Yapıların yangın dayanımlarının incelenmesindeki bu ilk adım, tüm bu parametrelerin değerlendirilmesi ve hesabının yapılması ile gerçekleştirilebileceği gibi genel olarak basitleştirilerek tanımlanmış nominal sıcaklık-süre ilişkisi de kullanılmaktadır (Şekil 1). Yapıların yangın dayanımı hesaplarında, zaman ve sarf edilen çabanın daha az olmasından dolayı çoğunlukla belirtilen nominal sıcaklık-zaman ilişkisi tercih edilse de bu seçim gerçekten uzak ve konservatif sonuçlara neden olmaktadır. Yangına ilişkin tüm parametrelerin göz önüne alınarak hazırlandığı gerçek sıcaklık-süre ilişkisinin kullanılması ise her ne kadar kendisinin belirlenmesinde çok daha fazla zaman ve yoğun emek harcanması gereksinimi olsa da daha doğru sonuçların elde edilmesine ve yapısal yangın tasarımının eleman boyutlarına yansması anlamında daha ekonomik çözümlere ulaşılmasına izin vermektedir. Sıcaklık-süre ilişkisinin belirlenmesinin ardından, yangının yapı ve yapı elemanları üzerindeki etkilerinin hesaplanması aşaması gerçekleştirilmekte ve olası yangın durumunda, yangın sonunda veya istenilen belirli bir süre yapının güvenli ayakta kalması sağlanmaktadır.

Bu çalışmada, yapısal yangın tasarımının daha doğru ve eleman boyutlaması adına daha ekonomik biçimde yapılmasını sağlayan ve yangına karşı güvenli yapı tasarımının ilk adımını oluşturan, gerçek sıcaklık-süre eğrisinin elde edilme sürecindeki temel parametrelerinden biri olan, yanıcılara ait kalorifik değerlerin ve yangın tasarım yükünün değerlendirilmesi ve karşılaştırılması sunulmaktadır. Bu amaçla konu ile ilgili yönetmelikler (Eurocode 1, 1-2 (3), Handbook on Building Fire Codes – Indian Codes (4)), yangın araştırmalarında söz sahibi uluslararası kuruluşların (Handbook of Fire Protection Engineering – SFPE (5), International Fire Engineering Guidelines – IFEG (6)) hazırladığı kılavuzlar incelenmiştir.

Tasarım Yangın Yükünün Belirlenmesi

Bu bölümde, çeşitli yönetmelik ve tasarım kılavuzlarında tasarım yangın yükü yoğunluğunun tespitine yönelik ifadeler yer almaktadır. Yangın yükü, genel olarak olası yangın durumunda ortamdaki yanıcıların verebileceği toplam enerji miktarı olarak tanımlanmaktadır. Standartlarda ve kılavuzlarda, bu değer hesaplanması, yangın yükü yoğunluğunun, yani birim alana düşen yangın yükünün değerlendirmesi ile gerçekleştirilmektedir. Yapılarda olduğu gibi belirli bir hacim içerisinde gerçekleşebilecek kompartıman yangınlarında tasarım yangın yükü ve yük yoğunluğunun belirlenmesi, temel olarak kompartımandaki yanıcı miktarının tespitine, belirlenen yanıcıların yanma sırasında ne kadar ısı enerjisi verebildiğini gösteren kalorifik değerlerine (1/kg olarak tanımlanmaktadır), yanıcıların tutuşabilme özelliklerine, yangının etkinleşmesine karşı alınmış

önlemlerin durumuna (havalandırma, yangın alarmı ve tespit sistemleri veya su püskürtücüler, insan müdahalesi, duman tahliye sistemleri vd.) ve yangının gerçekleştiği alana bağlıdır (2).

Avrupa Birliği yönetmelikleri kapsamında Eurocode 1, 1-2’de (3), yangın yükü yoğunluğunun hesabında .

$$q_{f,k} = \sum (\psi_i H_{ui} M_i) / A_f \quad (1)$$

$q_{f,k}$: yangın yükü yoğunluğu (MJ/m²).

M_i : i malzemesinin kütlesi (kg).

H_{ui} : i malzemesinin net kalorifik değeri.

ψ_i : i malzemesinin korunan yangın yükünün değerlendirilmesi faktörüdür ve isteğe bağlı olarak göz önüne alınmaktadır. Bu değer 0 (yangının gerçekleştiği süre içerisinde tam koruma) ile 1 (ısı salınımı sırasında korumanın etkisi olmadığı durum) arasında değişir. Çoğu pratik uygulama için bu değerin 1 alınması gerçekçi bir değerdir.

A_f : kompartımanın taban alanı (veya kompartıman iç yüzey alanı $A_{t,i}$). Kullanılan alan parametresine göre yangın yükü yoğunluğunun değerlendirme büyüklüğü değişmekte, yangın yoğunluğu taban alanı veya toplam yüzey alanı olarak ayrı ayrı değerlendirilmektedir.

Eurocode1, 1-2 (3) uyarınca, Denklem 1’de belirtilen ifade ile karakteristik yangın yükü belirlendikten sonra, tasarıma esas yangın yükü değeri yapının kullanım özellikleri ve yangına karşı mevcut önlemler göz önüne alınarak belirli katsayılarla revize edilerek, tasarım yangın yükü belirlenir.

$$q_{f,d} = \delta_{q1} \delta_{q2} \delta_n m_i q_{f,k} \quad (2)$$

$q_{f,d}$: tasarım yangın yükü yoğunluğu (MJ/m²)

δ_{q1} : kompartıman alanına bağlı yangın risk faktörü. Daha büyük alana sahip kompartımanlarda, yangın şiddetinin daha büyük olması durumunu hesaba dahil eden katsayı. Tablo yardımı ile elde edilmekte olup, ara değerler logaritmik interpolasyon yapılır.

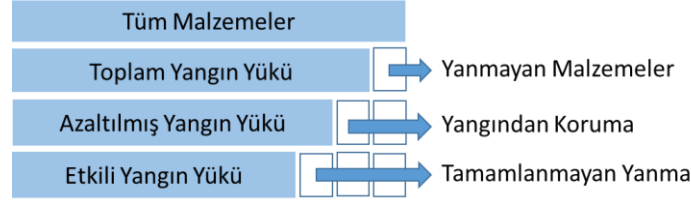
δ_{q2} : kompartıman kullanım amacına bağlı yangın risk faktörü. (Tablodan alınmaktadır)

δ_n : kompartımanda bulunan yangınla aktif mücadele önlemlerinin etkisini hesaba dahil eden katsayısı. Yapıda bulunabilecek 10 adet aktif yangınla mücadele önlemine ilişkin yönetmelikte verilen seçeneklere göre değişmekte olan değerlendirme katsayılarının çarpımına eşittir. Bu aktif önlemler, otomatik su ile söndürme sistemi, su besleme hattı miktarı, ısı algılamalı otomatik yangın detektörü, duman algılamalı otomatik yangın detektörü, itfaiyeye otomatik uyarı sistemi, itfaiyeye varlığı ve yakınlığı, güvenli erişim rotası kuralları, ilk müdahale aletlerinin varlığı, merdivenlerde duman tahliye sistemi varlığı şeklinde sıralanmıştır.

m_i : tanımlanan malzemenin yanma faktörü (selülozik maddeler için genelde 0.8 alınır).

Yangından Koruma Mühendisleri Birliği’nin (SFPE) hazırlamış olduğu Yangından Koruma Mühendisliği El Kitabı’nda (5) yangın yükü, temel olarak aynı prensiplere bağlı olarak hesaplanmaktadır. SFPE El kitabına göre yangın yüküne ilişkin değerlendirme, aynı belgede yer almakta olan Şekil 2’de yer alan şemaya göre yapılmaktadır. Yapıda oluşabileceği öngörülen kompartıman yangınında, kompartımandaki tüm malzemelerin yanıcı olamayacağı, yanıcı olan kısmın

belirli bir oranının yangın koruma önlemleri ile yanma aşamasına geçemeyeceği, yangına dahil olan yanıcıların da bir kısmının da tamamen yanamayacağı öngörüsüyle, kalan yanıcı malzemeler üzerinden etkili yangın yükü değerlendirmesi gerçekleştirilmektedir (5).



Şekil 2. Yangın yüküne ilişkin değerlendirmenin genel hatları (5)

SFPE el kitabında (5) yangın yükü hesabı, Denklem 3 ile tanımlanmaktadır. Kompartımandaki yanıcı malzemelerin değerlendirilmesi, ilgili malzemelerin üretim ve yanıcılık özelliklerine göre yapılmaktadır ve bu aşamada malzeme standartlarından yararlanılmaktadır. Günümüzde malzeme kullanımında, malzemelerin yanıcılık ve yangına durumunda gösterdikleri reaksiyon, testler sonucu belirlenmiş ve sınıflandırılmış durumdadır. İlgili yönetmelikler yangın yükü hesaplarında kullanılmaktadırlar. Buna göre SFPE el kitabında (5), Şekil 2’de gösterilen şema doğrultusunda azaltılmış yangın yükü değerleri, Denklem 4 uyarınca belirlenmektedir.

$$q = \sum (m_i H_i) / A \quad (3)$$

q : bölmenin içerisindeki yangın yükü yoğunluğu (toplam yangın yükü)
 m_i : yanıcı i malzemesinin kütlesi (kg)
 H_i : i malzemesinin kilogram başına düşen yanma ısı veya kilogram başına yanma sırasında salınan özgül enerji (MJ/kg – bu çalışmadaki genel ifadeyle kalorifik değer)
 A : yangın bölmesinin alanı (ilgili belgede alan olarak kompartıman taban alanı ve yüzey alanı ayrı ayrı ifade edilmiştir)

$$q = q_{\text{korunmayan}} + \sum (\psi_{p,i} q_{i,\text{korunan}}) \quad (4)$$

$q_{\text{korunmayan}}$: yangına karşı korunma bulunmayan malzemelerin yangın yükü yoğunluğu
 $q_{i,\text{korunan}}$: yangına karşı korunma bulunan malzemelerin yangın yükü yoğunluğu
 $\psi_{p,i}$: yangına karşı korunma işlemindeki azalma çarpanı (0 ile 1 arasında değişmektedir)

Kompartımanda mevcut malzemelerin özelliklerine göre tamamında yanma işlemi gerçekleşmeyebilir (ahşap malzemenin dışının yangın sırasında kömürleşerek doğal koruma sağlaması gibi). Bu etki sadece malzeme özelliklerine bağlı olmayıp, yanıcı malzemenin geometrik özelliklerine ve bulundukları konuma da bağlıdır. Bu durum göz önüne alındığında kompartımanda bulunan malzemelerin yanmaya katılımları, genelde bütün olarak gerçekleşmemektedir ve etkili yanma miktarı ile buna bağlı etkili yangın yükünün değerlendirilmesi gerekmektedir. SFPE el kitabında (5) bu durum Denklem 5 ile gösterildiği biçimde ifade edilmiştir. Bu değer Eurococe 1 1-2’de (3) yer alan m_i katsayısı ile karşılaştırılabilir.

$$q_{\text{eff}} = \chi q \quad (5)$$

q_{eff} : efektif yangın yükü yoğunluğu

χ : malzemenin tutuşma faktörü
 q : düşürülmüş yangın yükünden gelen yangın yükü yoğunluğu

Kanada, Amerika Birleşik Devletleri, Yeni Zelanda ve Avustralya ülkelerinin yapı şartnamelerini hazırlayan kurumlarınca oluşturulan kurul tarafından hazırlanan ve adı geçen ülkelerdeki pratiği göz önüne alan Uluslararası Yangın Mühendisliği Kılavuzu'nda (IFEG, 6) da Denklem 3'de yer alan hesap ilkesi yer almaktadır. Gerek SFPE'nin el kitabında (5) gerekse belirtilen Uluslararası Yangın Mühendisliği Kılavuzu'nda (6) kullanılan kalorifik değerler, nem açısından normal değerleri ifade etmektedir.

Hindistan standartları içerisindeki yapısal yangınla ilişkili kodlarda yangın yükü değerlendirmesi, detaylı formülasyonlar yerine doğrudan tablolaştırma yoluyla verilmektedir. Söz konusu değerler Tablo 1'de görülmekte olup bu değerler, aynı miktarda ahşabın vereceği yangın yüküne olan oranı ifade eden, ahşap eşdeğeri şeklinde ifade edilmiştir (4).

Tablo 1. Hint yönetmeliklerinde yangın yükü yoğunluğu tablosu (4)

Yapı Türü	Yangın Yükü Yoğunluğu (ahşap eşdeğeri kg/m ²)
1. Konut (A1 & A2)	25
2. Konut (A3'den A5'e)	25
3. Enstitü ve Okul (B & C)	25
4. Assembly (D)	25-50
5. Business (F)	25-50
6. Mercantile (F)	250'ye kadar
7. Endüstriyel (G)	150'ye kadar
8. Depo ve Riskli (H & J)	500'e kadar

Tablo 1'de verilen değerler için bazı sınırlamalar bulunmaktadır. A1, A2, G3 ve H & J kullanımlarına 15 metreden yüksek yapılarda; B, C, D & F kullanımlarına 30 metreden yüksek yapılarda; G kullanımlarına 18 metreden yüksek yapılarda; A3 ve A4 kullanımlarına 60 metreden yüksek yapılarda izin verilmemektedir. Ayrıca A5, A6 ve E için yükseklik sınırı yoktur. Bunlara ilave olarak ilgili tablonun kullanımında, kapı veya pencere açıklığının maksimum genişliği veya yüksekliği 2.75 m olacak şekilde, alanı 5.6 m²'den fazla olmamalıdır.

Farklı Yanıcı Malzemelere Ait Kalorifik Değerler

Bu bölümde, yangın yükü ve yangın yükü yoğunluğu hesabına temel teşkil eden, yangının büyüklüğüne ve süresine etki eden önemli etkenlerden biri olan bazı malzemelere ait kalorifik değerler, çalışmada incelenen yönetmelik ve kaynaklar ışığında verilmiştir. Kalorifik değer, ilgili malzemenin birim ağırlığına denk gelen (kilogram), yanma sırasında açığa çıkartacağı özgül enerji (MJ/kg) olarak tanımlanmaktadır. Eurocode 1 1-2 (3), Uluslararası Yangın Mühendisliği Kılavuzu (IFEG, 6), Yangından Koruma Mühendisliği El Kitabı (SFPE, 5) ve Hindistan Standartlarında (4) yer

alan aynı malzemelere ilişkin kalorifik değerler, Tablo 2’de görülmektedir. Tabloda ayrıca, Hint Yönetmeliklerindeki genel yaklaşım olan ve akla yakın derecelendirme ile karşılaştırma imkanı sunan, ahşap eşdeğeri kalorifik değerleri de verilmiştir. Tablo 2’de, sunulan kalorifik değerler açısından aynı malzeme için en büyük değer, koyu renk ile gösterilmiştir.

Tablo 2. Tipik malzemeler ait kalorifik değerler (MJ/kg)

	Eurocode1 1-2 (3)	Uluslararası Yangın Mühendisliği Kılavuzu (6)	Yangından Koruma Mühendisliği El Kitabı (5)	Hint Yönetmelikleri (4)	Ahşap Eşdeğeri (4)
Katılar					
Antrasit	30	34	30,5-34,2	28,6	1,66
Asfalt	40	41	-	38,3	2,13
Bitümen	-	42	-	33,4	1,9
Karbon	30	-	32,8	32,1	1,83
Selüloz	-	17	16,12	16,5	
Mangal kömürü	30	35	33,2-34,2	28,4	1,61
Kıyafetler	20	19	-	-	-
Kömür/Kok kömürü	30	31	28-31	27,5	1,56
Mantar tıpası	20	29	26,1	-	-
Pamuk	20	18	16,5-20,4	15,8	0,9
Deri	20	19	18,2-19,8	17,6	1
Muşamba	20	20	-	-	-
Kağıt	20	17	16,3-17,9	15,4	0,88
Parafin mumu	-	47	46,2	39,6-44	2,3-2,5
Turba	-	-	16,7-21,6	20,9	1,19
Kauçuk köpük	-	37	33,9-40,6	-	-
Kauçuk lastik	30	32	32,6	37,4	2,13
İpek	20	19	-	-	-
Hasır/saman	20	16	15,6	13,2	0,75
Ahşap	17,5	18	18-20	17,6	1
Yün	20	23	20,7-26,6	19,6-21,6	1,11-1,23

Tablo 2-Devamı. Tipik malzemeler ait kalorifik değerler (MJ/kg)

	Eurocode1 1-2 (3)	Uluslararası Yangın Mühendisliği Kılavuzu (6)	Yangından Koruma Mühendisliği El Kitabı (5)	Hint Yönetmelikleri (4)	Ahşap Eşdeğeri (4)
Sıvılar					
Benzin	45	44	44,1	41,6	2,36
Dizel	45	41	-	-	-
Keten tohumu yağı	-	39	39,3	-	-
Metanol	30	20	19,8	-	-
Zift (katran)		38	-	35,2	2
Heksan	-	-	44,4	44,9	2,55
Oktan	-	-	44,8	45,3	2,58
Pentan	-	-	45,3	46	2,61
Aseton	-	-	30,8	29,7	1,69
Asetaldehit	-	-	25,07	25,1	1,43
Benzen	40	40	39,9	39,6	2,25
Benzil alkol		33	32,93	-	-
Etil alkol	30	27	-	28,4	1,61

Gaz yağı	-	-	43,1	42,9	2,44
Selüloz asetat	-	-	18,8	17,8	1,01
Gazlar					
Asetilen	-	48	48,2	-	-
Bütan	50	46	45,7	47,1	2,68
Karbon monoksit	-	10	10,1	-	-
Etan	50	-	47,4	49,1	2,79
Etilen	45	-	47,17	47,7	2,71
Formaldehit	-	-	17,3	17,6	1
Büten	45	-	45,3	-	-
Hidrojen	-	120	119,9	134,2	7,63
Propan	50	46	46,3	47,3	2,69
Metan	50	50	50	52,8	3
Etanol	30	27	26,8	-	-
Plastikler	-	-	-	-	-
ABS (plastik)	35	36	-	-	-
Akrilik	-	28	30,7	-	-
Selüloid	-	19	16,4-19,2	-	-
Epoksi	-	34	31,43	-	-
Fenol formaldehit	-	29	27,9-31,6	-	-
Polyester	30	31	-	22	1,25
Polietilen	40	44	43,1	48,4	2,75
Polistiren	40	40	39,7	41,8	2,38
Poliizosiyanurat köpük	-	24	22,2-26,2	-	-
Polikarbonat	-	29	29,78	-	-
Polipropilen	40	43	43,2	48,4	2,75
Poliüretan	-	23	22,7	35,2	2,00
Polyurethane foam	-	24	22,2-26,2	-	-
Polivinilklorür (PVC)	20	17	16,9	20,9	1,19
Formaldehit üre	-	15	14,61	-	-
Formaldehit üre köpük	-	14	14,8	-	-
Propilen	45	-		46,2	2,53
Polyamid (nylon)	-	-	26,19	22	1,25
Polimetilmetakrilat	-	-	24,88	24,6	1,4

Sonuçlar

Bu çalışmada, yapılarda kompartıman türü yangına karşı güvenlik için gerçekleştirilen hesapların ve değerlendirmenin temelini oluşturan, yangın yükü/ yangın yük yoğunluğu hesapları ve yanıcı malzemelere ait kalorifik değerler, çeşitli şartname ve klavuzlar ışığında karşılaştırmalı olarak sunulmuştur. Yangın yükü ve yangın yük yoğunluğu genel olarak incelenen tüm belgelerde, yanıcı malzemelerin miktarı ve bu malzemelere ilişkin, yangın sırasında özgül enerji yayma potansiyeli olan kalorifik değerleri ile çarpımından elde edilmektedir. Bunun dışında yangın yükünü belirleyen diğer faktörlerin, incelenen belgelerde farklı ölçülerde hesaba dahil edildiği görülmüştür. Yanıcı malzemelere ilişkin yanma özelliklerinin, tam yanma durumunun ve malzemelerin yangına karşı korunmuş olması konularının en etkili biçimde Yangından Koruma Mühendisliği El Kitabı'nda (SFPE, 5) yer aldığı görülmüştür. Bununla birlikte incelen belgeler arasında, yangın risk belirlemesinin ve yangına karşı yapıda bulunan aktif koruma etkenlerinin en etkili biçimde Eurocode 1 1-2'de (3) hesap yöntemine dahil edildiği anlaşılmıştır. Bu durumun, Eurocode 1 1-2'ye (3) göre yangın yükü tasarımını daha gerçekçi hale getirdiği düşünülmektedir. Hint yönetmeliklerin de ise

yangın yükü hesabının, oldukça basit hale getirilmiş olduğu, sadece tablodan seçim işlemine dayandığı, bu durumun da güvenilirlik ve kesinlik açısından soru işaretleri uyandırdığı öngörülmektedir. Kalorifik değerler açısından incelenen belgelerin farklılık gösterdiği, bununla birlikte genel olarak değerlerde çok büyük farklılıkların olmadığı tespit edilmiştir (Bazı tekil değerlerde %20'lere varan farklar bulunmaktadır). Buna rağmen test sonuçları ile elde edilmiş olan bu rakamlarda, küçük de olsa farklılıkların bulunması dikkat çekicidir. Test ortamının ve şartlarının farklılığının bu sonuca yol açtığı düşünülmektedir.

Referanslar

- [1] Structural Fire Loads - Theory and Principles, (2012) Razdolsky, L., The McGraw-Hill Companies
- [2] Structural Design For Fire Safety, Andrew H. Buchanan and Anthony K. Abu, 2017, John Wiley & Sons, Ltd.
- [3] EN 1991-1-2 (2002). Eurocode 1: Actions on structures - Part 1-2: General actions - Actions on structures exposed to fire. CEN, European Committee for Standardization, Brussels, Belgium
- [4] Handbook on Building Fire Codes, IITK-GSDMA-Fire05-V3.0, (2005) Menon, G.B., Vakil, J.N., Final Report, IITK-GSDMA Project on Building Codes
- [5] Handbook of Fire Protection Engineering, (2016) Society of Fire Protection Engineers - SFPE, Springer
- [6] International Fire Engineering Guidelines (2005th ed.), Ramsay, G.C., He, Y., Taylor, P., Horason, M., and Verghese, D. Canberra, A.C.T: Australian Building Code Board

Yangın ve patlama potansiyeli olan tehlikeli ekipmanların belirlenmesi: dow indeksi

Merve ERCAN KALKAN¹, Kadriye OKTOR², Necmi ÖZDEMİR³

¹Kocaeli Üniversitesi Mühendislik Fakültesi Kimya Mühendisliği Bölümü

²Kocaeli Üniversitesi Mühendislik Fakültesi Çevre Mühendisliği Bölümü

³Kocaeli Üniversitesi Mühendislik Fakültesi Elektrik Mühendisliği Bölümü

Özet: Büyük endüstriyel kazalar, olma olasılıkları düşük, ancak gerçekleşmeleri halinde etkileri yıkıcı olabilecek olaylardır. Büyük endüstriyel kazalar genellikle yangın, patlama ve toksik yayılım şeklinde meydana gelmektedir. Özellikle yangınlar, taşıdıkları yüksek ısı akısı potansiyeli nedeniyle diğer ekipmanları da etkileyebilmekte ve bu nedenle patlama ve toksik yayılım gibi ikincil ve hatta üçüncül olayların oluşmasına da neden olabilmektedir. Yangın risklerinin proaktif olarak yönetilmesi ise yangın potansiyeli taşıyan ortamların belirlenmesi ile mümkündür. Dow Yangın ve Patlama İndeksi, bu amaçla yaygın olarak kullanılan bir metodolojidir. Yöntem, prosese ilişkin genel ve özel tehlikeleri dikkate alırken, aynı zamanda kimyasal maddelerin doğası gereği taşıdığı sağlık tehlikesi, reaktivite ve yanıcılık gibi unsurları da hesaba katmaktadır. Prosese ilişkin genel tehlikeler birçok prosese uygulanabilecek altı öğeden oluşmaktadır. Bunlar ekzotermik kimyasal reaksiyonlar, endotermik prosesler, malzeme aktarımı ve transferi, kuşatılmış (etrafı çevrili) veya kapalı alanlar, erişim, drenaj ve döküntü kontrolüdür. Yangın ve patlama olaylarının temel nedeni olarak görülen özel proses koşulları ise toksik (zehirli) malzemeler, atmosferik basıncın altında çalışma, alevlenme aralığında veya yakınında çalışma, toz patlamaları, güvenli tahliye basıncı, düşük sıcaklık, alevlenebilir/kararsız madde miktarı, korozyon ve aşınma, sızıntı (bağlantı yerleri ve ambalajlama), ateşli ekipmanların kullanımı, sıcak yağlı ısı değiştirici sistemleri ve döner ekipman kullanımı olarak dikkate alınmıştır. Genel ve özel proses tehlikelerinin metodolojiye uygun olarak hesaplanması ile elde edilen değerler, malzeme faktörü birlikte hesaplanır, böylece yangın ve patlama indeksi değeri nitel ve nicel olarak elde edilir. Bu değer, seçilen proses ekipmanının yangın ve patlama açısından olası risklere karşı önceliklendirilmesinde kullanılır. Bu çalışmada, endüstriyel bir işletmede yangın ve patlama riski taşıyan ekipmanların belirlenmesi amaçlanmıştır. Metodoloji olarak DOW Yangın ve Patlama İndeksi (DOW F&EI)'nden yararlanılmıştır. Büyük hasar ve yaralanmalar ile ekonomik kayıplara neden olabilecek yangın ve patlama potansiyeli taşıyan ekipmanların önceden belirlenmesi, yangın risklerinin yönetilmesinde birincil öncelik olacaktır. Ayrıca fabrika tasarımı ve kurulumu aşamasında yangın ve patlama indeksinin hesaplanması halinde, doğuştan güvenli tasarım hedefine ulaşılabacaktır.

Anahtar kelimeler: yangın, patlama, risk, Dow İndeksi

Hazard Classification of Equipments: DOW F&E Index

Abstract: Major industrial accidents are low probability and high consequence events. These events could occur in the form of fire, explosion and/or toxic release. Fires, especially, have the potential of high heat radiation to equipments and could cause secondary and tertiary events .such as fires, explosions and toxic releases. It is possible to manage fire risk with the definition of equipments, which have the high fire potential by using proactive approaches. There have been some methods to define high-risk potential equipments. Dow Fire & Explosion Index Methodology is a commonly used method for this purpose. The method considers general and special process hazards as well as health, reactivity and flammability properties of chemicals. General process hazards are consist of six key elements: exothermic chemical reactions, endothermic processes, material handling and transfer, enclosed or indoor process units, access and drainage and spill control. Twelve special process hazards are considered as toxic material(s), sub-atmospheric pressure, operation in or near flammable range, dust explosion, pressure, low temperature, quantity of flammable/unstable material, corrosion and erosion, leakage, joints and packing, use of fired equipment, hot oil heat exchange system and rotating equipment. Special process hazards could be directly or indirectly responsible for fire and explosions. Fire and explosion index is estimated considering general, special process hazards and material factor. F&EI Index is a guide to prioritize process equipments concerning fire and explosion risks. The main purpose of this study is to define equipments that have high fire and explosion risks at an industrial facility. Dow F&EI methodology was followed for this purpose. Classification of hazardous process equipments to prevent catastrophic events and their effects is the point of origin to manage fire risks. If the methodology would perform during the plant design and installation processes, inherently safer process goal would also be achieved.

Keywords: fire, explosion, risk, Dow Index

1.Giriş

Teknoloji ve sanayinin hızla gelişmesi bir yandan insanoğlunun hayatını kolaylaştırmakta ancak diğer yandan bu gelişmenin plansız ve ani oluşu da sanayi bölgeleri ve yaşam alanlarının iç içe geçmesi nedeniyle başta sağlık ve çevre olmak üzere çeşitli sorunları beraberinde getirmektedir. Özellikle sanayileşme ile birlikte kimyasal maddelerin üretimi, kullanımı, depolanması ve taşınması nedeniyle kimyasal etkilenim (maruziyet) kaçınılmaz hale gelmiştir[1]. Tehlikeli kimyasallar patlayıcı, oksitleyici, çok kolay alevlenir, kolay alevlenir, alevlenir, çok toksik, toksik, zararlı, aşındırıcı, tahriş edici, alerjik, kanserojen, mutajen, üreme için toksik ve çevre için tehlikeli özelliklerden bir veya birkaçına sahip madde ve/veya karışımları kapsayan geniş bir aileyi temsil etmektedir. Yukarıda bahsedilen özellikleri nedeniyle de kimyasal maddeler sadece bu maddeleri doğrudan kullanan kişi ya da işletmeleri değil, olası büyük endüstriyel kazalar halinde kitleleri etkileyebilecek potansiyele sahiptir. Büyük endüstriyel kazalar genellikle yangın, patlama, toksik yayılım veya bu olayların birkaçının farklı izlencelerle meydana gelmesi şeklinde gerçekleşmektedir[2,3].

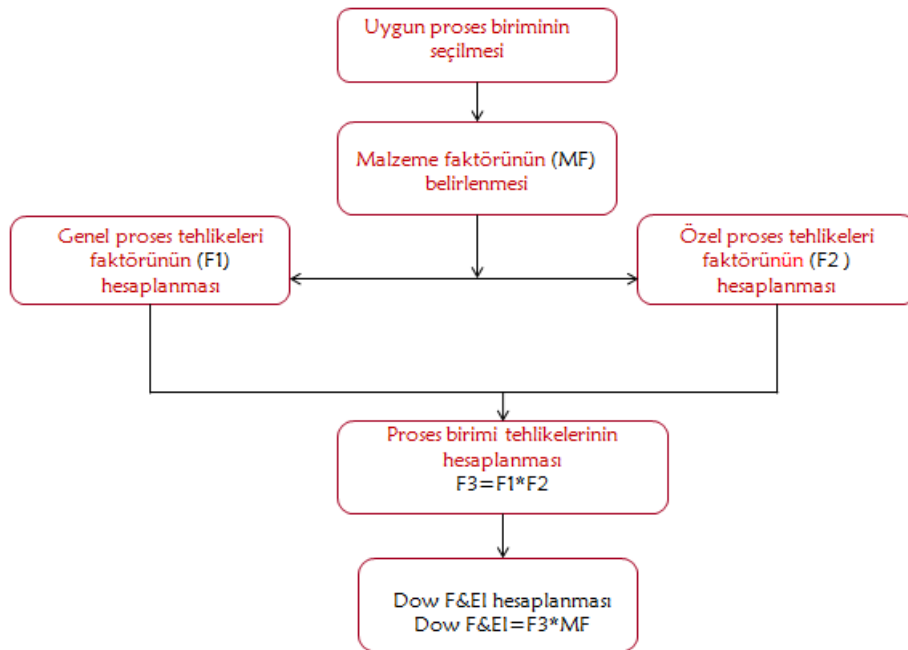
Ülkemizde, 30.12.2013 tarih ve 28867 No’lu Resmi Gazete’de yayınlanan “Büyük Endüstriyel Kazaların Önlenmesi ve Etkilerinin Azaltılması Hakkında Yönetmelik”, tehlikeli maddeler bulunduran kuruluşlarda büyük endüstriyel kazaların önlenmesi ve muhtemel kazaların insanlara ve çevreye olan zararlarının en aza indirilmesi amacıyla, yüksek seviyede, etkili ve sürekli korumayı sağlamak için

alınması gerekli önlemler ile ilgili usul ve esasları belirlemektedir. Yönetmelik, proses içerisindeki tehlikeli ekipmanların belirlenmesi ve gruplandırılması ile belirlenen tehlikeli ekipmanlar için senaryo edilen her bir büyük kazanın her türlü sonucunun meydana gelme frekansını 1×10^{-4} /yıl seviyesine veya bu seviyeden daha küçük bir seviyeye indirilmesi gerektiğini belirtmektedir. [4] Burada tehlikeli ekipman belirlemenin amacı, üzerinde büyük çaplı kaza senaryolarının tanımlanabileceği ekipmanın seçilmesidir [5]. Bu amaçla kullanılan yöntemlerden birisi de Dow Yangın ve Patlama İndeksi (Dow F&EI)'dir[6-8].

2. Metodoloji ve Senaryo

2.1. Metodoloji

Bu çalışmada, tehlikeli ekipmanları belirlemek ve önceliklendirmek amacıyla Dow F&EI kullanılmıştır. Yöntemin amacı, yangın, patlama ve reaktivite kaynaklı olası kazaların tahmini zararlarını belirlemek, kazaya neden olacak veya kazanın etkilerini arttıracak ekipmanı belirlemek ve risk potansiyelini paylaşmaktır. F&EI indeksinde izlenen yol Şekil 1.'de özetlenmiştir[9].



Şekil 1: Dow Yangın ve Patlama İndeksi hesaplamada izlenen yol

Referans Kılavuz[9]'dan uyarlanmıştır

Uygun proses (süreç) biriminin seçilmesinde kimyasal enerji potansiyeli, proses birimindeki tehlikeli madenin miktarı, işletme koşulları (basınç ve sıcaklık), geçmişte yangın ve patlama ile sonuçlanan olaylar, tesis devamlılığı için kritik üniteler ve prosesin yatırım değeri dikkate alınmıştır.

Malzeme faktörünün (MF) belirlenmesi, yangın ve patlama indeksinin hesaplanması için temel başlangıç noktasıdır. MF, NFPA (National Fire Protection Agency) yangın ve patlama derecelendirmeleri N_F ve N_R verilerinden elde edilir. Dow Yangın ve Patlama İndeksi, Tehlike Sınıflandırma Kılavuzu, Ek- A'da çeşitli kimyasallar için MF listesi mevcuttur.

2.1.2. Genel Proses Tehlikelerinin Belirlenmesi

Genel Proses Tehlikeleri, kayıp içerikli bir olayın büyüklüğünü belirlemede birinci derecede rol oynar. Genel Proses Tehlikeleri, birçok prosese uygulanabilecek 6 öğeden oluşur.

- A. Ekzotermik kimyasal reaksiyonlar,
- B. Endotermik prosesler
- C. Malzeme aktarımı ve transferi
- D. Kuşatılmış (etrafı çevrili) veya kapalı alanlar
- E. Erişim
- F. Drenaj ve döküntü kontrolü

“Genel Proses Tehlikeleri Faktörü” (F1) belirlenirken yukarıda sayılan öğelerin her birinin seçilen proses ve/veya proses birimine uygunluğu değerlendirilir. Dow Yangın ve Patlama İndeksi, Tehlike Sınıflandırma Kılavuzu referans alınarak her bir tehlike için Tablo 1.’de belirtilen uygun puan (penaltı faktörü) atanır. Genel tehlikeler için belirlenen puan sütunundaki rakamlar, temel faktör olan 1 değerine eklenir ve F1 değeri elde edilir.

2.1.2. Özel proses tehlikelerinin belirlenmesi

Özel proses tehlikeleri, kaybın gerçekleşme olasılığına birinci derece etkisi olan faktörlerdir. Yangın ve patlama olaylarının temel nedeni olarak görülen özel proses koşullarını içerir. Bu bölüm 12 öğeden oluşmaktadır:

- A. Toksik (zehirli) malzemeler
- B. Atmosferik basıncın altında çalışma
- C. Alevlenme aralığında veya yakınında çalışma
- D. Toz patlamaları
- E. Relief pressure (güvenli tahliye basıncı)
- F. Düşük sıcaklık
- G. Alevlenebilir/Kararsız madde miktarı
- H. Korozyon ve aşınma
- İ. Sızıntı (bağlantı yerleri ve ambalajlama)
- J. Ateşli ekipmanların kullanımı
- K. Sıcak yağlı ısı değiştirici sistemleri
- L. Döner ekipman

“Özel Proses Tehlikeleri Faktörü” (F2) belirlenirken yukarıda sayılan öğelerin her birinin seçilen proses ve/veya proses birimine uygunluğu değerlendirilir. Dow Yangın ve Patlama İndeksi, Tehlike Sınıflandırma Kılavuzu referans alınarak her bir tehlike için Tablo 1’de belirtilen uygun puan (penaltı faktörü) atanır. Özel proses tehlikeleri için belirlenen puan sütunundaki rakamlar, temel faktör olan 1 değerine eklenir ve F2 değeri elde edilir.

2.1.3. Proses Birimi Tehlike Faktörünün Belirlenmesi

“Proses Birimi Tehlike Faktörü” (F3), “Genel Proses Tehlikeleri Faktörü” (F1) ve “Özel Proses Tehlikeleri Faktörü” (F2)’nin çarpımıdır. F3, 1 ile 8 aralığında değer almaktadır. F3 için 8’den büyük bir değere elde edilmesi halinde, 8 alınmalıdır.

2.1.4. Yangın ve Patlama İndeksinin (F&EI) Belirlenmesi

Yangın ve Patlama İndeksi (F&EI), bir olay sonrası tesiste meydana gelebilecek hasarın tahmininde kullanılır. Tablo 2, F&EI'nin bağlı olarak derecelendirmesi hakkında fikir vermektedir. Yüksek tehlikeli alanlar için bir HAZOP çalışmasının yapılması önerilmektedir.

Tablo 1: Dow F&EI Kılavuz Tablo ,Referans [9]'dan uyarlanmıştır.

DOW YANGIN VE PATLAMA İNDEKSİ (Y&Pİ)					
FİRMA			DÜZENLEYEN		
BÖLÜM			ONAYLAYAN		
PROSES			TARİH		
KİMYASAL ADI					
MALZEME FAKTÖRÜ (AÇIKLAMALAR...					
1. Genel Proses Tehlikeleri				Puan Aralığı	Puan
	Temel Faktör			1.00	1.00
A.	Egzotermik Kimyasal Reaksiyonlar			0.30-1.25	
B.	Endotermik Prosesler			0.20-0.40	
C.	Malzeme Aktarımı ve Transferi			0.25-1.05	
D.	Kuşatılmış (etrafı çevrili) veya kapalı alanlar			0.25-0.90	
E.	Erişim			0.20-0.35	
F.	Drenaj ve döküntü kontrolü			0.25-0.50	
Genel Proses Tehlikeleri Faktörü (F1)					
2. Özel Proses Tehlikeleri					
	Temel Faktör			1.00	1.00
A.	Toksik Malzeme(ler)			0.20-0.80	
B.	Vakum Basıncı (<500 mmHg)			0.5	
C.	C. Alevlenme aralığında veya yakınında çalışma				
	1. Tank Çiftliğinde Yanıcı Sıvıları Depolama			0.5	
	2. Proses Bozulması veya Buhar Tahliye Problemi			0.3	
	3. Sürekli Yanma Aralığında			0.8	
D.	Toz Patlaması			0.25-2.00	
E.	Basınç İşletme BasıncıkPa Rahatlatma ValfikPa				
F.	Düşük Sıcaklık			0.20-0.30	
G.	Alevlenebilir/Kararsız Malzeme Miktarıkg				
	1. Prosesteki sıvı veya gazlar				
	2. Depolanan sıvı veya gazlar				
	3. Prosesteki tutuşabilir katı veya tozlar				
H.	Korozyon ve Aşınma			0.10-0.70	

I.	Sızıntı - Bağlantı Yerleri	0.10-1.50	
J.	Ateşli Ekipman Kullanımı		
K.	Sıcak Yağlı Isı Değiştiriciler	0.15-1.15	
L.	Döner Ekipmanlar	0.5	
Özel Proses Tehlikeleri Faktörü (F2)			0
Proses Birimi Tehlike Faktörü (F1*F2)=F3			
Yangın ve Patlama İndeksi (F3*MF=Y&Pİ)			

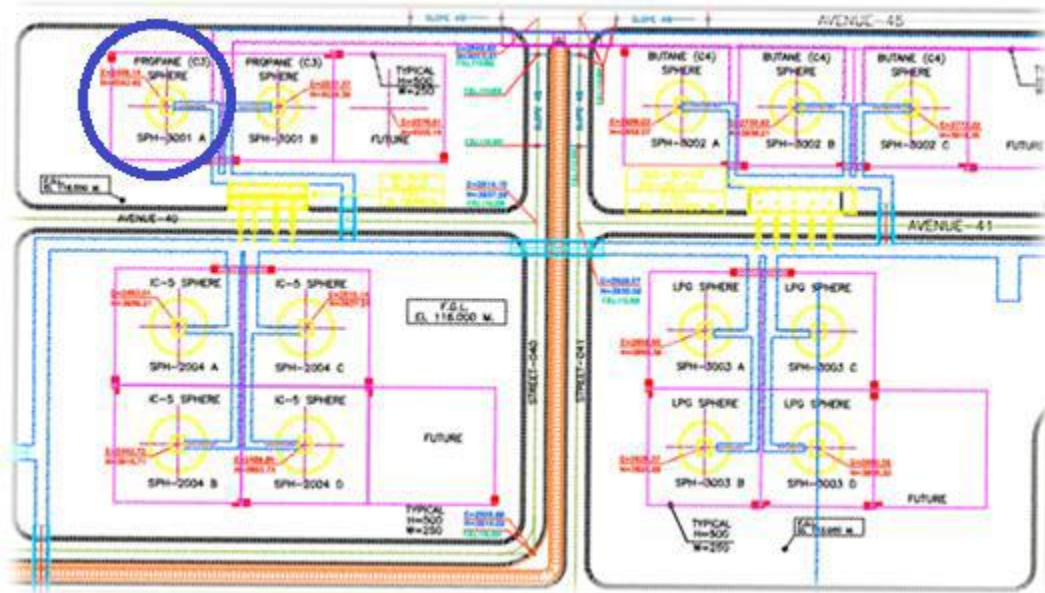
Uygulanamaz Tehlikeler için 0 puan değerini kullanınız

Tablo 2: F&EI için tehlike derecelendirmesi [9]

F&EI İndeks Değeri	Tehlike derecesi
1-60	Hafif
61-96	Moderate
97-127	Orta seviyeli (Intermediate)
128-158	Ağır (Heavy)
159 ve üzeri	Ciddi (Severe)

2.2. Senaryo

Bu çalışma kapsamında, bir rafineride bulunmakta olan karbon çeliğinden yapılmış ve 15,5 m çapında, 18 m yükseklikte ve 12,8 bar basınç ve 40°C'de işletilmekte olan bir propan depolama tankı[10], DOW F&EI yöntemi ile değerlendirilmiş ve yangın ve patlama indeksi hesaplanmıştır. Hesaplama kullanılan malzeme faktörü ve özellikleri Tablo 3'de yer almaktadır.



Şekil 2: Senaryo kapsamında F&EI açısından değerlendirilen depolama tankı [10]

Tablo 3: Malzeme faktörü ve özellikleri [9]

Madde	MF	Hc [BTU/Lb]10 ³	NFPA Sınıflandırması			Flaş Noktası (F)	Kaynama Noktası (F)
			N(H)	N(F)	N(R)		
Propan	21	19,9	1	4	0	Gaz	-44

3. Bulgular

Propan içerikli tank, depolama amaçlı kullanıldığından ‘Genel Proses Tehlikeleri’ bölümünde Endotermik ve Ekzotermik reaksiyon kalemlerine “0” puan atanmıştır. Malzeme aktarımı ve transferi, N(F) 4 sınıfında alevlenebilir sıvı veya gaz kullanılması nedeniyle 0,85 olarak değerlendirilmiştir. Depolama tankının kapalı ve veya kuşatılmış/kısıtlanmış bir alanda yer almaması nedeniyle bu bölüme “0” puan atanmıştır. Acil durumlarda tanka karayolu ile erişim sağlanabilmektedir, ancak işletmenin büyüklüğü dikkate alındığında ihtiyaten 0,2 puan atanmıştır. Drenaj döküntü kontrol sistemi mevcut olmakta ancak tank ile birlikte diğer ekipmanlar da aynı havuzda yer almaktadır, bu nedenle ilgili bölüme 0,5 puan atanmıştır.

Özel Proses Tehlikeleri incelendiğinde, malzemenin sağlıkla ilgili N(H) değeri 1 olup, bu bölüme atanan puan 0,2’dir. Vakum basıncı uygulanmadığından bu bölüme “0” puan atanmıştır. Alevlenme aralığında ve yakınında çalışma bölümü, N(F) 4 özelliğinde malzeme depolanması nedeniyle 0,5 olarak atanmış, toz patlaması senaryo için uygulanabilir olmadığından “0” değeri atanmıştır. Sıvılaştırılmış alevlenebilir gazlar için çalışma basıncı ve çalışma basıncının 1,5 katına set edilmiş patlama disk basıncı için atanan değer oranlanması ve sıvılaştırılmış alevlenebilir gazlar için düzeltme faktörü olarak önerilen 1,3 ile çarpılmasını öngörülmektedir. Bu şekilde hesaplanan değer 1,09 olarak belirlenmiştir. Düşük sıcaklık uygulanabilir olmadığından “0” puan atanmıştır. Depolanan alevlenebilir malzeme miktarı Kılavuz’daki 4 No’lu grafikten, sıvılaştırılmış gazlar için kullanılan eğri dikkate alınarak 0,43 okunmuştur. Korozyon ve aşınma minimum kabul edilerek 0,1 alınmıştır. Sızıntı ve bağlantı yerlerinde minör kaçaklar olabileceği dikkate alınarak bu bölüme 0,1 atanmıştır. Ateşli ekipman ve ısı değiştirici kullanımı söz konusu olmayıp bu bölümlere 0 değeri atanmıştır. Sistemde pompa bulunması nedeniyle döner ekipmanlar bölümüne de 0,5 değeri atanmıştır. F1, F2 ve F3 değerleri Tablo 4’te görülmektedir.

Tablo 4: Senaryoya ilişkin bulgular

Hesaplanan Değer	Puan
F1	2,55
F2	3,92
F3	8
F&EI	168

4. Sonuçlar ve Tartışma

Tablo 4’te hesaplanan F&EI indeks değeri, ekipmanın belirtilen proses/depolama koşullarında ciddi seviyede tehlikeli olduğunu göstermektedir. Basınç altında sıvılaştırılmış propan depolama örneğinde olduğu gibi, tehlikeli kimyasallar üreten ve depolayan tesislerdeki her bir ekipman, tehlike derecelendirmesine tabi tutulmalıdır. Yüksek derecede tehlikeli olan, büyük endüstriyel kazalara neden olma potansiyeli olan bu ekipmanlar ileri risk değerlendirme yöntemleri ile detaylıca incelenmeli ve gerekli önlemlerin alınması sağlanmalıdır.

Referanslar

1. Ercan Kalkan M., Deniz V., Dow Chemical Exposure Index Methodology, International Congress on Occupational Safety and Security, 2016.
2. Crowl D. A.; Louvar J. F.; Chemical Process Safety Fundamentals with Applications, 1990, 181-183.
3. Casal, J.; Evaluation of the Effects and Consequences of Major Accidents in Industrial Plants, First Edition, Elsevier, 2008, 119-137.
4. Büyük Endüstriyel Kazaların Önlenmesi ve Etkilerinin Azaltılması Hakkında Yönetmelik, Tarih:30.12.2013, Resmi Gazete No: 28867.
5. T.C. Çalışma Ve Sosyal Güvenlik Bakanlığı, İş Teftiş Kurulu Başkanlığı, Kimya Sanayi Sektöründe Seveso II Direktifi Kapsamındaki Endüstrilerde Kaza Riski Değerlendirme Metodolojisi, Yayın No 55, 2012, Ankara.
6. Gupta,J, P., Application of Dow Fire & Explosion Index, hazard classification guide to process plants in developing counties, J. Loss Prev. Vol 10, No:1, 7-15, 1997.
7. Etowa , C.B. Amyotte, P R., Pegg M J., Khan, F.I., Quantification of inherently safety aspects of the Dow indices, J. Loss Prev. Vol 15, 2002.477-487
8. Gupta J.P., Khemani G., Mannan M. S., Calculation of Fire and Explosion Index (F&EI) value for the Dow Guide taking credit for the loss control measures, Journal of Loss Prevention in the Process Industries 16 (2003) 235–241.
9. Dow's Fire & Explosion Index Hazard Classification Guide, Seventh Edition, 1994.
10. Nazari S., Karami, N., Moghadam, H., Nasiri, P., Consequence Analysis of BLEVE Scenario in the Propane Tank: A Case Study at Bandar Abbas Gas Condensate Refinery of Iran, *International Journal of Scientific Engineering and Technology*, Volume No.4 Issue No.9, 2015.pp:472-475.

İş güvenliği uygulamalarının yaygınlaştırılmasının yangından korunmaya katkıları

Necmi Özdemir ¹, İlbeyi Kılavuz ^{2,*}

¹ *University of Kocaeli, Engineering Faculty, Department of Electrical Engineering,
41380, Kocaeli, TURKEY, nemci.ozdemir@kocaeli.edu.tr*

² *University of Kocaeli, Ford Otosan İhsaniye Automotive Vocational School, 41680,
Kocaeli, TURKEY, ilbeyi@kocaeli.edu.tr*

Özet: İşçi sağlığı ve iş güvenliği uygulamaları, yasal zorunluluklar ve bu konudaki çabaların artması sayesinde ülkemizde gün geçtikçe yaygınlaşmaktadır. Pek çok işyerinde bu zorunluluklar ve bilinçlenmenin artması sebebiyle artan sayıda önlemler alınmaktadır. 50 ve daha fazla çalışanı bulunan işyerlerinde İş Sağlığı ve Güvenliği Kurulu oluşturulması zorunluluğunun gelmesi ve çalışanların ciddi tehlikeyle karşı karşıya kaldığında çalışmaktan kaçınma hakkı kullanabilmesi, önceden risk değerlendirmesi yapılması zorunluluğu gibi pek çok önlem çalışanların sağlığını korumakta büyük önem göstermektedir. İş sağlığı ve güvenliği kurullarının risk değerlendirmesi yapması, acil durum planlamaları yapılması gibi zorunluluklar daha önce bu duruma gereken önemi vermeyen işyerlerinin kendini düzeltmesini ve eksikliklerini azaltmasını sağlamıştır. İş güvenliği uzmanlığı kurslarında patlama ve yangından korunma, elektrik riskleri ve tehlikeleri, kişisel koruyucu donanım kullanımı, risk yönetimi, fiziksel risk etmenleri, Kaynak işlerinde iş sağlığı ve güvenliği, bakım onarım işlerinde iş sağlığı ve güvenliği gibi konular işlenmektedir. Bu çalışmada bu işlenen konuların yangınla mücadele konusundaki katkıları incelenmeye çalışılmıştır.

Contribution of occupational safety applications on fire prevention

Abstract: Workers health and occupational safety applications are becoming more common due to regulations and developing of experience in Turkey. Number of precautions are increasing thanks to regular obligations and developing consciousness. In businesses where 50 or more employees work Workers Health and Occupational Safety Council must be organized, also workers can resist working if a serious hazardous situation occurs, risk assessment must be issued before operations have begun and these precautions has great positive effect on workers' health. Preparing risk assessment files Workers Health and Occupational Safety Councils help businesses to fix themselves and decreasing the insufficiency. In compulsory courses for occupational safety experts subjects including explosion and fire prevention, electrical risks and dangers, personal protective equipment, risk assessment, physical risk factors, safety in welding operations, work health and safety in maintenance are discussed. In this study effect of these subjects on fire prevention are tried to be investigated.

1. Giriş

30.06.2012 tarihinde Resmi Gazete’de yayımlanarak altı ay sonra yürürlüğe giren 6331 sayılı İş Sağlığı ve Güvenliği Kanunu [1] kamu ve özel sektöre ait işyerlerinde iş sağlığı ve iş güvenliğinin sağlanması ve mevcut sağlık ve güvenlik şartlarının iyileştirilmesi için işveren ve çalışanların görev, yetki, sorumluluk, hak ve yükümlülüklerini düzenlemek amacıyla oluşturulmuştur. Bu kanun birkaç istisna haricinde kamu ve özel sektöre ait tüm işlere ve işyerlerine, bu işyerlerinin bu işyerlerinin işverenleri ile işveren vekillerine, çırak ve stajyerler de dâhil olmak üzere tüm çalışanlarına faaliyet konularına bakılmaksızın uygulanmaktadır. Bu kanun çerçevesinde İş güvenliği uzmanı ve işyeri hekimleri tanımlanmıştır. İşyeri hekimi; iş sağlığı ve güvenliği alanında bakanlıkça yetkilendirilmiş, işyeri hekimliği belgesine sahip hekim tanımlanmaktadır. İş güvenliği uzmanı ise Usul ve esasları yönetmelikle belirlenen belge sahibi müfettişler, mühendislik ya da mimarlık eğitimi veren fakültelerin mezunlarını ve teknik elemanını tanımlanmaktadır. İş güvenliği uzmanları ve İşyeri hekimleri çalışanların ve işin güvenliği ile ilgili mevzuatı takip ederek işverene ilgili konularda rehberlik ve tavsiye hizmeti yürütür.

2. İş Güvenliği Uzmanlarının Görev Yetki ve Sorumlulukları

İş güvenliği uzmanları, iş güvenliği uzmanı olmak için gerekli minimum şartı taşıyanlar arasından yetkilendirilmiş bir kurs merkezinde teorik kısmı 180 saat ve uygulama kısmı 40 saatten aşağı olmayacak şekilde 220 saatten az olmamak kaydıyla eğitim almış kişilerden daha sonra yapılacak merkezi sınavdan en az 70 puan alan kişilerdir. [2] İş güvenliği uzmanlığı tecrübe yeterlilik ve çalışma sürelerine göre A sınıfı, B sınıfı ve C sınıfı olmak üzere 3 sınıfa ayrılmıştır. Bu sınıflar ayrıca çalışılacak işyerine göre de az tehlikeli, tehlikeli ve çok tehlikeli işyerlerinde çalışacak uzmanların tayininde de kullanılmaktadır.

İş güvenliği uzmanlarının görevleri ilgili mevzuatta Rehberlik, Risk Değerlendirmesi , çalışma ortamı gözetimi, eğitim, bilgilendirme ve kayıt ve ilgili hekimlerle işbirliği şeklinde sıralanmıştır [2]. Bu sıralamanın içeriğine bakılırsa:

a) Rehberlik;

1) İşyerinde yapılan çalışmalar ve yapılacak değişikliklerle ilgili olarak tasarım, makine ve diğer teçhizatın durumu, bakımı, seçimi ve kullanılan maddeler de dâhil olmak üzere işin planlanması, organizasyonu ve uygulanması, kişisel koruyucu donanımların seçimi, temini, kullanımı, bakımı, muhafazası ve test edilmesi konularının, iş sağlığı ve güvenliği mevzuatına ve genel iş güvenliği kurallarına uygun olarak sürdürülmesini sağlamak için işverene önerilerde bulunmak.

2) İş sağlığı ve güvenliğiyle ilgili alınması gereken tedbirleri işverene yazılı olarak bildirmek.

3) İşyerinde meydana gelen iş kazası ve meslek hastalıklarının nedenlerinin araştırılması ve tekrarlanmaması için alınacak önlemler konusunda çalışmalar yaparak işverene önerilerde bulunmak.

4) İşyerinde meydana gelen ancak ölüm ya da yaralanmaya neden olmayan, ancak çalışana, ekipmana veya işyerine zarar verme potansiyeli olan olayların nedenlerinin araştırılması konusunda çalışma yapmak ve işverene önerilerde bulunmak.

b) Risk değerlendirme;

1) İş sağlığı ve güvenliği yönünden risk değerlendirme yapılmasıyla ilgili çalışmalara ve uygulanmasına katılmak, risk değerlendirme sonucunda alınması gereken sağlık ve güvenlik önlemleri konusunda işverene önerilerde bulunmak ve takibini yapmak.

c) Çalışma ortamı gözetimi;

1) Çalışma ortamının gözetiminin yapılması, işyerinde iş sağlığı ve güvenliği mevzuatı gereği

yapılması gereken periyodik bakım, kontrol ve ölçümleri planlamak ve uygulamalarını kontrol etmek.

2) İşyerinde kaza, yangın veya patlamaların önlenmesi için yapılan çalışmalara katılmak, bu konuda işverene önerilerde bulunmak, uygulamaları takip etmek; doğal afet, kaza, yangın veya patlama gibi durumlar için acil durum planlarının hazırlanması çalışmalarına katılmak, bu konuyla ilgili periyodik eğitimlerin ve tatbikatların yapılmasını ve acil durum planı doğrultusunda hareket edilmesini izlemek ve kontrol etmek.

ç) Eğitim, bilgilendirme ve kayıt;

1) Çalışanların iş sağlığı ve güvenliği eğitimlerinin ilgili mevzuata uygun olarak planlanması konusunda çalışma yaparak işverenin onayına sunmak ve uygulamalarını yapmak veya kontrol etmek.

2) Çalışma ortamıyla ilgili iş sağlığı ve güvenliği çalışmaları ve çalışma ortamı gözetim sonuçlarının kaydedildiği yıllık değerlendirme raporunu işyeri hekimi ile işbirliği halinde hazırlamak.

3) Çalışanlara yönelik bilgilendirme faaliyetlerini düzenleyerek işverenin onayına sunmak ve uygulamasını kontrol etmek.

4) Gerekli yerlerde kullanılmak amacıyla iş sağlığı ve güvenliği talimatları ile çalışma izin prosedürlerini hazırlayarak işverenin onayına sunmak ve uygulamasını kontrol etmek.

5) Bakanlıkça belirlenecek iş sağlığı ve güvenliğini ilgilendiren konularla ilgili bilgileri, İSG KATİP'e bildirmek.

d) İlgili birimlerle işbirliği;

1) İşyeri hekimiyle birlikte iş kazaları ve meslek hastalıklarıyla ilgili değerlendirme yapmak, tehlikeli olayın tekrarlanmaması için inceleme ve araştırma yaparak gerekli önleyici faaliyet planlarını hazırlamak ve uygulamaların takibini yapmak.

2) Bir sonraki yılda gerçekleştirilecek iş sağlığı ve güvenliğiyle ilgili faaliyetlerin yer aldığı yıllık çalışma planını işyeri hekimiyle birlikte hazırlamak.

3) Bulunması halinde üyesi olduğu iş sağlığı ve güvenliği kuruluşuyla işbirliği içinde çalışmak,

4) Çalışan temsilcisi ve destek elemanlarının çalışmalarına destek sağlamak ve bu kişilerle işbirliği yapmak,

olarak tanımlanmıştır.

3. İş Güvenliği Eğitim Konuları

İş güvenliği uzmanlığı eğitim programı ülkemizde Çalışma ve Sosyal Güvenlik Bakanlığı tarafından belirlenmektedir [3]. Derslerin en az 90 saatlik kısmının yüzyüze yapılması, uzaktan eğitim ile yapılan 90 saatlik kısmının en az %10'luk kısmının ise eşzamanlı yapılması mecburidir. Ders takibinde devama büyük önem verilmekte olup derslere minimum devam oranı %90'dır. Adayların derse devamları ilgili Bakanlık yetkililerince yapılan habersiz kontroller ile takip edilmektedir.

İş güvenliği uzmanı olacak adaylar içlerinde aşağıdaki konular başta olmak üzere 50 civarında konu hakkında eğitim almaktadır: [4]

1) İş Sağlığı ve Güvenliğine Genel Bakış ve Güvenlik Kültürü

2) Türkiyede ve dünyada iş sağlığı ve güvenliği

3) Temel hukuk

- 4) İş hukuku
- 5) İSG kurulları
- 6) Risk yönetimi ve değerlendirmesi
- 7) Çalışma ortamı gözetimi
- 8) Fiziksel Risk Etmenleri
- 9) Kimyasal Risk Etmenleri
- 10) Biyolojik Risk Etmenleri
- 11) Psikososyal Risk Etmenleri
- 12) Korunma Politikaları
- 13) Kaynak işlerinde iş sağlığı ve güvenlik
- 14) Elektrikle çalışmalarda iş sağlığı ve güvenliği
- 15) Bakım onarım işlerinde iş sağlığı ve güvenliği
- 16) Yangın
- 17) Acil Durum Planları
- 18) Sağlık ve Güvenlik İşaretleri
- 19) Havalandırma ve İklimlendirme Prensipleri
- 20) İş kazaları
- 21) İş güvenliği yönünden yapılması gereken kontroller ve düzenlenecek belgeler

Bu eğitim konuları arasında Risk Değerlendirmesi, Yangın, Acil Durum Planları ve İş kazaları eğitimleri de bulunmaktadır. Özellikle risk değerlendirmelerinin yapılması gündelik hayatta iş yoğunluğu içerisinde önemsenmeyen ancak ciddi tehlikelerin oluşmasına potansiyel sağlayabilecek olumsuzlukların giderilmesine büyük katkı sağlamaktadır.

4. Yangın ve Korunma Yöntemleri Eğitimi

Yangın eğitimleri C sınıfı İş Güvenliği Uzmanları için yüzyüze eğitimde 5 saatten ve toplamda 10 saatten az olmayacak şekilde verilmektedir [5]. Yangın eğitimi yanmanın tanımı Şekil 1.'de görülen yanma üçgeni (fire triangle) ile başlar ve tehlike doğuran önü alınamayan ve istenmedik zararlar doğuran yanmanın yangın olduğu bilgisi ile devam eder.



Şekil 1. Yanma üçgeni (Fire triangle) [6]

Yangın sınıfları kendi içinde

- 1- A sınıfı yangınlar – Katı madde yangınları
- 2- B sınıfı yangınlar – Sıvı madde yangınları
- 3- C sınıfı yangınlar – Gaz madde yangınları
- 4- D sınıfı yangınlar - Hafif ve Aktif Metaller
- 5- F sınıfı yangınlar – Pişirme gereçlerindeki pişirme ortamı (bitkisel veya hayvansal sıvı ve katı yağlar) yangınları
- 6- E sınıfı yangınlar – Elektrik ekipmanı yangınları



Şekil 2. F sınıfı yangın örneği yemek pişirilen ortam yangını [7]

olarak tanımlanır. Ancak bu tanımlamalardan sadece ilk dört tanesi Binaların Yangından Korunması Hakkında Yönetmelik'te [7] tanımlanmıştır. TS EN 2 ve TS EN 2/A1 standartlarında da yangın sınıfları ile ilgili tanımlama yapılmıştır.

Binalarda çıkan yangınların söndürülmesi için taşınabilir söndürme cihazları ve tipleri de ilgili yönetmelikte belirtilmiştir. Bu yönetmeliğe göre

- a) A sınıfı yangın çıkması muhtemel yerlerde, öncelikle çok maksatlı kuru kimyevi tozlu veya sulu,
 - b) B sınıfı yangın çıkması muhtemel yerlerde, öncelikle kuru kimyevi tozlu, karbondioksitli veya köpüklü,
 - c) C sınıfı yangın çıkması muhtemel yerlerde, öncelikle kuru kimyevi tozlu veya karbondioksitli,
 - ç) D sınıfı yangın çıkması muhtemel yerlerde, öncelikle kuru metal tozlu
- söndürücülerin bulundurulması gerekmektedir.

Ayrıca yangın eğitimi içeriğinde yangın tüplerinin periyodik bakıma ihtiyacı olduğu, bu periyodik bakımların süreleri, yangın söndürücünün nasıl kullanılması gerektiği, kullanılan yangın söndürücülerin sonrasında hangi işleme tabi tutulması gibi konular da işlenmektedir.

Acil durum planları içinde belirli ekiplerin hazırlanması zorunludur. Bu ekipler

1. Söndürme ekibi
2. Kurtarma ekibi
3. Koruma ekibi
4. İlk yardım ekibi

olarak sınıflandırılmıştır.

Bu ekiplerin kurulması ve eğitimlerinin tamamlanması olası yangınların önlenmesi ve her türlü önlemin alınmış olmasına rağmen bir yangın durumunda hızlı müdahale ve minimum zararlar yangının söndürülmesini sağlamaya yardımcı olacaktır.

5. Sonuç

2013 yılında yürürlüğe giren 6331 sayılı İş Sağlığı ve Güvenliği Kanunu sayesinde kamu ve özel sektöre ait işyerlerinde işçi sağlığı ve iş güvenliği şartlarının iyileştirilmesi için çalışmalar yapılmaktadır. Bu kapsamda görevli olan İş Güvenliği Uzmanları belirli bir akademik birikime sahip olan kişilerden seçildikten sonra uzun süreli teorik ve pratik bir eğitimden geçtikten sonra merkezi bir sınavla uzman olmaya hak kazanmaktadırlar. Bu eğitimin içinde yangının tanımı, yangınla mücadele, yangın söndürme ekipmanları ve yangın söndürme metotları anlatılmaktadır. Bu sayede İş güvenliği uzmanları Risk Analizleri'nin daha katkı sağlayacak şekilde yapılmasına yardımcı olmaktadır. Ayrıca işyeri içinde oluşturulan yangınla mücadele ekipleri ile de yangın riskleri ciddi oranda azaltılmaktadır.

Kaynaklar

- [1] İş Sağlığı ve İş Güvenliği Kanunu (Kanun numarası 6331). <http://www.mevzuat.gov.tr/MevzuatMetin/1.5.6331.pdf> (Ziyaret tarihi 20.04.2017)
- [2] İş Güvenliği Uzmanlarının Görev, Yetki, Sorumluluk Ve Eğitimleri Hakkında Yönetmelik ,ÇSGB, Resmi Gazete 29 Aralık 2012
- [3] www3.csgb.gov.tr/csgbPortal/ShowProperty/.../isggm/dosyalar/igutemelegitim30-5-2015 (Ziyaret tarihi 26.04.2017)
- [4] http://www.damarakademi.com/isguzmanligi.php?gclid=CjwKEAjwutXIBRDV7-SDvdiNsUoSJACIITqIL-ddJnYa3KgDnWiHayQNvKcmegEgF1lq1EpBsVkULxoCepHw_wcB (Ziyaret Tarihi 26.04.2017)
- [5] <http://www3.csgb.gov.tr/csgbPortal/ShowProperty/WLP%20Repository/isggm/dosyalar/igutemelegitim30-5-2013> (Ziyaret Tarihi 26.04.2017)
- [6] <http://kimyaca.com/wp-content/uploads/2013/12/fire-triangle2.jpg> (Ziyaret Tarihi 26.04.2017)
- [7] <http://www.inews880.com/syn/104/133473/london-fire-department-noticing-spike-in-cooking-related-fires> (Ziyaret Tarihi 26.04.2017)

Yangın önlemede istatistiksel verilerin kullanımı

Orhan Oduncu¹, Necmi Özdemir¹

¹ *University of Kocaeli, Engineering Faculty, Department of Electrical Engineering, 41380, Kocaeli, TURKEY*
nemci.ozdemir@kocaeli.edu.tr

Özet: Ülkemizde çıkan yangınlara bakıldığında birbirlerine benzedikleri ve neredeyse tekrardan ibaret oldukları gözlenmektedir. Bu açıdan bakıldığında yaşanan yangınlardan yeterli ders alınmadığı ve bir daha yaşanmaması için geleceğe ışık tutacak tecrübe ve bilgilerin istenilen seviyede muhafaza edilmediği değerlendirilmektedir. Başka bir sorun ise muhafaza edilen bilgi ve tecrübeler istenilen zamanda ulaşılmaması, bilgilerin ulaşılabilir olmaması yaşanan olaylardan çıkarılmış derslerin yangın önlemede kullanılmamasına neden olmuştur. Bu kapsamda değerlendirildiğinde yangın istatistiklerinin saklanması ve paylaşılması yangın önlemek için gerekliliğini ortaya çıkarmaktadır.

Bu bildiride, İstanbul'da meydana gelen (2012-2017 yılları) yangınlara ait istatistikler; yangın sayısı, yangın çıkış sebepleri, can kaybı ve maddi zarar açısından incelenmiştir. Yangın önlemede yaşanan ve edinilen tecrübelerin yangın istatistikleriyle ele alınıp, yangınların önlenmesinde bu istatistiklerin önemine dikkat çekilmektedir.

Çalışma sonunda, yangın istatistiklerinin tutulmadığı ülkemizde sadece İstanbul Büyükşehir Belediyesi tarafından çalışmalar yapıldığı, bu çalışmaların ülke geneline yayılmasının fayda sağlayacağı kanısına varılmıştır.

Anahtar Kelimeler: Yangın İstatistikleri, Yangın Çıkış Sebepleri, Yangında Can Kaybı, Yangında Maddi Zarar

Abstract: We can clearly see that fires in our country are similar and almost always repeating themselves. So lesson is not been learnt and it is been evaluated that the knowledge and experience for prevent the incident is not been recorded. Another problem is we can not access the information and experience in time so others can't prevent similar incidents. We can understand that the fire incident statistics should be stored and shared to prevent further incidents.

In this announcement, statistics of fire happened in Istanbul between 2012 and 2017 has been investigated for number of fire, reason for fire, casualties and property damage. Obtained experiences on fire preventing should be addressed and statistics should be highlighted to its importance.

In the end of research, fire statistics are not recorded in our country, only İstanbul Büyükşehir Belediyesi researched fire statistics. Its been decided to fire researches should be done across the country.

Key Words: Fire Statistics, Causes of Fire, Casualties on Fire, Property Damage on Fire

1.Giriş

Yangın ısı oksijen ve yanıcı maddenin bir araya gelmesiyle oluşan kimyasal olayın kontrol dışına çıkması olarak tanımlanabilir. [1].Yanma sonunda; yanıcı maddenin niteliğine göre değişen miktarlarda, ısı, ışık, duman ve yangın gazları ortaya çıkar. Acıgacikan bu unsurlar, yangın kontrol altına alınamadığı veya söndürülemediği takdirde, iletim, taşınım ve ışınilma, ortamdaki herşeyi ve komşu ortamları da yakar. Büyük mal ve insan kayıplarına yol açar. Artan nüfus ve gelişen endüstriye paralel olarak yangın sayılarında bir artış olmaktadır. Bu artış insan yaşamını ve toplum refahını olumsuz yönde etkilemektedir.

İstatistik, belirli bir amaç için verilerin toplanması, sınıflandırılması, çözümlenmesi ve sonuçların yorumlanması ile ilgili teknik ve yöntemleri içeren bir bilim dalıdır[2].Tutulan İstatistiklerin yardımı ile makul geleceğe bakabilir, hedeflenen planlar gerçekleştirilebilir.

2.Yangın İstatistikleri İle Yapılan Uluslararası Çalışmalar

Geçmişten günümüze yangın istatistikleri konusunda pek çok çalışma yapılmıştır. Uluslararası Yangından Korunma ve Söndürme Teknik Komitesinin (CTIF) 40 ülkeden aldığı verilere göre yayınladığı raporda 1993-2014 yılları arasında yaklaşık 83 milyon yangının rapor edildiği ve bu yangınlarda yaklaşık 1 milyon kişinin öldüğü ve 2,6 milyar insanın bu yangınlardan zarar gördüğü belirtilmiştir. [3]

NFPA her yıl dergilerinde kayıtlara geçmiş Sivil, İtfaiyeci ölüm ve yaralanmalarının istatistiklerini yayınlamaktadır. Bu istatistikler incelendiğinde, en fazla yangının olduğu mekânlar; salon, yatak odası ve mutfak iken, en öldürücü malzemelerin ise kumaş ve yanıcı sıvılar olduğu belirlenmiştir. Malzemelerin tutuşmasına sebep olan faktörlerin başında çocukların kibrit ile oynaması ve sigara gelmektedir. Binalarda yangın sırasında kaçabilmeyi etkileyen faktörler, kıyafetlerin tutuşması ve kaçmak için yeterli zamanın bulunamaması, yaralanmaya sebep olan şartlardan bazılarının ise yatalak veya çok yaşlı olmak, ilaç ya da alkol almış olmak ve uyuyor olmaktır. [4]

Amerika’da Ulusal Yangın Olay Raporlama Sistemi (NFIRS) itfaiyelerden gelen raporları elektronik ortamda toplamaktadır. Bu raporlar U.S Fire Administration (ABD yangın idaresi) tarafından incelenmekte ve yıllık istatistiki rakamlar yangın kayıpları günlük ve aylık yangın sıklıkları, yangın kaynaklı yaralanma ve ölüm sayıları; ırk,cinsiyet ve yaşa göre analiz edilmektedir. [5]

İngiltere’de yangın istatistikleri içeriği standart yangın raporunda toplanan verilere dayanmaktadır. [6] İstatistikler itfaiye raporları incelendikten sonra elektronik ortamda Olay Raporlama Sistemine (IRS) kaydedilmektedir.Bu istatistikler yıllık,üçer aylık dönemlerde yayımlanmaktadır.

Avusturya’da yapılan araştırmada yılda yaklaşık 25.000 yangının meydana geldiğini ölüm nedenleri istatistiklere % 80 duman ve % 20 alevlerden ve diğer nedenlerden kaynaklandığı tespit edilmiştir. Bu istatistik duman alarmlarının yaşam alanında zorunlu ihtiyaç olduğunu vurgulamaktadır. Yakın gelecekte yeni binalar için duman algılama alarmlarının zorunlu bir hale geleceği düşünülmektedir. [7]

3. Ulusal Yangın İstatistikleri

Ülkemizde ne yazık ki yangın istatistiklerine dair basılı bir doküman bulunmamaktadır. Her il belediyesinde bulunan İtfaiye Daire Başkanlıkları’nda yangın kayıtları tutulmaktadır. Ve bu kayıtlar 2011 yılına kadar T.C. Başbakanlık Afet ve Acil Durum (AFAD) Yönetimi Başkanlığı’na gönderilmiştir. 2011 yılından sonra AFAD’a herhangi bir veri gönderilmemiştir. Ayrıca istatistiklerin toplanmasında kullanılması gereken Yangın Sonrası İşlemler TS 9870, Yangın İstatistiği Kuralları TS10108 ve Yangın Kaynaklı Afetlerde Sevk ve İdare Esasları TS 9871 standartları Şubat 1992 yılından sonra güncellenmemiştir.

Bu bildiride, İstanbul'da meydana gelen (2012-2017 yılları) yangınlara ait istatistikler; yangın sayısı, yangın çıkış sebepleri, can kaybı ve maddi zarar açısından incelenmiş ve yangın önlemede tutulacak her ayrıntının istatistiklere girmesinin gerekliliğine dikkat çekilmiştir.

3.1 İstanbul 2012-2017 Yılı Yangın Sayıları

Tablo 1. Yıllara Göre Yangın Sayıları

Yıl		Yangın (Sayı)								
		Yapısal yangınlar					Yapısal olmayan yangınlar			
		Konut	Fabrika	Diğer Bina	Araç	Toplam	Ot	Çöp	Orman Fundalık	Genel Toplam
2012		5.129	136	7.069	1.524	13.858	7.442	4.033	136	25.469
2013		4.902	159	7.853	1.601	14.515	7.969	5.099	134	27.717
2014		5.261	123	7.869	1.689	14.942	3.008	4.830	68	22.848
2015		5.869	157	8.957	1.903	16.886	4.596	5.212	284	26.978
2016		5.910	153	8.887	1.940	16.890	6.110	5.430	156	28.586
2016 Ocak		640	15	948	196	1.799	5	306	0	2.110
2017 Ocak		684	15	929	162	1.789	4	282	1	2.076
Sayısal Değişim	2016 Ocak 2017 Ocak	44↑	0	-20↓	-34↓	-10↓	-1↓	-24↓	1↑	-24↓
	2012 Yılı 2016 Yılı	781↑	17↑	1.818↑	416↑	3.032↑	1.332↓	1.397↑	20↑	85↑
Oransal Değişim	2016 Ocak 2017 Ocak	7%↑	0%	-2%↓	-17%↓	-1%↓	-20%↓	-8%↓	0%	-2%↓
	2012 Yılı 2016 Yılı	15%↑	13%↑	26%↑	27%↑	22%↑	-18%↓	35%↑	15%↑	1%↑

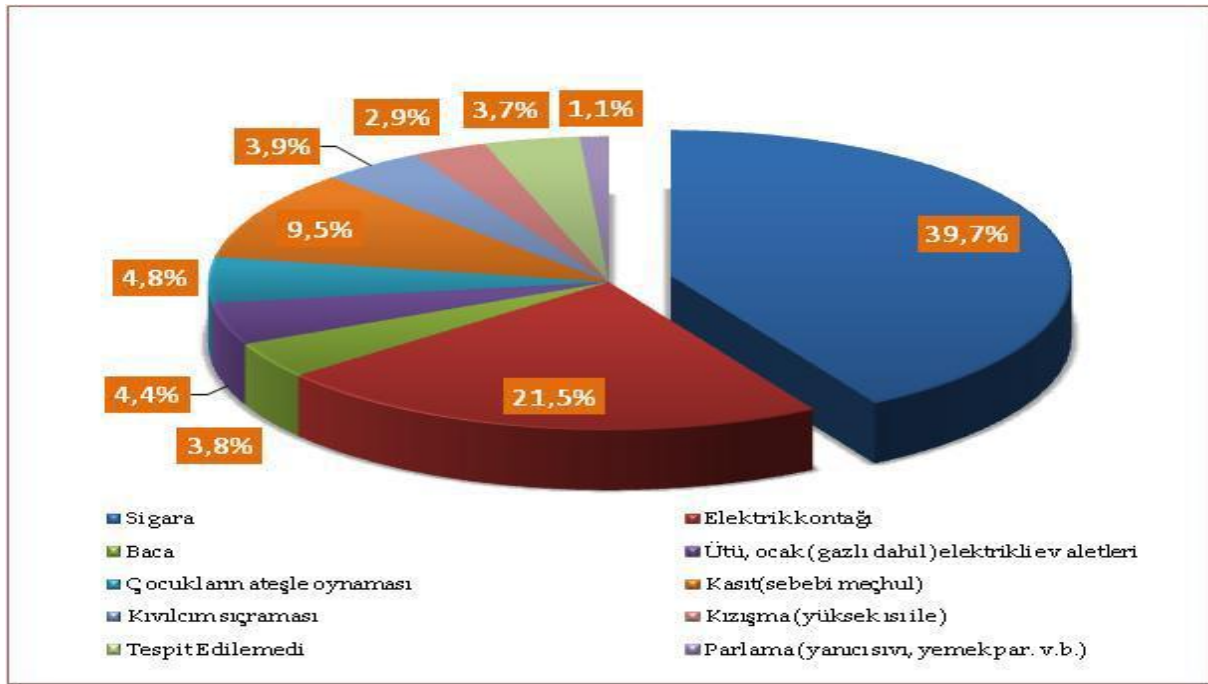
2017 Yılı Ocak ayı itibariyle İstanbul'da;684 konut, 15 Fabrika,928 diğer bina, 162 araç, 4 ot, 282 çöp,1 orman fundalık yangına müdahale edilmiştir. Tablo 1.'de görüldüğü üzere tüm yangınlarda bir önceki yılın aynı dönemine göre %2' azalış ve 2016 yılı sonu itibariyle de 2012 yılına göre %12'lik bir artış olmuştur. Buna rağmen genel olarak yapısal yangınlarda bir önceki yılın aynı dönemine göre %1'azalış,Fabrika yangınlarında da %'0, Konut yangınlarında ise %7'lik artış gerçekleşmiştir. Aynı dönem için ot yangınlarında %20', çöp yangınlarında %8'lik azalış, Orman-Fundalık Yangınlarında ise %0'düzeyinde kaldığı görülmektedir. Yine 2012-2016 döneminde meydana gelen yangınların ortalaması göz önüne alındığında her yıl meydana gelen yangınların yaklaşık %20,7'sini konut, %0,6'sını Fabrika,%31'ini diğer bina, %6,6'sını araç, %21,9'unu ot, %18,7'sini çöp ve %0,6'sını ise orman-fundalık yangınları oluşturmaktadır. [8]

3.2 Yangın Sebepleri

2011-2016 altı yıllık dönemin ortalaması göz önüne alındığında ilk üç sırada yangınların yaklaşık %44,0'ının sigara, %20,9'unun elektrik kontağı ve %9,5'inin kasıt(sebebi meçhul) nedenlerinden kaynaklandığı gözlemlenmiştir. 2016 yılına baktığımızda ise; ilk üç sırada %39,7'ile sigara,%21,5'ile elektrik kontağı,%9,5'ile kasıttan kaynaklandığı görülmektedir. 2011-2016 yıllarında sigara kaynaklı yangınlarının sayısının toplam yangınların içindeki oranı % 50-55 bandında iken 2011 sonrası %45-50 seviyesine indiği gözlemlenmektedir. Bu düşüşte Sağlık Bakanlığının ülke çapında yürütmüş olduğu "Dumansız hava sahası" uygulaması sonucu sigara kullanımındaki düşüş ve İstanbul İtfaiyesinin yürütmüş olduğu farkındalık artırma ve bilinçlendirme çalışmalarının etkisi olduğu yorumu yapılabilir. [8]

Tablo 2. Yangın Kaynağı (2012-2017)

Kaynak	Yıl									
	2012		2013		2014		2015		2016	
	Sayı	Yüzde	Sayı	Yüzde	Sayı	Yüzde	Sayı	Yüzde	Sayı	Yüzde
Sigara	12399	48,7%	13010	46,9%	9168	40,1%	10532	39,0%	11341	39,7%
Elektrik kontağı	5012	19,7%	5133	18,5%	5360	23,5%	6564	24,3%	6155	21,5%
Kasıt	865	3,4%	1454	5,2%	1340	5,9%	2058	7,6%	2729	9,5%
Çocukların ateşle oynaması	1389	5,5%	2097	7,6%	749	3,3%	1159	4,3%	1374	4,8%
Diğer	835	3,3%	707	2,6%	863	3,8%	823	3,1%	1276	4,5%
Ütü, ocak (gazlı dâhil) elektrikli ev aletleri	1242	4,9%	1190	4,3%	1189	5,2%	1245	4,6%	1272	4,4%
Kıvılcım sıçraması	932	3,7%	967	3,5%	903	4,0%	1021	3,8%	1122	3,9%
Baca	1144	4,5%	2097	4,7%	749	5,0%	1185	4,4%	1093	3,8%
Tespit Edilemedi	395	1,6%	762	2,7%	830	3,6%	956	3,5%	1060	3,7%
Kızışma (yüksek ısı ile)	714	2,8%	677	2,4%	961	4,2%	1107	4,1%	842	2,9%
Parlama (yanıcı sıvı (yemek parlaması vb.))	542	1,6%	422	2,7%	351	1,5%	328	1,2%	322	1,1%
Toplam	25.469	100%	27.717	100%	22.848	100%	26.978	100%	28.586	100%



Şekil 1. Yangın Kaynaklarının Tüm Yangınlar İçindeki Oranı

İstanbulda 2012-2017 yılları arasında meydana gelen yangınların çıkış sebepleri incelendiğinde; en büyük oranın % 39,7 ile “Sigara ve kibrit” olduğu görülmüştür (Şekil 2). İnsanların sigaralarını söndürmeden çöp kutularına veya balkondan dışarıya atması yangınlara sebep olmaktadır. [9]

4. Sonuç Ve Öneriler

İstanbul’da meydana gelen yangın sayıları 2012-2017 yılları arasında incelendiğinde; genel olarak fazla bir artışın söz konusu olmadığı 25000 ila 28000 arasında değiştiği gözlemlenmiştir. Nüfus ve enerji tüketiminin yangın sayıları üzerindeki artışa doğrudan etkisi bulunmaktadır.

Yangın çıkış sebepleri araştırıldığında en önemli faktörün sigara olduğu görülmüştür. Bu bağlamda halkın bilinçlendirilmesi ile yangın sayılarında azalma olacağı düşünülmektedir.

Yangınlarda meydana gelen can kayıpları incelendiğinde; hayatını kaybeden kişilerin sadece sayılarına yer verildiği görülmüştür. Bu kimselerin halktan mı yoksa itfaiye görevlilerinden mi olduğu bilinmemektedir. Ölenlerin yaş, cinsiyet ve ölüm şekilleri özellikle alev ve duman ölümleri hakkında detaylı bir istatistik tutulması gerekmektedir.

Yapılan bu çalışma sonunda Türkiye’de yangın istatistikleri konusuna yeteri kadar önem verilmediği görülmüştür. ABD ve Avrupa Birliği ülkelerinde her yıl meydana gelen yangınlarla ilgili raporlar hazırlanıp elektronik ortamda paylaşılmaktadır. Türkiye’de sadece İstanbul Büyükşehir Belediyesi, Ankara Büyükşehir Belediyesi ve İzmir Büyükşehir Belediyesi tarafından son yıllarda detaylı istatistikler tutulmakta ve bu verilerin daha da detaylandırılması gerektiği düşünülmektedir.

Yapılan bu araştırmada Yangın Sonrası İşlemler TS 9870, Yangın İstatistiği Kuralları TS10108 ve Yangın Kaynaklı Afetlerde Sevk ve İdare Esasları TS 9871 gibi standartların güncellenmesi ve itfaiye tarafından tutulacak raporların her şehirde aynı olmasının daha sağlam bir istatistik elde edileceği düşünülmektedir.

Bu bağlamda ülkemizde; yangınların kayıt altına alınmasını sağlayacak ortak bir veri tabanının oluşturulması, kullanılması, her yıl sonunda yangın istatistikleri raporlarının tutulmasının ve paylaşılmasının doğru olacağı düşünülmektedir.

Kaynaklar

- [1] Demirel, F., Binalarda Yangın Güvenliği, Yayınlanmamış Ders Notları, Gazi Üniversitesi, 2011.
- [2] Saraçbaşı, T, Kutsal, A., Betimsel İstatistik, Hacettepe Üniversitesi FenFakültesi Yayınları 17, Ankara, 1987.
- [3] Brushlinsky, N.N., Sokolov, S.V., Wagner, P., Hall, J.R., World Fire Statistics, Report no:21, The Center of, Fire Statistics of CTIF, 2016.
- [4] NFPA, “Fire Loss in the United States During 2014,” September 2015
- [5] U.S Fire Administration working for a fire safe America fire statistics report 2016
- [6] U.K Fire IRS 2016
- [7] Heiße Zahlen Eine kleine Brandschadenstatistik 2016
- [8] İstanbul Büyükşehir Belediyesi İtfaiye Daire Başkanlığı resmi web sitesi, <http://www.ibb.gov.tr/>
- [9] Tüyak 2011 Yangın Ve Güvenlik Sempozyumu Bidiriler Kitabı “Türkiye Ölçeğinde Yangın İstatistikleri Üzerine Bir Araştırma”



Chapter – 3

Combustion

Evaluation of Mathematical Models of Devolatilization for Numerical Simulations of Pulverized Coal Combustion

E. Kapusuz^{1,2,*}, B. Yilmaz¹, Y. Yükselentürk¹, İ. Gökalp²

¹ Marmara University, Department of Mechanical Engineering, İstanbul, Turkey

² Institut de Combustion, Aérothermique, Réactivité et Environnement, ICARE-CNRS
Orléans, France

*corresponding author: Erinc Kapusuz (erinc.kapusuz@gmail.com)

Abstract: Devolatilization is a conversion process from solid to gas phase, taking place at the initial stage of combustion of solid fossil fuels. Mathematical modeling of devolatilization plays an important role in prediction of ignition and flame development in the solid fuel combustion simulations.

A numerical study of coal combustion is carried out with special emphasis on the devolatilization modeling. In the study, mass loss predictions are compared for different heating rates for the selected devolatilization models available in literature. The influence of different devolatilization models on the simulation results of a pulverized coal jet flame is presented with their comparisons to the experimental data.

Keywords: Devolatilization model, pyrolysis, pulverized coal combustion, CFD modeling

1. Introduction

The combustion of coal involves several elementary processes such as particle turbulent dispersion, heat transfer between particles and the continuous phase, devolatilization of gaseous species, gas phase reactions and heterogenous reactions [1-3]. Devolatilization process is the first chemical conversion stage in the combustion of coal, resulting in release of gaseous species and tar [4]. As much as 50% by weight of the coal particle may volatilize and burn in the gas phase. Therefore, prediction capability of the ignition and heat released along the flame in the numerical simulations of pulverized coal combustion depend on the models defining yield rates of volatile products during devolatilization and the kinetic models used for describing the homogenous reactions.

The present work aims to evaluate the commonly used global devolatilization models of single-first-order reaction (SFOR) model [5] and two competing reactions (TCR) model [6], in comparison to using the more sophisticated chemical percolation devolatilization (CPD) network model [7]. As a preliminary study, effect of heating rate on the devolatilization models is presented. The selected devolatilization models are implemented in the numerical simulation of a lab scale pulverized coal jet flame and compared with the experimental results in terms of predictive capability.

2. Mathematical models of devolatilization

2.1. Global Models

The single reaction model [5] is widely used and can give good estimation of the volatile yields. Single first order reaction model calculates the overall devolatilization rate by means of the following expression:

$$\frac{dV}{dt} = (V_f - V)A_v \exp\left(-\frac{E_v}{RT_p}\right) \quad (1)$$

In the model equation, V is the volatile yield on a dry-ash free basis, kinetic rate is defined by Arrhenius type equation with pre-exponential factor A_v and activation energy by E_v , T_p is the temperature of particle, and the final volatile matter yield is V_f .

Two-competing reactions model proposed by Kobayashi [6] is an alternative global model. In this model, two parallel first order competing reactions are used for predicting volatile yield as represented in Fig. 1. One reaction is slower and initiates at lower temperatures due to low activation energy and the second one is a prompt reaction that dominates at higher temperatures.

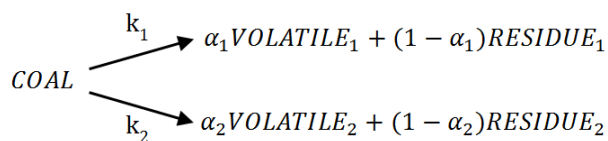


Fig.1. Two competing reaction mechanism of coal devolatilization proposed by Kobayashi [6]

The α_1 and α_2 are the mass stoichiometric coefficients for the asymptotic volatile yields of corresponding reactions, and k_1 and k_2 denote the Arrhenius type reaction rates. The rate equation for the devolatilization is described by the following relation.

$$\frac{dV}{dt} = \alpha_1 A_1 \exp\left(-\frac{E_1}{RT_p}\right) + \alpha_2 A_2 \exp\left(-\frac{E_2}{RT_p}\right) \quad (2)$$

Table 1. Two competing reactions model parameters proposed by Kobayashi [6] and Ubhayakar [10]

	α_1	A_1	E_1 (j/kmol)	α_2	A_2	E_2 (j/kmol)
Kobayashi	0.3	2×10^5	1.05×10^8	1	1.3×10^7	1.67×10^8
Ubhayakar	0.39	3.7×10^5	7.36×10^7	0.8	1.46×10^{13}	2.51×10^8

2.2. Network Models

There are three network models widely utilized in numerical simulations of coal combustion; namely, Chemical Percolation Devolatilization (CPD) model [7], Functional Group Depolymerization Vaporization Cross-Linking (FG-DVC) model [8] and Distributed Energy Chain Statistics (FLASHCHAIN) model [9]. Among the network models, CPD model is used in this work. The CPD model is built upon the representative description of the coal as an array of aromatic clusters interconnected by chemical bridges some of which are labile bonds that break during devolatilization, while others remain intact at high temperature. The formation of tar precursors, char and light gas, is modeled by reaction scheme shown in Fig. 2. Labile bridge population in the network is represented by ϵ . As the coal is heated, labile bridge forms the activated bridge intermediate ϵ^* with a slow reaction rate of k_b . Activated bridge intermediate decomposes by two competing reactions, one is forming two broken bridges δ with reaction rate k_δ , other one is generating a stable char bridge c and two moles of light gases g_2 with reaction rate k_c . Broken bridges generated from reactive intermediate decompose into light gas g_1 with a consecutive reaction with rate of k_g .

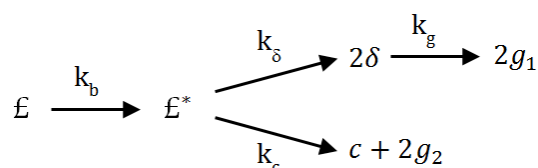


Fig.2. Reaction mechanism of coal devolatilization in the CPD model [7]

3. The Effect of Heating Rate on Devolatilization

In pulverized coal applications, particle sizes are very small ($100\mu\text{m} <$); hence, initial particle heat up can be very high in the range of 10^3 to 10^6 K/s [15]. Heating rate effect is investigated by numerical

integration of the volatile yields for the chosen devolatilization models with different heating rates that can be expected in a pulverized coal boiler environment. Volatile yields are given for Newlands coal that is also used in the simulated experiment with properties given in [16].

The CPD network model and the two-competing-reactions global model can predict the higher yield of volatiles with increasing heating rate, however single first order reaction model does not consider this effect and final volatile yield must be explicitly specified. SFOR model parameters are optimized using the results of CPD network devolatilization model [17-18]. The SFOR model volatile yield predictions and optimized Arrhenius rate parameters are represented in Fig. 4.

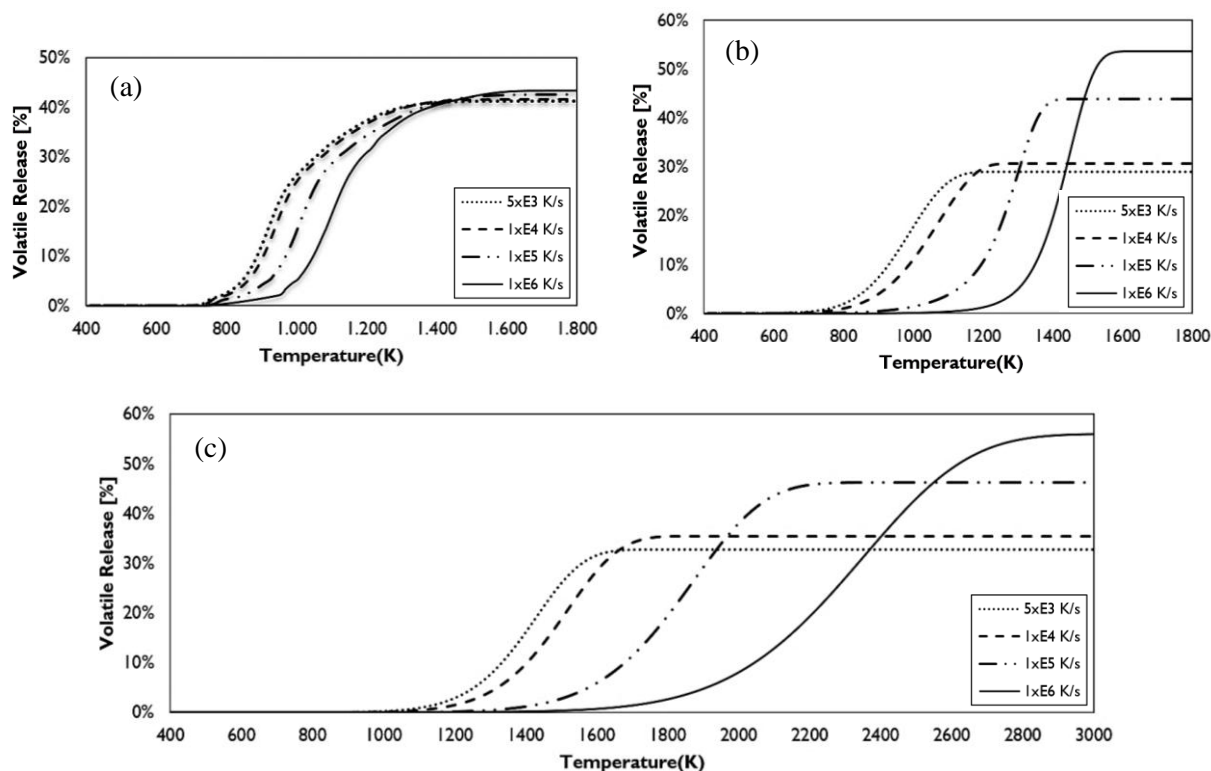


Fig. 3. Predicted yield of volatiles by (a) CPD model (b) TCR model with Ubhayakar parameters (c) TCR model with Kobayashi parameters for varying heating rates from 5×10^3 to 10^6 K/s

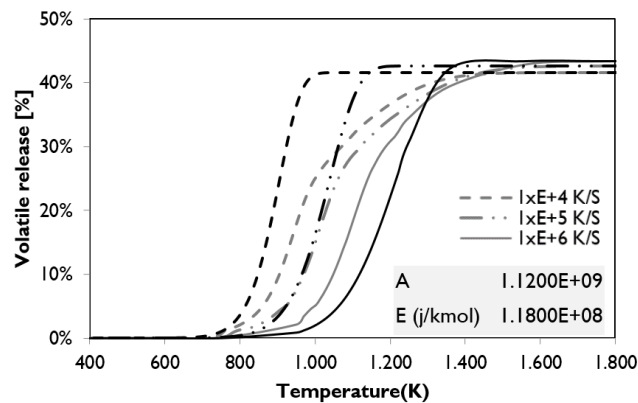


Fig. 4. Predicted yield of volatiles by SFOR model in comparison to CPD model predictions used for optimization of the SFOR model rate parameters

4. Numerical Simulation of a Pulverized Coal Flame

4.1. Simulated Pulverized Coal Flame

The CRIEPI's pulverized coal jet burner [6] experiment is shown in Fig. 5. Experimental conditions are summarized in Table 3.

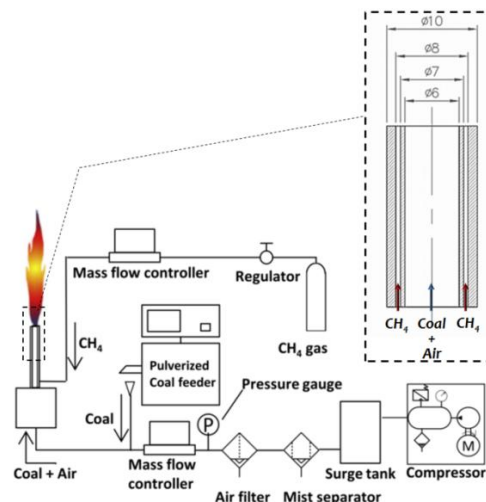


Fig. 5. CRIEPI's pulverized coal flame experimental configuration, adapted from [16]

4.2. Mathematical Model Description of Pulverized Coal Combustion

Devolatilization models are mentioned previously, in addition, governing models of both coal combustion and the flow field used within the well-known CFD software FLUENT are given in Table 4.

Table 3. Experimental conditions for the simulated pulverized coal flame [16]

Pulverized-coal feed rate	1.49x10 ⁻⁴ kg/s
Air flow rate	1.80x10 ⁻⁴ m ³ /s
CH ₄ flow rate	2.33x10 ⁻⁵ m ³ /s
Thermal input of coal*	4.19 kW
Thermal input of CH ₄ *	0.83 kW
Bulk equivalence ratio	6.09
Reynolds number	2544
*Based on lower heating value	

Table 4. Sub-models used in the numerical simulation of pulverized coal flame

4.2.1. Volatile Species (obtained from CPD model)						
H ₂ O	CO ₂	CH ₄	CO	other	tar	Σ
%6.15	%1.54	%5.06	%2.43	%8.59	%24.33	%48.1
4.2.2. Gaseous Reactions - units [m3,s ,K, kmol]						
Reaction	Reaction order			A	b	E
1 C ₈ H ₈ + 6O ₂ → 8CO + 4H ₂ O	[C ₈ H ₈]			3.8e7	0	5.55e7
2 CH ₄ + 1.5O ₂ → CO + 2H ₂ O	[CH ₄] ^{0.7} [O ₂] ^{0.8}			5.01e11	0	2.00e8
3 C ₃ H ₈ + 3.5O ₂ → 3CO + 4H ₂ O	[C ₃ H ₈] ^{0.7} [O ₂] ^{0.8}			1.5e10	0	8.7e7
4 CO + 0.5O ₂ → CO ₂	[CO] [O ₂] ^{0.25} [H ₂ O] ^{0.5}			2.23e12	0	1.7e8
5 CO ₂ → CO + 0.5O ₂	[CO ₂]			5.0e8	0	1.7e8
6 H ₂ + 0.5O ₂ → H ₂ O	[H ₂] ^{0.25} [O ₂] ^{1.5}			7.9e10	-1	1.47e8
4.2.3. Turbulence Chemistry Interaction						
Eddy Dissipation Concept Model [22]						
4.2.4. Char Combustion (Heterogeneous reactions)						
Kinetics-Diffusion Limited Models[23]						
4.2.5. Radiation						
Discrete ordinates [24] angular discretization 4×4, Weighted Sum of Gray Gases [25]						
4.2.6. Turbulence						
Reynolds Stress Transpor Model [27]						

5. Results and Discussion

The numerical simulation of pulverized coal combustion is carried out using CFD code FLUENT version 15.2. Domain size and mesh configuration is shown in Fig. 6. The computational domain has a total length of 240 mm (40D) and a diameter changing from 60 mm (10D) to 108 mm (18D). 1/4th of the domain is modeled by utilizing symmetry boundary conditions. Mesh dependency was examined by comparing results of structured grids with number of cells of 0.32 M, 0.64 M and 1.28 M, negligible difference is observed and 0.64 M is chosen for further study.

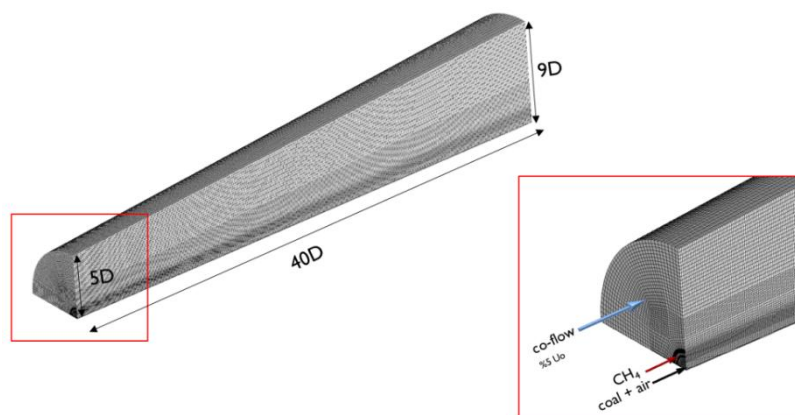


Fig. 6. Numerical grid used in the simulation of CRIEPI pulverized coal flame

5.1. Devolatilization Region

Fig. 7. shows the regions of volatile release in the 180 mm region where experimental measurements are taken and shown next to the flame image. It is observed that, SFOR model with optimized rate parameters closely match the CPD model devolatilization release region. For the TCR model with Kobayashi parameters, delay in devolatilization is observed as expected and devolatilization is not completed in the measurement domain.

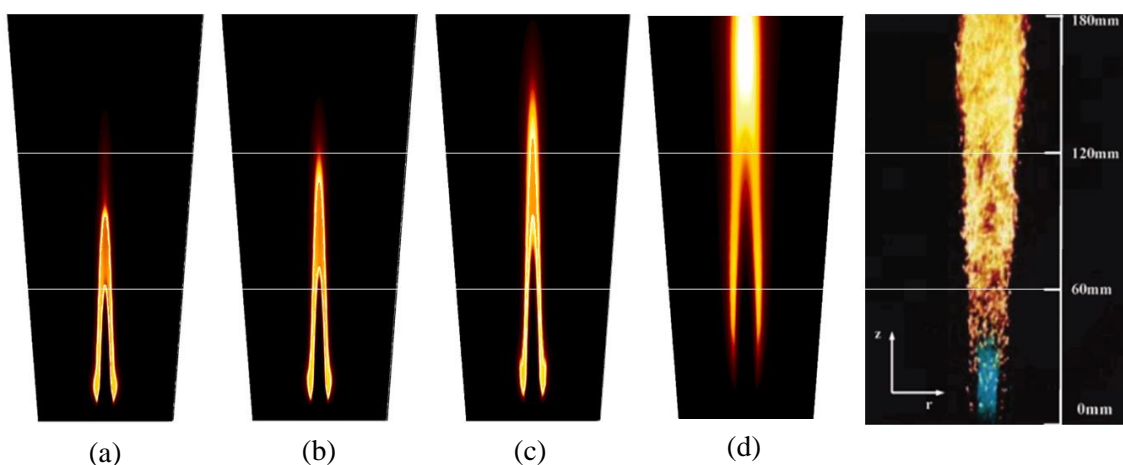


Fig. 7. Comparison of volatile release region predicted in the numerical simulation by different devolatilization models (a) CPD (b) SFOR (c) TRC-U (d) TCR-K

5.2. Temperature distribution

Fig. 8. shows the axial temperature profile of mean particle temperature from the experiment and the simulation. Pyrometer temperature measurement is compared with temperature of randomly selected 3000 particle sample in a radial distance and gas temperature at the domain axis and gas temperature at a radial offset where temperature distribution is at maximum (8-10mm). The clustering of scatter point

temperature data gives a comparison to pyrometer measurement. With respect to this criterion, TCR model with Kobayashi parameters resulted in prediction of particle temperature data in better agreement with the experimental measurements.

The temperature distribution across the cross-section of the computational domain is shown in Fig. 9. The temperature profiles exhibit close similarity for CPD, SFOR and TCR-U models. High temperature region is more distant from the central axis and broader in these models compared to TCR-K model. Even though the volatile release region is very different for TCR-K model, effect on temperature profile is less noticeable.

5.3. Species Concentration

The distribution of oxygen mole fraction on the central axis is compared to experimental measurement in Fig. 10. Rapid consumption of oxygen is observed in the numerical simulation results compared to the experimental data.

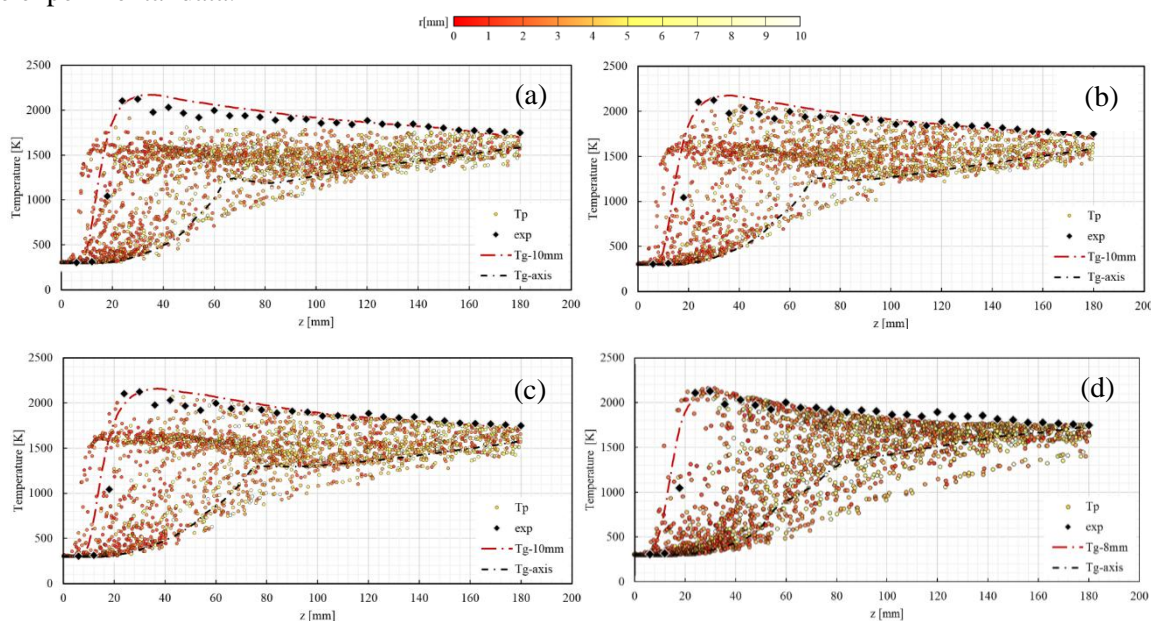


Fig. 8. Comparison between experimental temperature measurements and numerical simulation predictions with different devolatilization models (a) CPD (b) SFOR (c) TRC-U (d) TCR-K

The oxygen distribution along the central axis is not highly influenced by the utilization of different devolatilization models, however with the TCR-K model slightly slower oxygen consumption rate is predicted. The overestimation of oxygen consumption rate in the simulations is attributed to lack of a detailed chemical mechanism including dissociation reactions. Also, experimental error due to spatial resolution of the suction sampling is possible.

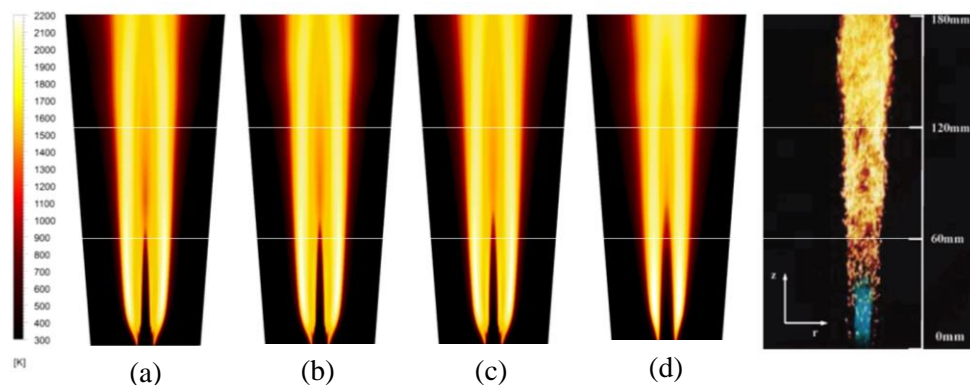


Fig. 9. Comparison of gas temperature distribution from CFD simulation results with different devolatilization models and experimental image of the flame (a) CPD (b) SFOR (c) TRC-U (d) TCR-K

Fig. 11 compares the CO_2 mole fraction on the central axis along the flame. CO_2 mole fraction closely match the experimental measurements however rapid consumption of oxygen result in over-production of the CO_2 at the initial data points. Again, the effect of devolatilization models does not seem prominent.

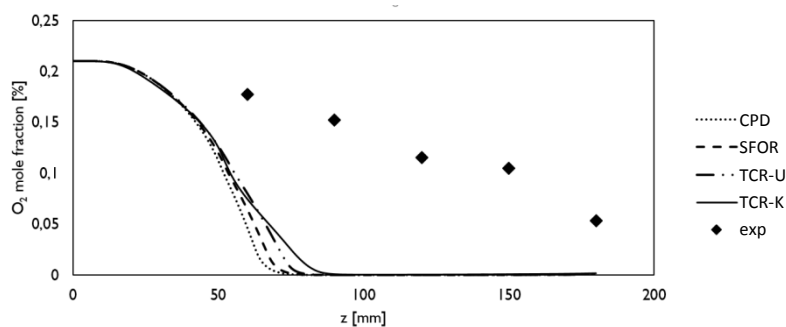


Fig. 10. Distribution of O_2 concentration on the central axis

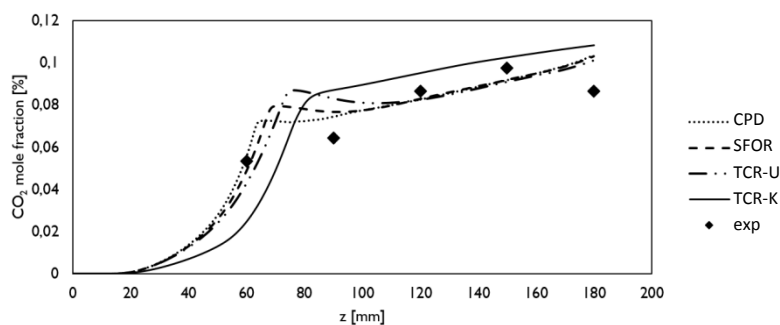


Fig. 11. Distribution of CO_2 concentration on the central axis.

6. Conclusions

In this study, global and network models for mathematical modeling of devolatilization are investigated in a numerical framework. Cross comparison is carried out between numerical results obtained by different devolatilization models and the experimental data. Influence of devolatilization models on the volatile release region, temperature of particles and gaseous species concentration is evaluated.

For the studied flame configuration of lab-scale round jet flame, prediction of the delayed and slower rated devolatilization model with two-competing rates proposed by Kobayashi was in better agreement with the experimental particle temperature measurement. In the numerical simulations of turbulent pulverized coal jet flame, the gaseous temperature and species field was not highly sensitive to the selection of devolatilization model. O₂ species consumption rate was too high in the central axis of the flame in the numerical simulations compared to the experimental distribution.

References

- [1] Williams A., Pourkashanian M., Jones J.M. The Combustion of Coal and Some Other Solid Fuels. *Proceedings of the Combustion Institute* (2000) 28:2141-2162.
- [2] Prado G. (ed.), LaHaye J. Fundamentals of the Physical-Chemistry of Pulverized Coal Combustion. Martinus Nijhoff Publishers, Dordrecht (1987).
- [3] Eaton A.M., Smoot L.D., Hill S.C., Eatough C.N. Components, formulations, solutions, evaluation, and application of comprehensive combustion models. *Prog Energy Combust Sci* (1999) 25:387–436.
- [4] Schlosberg R.H. (ed.). Chemistry of Coal Conversion. Springer Science+Business Media, LLC, New York (1985).
- [5] Badzioch S. and Hawksley P.G.W. Kinetics of Thermal Decomposition of Pulverized Coal Particles *Ind Eng Chem Process Design and Development* (1970) 9:521-530.
- [6] Kobayashi H., Howard J. B., Sarofim A. F. Coal Devolatilization at High Temperatures. 16th Symp (Int'l) on Combustion. The Combustion Institute (1976).
- [7] Grant D.M., Pugmire R.J., Fletcher T.H., Kerstein A.R. Chemical Model of Coal Devolatilization Using Percolation Lattice Statistics. *Energy & Fuels* (1989) 3:175-186.
- [8] Serio M.A., Hamblen D.G., Markham J.R., Solomon P.R. Kinetics of Volatile Evolution in Coal Pyrolysis: Experiment and Theory. *Energy & Fuels* (1987) 1:138-152.
- [9] Niksa S., Kerstein A.R. FLASHCHAIN Theory for Rapid Coal Devolatilization Kinetics. 1. Formulation. *Energy & Fuels* (1991) 5:647-665.
- [10] Ubhayakar S.K., Stickler D.B., Von Rosenberg C.W., Gannon R.E. Rapid devolatilization of pulverized coal in hot combustion gases. *Symp (Int) Combust* (1977) 16:427-436.
- [11] Yamamoto K., Murota T., Okazaki T., Taniguchi M. Large eddy simulation of a pulverized coal jet flame ignited by a preheated gas flow. *Proc Combust Inst* (2011) 33:1771–8.

- [12] Niksa S., Lau C.W. Global rates of devolatilization for various coal types. *Combust. Flame* (1993) 94:293-307.
- [13] Genetti D.B. An Advanced Model of Coal Devolatilization Based on Chemical. Brigham Young University. MSc Thesis (1999).
- [14] Anthony D.B., Howard J.B., Hottel H.C., Meissner H.P. Rapid devolatilization of pulverized coal. *Symp (Int) Combust* (1975) 15:1303-1317.
- [15] Prado G., Corbel S., Lahaye J. Modelling of Coal Devolatilization with a Non-Linear Heating Rate. In: *Fundamentals of the Physical-Chemistry of Pulverized Coal Combustion*. Volume 137 of the series NATO ASI Series (1987) 152-158.
- [16] Hwang S.M., Kurose R., Akamatsu F., Tsuji H., Makino H., Katsuki M. Application of Optical Diagnostics Techniques to a Laboratory-Scale Turbulent Pulverized Coal Flame. *Energy & Fuels* (2005) 19:382-392.
- [17] Richards A.P., Fletcher T.H. A comparison of simple global kinetic models for coal devolatilization with the CPD model. *Fuel* (2016) 185:171–180.
- [18] Stein O.T., Olenik G., Kronenburg A., Marincola F.C., Franchetti B.M., Kempf A.M., Ghiani M., Vascellari M., Hasse C. Towards Comprehensive Coal Combustion Modelling for LES. *Flow Turbulence Combust* (2013) 90:859–884.
- [19] Solomon P.R., Hamblen D.G., Carangelo R.M., Serio M.A., Desphande G.V. General model of coal devolatilization. *Energy & Fuels* (1988) 2:405-422.
- [20] Serio M.A., Hamblen D.G., Markham J.R., Solomon P.R. Kinetics of volatile evolution in coal pyrolysis: experiment and theory. *Energy & fuels* (1987) 1:138-152.
- [21] Wetbrook C.K. and Dryer F.L. Simplified Reaction Mechanisms for the Oxidation of Hydrocarbon Fuels in Flames. *Combustion Sci and Tech* (1981) 2:31-43.
- [22] Magnussen B.F. On the Structure of Turbulence and a Generalized Eddy Dissipation Concept for Chemical Reaction in Turbulent Flow. Nineteenth AIAA Meeting, St. Louis (1981).
- [23] ANSYS FLUENT 15.0 User's Guide, ANSYS Inc. (2014).
- [24] Fiveland W.A. Discrete Ordinate Methods for Radiative Heat Transfer in Isotropically and Anisotropically Scattering Media. *J. Heat Transfer* (1987) 109:809-812.
- [25] Smith T.F., Shen Z.F., Friedman J.N. Evaluation of coefficients for the weighted sum of gray gases model. *J Heat Transfer* (1982) 104:602–608.
- [26] Launder B.E., Reece G. J., Rodi W. Progress in the Development of a Reynolds-Stress Turbulent Closure. *Journal of Fluid Mechanics* (1975) 68:537-566.
- [27] Lasher W.C. Reynolds stress model assessment using round jet experimental data. *International Journal of Heat and Fluid Flow* (1994) 15:357-363.
- [28] Bermudez A., Ferrin J.L., Linan A., Saavedra L. Numerical simulation of group combustion of pulverized coal. *Combustion and Flame* (2001) 158:1852-1865.

The numerical and experimental investigation of a monoblock natural gas burner for reducing NO_x emissions

Engin Uza^{*1,2}, Barış Yılmaz¹

¹ Marmara University, Mechanical Engineering Dept., 34722 Kadikoy, Istanbul, TURKEY

² ECOSTAR Combustion Systems, 59860 Corlu, Tekirdag, TURKEY

(E-mail: engin_uza@hotmail.com , byilmaz@marmara.edu.tr)

Abstract: Fossil fuels, made up of ancient and decomposed organic materials, are still the major source of the energy production. Steady increase of energy consumption causes to increase in fossil fuel usage and that result in unpleasant effects on human beings and the environment. The fuels utilized in the power generation, especially in industrial scale applications, are almost hydrocarbons which consist of carbon and hydrogen in their molecular structure. In combustion of fossil fuels; main combustion products are carbon dioxide, hydrogen oxide, carbon monoxide, nitric oxide and sulphur oxide which are identified as the main suspects of the environmental damage. Among the most important topics in combustion science and engineering are using the energy more efficiently and decreasing the flue gas emissions.

The computational fluid dynamics (CFD) is an effective tool to optimize conventional designs and to develop new products. Using CFD during the design cycle, makes accurate prediction, shorten design time and reduce product development cost in industrial product development and academic researches.

In this study, an industrial scale gas burner, namely ECO-45, was investigated numerically. The burner and the assembled combustion chamber have been modelled using FLUENT software. The studied low NO_x gas burner satisfies also the standards defined in TSE EN 676:2000 Class-3. The NO_x level of less than 80 mg/kWh has been aimed to be obtained. Both the velocity and temperature fields are calculated and represented in terms of contour plots. The emissions at the exit of the combustion chamber and chamber-wall temperatures have been obtained. The numerical model results were validated with available experimental measurements obtained from test facilities in ECOSTAR company. The fruitful results have been achieved for reducing the NO_x levels.

Keywords: Combustion, NO_x reduction, CFD, Burner, Energy efficiency,

1. Introduction

Steady increase of energy consumption causes to increase fossil fuels usage in energy production and that causes unpleasant effect to human beings and the environment. The use of

energy more efficiently and the decrease of flue gas emissions are the most important topics in science and engineering recently.

Combustion is the controlled exothermic chemical reaction which provides heat and energy as a result of the reaction between fuel and oxidizer. Nowadays, most of the energy production is still being done by using fossil fuels which are made up ancient, decomposed organic materials. For starting combustion process, fuels need an oxidizer and an ignition source.

The fuels in the power generation in industrial applications are almost hydrocarbons (C_xH_y). Hydrocarbons are organic compounds consisting carbon and hydrogen in their molecular structure. Hydrocarbons can be found in the form of gases, liquids, and solids.

1.1 Combustion Products

In combustion of hydrocarbon fuels, the products of combustion are distinctly identified as a source of environmental damage. The main combustion products are carbon dioxide, hydrogen oxide, carbon monoxide, nitric oxide and sulfur oxide (in case of solid fuels). Main pollutants are nitric oxide and sulfur oxide but recently even carbon dioxide considered harmful and have a significant effect on atmosphere and concerns rising in global greenhouse effect.

Carbon dioxide (CO_2) is one of the main products of hydrocarbon combustion. Higher the percentage of carbon dioxide in combustion product means higher energy output of combustion process. Lower CO_2 level causes higher fuel consumption due to the inefficient combustion and it increases the energy production costs.

Oxygen (O_2) availability in flue gas emission means excess air is supplied to the combustion process to be ensured to complete combustion. Higher oxygen concentration causes to reduction in efficiency, on the other hand lower oxygen concentration may cause incomplete combustion.

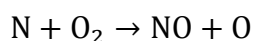
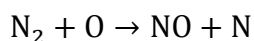
Carbon monoxide (CO) is the indicator of the incomplete combustion and it is colorless, odorless, and tasteless gas. It has nearly the same density as air and it can easily mix into the air.

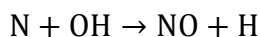
Nitric oxides (NO_x) emissions consists of nitric oxide (NO) and contains nitric dioxide (NO_2) and nitrous oxide (N_2O).

1.2 NO_x Mechanisms

Thermal NO mechanism that is well known as **Zeldovich Mechanism** is the largest contributor to NO_x emissions and formed by oxidation of atmospheric nitrogen contained in combustion air at high temperatures. Flame temperature directly affects the thermal NO_x emissions, under high temperature conditions; $T > 1500K$, nitrogen in combustion air is oxidized. Enriched oxygen combustion and preheated combustion air temperature directly affect flame temperature and thermal NO formation.

Zeldovich mechanism is;





The Prompt Mechanism is fast reaction between hydrocarbon and nitrogen in combustion air to form hydrocyanic acid (HCN) and known as **Fenimore Mechanism**. Hydrocyanic acid reacts with nitrogen and oxygen in combustion air and form NO_x . Prompt mechanism reactions are very complicated and consist of hundreds of reactions. Prompt NO_x is an important factor of NO_x formation in low temperature and under stoichiometric combustion. Prompt NO_x is the small portion of the total NO_x emissions and its control is important to reach single digit NO_x emission values.

Fuel NO_x is formed by oxidation of nitrogen in fuel and oxygen in the air. Gaseous fuels such as natural gas, propane are no bound nitrogen fuels. During the combustion of the liquid fuels and solid fuels that are consisted of fuel-bound nitrogen, 20%-50% of NO_x is formed due to the fuel NO_x . Fuel NO_x is generally important in non-premixed combustion, in premixed combustion, fuels that are used in non-premixed combustion is generally gaseous fuels that contain little amount of nitrogen or no bound nitrogen.

2. Material and Method

In this study, the combustion of natural gas has been examined using both numerical and experimental methods. A sample burner was chosen and then modelled using Fluent software. Fluent is a well-known commercial program used in both academic and industrial modeling studies. Numerical results have been validated with available experimental data.

2.1 Experimental Setup

In order to measure the temperature levels at different locations of the combustion chamber and the flue gas emissions, the experimental setup located in ECOSTAR company is utilized. Test setup technical specifications are being explained in the **Figure 2.1**.

The following operating parameters are being measured during the tests in line with PLC controlled test units;

- Fuel flow rate, fuel supply temperature and pressure,
- Cooling water flow rate, cooling water inlet and outlet temperature,
- Flue gas emissions (CO , CO_2 , O_2 , NO_x , SO_x)
- Flue gas temperature,
- Boiler back pressure,
- Fuel and combustion air pressure,

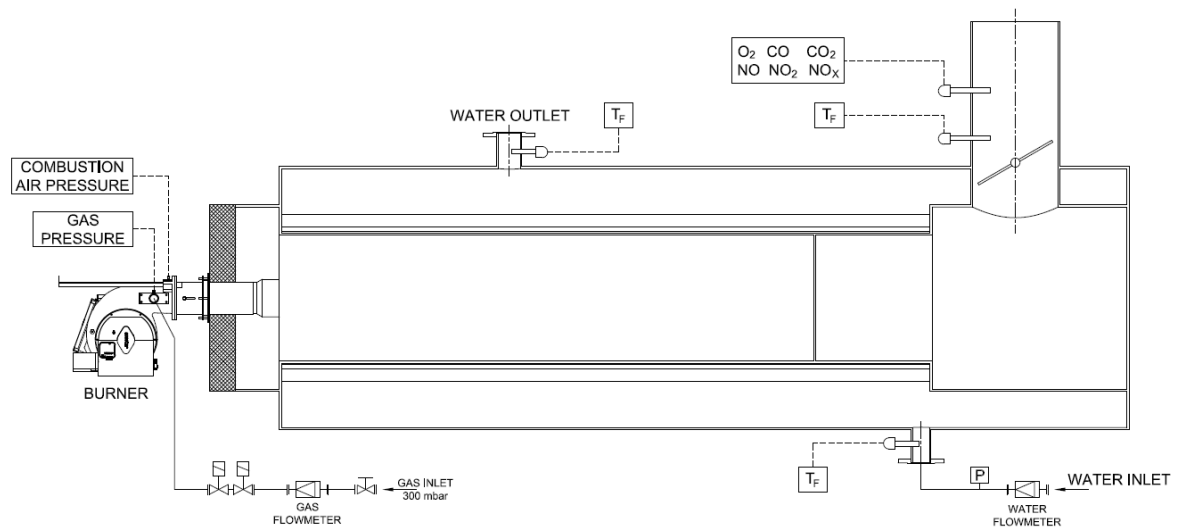


Figure 2.1. Test setup and measured operating parameters of the test setup

In this study, ECOSTAR ECO-45 G C burner is considered. It is a non-premixed type, monoblock modulating and natural gas/LPG burner. General specifications of ECO-45 G C burner is listed in **Table 2.1.**

Table 2.1. Burner Technical Specifications

BURNER TYPE	CAPACITY		CAPACITY		NATURAL GAS CONSUMPTION		FAN MOTOR POWER	MAIN SUPPLY
	Min. kcal/h	Max. kcal/h	Min. kW	Max. kW	Min. Nm ³ /h	Max. Nm ³ /h	kW	VAC
ECO 45 G C 2	172,000	645,000	200	750	20.8	78.2	0.75	3N 380
ECO 45 G C 2/L	172,000	749,920	200	872	20.8	90.9	0.75	3N 380
ECO 45 G C 2a	172,000	860,000	200	1,000	20.8	104.2	1.1	3N 380
ECO 45 G C 2b	172,000	1,032,000	200	1,200	20.8	125.1	1.5	3N 380

2.2 Numerical Model

Numerical studies are performed using ANSYS-Fluent CFD solver. Geometries for the solutions are modelled in Solidworks. Modelled geometry imported to **ANSYS Design Modeler** and fluid volume is created and then created fluid volume is imported to **ANSYS Mesh** and then mesh is generated. Generated mesh is imported to **ANSYS Fluent** solver. Cold flow and reactive analysis are done in Fluent by using calculated boundary conditions and experimental datas.

Burner geometry has complicated parts due to the its design and operation principle. For CFD analysis burner geometry is simplified. Simplifications that are done in geometry is;

1. Ignition electrode and ionization electrode are not modelled,

2. Burner body and other equipment are not used in modelled geometry,
3. Geometrical simplifications are done in diffuser wings,
4. Fixing plate of the flame tube extension is not modelled.

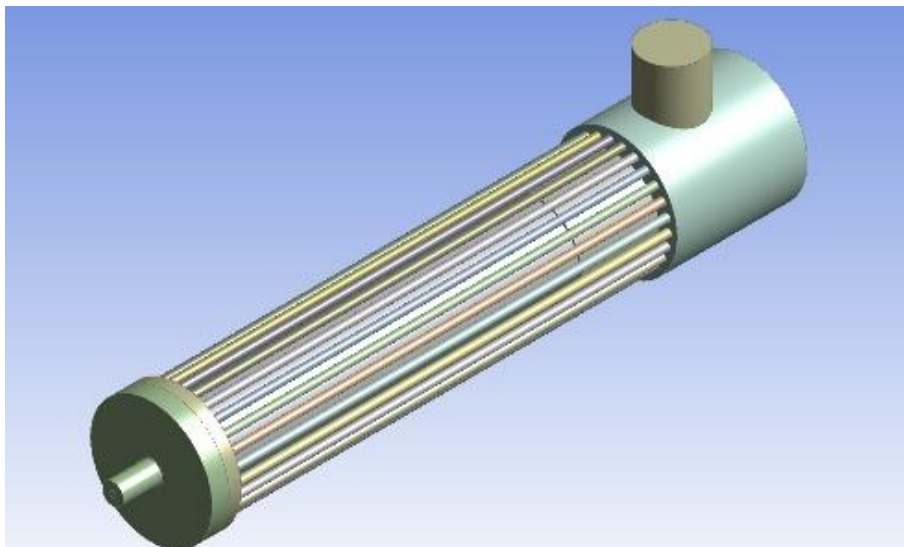


Figure 2.2. Fluid volume of the geometry in ANSYS Desing Modeler

Mesh independency studies are done with four different meshed geometries that are prepared to find the suitable quality and mesh element number. Details of the burner combustion head are directly affected the mesh quality and mesh number. During the mesh independency studies, element sizes in burner head and related combustion chamber parts where the combustion occurs, are changed to improve mesh quality.

Table 2.2. Mesh element number and mesh quality of the first geometry

Mesh Name	Element Number	Skewness (Maksimum)	Orhogonal Quality (Minimum)
Mesh-1	5961246	0.84834	0.22609
Mesh-2	5522284	0.87171	0.21169
Mesh-3	4789363	0.89912	0.18363
Mesh-4	4399183	0.93495	0.08915

Cold flow analysis done for the four-different mesh option cold flow analysis comparison graph for the first geometry is shown in **Figure 2.3**. Velocities in axial direction of the combustion chamber are compared for four-different meshed geometries.

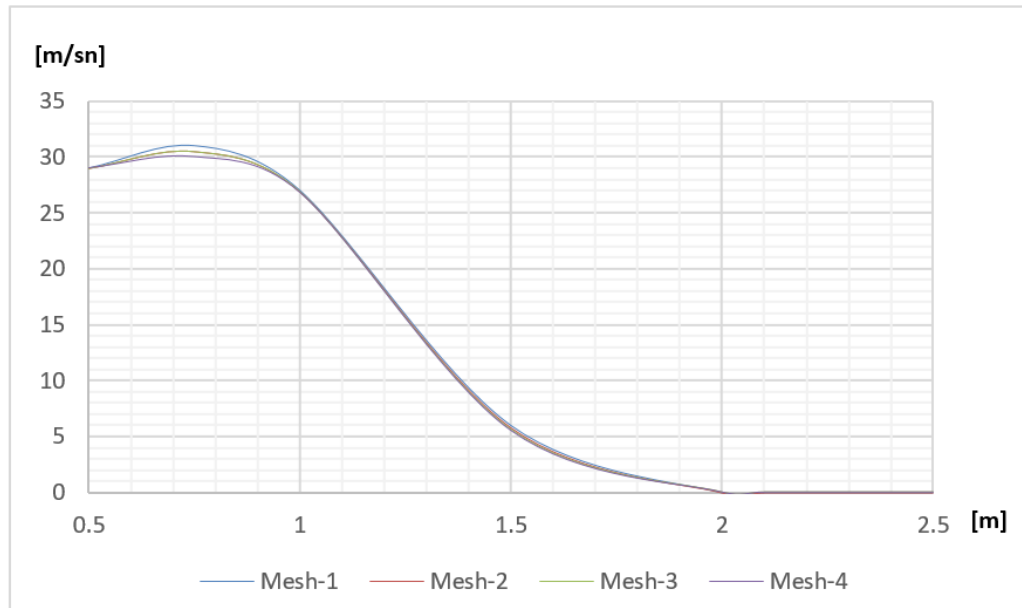


Figure 2.3. Axial Velocity [m/s] versus position [m]

Mesh-3 is found accurate enough for further studies. Mesh-3 is used for the numerical studies. Details of Mesh-3 are shown in **Figure 2.4**.

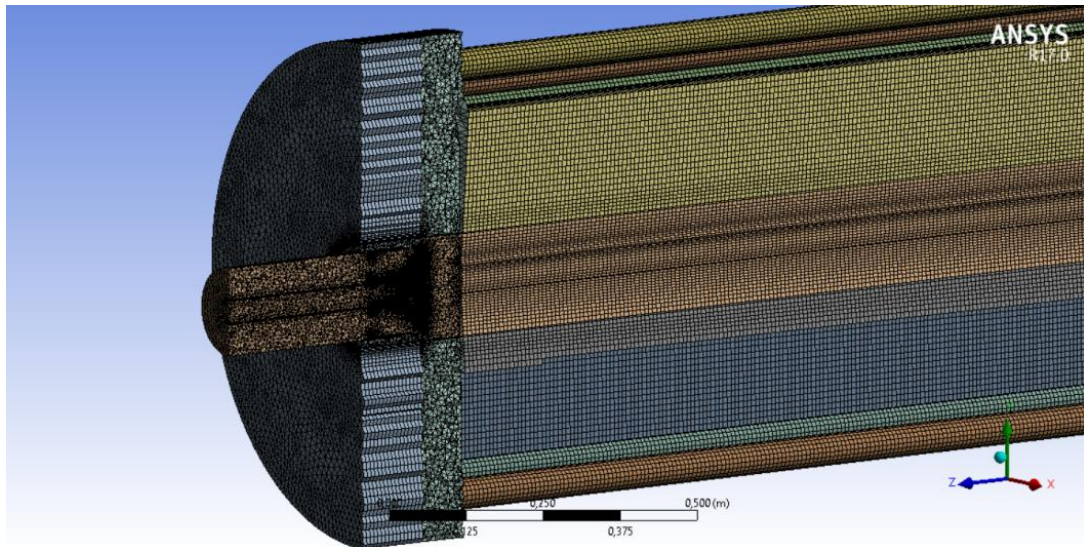


Figure 2.4.Details of Mesh-3 for the first geometry

Mass flow inlet boundary condition is used for both fuel inlet and air inlet during the numerical studies. Pressure outlet boundary condition is defined for the outlet.

Turbulent flow was modelled by using **k-ε turbulent model**. **PDF-Flamelet** combustion model and **DO** radiation model were used during the numerical studies. **Mass flow inlet** was used for the both fuel and air inlet conditions calculated **heat flux** is defined for the hot-water boiler due to unknown wall temperature. **Pressure outlet** boundary condition was defined as outlet boundary condition.

3. Results

First reactive analysis case studies were done in different excess air values for high load. For the mixed natural gas and %100 methane; 125.1 Nm³/h gas consumption. The comparison of numerical and experimental studies for the **first reactive analysis case studies** for natural gas are shown in Table 3.1 .

Table 3.1. First reactive analysis case studies and experiments comparisons

Case Experiment	Fuel Type	Gas Consumption	λ	O ₂	CO ₂	NO _x
		Nm ³ /h	-	%	%	ppm
Case-1	Mix Natural Gas	125.1	1.1	1.61	10.7	61.2
Experiment-1	Mix Natural Gas	125.1	1.1	2	10.41	66
Case-2	Mix Natural Gas	125.1	1.2	3.3	9.6	61.6
Experiment-2	Mix Natural Gas	125.1	1.2	3.5	9.76	63
Case-3	Mix Natural Gas	125.1	1.3	4.26	9.03	53.32
Experiment-3	Mix Natural Gas	125.1	1.3	4.9	8.77	57
Case-4	Mix Natural Gas	125.1	1.4	5.61	8.11	55.53
Experiment-4	Mix Natural Gas	125.1	1.4	6	8.18	51

Differences in experiments and numerical studies are found to be $\Delta O_2 \sim 7\%$, $\Delta CO_2 \sim 2\%$, $\Delta NO_x \sim 12\%$. Mix natural gas numerical study results are closer when compared with the methane case study to the experimental results.

Second reactive analysis case studies were done in the same excess air value; $\lambda=1.2$, for different burner loads. Numerical studies and experimental studies are compared for the **second reactive analysis case studies** for natural gas. Results are shown in Table 3.2 and Figure 3.1.

Table 3.2. Second reactive analysis case studies and experiments comparisons

Case Experiment	Fuel Type	Gas Consumption	λ	O ₂	CO ₂	NO _x
		Nm ³ /h	-	%	%	ppm
Case-6	Mix Natural Gas	50	1.2	3.5	9.48	46.54
Experiment-6	Mix Natural Gas	50	1.2	3.5	9.44	57
Case-7	Mix Natural Gas	75	1.2	3.5	9.83	56.86
Experiment-7	Mix Natural Gas	75	1.2	3.4	9.72	65
Case-8	Mix Natural Gas	100	1.2	3.5	9.50	49.7
Experiment-8	Mix Natural Gas	100	1.2	3.5	9.55	61
Case-2	Mix Natural Gas	125.1	1.2	3.3	9.6	61.6
Experiment-2	Mix Natural Gas	125.1	1.2	3.5	9.76	63

Differences in experiments and numerical studies are found to be $\Delta O_2 \sim 5\%$, $\Delta CO_2 \sim 2\%$, $\Delta NO_x \sim 18\%$.

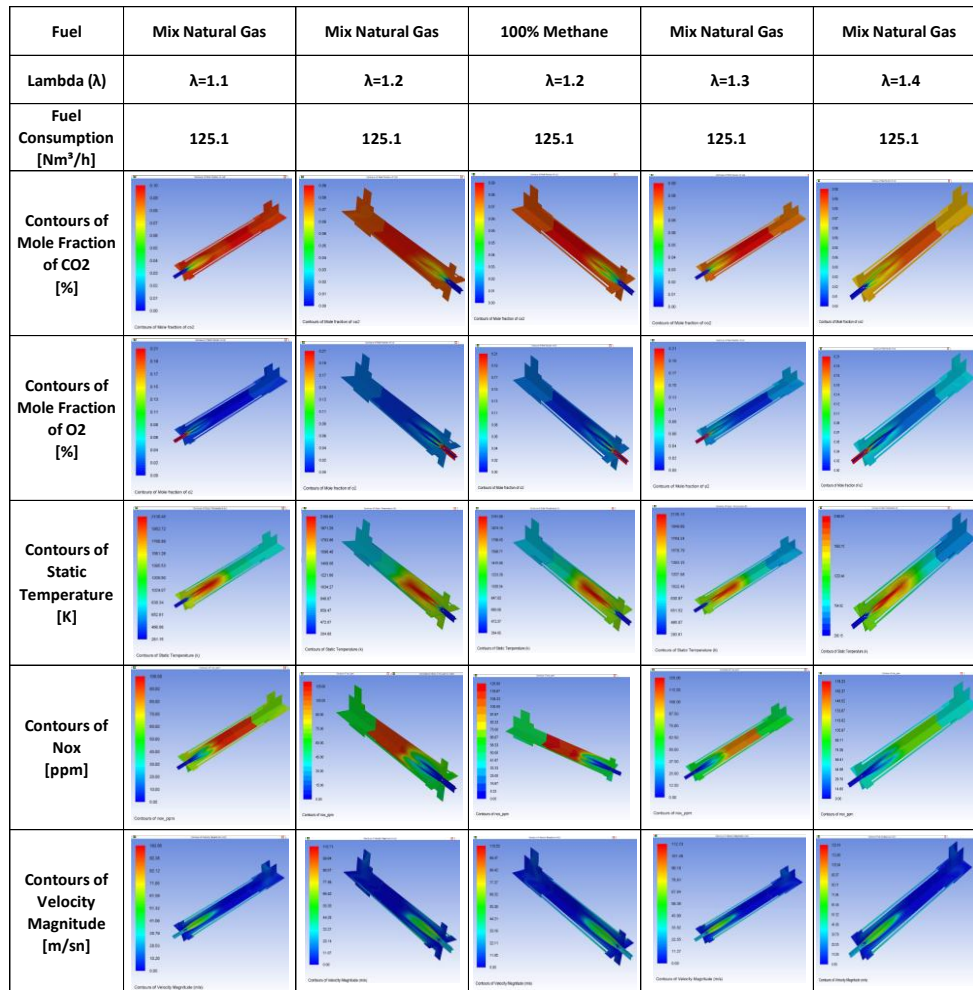


Figure 3.1. Contour plots of the numerical study results for the first geometry

4. Conclusion

The numerical studies of a burner and modified burner geometries have been performed in this study. The numerical studies have been performed initially for the mesh independency. The accurate enough mesh number and size have been determined by comparing four mesh cases. Then reactive case studies have been performed with this mesh.

In the first reactive analyses and experiments which were done with mix natural gas and 100% methane. Numerically it is observed that temperature distribution and CO₂, O₂ values are similar when %100 methane and mix natural gas are compared. However calculated NO_x values compared with the experimental values, mix natural gas reactive analysis results are found closer to the experimental data. For this reason, mix natural gas were used in the other cases.

In the second reactive analyses and experiments which were done with mix natural gas in different



burner outputs. Experiments and reactive studies were showed that less than 10 ppm difference occurs between high load and low load when the measured NO_x values compared.

5. References

- [1] Charles E.B., (2013) The John Zink Hamworthy Combustion Handbook Fundamentals Vol.1, 2nd Edition, CRC Press, Oklahoma
- [2] Basu P., Kefa C., Jestin L. (2000) Boilers and Burners Desig and Theory, 1st Edition, Springer, New York
- [3] Strehlow R.A., (1993) Combustion Fundamentals, 1st Edition, Krieger Pub Co,
- [4] McAllister S., Chen J., Fernandez-Pello A.C., (2011) Fundamentals of Combustion Proceses, 1st Edition, Springer, New York
- [5] Bayrakli İ., UZA E., (2016) ECOSTAR Burner & Combustion Technical Handbook, 2nd Edition Termo Isı A.Ş, Istanbul
- [6] EN 676:2008 Automatic Forced Draught Burners for Gaseous Fuels
- [7] Natural Gas Density Calculator, <http://www.unitrove.com/engineering/tools/gas/natural-gas-density>
- [8] Natural Gas Calorific Value Calculator, <http://www.unitrove.com/engineering/tools/gas/natural-gas-calorific-value>
- [9] Poinot T., Veynante D., (2001) Theoretical and Numerical Combustion, 1st Edition, Edwards, Philadelphia
- [10] Ansys Inc. (2016) Fluent Combustion Training Notes, 1st Edition, Ansys Inc., Canonsburg

Simulational Energy Analyses of Hybrid Vehicle's Electric Engine

Bahattin TANÇ¹, HüseyinTuran ARAT^{1}, Ertuğrul BALTACIOĞLU¹, Kadir AYDIN²*

¹ *Faculty of Engineering and Natural Sciences, Iskenderun Technical University*

² *The Faculty of Engineering and Architecture, Cukurova University*

hturan.arat@iste.edu.tr

Abstract: Today, complicated industry and manufacturers need simulation programs to reduce both the cost of test sets and to use time with the highest efficiency. Simulation systems and modeling phenomena are improve the significances on the product areas. Especially in automotive sector, before the production, the simulation and prototyping procedure is playing a highly important role. With this, AVL-Cruise simulation tool is chosen for this study that it is the one of the most comprehensive simulation program for automotive researchers and applicators. In addition, thanks to keeping up with evolving technology structure, this program can be easily implemented in hybrid vehicle simulations. In this study, a based modeled hybrid engine has created with 1.5 L, four cylinders gasoline engine and electric motor (10 kW) which equipped with appropriate generator. Energy analysis based on the changes of the CVT and manual transmission of a hybrid motor was run under 1750 rpm then the results of simulational data were examined and compared with each other. Sankey diagrams were used to illustrate the difference and consumptions of energy scale of the vehicle with the selected boundary conditions. As a result, it has been concluded that the energy consumption of the automatic transmission is more advantageous than the manual transmission under this study's test conditions.

Keywords: AVL-Cruise, energy analyses, cvt, manual transmission, hybrid vehicles

1. Introduction

The gradual decline of global oil reserves, in addition to stringent emission regulations around the world, has made even more critical the need for improved vehicular fuel economy [1]. Hybrid Electric Vehicle (HEV) is an attractive and promising solution to the problems of air pollution and petroleum shortage [2].

HEV's powertrain utilize an energy buffer, typically a battery and/or a supercapacitor, and one or more electric machines (EM) to supplement the output of the internal combustion engine (ICE). The multiple power sources open the possibility to further improve operational efficiency and customize vehicle powertrain. However, this also increases vehicle complexity, bringing into play many vehicle attributes, such as design, operation, performance, lifetime, and the interplay with the infrastructure, such as systems for navigation, traffic information, and the electric grid [3].

The essential function of a modern powertrain is to deliver torque to the road-tyre interface while providing high efficiency, and excellent ride quality. System design, and in particular, engine and transmission control design are the primary tools available to deliver these requirements. The shift

transients are the result of discontinuities in speed, torque, and inertia present during shifting. These discontinuities must be minimized to reduce the transient response of the powertrain [4].

Transmission system is very important and complex for all vehicles especially HEV. Wurm et.al explained the importance of this phenomenon as; “One important trend for hybrid vehicles is hybridization of transmission, in which motors were built into the transmission. All mainstream types of transmissions – manual transmission (MT), automatic transmission (AT), automated manual transmission (AMT), dual-clutch transmission (DCT) and continuously variable transmission (CVT) – have hybridized versions” [5].

Continuously variable transmission (CVT) consists of two pulleys flexible in their diameter and a belt wrapped around them. The pulley, which is connected to the engine crankshaft is called drive pulley. The other pulley is attached to the drive shaft and is denoted as driven pulley. The torque, provided by the engine, is transmitted by the belt. The major advantage of this system is that the transmission ratio can be changed without interrupting the torque output. CVTs are widely spread in the recreational vehicle industry like all-terrain-vehicles or snowmobiles [6]. The Continuously Variable Transmission can convert every point on the engine’s operating curve to an operating curve of its own, and every engine operating curve into an operating range within the field of potential driving conditions. Its advantage over conventional fixed-ratio transmissions lies in the potential for enhancing performance and fuel economy while reducing exhaust emissions. However, full exploitation of this theoretical capability would entail overdrive factors that are not realizable up to now [7].

In this preliminary theoretically study, the effect of different transmission systems on HEV energy performance were simulated. MT and CVT were selected and run with the same HEV for determining the differences for energetic perspective. It is observed that the results are consistent with the studies in the limited literary survey [1-8] on the subject.

2. Simulation Method

There are many simulation programs used today. The aim of the simulation programs is to model and develop the design. It is possible to use advanced simulation techniques which can give the closest result to the real-life conditions of the simulation studies. The AVL program is designed to give the nearest results with advanced simulation techniques thanks to its high integration capability with test equipment.

The AVL program consists of five sub-programs; AVL Fire, AVL Boost, AVL Cruise, AVL Cruise M, AVL Excite.

AVL CRUISE is usually used for drive and motor development calculations and also for energetic optimizations. Fuel consumption and emissions are used to determine the vibrations of driving links, driving performance (acceleration and flexibility), transmission (gear) organs, braking performance and also bulk loads in stress calculations [8].

In this simulation study, a 1460 cm³ 4-cylinder gasoline engine and a 10 kW power electric motor were used as a hybrid.

The component Gearbox contains a model for a gearbox with different gear steps. You can define as many gears as you want. For every gear it is possible to define the transmission ratio, the mass moments of inertia, and the moment of loss. In the component for manual gearboxes, the engine torque will be turned into a power take-off torque by considering the transmission, the mass moments of inertia, and the moment of loss [7].

The gearbox can be used for a manual or automatic gearbox. When used as an automatic gearbox, the gear shifting process will be controlled by the control module gearbox control or gearbox program. The driver will do this task when used as a manual gearbox.

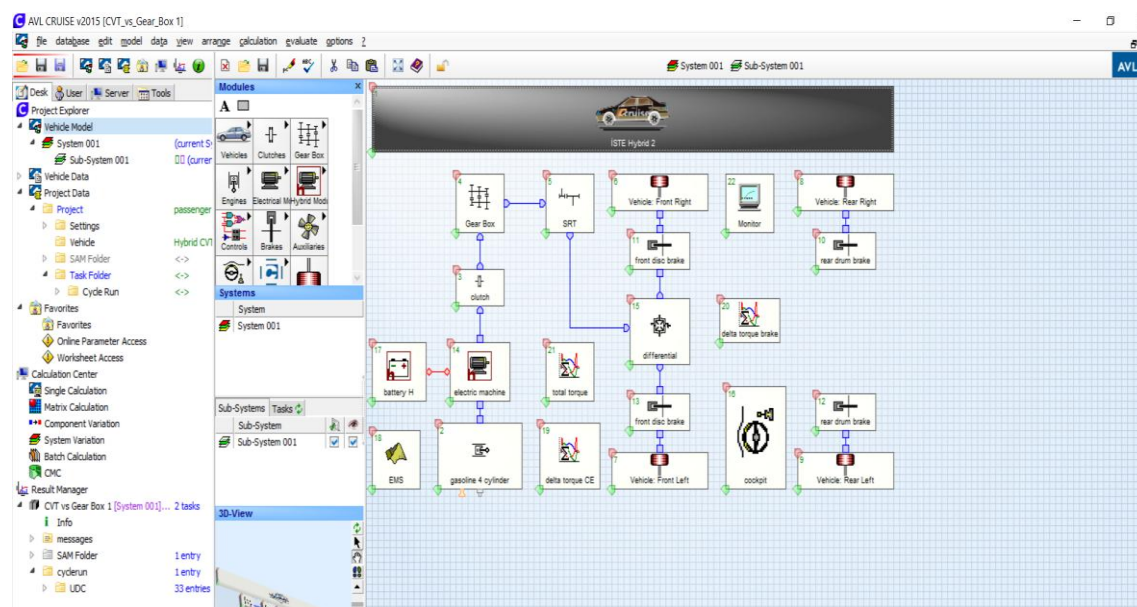


Figure 1. AVL Cruise Vehicle Model

With the model of the CVT gearbox included in AVL CRUISE it is possible to change the transmission between two user-defined threshold values. The adjusting speed between different transmissions is internal fixed at a constant value.

The change in transmission is done in form of a kinematic coupling. The advantage of this is that there is no additional degree of freedom. Thereby the calculation time is decreasing. The disadvantage is that the transitions might be not real harmonic and that there is the need to change the equation system for every change in transmission.

The manual gearbox and CVT data used are shown in table 1 and table 2 below.

Table 1. Manuel Gearbox Table

Gear	Transmission Ratio	Inertia Moment In	Inertia Moment Out	Number of Teeth Input	Number of Teeth Output
1	3,90909	0,0015	0,005	11	43
2	2,10526	0,0015	0,005	19	40
3	1,3871	0,0015	0,005	31	43
4	1,02326	0,0015	0,005	43	44
5	0,813953	0,0015	0,005	43	35
6	0,673913	0,0015	0,005	49	31

Table 2. CVT Table

Adjustment Time (s)	Switching Threshold	Inertia Moment In	Inertia Moment Out	Minimum Ratio	Maximum Ratio
2,5	0,04	0,035	0,045	0,5	2,8726

3. Results and Discussion

In this section, the energy optimization approach and selected results were compared and explained under the differences between simulations of the 6-speed manual gearbox and the CVT with the helped of AVL Cruise software simulation.

CVT transmission ratio and Manuel transmission ratio are compared in Figure 2. The CVT transmission ratio has progressed continuously in a fluctuating form between 2.8 to 1.1. The manual transmission ratio steadily progresses according to table 1 in each gear range.

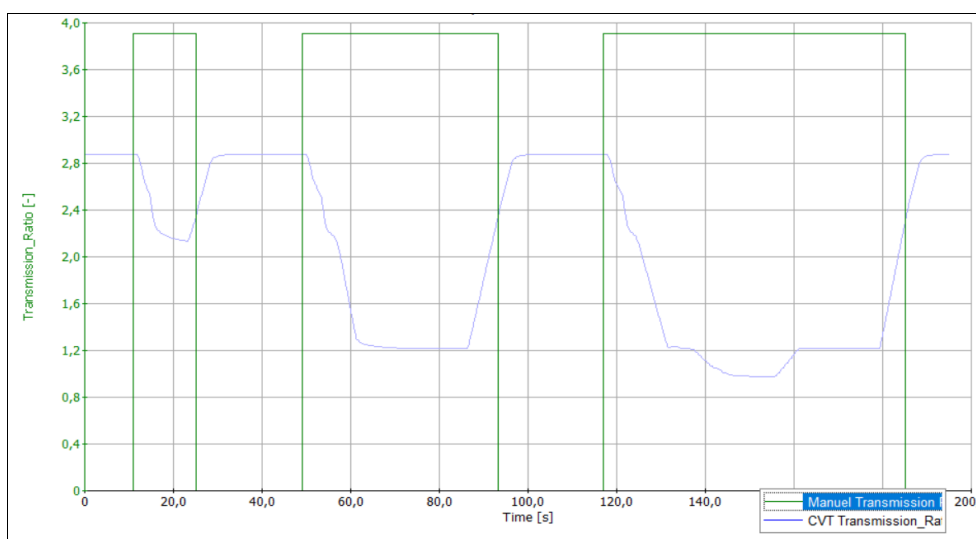


Figure 2. CVT Transmission Ratio and Manuel Transmission Ratio

CVT speed input and speed output, MT speed input and output have shown in Figure 3. The ratio of the speed input to the speed output gives the gear ratio. While this ratio can be easily determined in manual gears, instant rates are seen for CVT gears.

Sankey Diagrams are attention grabbing flowcharts that help in quick visualization of the distribution and losses of material and energy in a process. The width of the lines used in drawing the flowchart is proportional to the quantum of material or energy [9]. For a specific instantaneous Sankey values, The CVT battery potential is not lower than 30% but MT decreases this values up to 25%. Figure 4 illustrated that the CVT battery potential is more preferable energy optimization rather than MT. Results on whole simulational Sankey cycle the values on battery potential energetic outputs similar to instantaneous values.

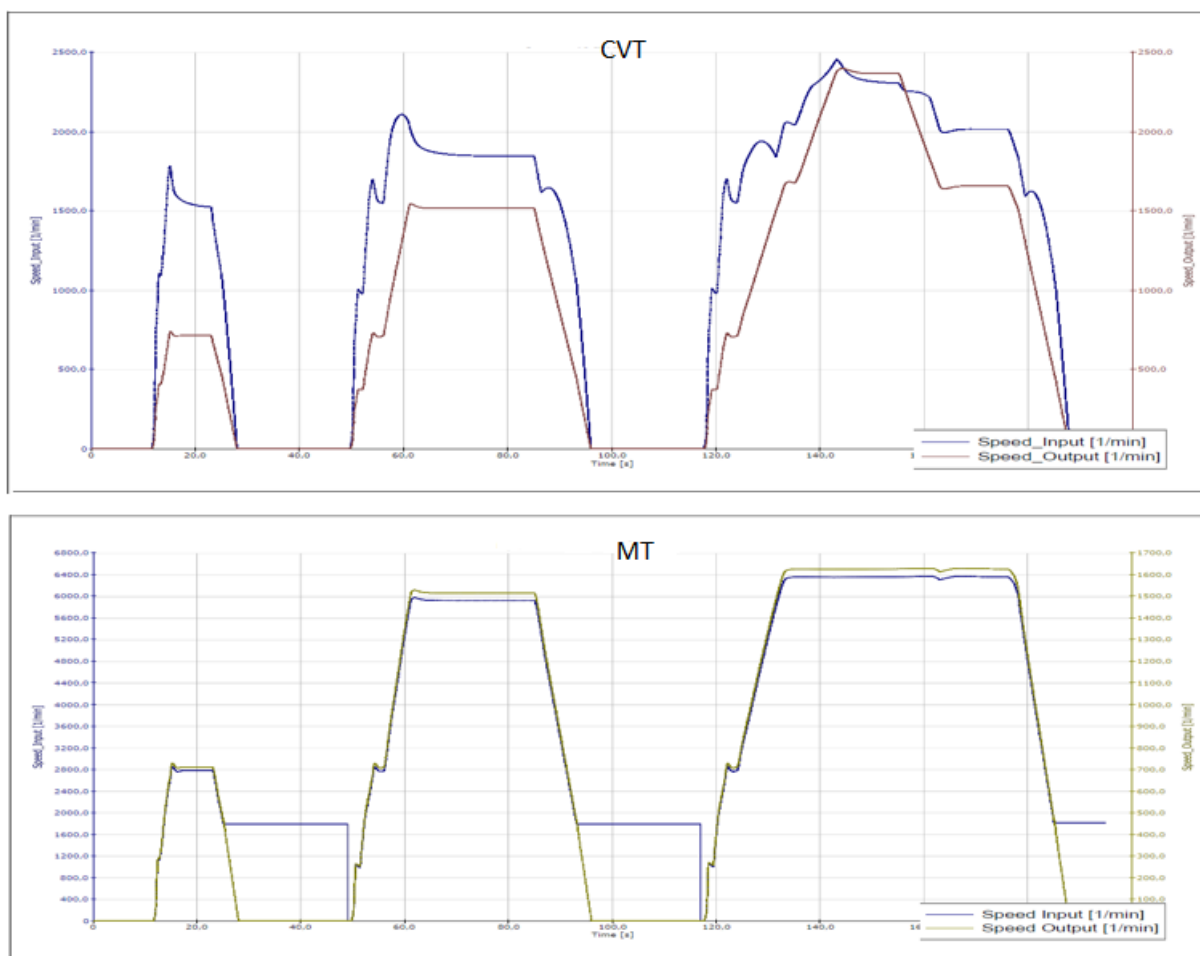


Figure 3. CVT Speed Input and Speed Output/ Manuel Speed Input and Speed Output

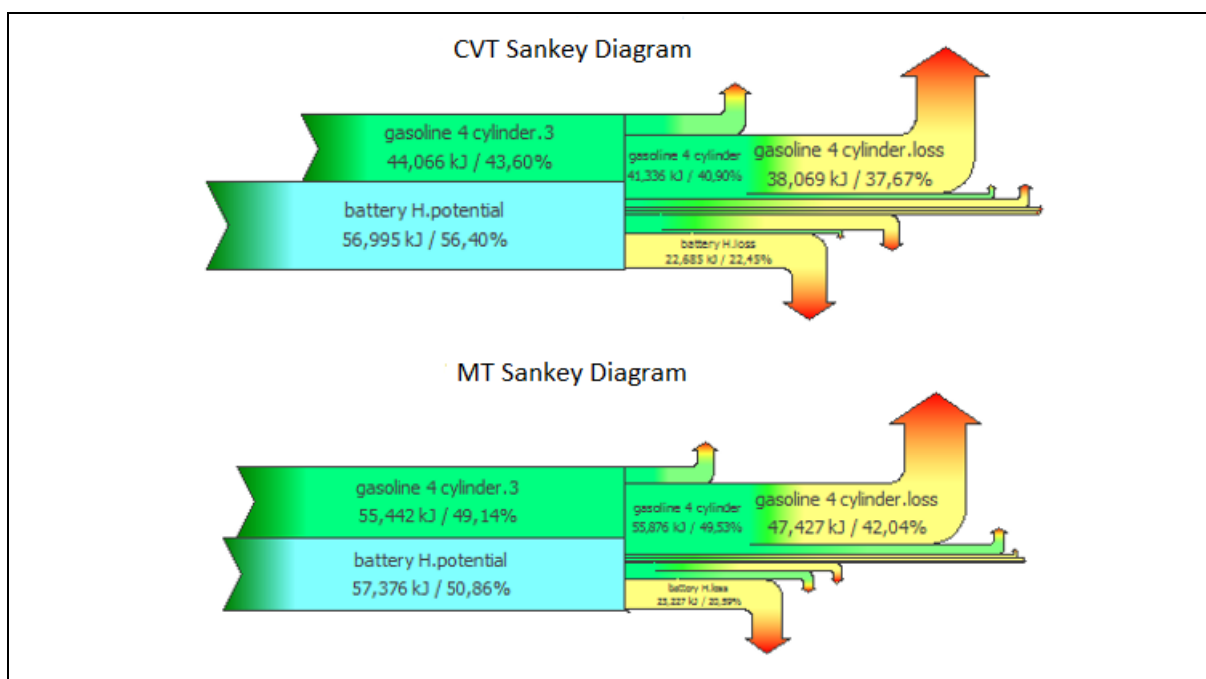


Figure 4. Sankey diagram of CVT and MT

4. Conclusion

In this study, a HEV with 10 kW electric motor and 1460 cm³ 4-cylinder gasoline ICE was simulated in AVL Cruise for identifying the energetically comparing of two different gearbox systems, CVT and Manual Transmission. The CVT system has been found to have very variable gear ranges, which is consequently more efficient in both fuel consumption and driving comfort than manual transmission. The energy and torque losses in manual transmission shifting time are much higher than CVT systems. Foreseeing an energetic perspective, the instantaneous values of system graphed and illustrated with Sankey diagrams. The CVT shifting system gives 5% more efficient results than the manual gearbox when using the battery potential at a same specific instantaneous time. According to this study outputs, the CVT has showed preferred criteria on speed and energy variations for choosing an HEV transmission when compared between manual one.

Acknowledgements: This study was conducted with AVL Cruise simulation program. We are grateful to AVL-AST, Graz, Austria to provide us this program within the scope of UPP (University Partnership Program)

References

- [1] Wisdom, E., Bannister, C., *Modelling and control of hybrid electric vehicles (A comprehensive review)*, Renewable and Sustainable Energy Reviews 74 (2017): 1210-1239.
- [2] Bingzhao, G., Qiong, L., Yu, X., Lulu, G., Hong, C., *Gear ratio optimization and shift control of 2-speed I-AMT in electric vehicle*, Mechanical Systems and Signal Processing 50 (2015): 615-631.
- [3] Nikolce, M., Hu, X., Egardt, B., *Computationally efficient energy management of a planetary gear hybrid electric vehicle*, IFAC Proceedings Volumes 47.3 (2014): 4831-4836.
- [4] Mohamed.,A., Peter, T., Paul, W., Nong, Z., *Dynamic modelling and simulation of a manual transmission based mild hybrid vehicle*, Mechanism and Machine Theory 112 (2017): 218-239.
- [5] Johannes, W., Matthias, F., Micheal., G., Esa, V., Christoph, H., *Advanced heat transfer analysis of continuously variable transmissions (CVT)*, Applied Thermal Engineering 114 (2017): 545-553.
- [6] Guang, W., Dong, Z., *Design, analysis and modeling of a novel hybrid powertrain system based on hybridized automated manual transmission*, Mechanical Systems and Signal Processing 93 (2017): 688-705.
- [7] Varga, B. O., et al. *Electric and plug-in hybrid vehicles—advanced simulation methodologies*, chapter7 (pp. 477–524)." (2015): 978-3.
- [8] Cruise, A. V. L. *Users guide*, AVL List GmbH, Graz, Austria, Document 04.0104 (2011).
- [9] <http://www.sankey-diagrams.com/sankey-definitions>

Kinetics Study of Adiyaman-Golbasi Lignite During Oxygen Enriched Combustion

Özlem UĞUZ¹, Hanzade HAYKIRI-AÇMA¹, Serdar YAMAN^{1,*}

¹Department of Chemical Engineering, Chemical and Metallurgical Engineering Faculty,
Istanbul Technical University

yamans@itu.edu.tr

Abstract: Turkey has vast reserves of lignites which have low calorific values as well as high contents of moisture, sulphur and mineral matter. Thus, burning lignites in thermal power plants in conventional ways causes drastic emissions into the atmosphere. Furthermore, ascending energy demand as a result of growing economy and increasing population growth rate requires producing more energy by burning coals. In this regard, clean coal technologies are addressed to lessen the emissions and increase efficiency. Oxygen enriched coal combustion is one of the clean coal technologies. By using this technology, oxygen content in the combustion atmosphere is adjusted to more than 21 vol% and the share of inert nitrogen gas in the mixture is reduced. This situation allows the existence of less nitrogen gas to carry heat through the stack and minimize the heat loss in the furnace. Recovering heat induces energy efficiency and cut down emissions released to the atmosphere. This study is based on establishing solid state kinetic models to determine the kinetic parameters of Adiyaman-Golbasi lignite samples which were burnt in a horizontal tube furnace in oxygen enriched conditions. In order to perform experiments, lignite sample from Adiyaman-Golbasi region was crushed and sieved to a grain size smaller than 250 µm. Each 5 g of sieved samples was then placed in a silica crucible inside the horizontal tube furnace which was heated to 200°C, 400°C and 600°C at a heating rate of 10°C/min under the flow of oxygen/nitrogen mixtures having 21%O₂+79%N₂, 30%O₂+70%N₂, 40%O₂+60%N₂, and 50%O₂+50%N₂ by volume. After that, TGA and DTG analyses were carried out by using Thermal Analyzer in dry air atmosphere with a heating rate of 40°C/min until temperature reached to 900°C for all of the original sieved sample and burned samples under the conditions mentioned above. From TGA-DTG curves, degrees of conversion for all samples were calculated. After calculating degrees of conversion, related functions were determined for each tested reaction models. By using Coats-Redfern method, kinetic parameters were obtained. According to the results, it was found that most of the samples obeyed the 1st order reaction model. It was also seen that changing oxygen/nitrogen concentrations inside the combustion atmosphere played an important role at high temperatures. Moreover, it was concluded that the samples which were burned at high temperatures had relatively high activation energies which pointed out the existence of an unburned portion inside the sample.

Keywords: Coal, coats-redfern method, oxygen enriched combustion, reaction kinetics.

Nomenclature and Symbols

α	degree of conversion
A	pre-exponential factor (min^{-1})
CR	Coats-Redfern method
E_a	activation energy (kJ/mol)
OEC	oxygen enriched combustion
R	universal gas constant (J/mol.K)
T	Temperature (K)
TGA	thermogravimetric analysis
t	time (min)

1. Introduction

Energy is a fundamental need for human-being and the prosperity of a country is often determined by the amount of the energy production and consuming with the least hazard to the environment. Coal is known to be the fundamental element in the formation and advancement of the industrial revolution in the world. The leading countries of today are the ones that started to utilize the coal to produce energy in the 19th century. Coal still has its popularity among the other energy sources and is generally used in electrical power plants in combustion process [1].

The combustion process of pulverized coal includes two steps. The first one is called devolatilization or pyrolysis, which takes place during initial heating, and the second one is the subsequent combustion of the porous, solid residue obtained from the first step. According to devolatilization process, pulverized coal sample is heated in inert or oxidizing conditions. Thus, some changes in the structure of coal particle will be detected such as softening of particle and moisture release with increasing temperature. Raising temperature further causes emission of gases and evolution of heavy tarry substances. During this stage, coal may lose up to 70-80% of its initial weight. The mass which is left after devolatilization which is rich in carbon content is called “char”. After the devolatilization stage is over, char combustion takes place. The time needed for the combustion of a char particle is more prolonged than devolatilization, which ranges from 30 ms to over an hour. This situation causes the char combustion process to be the rate determining step most of the time. Char combustion predominantly depends on the physical structure of coal, including pore surface, pore area, particle size and inorganic content [2].

Turkey has vast coal reserves which are spread all over the country. However, the qualities of these coals are often regarded low since they have low calorific values with high amount of water and mineral matter. These kinds of coals are named as lignites. The energy efficiency of burning lignites is not high. Moreover, they emit lots of hazardous emissions to the atmosphere when they are burned [3]. In order to reduce emissions and provide an efficient burning, clean coal technologies have been developed. Oxygen enriched combustion (OEC) is one of these technologies. OEC can be defined as a combustion method where combustion is carried out using oxygen-enriched atmosphere. By increasing oxygen concentration in the atmosphere, temperature inside the furnace also increases resulting in a loss of emissions and improved efficiency [4, 5].

Kinetics analysis of combustion gives important information on the combustion mechanism and the efficiency. The kinetics analysis can be investigated in two parts: Model-free and model-fitting. In order to determine the kinetic parameters, model-fitting methods are more commonly used. Coats-Redfern (CR) method is the most popular one among the model-fitting methods. This method uses the data obtained from TGA analysis, which yields the weight loss vs. temperature curve. According to the TGA curve, degree of conversion (α) can be calculated for different temperatures. For each predicted reaction model (reaction order ($n=1, 1/3, 1/2, 2/3, 2$), diffusional (1-D, 2-D, 3-D

(Ginstling-Brounshtein), contracting geometry (contracting area, contracting volume), nucleation (Avrami-Erofeev $n=2$, Avrami-Erofeev $n=3$), related $g(\alpha)$ functions are determined. CR method plots $1/T$ vs. $\ln(g(\alpha)/T^2)$. From the slope and the intercept of the straight line, activation energy (E_a) and pre-exponential factor (A) can be calculated, respectively [6].

2. Material and Methods

2.1. Material and Sample Preparation

Adiyaman-Golbasi (AG) coal basin, which was formed on Late Pliocene or Early Pliocene periods, is located in the East Anatolian Fault Zone of Turkey [7]. The collected raw lignite from Adiyaman-Golbasi coal seam was crushed with a hammer first. After that, the lignite was left in the air atmosphere for one day. The air-dried lignite sample was then ground with a ring mill to reduce the particle size below 250 μm .

2.2 Methods

Each 5 grams of ground AG sample was placed in a crucible made of silica which was placed in the middle of a horizontal silica tube inside the horizontal tube furnace. Horizontal tube furnace had connection with oxygen and nitrogen gas cylinders with plastic pipes. The total flow rate was set 100 ml/min with the oxygen (O_2) and nitrogen (N_2) shares of 21 ml/min O_2 +79 ml/min N_2 , 30 ml/min O_2 +70 ml/min N_2 , 40 ml/min O_2 +60 ml/min N_2 and 50 ml/min O_2 +50 ml/min N_2 . After adjusting the ratios of O_2 and N_2 , the furnace atmosphere was allowed to come into equilibrium with the adjusted atmosphere for 20 min. The heating rate (10°C/min), final temperatures (200°C, 400°C and 600°C) and the hold time at the final temperature (60 min) were introduced to the PID controller. After the heating is over, the sample was left to cool down in its own adjusted atmosphere. Proximate analyses were carried out by Thermal Analyzer for the ground untreated sample and burned samples. To do this, approximately 10 mg of each sample was put in a sample holder made of platinum. The sample was heated from ambient temperature to 105°C and kept constant at this temperature for 10 minutes for the moisture removal. After that, temperature was increased to 900°C with a heating rate of 40°C/min under nitrogen atmosphere. The atmosphere was kept isothermal at 900°C for 7 min to ensure that devolatilization is complete. Finally, temperature was reduced to 755°C under dry air with the cooling rate of 20°C/min until the ash yield ceased. Combustion experiments were carried out by using Thermal Analyzer. 10 mg of each sample was heated from ambient temperature to 900°C with a heating rate of 40°C/min under dry air atmosphere and kept constant at this temperature until the mass loss was over.

3. Results and Discussion

Table 1 gives the proximate analysis results of untreated AG lignite sample and the treated samples at given conditions. Proximate analysis yields moisture, volatile matter, fixed carbon and ash contents of all samples in wt% basis.

Table 1 indicates that untreated AG lignite sample had a high moisture and ash with low fixed carbon content. Increasing treatment temperature to 200°C caused an effect similar to torrefaction. Upon treatment at 400°C, combustion process started to take place and increasing oxygen percentage in the oxidizing atmosphere resulted in a more efficient burning in accordance with ash content reaching up to 71.50% of the total sample weight. Raising the final treatment temperature to 600°C provided a complete burning of the sample under conditions of 30% O_2 , 70% N_2 . Ash yield reached 91.27% when the oxygen fraction was 0.5 at this temperature. From the results obtained from Table 1, it can also be concluded that increasing O_2 concentration in the furnace can decrease fixed carbon and volatile matter contents to a high extent.

Table 1. Proximate analysis results.

Conditions	Moisture (%)	Volatile matter (%)	Fixed carbon (%)	Ash (%)
Untreated lignite sample	30.80	30.90	17.00	21.30
200°C – dry air	3.95	42.49	22.58	30.98
200°C- 30%O ₂ ,70%N ₂	3.97	42.24	23.96	29.83
200°C-40%O ₂ , 60%N ₂	4.03	41.50	23.50	30.97
200°C-50%O ₂ , 50%N ₂	4.43	41.37	25.23	28.97
400°C-dry air	6.60	30.40	11.50	51.50
400°C-30%O ₂ , 70%N ₂	6.60	28.70	5.30	59.40
400°C-40%O ₂ , 60%N ₂	5.00	25.30	1.00	68.70
400°C-50%O ₂ , 50%N ₂	3.90	24.20	0.40	71.50
600°C-dry air	4.10	19.50	1.70	74.70
600°C-30%O ₂ , 70%N ₂	1.80	14.40	0	83.80
600°C-40%O ₂ , 60%N ₂	1.40	7.50	0	91.10
600°C-50%O ₂ , 50%N ₂	1.58	7.15	0	91.27

Figure 1 and Figure 2 show the TGA and DTG curves for the burning untreated AG lignite under dry air conditions, respectively.

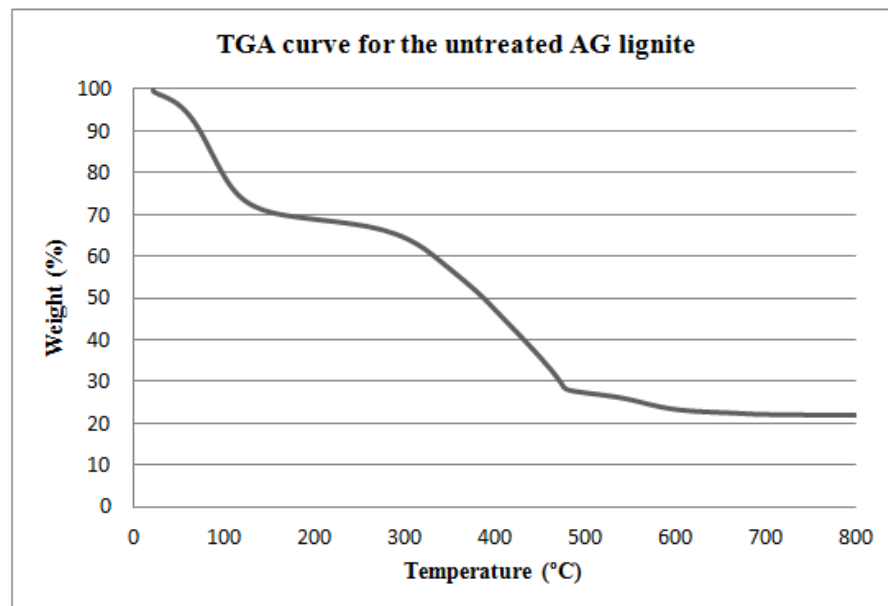


Figure 1. TGA curve for the untreated AG lignite.

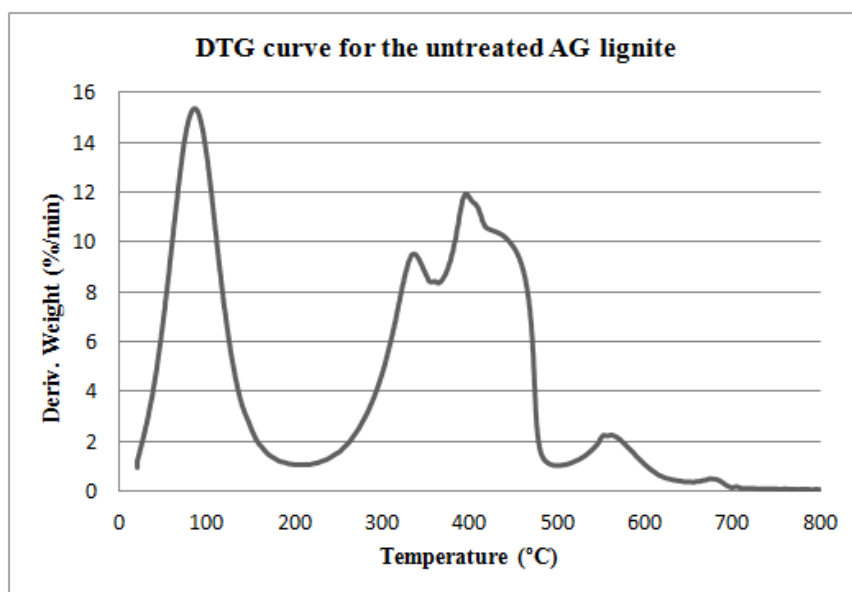


Figure 2. DTG curve for untreated AG lignite.

Figure 1 and Figure 2 are used to determine kinetic parameters for untreated AG lignite. The first peak seen at around 100°C indicates the moisture loss. Semi-detached peaks in the interval of 250°C-500°C points out the volatile matter combustion and char combustion, respectively. Thus, these two regions can be investigated in two separate parts in kinetics analysis calculations.

Table 2 and Table 3 show the calculated kinetic parameters for untreated AG lignite for volatile matter combustion region and char combustion region, respectively. It was seen that A and E_a values were higher in the char combustion region in comparison with volatile matter combustion region.

Table 2. Calculated kinetic parameters for untreated AG lignite for the volatile matter combustion region.

Reaction model	E_a (kJ/mol)	A (min^{-1})	r^2
Reaction order			
1st order	104.9194	1.6953×10^9	0.9821
1/3rd order	88.8394	3.6777×10^7	0.9577
1/2nd order	92.3148	8.4465×10^7	0.9662
2/3rd order	96.1394	2.1034×10^8	0.9734
2nd order	140.2307	6.8546×10^{12}	0.9543
Diffusional			
1-D	175.0514	9.4455×10^{14}	0.9449
2-D	186.1927	6.4408×10^{15}	0.9608
3-D(Ginstling-Brounshtein)	191.1979	4.6098×10^{15}	0.9668
Contracting geometry			
Contracting area	92.3148	4.2235×10^7	0.9662
Contracting volume	96.1394	7.0115×10^7	0.9734
Nucleation			
Avrami-Erofeev n=2	47.7587	6.1153×10^6	0.9780
Avrami Erofeev n=3	28.7038	116.0331	0.9725
Avrami Erofeev n=4	19.1763	11.5932	0.9648

Table 3. Calculated kinetic parameters for untreated AG lignite for the char combustion region.

Reaction model	E _a (kJ/mol)	A (min ⁻¹)	r ²
Reaction order			
1st order	142.1596	2.9469*10 ¹⁰	0.9631
1/3rd order	103.7803	1.9621*10 ⁷	0.8730
1/2nd order	111.1802	8.1507*10 ⁷	0.8992
2/3rd order	119.8936	4.3175*10 ⁸	0.9244
2nd order	246.8130	8.7561*10 ¹⁸	0.9274
Diffusional			
1-D	195.6628	6.9340*10 ¹³	0.8409
2-D	216.6816	1.8558*10 ¹⁵	0.8792
3-D(Ginstling-Brounshtein)	227.4487	3.1043*10 ¹⁵	0.8980
Contracting geometry			
Contracting area	111.1802	4.0755*10 ⁷	0.8992
Contracting volume	119.8936	1.4390*10 ⁸	0.9244
Nucleation			
Avrami-Erofeev n=2	65.2356	3.4035*10 ⁴	0.9559
Avrami Erofeev n=3	39.5957	281.0030	0.9465
Avrami Erofeev n=4	26.7749	22.1627	0.9341

E_a and A values in Table 2 ranged between 19.1763-191.1979 kJ/mol and 11.5032- 4.6098*10¹⁵ min⁻¹, respectively. 1st order reaction model yielded the highest r² value, 0.9821, and can be regarded as the most suitable mechanism in the volatile matter combustion region. E_a and A values given in Table 3 ranged between 26.7749-246.8130 kJ/mol and 22.1627-8.7561*10¹⁸ min⁻¹, respectively. The linearity of reaction models for char combustion decreased slightly compared with the volatile matter combustion region. However, the dominant mechanism remained the same as the one of volatile matter combustion region; 1st order reaction model gave the best fit to the data with r² value of 0.9631. Dominant kinetic models and calculated kinetic parameters for these models for volatile matter combustion and char combustion regions are presented in Table 4.

Table 4. Dominant kinetic models and calculated kinetic parameters for treated samples for volatile matter combustion and char combustion region.

Conditions	Dominant model	r ²	E _a (kJ/mol)	A (min ⁻¹)
Volatile matter combustion region				
200°C – dry air	1 st order	0.9898	113.0093	8.7543*10 ⁹
200°C- 30%O ₂ ,70%N ₂	1 st order	0.9836	110.5316	2.7480*10 ⁹
200°C-40%O ₂ , 60%N ₂	1 st order	0.9826	101.4191	3.5720*10 ⁸
200°C-50%O ₂ , 50%N ₂	1 st order	0.9824	107.6881	2.1663*10 ⁹
400°C – dry air	1 st order	0.9898	106.1583	5.8860*10 ⁷
400°C- 30%O ₂ ,70%N ₂	1 st order	0.9711	119.7357	2.7678*10 ⁸
400°C-40%O ₂ , 60%N ₂	n/a	n/a	n/a	n/a
400°C-50%O ₂ , 50%N ₂	n/a	n/a	n/a	n/a
600°C-dry air	1 st order	0.9793	108.6027	4.5401*10 ⁷
600°C- 30%O ₂ ,70%N ₂	n/a	n/a	n/a	n/a

600°C-40%O ₂ , 60%N ₂	n/a	n/a	n/a	n/a
600°C-50%O ₂ , 50%N ₂	n/a	n/a	n/a	n/a
Char combustion region				
200°C – dry air	Contracting vol.	0.9857	105.7176	5.1117*10 ⁸
200°C- 30%O ₂ ,70%N ₂	Contracting vol.	0.9729	102.1840	1.3036*10 ⁸
200°C-40%O ₂ , 60%N ₂	Contracting vol.	0.9728	95.0003	2.6128*10 ⁷
200°C-50%O ₂ , 50%N ₂	Contracting vol.	0.9771	100.0971	1.2021*10 ⁸
400°C – dry air	1 st order	0.9821	386.0293	7.7641*10 ²⁴
400°C- 30%O ₂ ,70%N ₂	1 st order	0.9780	401.8932	3.2746*10 ²⁵
400°C-40%O ₂ , 60%N ₂	1 st order	0.9795	306.3108	1.1623*10 ¹⁸
400°C-50%O ₂ , 50%N ₂	1 st order	0.9577	264.8386	1.1623*10 ¹⁶
600°C-dry air	1 st order	0.9748	296.7160	2.8289*10 ¹⁸
600°C- 30%O ₂ ,70%N ₂	1 st order	0.9653	143.1823	1.0490*10 ⁹
600°C-40%O ₂ , 60%N ₂	n/a	n/a	n/a	n/a
600°C-50%O ₂ , 50%N ₂	n/a	n/a	n/a	n/a

Table 4 shows that the most dominant mechanism for the treated samples was the 1st order reaction model except for the samples treated at 200°C for char combustion region. This might be due to the torrefaction effect of treating the sample at this temperature which causes contracting of volume. For the volatile matter combustion region, there was no data available for the samples of 400°C-40% O₂, 60%N₂, 400°C-50% O₂, 50%N₂, 600°C-30% O₂, 70%N₂, 600°C-40% O₂, 60%N₂, 600°C-50% O₂, 50%N₂ and for the char combustion region, for the samples of 600°C-40% O₂, 60%N₂ and 600°C-50% O₂, 50%N₂. The unavailability of the data for these samples is because of the very slight peaks for the corresponding regions.

4. Conclusion

This study showed that oxygen enriched combustion was an important method to increase the burning performance in the furnace and kinetic parameters are important indicators of the burning efficiency. Calculating kinetic parameters for the residue samples after burning in the horizontal tube furnace gave information about the unburned portion of these samples. Moreover, it was seen that samples had lower E_a values in the volatile matter combustion region in comparison with char combustion region. Treatment temperature and oxygen concentration played an important role on the proximate analysis results, which directly affected the dominant kinetic models, E_a and A values. Furthermore, it was seen that 1st order reaction model gave the best linearity for the majority of the samples.

References

- [1] Yılmaz, A.O., Uslu, T., *The role of coal in energy production-Consumption and sustainable development of Turkey*, Energ Policy 35 (2007) 1117-1128.
- [2] Smoot, L.D., Smith, P.J., *Coal combustion and gasification*, The Plenum Chemical Engineering Series, 1st ed., New York, 1985.
- [3] Toprak, S., *Petrographic properties of major coal seams in Turkey and their formation*, Int J Coal Geol 78 (2009) 263-275.
- [4] Kayahan, U., Özdoğan, S., *Oxygen enriched combustion and co-combustion of lignites and biomass in a 30 kWth circulating fluidized bed*, Energy 116 (2016) 317-328.

-
- [5] Shen, G., Wang, Z., Wu, J., He, T., Li, J., Yang, J., Wu, J., *Combustion characteristics of low-rank coal chars in O_2/CO_2 , O_2/NO_2 and O_2/Ar by TGA*, Journal of Fuel Chemistry and Technology 44 (2016) 1066-1073.
- [6] Wang, G., Zhang, J., Shao, J., Liu, Z., Zhang, G., Xu, T., Guo, J., Wang, H., Xu, R., Lin, H., *Thermal behavior and kinetic analysis of co-combustion of waste biomass/low rank coal blends*, Energy Conversion and Management 124 (2016) 414-426.
- [7] Karayığit, A.İ., Oskay, R.G., Tuncer, A., Mastalerz, M., Gümüş, B.A., Şengüler, I., Yaradılmış, H., Tunoğlu, C., *A multidisciplinary study of the Gölbaşı-Harmanlı coal seam, SE Turkey*, International Journal of Coal Geology 167 (2016) 31-47.

Effects of using different electric motors on hybrid engine's performance

Nuri YÖNETİ, Bahattin TANÇI, Hüseyin Turan ARATI,*

1 Faculty of Engineering and Natural Sciences, Iskenderun Technical University

* *turan.arat@iste.edu.tr*

Abstract: In the last decades, general community have get accustomed to hybrid vehicles that powered not only by an internal combustion engine (fuelled via gasoline, diesel or gas), but also by an electric motors. Hybrid Electric Vehicles (HEV) has an important opportunity for improving engine's performance besides reducing gas emissions and fuel consumptions. In the production & manufacturing steps of HEVs, simulation and modeling criteria's playing a significant role. Especially, choosing the eclectic motor of hybrid engine has depends on many parameters. For making preferable selection, simulation techniques help researchers for choosing and comparisons of these different electric motors. In this study; AVL Cruise simulation tool is used for analyzing the performance of hybrid engines which had 3 different electric motors and compared the effectiveness of these motors to whole hybrid engine. The based model of 4 cylinders, 4 strokes, 1.5 L, gasoline engine is selected for combustion engine. Three different electric motors were selected with 15, 20, 25 kW and they equipped with appropriate generators. Simulation results and mathematical models were also graphed and explained. The engine torque, power, fuel consumption, battery energy, electric energy in/outputs were explained and compared each other. As a result; for a specific energy/power approach; the 20kW electric motor has more preferable engineering properties when compared with the others. Another important result obtained from this work is that, AVL simulation tool can be successfully used in the modeling of hybrid vehicles and their components.

Keywords: AVL-Cruise, Hybrid Electric Vehicle, Electric Machine, Engine Performance

1. Introduction

Today, one of the most interesting technologies in the world is undoubtedly hybrid vehicles. It is well recognized today that hybrid electric vehicle (HEV) and electric vehicle (EV) technologies are vital to the overall automotive industry and also to the user, in terms of both better fuel economy and a better effect on the environment. Over the past decade, these technologies have taken a significant leap forward [1]. Interesting engineering properties, integrated with different engineering departments and complicated design have been raising the light of the future perspective of HEVs in transportation area.

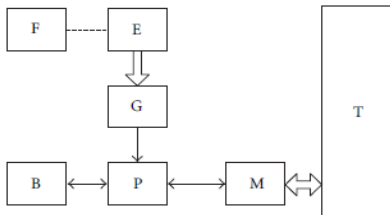
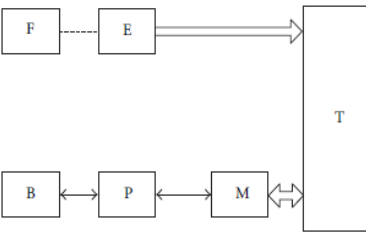
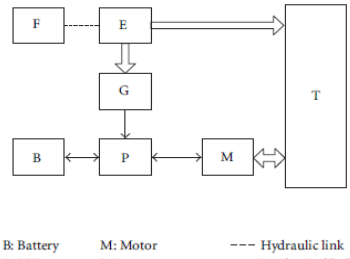
Generally HEV defines as the vehicle has included both an Internal Combustion Engine (ICE) and an electrical machine (EM), while the energy sources are fossil fuel for ICE and batteries for EM. The major challenges for HEV design are managing multiple energy source, highly dependent of driving cycles, battery sizing and battery management. The architecture of a hybrid vehicle is usually defined as the connection between the components of the vehicle traction, and then the energy flow path [2].

Hybrid electric vehicle architecture consisting as; series hybrids, parallel hybrids and parallel-series (power split) hybrids. Table 1 illustrated and explained the differences and benefits of these architectures on HEV.

For a specific determination of a HEV, automakers and researchers uses the “*hybridization ratio*” for new concepts. [1] reported this item briefly as “the hybridization ratio is defined as the ratio of electric power to the total powertrain power”. The concepts are usually related to the power rating of the main electric motor and commonly called *full hybrid*, *mild hybrid*, and *micro hybrid*. The typical rating of electric motors used in micro hybrids is less than 10 kW, mild hybrid is between 10 and 50 kW and full hybrid passenger car is approximately 50–75 kW. For example of a hybridization ratio, a HEV with a motor rated at 25kW and an engine rated at 75kW will have a hybridization ratio of $25/(25+75)\text{kW}=25\%$. [1]

HEV have new technology and complicated strategy; thus for a specific part of HEV i.e.; for battery or generator or range extender systems; limited literature has meet us. Detailed experiments have been continued on HEVs. In this time, researchers thanks for the modeling and simulation tools for helping the status of the system identification and foresight approaches before the prototyping and manufacturing.

Table 1. Benefits and Architecture of HEV [4]

Series	Parallel	(Power-Split or Series-Parallel)
 <p>(a) Series HEV.</p>	 <p>(b) Parallel HEV.</p>	 <p>(c) Combination HEV.</p> <p> B: Battery M: Motor --- Hydraulic link E: ICE P: Power converter — Mechanical link F: Fuel tank T: Transmission — Electrical link G: Generator </p>
<p>The series HEV is composed of ICE, generator, power converter, motor, and battery. There is no mechanical connection between ICE and transmission, thus ICE can operate at maximum efficient point by regulating the output power of battery to satisfy the required power of vehicle.</p>	<p>The parallel HEV allows both the electric motor and ICE to deliver power in parallel to drive the vehicle and there is mechanical connection between ICE and transmission, and thus the ICE’s rotational speed depends on the driving cycle.</p>	<p>Combination HEV incorporates the features of both series and parallel HEV, an additional mechanical connection between ICE and transmission is added compared with the series hybrid, and also an additional generator between ICE and power converter is added compared with the parallel hybrid.</p>

Especially for decade, the simulational studies were focused the effectiveness of HEV’s components and theirs engineering efficiency. Simulation methods and modeling systems helped researchers for determination of these components selection. Electric motors capacities and theirs capabilities are very important for selection and applications. For this, the different electric motors properties were compared each other and add the literature. Some researchers and applicators add their experiences and valuable results about the electric motors and generators in HEV’s [1-7]. For a minimized and specialized literature, that related our topic, is achieved by Bent Sørensen, who studied about effect of different parameters to batteries charging time and given a detailed comparison study about hybrid

vehicle's performance. He mentioned that, as the fuel cell rating goes up and the needed battery capacity down, there are larger excursions in the battery state of charge during the driving cycle [3].

In order to contribute to the study of this important situation, this simulational study aimed and modeled with; 4 cylinders, 4 strokes, 1.5 L, gasoline engine which is selected for combustion engine and three different electric motors were selected under 15, 20, 25 kW which they equipped with appropriate generators with the helped of AVL- Cruise.

2. Simulation Model

In general terms, the simulation process can be defined as all functional and/or operational activities on a model that representing the image of a source system necessary to be analyzed. [5]

There is a graphical user interface (GUI) in AVL CRUISE that has the function of allowing the user to build the vehicle model or modify the basic AVL CRUISE model [6]. Figure 1 is the model of the range-extended electric vehicle in parallel configuration, which has main components such as the internal combustion engine, generator, electric motor and battery. Each box in the model represents a component of the vehicle where the user can input data. Blue lines indicate the mechanical connection between components of the vehicle, red lines indicate electrical connections and black ones indicate the main components of the range-extended electric vehicle.

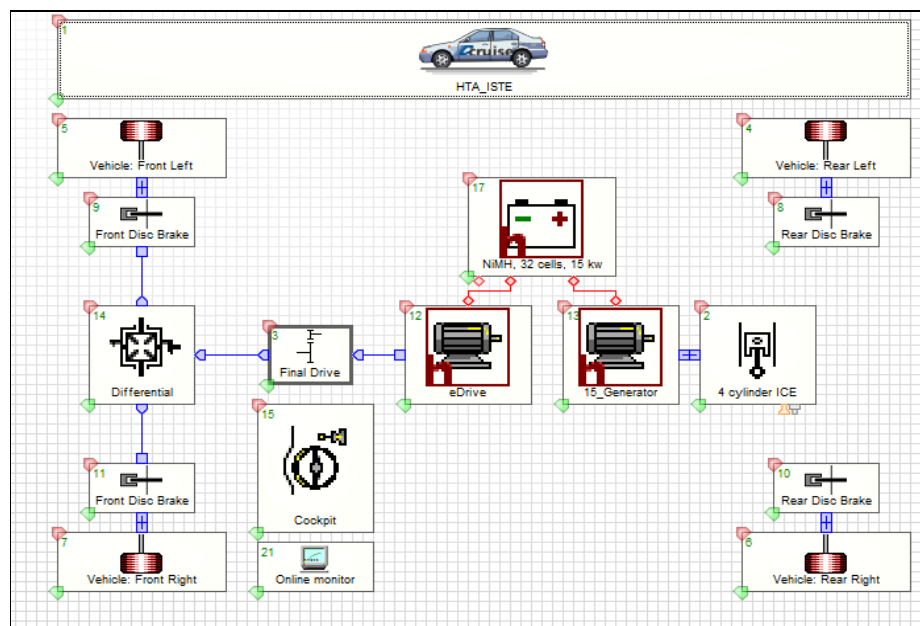


Figure 1. AVL Cruise Vehicle Model

After modeled the vehicle, user specified the input data. In Table 2., the modeled vehicles input data is given. From specific programming and mathematical approaches form AVL, the range extender parallel configuration HEV is run for calculation.

Determining the effectiveness of HEV battery results; driving cycle is selected as FTP-75 (Federal Test Procedure) for fuel economy. In a vehicle simulation; driving cycles can be used to compare the performance of vehicle; total fuel consumptions and emissions. For battery tests; driving cycles is handled on a chassis dynamometer [7].

Table 2. Simulational inputs for HEV

Components	15 kW	20 kW	25 kW
Battery [7]	32 Cells NiMH Max. charge :4.4 Ah, Nominal Voltage: 3.6 Max. Voltage: 4.1 V Min. Voltage: 3.0 V	60 Cells NiMH Max. charge :5.0 Ah, Nominal Voltage: 3.7 Max. Voltage: 4.15 V Min. Voltage: 3.0 V	72 Cells NiMH, Max. charger:5.3 Ah, Nominal Voltage: 3.0 Max. Voltage: 4.15 V Min. Voltage: 3.0 V
ICE	4 cylinder, 4 strokes, Idle 800 rev/min., Max. Speed: 5600 rpm, without charger		
E-Motor & Generator	PSM type, Nominal voltage: 220V, Max. Speed: 6000 rpm., Inertia moment: $4,04 \times 10^{-4}$ kg*m ² Initial temp.:20°C, layout temp.:70°C		

3. Results

Effects of different battery usage on different electric machines are compared each other in this section. Figure 2 and 3 give the outputs of the simulational data. Battery, ICE, E-machine and driving cycle sections performed and compared each other in coupled figures for easily understanding.

In a HEV, battery and e-machine components selection is playing a very important role for determining the energy input & output, current, voltage, state of charge (SoC), ICE performance and one of the most important items on fuel consumption values.

According to [5], “The generator (alternator) must provide the vehicle electrical system with a sufficient supply of current under all operating conditions in order to ensure that the State of Charge (SOC) in the engine storage device (battery) is consistently maintained at an adequate level. The object is to achieve balanced charging, i.e., the curves for performance and speed–frequency response must be selected to ensure that the amount of current generated by the alternator under actual operating conditions is at least equal to the consumption of all electrical equipment within the same period”. This system determination gives the valuable selection on HEV electric machine or electric motors. The model of the electric machine contains two components, the inverter and the electric motor. The Electric Machine component can be used either as an electric motor or as a generator.

In figure 2, the E-motor results can be seen as a function of; total input and output energy with the addition of batteries total input output charges. It can be clearly shown in figure 2, the top values on

input and output on energy scale is performed on 20 kW. Especially the differences on input and output values ratio is higher than 15 and 25 kW. Ratio of input and output energy values are 3.5, 3.9 and 3.4 for 15, 20 and 25 kW e-motors respectively. This influenced the effectiveness values of energy outputs. Additionally, the input energy values indicate the issue of the only time the torque assist hybrid is using the motor solely is during the braking and starting phases that can be seen by the figure's orange lines. Even this situation; for 20 kW of electric motor the balancing of the input and output values shown in higher efficiency and performance.

In the lower part of Figure 2, the driving cycle versus timing and distances were given. Fuel consumption and electrical consumption values of HEVs can be seen briefly. For all car included HEV, the consumption of fuel, electric and energy is the major dominant for automakers. For a complicated HEV, affected the total fuel consumption (both ICE and E-machine) and electric consumption are controlled by energy management systems. In figure it can be clearly seen that, the 20 kW electric machine HEV give more preferable results when compared with others. One of the most important factors affecting this criteria is the fact that 15 kW of HEV is not effective due to insufficient effect on fuel consumption (especially the selected driving cycle and low power) and 25 kW HEV has a high fluctuation variation due to high speeds and elapsed time that effect the energy losses ratings. For this simulation, under FTP75 driving cycle, fuel consumption of all engines values are 9.7, 9.2 and 11.4 (l/h) for 15, 20 and 25 kW respectively. Additionally, comparison of electric consumption on 15, 20 and 25 kW is obtained with the results of 8.0, 4.3 and 6.5 kW respectively. Both fuel and electric consumption under this driving cycle, 20 kW is more advantages rather than others.

Torque, Power and engine speed of ICE is given in figure 3. Maximum torque values of results can be listed as 37, 39 and 35 kW for 15, 20 and 25 kW respectively for a specific timing. In the battery results which seen in the bottom of the figure 3, the voltage, current, charge and SoC values are presented. The State of Charge (SoC) point was set at 40% of battery capacity, which means that the electronic management system controlled the range-extended engine to turn on the gasoline engine and recharge the battery. The minimum amplitude changing is graphed by 20 kW due to the better balancing on HEV components.

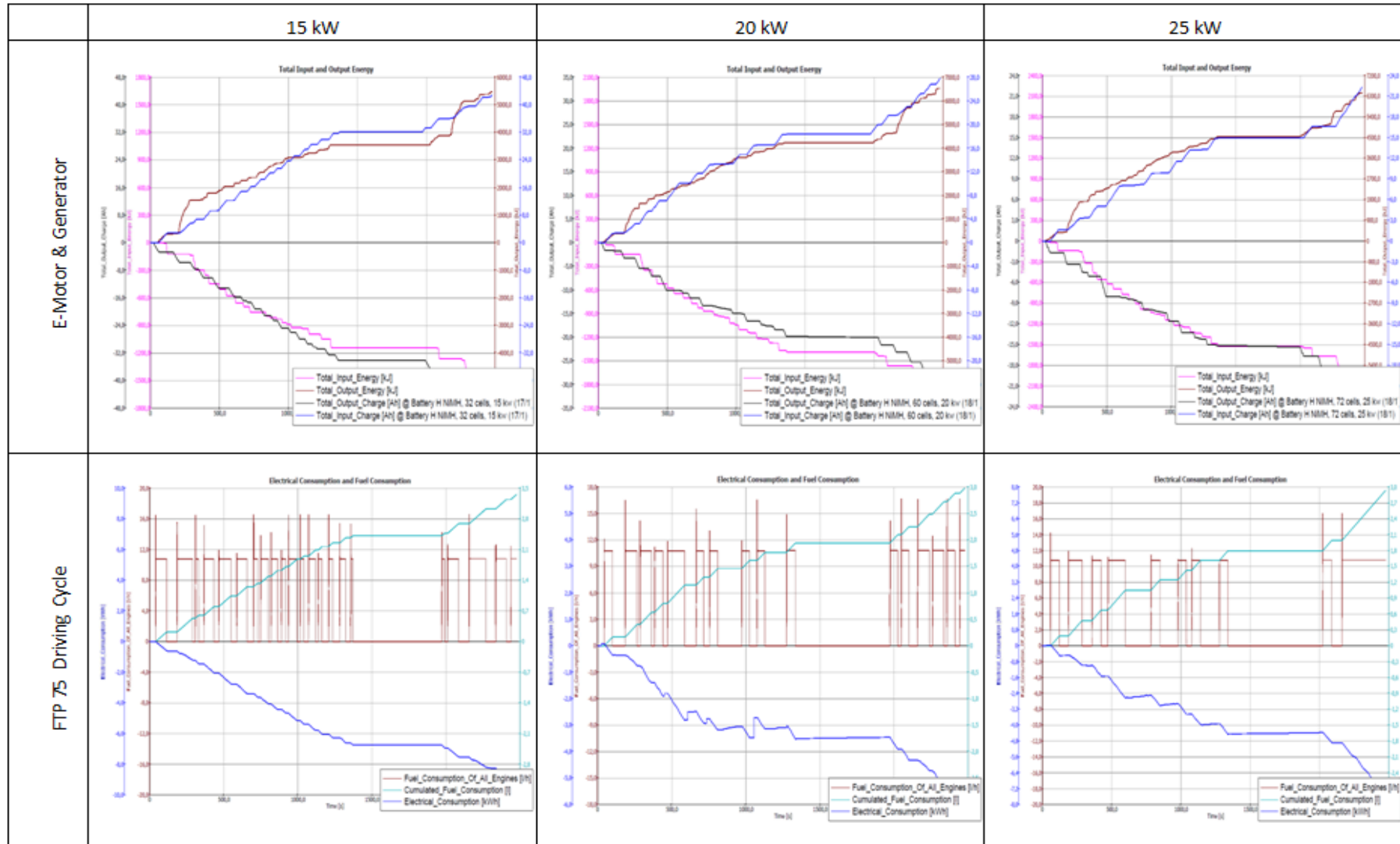


Figure 2. Results and Comparison of 15, 20 and 25 kW battery included HEVs (E-machine and Driving cycle)

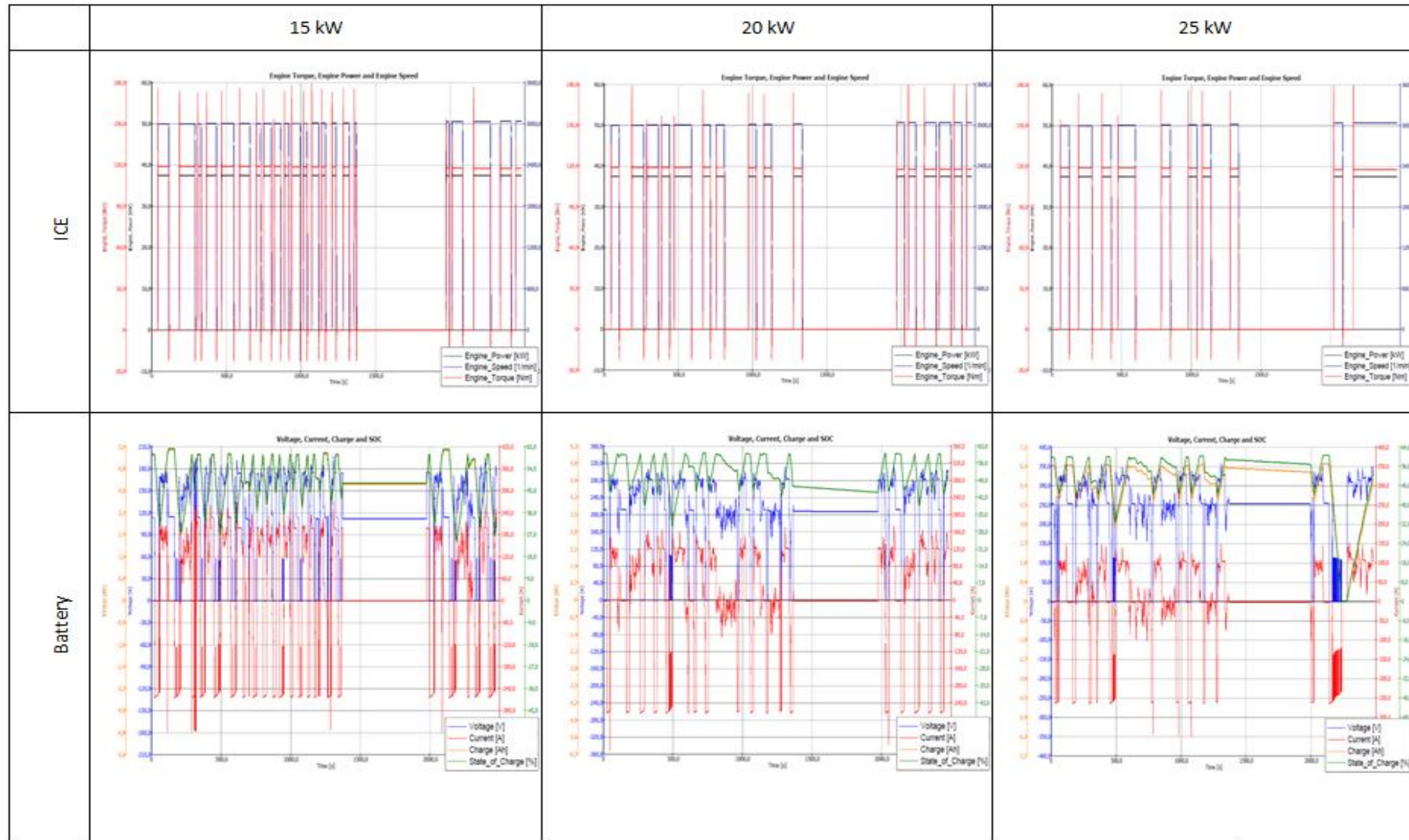


Figure 3. Results and Comparison of 15, 20 and 25 kW battery included HEVs (ICE and battery)

4. Conclusion

Based on the simulation results, the range-extended HEV model using 20 kW electric motor has the best performance compared to the other modeled HEV which used 15 and 25 kW electric motor and different battery scales. The simulation results were given detailed and compared with E-machine, Driving cycle, ICE and battery perspective. This HEV (20 kW) model has the lowest fuel and electrical consumption of the electrical motor compared to the other models and this model has the highest energy input and output energy ratio when compared the others.

For a specific energy/power approach under the assumption of the modeled simulated HEV; the 20kW electric motor has more effectiveness engineering properties when compared with the others. Another important result obtained from this work is that, AVL simulation tool can be successfully used in the modeling of hybrid vehicles and their components.

Acknowledgements: This study was conducted with AVL CRUISE simulation program. We are grateful to AVL-AST, Graz, Austria to provide us this program within the scope of UPP (University Partnership Program). Additionally authors acknowledge the U.S. Department of Energy's subunits National Renewable Energy Laboratory (NREL) and Argonne National Laboratories for the helped of using data on Downloadable Dynamometer Database.

References

- [1] Chris, Mi., M. Abul, Masrur., David, Wenzhong Gao. "Hybrid Electric Vehicles Principles and Applications With Practical Perspectives". *John Wiley & Sons, Ltd*, (2011)
- [2] Massimo, Barcaro., Nicola, Bianchi., Freddy, Magnussen., "PM Motors for Hybrid Electric Vehicles" *The Open Fuels & Energy Science Journal*, 2, (2009), 135-141.
- [3] Sørensen, Bent., "On the Road Performance Simulation of Battery, Hydrogen, and Hybrid Cars", *International Journal of Hydrogen Energy*, 32, 6, (2007), 683-686.
- [4] Caiying, Shen., Peng, Shan., Tao, Gao., "A Comprehensive Overview of Hybrid Electric Vehicles", *International Journal of Vehicular Technology*, doi:10.1155/2011/571683, (2011)
- [5] Bogdan, Ovidiu Varga., Florin, Mariasiu., Dan, Moldovanu., Calin, Iclodean., "Electric and Plug-In Hybrid Vehicles: Advanced Simulation Methodologies" *Springer*, DOI: 10.1007/978-3-319-18639-9, (2015).
- [6] Bambang, Wahono., Arifin, Nur., Widodo, Budi Santoso., Achmad, Praptijanto., "A comparison study of range-extended engines for electric vehicle based on vehicle Simulator", *Journal of Mechanical Engineering and Sciences*, 10,1, (2016), 1803-1816.
- [7] "Transportation Secure Data Center." (2017). National Renewable Energy Laboratory. Accessed April 4, 2017: www.nrel.gov/tsdc.
- [8] AVL-CRUISE Users Guide, AVL, V2015.

Oxy-fuel combustion of low calorific value coal gases: burner modifications and flame characteristics

Mustafa İLBAŞ^{1,*}, Abdulkadir BEKTAŞ² and Serhat KARYEYEN¹

¹Gazi University, Technology Faculty, Department of Energy Systems Engineering, 06500 Teknikokullar, Ankara, Turkey

² Gazi University, Graduate School of Natural and Applied Science, 06500 Teknikokullar, Ankara, Turkey

* ilbas@gazi.edu.tr

Abstract: Nowadays, using oxygen instead of air in a burning process is being widely discussed as an option to reduce fuel consumption and CO₂ emissions and to be expected to improve the thermal efficiency and combustion performances. The main goal of this study is to focus on the oxy-fuel combustion behaviors of low calorific value coal gases. The present work investigates oxy-fuel combustion of low calorific value coal gases including CO, CO₂ and NO_x components in the existing burner and the combustor. The coal-derived low calorific value coal gases (syngases) have been properly oxy-combusted using the new type of burner. Temperature and emission values have been experimentally measured and investigated on different axial and radial positions by using thermocouples and a flue gas analyzer throughout the combustion chamber. The burner walls were overheated due to using of pure oxygen instead of air during combustion when the turbulator position of the burner was further to the burner exit (7 cm). Because of that, the turbulator position of the burner has also been changed as a small modification to alleviate overheating of the burner walls and hence, it has been approached to the burner exit (2 cm). All experiments have been performed under a thermal power of 10 kW and an oxygen/fuel ratio of $\lambda=1,2$ combustion conditions for both turbulator distances of 7 cm and 2 cm. The experimental results show that the maximum temperature value was measured and determined to be 1323 K for the generator gas combustion under the combustion condition of 7 cm of the turbulator distance. On the same terms, the temperature of 1185 K was measured for the turbulator distance of 2 cm. In similar conditions, the maximum temperature level was observed of 1166 K for the blast-furnace gas combustion under the combustion condition of 7 cm of the turbulator distance. Similarly, the temperature of 946 K was measured for the turbulator distance of 2 cm. It is consequently concluded that the flame that has emerged under the combustion condition of 2 cm of the turbulator distance is wider and smoother than that of the flame showing up under the combustion condition of 7 cm of the turbulator distance. CO, CO₂ and NO_x emissions have also been determined on different axial and radial positions. According to the measurements, it has been demonstrated that CO₂ and NO_x decrease while CO increase on the axial measurements as the turbulator distance is approached to the burner exit.

Key words: Oxy-fuel combustion, Coal gases, Burner, Modification.

1. Introduction

Fossil fuels are limited as it is known. In particular, the predicted consumption times for oil and natural gas are less than that of coal and biomass. For this reason, it is very important to increase the use of local and/or renewable energy resources such as coal and biomass. However, there are some challenges such as direct use of these solid fuel types and some problems such as pollution. So, it is more suitable to obtain gaseous fuels from these resources and to use these fuels as alternative fuels. By-product / products resulting from the coking of coal, synthesis gases obtained by gasification of coal and biomass are rather more convenient. Even so, combustion performance of these fuels are somewhat farther away from that of natural gas due to their lower calorific values as well as they are able to be burned with air. For all these reasons, it will be very important to burn these synthesis gases under oxy-combustion conditions with pure oxygen and to investigate combustion and emission parameters of them.

Oxy-fuel combustion is a process of burning a fuel using pure oxygen instead of air as the primary oxidant. Since the nitrogen component of air is not heated, fuel consumption is reduced, and higher flame temperatures are possible. The primary use of oxy-fuel combustion has been widely in welding and cutting of metals, in particular, steel, since oxy-fuel allows higher flame temperatures than that of air-fuel flame. Oxy-fuel combustion has substantial advantages over traditional air-fired plants. Among these are: the mass and volume of the flue gas are reduced by approximately 75%, because the flue gas volume is reduced, less heat is lost in the flue gas, the size of the flue gas treatment equipment can be reduced by 75%, the flue gas is primarily CO₂, suitable for sequestration, the concentration of pollutants in the flue gas is higher, making separation easier, heat of condensation can be captured and reused rather than lost in the flue gas, because nitrogen from air is absent, nitrogen oxide production is greatly reduced [1].

There are many studies related to oxy-fuel combustion. For instance, the characteristics of char reactions, flames, gas emissions (CO, NO_x and SO_x) and temperature distribution have been investigated under oxy-fuel combustion conditions [2]. Çekiç [3] have determined how amount of O₂ in the air affects the calorific value of the Tekirdağ lignite. Krieger et al. [4] have performed CFD simulations of propane/syngas under different oxy-fuel combustion conditions. They have concluded that the temperature level of the oxy-propane flame is higher than that of the air-propane flame. Huynh and Kong [5] have combusted different syngases obtaining from three biomass and investigated their NO_x emission levels under oxygen-enriched air and steam combustion conditions. Bongartz and Ghoniem [6] have performed chemical kinetics of a gas mixture including CH₄, CO₂ and H₂S. Nemitallah and Habib [7] have conducted an experimental and numerical studies to investigate an atmospheric diffusion oxy-combustion flame in a gas turbine model combustor. de la Torre et al. [8] have conducted an experimental study so as to determine radiative heat release properties from oxy-syngas and oxy-methane flames. They have concluded that the effects of CO₂ diluent, impact of equivalence ratio, percentage of H₂ in the fuel, and firing input on the flame's radiative heat release ratio. Ranga Dinesh et al. [9] have scrutinized numerical studies using three-dimensional direct numerical simulations. They have found out that syngas are burned with oxygen better.

Although there are several studies regarding oxy-fuel combustion of syngas as mentioned above, experimental studies related to oxy-syngas combustion are limited. Especially, there are still not enough experimental studies on oxy-fuel combustion of low calorific value coal gases. Moreover, it is aimed to burn syngas with pure oxygen under more stable flame conditions by through making an improvement on the existing syngas burner in the present study.

2. Experimental System

Coal-derived low calorific value syngases have been combusted with pure oxygen via the existing low calorific value syngas burner in the present study [10]. The existing burner and the movable turbulator are clearly illustrated in Fig. 1. This burner is a diffusion flame burner and oxygen and fuel streams are coaxially supplied in it. There are two different types of oxygen inlets to the combustor on the burner. The first oxygen inlets have 15 angles to provide flame stabilization via tangential velocity as well as the second oxygen inlets are comprised of annular inlets. There are 10 and 9 angular oxygen inlets and annular oxygen inlets on the burner, respectively. The fuel inlet is designed to be a radial inlet to the combustor in order to achieve a better fuel/oxygen mixture to enhance the combustion performances of coal-derived low calorific value syngases under oxy-fuel combustion conditions due to their low calorific values.

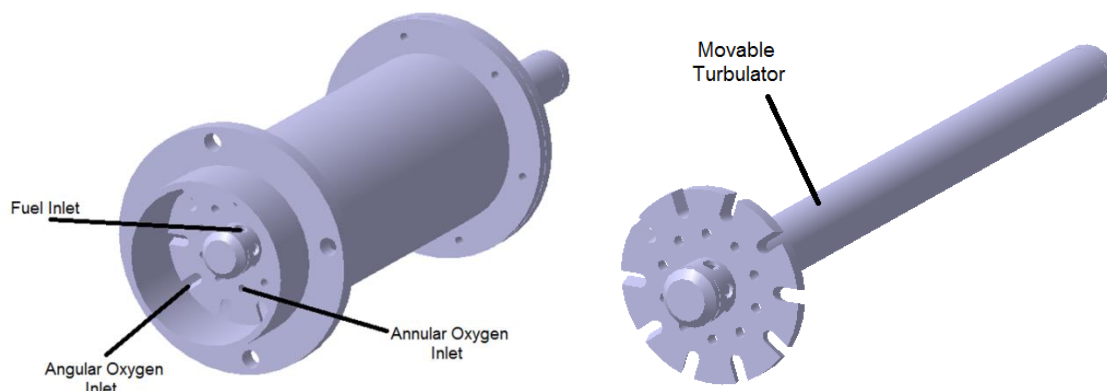


Figure 1. The existing syngas burner and the movable turbulator

Table 1 shows the main properties of coal-derived low calorific value syngases by volume. The coal-derived low calorific value syngases have high amounts of nitrogen as well as some carbon monoxide and hydrogen as combustible components, shown in Table 1.

Table 1.Coal-derived low calorific value syngases [10]

	<i>H₂</i> (%)	<i>CH₄</i> (%)	<i>CO</i> (%)	<i>CO₂</i> (%)	<i>N₂</i> (%)	<i>LHV</i> (<i>kcal/m³</i>)	<i>Density</i> (<i>kg/m³</i>)
Generator Gas	12	0,5	28	5	54,5	1124	1,070
Blast-Furnace Gas	2	-	30	8	60	900	1,200

The schematic view of the existing combustion system equipped with the existing burner is illustrated in Fig. 2. High pressure fuel cylinders, which were prepared in desired percentages as indicated in Table 1, and an oxygen cylinder have been integrated in order to supply the coal-derived low calorific value syngases and the pure oxygen to the existing burner. This system comprises of two gas lines including the coal-derived low calorific value syngas and oxygen lines. These lines consist of regulators, manometers, solenoid valves and float type flowmeters. The regulators have been placed on the system to regulate gas and oxygen pressures. Gas and oxygen pressures have also been periodically tracked in the lines by means of the manometers in order to control gas and oxygen pressures during the experiments. Solenoid valves have been integrated into the system to prevent gas flows when the flame at the burner front is absent. Moreover, this combustion system incorporates float type flowmeters in all lines in order

to achieve the desired gas and oxygen flow rates.

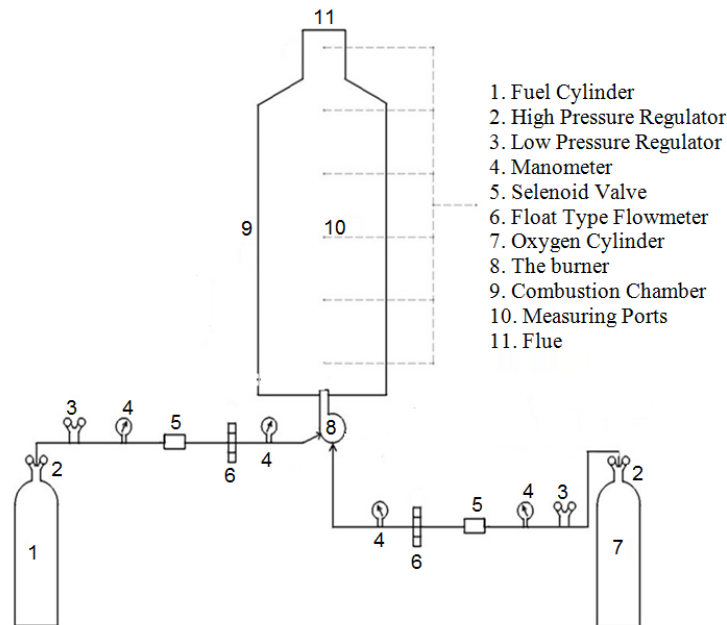


Figure 2. Layout of combustion system

A general view of the existing combustion chamber is clearly shown in Fig. 3. The length and diameter of the combustion chamber are fixed at 100 cm and 40 cm, respectively. The combustion chamber consists of a sight glass made of tempered glass to track the flame during the experiments. It has also five measuring ports. These measuring ports are located on the combustor wall where the thermocouples have been positioned in order to measure temperatures and emissions on different axial and radial positions in the combustor. The first measuring port is designed to determine the flame characteristics of the coal-derived low calorific value syngases and location of this measuring port is 10 cm away from the origin on the axis. The other four measuring ports are placed at intervals of 20 cm from the first measuring port on the same directions.

Ceramic coated R-type thermocouples capable of withstanding high temperatures up to 1700°C were used to measure temperature values throughout the combustion chamber. The diameters of thermocouples are of 5 mm. These thermocouples have been fixed with threaded connections to the combustor wall with a thickness of 4 mm. Emission values have also been measured on different axial and radial positions via the same measuring ports through a flue gas analyzer.

2. Results and Discussions

The combustion performances and emission characteristics of the low calorific value coal gases have been experimentally investigated under oxy-fuel combustion conditions in the present study. Moreover, the turbulator position of the burner has also been changed as a small modification in order to alleviate overheating of the burner walls due to usage of the pure oxygen as an oxidant and therefore, the turbulator position has been modified from the distance of 7 cm to the distance of 2 cm based on the burner exit.

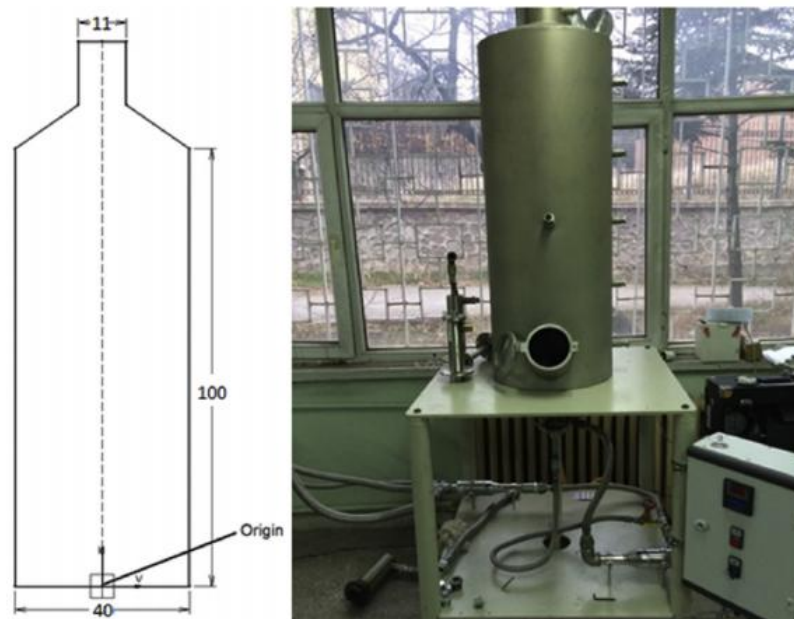


Figure 3. A general view of the existing combustion chamber

Temperature and emission values have been measured on different axial and radial positions by means of measuring ports located on the combustor wall throughout the combustor. At high temperatures, the radiation correction is essential to determine the temperature levels precisely. In particular, radiative heat transfer takes places from the flame to the combustor wall. Mean bulk velocities were calculated theoretically in the flame front taking into account fuel and oxygen velocities. Then, correction was performed for each axial and radial measurement based on the measured combustor wall temperatures. Therefore, it was computed to be between 2–50 K depending on the measured axial, radial and wall temperatures in the combustor.

2.1. Temperature Measurements

Axial and radial temperature values have been measured by using ceramic coated R-type thermocouples throughout the combustor in the present study. Axial temperature measurements are given in Fig. 4. According to the Figure 4, it can be readily said that the maximum temperature value emerges for generator gas combustion in the flame region under the combustion condition of 7 cm of the turbulator distance. This corrected value is of 1378 K. The flame temperature of the blast-furnace gas was also determined as of nearly 1200 K. However, the flame temperatures of the coal gases decrease considerably when the turbulator is moved to the burner exit (2 cm). This conclusion may be explained with flame structures of the generator and blast-furnace gases shown in Figure 5 and 6, each of which represents the flame photographs of these coal gases under all oxy-fuel combustion conditions in this study. The flame temperatures are higher under the combustion condition of 7 cm of the turbulator distance for both fuels as fuel/oxygen mixture has been achieved better under this condition. It can be also said that the low calorific value coal gas flames are gathered when the turbulator is positioned 7 cm away from the burner exit. Similar results have been observed on other axial positions. For instance, at 30 cm axial distance, temperature value of the generator gas flame was measured of 1146 K under the combustion condition of 7 cm of the turbulator distance whereas temperature value of the generator gas flame was determined as of 1120 K under the combustion condition of 2 cm of the turbulator distance. The temperature levels for all combustion conditions decrease gradually towards the combustor outlet at the center of the combustor because of convective and especially radiative heat transfers.

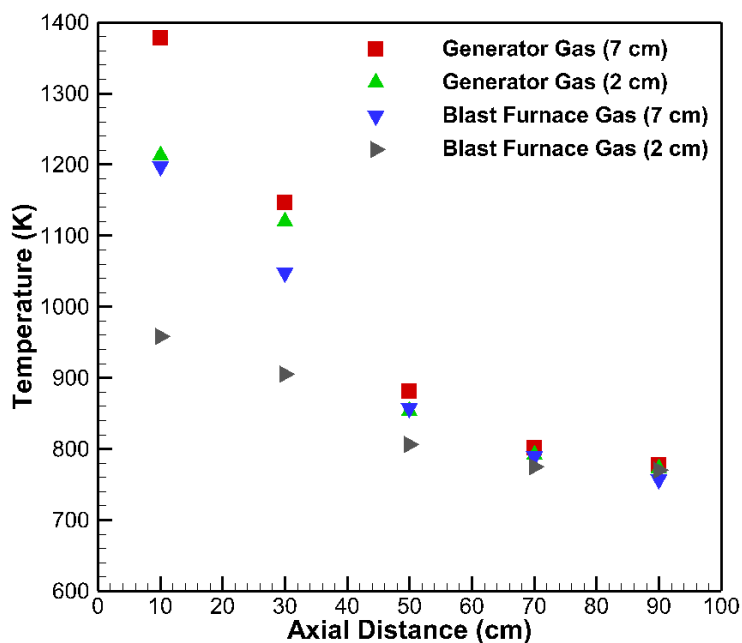


Figure 4. Axial Temperature Measurements

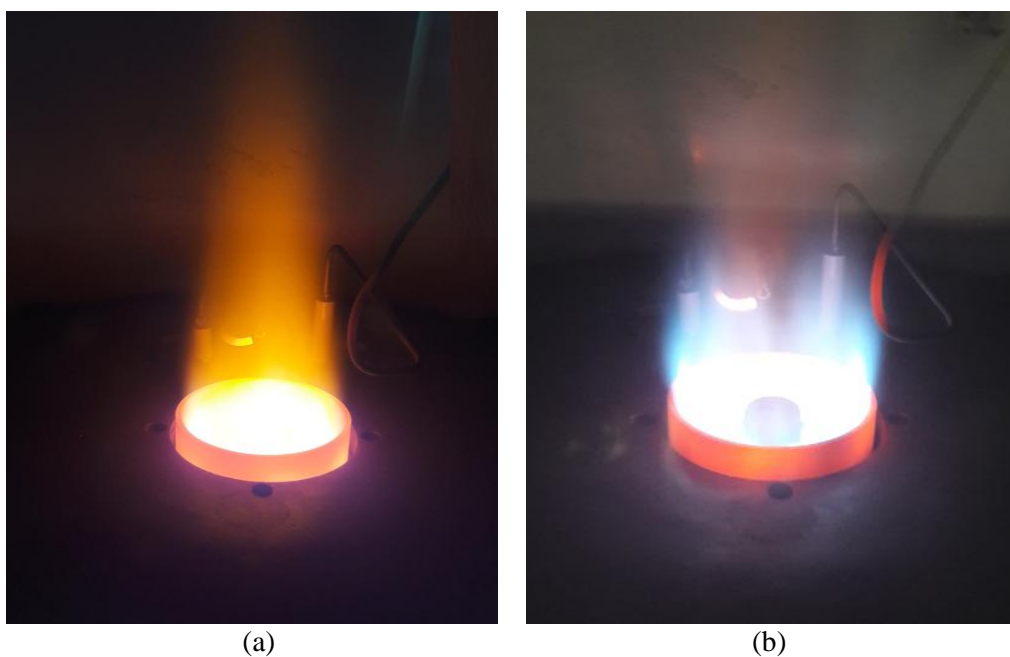


Figure 5a. The generator gas flame photograph for the turbulator distance of 7 cm

Figure 5b. The generator gas flame photograph for the turbulator distance of 2 cm

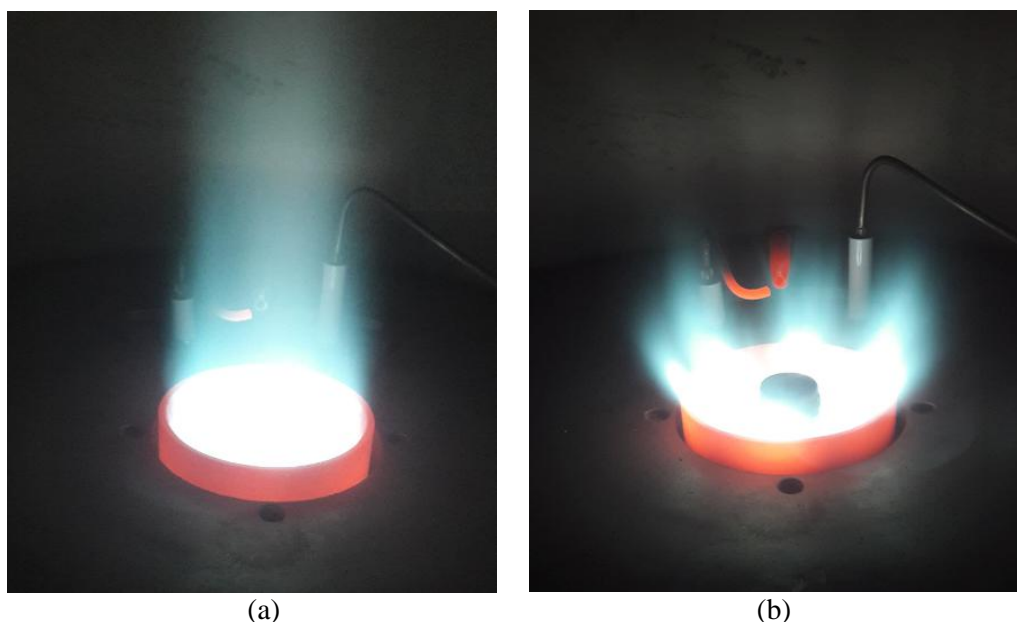


Figure 6a. The blast-furnace gas flame photograph for the turbulator distance of 7 cm
Figure 6b. The blast-furnace gas flame photograph for the turbulator distance of 2 cm

In contrast to axial measurements, according to the radial measurements (Fig. 8), it may be said that the temperature levels increase when the turbulator is located 2 cm away from the burner exit. For instance, at radial measurements acquired from an axial distance of 10 cm, temperature value of the generator gas was measured of almost 700 K under the combustion condition of 7 cm of the turbulator distance while temperature value of the generator gas flame was determined as of nearly 930 K under the combustion condition of 2 cm of the turbulator distance. This conclusion may be explained with flame structures of the generator and blast-furnace gases shown in Figure 5 and 6 just as it is at the axial measurements. The flame under the combustion condition of 2 cm of the turbulator distance is wider and closer to the measuring points compared to the other condition. By the way, it can be concluded that modification to alleviate overheating on the burner walls serves increment of the combustion performances of the low calorific value coal gases under oxy-fuel combustion conditions.

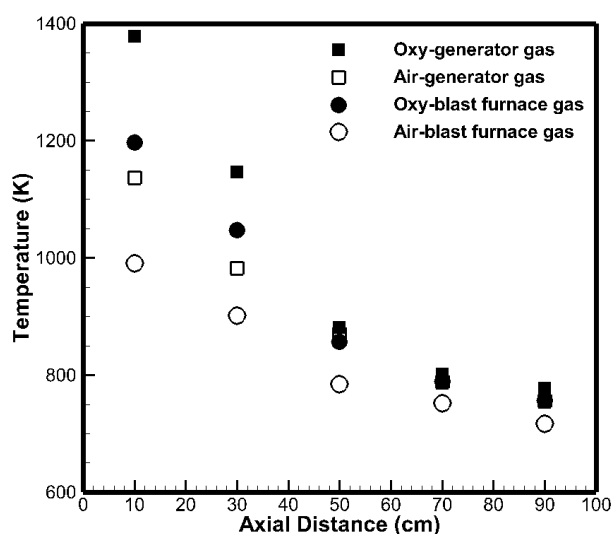


Figure 7. Comparison of oxy-fuel and air-fuel temperature distributions

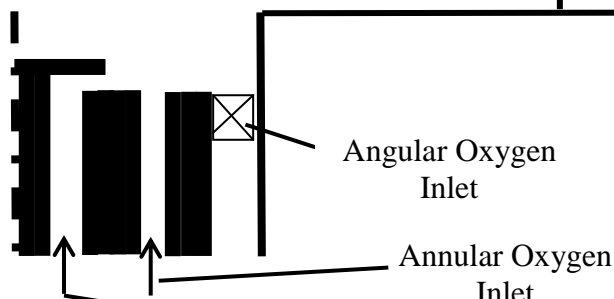
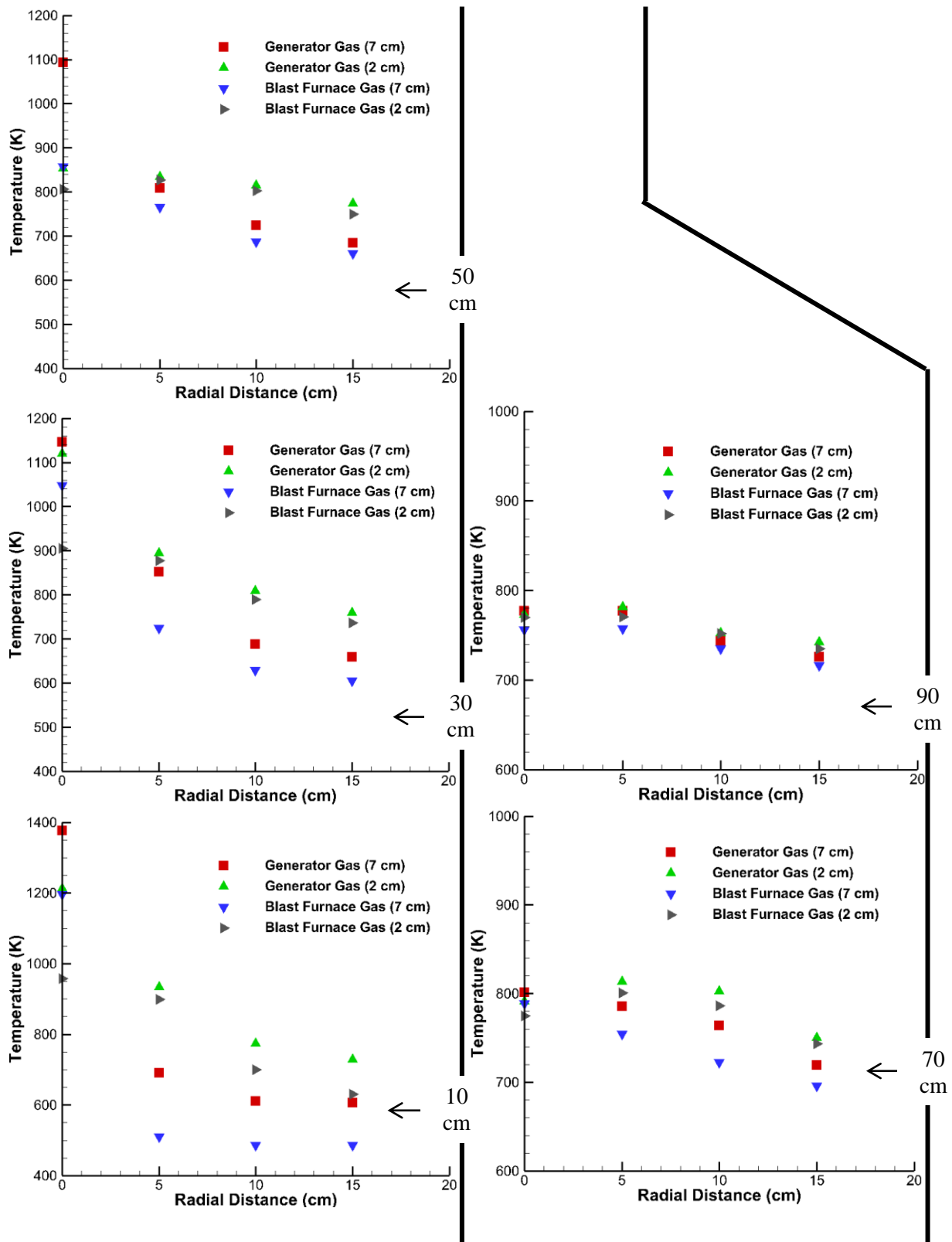


Figure 8. Radial temperature measurements throughout the combustor

Figure 7 shows comparison of axial temperature measurements that have been obtained under oxy-fuel and air-fuel combustion conditions. The results acquired under air-fuel combustion conditions are reported by Karyeyen and İlbaş in the literature [10]. According to the Figure 7, it can be readily said that burning gases with oxygen enhances the flame temperatures of the low calorific value coal gases significantly. In particular, the flame temperatures of these gases increase by around 20% when combustion is taken place with pure oxygen.

2.2. Emission Measurements

Emissions such as NO_x , CO and CO_2 have also been measured on the same axial and radial positions by a flue gas analyzer within the present study. Figure 9 shows NO_x emission values throughout the combustor. As can be seen in Figure 9, the maximum NO_x level emerges for the generator gas combustion in the flame region under the combustion condition of 7 cm of the turbulator distance (219 ppm). This result is directly related to the measured temperature value of it (Fig. 8.). Likewise, it is also seen in combustion of the blast-furnace gas. However, when it is examined the same figure again, it can be seen that the measured NO_x levels for the generator and blast-furnace gases ascend relatively when the turbulator position of the burner has been changed. But yet, these slight increments have not been so much compared to changes in temperature levels although NO_x levels are directly related to temperature levels. Therefore, it can be concluded that modification is not high NO_x emission problem under oxy-fuel combustion of the low calorific value coal gases.

Figure 10 gives CO_2 emission measurements throughout the combustor. The maximum CO_2 level shows up during generator gas combustion in the flame zone under the combustion condition of 7 cm of the turbulator distance as oxygen-fuel mixture is better inside the burner. CO_2 levels decrease gradually at the center of the combustor while it increases slightly at regions in near the combustor wall as the burner fuel inlet is radial inlet. It can also be seen that CO_2 levels decrease as the turbulator of the burner is moved to the burner outlet. Thus, it can be concluded that modification does not increase CO_2 emission levels under oxy-fuel combustion of the low calorific value coal gases just as it is in NO_x emissions.

CO emission measurements are also illustrated in Figure 11 in the present study. In general, CO emission levels are high for all combustion conditions in the flame region. Then, it decreases gradually towards the combustor outlet. The maximum CO formation emerges during blast-furnace gas combustion throughout the combustor under the combustion condition of 7 cm of the turbulator distance excluding the flame region. It is also revealed that CO levels decrease generally throughout the combustor as the turbulator of the burner is moved to the burner outlet.

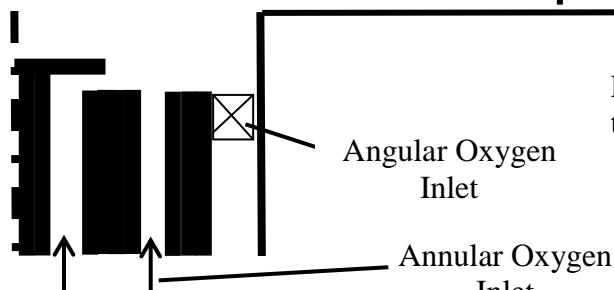
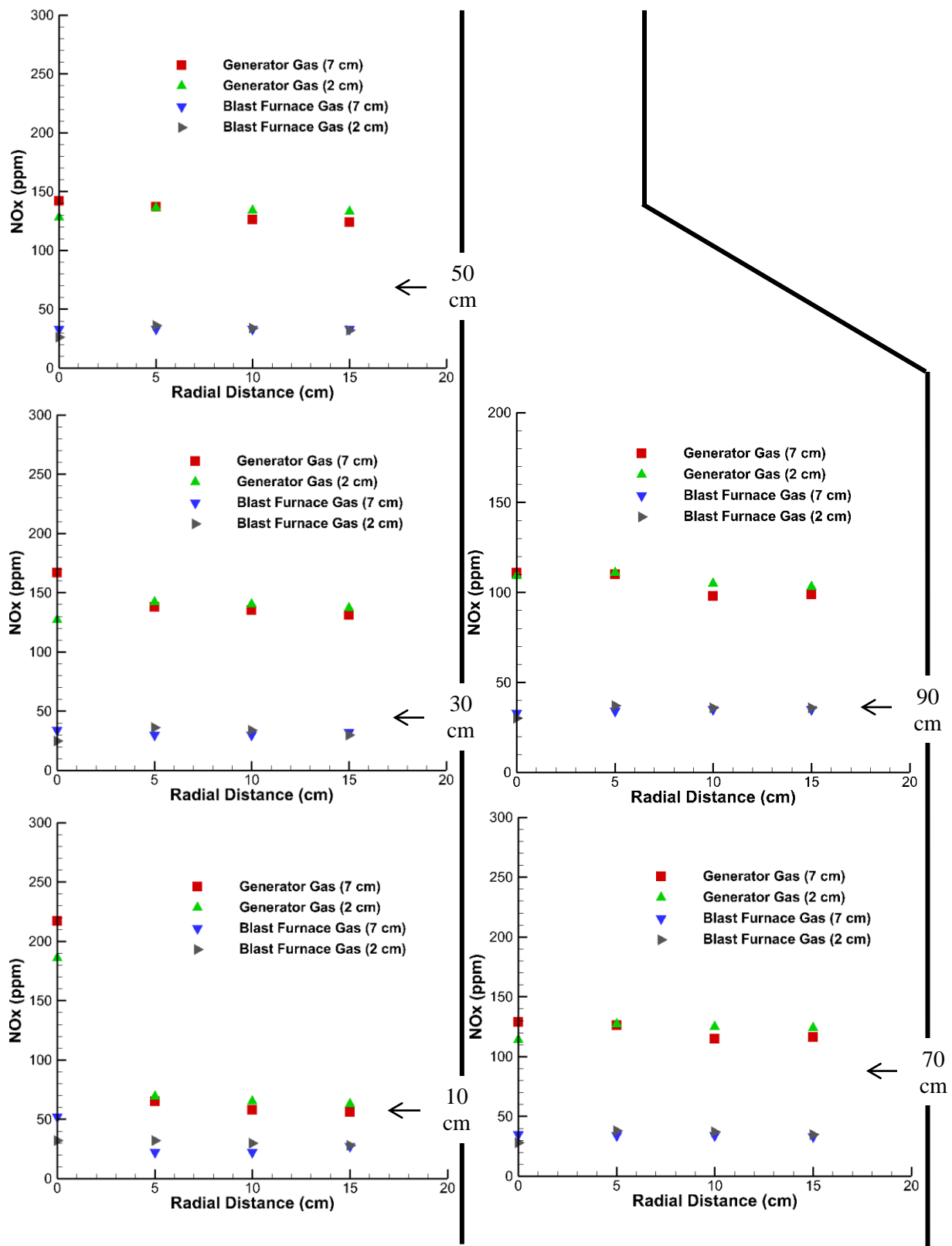


Figure 9. Radial NO_x measurements throughout the combustor

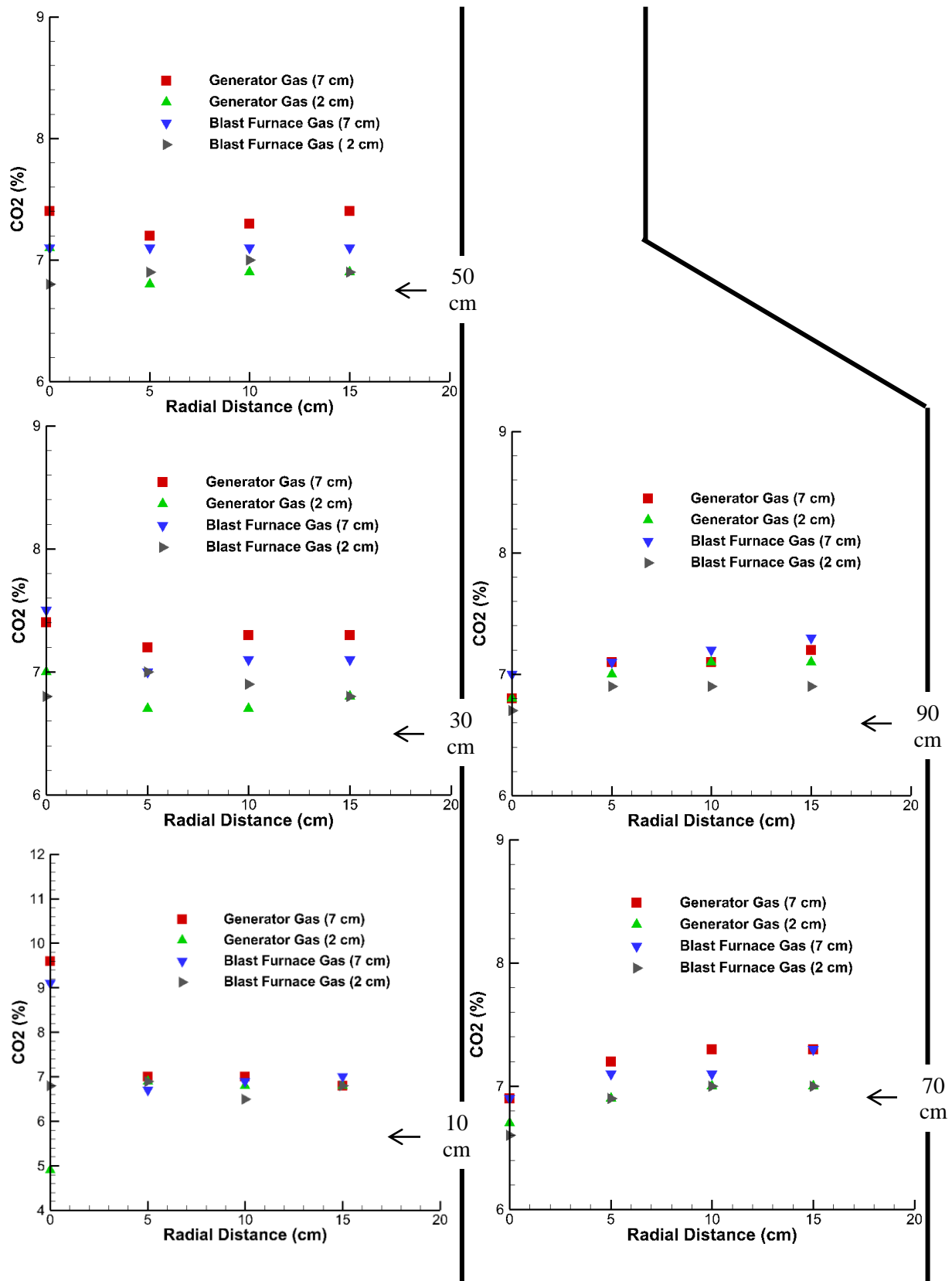


Figure 10. Radial CO₂ measurements throughout the combustor

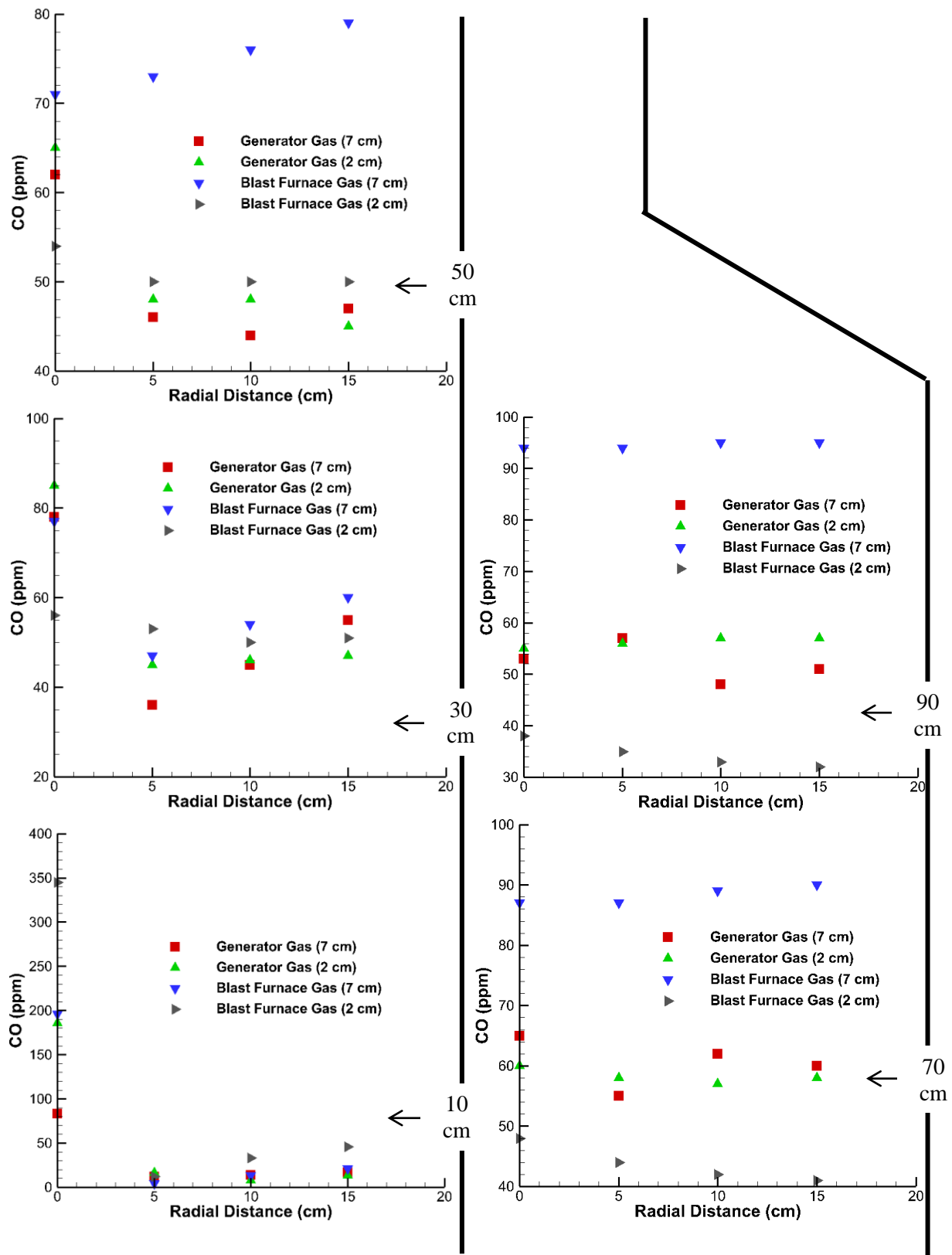


Figure 11. Radial CO measurements throughout the combustor

3. Conclusions

Air-fuel combustion of the low calorific value coal gases (generator and blast-furnace gases) has been previously studied and obtained very interesting results. These results have contributed to the literature. With this study, oxy-fuel combustion of these gases has been experimentally investigated by using the existing burner and the combustion and emission characteristics of these gases have been determined on this. Moreover, the turbulator position of the burner has been changed from the distance of 7 cm to the distance of 2 cm based on the burner outlet so as to alleviate overheating of the burner walls and the effects of this movement have also been investigated on the temperature and emission distributions of the low calorific value coal gases throughout the combustor. Therefore, some important results obtained from the present study are presented below.

The maximum flame temperature emerges during the generator gas combustion under the combustion condition of 7 cm of the turbulator distance. The flame temperatures are higher under the combustion condition of 7 cm of the turbulator distance for both fuels as fuel/oxygen mixture has been achieved better under this condition. However, the radial temperature values are slight different as the low calorific value coal gas flames are wider when the turbulator is positioned 2 cm away from the burner exit. The measured temperature values obtained from radial positions increase as the turbulator position of the burner is moved. Therefore, it can be demonstrated that modification to alleviate overheating on the burner walls serves increment of the combustion performances of the low calorific value coal gases under oxy-fuel combustion conditions. When oxy-fuel combustion is compared to air-fuel combustion, it can be readily concluded that the combustion performances of the low calorific value coal gases enhance considerably.

When the NO_x emission levels are evaluated in the present study, it can be revealed that the measured NO_x levels for the generator and blast-furnace gases ascend relatively when the turbulator position of the burner has been changed. But still, these slight increments have not been so much compared to changes in temperature levels although NO_x levels are directly related to temperature levels and it may be said that modification is not high NO_x emission problem under oxy-fuel combustion of the low calorific value coal gases. When CO₂ and CO emissions are evaluated, it can be revealed that modification does not increase CO₂ emission levels under oxy-fuel combustion of the low calorific value coal gases just as it is CO emissions.

In summary, the low calorific value coal gases can be used in the existing syngas burner under oxy-fuel combustion conditions. But, the modification, which means that the turbulator is moving, is essential to alleviate overheating of the burner walls and it has been demonstrated that this modification enhances the combustion performances of the low calorific value coal gases while it effects their emission levels slightly.

Acknowledgement: The authors gratefully acknowledge financial support from TUBITAK (Project Number: 114M668).

References

- [1] https://en.wikipedia.org/wiki/Oxy-fuel_combustion_process [accessed on 02 April 2017].
- [2] S. Park, J.A. Kim, C. Ryu, T. Chae, W. Yang. “Combustion and heat transfer characteristics of oxy-coal combustion in a 100 MWe front-wall-fired furnace” *Fuel*, 106 (2013), pp. 718–729
- [3] Çekiç, Y. Determination of optimum temperature and oxygen content by burning Tekirdağ malkara lignite coal at different temperature and different oxy fuel conditions, Master Thesis, İTÜ, Institute of Science and Technology, 2015.
- [4] Krieger G. C., Campos A. P. V., Takehara M. D. B., Alfaia da Cunha F., Gurgel Veras C.A. “Numerical simulation of oxy-fuel combustion for gas turbine applications” *Applied Thermal engineering*, 78, (2015) 471-481.
- [5] Cuong V. H., Song-Charng K. “Combustion and NO_x emissions of biomass-derived syngas under various gasification conditions utilizing oxygen-enriched-air and steam” *Fuel*, 107, (2012) 455-464.
- [6] Bongartz, D., Ghoniem A. F. “Chemical kinetics mechanism for oxy-fuel combustion of mixtures of hydrogen sulfide and methane” *Combustion and Flame*, 162, (2015) 544-553.
- [7] Habib, M. A., Salaudeen, S. A., Nemitallah, M. A., Ben-Mansour, R., Mokheimer, E. M. A. “Numerical investigation of syngas oxy-combustion inside a LSCF-6428 oxygen transport membrane reactor”, *Energy*, 96, (2016) 654-665.
- [8] de la Torre, M., Chowdhury, A. S. M. A., Love, N., Choudhuri, A. “Radiative heat release from premixed oxy-syngas and oxy-methane flames”, *Fuel*, 166, (2016) 567-573.
- [9] Ranga Dinesh, K. K. J., van Oijen J. A., Luo K. H., Jiang X. “Near-field local flame extinction of oxy-syngas non-premixed jet flames: A DNS study”, *Fuel*, 130, (2014) 189-196.
- [10] S. Karyeyen, M. Ilbas, Turbulent diffusion flames of coal derived-hydrogen supplied low calorific value syngas mixtures in a new type of burner: An experimental study, *International Journal of Hydrogen Energy*, 42 (2017) 2411-2423.

Evaluation of combustion and NO_x formation in a gas turbine combustor by changing primary zone length

Melih Yıldız^{1,*}, Mürüvvet Kurt², Bilge Albayrak Çeper¹

¹*Erciyes University, Faculty of Engineering, Department of Mechanical Engineering, 38039 Kayseri, Turkey*

²*2nd Air Supply Maintenance Center Command, 38040 Kayseri, Turkey*

Abstract: This paper presents the numerical study which focuses on the investigation of temperature distribution and, NO_x formation in a micro-gas turbine combustor. The combustor consists of primary and secondary zones for the flow field and combustion process. The primary zone length is one of the crucial design parameters which change the flow characteristics and combustion development. Therefore, the three-dimensional numerical study was carried out to investigate how the temperature distribution and NO_x formation are affected with the change in the length of primary zone for different excess air ratios. In this study, CFD-Fluent program which uses the finite volume method was used as an analysis tool. The results show that the lowest NO_x values are obtained when the primary zone length is 110 mm.

Keywords: Combustor, NO_x, CFD, Swirling

1. Introduction

In today's world, energy shortage problems have become a major concern indicating the need to use our resources more efficiently. Using of micro-gas turbine providing the efficient use of energy is gaining importance in the world. Micro-turbines reach the gas turbine technologies in smaller sizes, so they are a type of combustion turbine that produces both heat and electricity in relatively small scale. Their applications and broad explanations are summarized by Capehart[1]. Micro-turbines offer several potential advantages compared to other technologies for small-scale power generation, such as higher power-to-weight ratio, low emissions (NO_x emissions <9-50 ppm) and few, or just one, moving part[2-3].

Extensive research about the use of internal combustion small gas engine on the micro combined heat and power generation has been done on the last decade. Despite using a known technology, noise, emission and maintenance problems haven't been solved completely yet. For this reason, studies and technological developments make micro-power producers more efficient, greener and cheaper [4].

The work carried out by Furuhashi et al.[5], which is one of the studies on micro-gas turbine combustor, was regarded as a reference model for the current study. Therefore, the design of the geometric model was created considering the main dimensions of the combustor. The effect of the change in the primary zone length for three different excess air ratios was analyzed using CFD-Fluent program. The results were investigated in terms of temperature distribution and NO_x formation.

2. Numerical Analysis

In this study, the combustion in a kerosene-fueled can-type combustor was analyzed for values of primary zone length, 90, 110 and, 130 mm with different air excess ratios(λ), 1.30, 1.50 and 1.70. The combustor consists of primary and secondary combustion zones, and these zones were connected by a throat. A swirler was set between the primary and secondary combustion zones. In order to enhance the recirculation of burned gas in the primary combustion zone, the combustion air was introduced through the swirler and, forced to flow upward to the combustor bottom, from where fuel spray was supplied through a nozzle. The geometric model and, the mesh structure were created by using GAMBIT as shown in Figure 1.

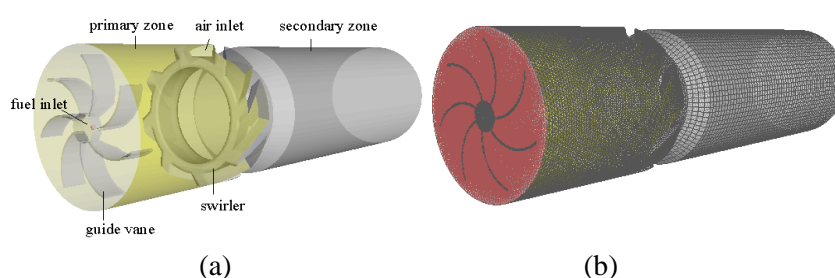


Figure 1. (a) Geometric model, (b) mesh structure of the model

After creating the necessary models for numerical solution, Governing Equations, momentum, energy and continuity, are solved with the submodels including k- ϵ RNG turbulence, P1 radiation and, Eddy-Dissipation combustion models. The fuel content is assumed to be free of nitrogen and modeled only with thermal and prompt NO_x formation mechanisms [6].

3. Results and Discussions

The streamlines obtained in the combustor are given in Fig.2. As seen in the figure, the air passes through the swirler wings to gain speed in the tangential direction and enter the primary zone. The air reaching the guide blades in the primary zone is directed towards the fuel inlet and fuel-air mixture is provided.

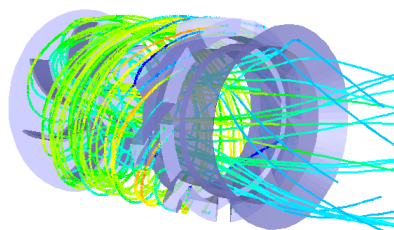


Figure 2. Streamlines in the combustor

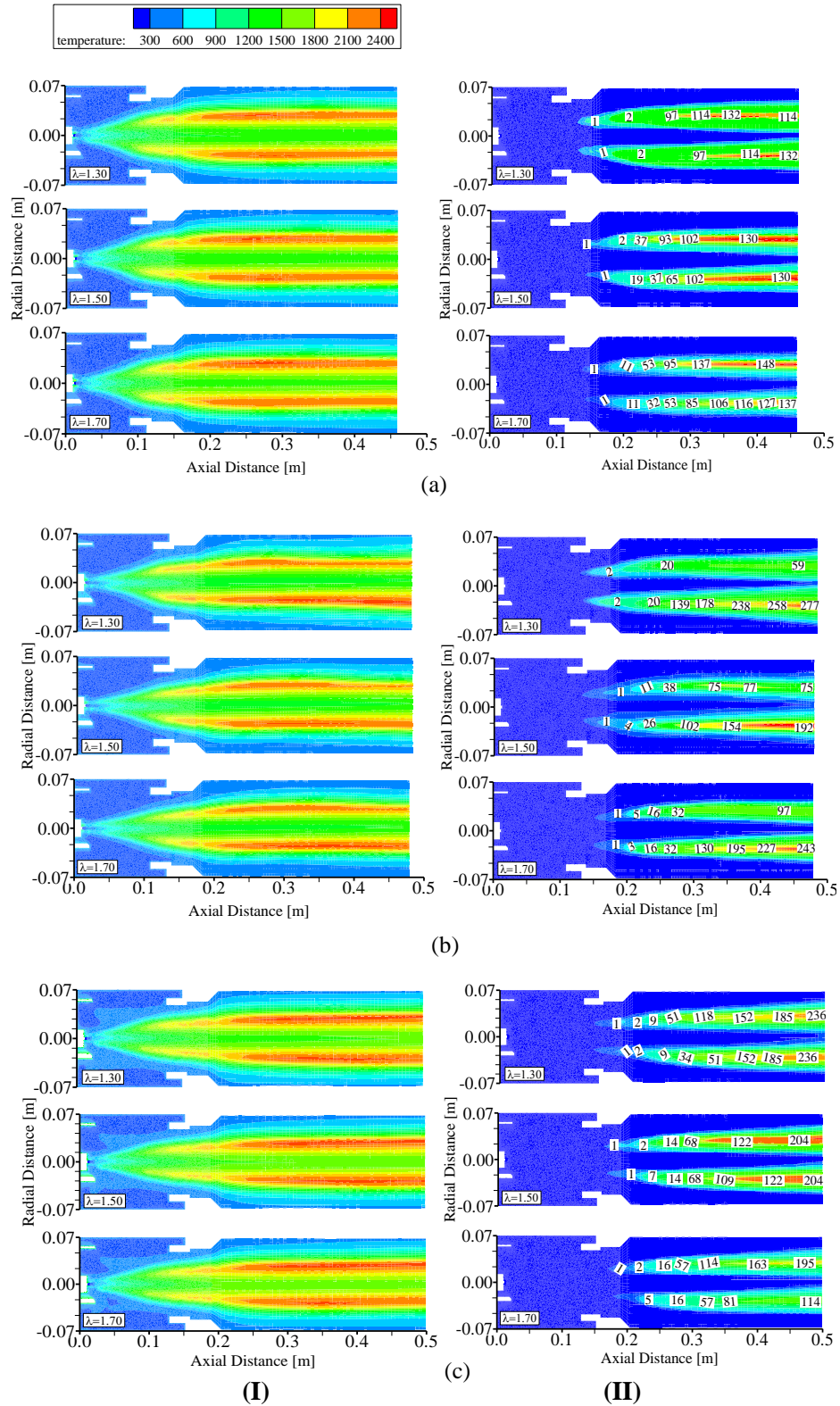


Figure 3. Temperature distribution(I) and, NOx formation(II)
(a)PZL=90 mm, (b) PZL=110 mm, (c) PZL=130 mm

Figure 3 shows the temperature distribution through the combustor zones for primary zone length (PZL), 90, 110 and, 130 mm with different excess air ratio (λ). Figure 4 also illustrates NOx formation in the combustor for all cases.

As seen from the temperature distributions, the primary region is composed of cold regions. The temperature values in the secondary zone reached maximum values with flame development. As the PZL increases, the average temperature in the primary zone is higher and, the flame length in the secondary zone is higher. It is observed that the NOx concentration does not occur in the primary zone, whereas the formations in the secondary zone reach the highest level due to high temperature.

The temperature values in the secondary zone reached maximum values with flame development. As the excess air ratio increases, the temperature values decrease. Particularly cold regions near the boundary have expanded with increasing excess air ratio. The temperature values in the high temperature region decrease by a certain value as the excess air ratio increases. The NOx emissions and maximum temperature values obtained at the combustor outlet at different values of the PZL are shown in Figure 5.

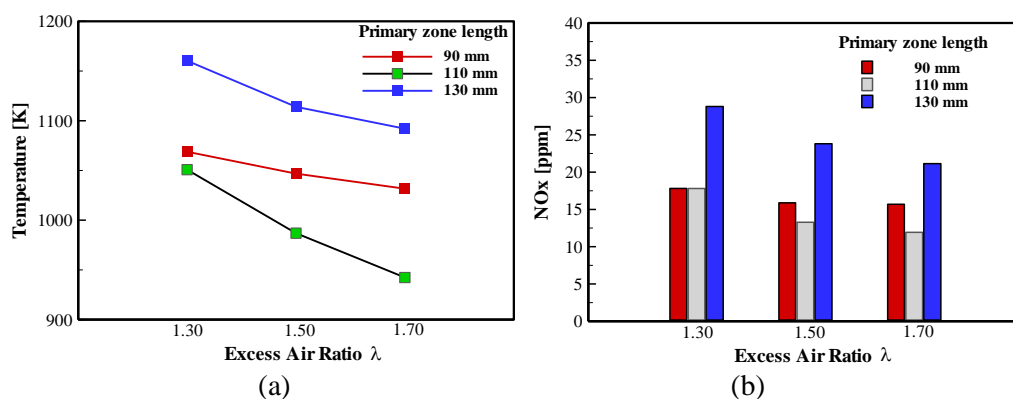


Figure 5. The average temperature (a) and, (b) NOx emissions at the combustor outlet.

4. Conclusions

In this study, a kerosene fueled micro-gas combustor was numerically studied for ZPL=90, 110 and 130 mm at different excess air ratios $\lambda=1.30$, 1.50 and 1.70. The results obtained are summarized below:

- In the case of PZL=130 mm, the temperature distribution is higher than those at other lengths of primary zone. This geometry makes the high temperature zone in the combustion chamber closer to the combustion nozzle.
- At the combustor outlet, the highest values of mass-average NOx concentrations were observed at the lowest air excess ratio. NOx emission values were obtained about 18 ppm and, 28 ppm for both 90 and 110 mm, 130 mm of PZL respectively.
- Similar to the change in temperature, the NOx concentration values for PZL = 130mm were found to be higher than those for others and, it was also observed to increase by almost 60%.

As a result, the temperature and NO_x concentrations at the combustor outlet at PZL=110 mm are lower than those at other lengths and, therefore; it is considered that the optimum length of the primary zone in terms of NO_x concentration is 110 mm.

References

- [1] Capehart B.L. Microturbines. Available from: <http://wbdg.org/resources/microturbines>.
- [2] Decuyper R., Verstraete, D. Micro Turbines from the Standpoint of Potential User. VKI RTO-AVT131, Micro Gas Turbines, March 14-18, 2005, Rhode-St-Genèse, Belçika.
- [3] Erbay L.B., İnal L., Öztürk M.M. Akışkan-Mikroelektromekanik Sistemler. Mühendis ve Makine Dergisi, 2006, Vol: 47, no: 556, p.13-33.
- [4] Derbentli T. Bileşik Isı-Güç Üretiminin Küçük Ölçeklerde Uygulanabilirliği. 2012 Türkiye Enerji Konferansı Bildirileri, p. 44-49.
- [5] Furuhashi T., Amano S., Yotoriyama K., Arai M. Development of can-type low NO_x combustor for micro gas turbine (fundamental characteristics in a primary combustion zone with upward swirl), Fuel, 86; (2007) 2463–2474.
- [6] Fluent 6.3 User's Guide, 2006. Fluent Incorporated, Centerra Resource Park, 10. Cavendish Court, Lebanon, NH 03766, USA.

Numerical investigation on combustion behavior of premixed hydrogen/air flames in a micro combustor with varying geometric properties: part - I effect of backward facing step and cavity

^{1*}Harun Yilmaz, ²Omer Cam, ³Mustafa Ilbas, ²İlker Yilmaz

¹ *Erzincan University, Civil Aviation College, Airframe - Powerplant Department, Erzincan, 24000, Turkey*

² *Erciyes University, Fac. of Aeronautics and Astronautics, Airframe - Powerplant Dept., Kayseri, 38039, Turkey*

³ *Gazi University, Technology Fac., Dept. of Energy Systems Engineering, Teknikokullar, Ankara, 06500, Turkey*

* E-mail: hyilmaz@erzincan.edu.tr

Abstract: Main challenges for fuel efficient micro scale combustion are rooted from size restriction of micro combustors which results with inappropriate residence time of fuel air mixture and intensified heat losses due to relatively higher surface to volume ratio. One way of increasing energy output of such combustors is optimizing combustor geometry. In this study, effect of combustor geometric properties to combustion behavior of premixed hydrogen/air mixtures is numerically investigated. For this purpose, an experimentally tested micro combustor's geometric properties were modified by establishing a backward facing step which is varying distance from combustor inlet and has varying step height and establishing a cavity with constant length to depth ratio and which is varying distance from combustor inlet. Modeling and simulation studies were performed using ANSYS Design Modeler and Fluent programs, respectively. Combustion behavior was analyzed by means of centerline and outer wall temperature distributions, amount of heat transferred through combustor wall and conversion ratio of input chemical energy and to utilizable heat. Turbulence model used in this study is Renormalization Group (RNG) k- ϵ . Multistep combustion reaction scheme with 9 species and 19 steps was simulated using Eddy Dissipation Concept model (EDC). Results showed that backward facing step in the flame region alters reaction zone distribution, flame length and shape and consequently temperature value and distribution throughout the combustor. Lastly cavity was found to slightly increase peak temperature value.

Key words: Micro scale combustion, combustor geometry, backward facing step, cavity

1. Introduction

Increasing functionalities of up to date microelectronic devices require compact and powerful energy sources. Compared to conventional batteries, conversion of fuel bound chemical energy to applicable forms of energy via micro combustors can meet high density energy demand of micro devices. When we consider battery disposal, micro combustors can also meet this demand in an environmentally friendly manner [1]. To answer increasing energy demand, many researchers developed various forms of micro combustor based power generators and studied combustion and emission behavior of these combustors both numerically and experimentally.

Akhtar et al. simulated hydrogen air combustion in a micro combustor by varying combustor cross section (circular, quadratic, triangular and trapezoidal), turbulence and combustion models (to find the most appropriate computational fluid dynamic model). They examined effect of these parameters on flow and flame behavior and concluded that Eddy Dissipation Concept model along with Reynolds Stress Model gives the most consistent simulation results with experimental data, an increment in inlet velocity increases wall temperature, trapezoidal and triangular cross sectional shaped combustors perform better with respect to combustion performance [2].

Hydrogen and hydrocarbon fuel combustion stability in a micro annular combustor with EGR (Exhaust Gas Recirculation) by means of quenching distance and flammability limits is numerically investigated by Lei et al. Results showed that a decrement in combustor diameter reduces flammability limits but with EGR, flammability limits widen; EGR also reduces quenching distance; the most effective energy conversion rate can be gained with 1 mm diameter combustor [3]

Li et al. conducted both numerical and experimental studies to examine combustion behavior of diffusion methane micro-jet flames in confluence air. Numerical simulations were carried out using 2D tube models which take flame-wall interactions into consideration. On the other hand, experimental studies were conducted measuring flame height, blow out and flame extinction limits at different mass flow rates. Numerical results showed a good agreement with experimental results and indicated that increasing confluence air velocity firstly broadens blow out limit then reduces it, extinction limit is not susceptible to confluence air velocity [4]

Miyata et al. conducted CH₄/air combustion simulation studies by varying inlet and wall temperature gradient in a 1 mm diameter micro channel which has wall temperature gradient in flow direction using DNS (Direct Numerical Simulation) method. Based on the inlet and wall temperature gradient, they observed flame iterant extinction- ignition behavior and concluded that this behavior brings in a phase in which total heat transfer rate through wall gets a negative value [5]

Jiang et al. added varying amount of CO to pure H₂ to investigate effect of CO addition on emitter power of a micro combustor. During numerical simulations, combustor length and combustor wall thickness were chosen as variable parameters. It was observed that the region where emitter power is high moves downstream with CO addition, an increment in CO mass fraction and inlet velocity decreases emitter power, maximum emitter efficiency can be achieved with 20 mm length and 0.4 mm wall thickness combustor [6]

Sarath et al. numerically examined methane/air diffusion flames in a micro combustor by adding a bluff body in central region of the combustor or on combustor wall, varying bluff body shape and bluff body position in stream wise direction at different methane mass flow rates. It was demonstrated that

fuel mass flow rate shifts reaction rates, fuel efficiency and the place where combustion takes place; with bluff body on the wall, combustion performance increases more than that of the bluff body in central region; moving bluff body settlement downstream reduces combustion performance; implemented bluff body shapes has no significant superiorities over each other [7].

Zhou et al. established an experimental setup to analyze performance of a micro combustor under various operating conditions and tried to improve its performance with electrical heating inside. Results revealed the significant impact of electrical heating on stability range of the studied H₂/air flames. With 1.05 and 4.70 W electrical heating, stability range (extinction and blow out limits) broadens from 0.362 – 6.52 to 0.178 – 7.66 and 0.126 – 9.43 L/min, respectively. Electrical heating also widens flammability limits [8]

Hosseini and Wahid performed simulation studies to investigate lean premixed and non-premixed CH₄/air conventional and flameless combustion mechanisms with respect to temperature distribution and flame stability in a micro combustor with or without a bluff body. It was shown that establishing a bluff body in the flame region increases stability range of the premixed conventional combustion flames, maximum temperatures for conventional and flameless combustion are 2200 and 1520 K, whereas maximum exhaust gas temperatures are 1300 and 1500 K, respectively; in flameless combustion regime outer wall temperature distribution is more uniform which indicates a positive effect on combustor service life [9].

Jimenez and Kurdyumov studied fuel lean H₂/air flames which freely propagate in a narrow channel using DNS method. They assigned channel distance (1 mm) and equivalence ratio (0.4) as constant parameters and varied fuel/air mixture mass flow rate and heat transfer conditions. They concluded that both symmetric and non-symmetric solutions can be attained based on the boundary conditions, symmetric flames are more prone to flame instabilities compared to non-symmetric counterpart, non-symmetric flames burn more intensively indicating a resistance to quenching [10].

Because of the intensive heat losses to environment and radical wall interactions, sustaining combustion process in a micro combustor in a stable and fuel efficient manner is a challenging issue. To overcome these challenges, micro combustor geometry can be optimized as a cheap and effective option. In this study, an experimentally tested micro combustors geometry was altered to achieve more energy output with respect to basic thermo photovoltaic system requirements by establishing a backward facing step which is varying distance from combustor inlet and has varying step height, and a cavity which is varying distance from combustor inlet and has a constant cavity length and depth.

2. Numerical Setup

2.1. Combustor Geometry

In this study, 3D micro combustor models were constructed using ANSYS/Design Modeler program and in these models, multistep hydrogen/air combustion was simulated using ANSYS/Fluent program. The combustor model has 18 mm length, 3 mm height, 9 mm width and 0.5 mm wall thickness as shown in Figure 1. Based on this model, micro combustor geometry was modified.

Combustor model with backward facing step can be seen in Figure 2. Backward facing step settlement was determined according to flame region (in the flame region, right after the flame region and outside the flame region which are 2, 4 and 6 mm away from combustor inlet, respectively). Step

heights were set as 0.5, and 0.75 mm. On the other hand, cavity length and depth (2 mm and 0.4 mm, respectively) were kept constant and the distance between cavity location and combustor inlet was varied (2, 4, and 6 mm). It can be seen in Figure 3.

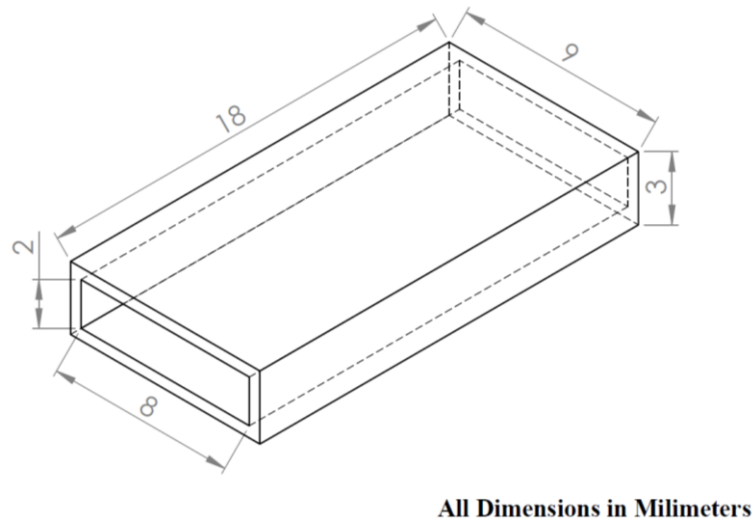


Figure 1. The physical domain of the combustor with straight channel.

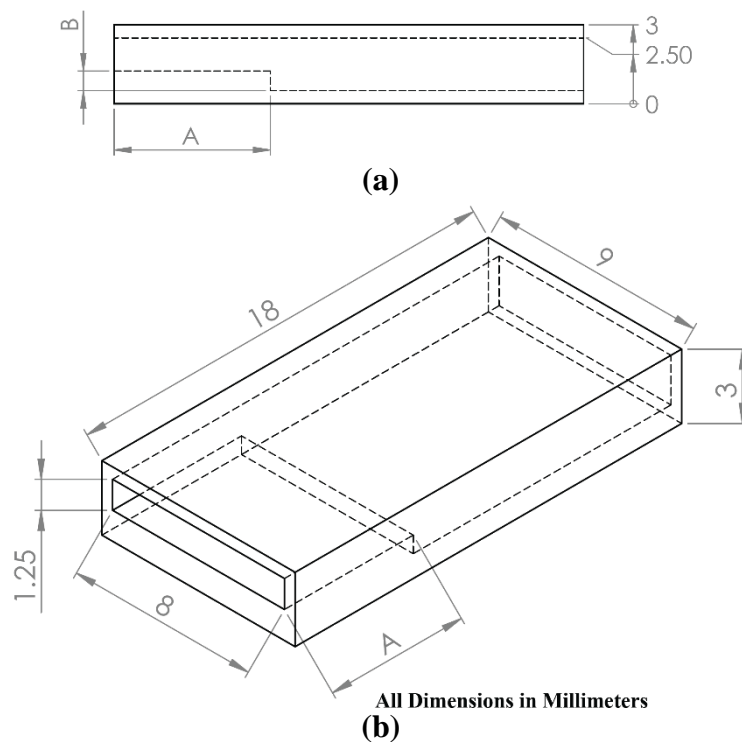


Figure 2. The physical domain of the combustor with backward facing step.
(a) Side view (b) Isometric view

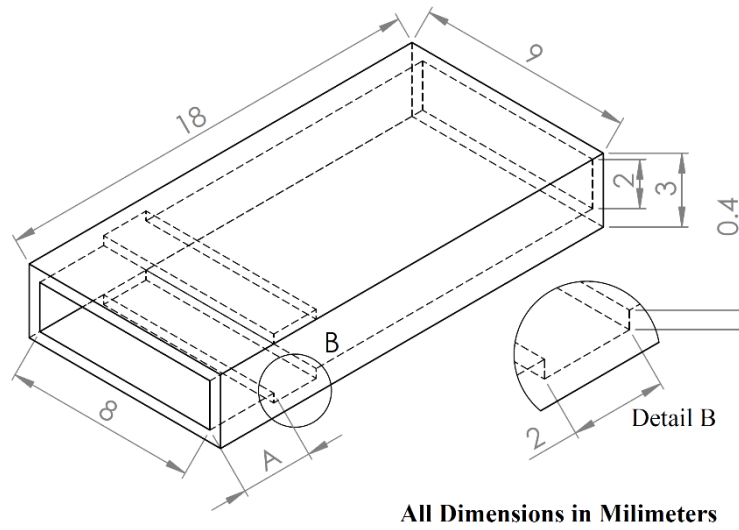


Figure 3. The physical domain of the combustor with cavity.

2.2. Mathematical Model

Steady state forms of the basic governing equations are solved and these equations are:

Continuity;

$$\frac{\partial(\rho u_j)}{\partial x_j} = 0$$

ρ , density; u_j , velocity component.

Momentum;

$$\frac{\partial \rho u_j u_i}{\partial x_j} = -\frac{\partial P}{\partial x_i} + \frac{\partial \tau_{ij}}{\partial x_j}$$

P , pressure; τ_{ij} , stress tensor.

Energy;

$$\frac{\partial(\rho u_j h)}{\partial x_j} = \frac{\partial}{\partial x_j} \left(k \frac{\partial T}{\partial x_j} - \sum_{i=1}^N h_i j_{ij} \right) + u_j \frac{\partial P}{\partial x_j} + S_h$$

h , enthalpy; k , thermal conductivity; T , temperature; S_h , fluid enthalpy source; j_{ij} , diffusion flux.

Species;

$$\frac{\partial(\rho u_j Y_i)}{\partial x_j} = -\frac{\partial J_{ij}}{\partial x_j} + R_i$$

Y_i , mass fraction of species i ; R_i , net production rate of species i via chemical reactions. All of the governing equations are discretized by a second order upwind scheme using finite volume and under relaxation method.

Assumptions for the simulations are (1) no work is done by pressure and viscous forces (2) no surface reaction (3) no gas radiation (4) no energy flux due to mass concentration gradients (5) no slip boundary condition at the combustor wall [11-13]. Multi step hydrogen air combustion (9 species and 19 steps) was modeled using EDC (Eddy Dissipation Concept) combustion model. As turbulence model RNG k- ϵ is chosen. Reaction scheme of hydrogen/air combustion and turbulence model can be found in Ref. [14-15], respectively.

2.3. Boundary Conditions

Hydrogen flux into the combustor set as 1200 ml/min and depending on the equivalence ratio (0.8) total hydrogen/air mass flow rate and mass fraction of reactant species are specified. So for the combustor inlet, mass flow inlet and for the outlet, pressure outlet boundary conditions are chosen, and for both hydraulic diameter (depending on the geometric variations) and turbulent intensity are identified. For combustor wall, mixed thermal condition is chosen to consider radiation and convective heat transfer. Convergence criteria is set as 10^{-6} .

2.4. Mesh Independency Study

Constructing a mesh structure which consists of sufficient number of elements for an accurate and least time and computational effort consuming simulation is very important. For this purpose, we constructed 5 different mesh structures which has 31104, 90640, 248832 and 486000 elements. Using these structures, we simulated H_2 /air combustion under same boundary and operating conditions, and compared predicted centerline temperature profiles (Figure 4). Results do not significantly change for the mesh structures which have 248832 and 486000 elements. So, mesh structure with 248832 elements was chosen.

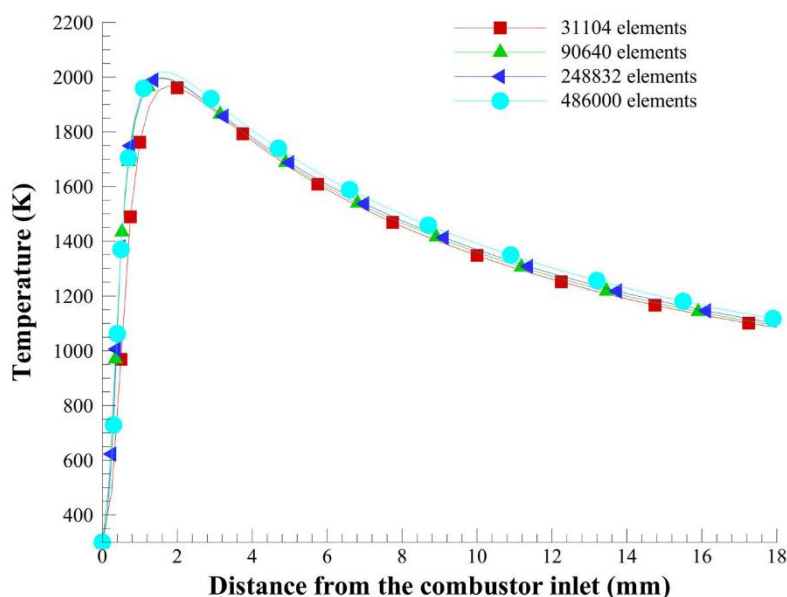


Figure 4. Mesh independency study.

2.5. Model Validation

To validate our model, predicted outer wall temperature values are compared with the numerical and experimental results of Ref. [16]. This comparison is illustrated in Figure 5. Predicted results showed a good agreement with published data and proved availability of our model. Discrepancies between numerical and experimental results are attributed to be rooted from assumptions for numerical simulations, limitations of experimental apparatus and size limitation of micro devices.

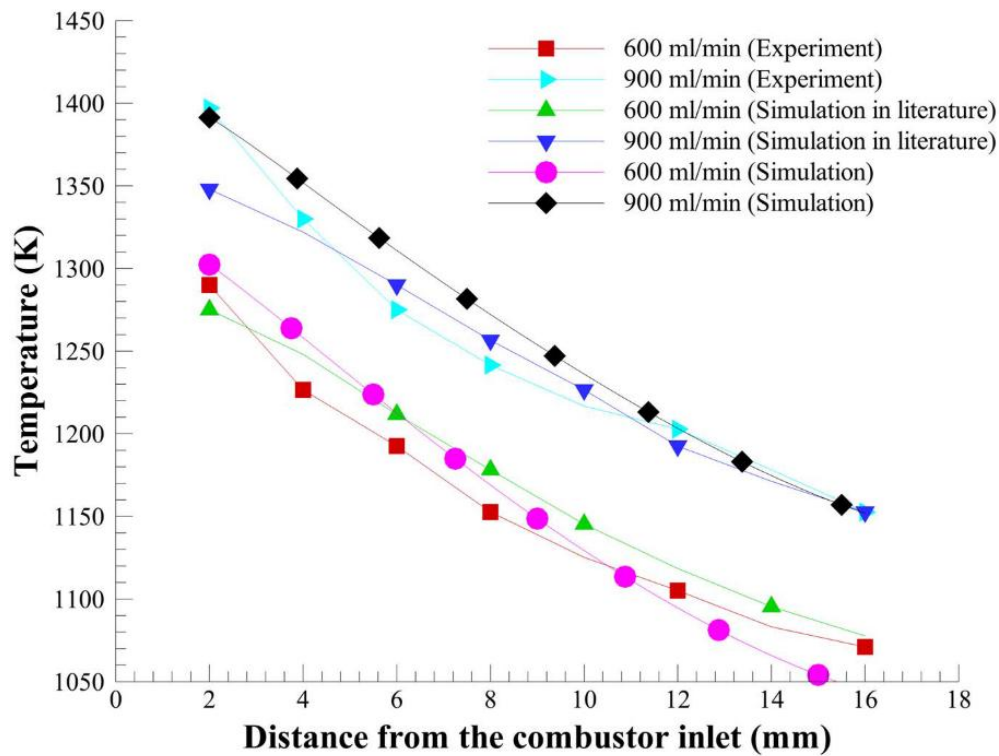


Figure 5. Validation of numerical model [Tang et al., 2015]

3. Results and Discussions

Main driving force of the heat transfer is flame temperature. Motivated by this and because being the cheapest option, a micro combustor's geometry is varied to be able to achieve high and uniform temperature output from combustor wall. In figure 6, centerline temperature profile of the combustors with backward facing step which is varying distance from combustor inlet (2, 4 and 6 mm) and has different step height (0.5 and 0.75) can be seen. When step height is 1.0 mm, combustor centerline overlaps inner side of the combustor wall and this situation causes misinterpretation of the results so centerline temperature profile of the combustor with 1 mm step height is excluded. Irrespective of step settlement and height, backward facing step increases maximum temperature value and temperature distribution throughout the combustor.

Temperature increment to peak temperature value in straight channel combustor occurs nearly six millimeters away from combustor inlet. With increasing step height and narrowing channel gap, this temperature increment moves upstream and combustion takes place in a narrow area right after combustor inlet. Temperature profiles of the combustors with backward facing step are nearly the same in terms of trend and value but these profiles differ starting from backward facing step

settlement. Sudden expansion of the flow area causes flame temperature to reduce then it increases. Towards the outlet of the combustor, all temperature profiles come to nearly the same trend and value again. Recirculating zone formed by sudden expansion develops mixing process and extends residence time. Therefore combustion products emanated from combustors with backward facing step exhaust at lower temperature compared to straight channel combustor.

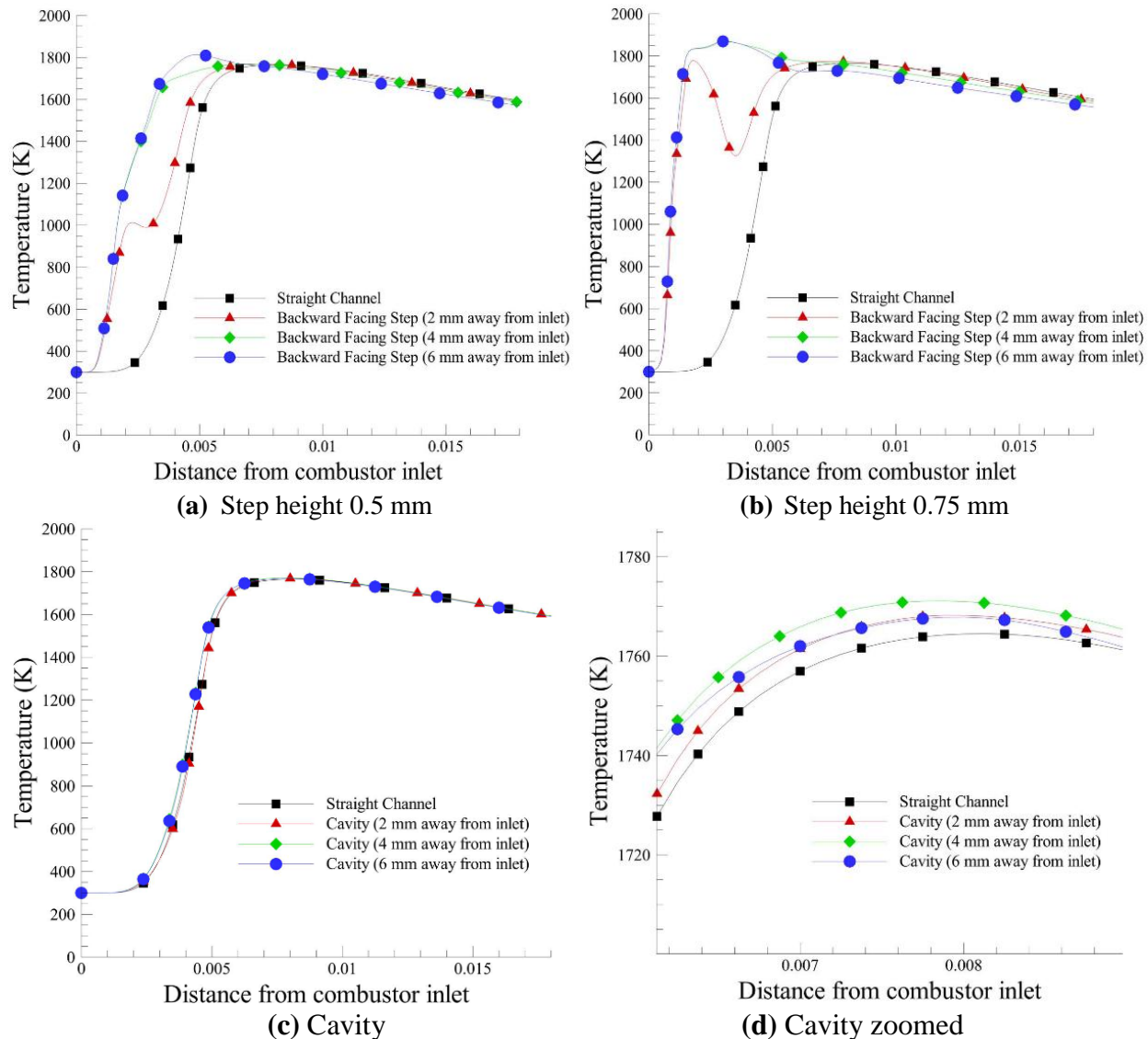


Figure 6. Centerline temperature profiles of the combustor.

From the centerline temperature profiles of the combustors with cavity, it can clearly be seen that this kind of cavity slightly increases peak temperature value and changes temperature distribution. Because this kind of cavity doesn't change reaction zone distribution (Figure 7).

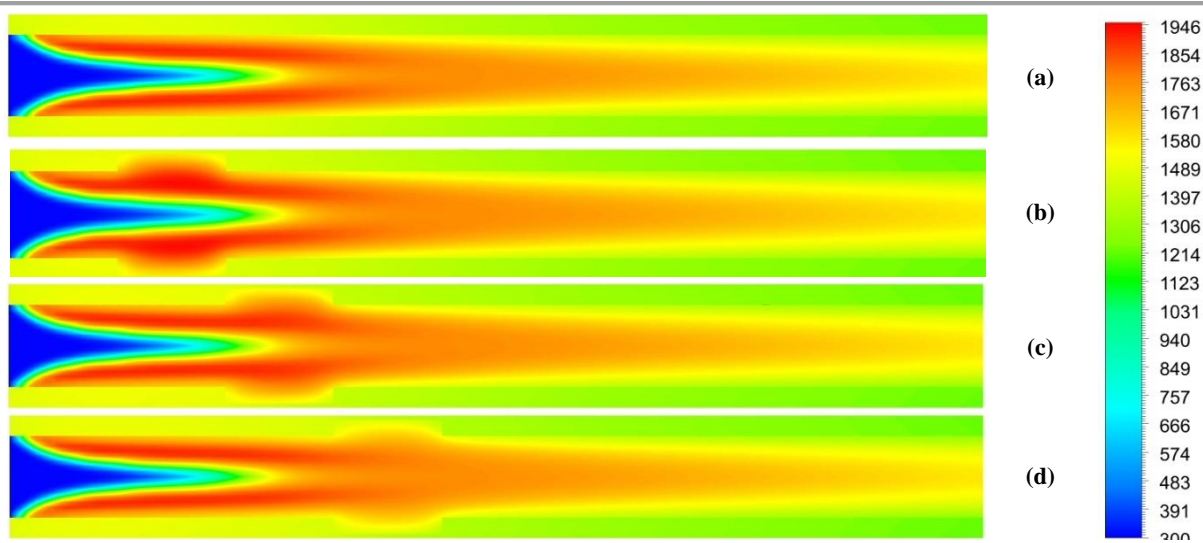
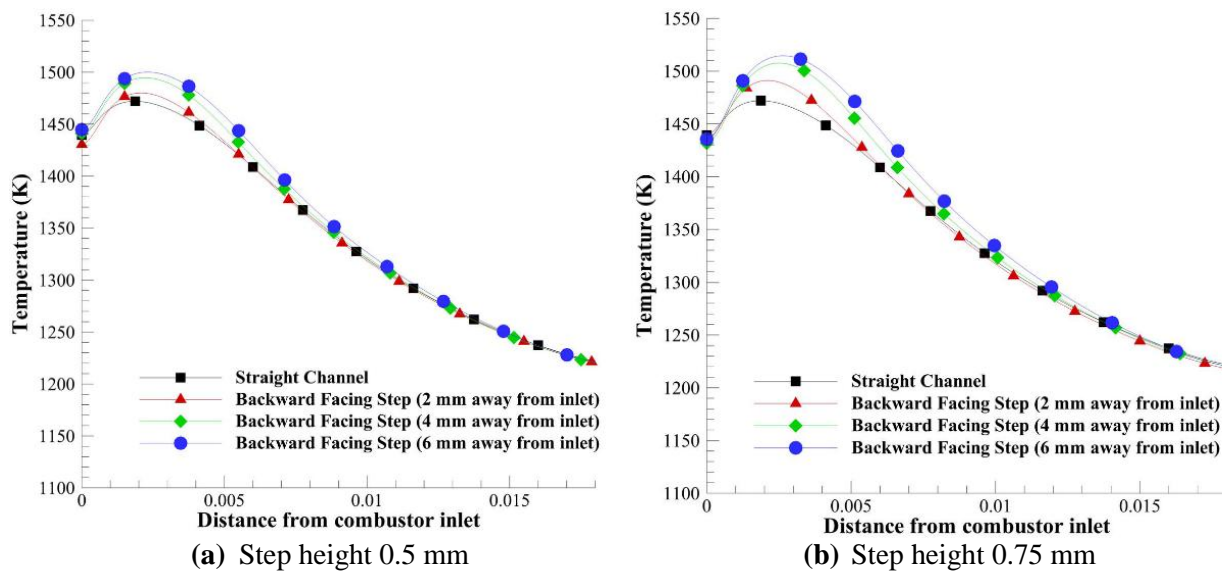


Figure 7. Temperature (K) contours with straight channel and cavity with 2, 4 and 6 mm away from inlet.

In figure 8, temperature profiles at the midline of the combustor outer wall can be seen. Backward facing step arrangement increases peak temperature value at the outer wall of the combustor and improves temperature distribution in a positive manner regarding basic thermo-photovoltaic system requirements. Temperature increment at the outer wall of the combustor rises with increasing step height and moving backward facing step settlement away from combustor inlet. On the other hand, mean temperature value at the outer wall and conversion rate of input chemical energy to utilizable transferred heat significantly change with backward facing step arrangement (Figure 9). This is because of the combined effect of backward facing step and narrowing channel height. As mentioned before, cavity barely alters outer wall temperature distribution.



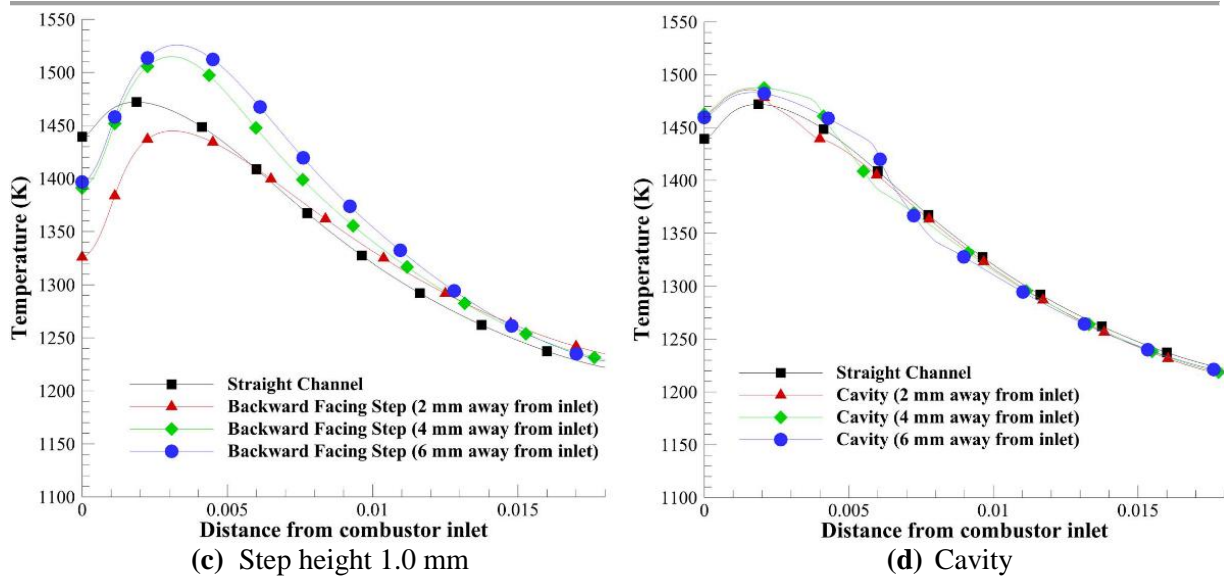


Figure 8. Wall temperature profiles of the combustor.

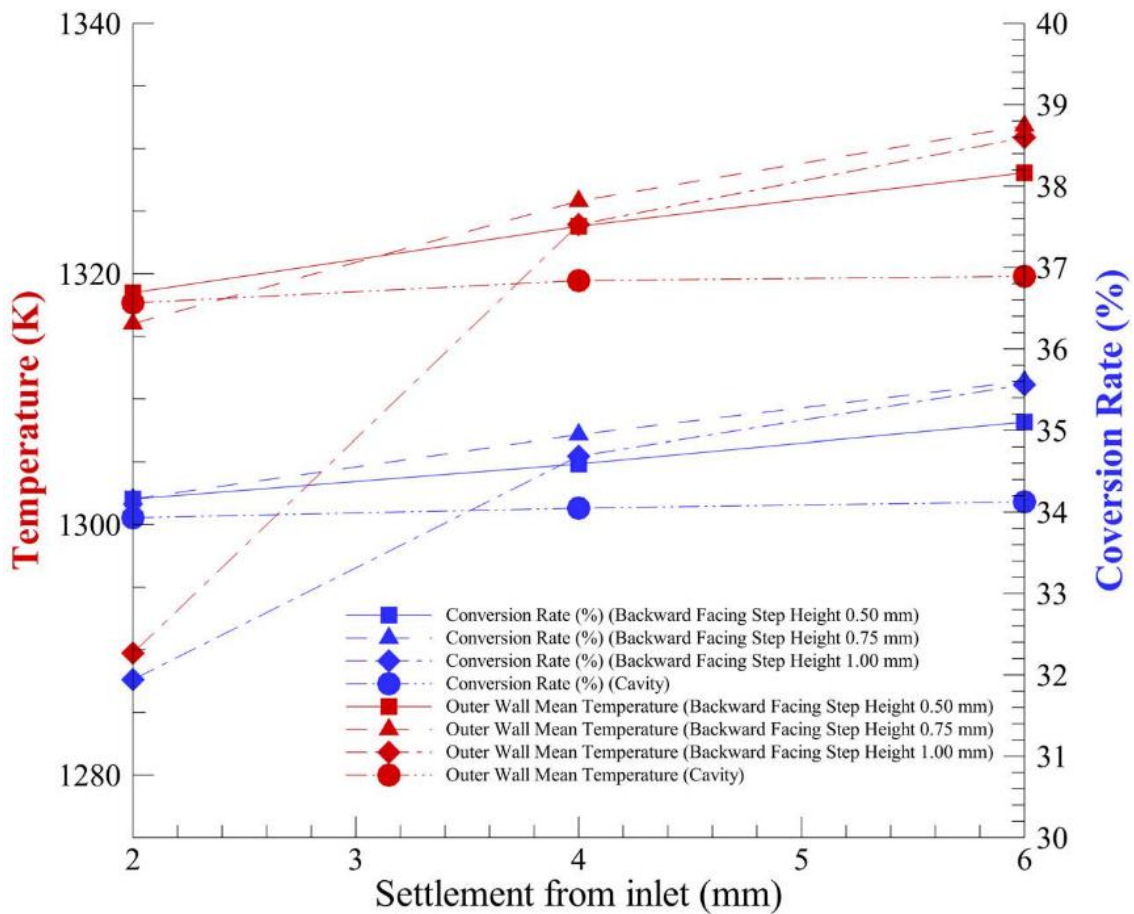


Figure 9. Change of outer wall mean temperature value and conversion rate of input chemical energy to utilizable heat with backward facing step settlement.

In figure 10 and 11, H_2 and H_2O mass fraction profiles along the centerline of the combustor can be seen. Consistent with the centerline temperature profiles, the area where H_2 is consumed and H_2O is formed moves upstream with backward facing step arrangement.

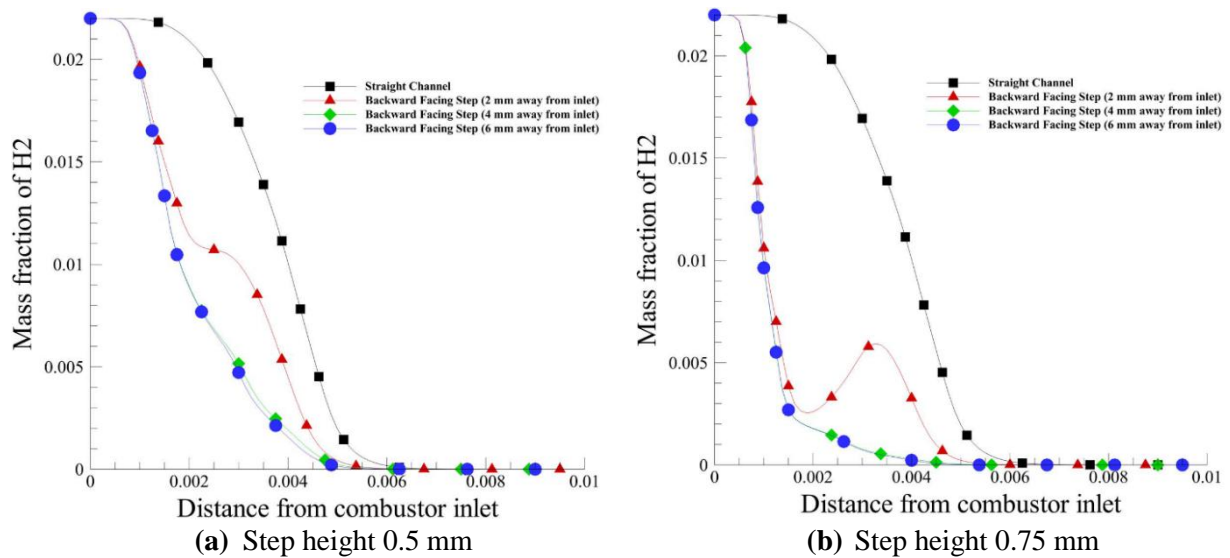


Figure 10. Mass fractions of H_2 .

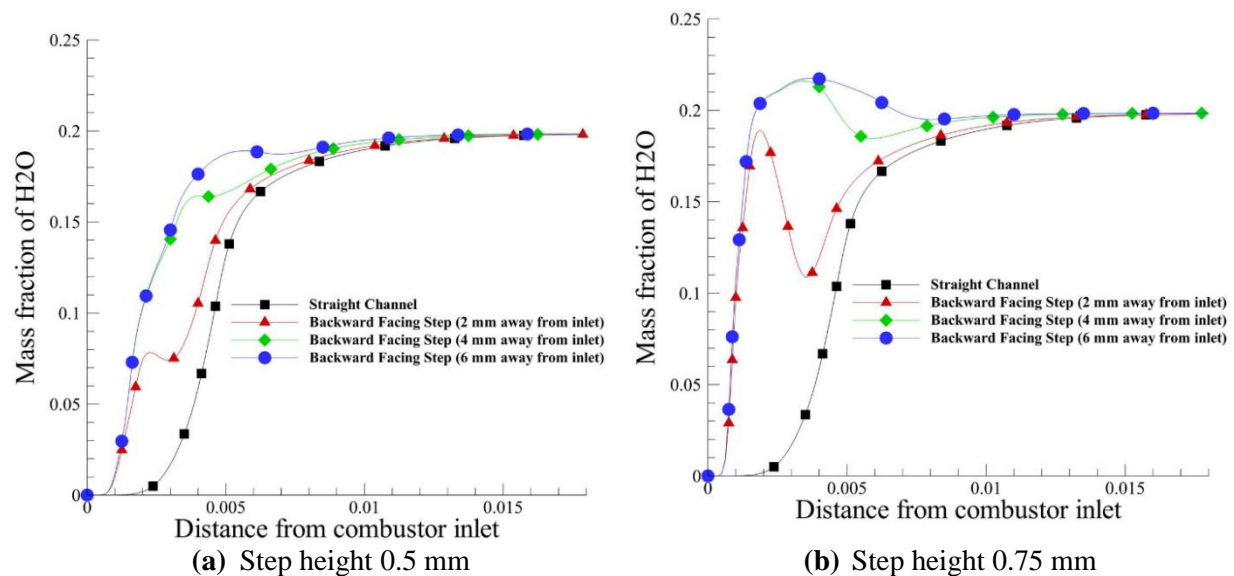


Figure 11. Mass fractions of H_2O .

4. Conclusions

In this study, a micro combustor's geometry is varied by establishing backward facing step (varying step height and distance from combustor inlet) and cavity to be able to achieve high and uniform temperature distribution from the outer wall of the micro combustor to better meet basic TPV requirements. For this purpose, different micro combustor models were constructed and hydrogen/air combustion is simulated in these models under the same boundary conditions. Results obtained from

this numerical study is validated against published experimental data [16] and showed that backward facing step arrangement alters temperature distribution throughout the combustor in an advantageously utilizable manner. This arrangement also increases outer wall mean temperature value and conversion rate of input chemical energy to utilizable heat. On the other hand, cavity slightly increases centerline and outer wall temperature distribution.

5. Acknowledgements

We would like to thank the Scientific and Technological Research Council of Turkey (TÜBİTAK-MAG-215M821) for its financial support.

References

- [1] S.K. Chou, W.M. Yang, K.J. Chua, J. Li, K.L. Zhang, Development of micro power generators—a review, *Applied Energy* 88:1 (2011) 1-16.
- [2] S. Akhtar, J.C. Kurnia, T. Shamim, A three-dimensional computational model of H₂–air premixed combustion in non-circular micro-channels for a thermo-photovoltaic (TPV) application, *Applied Energy* 152 (2015) 47-57.
- [3] Y. Lei, W. Chen, J. Lei, Combustion and direct energy conversion inside a micro-combustor, *Applied Thermal Engineering* 100 (2016) 348-355.
- [4] X. Li, J. Zhang, H. Yang, L. Jiang, X. Wang, D. Zhao, Combustion characteristics of non-premixed methane micro-jet flame in coflow air and thermal interaction between flame and micro tube, *Applied Thermal Engineering* 112 (2017) 296-303.
- [5] E. Miyata, N. Fukushima, Y. Naka, M. Shimura, M. Tanahashi, T. Miyauchi, Direct numerical simulation of micro combustion in a narrow circular channel with a detailed kinetic mechanism, *Proceedings of the Combustion Institute* 35:3 (2015) 3421-3427.
- [6] D. Jiang, W. Yang, K.J. Chua, J. Ouyang, J. Teng, Effects of H₂/CO blend ratio on radiated power of micro combustor/emitter, *Applied Thermal Engineering* 86 (2015) 178-186.
- [7] C.G. Sarath, M. Sreejith, R.V. Reji, Flow Field Predictions of Bluff Body Introduced Micro Combustor, *Procedia Technology* 24 (2016) 420-427.
- [8] J. Zhou, Y. Wang, W. Yang, J. Liu, Z. Wang, K. Cen, Improvement of micro-combustion stability through electrical heating, *Applied Thermal Engineering* 29:11 (2009) 2373-2378.
- [9] S.E. Hosseini, M.A. Wahid, Investigation of bluff-body micro-flameless combustion, *Energy Conversion and Management* 88 (2014) 120-128.
- [10] C. Jimenez, V.N. Kurdyumov, Propagation of symmetric and non-symmetric lean hydrogen–air flames in narrow channels: Influence of heat losses, *Proceedings of the Combustion Institute* (2016).
- [11] J.F. Pan, W.M. Yang, A.K. Tang, S.K. Chou, L. Duan, X.C. Li, Micro combustion in sub-millimeter channels for novel modular thermophotovoltaic power generators, *J. Micromech. Microeng.* 20:125021 (2010).
- [12] R. Fursenko, S. Minaev, K. Maruta, H. Nakamura, H. Yang, Characteristic regimes of premixed gas combustion in high-porosity micro-fibrous porous media, *Combustion Theory and Modelling* 14:4 (2010) 571-581.
- [13] D.G. Norton, D.G. Vlachos, Combustion characteristics and flame stability at the microscale: a CFD study of premixed methane/air mixtures, *Chemical engineering science* 58:21 (2003) 4871-4882.



-
- [14] P. Markatou, L.D. Pfefferle, M.D. Smooke, The influence of surface chemistry on the development of minor species profiles in the premixed boundary layer combustion of an H₂/air mixture, *Combustion science and technology* 79:4-6 (1991) 247-268.
- [15] Fluent Incorporated. ANSYS Fluent Theory Guide, version 15.0, 2013.
- [16] A. Tang, J. Pan, W. Yang, Y. Xu, Z. Hou, Numerical study of premixed hydrogen/air combustion in a micro planar combustor with parallel separating plates, *International Journal of Hydrogen Energy* 40:5 (2015) 2396-2403.

Numerical investigation on combustion behavior of premixed hydrogen/air flames in a micro combustor with varying geometric properties: part - II effect of multi-channel arrangement

^{1*}Harun Yilmaz, ²Omer Cam, ²Selim Tangoz, ²İlker Yilmaz

¹ *Erzincan University, Civil Aviation College, Airframe - Powerplant Department, Erzincan, 24000, Turkey*

² *Erciyes University, Fac. of Aeronautics and Astronautics, Airframe - Powerplant Dept., Kayseri, 38039, Turkey*

* E-mail: hyilmaz@erzincan.edu.tr

Abstract: Fuel efficient micro scale combustion can be achieved by optimizing micro combustor's geometric properties taking simplicity and easy manufacturability into consideration. In this study, effect of multi-channel arrangement on combustion behavior of premixed hydrogen/air flames is numerically investigated. A fabricated and tested micro combustor's geometric properties were revised with adding multi-channels to interior of the combustor. Distance between multi channels (channel gap distance), length of the channel and channel number were chosen as geometric variables. Multi-channel settlement was determined with respect to flame development and flame stability characteristics. All of the combustor models are constructed using ANSYS Design Modeler program and simulation studies are performed via ANSYS Fluent program. Centerline and outer wall temperature profiles, species distribution profiles, heat transfer characteristics and mixing degree of fuel air mixture are considered as investigating combustion behavior. Turbulence model used in this study is RNG (renormalization group) k- ϵ . Multistep combustion reaction scheme with 9 species and 19 steps was simulated using EDC (Eddy Dissipation Concept) model. Results revealed that multi-channel arrangement significantly improves temperature distribution on the outer wall of the combustor by means of value and uniformity. Compared to single channel combustor, outer wall mean temperature value increases with elongating channel length and narrowing channel gap.

Key words: Micro scale combustion, combustor geometry, multi-channel

1. Introduction

Growing demand for miniaturized mechanical and electro-mechanical devices requires a powerful energy source that can substitute conventional batteries which are unable to meet micro device necessities with respect to mass and volume restriction, and energy density. This demand motivated

many researchers to develop micro power sources which have high energy density, low weight and long service life. Mostly studied, developed, fabricated and tested micro power systems are micro gas turbines, micro rotary engines, micro thermoelectric systems and micro fuel cells [1].

Utilization of micro hydrocarbon or hydrogen combustion for electricity production brings in many advantages which are high energy content per unit mass and high energy production per unit volume even with low fuel and energy conversion efficiency [1]. Motivated by this, many researchers investigated micro combustion process both numerically and experimentally to further improve micro power generators in point of energy output of the overall system.

Park et al. developed a micro combustor which is surrounded by a chamber which has photovoltaic cell installation inside, and has a shield over its walls for exhaust gas recirculating and tested it both numerically and experimentally. Wall material of a combustor and the distance between photovoltaic cell arrangement and combustor wall (gap distance) determine the energy output of a thermo photovoltaic system (TPV). They also tried to optimize their system by varying the distance between photovoltaic cells and combustor wall. Results showed that a stable combustion with uniform outer wall temperature distribution can be achieved with heat recirculation, optimum operating conditions are $\phi=1$ (for propane/air mixture) and an inlet velocity of 3.9 m/s for a combustor with 12 mm gap distance [2].

Wenming et al. fabricated three SiC micro cylindrical combustors which have different wall thickness (0.4, 0.6, 0.8 mm). They kept combustor volume constant (0.113 cm^3) and varied hydrogen mass flow rate and hydrogen/air ratio. It is concluded that a decrement in wall thickness increases maximum electricity production, when combustor diameter is set as an invariable; combustor with 0.4 mm wall thickness provides 0.92 W electrical power output at 4.20 g/l hydrogen flux and 0.9 hydrogen/air ratio by sacrificing reliability of the overall system [3].

Sahota et al. investigated premixed CH_4/air flames in a micro combustor with 2 step backward facing to study effect of equivalence ratio and fuel/air mass flow rate on flame stabilization mechanisms by generating swirl (actively or passively) in main flow at the inlet of the combustor. It is shown that introducing swirl into the flow increases flame stability limits via recirculating hot products and reducing velocity, and this increment is the highest when swirl is introduced actively; active swirl generation technique can be used to control flame position and so desired temperature profiles can be gained; flame position is insensitive to equivalence ratio [4].

Wang et al. conducted experimental studies to examine stability limits of hydrogen/air flames in a quartz micro combustor, heat loss of which is controlled by external air at different temperatures (277, 380 and 1001 K). They concluded that when wind temperature is 380 K, stability limits broaden with decreasing heat losses to the environment; further increment in wind temperature (at 1001 K) makes flame more prone to blow off [5].

Su et al. developed a novel micro combustor with 2 cavities and simulated hydrogen/air combustion in this combustor to analyze thermal behavior of the new design. Equivalence ratio and some geometric parameters such as distance between cavities and cavity number (1 or 2) were set as variables. It is inferred that basic TPV requirements (high and uniform temperature distribution at the outer wall of the combustor) can be more effectively meet with new design; increasing outer wall temperature

improves radiant efficiency and the quality (in point of utility) of radiate photons; optimum distance between two cavities depends on inlet velocity [6].

Khandelwal and Kumar carried out experimental studies to investigate flame stabilization characteristics of premixed CH₄/air mixtures in a diverging channel by examining effect of equivalence ratio and mixture inlet velocity on flame anchoring position, flame shape, flame stability limits and exhaust gas emissions. They also used a burner to preheat divergent part of the channel to achieve positive temperature gradient in stream wise direction which is utilized for flame stabilization and concluded that inlet velocity and equivalence ratio alters flame propagation mode, rich flames are more resistant to flame instabilities compared to lean ones, flame front fluctuations causes incomplete burning and increases CO emissions [7].

Wan et al. numerically analyzed effect of combustor wall material thermal conductivity on combustion efficiency of lean hydrogen/air flames in a micro combustor with cavity. Results showed thermal conductivity has a non-monotonic effect on combustion efficiency; when thermal conductivity is the highest of the values tested, temperature distribution near inlet section of the combustor is also the highest which provides better preheating of the reactants thus flow velocity at the cavity exit increases and flame splitting limit reduces. Lastly, moderate values of wall thermal conductivity is found to be favorable for micro combustor with a cavity [8].

To investigate effect of equivalence ratio, inlet velocity and size of the combustor on combustion behavior of premixed CH₄/air mixtures, Feng et al. performed simulation studies in a micro combustor model with temperature gradient at outer wall of. They reported that inlet velocity significantly shifts reaction zone distribution but it slightly affects flame temperature. Size of the combustor has a great effect on combustion behavior of studied methane/air flames. When combustor size is small, it is hard to sustain combustion. But results revealed that with steady combustion can be sustained in a smaller size combustor by controlling outer wall temperature distribution [9].

Micro combustor is a vital component of a TPV system. High and uniform temperature distribution at the outer wall of the combustor is desirable for high energy output. Zuo et al. developed a micro cylindrical combustor with gradually reduced wall thickness in stream wise direction and modeled hydrogen/air combustion. They also numerically tested a micro combustor with a step under different conditions and compared both kinds. Numerical results showed that combustor with gradually reduced wall thickness performs better with respect to uniformity and value of outer wall temperature distribution in all equivalence ratios, hydrogen flow rates and inlet/outlet diameter ratios tested compared to combustor with a step; performance increment of the new design depends on combustor material [10].

In this study, premixed hydrogen air combustion is simulated in an experimentally tested micro combustor by introducing varying number and length of multi channels into the flow area, and keeping channel wall thickness constant to better meet basic TPV requirements which are high and uniform temperature distribution at the outer wall of the combustor.

2. Numerical Setup

2.1. Combustor Geometry

In this study, 3D micro combustor models were constructed using ANSYS/Design Modeler program and in these models, multistep hydrogen/air combustion was simulated using ANSYS/Fluent program. The combustor model has 18 mm length, 3 mm height, 9 mm width and 0.5 mm wall thickness as shown in Figure 1. Based on this model, micro combustor geometry was modified.

Combustor model with multichannel can be seen in Figure 2. Taking flame length into consideration, leading edge of the micro channels are set as 4 and 8 mm away from the combustor inlet. Number of multi-channels (4, 6, 8, 10) and channel gap distance is varied (0.44, 0.65, 1.0 and 1.70 mm). On the other hand channel wall thickness is kept constant (0.4 mm).

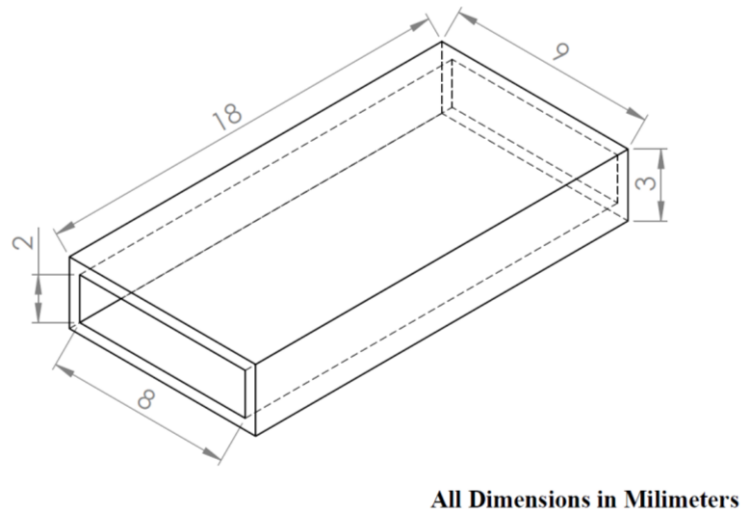


Figure 1. The physical domain of the combustor with straight channel.

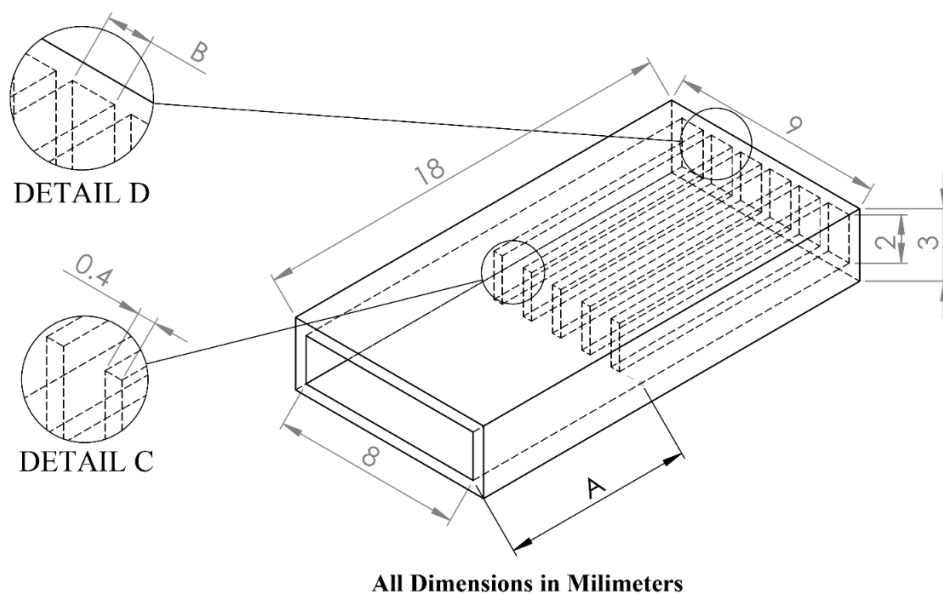


Figure 2. The physical domain of the combustor with multichannel.

2.2 Mathematical Model

Steady state forms of the basic governing equations are solved and these equations are:

Continuity;

$$\frac{\partial(\rho u_j)}{\partial x_j} = 0$$

ρ , density; u_j , velocity component.

Momentum;

$$\frac{\partial \rho u_j u_i}{\partial x_j} = -\frac{\partial P}{\partial x_i} + \frac{\partial \tau_{ij}}{\partial x_j}$$

P , pressure; τ_{ij} , stress tensor.

Energy;

$$\frac{\partial(\rho u_j h)}{\partial x_j} = \frac{\partial}{\partial x_j} \left(k \frac{\partial T}{\partial x_j} - \sum_{i=1}^N h_i j_{ij} \right) + u_j \frac{\partial P}{\partial x_j} + S_h$$

h , enthalpy; k , thermal conductivity; T , temperature; S_h , fluid enthalpy source; j_{ij} , diffusion flux.

Species;

$$\frac{\partial(\rho u_j Y_i)}{\partial x_j} = -\frac{\partial J_{ij}}{\partial x_j} + R_i$$

Y_i , mass fraction of species i ; R_i , net production rate of species i via chemical reactions. All of the governing equations are discretized by a second order upwind scheme using finite volume and under relaxation method.

Assumptions for the simulations are (1) no work is done by pressure and viscous forces (2) no surface reaction (3) no gas radiation (4) no energy flux due to mass concentration gradients (5) no slip boundary condition at the combustor wall [11-13]. Multi step hydrogen air combustion (9 species and 19 steps) was modeled using EDC (Eddy Dissipation Concept) combustion model. As turbulence model RNG k- ϵ is chosen. Reaction scheme of hydrogen/air combustion and turbulence model can be found in Ref. [14-15], respectively.

2.3. Boundary Conditions

Hydrogen flux into the combustor set as 1200 ml/min and depending on the equivalence ratio (0.8) total hydrogen/air mass flow rate and mass fraction of reactant species are specified. So for the combustor inlet, mass flow inlet and for the outlet, pressure outlet boundary conditions are chosen, and for both hydraulic diameter (depending on the geometric variations) and turbulent intensity are

identified. For combustor wall, mixed thermal condition is chosen to consider radiation and convective heat transfer. Convergence criteria is set as 10^{-6} .

2.4. Mesh Independency Study

To reduce computational time and effort, a mesh independency study is carried out. Five different mesh structures which include different number of elements (31104, 90640, 248832 and 486000 elements) are constructed and predicted centerline temperature profiles of these models are compared. It can be seen that centerline temperature profile of the mesh structure with 248832 elements is very similar to that of the 486000 element. So, mesh structure with 248832 elements is chosen. In this study, effect of combustor geometry on combustion performance is examined as mentioned before. Mesh structure of these models are arranged to have same mesh density to correctly analyze effect of geometry.

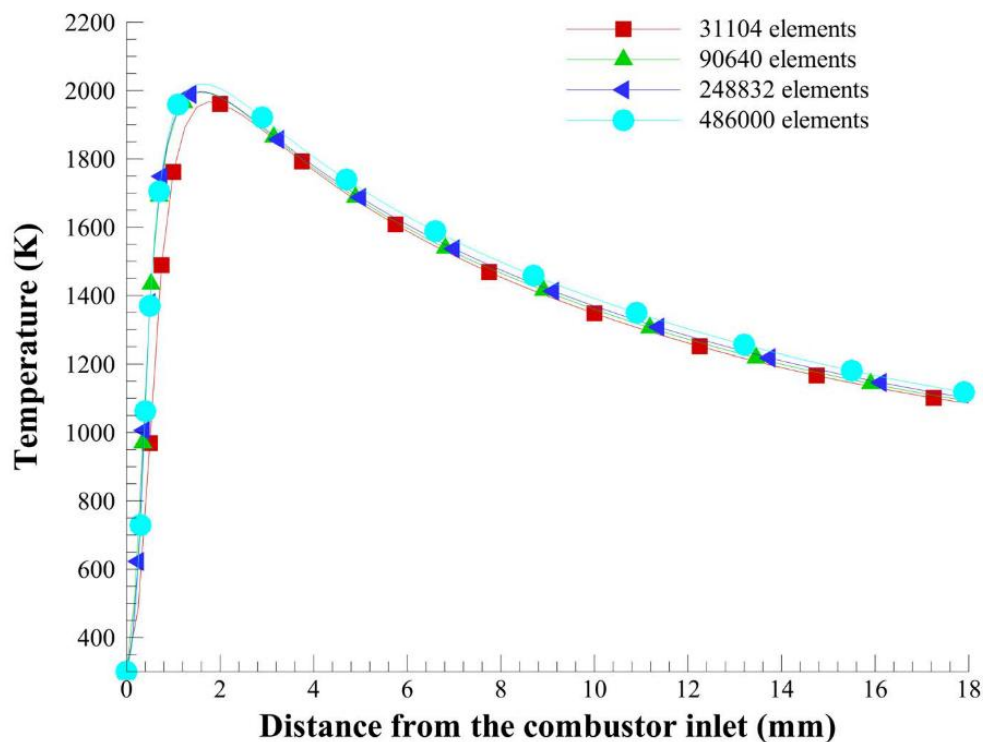


Figure 3. Mesh independency study.

2.5. Model Validation

Predicted outer wall temperature profiles are compared with the numerical and experimental results of Ref. [16] to validate availability of our model. This comparison can be seen in Figure 4. Predicted results showed a good agreement with published data. Discrepancies between numerical and experimental results are attributed to be rooted from assumptions for numerical simulations, limitations of experimental apparatus and size limitation of micro devices.

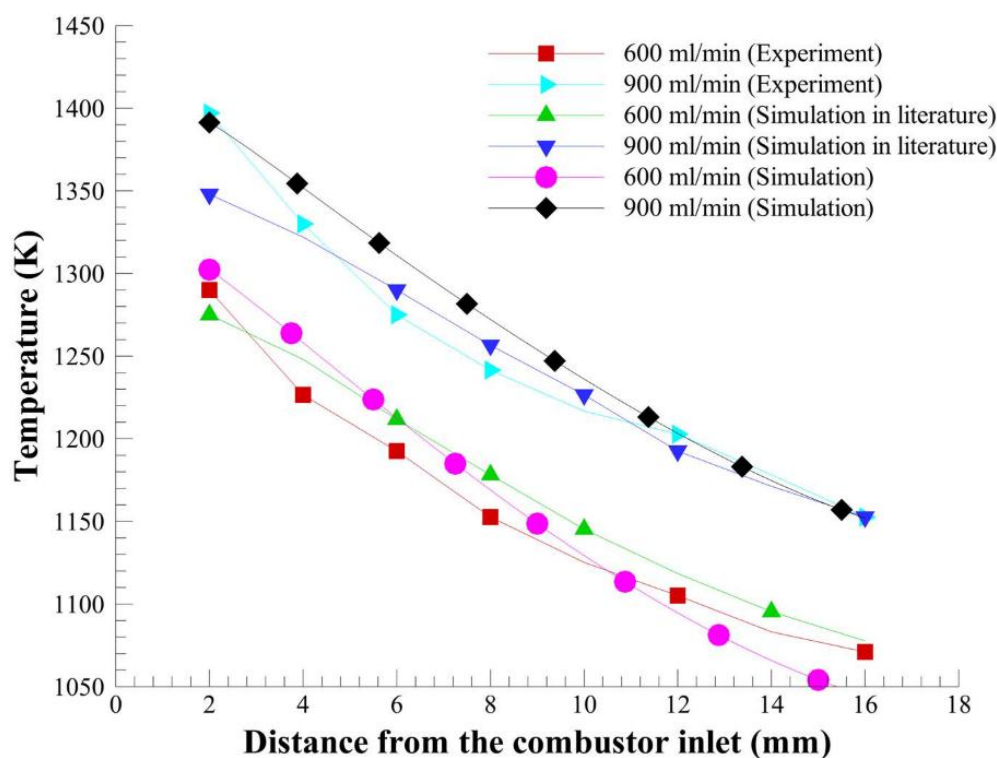


Figure 4. Validation of numerical model [Tang et al., 2015]

3. Results and Discussions

Micro power devices consist of three parts; a heat source, an emitter (combustor wall) and a photovoltaic cell. For GaSb cells, photons which has more than 1.7 μm wavelength cannot be exploited for electricity production and wasted. An increment in outer wall temperature improves emissive power and spectral distribution of photons [17]. In this study a micro combustor geometry is varied by adding varying number and length of multi-channels into the flow area to be able to achieve high and uniform energy output from outer wall of the combustor. Because, multi-channel arrangement is reported to provide better contact with hot combustion products and channel walls [16].

In figure 5, centerline temperature profiles of combustors with multi-channels and straight channel (2 mm channel height) can be seen. Because channel height and width do not change until multi-channel arrangement, temperature profiles of the all combustor models are the same until leading edge of the channel wall. Starting from multi-channel settlement, temperature profiles differ. Combustion products of the combustors with multi-channels exhaust at lower temperature than that of the straight channel combustor. This temperature decrement becomes more obvious with narrowing channel gap and can clearly be seen from temperature profiles of the combustors with 10 mm channel length. In straight channel combustor, chemical reactions take place in a small area near combustor inlet. With multi-channel arrangement, increasing flow speed moves reaction zone downstream and so combustion is completed in channels of the combustors with 14 mm channel length and this is why temperature decrement is indistinct for this combustor. Multi-channel arrangement also improves uniformity of temperature distribution throughout the combustor (Figure 6).

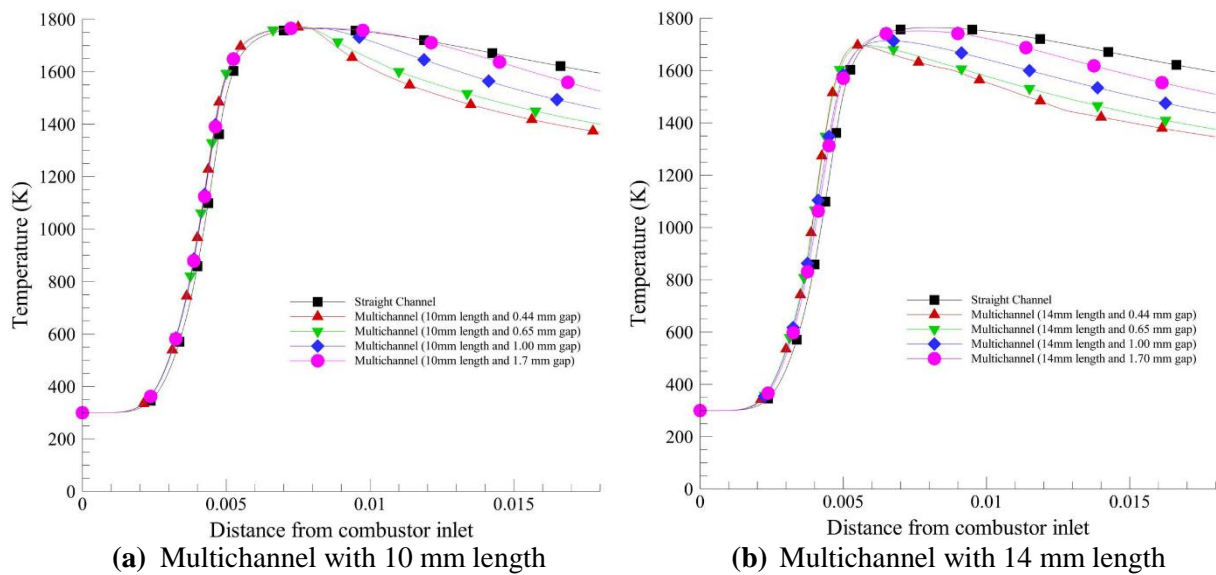


Figure 5. Centerline temperature profiles of the combustor.

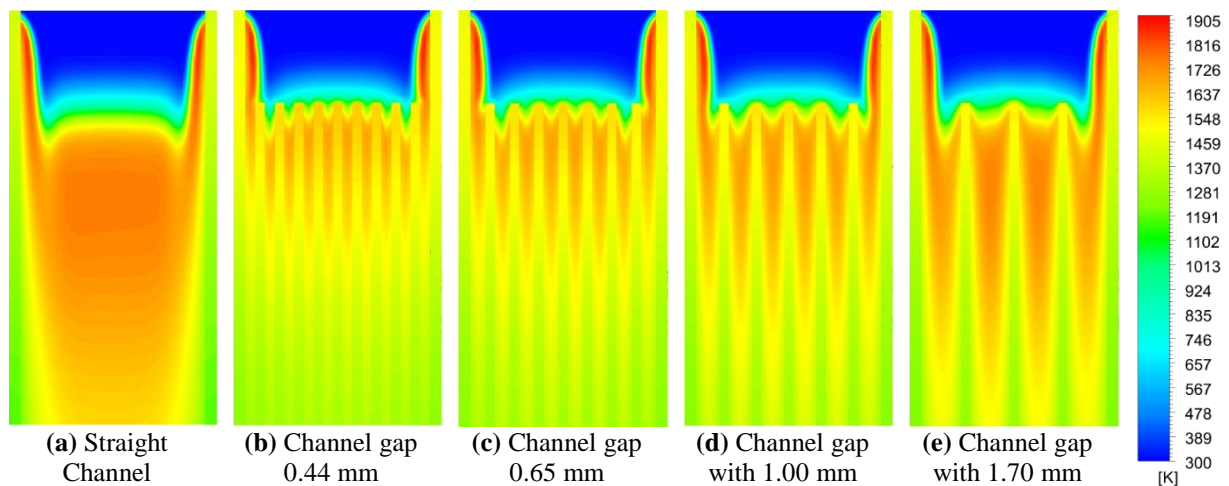


Figure 6. Temperature (K) contours with straight channel and multichannel with 14 mm length.

Multi-channel arrangement significantly improves temperature distribution on the outer wall of the combustor by means of value and uniformity. Compared to single channel combustor, outer wall mean temperature value increases with increasing channel length and narrowing channel gap. Combustor with 14 mm channel length and 0.44 mm channel gap has formed highest temperature distribution at the outer wall. This can clearly be seen from outer wall temperature contours (Figure 8), the area of hot temperature zone broadens with multi-channel arrangement and is the largest for the combustor with 14 mm channel length and 0.44 mm gap distance.

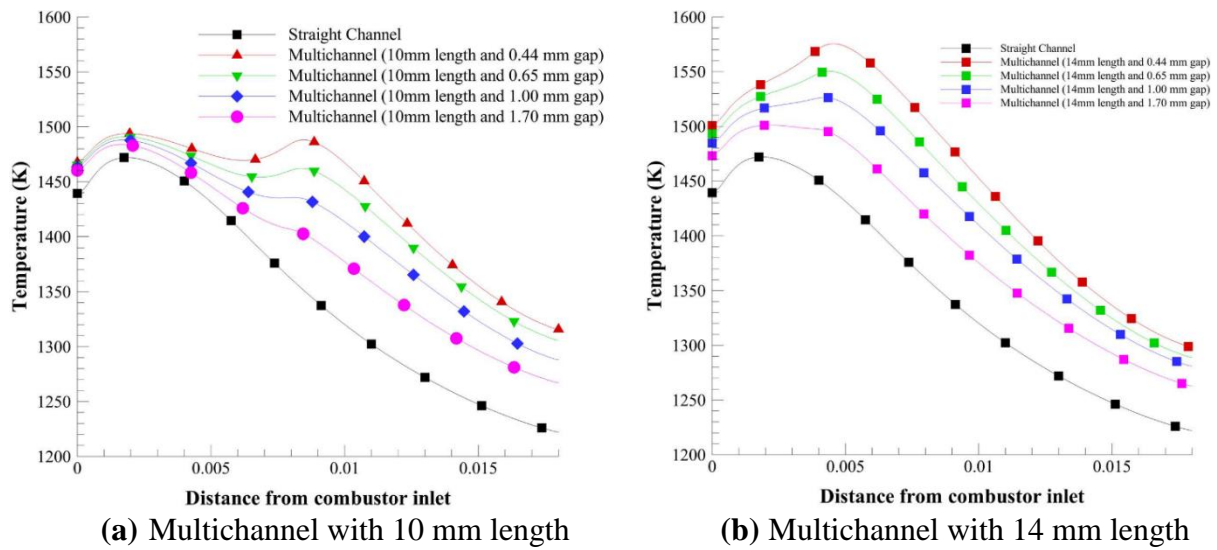


Figure 7. Wall temperature profiles of the combustor.

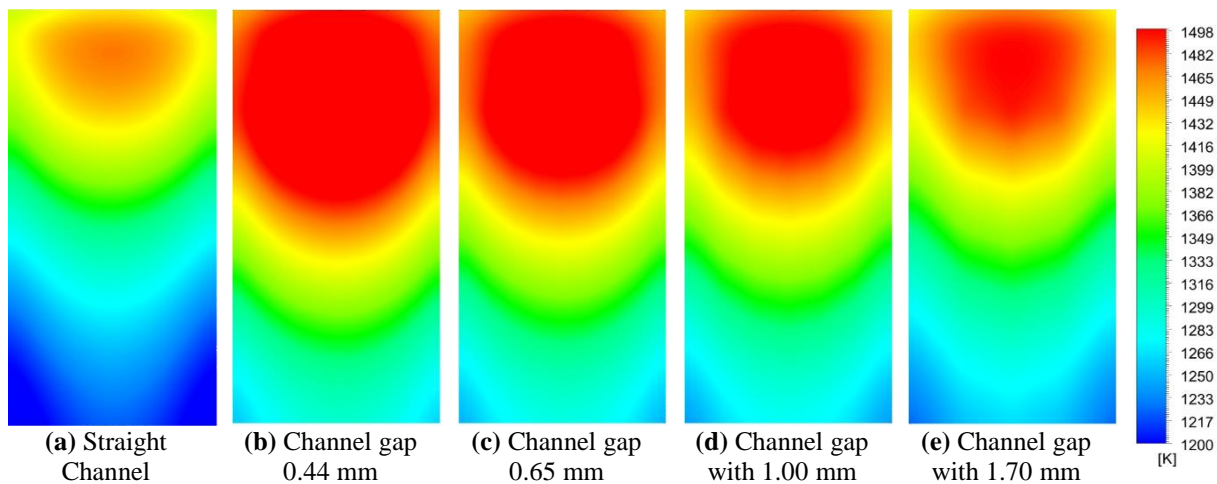
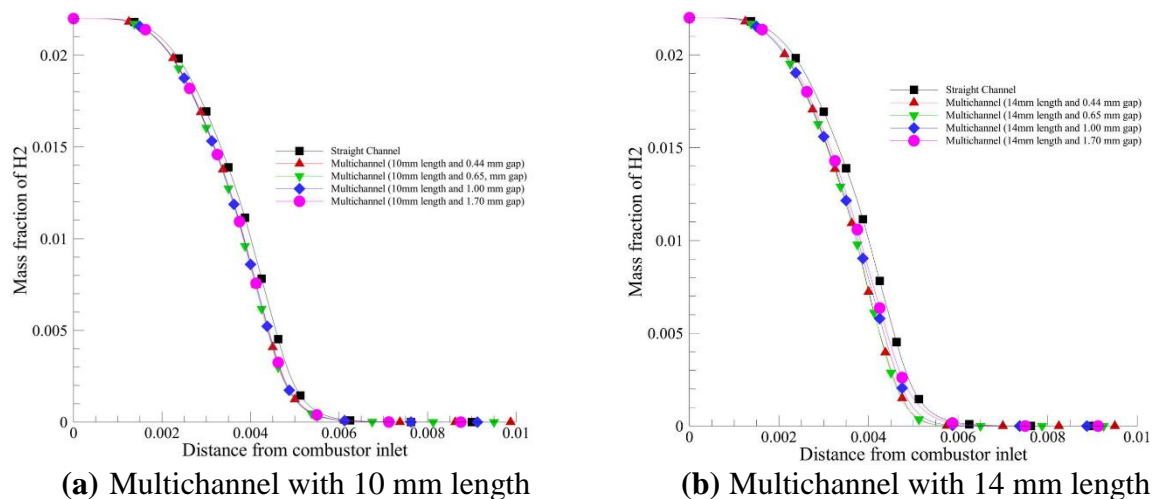
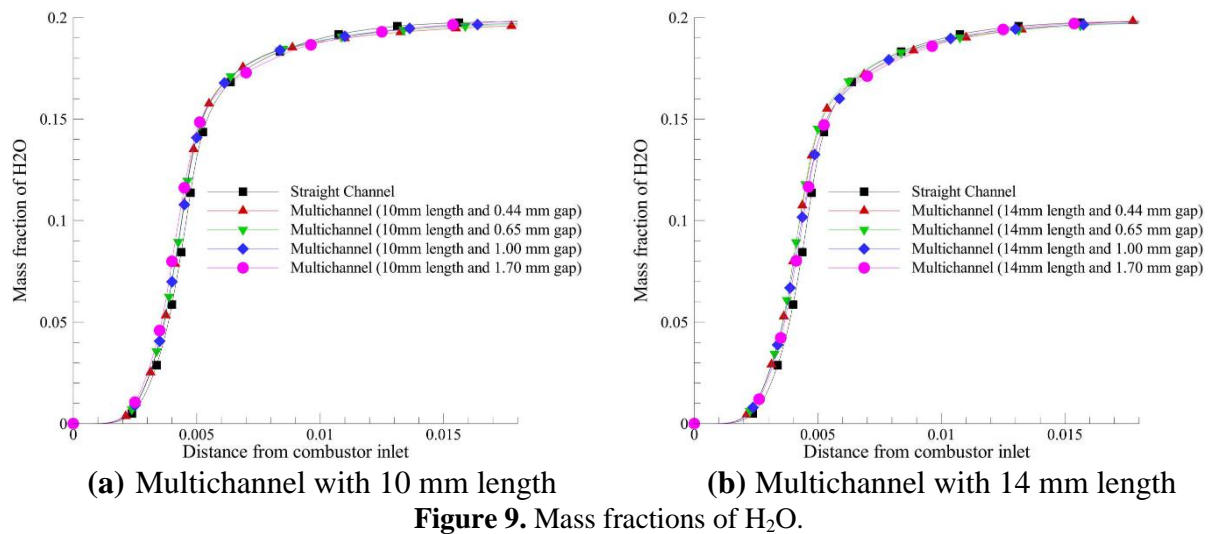


Figure 8. Wall temperature (K) contours with straight channel and multichannel with 14 mm length.

In figure 9 and 10, H_2 and H_2O mass fraction contours can be seen. H_2 mass fraction decreases sharply at a zone near inlet and H_2O mass fraction increases sharply at the same zone. H_2 consumption and H_2O formation trends are nearly the same for all combustor models tested implying that multi-channel arrangement doesn't alter reaction kinetics. But it alters heat transfer characteristics and so temperature distribution.



4. Conclusions

In this study, a micro combustor's geometry is modified by adding multi channels into the flow area. Multi-channel length and channel gap distance are set as variable parameters and different combustor models are constructed. Hydrogen/air combustion is simulated in these model with same boundary conditions. Numerical results are validated with data obtained from Ref. [16]. Results showed that multi-channel arrangement slightly alters temperature distribution throughout the combustor and peak temperature value but it significantly increases outer wall mean temperature value and improves uniformity of temperature distribution at the outer wall of the combustor. This arrangement also causes exhaust gas temperature to reduce.

5. Acknowledgements

We would like to thank the Scientific and Technological Research Council of Turkey (TÜBİTAK-MAG-215M821) for its financial support.

References

- [1] L.C. Chia, B. Feng, The development of a micropower (micro-thermophotovoltaic) device, *Journal of Power Sources* 165:1 (2007) 455-480.
- [2] J.H. Park, J.S. So, H.J. Moon, O.C. Kwon, Measured and predicted performance of a micro-thermophotovoltaic device with a heat-recirculating micro-emitter, *International Journal of Heat and Mass Transfer* 54:5 (2011) 1046-1054.
- [3] Y. Wenming, C. Siawkiang, S. Chang, X. Hong, L. Zhiwang, Effect of wall thickness of micro-combustor on the performance of micro-thermophotovoltaic power generators, *Sensors and Actuators A: Physical* 119:2 (2005) 441-445.
- [4] G.P.S. Sahota, B. Khandelwal, S. Kumar, Experimental investigations on a new active swirl based microcombustor for an integrated micro-reformer system, *Energy Conversion and Management* 52:10 (2011) 3206-3213.
- [5] Y. Wang, Z. Zhou, W. Yang, J. Zhou, J. Liu, Z. Wang, K. Cen, Instability of flame in micro-combustor under different external thermal environment, *Experimental Thermal and Fluid Science* 35:7 (2011) 1451-1457.
- [6] Y. Su, J. Song, J. Chai, Q. Cheng, Z. Luo, C. Lou, P. Fu, Numerical investigation of a novel micro combustor with double-cavity for micro-thermophotovoltaic system, *Energy Conversion and Management* 106 (2015) 173-180.
- [7] B. Khandelwal, S. Kumar, Experimental investigations on flame stabilization behavior in a diverging micro channel with premixed methane–air mixtures, *Applied Thermal Engineering* 30:17 (2010) 2718-2723.
- [8] J. Wan, A. Fan, H. Yao, W. Liu, Effect of thermal conductivity of solid wall on combustion efficiency of a micro-combustor with cavities, *Energy Conversion and Management* 96 (2015) 605-612.
- [9] L. Feng, Z. Liu, Y. Li, Numerical study of methane and air combustion inside a small tube with an axial temperature gradient at the wall, *Applied Thermal Engineering*, 30:17 (2010) 2804-2807.
- [10] W. Zuo, E. Jiaqiang, Q. Peng, X. Zhao, Z. Zhang, Numerical investigations on thermal performance of a micro-cylindrical combustor with gradually reduced wall thickness, *Applied Thermal Engineering* 113 (2017) 1011-1020.
- [11] R. Fursenko, S. Minaev, K. Maruta, H. Nakamura, H. Yang, Characteristic regimes of premixed gas combustion in high-porosity micro-fibrous porous media, *Combustion Theory and Modelling* 14:4 (2010) 571-581.
- [12] D.G. Norton, D.G. Vlachos, Combustion characteristics and flame stability at the microscale: a CFD study of premixed methane/air mixtures, *Chemical engineering science* 58:21 (2003) 4871-4882.
- [13] J.F. Pan, W.M. Yang, A.K. Tang, S.K. Chou, L. Duan, X.C. Li, Micro combustion in sub-millimeter channels for novel modular thermophotovoltaic power generators, *J. Micromech. Microeng.* 20:125021 (2010).
- [14] P. Markatou, L.D. Pfefferle, M.D. Smooke, The influence of surface chemistry on the development of minor species profiles in the premixed boundary layer combustion of an H₂/air mixture, *Combustion science and technology* 79:4-6 (1991) 247-268.
- [15] Fluent Incorporated. ANSYS Fluent Theory Guide, version 15.0, (2013).

- [16] A. Tang, J. Pan, W. Yang, Y. Xu, Z. Hou, Numerical study of premixed hydrogen/air combustion in a micro planar combustor with parallel separating plates, *International Journal of Hydrogen Energy* 40:5 (2015) 2396-2403.
- [17] W.M. Yang, S.K. Chou, C. Shu, Z.W. Li, H. Xue, Combustion in micro-cylindrical combustors with and without a backward facing step, *Applied Thermal Engineering* 22:16 (2002) 1777-1787.

Experimental Analysis of Turbulent Premixed Coal Gas Combustion

Serhat KARYEYEN¹, Mustafa İLBAŞ^{1,*}

¹Gazi University, Technology Faculty, Department of Energy Systems Engineering,
Teknikokullar

ilbas@gazi.edu.tr

Abstract: This study describes experimental studies of low-calorific value coal gas combustion under turbulent premixed combustion conditions. Any conventional natural gas burner is not convenient to burn a low calorific value coal gas efficiently and properly. Therefore, a newly generated premixed burner that can properly burn low calorific value coal gases has been designed and manufactured. This burner has also got a hydrogen pipe from which the hydrogen is supplied into the flame zone in order to enhance the flame temperatures of the low-calorific value coal gases. The flame of the blast-furnace gas was not observed without hydrogen supply due to absence of the enough combustible gases excluding CO during the experiments. However, the flame temperature of the generator gas was measured as of 947.1°C without hydrogen supply. It has been concluded that the flame temperatures of the low calorific value coal gases were enhanced as the hydrogen was supplied from the center of the newly generated burner to the flame zone. In addition to the temperature measurements, emissions such as NOX, CO and CO₂ were also examined by a flue gas analyzer in the combustor. The results show that the NOX emission levels increase as the hydrogen is supplied into the flame region because of thermal NOX mechanism. It has been also demonstrated that CO₂ levels ascend due to hydrogen addition. It can be eventually concluded that the new burner provides more stable flame and the hydrogen addition improves the combustion performances of the low calorific value coal gases under premixed combustion conditions.

Keywords: Coal gas, syngas, hydrogen, premixed combustion

1. Introduction

Combustion is one of the most common methods used in generating heat and electricity. Fossil fuels that are classified as solid, liquid and gas are normally consumed in combustion processes. However, the scientists estimate that fossil fuels run out of in the near future. It is especially said that crude oil and natural gas reserves are less than that of coal. On the contrary, coal reserves are abundant. In addition, their reserves are positioned comparatively evenly all over the World. Therefore, use of coal in heat and electricity production is getting more and more promising.

Coal gases are fundamentally derived from coal in gasification or carbonization processes and classified as low, medium and high calorific values. Low calorific value coal gases are mostly called as generator and blast-furnace gases. Air is directly blown over the coal in a gasification reactor resulting in the production of the generator gas which is composed chiefly of high amounts of nitrogen and carbon monoxide [1]. The blast-furnace gas, which consists mainly of nitrogen and carbon dioxide, is a by-product of blast furnaces when the iron ore is reduced with coke to metallic iron [2].

Premixed combustion is a promising combustion condition as fuel and oxidizer are mixed better in burner before entering to the combustor. There are many studies related to premixed combustion in

the literature. Bidi et al. [3], for instance, have modelled methane-air combustion considering radiation effect under premixed conditions in a cylindrical Chamber. The results show that the numerical simulation results with radiation model are in better agreement with the measurements under premixed combustion conditions. Schefer et al. [4] have studied combustion of hydrogen-enriched methane experimentally and numerically under lean premixed conditions. They have determined that hydrogen addition leads to a considerable effect on the flame structure. Singh et al. also [5] performed an experimental and numerical studies to determine laminar flame speeds of syngases at elevated temperature under premixed combustion conditions. In addition, they investigated the effect of water addition on their laminar flame speeds. They have concluded that flame speed ascends with up to 20 % H₂O addition and then descends with any further water addition. Daniele et al. [6] have conducted an experimental study to ascertain turbulent flame speeds of different syngases under premixed combustion conditions. It has been shown that S_T/S_L depends on preferential diffusive thermal effects considerably. It has also been demonstrated that S_T/S_L ratio increases as hydrogen content in the fuel mixture is increased. Halter et al. [7] investigated the effects of hydrogen addition into methane under premixed combustion conditions. They have concluded that not only instantaneous but also average flame characteristics are highly effected as a small amount of hydrogen is added into methane. Williams et al. [8] completed an investigation regarding effect of syngas composition in a optically accessible premixed swirl-stabilized combustor. They also scrutinized CO₂-diluted oxygen on performance of syngas. They have observed that the presence of hydrogen in the syngas mixture leads to more compact flame of which temperature increases.

Although there are several studies regarding syngas combustion under premixed conditions as it has been mentioned above, studies related to syngas combustion are limited. In particular, There is still not enough experimental studies related to low calorific value coal gases under premixed combustion conditions. Moreover, to supply hydrogen into a low calorific value coal gas flame is making very attractive. Therefore, a newly generated burner has been designed and manufactured to burn low calorific value coal gases and to supply hydrogen from the center of the burner into the flame region individually under premixed combustion conditions.

2. Experimental System

A new type of premixed flame burner has been designed and manufactured so as to determine combustion characteristics of low calorific value coal gases. The premixed burner was integrated to the existing combustion system [1]. This burner' sections have been designed and manufactured considering the densities and heating values of low calorific value coal gases. The generated new type of premixed burner is clearly illustrated in Fig. 1. This burner is a premixed flame burner where low calorific value coal gases and air are fully mixed before ignition. There are two different types of inlets to the combustor in the burner. The burner has 8 first type of inlets from which fuel-air mixture comes to flame region. The other type of inlet has been located on the burner to supply hydrogen to flame zone so that the combustion performances of the low calorific value coal gases enhance in the combustor.

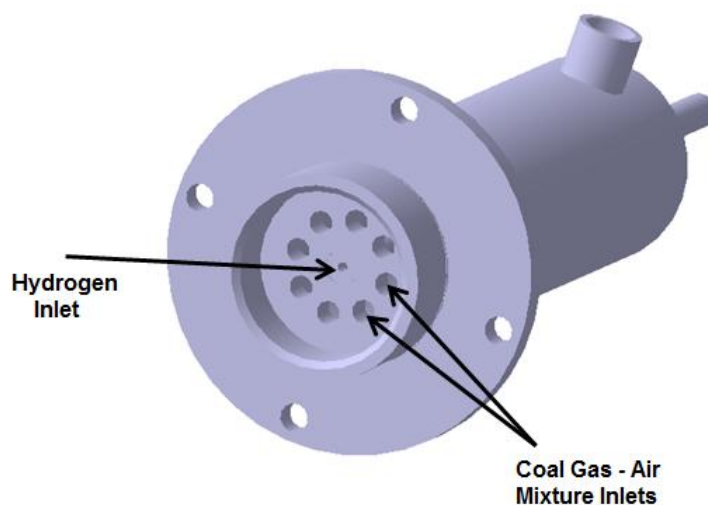


Figure 1. The new type of premixed burner

The schematic layout of the existing combustion system combined with the new premixed burner is illustrated in Fig. 2. The new type of burner has been mounted to the combustion chamber with a flange connection from the bottom of the combustion chamber. High pressure fuel cylinders, which were prepared in desired percentages as indicated in Table 1, have been integrated in order to supply the low calorific value coal gases to the system. This system is also composed of three gas lines including the low calorific value coal gas line, airline and hydrogen line. These lines consist of regulators, manometers, solenoid valves and float type flowmeters. The regulators have been placed on the system to regulate gas, air and hydrogen pressures. Gas, air and hydrogen pressures have also been periodically tracked in the lines by means of the manometers in order to control gas and air pressures during experiments. Solenoid valves have been integrated into the system to prevent gas flows when the flame at the burner front is absent. There is an air compressor so as to supply pressurized air in this system. Furthermore, the combustion system incorporates float type flowmeters in all lines in order to achieve the desired gas, air and hydrogen flow rates. Finally, it has also been equipped with a pilot ignition device (LPG: auxiliary fuel) and line to initiate first ignition in case the low calorific value coal gases may not be auto-ignited due to their low calorific values (in particular blast furnace gas).

A photograph of the combustion chamber is shown in Fig. 3. The length and diameter of the combustion chamber are fixed at 100 cm and 40 cm, respectively. The combustion chamber consists of a sight glass made of tempered glass, six measuring ports and a flue. Five measuring ports, by which temperature and emission values are determined during the experiments, are placed on the combustor wall. The other measuring port is also located on the flue in order to determine the flue gas temperature and emissions. The first measuring port that is positioned 10 cm away from the combustor inlet has been designed to determine the flame characteristics of low calorific value coal gases. Other four measuring ports are placed at intervals of 20 cm from the first measuring port to the combustion chamber outlet.

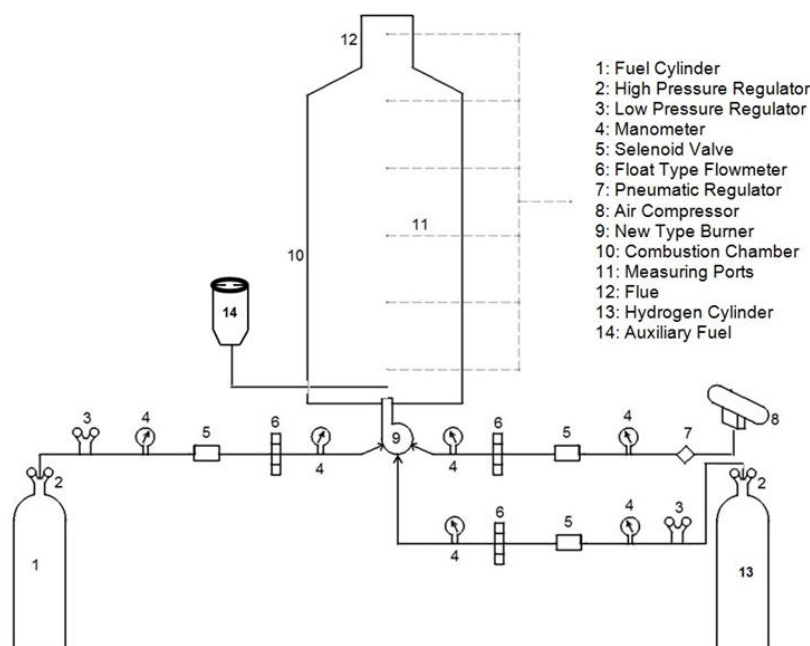


Figure 2. Layout of combustion system



Figure 3. Combustion chamber

Ceramic coated R-type thermocouples capable of withstanding high temperatures up to 1700°C were used to measure temperature values throughout the combustion chamber. The diameters of these thermocouples are 5 mm. These thermocouples have been fixed with threaded connections to the combustor wall with a thickness of 4 mm. Emission values have also been measured on the axial and radial distances and from the flue by a flue gas analyzer during the experiments.

Table 1 shows the main properties of low calorific value coal gases in volumetric basis. The low calorific value coal gases have high amounts of nitrogen as well as some carbon monoxide and hydrogen as combustible components, shown in Table 1. Table 1 also gives the properties of

hydrogen which has a high amount of energy compared to other conventional fuels as used in the present study.

Table 1. Low calorific value coal gases [1]

	<i>H₂</i> (%)	<i>CH₄</i> (%)	<i>CO</i> (%)	<i>CO₂</i> (%)	<i>N₂</i> (%)	<i>LHV</i> (kcal/m ³)	<i>Density</i> (kg/m ³)
<i>Generator Gas</i>	12	0,5	28	5	54,5	1124	1,070
<i>Blast-Furnace Gas</i>	2	-	30	8	60	900	1,200
<i>Hydrogen</i>	100	-	-	-	-	2422	0,084

3. Operating Conditions

All experiments were performed under thermal power of 10 kW and an equivalence ratio of $\phi = 0.83$ taking into account on the heating values of the low calorific value coal gases and the amount of supplied hydrogen. When the hydrogen was supplied to the flame region during experiments, amounts of the low calorific value coal supplied were decreased to maintain a thermal power of 10 kW considering the amount of supplied hydrogen. There were three different experiment conditions for each low calorific value coal gases. First, these fuels were solely used in order to provide a thermal power of 10 kW. Then, a part of the thermal power of 10 kW (2.5 kW and 5 kW) was provided from hydrogen during the experiments. For example, GGH1 (7.5 kW from the generator gas and 2.5 kW from the hydrogen), GGH2 (5 kW from the generator gas and 5 kW from the hydrogen), BFGH1 (7.5 kW from the blast-furnace gas and 2.5 kW from the hydrogen) and BFGH2 (5 kW from the blast furnace gas and 5 kW from the hydrogen) represent the combustion results of the generator and blast furnace gases with hydrogen as well as the GG and BFG mean combustion results of the generator and blast-furnace gases without hydrogen in next figures. However, the blast-furnace gas could not be ignited without hydrogen supply under premixed combustion conditions during the experiments because of its very low calorific value. In addition, combustion were performed under atmospheric pressures.

4. Results and Discussions

The combustion performances and emission characteristics of the low calorific value coal gases have been experimentally investigated under premixed combustion conditions in the present study. In addition, the hydrogen has been supplied from the center of the newly generated burner to the flame zone in order to enhance the combustion performances of the coal gases because of their low calorific value. Any problem such as flashback, flame lift off or blow-off were not observed during the experiments. There was no need auxiliary fuel (LPG) during the experiments. BFG could not be ignited without hydrogen as it has high amount of nitrogen and few amount of combustible components. The flames of coal gases (with and without hydrogen) were observed during the experiments through the sight glass (each experiment took approximately 45 minutes).

Temperature and emission values have been measured on different axial and radial positions by means of measuring ports located on the combustor wall throughout the combustor. At high temperatures, the radiation correction is essential to determine the temperature levels precisely. In particular, radiative heat transfer takes places from the flame to the combustor wall. Mean bulk velocities were calculated theoretically in the flame front taking into account fuel, air and hydrogen velocities (in particular hydrogen). Then, correction was performed for each axial and radial measurement. Thus, it was computed to be between 2–35 °C depending on the measured axial, radial and wall temperatures in the combustor.

4.1. Temperature Measurements

Axial and radial temperature values have been measured by using ceramic coated R-type thermocouples throughout the combustor in the present study. Figure 4 shows the axial temperature measurements of the low calorific value coal gases for both hydrogen supply and non-hydrogen supply conditions. The corrected generator gas (GG) flame temperature was determined as 947 °C. On the contrary, the blast-furnace gas flame temperature could not be determined for not being burned.

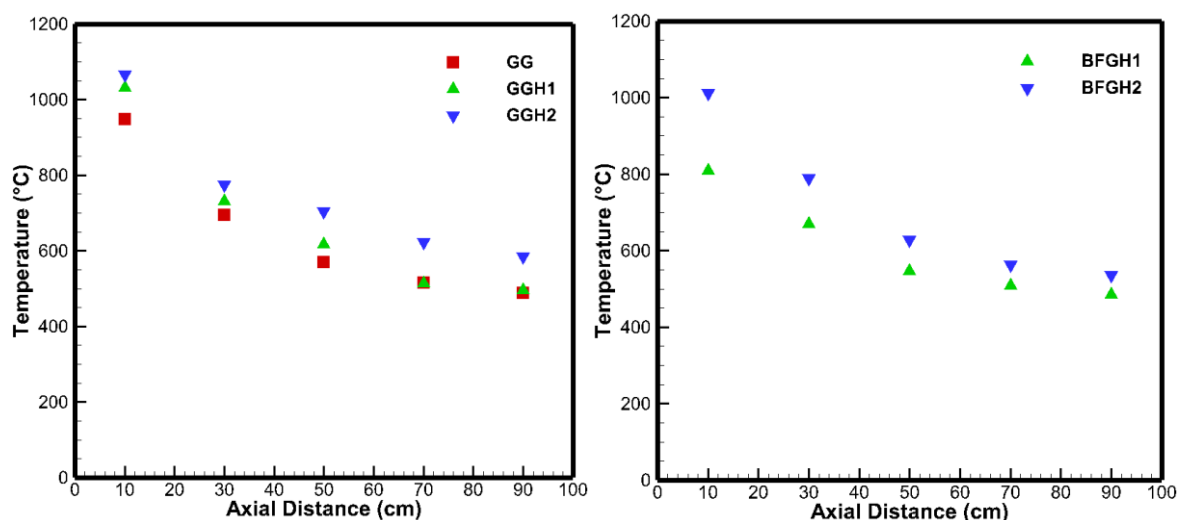


Figure 4. Axial temperature measurements

Figure 4 also gives some another results that represent the effects of the hydrogen supply on the combustion performances of the low calorific value coal gases from the center of the burner to the flame region. In addition, it is understood from Figure 4 that ignition of the blast-furnace gas has been taken place with hydrogen supply in the combustor. As can be clearly seen in Figure 4, the flame temperatures of GG and BFG enhance as hydrogen is supplied from the center of the burner to the flame zone. The corrected flame temperatures of these coal gases were determined to be 1030.9 °C for GGH1, 1064.9 °C for GGH2, 808 °C for BFGH1 and 1011.3 °C for BFGH2, respectively. It can be concluded that the hydrogen supply not only increases the combustion performances of the GG and BFG but also provides ignition of the blast-furnace gas under premixed combustion conditions throughout the combustor.

Figure 5 clarifies the corrected radial temperature measurements of the low calorific value coal gases and the effect of hydrogen supply on the radial temperature distributions throughout the combustor. Figure 5 indicates that temperature levels decrease drastically from the center of the combustor to the combustor wall at 10 cm axial distance as the combustor type is sudden expansion. The temperature value of GG has been measured and found to be 215.9 in the region closest to the combustor wall. Similarly, it can be readily said that the flame temperatures of GG and BFG increase as hydrogen is supplied from the center of the burner to the flame zone. Therefore, it can be concluded that the combustion performances of the low calorific value coal gases may be enhanced with supplying hydrogen. The temperature levels for all combustion conditions decrease gradually towards the combustor outlet due to radiative and convective heat transfers. However, the temperature differences between the center of the combustor and the combustor wall decrease towards the combustor outlet relatively. For example, the corrected temperature value of GGH2 was determined as of almost 585 °C while it was found to be nearly 524 °C, which means closer temperature levels comparatively in the combustor.

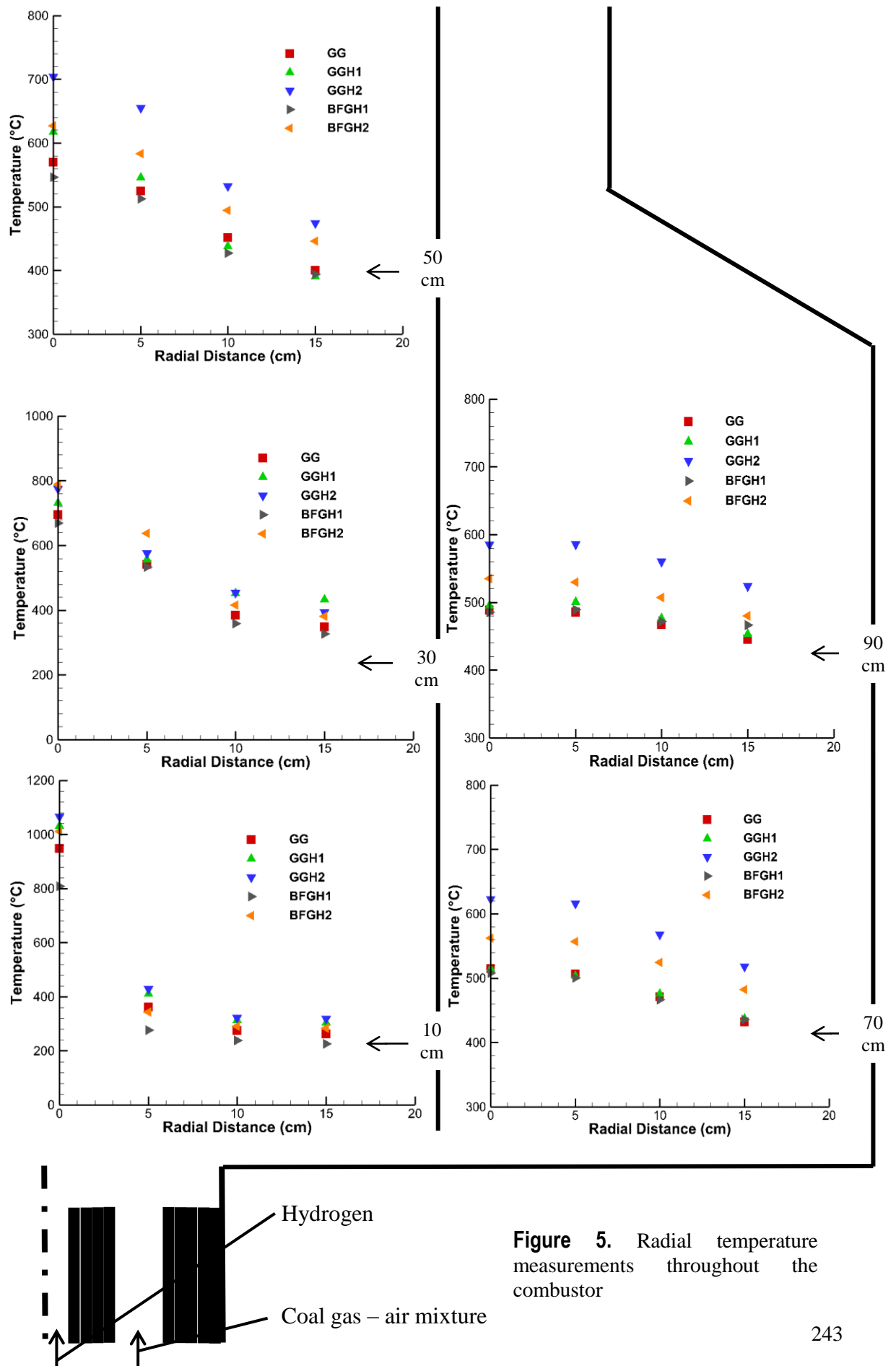


Figure 5. Radial temperature measurements throughout the combustor

4.2. Emission Measurements

Emissions have been measured using a flue gas analyzer within the combustor in the present study. To measure the emission values of low calorific value coal gases is vital in determining the emission parameters of these. In addition, To supply hydrogen to the flame zone affects pollutant formation considerably. There are three NO_x formation mechanisms that are known as thermal NO_x , prompt NO_x and fuel NO_x . Fuel NO_x results from the oxidation of fuel-bound nitrogen coming from the fuel. Thermal NO_x arises from the oxidation of molecular nitrogen during combustion in air and finally, prompt NO_x is thought to be formed by the reaction of N_2 with fuel fragments in the flame front [9].

The radial NO_x measurements of the generator and blast-furnace gases with and without hydrogen supply are shown in Figure 6. It can be understood from Figure 6 that the NO_x level of GG is very low in comparison to that of the natural gas flame due to its low flame temperatures. The NO_x value of GG was measured as 3 ppm in the flame zone. However, the amounts of NO_x formation increase rapidly as hydrogen is supplied to the flame and the NO_x value increases to 99 ppm in the flame zone under GGH2 combustion condition. This occurs as a result of the molecular nitrogen effect in the fuel as well as the contribution of molecular nitrogen in the air due to the thermal NO_x mechanism. This is because the flame temperature increases with supplying hydrogen. NO_x formed at a rate of 22 ppm in the flame region under the BFGH2 combustion condition.

Radial CO_2 distributions of the generator and blast-furnace gases with and without hydrogen are presented in Figure 7. Maximum CO_2 formations have been determined in the flame region. This is because of nearly completed combustion in this region. In addition, CO_2 formed higher values relatively when the generator and blast-furnace gases were combusted in the combustor. The main reason for high CO_2 emissions can be also account for the presence of CO_2 in fuels (up to 8 % by volume). In addition these findings, it can be seen that CO_2 measurement levels increase as the hydrogen is supplied to the flame region at the same time in Figure 7. This may be explained that hydrogen supply affects the conversion of CO (up to 30% in fuels) to CO_2 emissions significantly. The authors estimate that the main reason of this circumstance is the effect of conversion of CO to CO_2 when the presence of hydrogen in flame. Moreover, water gas shift reaction effect can not be ignored under GGH1, GGH2, BFGH1 and BFGH2 combustion conditions. This circumstance can also be seen in Figure 8. CO levels decrease gradually as hydrogen is supplied to the flame as can be seen in Figure 8. Radial CO measurements of the low calorific value coal gas flames are given in Figure 7. CO levels for all conditions decrease gradually towards the combustor outlet due to depletion of CO in the fuels.

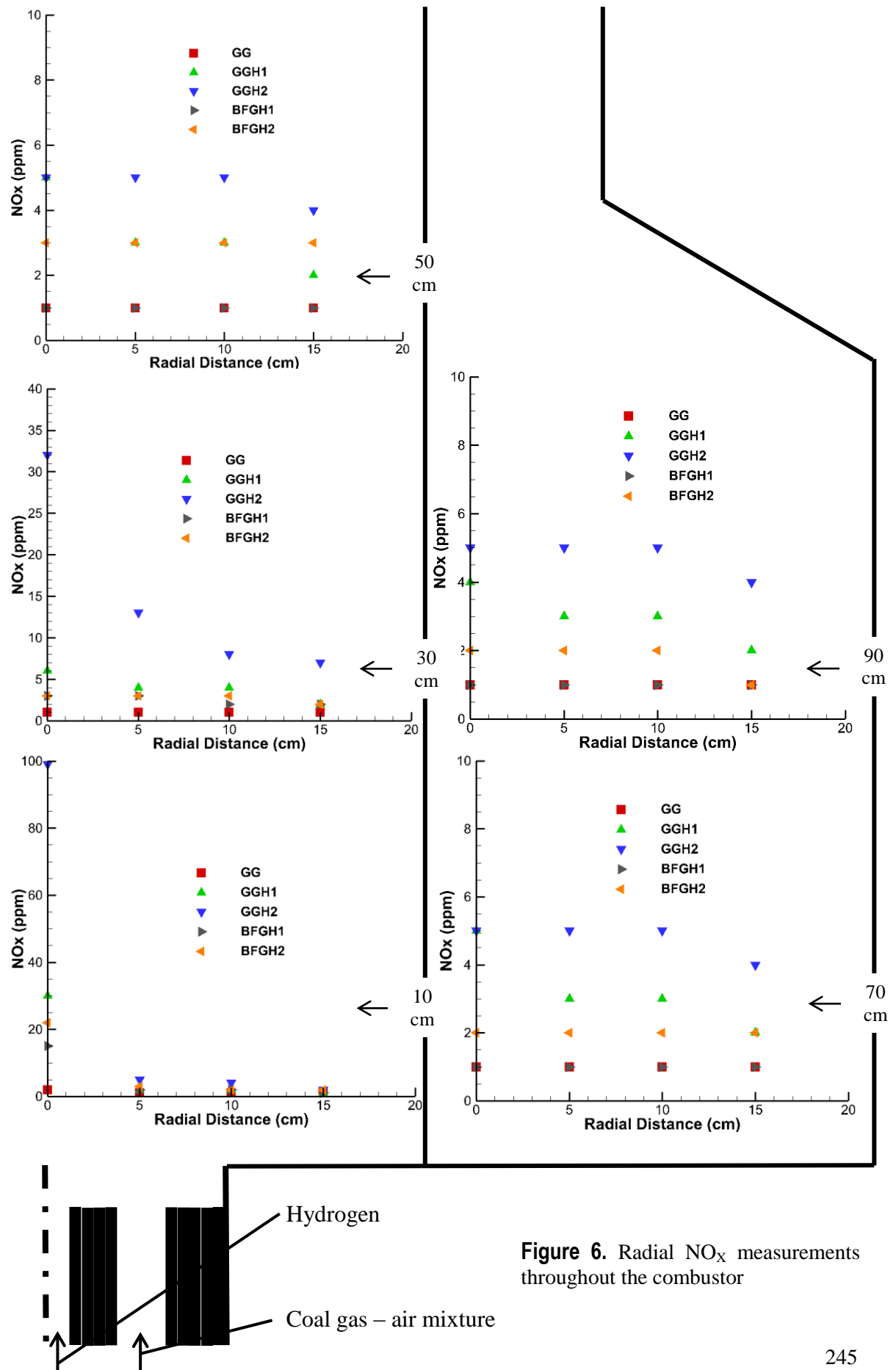


Figure 6. Radial NO_x measurements throughout the combustor

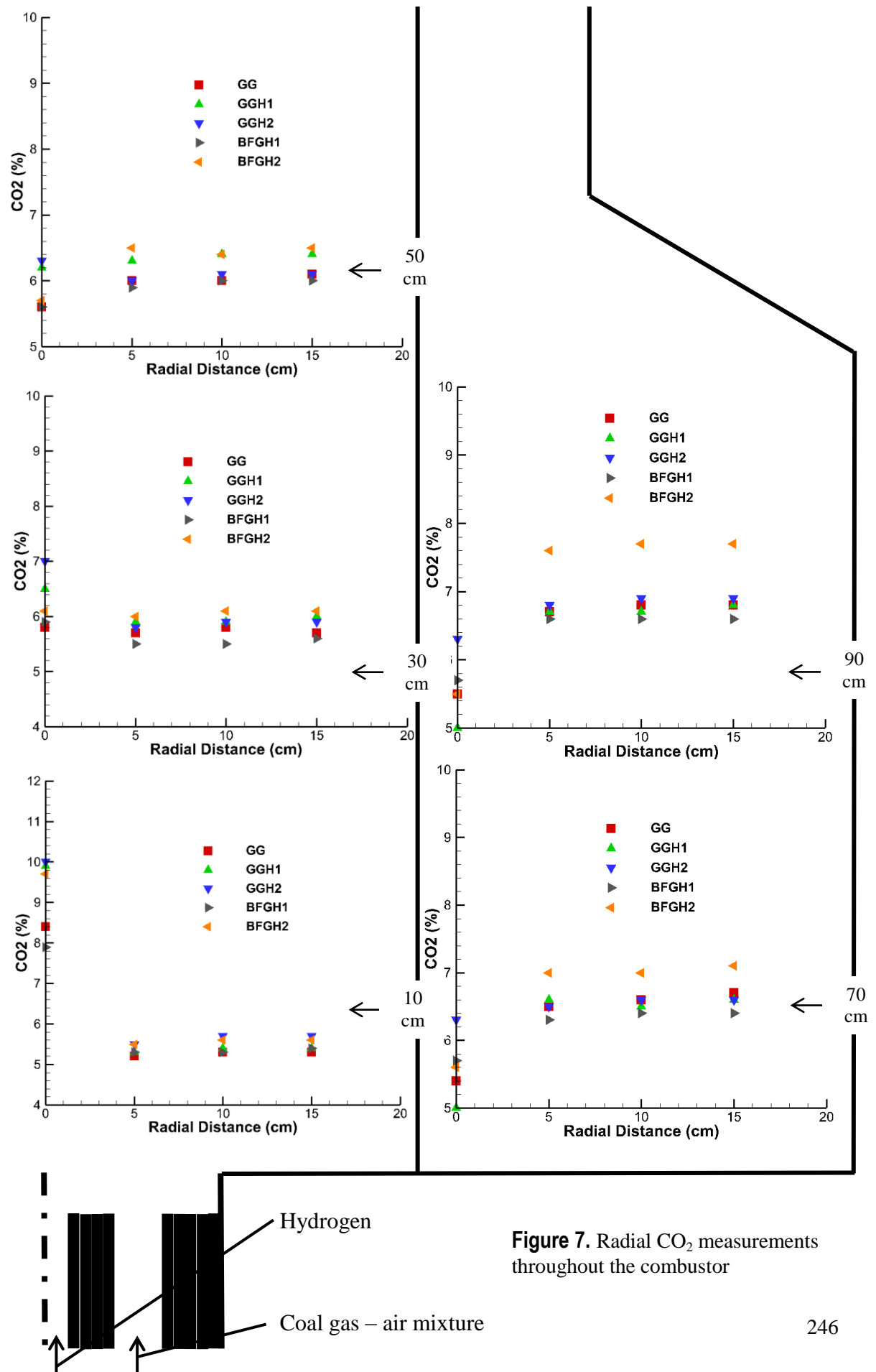
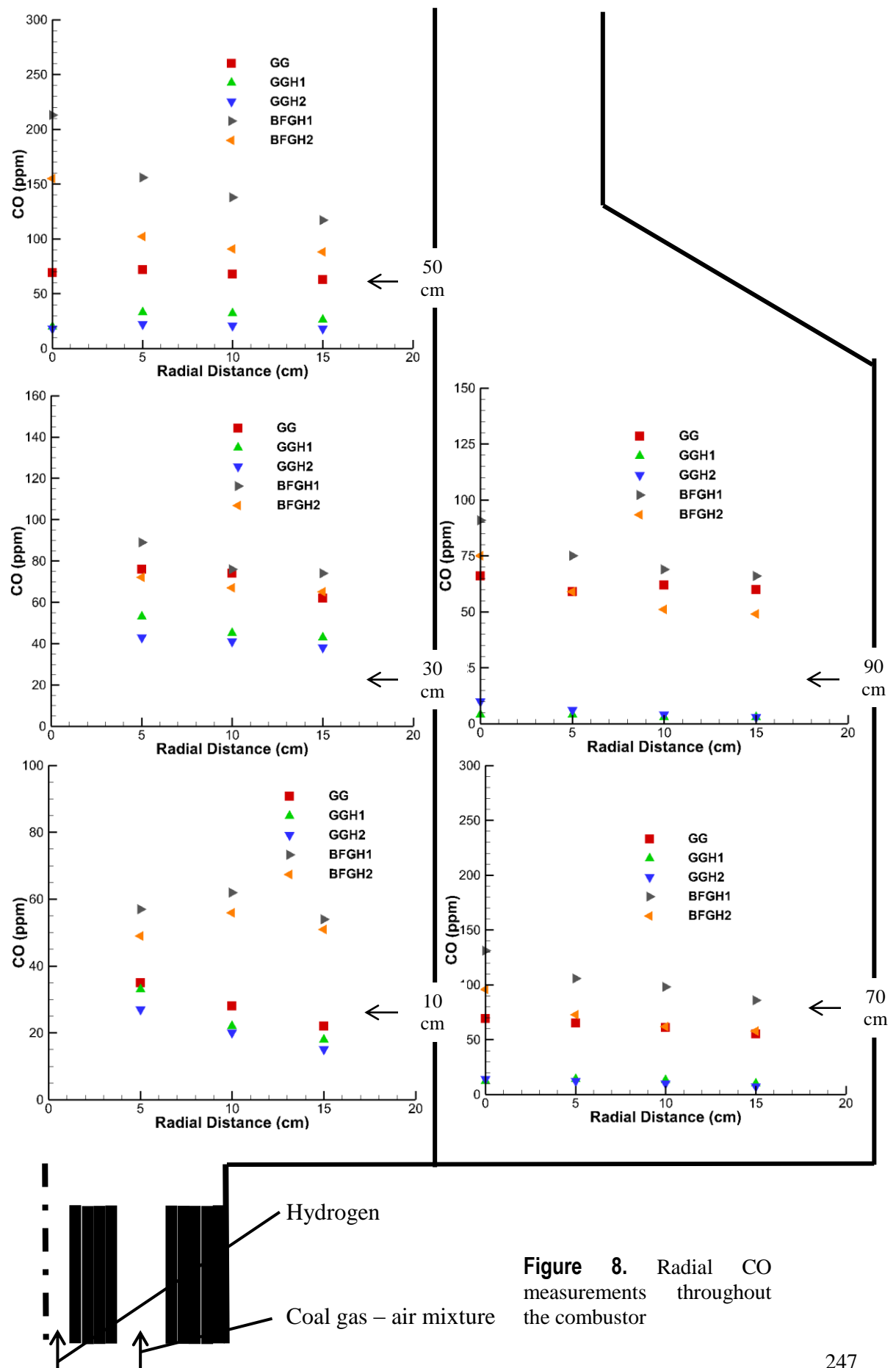


Figure 7. Radial CO₂ measurements throughout the combustor



5. CONCLUSIONS

An experimental study has been conducted in order to investigate the combustion behaviours of the low calorific value coal gases under premixed combustion conditions. In addition, hydrogen has been supplied from the center of the new type of burner to the flame so as to enhance the combustion performances of these coal gases. The experimental results bring about the following conclusions:

- The low calorific value coal gases have been properly consumed using the new type of burner coupled with the existing combustor under premixed combustion conditions. Yet, the blast-furnace gas could not be ignited without supplying hydrogen under premixed combustion conditions as it has high amount of nitrogen and few combustible components.
- It has been demonstrated that the flame temperatures of the low calorific value coal gases increase with supplying hydrogen.
- Although the NO_x level of the generator gas (3 ppm in the flame region) is quite lower in comparison to that of the natural gas flame due to its low flame temperatures, the amount of NO_x formation increases rapidly as hydrogen is supplied to the flame (99 ppm and 22 ppm under the GGH2 and BFGH2 combustion conditions, respectively).
- It has been demonstrated that hydrogen supply affects conversion of CO (in the syngases) to CO₂ significantly in combustion products.

Acknowledgement: The authors gratefully acknowledge financial support from TUBITAK (Project Number: 114M668).

References

- [1] Karyeyen, S., Ilbas, M., *Turbulent diffusion flames of coal derived-hydrogen supplied low calorific value syngas mixtures in a new type of burner: An experimental study*, International Journal of Hydrogen Energy, 42 (2017) 2411-2423.
- [2] https://en.wikipedia.org/wiki/Blast_furnace_gas [accessed on 09 March 2017].
- [3] Bidi, M., Hosseini, R., Nobari, M.R.H., *Numerical analysis of methane-air combustion considering radiation effect*, Energy Conversion and Management, 49 (2008) 3634-3647.
- [4] Schefer, R.W., Wicksall, D.M., Agrawal, A.K., *Combustion of hydrogen-enriched methane in a lean premixed swirl-stabilized burner*, Proceedings of the Combustion Institute, 29 (2002) 843-851.
- [5] Singh, D., Nishiie, T., Tanvir, S., Qiao, L., *An experimental and kinetic study of syngas/air combustion at elevated temperatures and the effects of water addition*, Fuel, 94 (2012) 448-456.
- [6] Daniele, S., Jansohn, P., Mantzaras, J., Boulouchos, K., *Turbulent flame speed for syngas at gas turbine relevant conditions*, Proceedings of the Combustion Institute, 33 (2011) 2937-2944.
- [7] Halter, F., Chauveau, C., Gökalp, I., *Characterization of the effects of hydrogen addition in premixed methane/air flames*, International Journal of Hydrogen Energy, 32 (2007) 2585-2592.
- [8] Williams, T.C., Shaddix, C.R., Schefer, R.W., *Effect of syngas composition and CO₂-diluted oxygen on performance of a premixed swirl-stabilized combustor*, Combustion Science and Technology, 180 (2008) 64-88.
- [9] Lieuwen, T.C., Yang, V., Yetter, R., *Synthesis Gas Combustion Fundamentals and Applications*, Taylor & Francis Group, Boca Raton, USA, 2010.

Diffuser Combustor to Study the Influence of Turbulence on Turbulent lean Premixed Flame

Ibrahim Thamer Nazzal¹, Özgür Ertunc¹

¹Ozyegin University

thamer.nazzal@ozu.edu.tr & ozgur.ertunc@ozyegin.edu.tr

Abstract: This work investigates the effect of the turbulence on the flame location of a turbulent lean premixed flame. k-epsilon model together with the coherent flame model are used to introduce the turbulence effect on combustion. It was seen that the turbulent length scale and turbulence intensity influence the flame location. In addition to the turbulence effect on combustion, turbulence caused flow separation, which in turn influence the flame location and topology. In order to avoid the flow separation of the diffuser combustor, a V shaped object is placed at the middle of diffuser combustor. It was seen that the flow separation is suppressed, when V-object is used inside the diffuser, consequently the flame is stabilized.

Keywords: Premixed turbulent flame, flame location, turbulence intensity, and turbulent length.

1. Introduction

Turbulent combustion is a complicated process due to the interaction between the turbulence and combustion. The understanding of the turbulent – combustion interaction is crucial to improve combustion devices such as gas turbines and the spark ignition engines [1]. In order to get better understanding and information required for the combustion – turbulent interaction, it is essential to select the suitable model.

There are several studies for the modeling of turbulent premixed flame that are related to the impact of turbulence on the flame, such as the coherent flame model. Flame area density is the main quantity of the coherent flame model which involve the effect of the turbulence on the flame within the source term of the species transport equation [2,3]. However, the impact of the turbulence on the flame and the effect of the flame on the turbulence are studied by many researchers [4-9]. Despite continuing efforts on turbulence-flame interaction, the influence of the turbulence on the flame location need to be investigated, while is highly relevant to many industrial applications. Therefore, this study will be about the flame location behavior under turbulence effect in a diffuser combustor.

2. Flame modelling

Coherent flame model and k-ε model is used to study the impact of the turbulent on the flame within the frame of the Reynolds-Averaged Navier-Stokes (RANS) equations. It should be noted that in combustion simulations RANS formulation is used like the Favre averaged equations to deal with the fluctuations of density, velocity, etc.. According to Favre-averaged density, species transport equation is written as follows:

$$\frac{\partial}{\partial t}(\bar{\rho}\tilde{c}) + \frac{\partial}{\partial x_i}(\bar{\rho}\tilde{u}_i\tilde{c}) = \frac{\partial}{\partial x_i}\left(\bar{\rho}D_t\frac{\partial\tilde{c}}{\partial x_i}\right) + \bar{w} \quad (1)$$

where \bar{w} is reacting term which is the main problem in the modeling of the turbulent combustion. This reacting term is solved in terms of the fuel mass fraction and flame area density according to the coherent flame model [3]. Therefore, a transport species equation is written in term of the flame area density as:

$$\frac{\partial}{\partial t}(\bar{\rho}\tilde{\zeta}) + \frac{\partial}{\partial x_i}(\bar{\rho}\tilde{u}_i\tilde{\zeta}) = \frac{\partial}{\partial x_k}\left(\bar{\rho}D_t\frac{\partial\tilde{\zeta}}{\partial x_k}\right) + \bar{w}_\Sigma \quad (2)$$

where ζ is the flame area density per unit mass. Where the second term of the equation (2) is the reacting term in terms of the flame area density Σ and it is formulated according to [1,3] as :

$$w_\Sigma = \alpha K_t \Sigma - \beta \frac{\rho_u Y_{ft} S_L \left(1 + \alpha \sqrt{k}/S_L\right)}{\rho Y_f} \Sigma^2 \quad (3)$$

3. Numerical simulation

The flame location is investigated under different turbulence intensities and turbulent length scales. Here, a diffuser burner is selected to achieve this study. The half angle of the diffuser expansion was 3° and the downstream of the diffuser was built as constant at outlet diameter with 40 cm length. However, Figure (1) indicates the details of this diffuser. Lean premixed propane is introduced into the diffuser with 0.3 m/sec velocity. The temperature and pressure are set as 300 °K and ambient pressure respectively for the initial condition and boundary conditions at the inlet and the outlet. While at the inlet, the turbulence intensity is varied gradually from 0.05 to 0.30, while the turbulent length scale is set to 1 cm and 10 cm.

STAR CCM+ version 11.02.009-R8 is used to perform the simulations of the cases. In addition, simulations had been conducted enough time to allow for stabilizing the location of the flame with the new value of turbulence intensity and turbulent length scale.

4. Results and discussion

The effect of the turbulent intensity and the integral length scale of turbulence on the flame location are shown in Figure (2). Here, the flame location is measured using the temperature at the centerline. Flame location is defined as the location where temperature is 1400 °K. It was observed that the flame location moves gradually towards the inlet of the combustor with an increase in the turbulence intensity and turbulent length scale. However, it was also observed that flow separation occurs in the diffuser combustor and this prevents the determination of the sole effect of turbulence on the flame location. For this reasons, a V- object is placed inside the diffuser. Figure (3) indicates the convolution integral of the flow with V- object and without for turbulence intensities (5% and 30%) and for turbulent length scale (1 and 10 cm). It can be observed that, the flame separation occurs without V-object, while the flow separation is eliminated with the use of V-object. It is evident, besides of the location of the flame, the topology of the flame is also influenced by the turbulent length scale and the turbulence intensity. It can be seen in Figure (2), the flame location became less sensitive to turbulence parameters at low turbulence intensity but highly sensitive when TI>25 % with V-object.

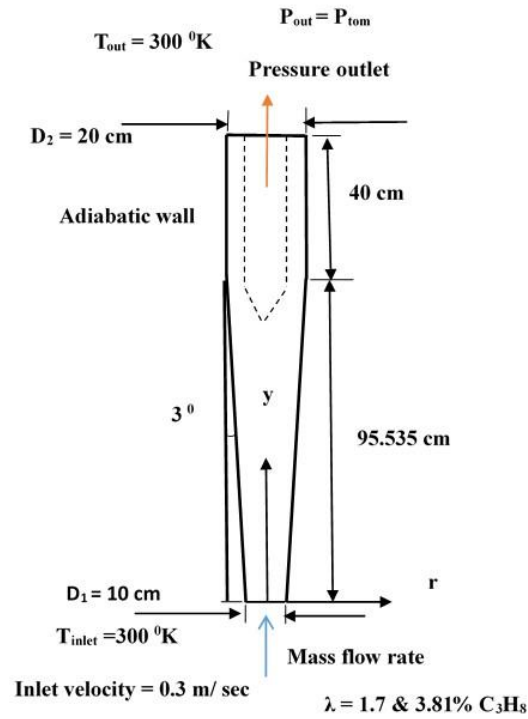


Figure 1. The geometry of the diffuser combustor and the boundary conditions

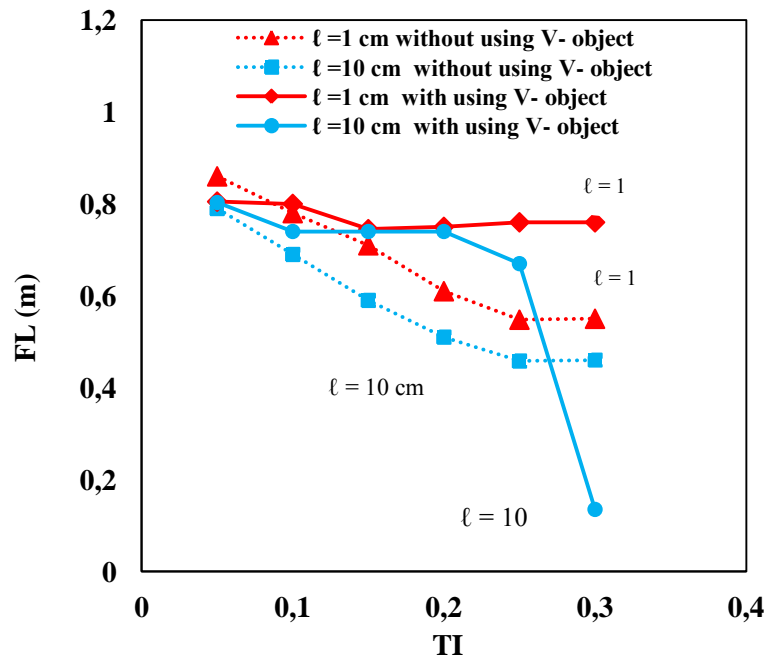


Figure 2. The flame location (FL) under various turbulence intensities (TI) and for 1 cm and 10 cm turbulent length scale (ℓ).

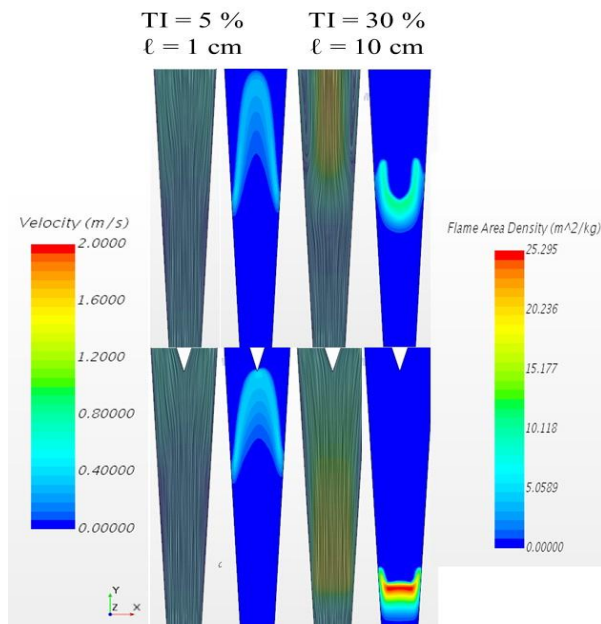


Figure 3. The contour flame area density and convolution integral of the flow for the turbulence intensities 5% and 30% and (1&10 cm)

Conclusions

It is shown that turbulent length scales and turbulence intensities effect the flame front. However, they can also trigger the flow separation which in turn can influence the flame location. In order to eliminate the effect of flow separation and study the sole effect of turbulence on the flame location, a v– object was placed inside the diffuser. It is shown that the flow separation is eliminated totally. The flame in the v-object case was less sensitive to the changes in turbulence properties at low turbulence intensities. However, after 25 % turbulence intensity, the flame location dropped drastically towards the inlet as expected. In general, this study shows that diffuser combustor with v-object can be used to study the effect of turbulence on the flame both numerically and experimentally.

Acknowledgments

The authors would like to acknowledge the Ozyegin University in Istanbul Turkey and Tikrit University in Tikrit, Iraq for supporting this work. The authors would also like to acknowledge the Scientific and Technological Research Council of Turkey (TÜBİTAK) for providing the financial support for this research with the 114C113 project. Authors would like to thank Prof. Dr. Bedii Özdemir for fruitful discussions.

Nomenclature

D	Diameter [m]
D_t	Mass diffusivity [m^2/s]
K_t	Flame stretch [$1/\text{s}$]
S_L	Laminar flame speed [m/sec]
u	Velocity [m/sec]
Y_{ft}	mass fraction [%]
Y_{res}	Residual of fuel mass fraction [%]
ℓ	Turbulent length scale [m]
ρ	Density [kg/m^3]
ρ_u	Density of the unburned [kg/m^3]
Σ	Flame area density per volume [m^2/m^3]
ς	Flame area density per mass [m^2/kg]
FL	Flame location
w	reacting term
TI	Turbulence intensity
w_Σ	Source term in terms of flame area density
α	Constant parameter of the CFM model
β	Constant parameter of the CFM model
\tilde{c}	Reaction Progress variable



References

- [1] N. Peters, turbulent combustion, Cambridge University, London, U.K, 2004.
- [2] Marble and Broadwell, ‘Coherent Flame Model for Turbulent chemical Reactions’, 1977, Project Squid Tech. Rep. TRW-9-PU. Purdue University, Indiana, USA.
- [3] C. Meneveau and T. Poinso, ‘Stretching and quenching of flamelets in premixed turbulent combustion’, Combustion and Flame, 86 (1991) 311–332.
- [4] S. Chaudhuri, a. Saha, and C. K. Law, ‘On flame-turbulence interaction in constant-pressure expanding flames’, Proceedings of the Combustion Institute, 35 (2014) 1331-1339.
- [5] U. Ahmed, ‘Flame Turbulence Interaction In Premixed Turbulent Combustion’, 2013, Ph.D. thesis, University of Manchester, U.K.
- [6] A. Steinberg, J. F. Driscoll, and S. Ceccio, ‘Turbulence–flame interactions the mechanisms of flame strain and wrinkling’, 44th AIAA/ASME/SAE/ASEE Joint Propulsion Conference & Exhibit 21 - 23 July 2008, Hartford.
- [7] Ö. Gülder and G. Smallwood, ‘Flame Surface Densities in Premixed Combustion At Medium To High Turbulence Intensities’, Combustion Science and Technology, 179 (2007) 191–206.
- [8] M. S. Boulahlib, M. Chekired & S. Boukebbab, ‘The turbulence effect on a lean premixed methane-air flame in a Bunsen burner’, WIT Transactions on Ecology and The Environment, 186 (2014) 719–727.
- [9] M. S. D. and J. B. B. A. J. Aspden, ‘Turbulence–flame interactions in lean premixed hydrogen: transition to the distributed burning regime’, J. Fluid Mech., 680 (2011) 287–320.

Numerical investigation on oxy enriched air combustion with methane fuel in combustion chamber of a boiler

Esenay ARSLAN¹; Selahaddin Orhan AKANSU¹; Nafiz KAHRAMAN¹; Melih YILDIZ¹

¹Erciyes University / Engineering Faculty / Department of Mechanical Engineering

Kayseri TURKEY

esenayarslan@erciyes.edu.tr; akansu@erciyes.edu.tr;

nafiz@erciyes.edu.tr; melihyildiz@erciyes.edu.tr

Abstract: In order to prevent climate change and global warming, which are the consequences of greenhouse gases, today, we are particularly interested in reducing exhaust emissions. In this study, improvement of the combustion emissions in the boiler will be provided achievement against both global warming and the prevention of environmental pollution. In addition, boiler efficiency may be increased by using enriched oxygen.

In practice, as the combustion conditions are not ideal, more air is needed than theoretically necessary to ensure a good combustion. The amount of excess air actually required depends on the type and composition of the fuel, the furnace or boiler design, the design and operating conditions of the burner.

In this study, the temperature distribution and emission values of the boiler chamber intended for decreasing the emission amount and increasing the efficiency are investigated within the scope of numerical investigation of the oxygen-enriched methane-air mixture in boiler at 6000000 kcal/h power. In the oxygen-enriched combustion, the exhaust heat thrown by N₂ decreases, the temperature values increase, CO and HC values decrease. However, firstly NO_x values increase and then decrease. The FLUENT code software program is used in this study. The analysis model is considered as three-dimensional and "k-epsilon realizable" turbulence model and "eddy-dissipation" combustion model are preferred for numerical study. Two - stage combustion of the methane - air mixture in the three - dimensional boiler model was analyzed. The excess air coefficient is selected as 1.0, 1.1 and 1.2 in the combustion analyzes enriched with oxygen. Also, for all cases, the oxygen enrichment percentages of the mixture are taken as 5%, 10%, 15% and 20% respectively.

The temperatures in the boiler outlet zone are compared for the different situations by the numerical study. Increasing the enrichment ratio also increased the boiler outlet temperature. In addition to the increase in temperature, the decrease in the emissions is obtained at the end of combustion.

Key words: methane-air mixture, oxygen enriched combustion, CFD

1. Introduction

Oxy-fuel combustion is the process of burning a fuel using pure oxygen instead of air as the primary oxidant. Since the nitrogen component of air is not heated, fuel consumption is reduced, and higher flame temperatures are possible. Historically, the primary use of oxy-fuel combustion has been in welding and cutting of metals, especially steel, since oxy-fuel allows for higher flame temperatures than can be achieved with an air-fuel flame.

There is currently research being done in firing fossil-fueled power plants with an oxygen-enriched gas mix instead of air. Almost all of the nitrogen is removed from input air, yielding a stream that is approximately 95% oxygen. Firing with pure oxygen would result in too high a flame temperature, so the mixture is diluted by mixing with recycled flue gas, or staged combustion. The recycled flue gas can also be used to carry fuel into the boiler and ensure adequate convective heat transfer to all boiler areas. Oxy-fuel combustion produces approximately 75% less flue gas than air fueled combustion and produces exhaust consisting primarily of CO₂ and H₂O (see .

The justification for using oxy-fuel is to produce a CO₂ rich flue gas ready for sequestration. Oxy-fuel combustion has significant advantages over traditional air-fired plants. Among these are:

- The mass and volume of the flue gas are reduced by approximately 75%.
- Because the flue gas volume is reduced, less heat is lost in the flue gas.
- The size of the flue gas treatment equipment can be reduced by 75%.
- The flue gas is primarily CO₂, suitable for sequestration.
- The concentration of pollutants in the flue gas is higher, making separation easier.
- Most of the flue gases are condensable; this makes compression separation possible.
- Heat of condensation can be captured and reused rather than lost in the flue gas.
- Because nitrogen from air is absent, nitrogen oxide production is greatly reduced.

Economically speaking this method costs more than a traditional air-fired plant. The main problem has been separating oxygen from the air. This process needs lots of energy, nearly 15% of production by a coal-fired power station can be consumed for this process. However, a new technology which is not yet practical called chemical looping combustion can be used to reduce this cost. At present in the absence of any need to reduce CO₂ emissions, oxy-fuel is not competitive. However, oxy-fuel is a viable alternative to removing CO₂ from the flue gas from a conventional air-fired fossil fuel plant. However, an oxygen concentrator might be able to help, as it simply removes nitrogen.

In industries other than power generation, oxy-fuel combustion can be competitive due to higher sensible heat availability.

Habib et al (1) numerically investigated syngas combustion and emission characteristics and compared with the case of pure methane combustion in a two-burner 200 MW package boiler. Different syngas compositions were considered for combustion with air. The results showed a combustion delay in case of pure methane combustion as compared to syngas combustion. The boiler exit temperature was found to increase with the increase of hydrogen content in the syngas. NO_x emission decreases by about 30% when the amount of excess air is increased from 5% to 25%, which is very promising.

To determine the influence of oxygen enrichment on soot formation and radiation, Shaddix et al (3) developed a non-premixed coannular burner in which oxygen concentrations and oxidizer flow rates can be independently varied, to distinguish the effects of turbulent mixing intensity from oxygen

enrichment on soot formation and flame radiation. The measurements show that soot formation increases as the oxygen concentration decreases from 100% to 50%, helping to moderate a decrease in overall flame radiation. The soot temperature decreases with a decrease in the oxygen concentration and increases with an increase in turbulent mixing intensity.

In the study, Heil et al (4) presents an experimental study on oxyfuel methane combustion with the aim to investigate the importance of the chemical effects of high CO₂ concentrations. Experiments have been carried out in a 25 kW furnace for flameless combustion which provides the possibilities to achieve stable combustion of methane within a wide range of oxygen concentrations in the CO₂/O₂ mixture at constant reactor temperature. The results obtained in this work demonstrated that by elimination of the influence of: molar heat capacity, CO₂ dissociation, and thermal radiation, it can be estimated that the observed effects of high CO₂ concentrations on combustion rates can be attributed to its participation in the chemical reactions. An increase of O₂ in oxyfuel led to a reduction of this impact, however, further investigations on the exact mechanism are necessary.

The oxygen-methane diffusion flame taking place in a gas turbine reactor was investigated experimentally with emphasis on flame stability by Habib et al (5). The oxidizer is a mixture of O₂ and CO₂ and the oxy-combustion process was studied at different equivalence ratios ranging from $\Phi = 0.5$ to 1.0 and different O₂/CO₂ mixture composition (100/0, 80/20, 60/40, 50/50, 40/60, 30/70 and 25/75). It was found that the flame is very stable at the equivalence ratio of 0.65. It was also found that both flame and flue gas temperatures are reduced with the increase of the equivalence ratio.

Cheong et al (6) reports on the NO and CO emission characteristics of counterflow combustion of methane simulated under MILD or/and oxyfuel conditions. Simulations using CHEMKIN are conducted for various injection conditions of fuel and oxidizer. It is observed that the NO emission of MILD-CO₂ combustion is ultra-low for all cases of investigation, even when increasing the combustion temperature up to 2000 K or adding more N₂ (up to 20%) to either the fuel stream (to simulate nitrogen-containing fuels like biomass) or the oxidizer stream (to simulate the air-ingress). A higher temperature allowed under MILD-CO₂ combustion suggests the improvement of energy efficiency for the MILD combustion technology. Moreover, the presence of steam in the oxidant reduces both NO and CO emissions of combustion for all cases.

Mardani et al (7) demonstrates a numerical study on the combination of Oxy-Fuel and MILD (moderate or intense low-oxygen dilution combustion) combustions, i.e. OXY-MILD. The N₂ of a hot oxidizer was replaced with CO₂ and H₂O in a MILD combustion test case. The study was conducted using a CFD analysis, a zero-dimensional well-stirred reactor analysis, and a reactors network analysis. In the CFD analysis, RANS equations with modified $k-\epsilon$ equations were solved for a 2D-axisymmetric computational domain. Results showed a decrease in temperature gradient, reaction rate, and Damköhler number under the OXY-MILD condition in comparison with the MILD one.

The aim of this study is to increase the end-of-combustion temperature and reduce emission values by adding oxygen to the methane fuel at different rates. In this study, oxy enriched combustion of the methane fuel was investigated on horizontal type boiler. In addition to the three different air excess coefficient values, the temperature and emission values that is obtained by considering the oxygen addition rates were compared.

2.Mathematical Model and Numerical Method

In this study Selnikel brand boiler ,that is seen in the figure 1, dimensions are taken into account in the modeling of the boiler. Furnace and combustion chamber parts of the boiler are only modeled to investigate temperature distribution.



Figure 1. Hot water boiler of Selnikel

The boiler power in the study is 6000000 kcal / h capacity and the technical data is shown in table 1.

Table 1. Technical information for boiler

Specifications	Values
Boiler type	Scotch
Boiler capacity	6000000 kcal/h
Boiler efficiency	%97
Fuel inlet	Ø20 mm
Air inlet	Ø150 mm
Outlet	Ø76 mm
Combustion chamber	Ø2000 mm
Furnace	Ø1250 mm
Length of boiler	5100 mm

The boiler used in the numerical study was modeled as three dimensional in Solidworks program. Boiler model and its section view are shown in figure 2.

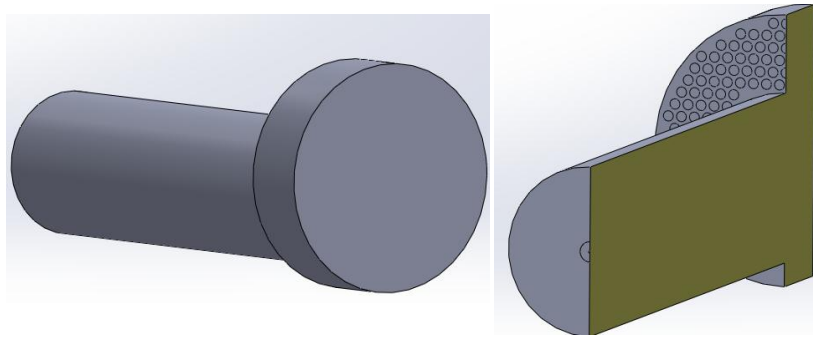


Figure 2. Isometric and section views of the model

The model has different fuel and air inlet and these regions are shown in Figure 3.

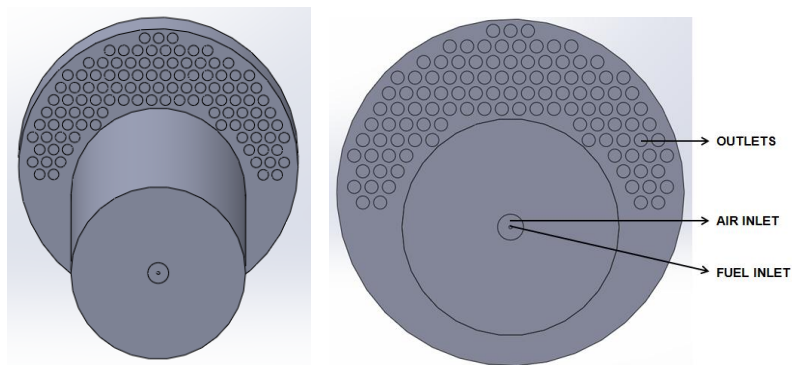


Figure 3. Inlet and outlet regions on the model

3D model has been meshed in fluent. Meshed model has shown in figure 4. Information about mesh and mesh quality are following;

Minimum Orthogonal Quality = 2.79813e-01

Maximum Aspect Ratio = 1.76826e+01

Table 2. Mesh size

Level	Cells	Faces	Nodes	Partitions
0	328312	670956	62133	1

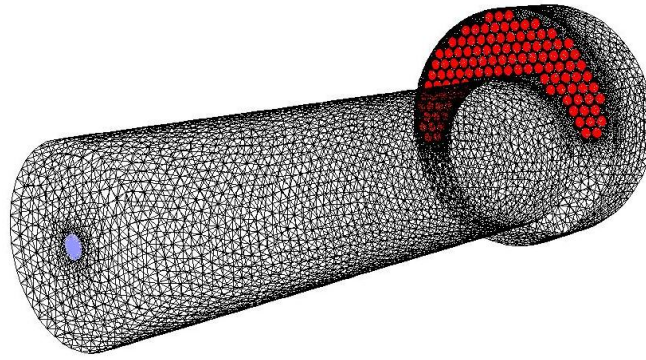


Figure 4. Mesh view of the model

The analysis is based on the steady-state, 3D continuity, momentum and energy equations. In the numerical study, k-epsilon realizable turbulence model is used. An eddy-dissipation combustion model is used for the two-stage combustion of methane fuel.

For the boundary conditions;

Inlet temperature: 300K

Furnace wall temperature: 424,86K

Inlet wall temperature: 300K

5%, 10%, 15% and 20% ratios were used to enrich the fuel in terms of oxygen. These ratios were analyzed considering the cases where the air excess coefficient is 1.0, 1.1 and 1.2. Table 3 has shown value of reactants according to different excess air ratios and oxygen enrichment rates.

Table 3. Air and fuel ratios for combustion

Excess Air Coefficient	Oxygen Rate	Mass Flow of CH ₄	Mass Flow of O ₂	Molar Ratio of O ₂
$\lambda=1$	Unenriched	0,129	2,223	0,22
	% 5 O ₂	0,129	2,142	0,228
	% 10 O ₂	0,129	2,068	0,235
	% 15 O ₂	0,129	2,001	0,243
	% 20 O ₂	0,129	1,939	0,25
$\lambda=1.1$	Unenriched	0,129	2,446	0,221
	% 5 O ₂	0,129	2,357	0,229
	% 10 O ₂	0,129	2,275	0,237
	% 15 O ₂	0,129	2,201	0,244
	% 20 O ₂	0,129	2,132	0,252
$\lambda=1.2$	Unenriched	0,129	2,668	0,222
	% 5 O ₂	0,129	2,571	0,23
	% 10 O ₂	0,129	2,482	0,238
	% 15 O ₂	0,129	2,401	0,245
	% 20 O ₂	0,129	2,326	0,253

3.Results and Discussion

The solution is considered to be sufficiently converged when the normalized residual of the algebraic equation is less than a prescribed value of 10^{-4} . These computations, performed on a PC Intel Core-i5 3.20 GHz, 1000 total iterations for each case and about 2,5–3 h CPU time.

Furnace temperatures in different cases have been compared according to obtained analysis results. Temperature distributions for furnace have been given in figure 5, figure 6 and figure 7. As it is seen in the figures increasing of oxygen rate in the mixture has provided increment on temperature values because the more mixture has been combusted in the boiler. At the same time, furnace temperature has increased in direct proportion to excess air coefficient.

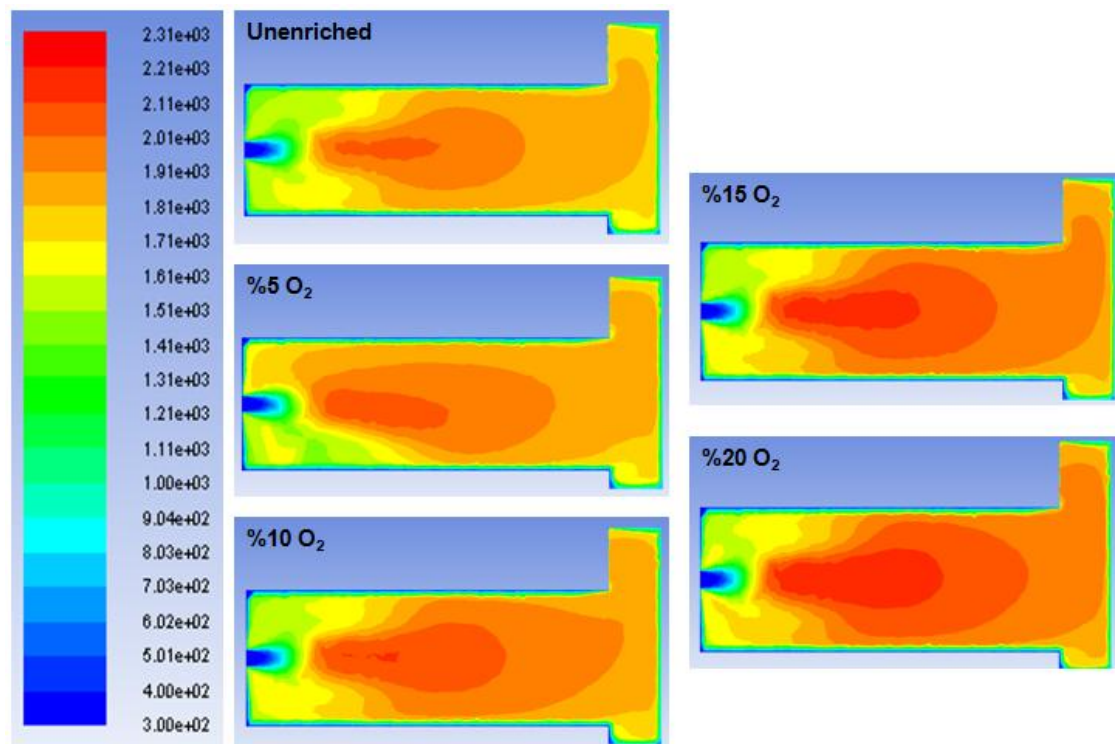


Figure 5. Temperature distributions for EAC value = 1.0

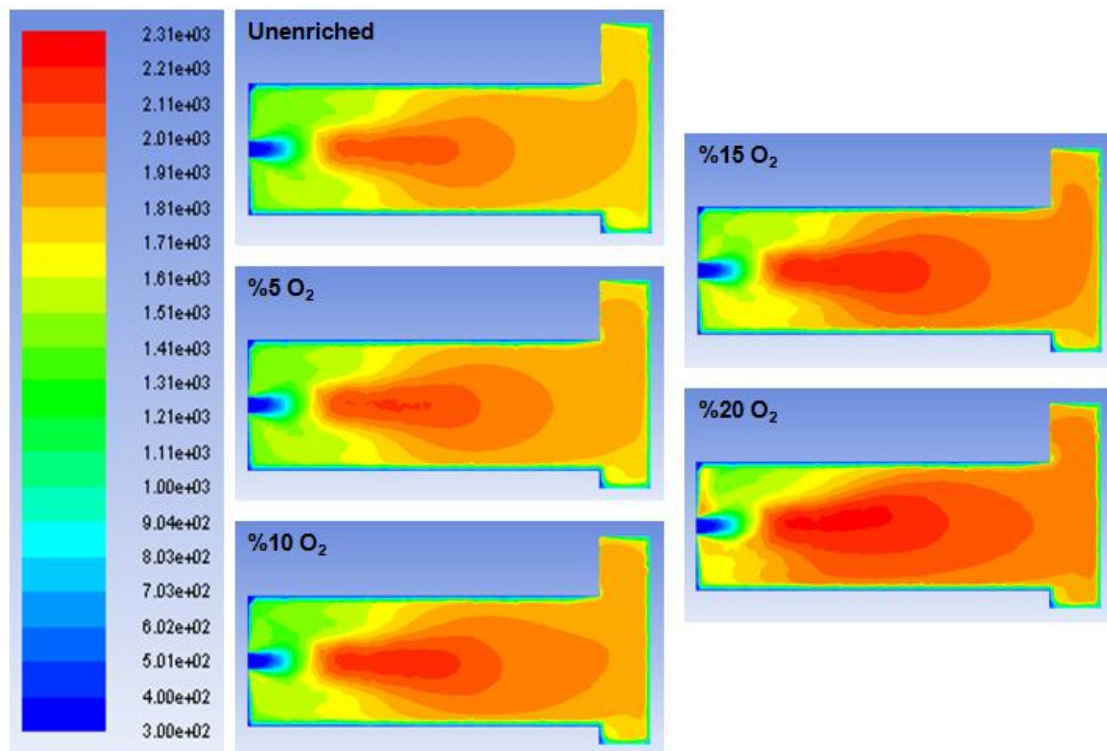


Figure 6. Temperature distributions for EAC value = 1.1

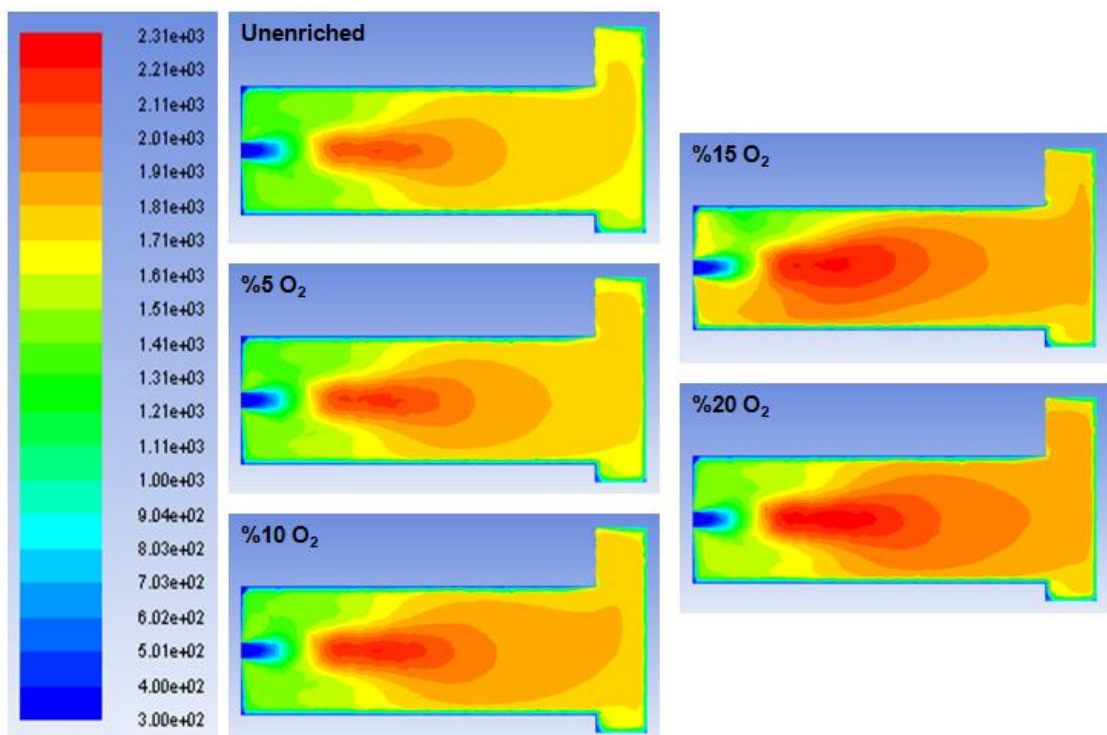


Figure 7. Temperature distributions for EAC value = 1.2

Maximum outlet temperature has been obtained for EAC value of 1,1 and %20 oxygen rate. As it is seen in the table 4, the lowest outlet temperature values are for EAC value of 1,2 and unenriched case.

Table 4. Obtained temperature values

Excess Air Coefficient	Oxygen Rate	Outlet Temperature (K)	Avarage Temperature (K)	Maximum Temperature (K)
$\lambda=1$	Unenriched	1706,84	1779,24	2039,66
	% 5 O ₂	1736,23	1815,65	2094,55
	% 10 O ₂	1762,43	1845,70	2122,51
	% 15 O ₂	1797,38	1883,52	2166,92
	% 20 O ₂	1822,57	1913,82	2202,57
$\lambda=1.1$	Unenriched	1692,84	1746,96	2087,91
	% 5 O ₂	1728,67	1780,40	2137,08
	% 10 O ₂	1757,08	1811,72	2185,38
	% 15 O ₂	1794,49	1861,05	2217,49
	% 20 O ₂	1828,23	1914,27	2265,40
$\lambda=1.2$	Unenriched	1609,73	1665,32	2132,18
	% 5 O ₂	1644,97	1705,23	2182,91
	% 10 O ₂	1680,68	1736,68	2230,48
	% 15 O ₂	1706,28	1819,35	2256,68
	% 20 O ₂	1741,37	1811,52	2314,87

Combustion gases as HC, CO, CO₂ and NO_x has been given in table 5. The increase in excess air coefficient has reduced the emissions.

Table 5. Emission values

Excess Air Coefficient	Oxygen Rate	HC Emissions	CO Emissions	CO ₂ Emissions	NO _x Emissions
$\lambda=1$	Unenriched	0.002541	0.000797	0.141755	1.893194e-05
	% 5 O ₂	0.003046	0.001005	0.146438	3.41634e-05
	% 10 O ₂	0.003312	0.000965	0.150443	6.651632e-05
	% 15 O ₂	0.003313	0.000943	0.155415	0.0001337609
	% 20 O ₂	0.003615	0.000980	0.159503	0.0002152814
$\lambda=1.1$	Unenriched	7.2360e-10	1.2707e-08	0.137590	8.439468e-05
	% 5 O ₂	8.0348e-10	1.4145e-08	0.142296	0.0001812557
	% 10 O ₂	8.2103e-10	1.4395e-08	0.146649	0.0003672701
	% 15 O ₂	1.3979e-09	2.3800e-08	0.150964	0.0005423053
	% 20 O ₂	1.6827e-09	2.7207e-08	0.157487	0.0007332292
$\lambda=1.2$	Unenriched	6.0576e-11	1.3016e-09	0.126446	6.989459e-05
	% 5 O ₂	7.7895e-11	1.6677e-09	0.130610	0.0001585545
	% 10 O ₂	9.7597e-11	2.0410e-09	0.135068	0.0003061678
	% 15 O ₂	2.0249e-11	4.6194e-10	0.140085	0.0006351819
	% 20 O ₂	1.5617e-10	3.2048e-09	0.143411	0.0009172218

4. Conclusions

Numerical analysis on the combustion chamber of a boiler has been performed for oxy enriched methane fuel. In this study, different excess air coefficients and oxygen enrichment ratios have been used to investigate temperature distributions and emissions. The following results have been achieved:

- Maximum furnace temperature has increased in direct proportion to excess air coefficient.
- For each excess air coefficient, increasing in oxygen enrichment rates has provided increment in outlet and maximum temperatures.
- Influence area of maximum temperature is wider for excess air coefficient value of 1.0 by comparison with others.
- HC, CO and CO₂ emissions have decreased by increasing of excess air coefficient.

References

- [1] Kiriishi, K., Fujimine, T., & Hayakawa, A. (2009, October). High efficiency furnace with oxy fuel combustion and zero-emission by CO₂ recovery. In 24th World Gas Conference (Vol. 5). International Gas Union Buenos Aires, Argentina.
- [2] https://en.wikipedia.org/wiki/Oxy-fuel_combustion_process
- [3] Habib, M. A., Mokheimer, E. M., Sanusi, S. Y., & Nemitallah, M. A. (2014). Numerical investigations of combustion and emissions of syngas as compared to methane in a 200MW package boiler. *Energy Conversion and Management*, 83, 296-305.
- [5] Shaddix, C. R., & Williams, T. C. (2017). The effect of oxygen enrichment on soot formation and thermal radiation in turbulent, non-premixed methane flames. *Proceedings of the Combustion Institute*, 36(3), 4051-4059.
- [6] Heil, P., Toporov, D., Förster, M., & Kneer, R. (2011). Experimental investigation on the effect of O₂ and CO₂ on burning rates during oxyfuel combustion of methane. *Proceedings of the Combustion Institute*, 33(2), 3407-3413.
- [7] Habib, M. A., Nemitallah, M. A., Ahmed, P., Sharqawy, M. H., Badr, H. M., Muhammad, I., & Yaqub, M. (2015). Experimental analysis of oxygen-methane combustion inside a gas turbine reactor under various operating conditions. *Energy*, 86, 105-114.
- [8] Cheong, K. P., Li, P., Wang, F., & Mi, J. (2017). Emissions of NO and CO from counterflow combustion of CH₄ under MILD and oxyfuel conditions. *Energy*, 124, 652-664.
- [9] Mardani, A., & Ghomshi, A. F. (2016). Numerical study of oxy-fuel MILD (moderate or intense low-oxygen dilution combustion) combustion for CH₄-H₂ fuel. *Energy*, 99, 136-151.



Chapter – 4

Corporate Presentations

Wind turbine fires

Necmi Cemal ÖZDEMİR(1)

Kocaeli Üniversitesi, Mühendislik Fakültesi, Elektrik Mühendisliği Bölümü

necmi.ozdemir@kocaeli.edu.tr

Fikret KIR(2)

Demo Fire Genel Müdürü

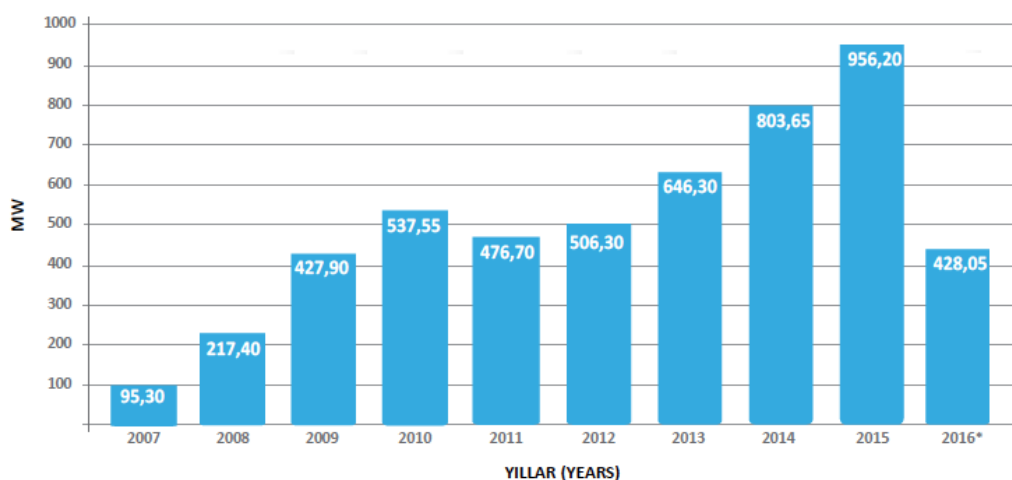
fikretkir@yahoo.com

The World has started looking for other energy resources besides fossil fuel-based energy sources to meet its ever increasing energy need. Investments on many new alternative energy sources have gained a huge increase in recent years.

One of the most invested and talked about sources is renewable or clean energy sources. There are many clean energy sources but one of the most important branches of renewable or clean energy is Wind Energy. Because wind energy emerges as one of the most cost effective investments in the renewable energy segment. For this reason, in recent years, electricity generation from wind energy has increased significantly. Wind Energy Plant investments in energy production continue to increase every year, and the share of energy generated from the Wind Energy plants in total energy production is increasing. Wind Energy sector; with the incentives provided to investors all over the World and its affordable price in installation and commissioning, and the free raw material costs; is showing an ever increasing popularity.

Also, wind energy has become one of the leading sectors in the renewable energy sector because of its ability to offer a sustainable energy solution.

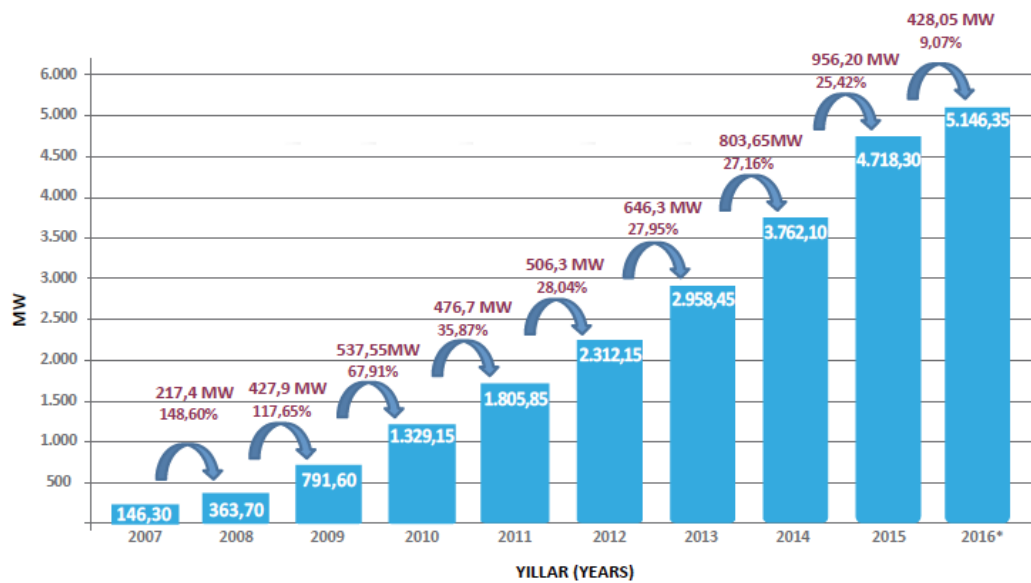
In our country, investments in the wind energy sector have shown a considerable increase. Our wind energy investments are increasing every day because of considerable investment incentives, and the constant increase in energy demand of country. According to TUREB data, an installation of 956.20 MWA in 2015 and an installation of 428 MWA in the first half of 2016 was established, and it is expected that this installation will exceed 1000 MWA by the end of 2016.



In total energy installation, the wind energy installation was 146 MWA in 2007 and it increased to 5.146 MWA in the first half of 2016. In other words, the share of wind energy in energy production is increasing every day. The number of wind energy plants in our country is 127 and 15 are operated by investors. The wind energy plants are mostly established in the

Marmara, Aegean and Mediterranean regions. Balıkesir, İzmir, maina and Hatay are the ones that receive the most wind energy investments. In addition, there are 54 new RES investments currently under construction, and the number of new investment companies investing in RES is also increasing everyday.

Türkiyedeki Rüzgar Enerjisi Santralleri için Kümülatif Kurulum *Cumulative Installations for Wind Power Plants in Turkey (MW)*



However, just like in every new sector, the wind energy sector faces a lot of challenges. One of those -in fact, is a concern for us as well- is fire. Due to the fact that it is a new sector, we do not have much knowledge and experience about fire, fire protection, fire prevention and fire risk management in wind energy sector. Scientifically only some hypotheses and limited experiments can guide us in this subject. Also, the statistic data can guide us in the wind energy sector on fire, fire protection, fire prevention and fire risk management.

Turbine Structure

First of all, knowing the wind energy turbine construction will help us in the basic assessment. Even though there are many brands and models, wind power plants are basically produced with similar technics.

Such as;

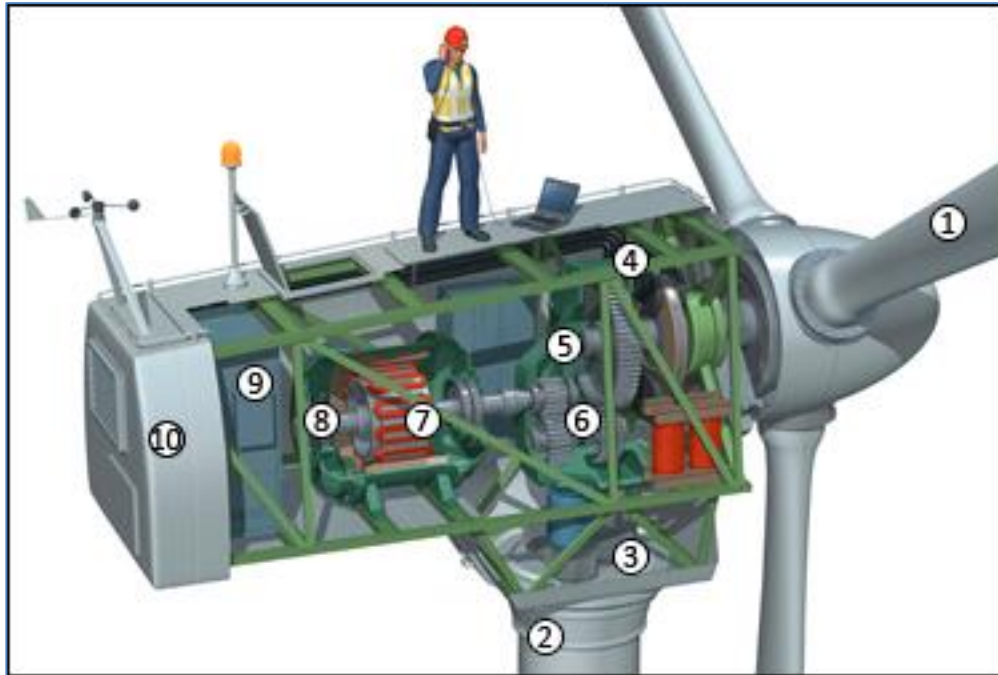
- 1- Wings: The wind that hits the wings, causes the wings to rotate. It is the component which the rotation motion happens at.
- 2-Tower: It is the component that's placed on top of the tower.
- 3- Yaw System: Allows the turbine to rotate in the wind direction.
- 4- Brake System: In case of emergency, it stops the movement of the rotor by a mechanical, electrical and hydraulically applied disk.
- 5- Low speed shafts: It is the mechanism in which low speed shafts are housed.
- 6- Gearbox: It houses the mechanism of low and high speed shafts. It increases the low speed rotary load for the high speed shaft, which comes from the low speed shaft that is connected to the rotor.
- 7- Generator: It converts mechanical energy into electricity.
- 8- High speed shaft; It is the mechanism which the high speed shafts are housed.

9- Nacelle Control Cabin: Stops or starts turbine at certain wind speeds.

10- Nacelle: It contains a gear box, low and high speed mill, generator, control unit and brakes.

11-Anemometer and Wind Gauge: Measures the wind speed and transmits it to the control system.

12-Lightning rod: Used for lightning protection.



Again as seen in the picture below; There are cable ways in the tower and transformer or connection box in many towers.



If we make an assessment in the frame of fire technic; the three main elements of the basic fire triangle; the fuel, oxygen, and ignition-heat source (electrical, mechanical and lighting), are located in the Nacelle section. Also the locations of flammable cables, the transformer or the control box in the tower section are the areas with the risk of fire.

There are many flammable materials in the manufacturing of the wind turbines that are lighter and used to reduce costs; Fiberglass reinforced polymers, foamed insulation and cables. Moreover, due to the large oil reservoirs that are used to lubricate mechanical parts, the fuel load on a turbine's nacelle is often too large.

When fire starts, the chances of fire intervention are very low because of the height of nacelle and the wind power plants are usually located in remote areas from the city.

Furthermore, because the turbine manufacturers do not share almost any technical details with the intention of protecting their proprietary technology, it is very difficult to carry out scientific studies for fire prevention. Turbine manufacturers do not share their technology nor they give information about system failures. The technical reports after fire accidents don't get shared as well in order to protect the reputation of the company. Because of that, it is not yet possible to assess the impact of fires on the global energy sector accurately. The sources of information we currently use are incomplete or contain general information and do not contain any special technical data that is not publicly available.

Fire Data

When we evaluate with known data; it can be said that about 25% to 35% of the damages that occur in wind turbines come from the fire accidents, which is a very high rate. The main

reason why the rate of fire is high is that the wind turbine materials are highly flammable. Many fires were not actually analyzed and reported, but at 90% of reported fires turbines that were exposed to fire became unusable. Generally, wings, nacelle, mechanical and electrical components have been damaged in great proportions. Fire damage to the wind energy plant is always serious because reaching to the turbine is hard and fire intervention is almost impossible.

It is known that wind turbine fire statistics have been recorded in Western countries since 1970. It's become evident that fire accidents have increased between 1995 and 2015. The main reason for this is the fact that the fire prevention technologies did not develop adequately despite the increase in power output of wind energy plants. Some of the turbine producers have declared that they are also working on this issue. Since this is a new sector in our country, there is almost no data that we can reach. Fire damage is already the highest rate of damage compared to almost every other sector in our country. Therefore, there are almost no measures, records and actual data in our country in the wind energy plant sector.

Combustion Sources

In order to understand wind turbine fires and to understand fire protection measures, it is first and foremost important to identify and understand the source and amount of fuel loads.

The fuel load on the nacelle part of the wind turbine is usually very high, but fire risk varies depending on the turbine type. The nacelle section usually contains the following components as a combustion source.

Nacelle Body :

Nacelle main body-wall construction include light but flammable or has low fire resistance materials like polymers and fiber materials. Typically, the nacelle part of the wind turbine is made of glass fiber reinforced plastic. The Glass fiber reinforced plastic material is the main element that increases the flame spread and the fire load. The epoxy resin used to bond and harden the composites when the Glass fiber reinforced plastic composite system is being constructed is a highly flammable material and it also releases highly toxic lethal gases during combustion. Nacelle has a lot of fire risks because there are many flammable, ignition equipment side by side in Nacelle, and there is no fire cell - zoning because of application difficulty.

Insulation Materials :

Insulation materials used in Nacelle manufacturing have potentially heavy fire load. The materials used for internal sound insulation, usually made of foam, are also an important part of the potential fire load. Foam insulation materials are not only highly flammable, they can easily suck spilled oil due to their spongy structure and thus create a greater potential for fire.

Wires :

The cables used for energy transmission, control, lighting etc. are already flammable materials. Low voltage electrical installation and the long electric cables carrying medium to high voltage from NASEL to the base of the tower, also have potential high fire loads. These cables are designed and installed in the form of Copper-Aluminum-Copper for economic reasons. This design is the reason of most of the fire accidents in wind energy plants.

Oils :

Furthermore, lubricants used in gear boxes, transformers and brake systems are materials that have potential for heavy fire loads. For example, up to 900 liters of oil can be found in a single 1.5 MW wind turbine. Nacelle gear system has 450 liters of grease. In addition to that, wastes containing uncleaned oil constitute an additional fire hazard. In direct drive turbines newly developed by some turbine manufacturers, there is no risk of fire from the gear system,

but there is still a large amount of oil used in other systems in Nacelle - such as hydraulic oils, lubricating oils.

Transformer:

The transformer, which can be found in the bottom of the boiler or sometimes in the nacelle on the top of the boiler, creates a serious potential fire load. For turbines below 1 MW, the transformer is located at the base of the tower. On the other hand, it is placed inside the nacelle on turbines above 1 MW. This situation increases the risk of fire in the nacelle to a higher level, and limits the possibility of fire intervention. However, when the transformer is on the ground it does not reduce the general fire risk. Because if the selected transformer is an oil type transformer, it can contain an average of 2500 liters of transformer oil.

Groups Of Transformers:

In the wind energy plants, the high-voltage transformer stations to which all turbine groups are connected also present a separate risk of fire, each of which may contain over 45,000 liters of transformer oil.

Fire Starting Sources

The most basic cause of fire in wind turbines is electrical current. However, fires that occur during repair and maintenance and mechanical sparks that originate from excessive friction are also common causes of fire accidents. It is possible to categorize the causes of fire in wind turbines as outsourced and internal sources.

Lightning strike is the primary cause of outsourced fire accidents. Statistics show that the lightning strike is the most common cause of outsourced fire accidents on wind turbines. Sea turbines operating in harsh weather conditions, multi-megawatt land turbines of over 100 meters in height and turbines placed at high altitudes all face high risk of a lightning strike. The risk of fire increases considerably when there is not enough lightning protection system.

Fire accidents that happen because not following safety guidelines or faulty work done by unqualified personnel during turbine maintenance is also categorized as outsourced fires. Though very rare, fire due to intentional sabotage and terrorist attacks are also categorized as outsourced fires.

Internal fires are fires arising from the system itself during design, installation, manufacturing and operation. These fires can occur due to electrical, mechanical and electromechanical parts. The table below shows the percentage of domestic fire.

FIRE STARTING REASON	% ORANI
Electrical system, Cables and connection equipment	24%
Electronic control system	18%
Sensing and control sensors belonging to the systems	10%
Hydraulic system and equipment	10%
YAW system (Nacelle guidance system by wind)	7%
Wings	7%
Mechanical braking system and equipment	5%
Rotor and shaft systems	5%
Generator system and equipment	4%
Gearbox	4%
Nacelle - Main compartment	4%
Drive system and equipment	2%

Turbine fire can start from a short circuit or over-current in the control system, electricity generation, transmission. Overheating and overloading of electrical and electronic components can lead to fire. Short circuits, arcs and inadequate electrical protection are common causes of fires in wind turbines. In order to avoid this risk, it is first necessary to design the project correctly, to use quality equipment, to tightly inspect the assembly works with the professionals, and to carry out the planned maintenance and inspection in a timely manner.

The occurrence of fires due to mechanical heating is also a serious risk. A fire may start if the flammable materials contact hot surfaces such as gearboxes and mechanical brakes, and the oil in an overheated gearbox may start to burn. In general, all equipment that has the potential to generate heat or contains flammable liquids is a potential source of fire. In wind turbines, systems such as generators, azimuth engines, gear boxes, hydraulic equipment are systems that are risky to start a fire.

Mechanical braking systems are also used when aerodynamic brakes in emergency situations are insufficient to stop the turbine. Mechanical brakes can reach very high temperatures during stopping turbine at high speeds, and can produce sparks, increasing the risk of fire.

It is also a risk of fire with oil spillage, hydraulic pump malfunctions, hydraulic hose punctures, and contact of flammable oils with hot surfaces.

Fire Precautions In Wind Turbines

There are no regulations in our country regarding fire precautions to be taken in wind turbines. BYKYH does not cover this subject anyway. Therefore, we can only refer to basic fire science and dynamics and information in the NFPA 850 standard book. In NFPA 850 booklet there is “Chapter 10 Identification and Protection of Hazards for Wind Turbine Generating Facilities”. Designs should be made to reduce the burden of fire with an accurate and good engineering solution and fire precautions should be taken seriously.

Fire prevention measures for wind turbines can be called passive measures and fire protection measures can be called active measures.

Passive Fire Protection Methods

1- The general piping system should be constructed in accordance with NFPA 30 rules and following points should be taken into consideration.

Piping installations must be rigid and fixed in such a way that they are not affected by vibrations.

Welded pipe connections, models with threaded connections, instrumentation tubes, pipes and indicators must be protected against accidental mechanical damage. All mechanical connections must be protected.

Pipe connections and piping should be passed through areas that will not leak into the electrical installation.

Systems must be constructed to collect oil spills in a way that cannot cause fire.

2- the whole turbine system must be protected with a SCADA-control-alarm-trip system which includes the following.

- Grid disturbance
- Yaw system limits and errors
- Brake system errors
- Vibration Abnormality
- Overspeed (including wind conditions)
- Temperature faults – (high temperature and temperature anomalies)
- Oil condition (gearbox / lubrication and hydraulic)

- Motor protection
 - Loss of communication between modules or with control center
 - Blade angles and battery status
- 3- Oils; Gearbox oils, Hydraulic and lubrication oils should not be easy to catch fire. The use of non-flammable hydraulic and lubrication oil is an important passive fire prevention choice. In addition to this, it is necessary to design pipe designs which will minimize the amount of oil to be used.
- 4- Cable connections and attachments; It is important to select the appropriate power and control cables in the tower or nacelle and to make the cable connections correctly. If the system has aluminum and copper cable connections, these connections must be done properly. All connections and attachments should be checked periodically.
- 5- Accumulator; in the system for the accumulator to be used for the backup power supply control system dry type should be selected and the necessary maintenances should be made in accordance with the standard guidelines.
- 6- Heaters; It is important that the electric heaters used in sections such as gearbox oil or in the nacelle are made to conform to the quality standards.
- 7- Lightning protection system; Wind turbines carry a very high risk of lightning due to their location and structure. Lightning damage in wind turbines can lead to great damage. These events, which usually result in fire, cause the destruction of the turbine, leading to massive financial losses. The wing breaks due to Lightning Fall and the resulting imbalance and destruction are frequently encountered. Lightning Damage risk should be minimized by taking some precautions.
- Inner Lightning Systems: These systems are circuit elements that take direct or indirect lightning strike to be safely transferred to the ground by protecting electronic devices in the building's interior.
- External Lightning Systems can be examined in two parts as lightning rod and Faraday cage. Faraday cages are used in nacelle in wind turbines. If we compare two systems, the faraday cage is a higher-cost system that must be used with lightning arresters to protect from the fringing effects of lightning discharge.
- 8- Grounding System: The most important thing to be considered in earthing systems is that the grounding resistance will rise over time. The most important factor affecting this is the corrosive effect. For this reason, the galvanized strips to be used in the base earthing must be stainless steel and their thickness must conform to DIN EN50164-2 standard. In our country these standards are stated in TS EN 62305. Furthermore, the use of corrosion bands at each connection point is important for plant sustainability. Basic grounding planning should be done with calculations made within the scope of the specific resistance obtained as a result of the construction of the wind energy plant ground survey. The system should be strengthened with chemicals that are able to freeze.
- 9- Equivalent Potential System; Equivalent potentialization is the most reliable grounding system. All groundings and metal sections in a system must be connected to each other by means of equipotential lines. Thus, the potential difference between grounding and any two metals can be avoided and equal potential is achieved at all points
- 10- Structurally hard to burn materials should be preferred in the production of nacelle. Material that does not spread flames should be chosen. During the design process, heat barrier on nacelle and passive stoppers should be put if possible.
- 11- It is very important to avoid as much as possible from the hot work carried out during maintenance, and to take measures if it has to be done. If possible such work should be carried out by cold procedures (cutting, screwing, cold bonding, etc.)

Active Fire Protection Methods (Systems that activate in the fire accident)

- 1-Fire Detection Systems
- 2-Fire Extinguishing Systems

1- Fire Detection Systems:

Designing of fire detection and alarm systems and keeping them in continuous operation is a very important precaution.

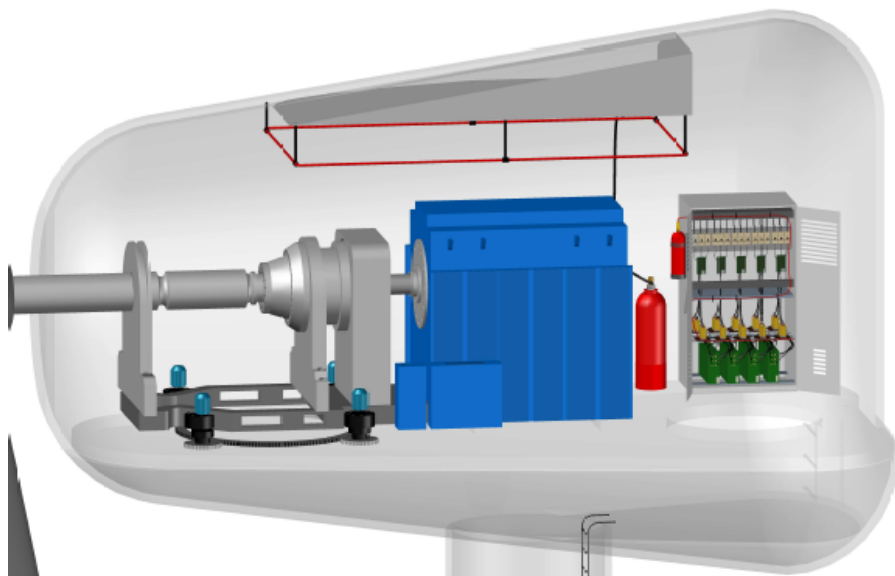
Fire alarm systems should be installed as interactive addressable, analogue addressable or general type in the nacelle, tower and in the transformer zone and apply the necessary automation scenario to reduce the fire propagation to the minimum after the system detects fire according to the determined fire scenario. It is important to select appropriate detectors and determine the correct scenario and add them to automation. Within the scenario; Shutdown of the fans, closing of the main switches, and closing of the oil valves.

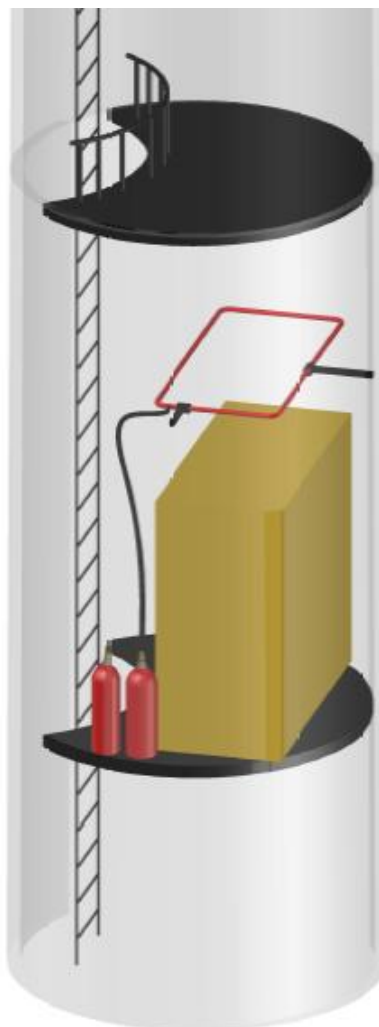
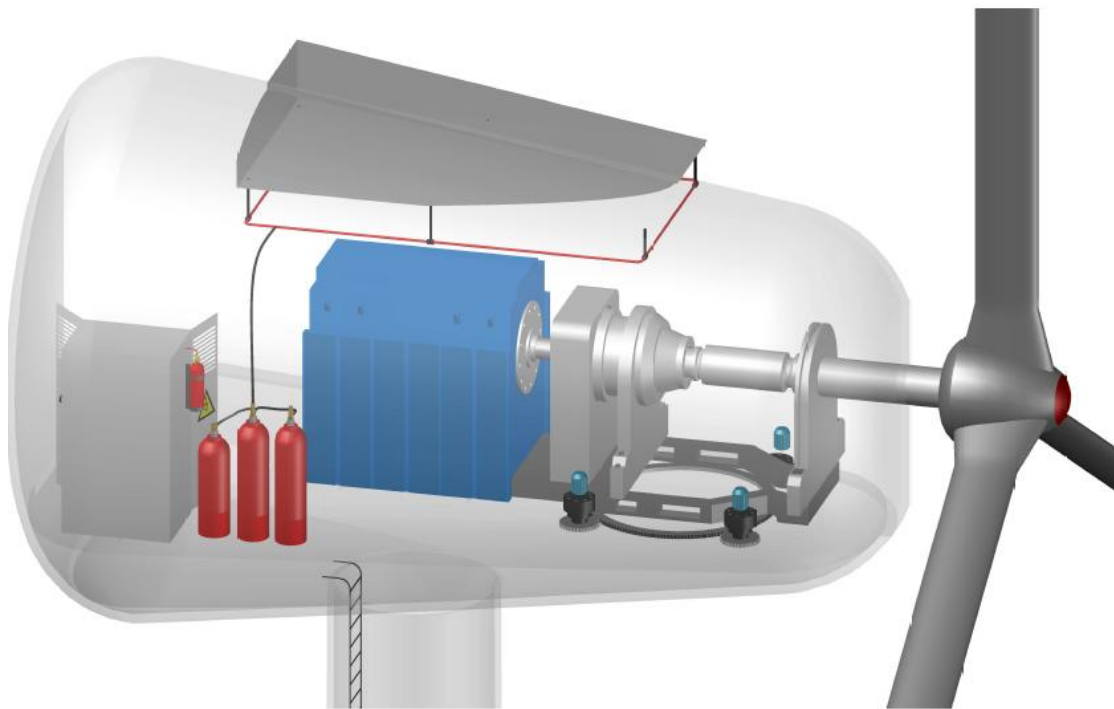
2- Fire Fighting systems:

The application of automatic fire extinguishing systems in wind turbines is very important in order to minimize the damage that can be caused by fire and to be able to extinguish the fire quickly at the start.

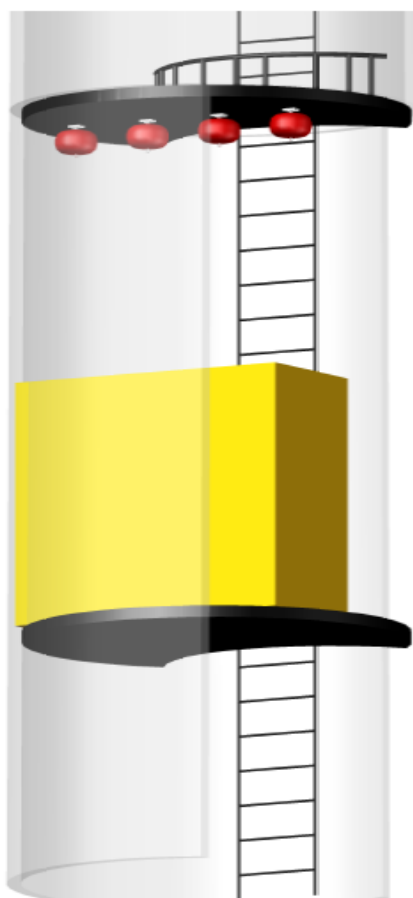
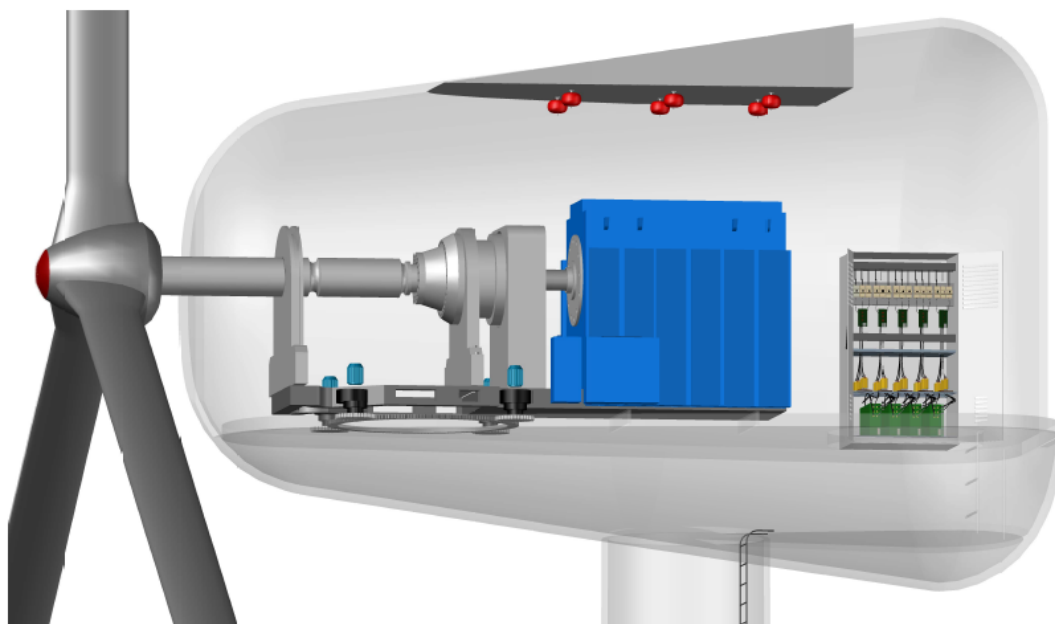
a- Gas Automatic Extinguishing Systems; Automatic gas extinguishing systems, which are commissioned in accordance with the cross zone independent sensors or connected to an alarm system, can be used in all Nacelle, in electrical panels and in transformer sections. Any of the gases listed as extinguishing agents in gas extinguishing systems can be used. One of the important points here is the necessity of closing the fans and air damper before the system starts. It is important of the leaktightness of the area to be extinguished in gas systems.

b- Watermist Extinguishing Systems; Automatic watermist extinguishing systems, which are commissioned in accordance with the cross zone independent sensors or connected to an alarm system, can be used in all Nacelle, in electrical panels and in transformer sections. The use of endothermically reactive - wet chemical agent additive systems will be a more effective solution. Low-pressure and conformant to non-pump standards must be designed.





c- Hanging Portable Automatic Extinguishing Systems; Suspended portable extinguishing systems that are automatically activated depending on the temperature can be used in all Nacelle, in electrical panels and in transformer sections. The use of endothermically reactive - wet chemical agent additive systems will be a more effective solution.





d- Pressurized Foam Extinguishing Systems; Automatic foamed extinguishing systems that come into commission depending on the cross zone independent perceived or connected to an alarm system can be used in all Nacelle. It must be designed in accordance with NFPA 11 standards. Not preferred for electrical systems.

Extinguishing systems can also be mixed, ie they can be applied to several different systems at the same time. Engineering design principles are important factor here. First, a proper risk analysis should be done and the most suitable automatic extinguishing system design should be done considering the turbine manufacturer's directives.

References

WIND TURBINE ACCIDENT AND INCIDENT COMPILATION REPORT 2016

NFPA 850

NFPA 70

NFPA 72

NFPA 101

NFPA 99

NFPA 550

OVERVIEW OF PROBLEMS AND SOLUTIONS IN FIRE PROTECTION ENGINEERING OF WIND TURBINES(SOLOMON UADILE,EVIO URBAN 1,RICK CARVEL,DAVID LANGE,GUILLERMO REIN)"Overview of Problems and Solutionsd in fire protection engineering of wind turbinesé presentation by dr Ricky carvel caevel from the university of edinburg at the 11th international aassociation of fire safety science (iafss)Symposium.

Yangın yayılımı etkileri düzleminde tünel yangınları - tunnel fire with HRR

Günümüzde karayolları ulaşımında en önemli konulardan biri tüneller ve geçitler haline gelmiştir. Günümüz teknolojik imkanların ve ihtiyaçların etkisiyle yüksek otomasyona sahip gelişmiş tüneller kara ulaşım dünyasına her geçen gün daha fazla girmektedir. Bu hızlı gelişim emniyet ve güvenlikle ilgili sorunları da beraberinde getirmektedir. Bu sorunların en önemlilerinden biri de bu yapılarda- tünellerde oluşabilecek yangın riskidir. Tünel içlerinde oluşabilecek bir yangından kaçış olanaklarının sınırlılığı, itfaiye olanaklarının yangına ulaşmasındaki zorluğu, insan gücünün kısıtlı olması nedeniyle yangın güvenliği ve yangınla mücadele açısından iyi planlanma ve eğitim gerekmektedir.

Tünel imalat ve işletmeciliğinde yangına karşı alınacak aktif ve pasif önlemler ile beraber yangınla mücadele önlemlerini de en iyi biçimde tasarlamak ciddi bir gerekliliktir.

Hayatımızın hemen hemen her kademesinde yaşanan yangın deneyimleri yangın güvenlik taktiklerinin, yönetmelik ve standartların oluşumunda etkili olmuştur. Bu nedenle çok geniş bir yelpaze içinde incelenebilecek olan bu konuda tünellerde yangın güvenliği ve risk durumları değerlendirmeye alınacaktır.

Heat Rate Release – Yangın Yayılımı ve yangın dinamiği baz alınarak tünellerde alınabilecek aktif ve pasif yangın güvenlik önlemlerinin performansa dayalı tasarımı üzerine çalışmak günümüzde en optimal çözüm olarak ortaya çıkmaktadır.

Hali hazırda Devlet ve il Yollarımızda ;

500m'den kısa tünel sayısı :113

500m-1000m arasındaki tünel sayısı :28

1000m-2000m arasındaki tünel sayısı :14

2000-3000m arasındaki tünel sayısı :3

3000m'den uzun tünel sayısı :1

Olmak üzere Toplamda 160 adet tünel bulunmaktadır.



Otoyollarımızda ;

500m'den kısa tünel sayısı :12

500m-1000m arasındaki tünel sayısı :9

1000m-2000m arasındaki tünel sayısı :3
2000-3000m arasındaki tünel sayısı :1
3000m'den uzun tünel sayısı :2
Olmak üzere Toplamda 27 adet tünel bulunmaktadır

2023 Yılında ise ülkemizdeki tünellerin sayısında ciddi bir artış olacaktır.

TÜNEL ENVANTER	SAYI (adet)		UZUNLUK (m)	
	>500m	Toplam	>500m	Toplam
DEVLET VE İL YOLLARI	46	160	74.528	102.394,68
OTOYOLLAR	15	27	38.386	44.353
YAPIM VE PROJE AŞAMASINDA	34	51	174.942	183.360
HEDEF (2023)	95	238	287.856	330.054,68

Ülkemizdeki istatistikler incelendiğinde, tünellerde, açık yollara göre daha az yangın çıkmaktadır. Çünkü tüneller, açık yollara göre daha iyi kontrol altında tutulan alanlardır. Burada aydınlatma ve işaretler normal yollara göre daha iyidir. Hava koşullarından araçların daha az etkilenmesi söz konusudur. Bütün bunlara rağmen ;
187'den fazla karayolu tüneli olduğu düşünülürse, buralarda çıkacak yangınların tahmin edilenden daha ciddi facialara ,yol açması söz konusu olabilir

PIARC (World Road Association) tarafından incelenen karayolu tünel kazalarında meydana gelen yangınların nedenleri şu şekilde sıralanmıştır.

- Elektrik arızaları (hafif araçlarda en sık olarak yangın sebebi),
- Fren balatalarında meydana gelen ısınmalar (ağır taşıtlardaki yangınların %60-%70'inin sebebi),
- Aracın kendi kendine alev almasına yol açan diğer arızalar.

Daha az karşılaşılan kaza nedenleri:

- Çarpışmalar,
- Tünel ekipmanındaki teknik hatalar,
- Tünellerde yürütülen bakım çalışmaları.

Tünelde meydana gelecek olası bir yangının boyutları yangın çıkan aracın yükü ve tipine bağlıdır.

- a. Özel araçlar (motor, kısa devre, karbüratör...)
- b. Ağır taşıtlar (lastik, fren, motor, branda...)
- c. Ağır taşıtların yükü
- d. Tehlikeli madde taşıyan taşıt yangınları.

SON 40 YILDA TÜNEL YANGINLARI

1975	Moorgate , Londra	44 ölüm	
1975	Mexico City Metro su	50 Ölüm	
1979	Nihonzaka Tüneli Japonya	7 Ölüm	189 Araç Hasarı
1982	Caldecott Tüneli , USA	7 Ölüm	
1984	Summit Tüneli, UK		Tren ve 13 tanker
1987	King's Cross , Londra	31 Ölüm	
1993	Serra a Ripoli , İtaya	4 Ölüm	11 HGV + 11 Araç Hasarı
1995	Bakü Metro su	260 Ölüm	
1996	Channel Tüneli - Manş		10 HGV
1999	Mont Blanc Tüneli , Fransa	39 Ölüm	34 Araç Hasarı
2000	Kaprun Tunel , Avusturya	155 Ölüm	
2001	St Gotthard Tüneli ,İsviçre	11 Ölüm	23 Araç Hasarı
2003	Daegu Metro ,Güney Kore	200 Ölüm	
2005	Frejus Tüneli , İtalya	2 Ölüm	4 HGV
2007	Burnley Tüneli , Avustralya		
2008	Channel Tüneli - Manş		650 metre hasar
2009	Eiksund Tüneli, Norveç	5 Ölüm	
2013	Bratli Tüneli , Norveç		5 Gün devam etti

Son 40 yılda yukarıdaki tabloda görüleceği üzere bir çok tünel yangını olmuştur.

Tünel yangınlarını standardize etmek mümkün olmadığı için yangınla mücadele konusunda alınabilecek önlemler için çeşitli deneyler ve önlem önerileri geliştirilmektedir.

Amerikan Ulusal Yangından Korunma Birliği (NFPA - National Fire Protection Association) karayolu tünellerinde alınacak önlemler hakkında standartlar getirmiştir.

NFPA 130, Standard for Fixed Guideway Transit and Passenger Rail System, 2010.

NFPA 502, Standard for Road Tunnels, Bridges and Other Limited Access Highways, 2011.

İngiliz Ulaştırma Bakanlığı (Department of Transport), karayolu tünellerinde dizayn kriterleri konusunda standart oluşturacak çalışmalar yapmıştır.

4 yılda bir toplanan Yol Kongrelerinin Daimi Uluslararası Birliği (Permanent International Association of Road Congresses) karayolu tünelleri konusunda özel teknik komite raporları yayınlanmaktadır.

Her ne kadar, TS 4156 / Ocak 1991, Umumi Yerlerde Yangından Korunma - Genel Kurallar yayınında otoparklar, terminaller, araçlar gibi bölümler varsa da bu önlemlerin **karayolu tünelleri yangın önlemleri konusu ile fazla bir özel bilgi –kurallar bulunmamaktadır.**

Tünellerde Yangınla Mücadele;

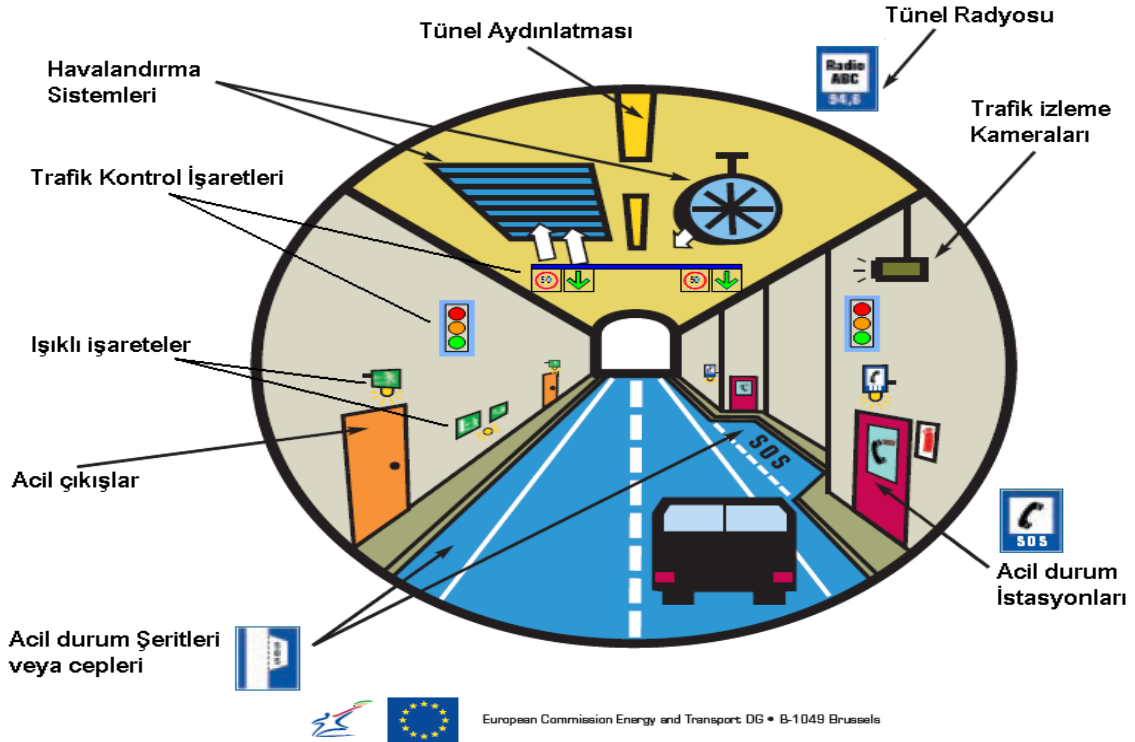
Tünel yangınları ile mücadele uygun ve gerekli ekipmanın tünelde bulunması ve kullanılmasından öteye tam bir risk yönetim çalışması gerekmektedir.

Yangınla mücadele sırasında trafik kontrolü, havalandırma, haberleşme, drenaj, acil durum ekipmanı, acil durum aydınlatması ve otomatik söndürme sistemeleri arasındaki esgüdüm çok önemli bir ver tutmaktadır.

Tünel Yangınları için Alınan Önlemler;

- 1- YAPISAL ÖNLEMLER
- 2- ALARM VE ALGILAMA SİSTEMLERİ
- 3- HAVALANDIRMA VE DUMAN TAHLİYE SİSTEMLERİ
- 4- ACİL DURUM İSTASYONLARI
- 5- ACİL AYDINLATMA SİSTEMLERİ – İŞARETLEMELER
- 6- CCTV İZLEME SİSTEMLERİ
- 7- ACİL HABERLEŞME SİSTEMLERİ
- 8- YANGIN SÖNDÜRME SİSTEMLERİ

Karayolu Tünellerinde Standart Güvenlik Sistemleri ve Ekipmanları



Yapısal Önlemler;

- Coğrafi koşullar uygunsa eğim %5 veya %5 den küçük olmalıdır.
 - Tünelin yapım karakteristiği izin veriyor ve aşırı maliyet getirmiyorsa acil şerit, sığınma cebi, yaya yolları ve acil haberleşme girintileri olmalıdır.
 - 1.500 m'den uzun çift tüplü tünellerde her 500 m'de bir acil servisler için enine geçişler olmalıdır.
 - Coğrafi koşullar uygunsa çift tüplü tünellerde çıkışlarda acil refüj geçişi olmalıdır.
 - Tüm tünel ekipmanlarının yangına dayanıklılık düzeyi, teknolojik imkanları ve bir yangın durumunda gerekli güvenlik fonksiyonlarının sürdürülmesi amacı dikkate alınarak yangına dayanıklı malzeme seçilmelidir.
- Yangının verebileceği zararları azaltmak için tünel yapı malzemesinin yangına ve sıcaklığa karşı mukavim olması gerekmektedir. Çelik kontrüksiyon bölümler en az iki saat süren yangına karşı dayanıklıdır olmalıdır.

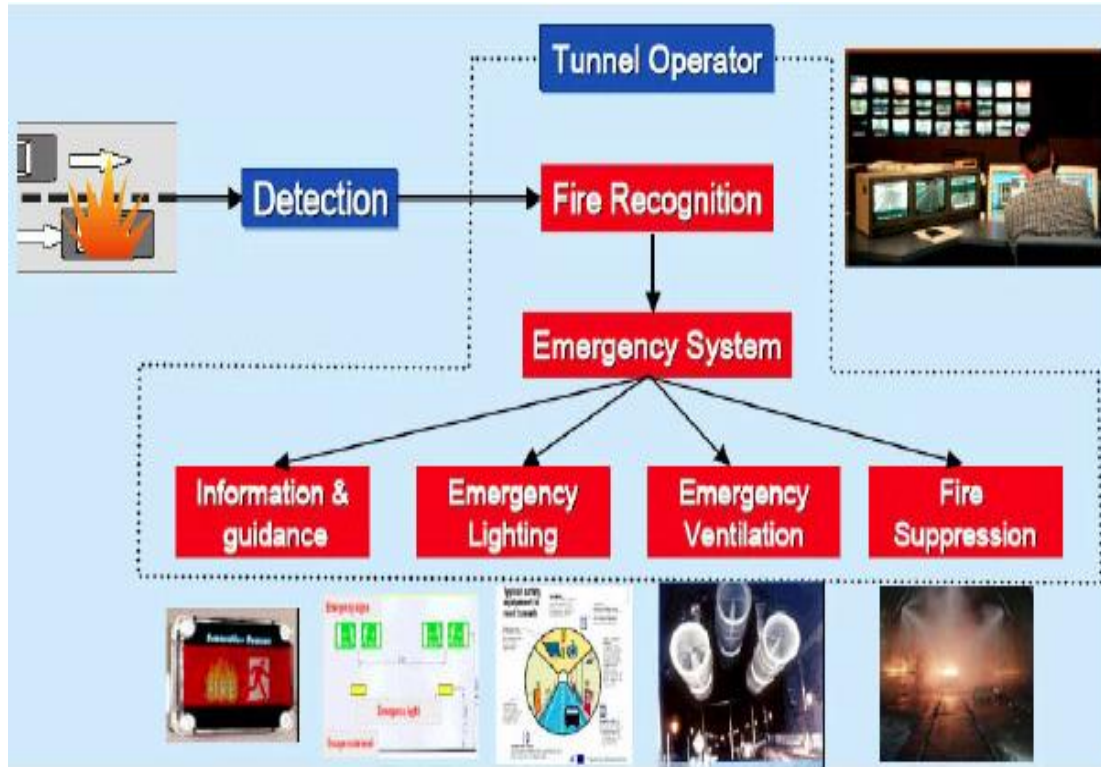
Tünel içindeki tüm kablolar alev iletmeyen, halojenden arıtılmış (sıfır halojenür) kablo olacaktır. Yanma deneylerinde HCl, HBr gibi halojen türü gaz ve SO₂, NO₂ gibi korozyona müsait gaz ve zehirli duman üretmeyeceklerdir.

Tünel içine kaplama yapılacaksa bu kaplamanın yanmaz malzemeden olması, duvarla arasında kalan boşlukta her 3 m'de bir yangın durdurucular konulması gibi konstrüktif önlemler de tünel dizaynının da yangınla mücadele bakımından göz önünde tutulması gerekli önlemlerdir.

Alarm ve Algılama Sistemleri;

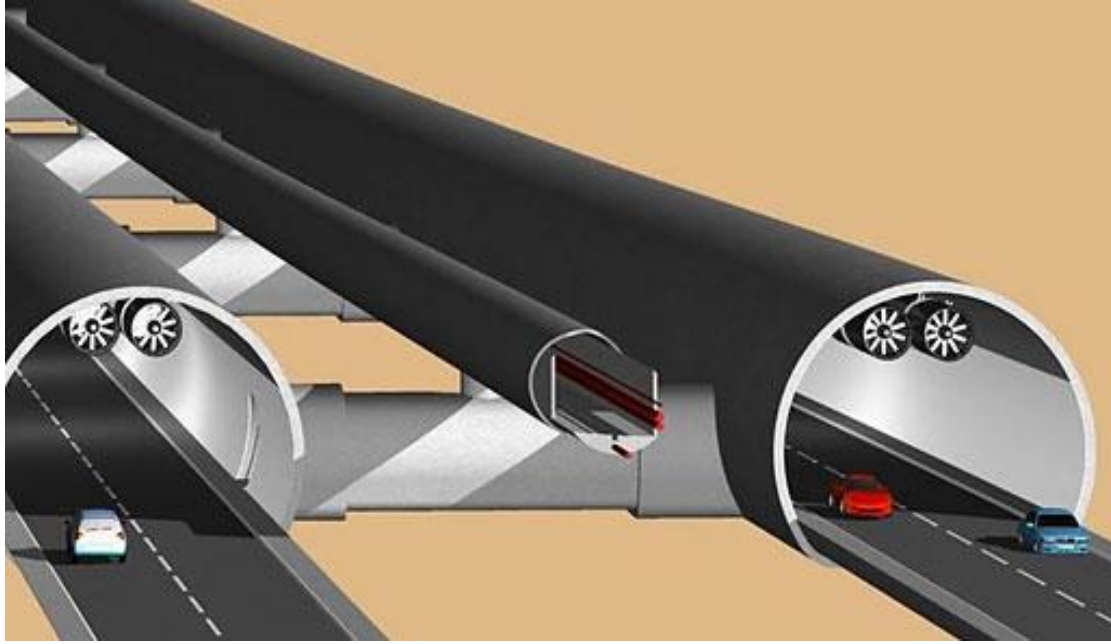
Tünellerde yangın algılama ve alarm sistemleri 1960'lı yıllardan bu yana kullanılmasına rağmen özellikle Avrupa'da 1999 ile 2001 yılları arasında yaşanan kazalar bu sistemlerin ne kadar önemli olduğunun daha çok anlaşılmasına sebep olmuştur.

Diğer taraftan klasik yangın algılama cihazlarının tünellerde erken algılamanın yanı sıra asılsız uyarılar verdiği/vereceği düşünülerek bu sistemlerin tesis edilmesi tereddüt konusu olmuştur.



HAVALANDIRMA VE DUMAN TAHLİYE SİSTEMLERİ ;

- 1.000 m'den uzun ve şerit başına 2.000 araçtan yüksek trafik hacmine sahip bütün tünellerde mekanik havalandırma sistemi tesis edilmelidir.
- 3.000 m'den uzun ve şerit başına 2.000 araçtan yüksek trafik hacmine sahip bütün tünellerde enine veya yarı enine havalandırma sistemi tesis edilmelidir.



Jetfan otomatik çalışma testi ;

Yangın algılama sistemine bağlı olarak otomatik devreye girme yada operatör tarafından elle başlatma şeklinde yapılır.

Sistem belirlenen senaryoya göre jet fanları çalıştırır ve tünelin sadece bir yönüne doğru duman tahliyesi yapacak şekilde çalışır.

Duman tahliyesi 4 metre / sn olacak şekilde jeftanlar çalışır.

Sistem testi 19 Lt Mazot ve 5 Lt benzin yakılarak yapılıyor. Yaklaşık 5 MW bir yangın gücü kullanılır.

ACİL DURUM İSTASYONLARI;

•En fazla 150 m’de bir acil haberleşme telefonu, kuru tip yangın söndürücü tüpü, acil durum butonu gibi ekipmanlar bulunan istasyonlar oluşturulmalıdır.

Tünellerde bulunan acil durum istasyonları içinde;

1 adet 6 LT KKT ABC tipi yangın söndürücü

1 adet 6 LT D tipi yangın söndürücü bulunmaktadır.

Bu YSC ler araç kullanıcılarının acil durumlarda kullanması amacı ile konulmaktadır. Ancak ABC yangın tipi ile D tipi yangını ayırabilecek sürücü nerdeyse yok gibidir.

Öneri ; ABCDK tipi endotermik söndürücülerin konmasıdır.



ACİL AYDINLATMA SİSTEMLERİ – İŞARETLEMELER ;

Bütün tüneller uzunluğuna bakılmaksızın aydınlatılmalıdır.

- Girişinden çıkışı görünen 500 m’den kısa tünellerde 2 kademeli (gece-gündüz) aydınlatma yapılabilir.

- Diğer tünellerde en az 6 kademeli harici ve dahili lüminansmetre ile kontrol edilebilen tünel içerisinde olduğu gibi giriş ve çıkış bölgelerinde de sürücülere yeteri gündüz ve gece görünürlüğü sağlayacak özelliklerde normal aydınlatma olmalıdır.

- Bir güç kaynağı arızası durumunda araçların tünel tahliye etmeleri için ve tünel kullanıcılarına asgari görünürlük sağlayan ve acil bir güç kaynağından sürekli beslenen bir güvenlik aydınlatması ve 1,5 m’den yüksek olmayacak şekilde tahliye işaret ışıkları ile acil durumda tüneli yürüyerek terk etmeleri için tünel kullanıcılarına kılavuzluk yapacak tahliye aydınlatması olmalıdır.

CCTV İZLEME SİSTEMLERİ ;

- 3.000 m’den uzun ve şerit başına 2.000 araçtan yüksek trafik hacmine sahip ve kontrol merkezi bulunan tünellerde yangın algılama, olay algılama, görüntülü izleme sistemi olmalıdır.

Tünellerde, güvenliği sağlamak ve olası saldırıları önlemek, trafik kazası araç bozulması veya yangın gibi olayları gözlemlemek ve tünelde bulunan cihazların görsel kontrollerini sağlamak amacıyla Kapalı Devre Televizyon Sistemi bulunmaktadır. Bu sistem aracılığı ile tüneller 7 gün 24 saat izlenmekte ve kaydedilmektedir. Tünellerde kameralar tünelin yapısına ve fiziksel özelliklerine göre kör nokta kalmayacak şekilde yerleştirilmektedir.

Kameralar operatörler tarafından canlı olarak izlenebildiği gibi otomatik olay algılama sistemi (AID) ile görüntü işlemeye tabi tutularak tünel içinde meydana gelen duran araç, tünel içinde yavaş, tünel içinde yabancı cisim gibi durumlar otomatik olarak algılanabilmekte ve operatöre bilgi verilmektedir.

ACİL HABERLEŞME SİSTEMLERİ;

Tünel ile kontrol merkezi arasında iletişimin sağlanması amacıyla tünel içinde belirli aralıklarda acil durum telefonları bulunmaktadır.

Bu telefonlar aracılığı ile kontrol merkezi ile doğrudan iletişime geçilebilmektedir.

Gelen telefon çağrıları SCADA sisteminde gösterilmekte ve kaydedilmektedir.

Her çağrı sonrasında SCADA sisteminde çağrı bilgilerini içeren bir rapor oluşturulmakta ve bu rapor operatör tarafından çağrı bilgilerine göre doldurulmaktadır.

YANGIN SÖNDÜRME SİSTEMLERİ;

Olası bir yangına müdahale edebilmek için tünel içinde yangın tüpleri ve hidrantlar bulunmaktadır.

Tünelde bulunan sulu yangın söndürme sistemi; yedekli pompalar, su basıncını dengelemek için jokey pompa, hidrantlar ve yangın dolaplarından oluşmaktadır.

Değerlerin standartların dışına çıkması veya sistemde bir arıza olması durumunda SCADA sistemi görsel ve sesli uyarı vererek operatörleri uarmaktadır. Böylece sulu yangın söndürme sisteminin her an hazır olması amaçlanmıştır.

Tünellerde meydana gelecek bir yangına müdahale için yerel itfaiye teşkilatı ile protokol yapılmakta ve olası bir yangında bu itfaiye teşkilatından yararlanılmaya çalışılmaktadır.

Ancak tüneller genellikle kırsal ve dağlık arazide olduğu için yerel itfaiyenin bölgeye ulaşması güç olmakta ve itfaiyenin ulaşım süresi ortalama olarak yarım saati aşmaktadır.

Tünel yangınları incelendiğinde bu sürenin çok uzun olduğu ortaya çıkmaktadır. Ayrıca itfaiyenin bir tünel yangınına müdahale edebilecek yeterli teçhizat, ekipman ve donanımına sahip olmadığı görülmektedir.

1999 yılında yayınlanan Dünya Yol Teşkilatı (World Road Association-PIARC) raporunda , tünellerde kurulacak otomatik yağmurlama sistemlerinin bir dizi sakıncasından bahsedilmiştir.

Bunlar, petrol türevleri ve kimyasallarla temasta patlama riski oluşturması, araç içi yangınlarda etkisinin zayıf olması, işletme maliyetinin yüksek olması, kaçanların görüş mesafesini düşürmesi olarak sayılabilir.

Teşkilat, 2000’li yıllarında ilk b.lümünde yaşanan felaketle sonuçlanan yangınlar ve UPTUN (Cost- Effective Sustainable and Innovative Upgrading Methods for Fire Safety in Existing Tunnels) gibi projelerin başlamasıyla, 2007 yılında yeni bir rapor yayınlamıştır.

Bu raporda, otomatik yağmurlama sistemlerinin yangınlarda bazı avantajlar getirebileceği belirtilmiştir.

2008 yılında detaylandırılan raporda, hızlı ve etkili bir algılama sistemiyle entegre edilen yağmurlama sistemlerinin, yangınlarda etkili olduğu belirtilmiştir.

Otomatik söndürme sistemleri araç içinde çıkan yangınları söndürme konusunda etkili değildir.

Ancak araçtaki yangının yayılma hızını yavaşlatarak, diğer araçlara sıçramasını engelleyecek, daha güvenli bir kaçış ortamı sağlayacaktır

Gerek konvansiyonel sprinkler sistemlerinde, gerekse su sisi sistemlerinde, tasarım yapılırken göz önünde bulundurulacak birtakım parametreler mevcuttur.

Bunlar; tünel geometrisi ve kesit alanı, trafik akışı (tek yönlü veya çift yönlü oluşu), tahmini yangın büyüklüğü, (tehlikeli madde geçişine izin verilen tüneller), kaçış yollarının tasarımı, havalandırma sistemi tipi, tünel izleme ve yangın algılama sistemleridir.

Sistemler tasarlanırken, tünelde olabilecek kaza senaryoları esas oluşturmalıdır.

Örneğin tek yönlü trafik olan tünellerde, kaza bölgesinden ileride olan araçların rahat bir şekilde tüneli terk edebileceği düşünülür.

Aksi yönde ise araç trafiği oluşacak ve yangın bu yönde yayılma eğilimi gösterecektir. İki yönlü trafiğin olduğu tünellerde ise trafik her iki yönde de oluşacaktır. Sprinkler sistemi zonlaması yapılırken, bu hususlar gözönünde bulundurulmalıdır.

Türkiye Yangından Korunma Yönetmeliği’ne göre karayolu veya demiryolu tünellerinde otomatik sulu söndürme sistemi bulunması zorunlu değildir.

Amerikan standartları NFPA 130 (Standard for Fixed Guideway Transit and Passenger Rail System, 2010) ve NFPA 502 (Standard for Road Tunnels, Bridges and Other Limited Access Highways, 2011)’de tünellerde otomatik sulu söndürme sistemlerini tarif etmektedir.

Sprinkler sistemlerinin zonlara bölünmesi, ÖNEMLİ bir yöntemdir. Burada zon büyüklüklerini ve kaç zonan aynı anda çalışabileceğini iyi belirlemek gerekir. Uygulamada genellikle iki ya da üç zonan aynı anda çalışacağı kabul edilir

Kaç sprinkler zonanın çalışacağını belirleyen, tüneldeki yangın algılama sistemidir. Algılama elemanları, uygun aralıklarla ve yeterli sayıda yerleştirilerek, sistem hassasiyeti kabul edilebilir düzeye ulaştırılmalıdır.

Pratikte sıkça başvuru olan yöntem, söndürme sistemlerinin, tünel operatörünün kontrolüne bırakılmaktadır.

Algılama sisteminden gelen alarm, tünel operatörü tarafından değerlendirilerek, uygun görülen sprinkler zonlarının elle devreye sokulması söz konusudur.

Bu sayede hatalı alarmların sonucunda söndürme sisteminin gereksiz yere devreye girmesi önlenmiş olur.

Söndürme sisteminin başlatılmasının, tüneldeki insanların boşaltılmasından sonra yapılması konusunda çeşitli görüşler bulunmaktadır.

Bir görüşe göre, tünel tamamen boşaltılmadan söndürme sisteminin başlatılmaması gerekmektedir.

Bir başka görüş ise, tünel boşaltma süresinin, kazanın oluş şekline ve insanların davranışına bağlı olduğu, dolayısıyla tüm insanların tüneli terk etme süresinin değişkenlik gösterebileceği, bu nedenle söndürme sisteminin çok geç çalışması nedeniyle etkili olamayacağıdır.

HRR VE PERFORMANSA DAYALI TASARIM ;

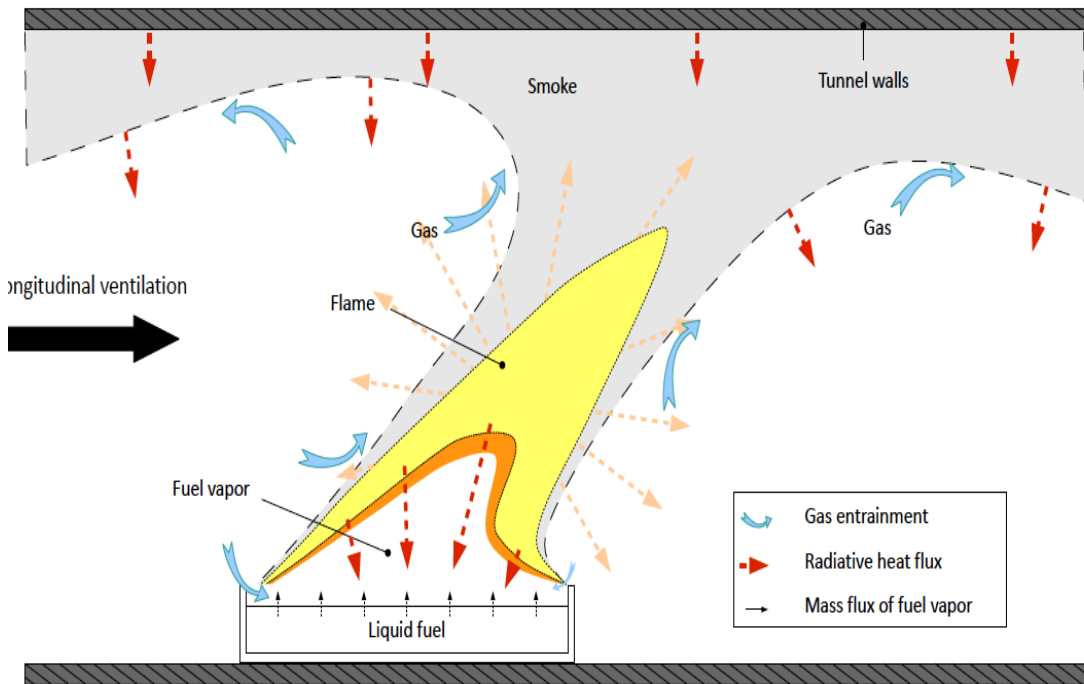
Sprinkler sistemlerinin performansını daha iyi kavrayabilmek için, yapılmış bazı büyük ölçekli yangın testlerini incelemek gerekir.

Yangının özelliğini etkileyen 3 faktör vardır.

Tünelin geometrik yapısı

Tünel havalandırma sistemi.

Poyansiyel Isı Yayılım Gücü / Heat Release Rate

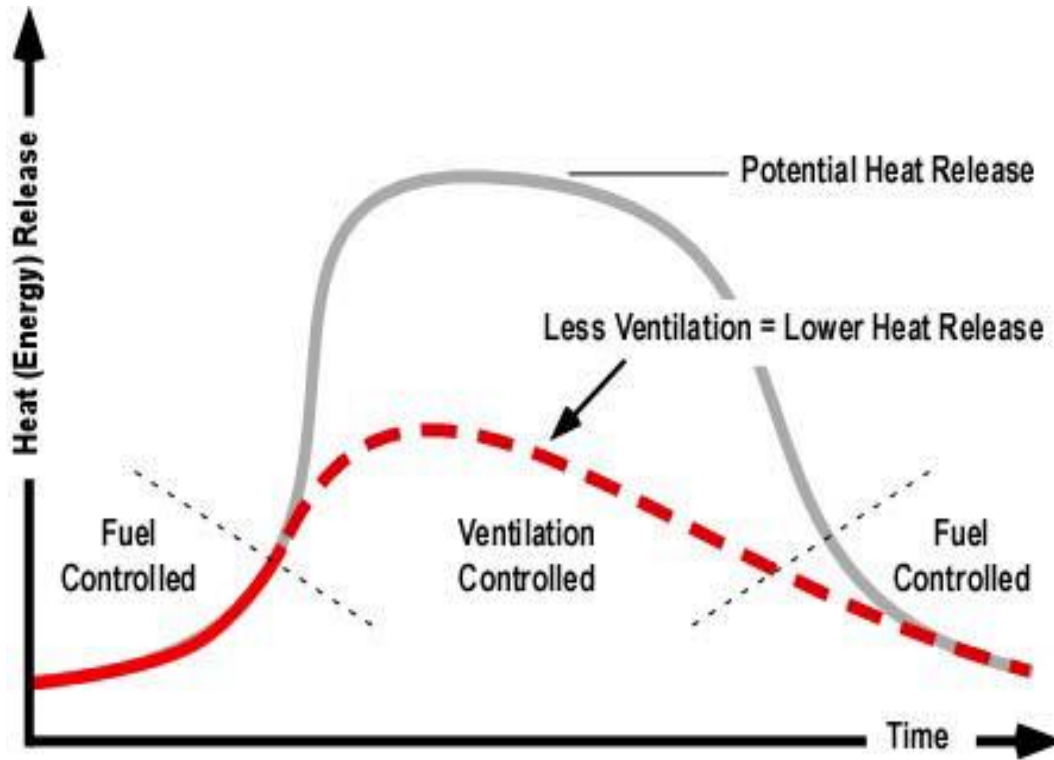


1970 lerde ; duman ile başa çıkmak için bir tasarım seçilirdi yani yangın ve tasarım havalandırma sistemini seçilirdi.

Modern sistemlerde ise ; Havalandırma akışı yangın davranışını ve boyutunu tanımlar . Ne tür yangın ile uğraşmak istiyoruz onu belirleriz.

Tünel Yangınlarının Dinamiği;

- 1- Tünelde yangınlar geçmiştekine göre daha hızlı geliyor ve ilerliyor.
- 2- İnsanlar genellikle vermesi gereken doğru tepkileri vermiyorlar.
- 3- Kurtarma ekipleri insanları kurtarmak için genellikle zamanında müdahale edemiyorlar.
- 4- Duman genellikle tünel yangınlarında ölümlere sebebiyet vermektedir.
- 5- İtfaiye olay yerine geldiğinde yaklaşmayı engelleyen ciddi bir ısı yayılımı olmaktadır.
- 6- Büyük tünel yangınlarının olduğu tünellerde genellikle havalandırma kontrol sistemi vardır.



İKİ BÜYÜK PROBLEM VAR

1- HGV Heavy Good Vehicle – Truck ; Yanma yükü yüksek yüklü büyük araçlar.

Gerçek yangınlar ile kabuller arasında ciddi farklar var

HRR dizayn parametreleri 30 MW ile 100 + MW arasında değişkenlik arz etmektedir.

2- ZAMAN

Yangınlar son derece hızlı büyümektedir.

Kabul edilen Tünel Yangın Boyutları şu şekilde sıralanabilir.

Araç Tipi	Tipik Yangın Yüğü (MJ)	Tipik Yangın Gücü (MW)	Notlar
Otomobil	3.000-3.900	2,5-5	Finlandiya'da yangın testlerinde kullanılan yüklerdir.
Otobüs	41.000	20	EUREKA(A pan-European network for market-oriented, industrial R&D) tarafından yangın testlerinde kullanılmıştır.
Yüklü Kamyon	65.000	20-30	
Ağır Yük Taşıyan Araç	88.000	30	
50 m ³ benzin taşıyan Tanker	1.500.000	300	Büyük boyuttaki yangınlar için Hollanda'da kabul edilen değerlerdir.

ESTIMATE HRR (MW) – YAKLAŞIK ISI YAYILIMI DEĞERLER TABLOSU					
	PIARC	FRENCH	NFPA	TESTS	REAL FIRE
CAR	2,5- 8	2,5- 8	5	2,5- 9	3-10
VAN	15	15			
BUS	20	20	20	29-34	36
HGV	20-30	30	20-30	15-203	300-400
TANKER	100	200	100	20-100	120-300

Tabloda görüldüğü üzere kabul edilen yaklaşık değerler , test değerleri ile gerçek yangınlarda ölçülen , meydana çıkan HRR değerleri arasında ciddi bir fark vardır. Bu fark ta tünel yangınları söndürme sistemlerinin tasarımının ne kadar zor ve hassas olduğunun bir ifadesidir.

Yangın Söndürme Sisteminden Beklenenler ; Genel olarak bir yangın söndürme sisteminden iki özellik beklenir.

- 1- Yangını söndürmek – Yangınla Mücadele
- 2- Yangının yayılmasını engellemek ; Yayılımı engellemek içinde
 - A.Gaz ve Yüzey Soğutma
 - B.Radyasyon etkisini zayıflatma
 - C.Oksijen Seyreltme
 - D.Duman etkisini azaltma

Gibi özelliklerin olması beklenmektedir.

Genel bir değerlendirme yapıldığında, su bazlı KLASİK köpüklü söndürme sistemlerinin, tünel yangınlarında kontrol modunda işlevinin olduğu, söndürme işlemini etkin bir şekilde gerçekleştiremediği söylenebilir.

Bu sistemlerin yapılması, tünelin ve içindeki her türlü tesisat/ekipmanın yapısal olarak korunması açısından faydalı görülüyorsa, uygulamaya geçilebilir.

Özellikle kanuni zorunluluğun olmadığı ülkemizde, böyle bir sistemin kurulum ve işletim maliyetleriyle,tünelin yangında uğrayacağı kayıp bedelinin karşılaştırılması, karar vermede etkin rol oynayacaktır

Büyük ölçekli test sonuçları genel olarak değerlendirilecek olursa, suyun soğutma etkisinin hem geleneksel sprinkler sistemlerinde, hem de su sisi sistemlerinde etkili olduğu anlaşılmaktadır.

Su bunu,hem yangının ısı yaymasını etkileyerek, hem de direkt olarak havayı soğutarak başarmaktadır.

Peki ya mist sistemin söndürme gücünü katkılar ile daha da arttırırsak , su bazlı , nfpa 18 wet agent katkılı yada endotermik söndürücü katkılı sabit sprinkler ve mist (sisleme) söndürme sistemleri tasarlırsak. Hem de tasarımlarımıza yeni teknolojik ürünleri de katabilirsek ciddi bir tasarım yoğunluğu elde etmiş oluruz.

YENİ TEKNOLOJİK ÜRÜNLER NE İŞE YARAR; Teknolojik ürünleri kullanmak aşağıdaki durumları güçlendirir.

Daha hızlı yangın söndürme

Daha kolay yangın söndürme

Performansa dayalı diyazni ciddi biçimde geliştirme

Bilimsel yenilikleri yakalama

Modern yöntemleri yakalama

YENİ TEKNOLOJİK ÜRÜNLERİ KULLANIRKEN DİKKAT;

Ulasal standartlara uygun mu ?

TSE

Ya da uluslararası standartlara uygun mu ?

UL , MPA DRESDEN , FM GLOBAL , VDS , NFPA v.b.

Yeterli bilgi , destek ve teknik uygulama detayına sahipmiyiz. Diyerek gerekli uygunluklara önem vermeliyiz.

Bu teknolojik ürünlerden biri endotermik wet chemical ürünlerdir.

ENDOTERMİK WET CHEMICAL NEDİR ?

Genelde toksik olmayan ve %100 biyolojik olarak parçalanabilen ürünlerdir.

yanma reaksiyonu üzerine su ile karıştırılarak uygulandığında ; yanma reaksiyonu üzerinden ısıyı ve hidrokarbonları ortadan kaldıran bir katalizör görevi görür.

Wet chemical ürünler endotermik reaksiyona girerek ; ısı alır , yakıt kaynağı hidrokarbonlarının yapısını parçalar.

Yeniden yanmayı engellemek için hidrokarbonları sarmalayarak hapseder.

Sudan 6 kat daha nüfuz yeteneği vardır ve 3 kat daha fazla btu- ısı alır.

Yangına müdahale sonrasında çok az su ve duman hasarı kalır.

Etkileyici bir termal bariyer son derece hızlı bir metal soğutma yeteneği vardır.

İnsanlara veya nesnelere uygulanabilir.

Büyük miktarda ısıyı bloke eder.

Konuyu maddeler halinde özetlemek gerekirse ;

1- YAPISAL ÖNLEMLER ; Doğru biçimde alınmalı ve HRR performansa dayalı tasarımlar daha projelendirme aşamasında yapılmalıdır.

2- ALARM VE ALGILAMA SİSTEMLERİ ; En uygun ve doğru seçilmiş bir algılama sistemi HRR düzleminde tasarlanmalıdır.

3- HAVALANDIRMA VE DUMAN TAHLİYE SİSTEMLERİ ; İyi test edilmiş , doğru tasarlanmış sistemler HRR baz alınarak tasarlanmalıdır.

4- ACİL DURUM İSTASYONLARI ; Uygun kalite testlerinden geçmiş olmalı ve sürekli kullanılabilir bir biçimde olmalıdır. İstasyonlarda ABCD yangınlarında etkili taşınabilir söndürme cihazları kullanılmalıdır.

5- ACİL AYDINLATMA SİSTEMLERİ – İŞARETLEMELER ; Hızlı tahliye kurallarına uygun olarak yapılmalıdır.

6- CCTV İZLEME SİSTEMLERİ ; Hem hareket ve hız hem de ısı değişikliklerine duyarlı sistemlerin yapılması önemlidir.

7- ACİL HABERLEŞME SİSTEMLERİ ; Sürekli çalışır durumda olmalıdır.

8- YANGIN SÖNDÜRME SİSTEMLERİ ; Klasik söndürme sistemleri yerine.

A- HRR esaslarına göre tasarlanmış

B- Zonlara ayrılmış

C- Gerektiğinde operatör tarafında aktive edilebilen

D- Tercihen Düşük Basıncılı WATERMIST sistemleri , Pompalı yada , Tüplü istasyonlu sistemleri kullanılmalı.

E- Watermist sistemlerin WET CHEMICAL Endotermik ürünler ile tasarlanması önem taşımaktadır.

Neden Watermist dersek;

Tünellerde yangın yükü parametrelerinin değişken olması nedeniyle yapılmış olan geleneksel sprinkler sistemi testlerinin yeterli olmaması durumu söz konusudur.

Genelde bu testleri 25MW yangına kadar yapmışlardır.

Nihonzaka tüneli yangınında (11 Temmuz 1979) sprinkler sistemi su tükeninceye kadar 1 saat boyunca yangını kontrol altına almayı başarmıştır fakat daha sonra yangın kontrolden çıkmış ve 7 gün boyunca devam etmiştir.

Düşük basınçlı su sisi 100 MW kadar test edildi ve yol tünellerinin korunması için uygun olduğu kanıtlandı.

Watermist Donatılmış Tüneller;

Country	Name of tunnel	Location	Name of tunnel
Austria	Mona Lisa Tunnel Felbertauern Tunnel	Boston, Massachusetts	CANA Northbound* CANA Southbound*
France	A86 Tunnel	Seattle Washington	Battery Street I-90 First Hill Mercer Island* Mt. Baker Ridge* I-5 Tunnel*
Italy	Brennero Tunnel Virgolo Tunnel	Vancouver, British Columbia	George Massey Tunnel
The Netherlands	Roermond Tunnel		
Norway	Vålreng Tunnel Fløyfjell Tunnel		
Spain	M30 Tunnels Vielha Tunnel		
Sweden	Tegelbacken Tunnel Klara Tunnel		

Yeni teknoloji ve sistemleri kullanmak bize ciddi bir tasarım yoğunluğu ve tünel güvenliği sağlayacaktır.

Fikret KIR

“VI Mühendislikte Yenilenebilir Yakıtlar, Yanma ve Yangın Konferansı FCE2017”

Securitas İtfaiye Hizmetleri Kurumsal Sunum

Uğur YERTUT / Genel Müdür

Securitas

Securitas, 1934 yılında bir güvenlik şirketi olarak İsveç’te kurulur. İsveç’te doğan küçük bir güvenlik firmasının hikâyesi, kıtalararasında üç kırmızı noktayı taşıyan, yüzbinlerce güvenlik görevlisine sahip, sektöründe dünya lideri Securitas’a kadar uzanır.

Yüzyılı aşan güven

Grubun Kuzey Amerika’daki kökleri eskilere; 1850’de Chicago’da kurulan Pinkerton Dedektiflik Bürosu’na dayanır. Misyonu koruma ve güvenlik olan Pinkerton, Amerika’da hızla tanınmaya başlar.

1934 yılına gelindiğinde ise, Avrupa’nın kuzeyinde güvenlik sektöründe yeni ve heyecan verici bir yapılanma dikkati çeker. Erik Philip Sörensen, İsveç’te, Helsingborg Nattvakt isimli bir firma kurar.

Değişmez değerler, değişmez marka

Kısa süre içerisinde İsveç’teki küçük güvenlik şirketlerini bünyesinde toplamaya başlayan firma, 1972 yılında bütün şirketleri tek bir isim ve çatı altında birleştirme kararı alır: Bu özel isim, “Securitas”tır.

Aynı zamanda “üç kırmızı nokta” logosunun yaratıldığı bu dönemde, noktaların her biri, Securitas’ın değişmez değerlerinin adını taşımaya başlar; bu değerler Dürüst, Dikkatli ve Yardımsever’dir.

Üç kırmızı noktanın seçimi, mors alfabesindeki “S” harfini simgelemesinden, Securitas ismi ise, Roma İmparatorluğu’nun koruyucu tanrısından esinlenir. 74 yıldır değişmeyen güçlü markanın sırrı, bu titiz seçimden ve markanın Securitas’ın değerleri ile birebir örtüşmesinden kaynaklanır.

Avrupa’dan Amerika’ya Securitas

Securitas markası, 1990’ların sonuna kadar Avrupa’da satın almalarla büyür ve lider pozisyona yükselir. 1999 yılına gelindiğinde ise, coğrafyasını Amerika’ya kadar genişletme kararı alan Securitas ile Pinkerton’un yolları kesişir.

Pinkerton Dedektiflik Bürosu’nu satın alan Securitas, 2000 yılında Amerika’nın en büyük ikinci güvenlik şirketi olan Burns’ü; takiben Wells, Fargo ve Loomis gibi kıymetli geleneklere sahip köklü kuruluşları da satın alır.

Güvenlik sektöründe dünyanın en büyük grubu haline gelen Securitas, satın aldığı kuruluşların uzmanlıkları sebebiyle, ihtisaslaşmış hizmet vermeye yönelik doğal bir strateji izler.

Grubun köklü yapısını; uzmanlaşmış güvenlik, devriye, alarm izleme, danışmanlık ve araştırma (Pinkerton) ile nakit para taşıma hizmetleri (Loomis) oluşturur. İsveç'te doğan küçük bir güvenlik firmasının hikâyesi, kıtalararasında üç kırmızı noktayı taşıyan, yüzbinlerce güvenlik görevlisine sahip, sektöründe dünya lideri Securitas'a kadar uzanır.

Bu gün Securitas güvenlik sektöründe dünyanın en büyük kuruluşu, bünyesinde 330.000 çalışanı ile 53 ülkede faaliyet göstermektedir.

Securitas Türkiye

Securitas Türkiye, 9 bölge ofisi, 8 şube müdürlüğü ofisi, 52 şube müdürü ve 353 idari personel ile Türkiye genelinde 650 projede, 2.200 hizmet noktasında 11.500'den fazla güvenlik görevlisi ile 75 şehirde hizmet veriyor.

1992 yılında, Türkiye özel güvenlik pazarında ilk kurulan şirketlerden biri olan DAK Güvenlik ile Securitas Türkiye'nin temeli atılmış oldu. 2006 yılına gelindiğinde DAK ile Kare Güvenlik Securitas Güvenlik Hizmetleri adı altında birleşti. Securitas Türkiye bugün, Securitas Avrupa Güvenlik Hizmetleri'ne bağlı olarak faaliyetlerini sürdürüyor.

- 2006 – Securitas Uzaktan İzleme Merkezi A.Ş.
- 2010 – ICTS Danışmanlık Firması (Satın Alınma)
- 2011 – Sensormatic Firması (Satın Alınma)
- 2011 – Securitas İtfaiye Hizmetleri A.Ş.
- 2011 – Loomis (CIT) (Satın Alınma)
- 2012 – Kontrol Hizmetleri AŞ.

Teknoloji ve bilgiyi, hizmetlerine entegre ederek hızla büyüyen Securitas, Türkiye pazarında bilgi lideri misyonunu koruyor. Uluslararası kalite ve deneyimlerini, yerel operasyon gücü ile birleştirerek öncülük ediyor.

Geniş hizmet ağı içerisinde;

- Deniz Limanları
- Endüstriyel Tesisler
- Petro-Kimya Endüstrisi
- Hava Limanları
- Plaza ve Rezidanslar
- Organize Sanayi Merkezleri olmak üzere yetişmiş uzman kadro ile maksimum fayda&minimum maliyet odaklı hizmet anlayışı içerisinde çalışarak,
- Yangın Risk analizi
- Yangın Algılama
- Yangın Müdahale
- Tahliye
- Arama&Kurtarma alanlarında sürdürülebilir bir gelecek için sorumluluklarının farkında olarak hizmetlerini devam ettirmektedir.

İş Ortaklarımız

Securitas olarak İtfaiye hizmeti verdiğimiz iş ortaklarımız arasında; 27 Multi Rol Güvenlik Görevlisi ile Kanyon AVM, 4 İtfaiye Personeli ve 10 Multi Rol Güvenlik Görevlisi ile Borusan Gemlik Liman, 1 Proje Müdürü, 3 İtfaiye Amiri ve 20 Acil Müdahale Timi Personeli ile Zorlu Center, her vardiya 9 devriye ve 4 yangın izleme personelinden oluşan ICF Antalya Havalimanı bazılarımızdır.

2017 Yılı ile birlikte Emaar Square (AMT), BASF Kimya A.Ş. (Watchman) ve JLL AVM İşletmesi Yangın Danışmanlığı (32 Ad AVM) başlayan projelerimiz arasındadır.

İtfaiye Hizmetleri Çözümlerimizde ana başlıklarımız;

İtfaiye Hizmetleri
İstasyon İşletmeciliği
Yangın Danışmanlığı
Yangın Risk Yönetimi
Hava-Deniz Limanları İtfaiyesi
Gözlemci (Watchman)
Acil Müdahale Timi (AMT) Hizmetleri
Bakım ve Kontrol
Multi Rol Görevlileri
Gerçek Zamanlı 7/24 Raporlama

Entegre Güvenlik Çözümleri

Securitas olarak amacımız, daha güçlü ve daha uzun süreli iş birliktelikleri için, uzmanlığımızı dünyadaki yeni güvenlik trendleri ile birleştirmek ve iş ortaklarımızın özelihtiyaçlarına en uygun güvenlik çözümünü, “tek sözleşme” ve “tek muhatap” ile sunmak.

Securitas Türkiye’nin özel güvenlik sektörüne kazandırdığı bu yeni hizmet modeli, “Entegre Güvenlik Çözümleri” olarak ifade ediliyor. Entegre güvenlik çözümlerinin yapı taşlarını; Uzman Güvenlik Hizmetleri, Teknoloji, Uzaktan İzleme Hizmetleri, Kontrol Hizmetleri ve Danışmanlık Hizmetleri oluşturuyor.



Yangına Nasıl Müdahale Etmeliyiz?

Bir yangın esnasında ilk 5 dakika çok önemlidir. İlk 5 dakikada ortamda bulunansıcaklık 555 C iken 10 dk. sonra 660 C ye ulaşmaktadır. Buda bize yangın esnasında sıcaklıkartışının ilk 5 dakikada çok hızlı bir ivme kazandığını göstermekte olup, ilk müdahalenin veyetişmiş/eğitilmiş insan gücünün önemini ortaya koymaktadır.

Acil Müdahale Süreçleri incelendiğinde, 5'inci Dakikada artık müdahaleye başlanma zorunluluğu ortaya çıkmış 10'uncu dakikada ise yangının kontrol altına alınması ve yangın sonrası eylemlerin devam ettiği bir safahat gözlemlenmektedir.

Günümüzde kamu itfaiyelerinin yangın yerine ulaşmasında birçok geciktirici faktörler rol oynadığından, ilk müdahale yangın yerinde bulunan kişiler tarafından yapılacağı gerçeğini ortaya çıkarmaktadır.

Unutmayın ki, her büyük yangın bir kıvılcımla başlar.

Yangın olaylarında istatistiklere bakıldığında ilk 5 dakikadan sonra ölüm olaylarının başladığı ve 12'nci dakikadan sonra hızla arttığı görülmektedir.

Yangın Risk Analizi;

Yangın Risk Analizinin özünü yangın öncesi planlama diye tabir edebiliriz. Analizi yapılan yerin yangına karşı önceden bünyesinde bulundurduğu riskleri tespit etmek ve bu yönde alınabilecekleri kontrol ederek eksik görülen hususları düzenlemek, oluşturulan senaryolara dayalı olarak planlı/plansız eğitim ve tatbikatlarla reaksiyon şekillerini pekiştirmek. Otomasyon bir sistemle risklere yönelik tespitler sürekli izlenir ve anında müdahaleler yapılır. Raporlama hizmeti sürekli bir faaliyettir.

İtfaiye Müdahale Modellemesi;

Her tesisin müdahale usulleri ve hassasiyetleri farklılık arz etmektedir. Bu aşamada Securitas İtfaiye ve Tesis Yönetimi ortak çalışma durumundadır. Securitas İtfaiye Tesis içi riskleri tespit ederken Tesis Yönetimi de acil durum eylem planlarını hazırlar. Bunun sonucunda uygun yangın müdahale yöntemi oluşturularak ortak plan hazırlanır. Bu altyapı çalışması bizi İtfaiyenin Müdahale Metodunun tespitine götürür.

İtfaiye Müdahale Modelinde dikkat edilecek hususlar;

Kaza ve Olay İstatistikleri
Yangın Senaryoları
Yangına Müdahale Noktaları
Müdahale Yolları
Primer Risk Noktaları
Sonuç Analizi
Müdahale Yöntemlerinin Tespiti
Tatbikat (Gece/Gündüz) İcrası

Sonuç

Securitas güvenlikte global bilgi lideridir. Uzman güvenlik hizmetlerinden, teknolojik çözümlere, danışmanlığa ve araştırmaya kadar uzanan geniş hizmet yelpazesinde; her iş ortağımızın özel ihtiyaçlarına uygun, en etkin güvenlik çözümlerini sunuyoruz. Küçük ve orta ölçekli işletmelerden, havalimanlarına kadar birçok alanda 54 Ülkede 330.000 çalışanımızla hizmette fark yaratıyoruz.

Dürüst | Dikkatli | Yardımsever

Endüstride yangın güvenliği ve uygulamaları

Uğur GÜLLÜ¹ and Bilge ALBAYRAK CEPER²

¹ *Erciyes University, Engineering Faculty, Dept. of Mechanical Engineering, Kayseri*

² *Erciyes University, Engineering Faculty, Dept. of Mechanical Engineering, Kayseri*

Corresponding Author: e-mail: balbayrak@erciyes.edu.tr

Özet: Yangın, çevresel risk taşıyan sadece çıktığı mahalde kalmayarak tüm binayı hatta eğer kontrol edilmezse gelişerek tüm bölgeyi etkisi altına alabilecek bir felakettir. Çalışmamızda bu büyük felaketin endüstride oluşturabileceği zararların en aza indirilmesi için alınan önlemler, bu önlemlerin uygulamaları ve getirileri üzerinde durulacaktır. Yangın koruma ve fabrikalarda yangın güvenliği sorununun sadece bir dizi yönetmelikle geçirilebilecek bir sorun değil, aksine mimari tasarım aşamasından başlayarak binanın ömrü boyunca devamlı kontrol altında tutularak araştırılması, öğrenilmesi ve uygulanması gereken bir zorunluluk olduğu konularına değinilmiştir. İdarecilerin bu yöndeki görev ve sorumlulukları hakkında yol gösterilmesine çalışılmış ve endüstriden bir örnek olarak Hes Kablo Fabrikasında yangına karşı alınan önlemler ve uygulamalar dan bahsedilmiştir.

1.Giriş

Yangın günümüzde üzerine alınan tedbirler açısından en önemli afet olayıdır. Yangın sonucunda can ve mal kaybı açısından çok büyük zararlar verilmesi sebebi ile yangın önleme faaliyetleri çalışmaları çok önemli bir hal almış ve bu konu üzerine birçok deneysel tezler de ortaya çıkarılmıştır. Yangın önleme sistemleri ve çalışmaları insan hayatı ve maddi manevi kayıpları önlemek açısından büyük önem arz etmektedir. Yangın oluşumuna ihmaller zincirinin sebep olacağı gibi ufak dalgınlıkların veya hataların da büyük kayıplara yol açması kaçınılmazdır. Yangın oluşumu açısından kolay sonlandırılması açısından zor bir olgu olması sebebiyle önlem alınmasını zorunlu kılan tehlikeli bir olaydır[1].

Bir yangından bahsedilebilmesi için öncelikle yanma olayının gerçekleşmiş olması gerekmektedir. Yanma kimyasal bir olaydır. Bütün maddeler oksitlenir; demir paslanır, kağıt sararır, gevrekleşir. Yangın veya tutuşma ısı ve ışığın meydana gelmesiyle hızlı bir oksitlenme olayının oluşumudur. Yangın; kontrolden çıkmış yanma olayıdır. Yanmanın gerçekleşmesi için de 3 önemli unsur gereklidir. Bunlar; yanıcı madde, ısı ve oksijendir.

Yanma başlamadan önce oksijen ve yanıcı madde mevcut miktarlarda bulunurlar. Uygun koşullar oluşunca yanma başlar. Yanıcı madde yanar ve daha çok ısı üretir. Artan ısı ise daha çok yanıcı maddeyi tetikler ve yanma olayını arttırır. Yanma bölgesinde oksijene ihtiyaç olduğu için bu bölgeye daha çok oksijen sürüklenir ve buradaki oksijen yanmanın ısını arttırır. Dolayısıyla daha çok yanıcı madde yanmaya katılır. Bu zincirleme reaksiyon bütün yanıcı madde bitene ve oksijen tükeninceye kadar devam eder[2].

2.Yangından Korunma

Yangından korunmada amaç, yangında bulunabilecek şahısların can güvenliğini sağlama, her türlü maddi kayıp ve hasarı önleme ve şayet yangın olayı gerçekleşirse bunu en azda tutma çalışmalarıdır[3].

2.1.Risklerin Belirlenmesi

Birçok endüstri sektörü üretimde kullanılan hammaddeler, yarı mamuller ve sonuç mamuller ile üretim bandı ve insan faktörü çerçevesinde yüksek yangın riski potansiyeline sahiptir. Günümüz endüstrisinde kullanılan teknolojinin ilerlemesi ile yüksek yangın riskine sahip malzemelerin kullanıldığı, işletmelerin iş hacimlerinin büyüdüğü, çalışan insan sayısının ve kullanılan enerjinin de bu oranda arttığı görülmektedir.

Tablo 1'de endüstride hizmet vermekte olan firmaların risk tablosu verilmiştir. Çevre, çalışan, sağlık ve güvenlik ile toplum etkileşimli risk ilişkileri gösterilmiştir.

Tablo 1. Risk Tablosu

Risk Kategorileri	Çevre	Sağlık ve Güvenlik	İşçi	Toplum
Risk anahtarı	Doğal Çevreye Etki	Çalışanın Sağlık ve Güvenliğini Etkisi	İşyeri Koşulları ve Çalışanların Sağlığına Etkisi	Toplum, halk sağlığı ve güvenliği, Geçim ve Çevre Etkisi
Tedarik zinciri riski	+		+	+
Hava salınımı	+	+		+
Tehlikeli maddeler	+	+		+
İş sağlığı ve güvenliği		+	+	
Su yönetimi ve atık su	+			+
Katı atık	+			+
Enerji tüketimi	+			
İşçi hakları			+	+
Ahlak ve rüşvet			+	+
Toplum ve sosyal riskler				+

3.Endüstride Alınan Yangın Önlemleri Ve Güvenliği

Dünya genelinde endüstriyel yangınlar sebep ve sonuçları dikkate alındığında büyük önem arz eden sektörlerdir. Tablo 2'de Türkiye'de ki olay mahali türlerine bağlı, yapısal ve yapısal olmayan yangınlar verilmiştir.

Tablo 2. Türkiye'de ki Yangın Olayları

Tablo 2. Yangınlar (2010-2015)										
Yıl	Yangın (Sayı)									
	Yapısal yangınlar					Yapısal olmayan yangınlar				Genel Toplam
	Konut	Fabrika İşyeri	Diğer Bina	Araç	Toplam	Ot	Çöp	Orman Fundalık	Toplam	
2010	4.815	122	5.922	1.396	12.255	4.333	3.409	49	7.791	20.046
2011	5.394	131	7.012	1.541	14.078	8.115	4.134	117	12.366	26.444
2012	5.129	136	7.069	1.524	13.858	7.442	4.033	136	11.611	25.469
2013	4.902	159	7.853	1.601	14.515	7.969	5.099	134	13.202	27.717
2014	5.261	123	7.869	1.689	14.942	3.008	4.830	68	7.906	22.848
2015	5.869	157	8.957	1.903	16.886	4.596	5.212	284	10.092	26.978
Sayısal Değişim	2014 2015	608↑	34↑	1.088↑	214↑	1.944↑	1.588↑	382↑	216↑	4.130↑
	2010 2015	1.054↑	35↑	3.035↑	507↑	4.631↑	263↑	1.803↑	235↑	6.932↑
Oransal Değişim	2014 2015	12%↑	28%↑	14%↑	13%↑	13%↑	53%↑	8%↑	318%↑	18%↑
	2010 2015	22%↑	29%↑	51%↑	36%↑	38%↑	6%↑	53%↑	480%↑	35%↑

Tablo incelendiğinde fabrikalardaki yangın oranları artış eğiliminde olup bunun büyük bir etkisi de gelişen sanayi nedeniyle fabrika sayısının artmasıdır. Yangına karşı alınan önlemlerin artmış olmasına

rağmen yangın sayılarındaki artış, yangın sayısının artışından çok artan fabrika sayıları olarak yorumlanabilir.

Türkiye’de oluşan yangın sebepleri istatistiklerinin görülebileceği Tablo 3 de insan faktörünün yangın olaylarında ne kadar etkili olduğu anlaşılmaktadır. 2010-2015 yıllarında çıkan yangınların sebeplerinde en büyük pay tüm yıllarda sigara sebepli yangınlar olarak karşımıza çıkmaktadır. Endüstri yangınları için de büyük tehlike arz eden sigara kullanımı birincil öncül olmaktan kendisini alamamaktadır.

Tablo 3. Türkiye’de yangın sebepleri

Tablo 3. Yangın Kaynağı (2010-2015)												
Kaynak	Yıl											
	2010		2011		2012		2013		2014		2015	
	Sayı	Yüzde	Sayı	Yüzde	Sayı	Yüzde	Sayı	Yüzde	Sayı	Yüzde	Sayı	Yüzde
Sigara	8.546	42,6%	13.032	49,3%	12.399	48,7%	13.010	50,5%	9.168	40,1%	10.532	39,0%
Elektrik kontağı	4.567	22,8%	4.771	18,0%	5.012	19,7%	5.133	18,3%	5.360	23,5%	6.564	24,3%
Kasıt(sebebi meçhul)	622	3,1%	985	3,7%	932	3,7%	1.454	3,2%	1.340	5,9%	2.058	7,6%
Ütü, ocak (gazlı dâhil) elektrikli ev aletleri	1.090	5,4%	1.130	4,3%	1.144	4,5%	1.190	4,2%	1.189	5,2%	1.245	4,6%
Baca	1.244	6,2%	1.422	5,4%	1.389	5,5%	1.298	5,1%	1.134	5,0%	1.185	4,4%
Çocukların ateşle oynaması	1.171	5,8%	1.543	5,8%	1.242	4,9%	2.097	5,7%	749	3,3%	1.159	4,3%
Kızışma (yüksek ısı ile)	561	2,8%	726	2,7%	714	2,8%	677	2,4%	961	4,2%	1.107	4,1%
Kıvılcım sıçraması	750	3,7%	860	3,3%	865	3,4%	967	3,6%	903	4,0%	1.021	3,8%
Tespit Edilemedi	235	1,2%	564	2,1%	542	2,1%	762	1,6%	830	3,6%	956	3,6%
Diğer	523	2,6%	731	2,8%	584	2,3%	505	2,3%	596	2,6%	537	2,0%
Parlama (yanıcı sıvı, yemek par. v.b.)	492	2,5%	440	1,7%	395	1,6%	422	1,9%	351	1,5%	328	1,2%
Trafo	245	1,2%	240	0,9%	251	1,0%	202	1,0%	267	1,2%	286	1,1%
Toplam	20.046	100%	26.444	100%	25.469	100%	27.717	100%	22.848	100%	26.978	100%

Endüstri de yangına karşı tedbirlerin ve önlemlerin alınmasında dikkat edilmesi gereken bazı hususlar[4];

- Yangın çıkmasının önlenmesi
- Yangının algılanması
- Yangının büyümesinin geciktirilmesi
- Duman hareketinin kontrol edilmesi
- Kaçış yollarının sağlanması
- Yangının başka hacimlere yayılmasının önlenmesi
- Oluşabilecek göçüklerin önlenmesi
- Yangının kontrol altına alınması
- Yangınla mücadele
- Yangın güvenlik idaresi

başlıkları altında toplanabilir.

Bir endüstri kuruluşu olan HES KABLO firması, 1974 yılında enerji kabloları üretmek üzere kurulmuştur. Geçen zaman içerisinde bakır haberleşme kablosu, fiber optik kablo, enerji kablosu, yüksek gerilim enerji kablosu, alüminyum iletken ve emaye bobin teli üretimini de kendi bünyesinde gerçekleştirmeye başlamıştır. Bunun yanı sıra, yarı mamül olarak kullanılan granül ve makara üretimini de kendi bünyesinde üretmektedir. İşletme 120,000 m²'si kapalı, 250,000 m² alandaki entegre tesisleri ile sanayiye katkı sağlamaktadır[5]. Hes Kablo fabrikasının yangın önleme ve güvenlik açısından aldığı önlemler alt başlıklar halinde sunulmuştur.

3.1. Yangın Yönetmeliği Uygulamaları

Endüstride yangına karşı alınacak önlemlerin belirli uygulamaları ve bu uygulamaların yürütülebilmesi için uyulması gereken gerekli yönetmelikler ve kurallar mevcuttur. Kuruluşundan itibaren çevre duyarlılığına gösterdiği hassasiyet ve yangın tedbirleri açısından sektöründe zirvede bulunan Hes Kablo, yangın önleme sistemleri ve tedbirleri açısından gerekli alt yapıya sahiptir. Ayrıca uygulamaları eksiksiz yerine getirmesiyle de örnek teşkil etmektedir.

a) Eğitim

Fabrikada, yangın yönetmeliği kapsamında personele yangınla alakalı alınması gereken eğitimler zamanında ve uzman ekip tarafından verilmektedir (Şekil 1). Eğitim alan personel içerisinde seçilen, yangın önleme ekibi, söndürme ekibi, kurtarma ekibi gibi ekipler oluşturulup personelin olası bir yangın halinde görevlerinin belirlenmesi sağlanmaktadır. Bu ekiplerin önceden belirlenmesi yangın durumunda yol açılacak can ve mal kaybını aza indirmekte ve oluşacak panik ortamını ortadan kaldırmayı hedeflemektedir. Verilen yangın eğitiminde yaşanmış yangın olaylarından örneklendirmeler aktararak yangın anında yapılması gereken davranışlar anlatılmaktadır.

b) Tatbikat

Personel aldığı eğitim sonrasında olası bir yangın durumuna karşılık almış oldukları eğitimi tatbikatlı olarak eğitilirler (Şekil 2). Yapılan tatbikatta yangını önleme çalışmaları, yangına müdahale ve kurtarma gibi olaylar canlandırılıp personelin bilinçlenmesi sağlanmaktadır.



Şekil 1. Yangın Eğitimi





Şekil 2. Yangın tatbikatı

3.2. Yangın Önlemleri

Fabrikalarda olası bir yangın durumunda can ve mal kaybının diğer bölgelerdeki yangın durumundan daha fazla olacağını bilinmektedir. Dolayısıyla alınması gereken yangın önlemleri de bir o kadar önemli ve artırılması gerekmektedir. Fabrikalarda yangına karşı çeşitli otomasyon sistemleri kurularak yangın önleme, söndürme, soğutma, kurtarma gibi durumlar için gerekli önlemler alınmaktadır. Bu tür sistemler için Hes Kablo'da bulunan yangın önleme sistemleri aşağıda sıralanmıştır.

a. Yangın dolapları ve yangın tüpleri

Yangın dolapları fabrika sahası içerisinde hemen her bölgede yer almakta ve bu dolapların içerisinde fabrikanın yangın hattından gelen basınçlı su bulunmaktadır (Şekil 3). Hes Kablo fabrikasında yangın hattının su basıncı yaklaşık 8 bardır. Yüksek basınçlı su yangın söndürme hortumundan çıktıktan sonra yüksek bölgelere ulaşabilmesi için basınçlandırılır. Yangın dolapları kırmızı renklidir ve önüne malzeme ve başka çeşitli materyaller konulmayacak şekilde uygun bir duvara yerleştirilmiştir.



Şekil 3. Yangın dolabı

Ayrıca firmada makine bazında yangın dolapları ve yangın söndürücü tüpler bulundurulmaktadır (Şekil 4). Bu durum olası bir yangın anında makine operatörlerinin ilk müdahaleyi yapmasını kolaylaştırmak ve meydana gelebilecek hasarı en aza indirmeyi amaçlamaktadır.



Şekil 4. Makine bazında yangın dolabı ve yangın tüpü uygulaması

Makinelerin elektrik aksamı parçalarını panolarını ve panoların içerisinde bulunan olası bir yangın durumunda sudan, köpükten etkilenebilecek elektronik cihazların korunabilmesi için firma özel üretim

“halokarbon” tip söndürme tüpü uygulamasını kullanmakta olup, cihazların zarar görmemesi için gerekli önlemleri almıştır (Şekil 5).



Şekil 5. Halokarbon tüp uygulaması

Yangın riski oluşturması muhtemel her alanda tedbirleri elden bırakmayan Hes Kablo, bakım onarımında kullanılan, kaynak makinelerinde ve oksijen kaynağı araçlarında yangın söndürme tüplerini her zaman hazır bulundurup anında müdahale ile oluşabilecek zararları en aza indirmeyi hedeflemektedir (Şekil 6).



Şekil 6. Yangın riskli mobil cihazlarda yangın tüpü uygulaması

b. Köpük dolapları

Köpük uygulaması alevlenmesi kolay olan yangınlarda sudan daha etkilidir. Hes Kablo firmasında yangın riskinin fazla olduğu bölümlerde, doğalgaz bağlantılı makinelerin çalıştığı ortamlarda ve alevlenme riski fazla maddelerin olduğu bölümlerde yangının kontrol altına alınmasında etkili bir yöntem olan köpük dolapları sistemsel olarak kurulmuş ve uygulanmaktadır (Şekil 7).



Şekil 7. Hes Kablo’da Köpük Dolabı Uygulaması

c. Elektrikli yangın hattı pompa sistemi

Yangın hattı pompa sistemi, fabrikada bulunan yangın önleme sistemlerindeki su ihtiyacını karşılamak ve basınçlandırmak için kurulmuştur. Hatta basınç sağlayan pompalar, hatta oluşan olası bir basınç kaybında otomatik devreye girerek sistemdeki eksilmiş suyu tamamlar ve gerekli basınca getirirler. Basınç bilgilerine göre çalışan sistem yangın hattında sürekli su bulunmasını sağlar. Dolayısıyla olası bir yangın durumunda yangın önleme hızlandırılmış olur (Şekil 8).

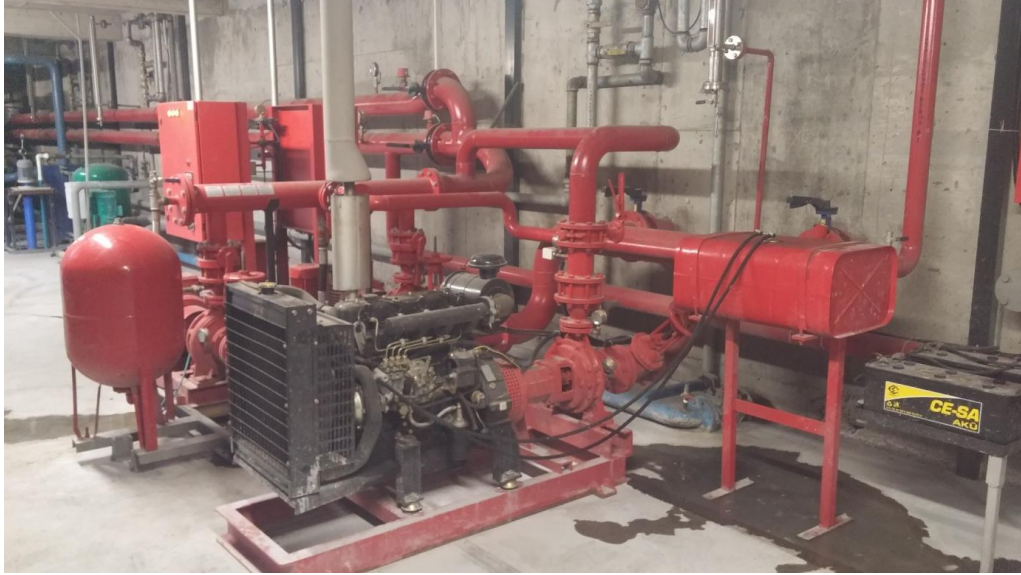
d. Dizel yangın hattı pompa sistemi

Dizel yangın hattı pompa sistemi aynı elektrikli pompa sistemi gibi yangın hattında bir diğer yoldan su ve basınç sağlamaktadır. Elektrikli pompanın elektrik kesilmesi durumunda çalışmaması durumunda hattaki sensörler devreye girerek dizel motorunun çalışması sayesinde pompalar hatta su ve basınç

sağlarlar. Böylelikle yangın durumunda elektrik kesilmiş olsa bile alınmış olan bu önlemle yangın hattından yangının önlenmesi, can ve mal kaybının en aza indirilmesi sağlanmış olur.



Şekil 8. Fabrika da ki elektrikli yangın önleme sistem pompaları



Şekil 9. Fabrika da dizel motorlu yangın önleme sistemi pompası

e. Yangın algılayıcı ve adrese dayalı alarm sistemi

Yangın algılayıcıları, yangın durumunda çıkan dumandaki partiküllerin durumuna göre yangın olup olmadığını algılayan ve alarmı çalıştıran sistemlerdir. Yangın algılayıcıları, optik duman algılayıcısı,

ışın (Beam) tipi algılayıcılar, alev algılayıcılar hava emmeli hassas duman algılama sistemi, ısı algılayıcılar, ısı artış algılayıcılar şeklinde sınıflandırılır[6].

Fabrikada yangın algılayıcı sistemler, detektörler her alana kurularak alarm sisteminin çalıştırılması ve yangına karşı müdahale edilmesi sağlanmıştır. Adrese dayalı yangın alarm sistemi ile firmanın uydu görüntüsü itfaiye sitemine gönderilerek olası bir yangın durumunda hızlı haberleşme ve yer tespiti sağlanıp yangının meydana getirebileceği kayıplar en aza indirilmesi hedeflenmektedir.

Sonuçlar

Sonuç olarak endüstride yangınların önlenmesi, gecikmeden fark edilmesi, erken ve etkin müdahalenin yapılabilmesi, sirayetin önlenmesi ve organize bir tahliyenin sağlıklı olarak yapılabilmesi için fabrikaların gereken hassasiyeti göstermesi gerekmektedir. Yangın önleme tedbirlerinin alınması, bunların önceden planlanması, personelin eğitilmesi, tatbikatların yapılması, prosedürlerin tarif edilmesi ve ekipmanların tedarik edilmesine ihtiyaç vardır.

Fabrikada yangın güvenlik sistemlerinin periyodik bakımları ve testleri zamanında yapılmalı ve her zaman çalışır durumda bulundurulmalıdır. Müessesenin elektrik ve mekanik sistemlerinin de gerekli bakım ve kontrolleri yangın güvenliği açısından çok önemlidir. Tahliye tatbikatlarında; sistemler ayrıca test edilmelidir. Alınacak bu tedbirler sayesinde can ve hasar kaybının minimuma inmesi sağlanabilecektir.

Kaynaklar

- [1] Yorulmaz G., Yangından Korunma ve Binalarda Yangın Güvenliği Önlemleri, Yüksek Lisans Tezi, Selçuk Üniversitesi, 2001.
- [2] Cerbezer F., Mimari Tasarım ve Malzeme Yönünden Yangın Güvenliği, İstanbul Büyük Şehir Belediyesi İtfaiye Müdürlüğü Yayınları, İstanbul.
- [3] Sunar Ş., Yangından Korunma ve Bina Yangın Güvenliği İlkeler Çelişkiler Gerçekler, İstanbul Teknik Üniversitesi Mimarlık Fakültesi, İstanbul.
- [4] Becan, A.S., Yangınla Mücadelede Aktif ve Pasif Yöntemler, İtfaiye 110 Dergisi sayı 10
- [5] www.hes.com.tr , Firma Profili.
- [6] www.essed.com.tr , Yangın Alarm Sistemleri.

SİSAR MÜHENDİSLİK

YANGIN ve GÜVENLİK SİSTEMLERİ
MADENCİLİK TEKSTİL TURİZM İNŞAAT
SANAYİ ve TİCARET LTD.ŞTİ.



AEROSOLLÜ SİSTEMLER:



FP 20 S

FP 40 S

FP 80 S

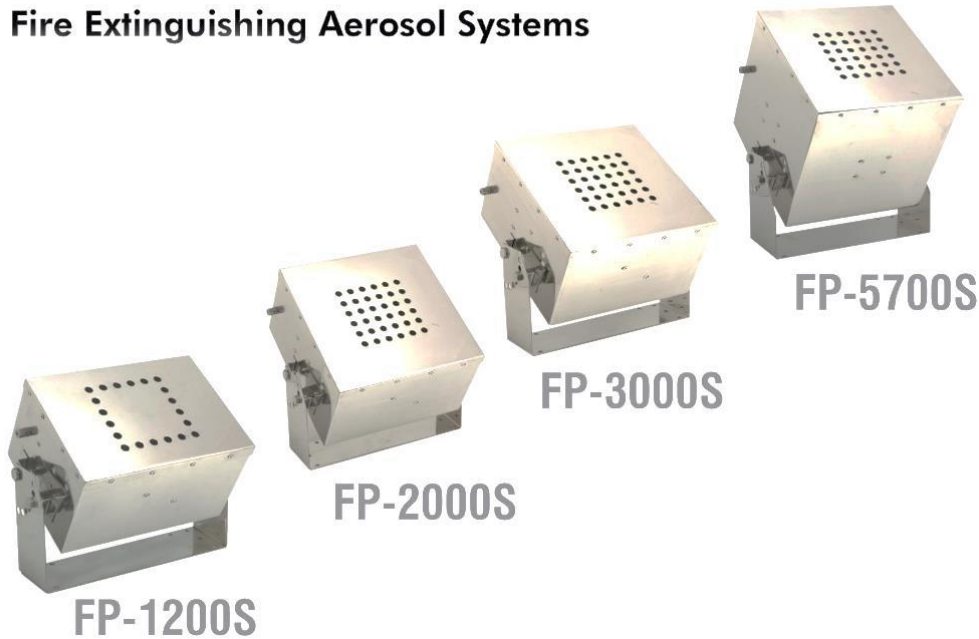
FP 100 S

FP 200 S

FP 500 S

FirePro®

Fire Extinguishing Aerosol Systems



FP-1200S

FP-2000S

FP-3000S

FP-5700S

Aerosol nedir? FirePro genel söndürme prensibi nasıl çalışır?

Aerosol: 10 mikrondan küçük katı taneciklerin gaz içinde yayılma olayına aerosol denir. Aerosol katısı hedef bölgeye tetikleyiciler yardımıyla inert bir gaz ile dağıtılır. Bu dağılma işleminden sonra katı partikülleri hızla hedefleri ile süratle etkileşime girerler.

FirePro aerosol katısı potasyum esaslıdır. Potasyum yapısı itibariyle bir alkali metaldir ve oldukça iyonik yani bileşik oluşturma isteği fazla olan bir elementtir.

Potasyum; deniz suyunda 0,380 g/kg oranında bulunan, insan sağlığına zararsız bir elementtir. Her insan başta sinir sisteminin ihtiyacı olmak üzere her gün 3,5 mg potasyuma ihtiyaç duyar.

ISO 14001 belgesine sahip FirePro potasyum esaslı olduğu için; toksik ve iletken olmayan oksijen bağlamayan ve ozon tabakasına zarar vermeyen, küresel ısınma etkisi ve karbon ayak izi bırakmayan bir malzemedir.

Genel olarak yangın, O, H, OH radikallerinin zincirleme reaksiyonları sonucu ortaya çıkar. Aerosolün birinci adımında inert gazlar (N_2 , H_2O , CO_2) mikro boyutlarda başta K_2CO_3 içeren partiküller ortaya çıkarır. Aerosolün ikinci adımında ise söndürme işlemi başlamıştır, ortaya çıkan potasyumun çeşitli formasyonları hızla K_2CO_3 'ten ayrılarak daha iyonik ve bileşik oluşturma isteğinde oldukları yangın radikalleriyle (C, H, OH) kararlı bileşikler (KOH vb.) oluştururlar ve yangın oksijeni boğmadan söndürülür.



Neden Firepro?

Firepro yapı itibariyle çevreye zararsız katı parçacıklar (aerosol) ihtiva eder. Bu aerosol, tetikleyici olan durumlarda içindeki potasyum yardımıyla yangın radikallerini (C, CO, OH) bağlayarak yanmayı engeller.

Öyle ki; Yangın söndürme sırasında mevcut söndürücüler oksijen boğma yöntemiyle söndürme yapmaktadır. Firepro yapısı itibariyle oksijene dokunmadan diğer bileşenleri engelleyerek yangını söndürür.

Ülkemizde gelişmekte olan çevre bilincinin de etkisiyle, çevre yönetmelikleri ve standartları, firmaların her durumda çevreye zararı en az olan malzemelerin kullanımını desteklemektedir. Aerosollü yangın söndürme sistemleri önümüzdeki yıllar içinde firmalar için zorunluluk haline gelecek ve bu sistemler bizim ülkemizde de yaygınlaşacaktır.

Firepro yangın söndürme sistemleri, öncelikli olarak her tür CO₂ ve FM200 ihtiva eden yangın sisteminin yerine daha az bir masrafla ve çok daha fazla yer ve zaman kazancıyla, bütün yangın türlerine de etkili olduğundan her tür yapıya, trafo ve pano odalarına, teknelere, motor sistemlerine kurulabilmektedir.

ISO 14001 belgesi ve UL standardına sahip olan firepro aerosol yangın söndürme sistemlerini, 6 kıta ve 66 ülkeden sonra ülkemize getirmiş olmanın haklı gururunu yaşıyoruz.

FirePro Uygulama alanları,

- Makine dairesi
- Kontrol odaları
- Alçak gerilim istasyonları
- Bilgisayar odaları
- Bilgi-işlem odaları
- Veri merkezleri
- Elektrik panoları, kabinleri
- Yatlar, Gemiler
- Yükseltilmiş zeminler
- Asma tavanlar
- Motorlu araçlar
- Elektrik odaları
- Haberleşme santralleri





Chapter – 5

Abstracts

Atrium binalarda duman emiş fanı seçiminin hesaplamalı akışkanlar dinamiği yöntemi ile belirlenmesi

Gökhan Coşkun¹, İsmet YÜZÜCÜ², Usame Demir^{1,*}, Hakan S. Soyhan^{1,3}

¹Department of Mechanical Engineering, Sakarya University, Sakarya, Turkey

²Institute of Natural Sciences, Sakarya University, Sakarya, Turkey

³Team-SAN Co, Technocity at Sakarya University, Sakarya, Turkey

Özet: Bu çalışmada Sakarya Üniversitesi Mühendislik Fakültesi M-4 Binasının zemin katında bulunan elektrik kat dağıtım panosunda ortaya çıkabilecek elektrik kaçağı veya aşırı yüklenme nedeniyle, fazla ısınan ana şalter ve plastik kabloların tutuşması sonucu ortaya çıkabilecek yangın modellenmiştir. Yangının modellenmesi için "Hesaplamalı Akışkanlar Dinamiği yazılımı olan "Fire Dynamic Simulator (FDS)" kullanılmıştır. Belirtilen nedenlerle oluşabilecek bir yangında dumanın ilerleyişi modellenerek can kayıplarını ortadan kaldıracak tedbirlerin tespit edilmesi ve gerekebilecek fiziki düzenlemelerin ortaya çıkarılması amaçlanmaktadır. Yoğun insan bulunan bir bina olması, kablo yangınlarında aşırı derecede duman oluşması ve duman tahliyesi için, ters basınçlandırma sistemi uygulanamaması nedeniyle bu çalışmada öneri olarak atriumun çatı kısmında duman tahliye fanı eklenmesi düşünülmüş ve üç farklı duman tahliye debisi için analizler gerçekleştirilmiştir. Duman tahliye fanının olması durumunda artan fan debisi ile birlikte duman yoğunluğunun azaldığı tespit edilmiştir.

Anahtar kelimeler: Yangın Modelleme, Duman Emiş Fanı, FDS

Canola based biodiesel production using microwave technology

Veli Gokhan Demir¹, Hakan Serhad Soyhan², Hayrettin Yuksel¹

Abstract: Canola is one the most preferred feedstock in biodiesel production because of its important advantages such as high oil content, superior flow in cold weather, oxidative stability, carbon sequestration, quality standards etc. In addition, canola has the highest productivity per hectare in Europe region, so in relation to the oil feedstock, canola oil was used for obtaining biodiesel in this study. The alkali-catalyzed transesterification reaction was carried out in our own design pilot scaled microwave assisted reactor. According to the results, canola oil based biodiesel meeting the main fuel properties of EN 14214 biodiesel standards with 98.00% ester content, 0.885 g/cm³ density, 4.612 mm²/s and 95.95 ester yield was produced in 5 min reaction time (approx. 12 times less than conventional production methods require) with 95.95% product yield. Consequently, it was observed that microwave technology fairly contributed to the reaction rate and product yield; hence this highly efficient technology can be applied in commercial biodiesel productions in order to decrease the biodiesel production costs.

Keywords: Canola Oil, Transesterification, Microwave, Biodiesel

¹ Corresponding author: Balıkesir University, Department of Mechanical Engineering, 10100, Balıkesir, Turkey.
veligokhandemir@balikesir.edu.tr

¹ Balıkesir University, Department of Environmental Engineering, 10100, Balıkesir, Turkey.

² Sakarya University, Department of Mechanical Engineering, 54187, Sakarya, Turkey.

Effect of side ports on the flow field of a rotary engine

Ozgur Oguz TAŞKIRAN¹, Alper Tolga CALIK², Osman Akın KUTLAR²

¹ *Design Project Office, Istanbul Naval Shipyard*

² *Automotive Division, Faculty of Mechanical Engineering, Istanbul Technical University*

Abstract: Wankel engine as an industrialized rotary engine has advantages of being simple and having high specific power compared to reciprocating engines. These advantages enable Wankel engine to be used in small aircrafts, unmanned air vehicles, boats, automobiles, motorcycles and light-weighted devices. However, both rotary and reciprocating engines have to overcome 21st century challenge of internal combustion engines which is reducing both emission and fuel consumption. As the emission restrictions get more and more stringent, investigations of flow pattern, mixture formation and stratification in internal combustion engines come into prominence. Thus, air movements flowing through the intake ports have importance on generating flow pattern inside the combustion chamber. In addition, air flow inside the combustion chamber is one of the basic factors that affect the efficiency of rotary engines.

Similar to reciprocating engines, rotary engines may have tumble and swirl motion which depend on intake air flow, intake channel, shape and position of rotor pocket. The flow pattern inside the combustion chamber also changes according to peripheral ported engines and side ported ones. In this study, air flow inside a double-side-ported rotary engine is investigated by using Computational Fluid Dynamic (CFD) techniques. For this purpose, rotary engine with 4 inlet and 2 exhaust ports were numerically modeled in Ansys Fluent. In contrast to Wankel engine simulations reported in the literature, this study has double side intake and exhaust ports including geometry of port channels. Channel geometries were added to obtain accurate inlet velocity vectors of air flowing to the combustion chamber.

Application of a dynamic mesh that is simulating eccentric motion of rotor as it compressing and expanding the volume in the combustion chamber is a challenging task of the numerical modeling. In addition, apex seals have to be properly modeled to ensure gas tightness of separated combustion chambers. These problems were overcome by using a User Defined Function that enables mesh and rotor movements. Different mesh sizes were applied to get best balance between the computer time and accurate converging solutions. Numerical results are validated by comparing experimental data presented in the literature. After validation of the numerical study, effects of side ports and rotor speed on air motion were investigated. In order to obtain effect of side ports, various cases were conducted by setting ports as open and/or closed in a methodological manner.

Corresponding Author:

Özgür Oğuz TAŞKIRAN

Design Project Office, Turkish Naval Forces

Istanbul Naval Shipyard, 34890 Pendik/Istanbul

ootaskiran@hotmail.com

Volumetric efficiency which is an important parameter describing flow characteristics of the engine is obtained for each case. The effecting parameters such as rotor speed, open/close condition and location of the inlet ports were analyzed by using numerical solutions. In line with the expectations, the results showed that volumetric efficiency increases as the rotating speed increases. However, after reaching a certain limit of rotating speed, open period of intake ports becomes insufficient for charge air and then, volumetric efficiency decreases for higher rotating speeds. Meanwhile, a three-dimensional dynamic simulation of the flow were investigated for swirl and tumble motions for each simulation case. The results revealed that swirl and tumble motions were together formed in one side-ported simulations. When air entrance is allowed from double-sided-ports, tumble motion is seem to be prevented by opposing air flow. Though, the formation of twin swirl was observed during the last section of intake period, one of them vanishes just after closing of intake ports. The swirl center is located in front of the combustion chamber at low rotor speeds and its location moves backwards at higher rotor speeds.

The numerical results including distributions of pressure, temperature, velocity and streamlines are presented to develop insight into the effective parameters of mixture formation. Based on the simulations, volumetric flow rate of the side ports are discussed as well. Due to the limited data presented in the literature, this study gives valuable information about the flow field of side ported rotary engines by revealing effecting parameters on formation and development of air motions.

Keywords: CFD, air flow simulation, rotating speed, side-ported rotary engine

Acknowledgement: This work has been supported by TUBITAK (Turkish Scientific and Technical Research Council), Project no: 115M690.

CFD Investigation of twin swirl application to diesel engine

Alper Tolga CALIK¹, Ozgur Oguz TAŞKIRAN², Rafiğ MEHDIYEV³

¹ Automotive Division, Faculty of Mechanical Engineering, Istanbul Technical University

² Design Project Office, Istanbul Naval Shipyard

³ Mechanical Engineering, Faculty of Engineering, Gebze Technical University

Abstract: Studies related to improving efficiency and reducing emission levels of ICEs have showed a remarkable improvement by introducing Common Rail (CR) electronic fuel injection system to the market. CR system itself and required after treatment system are not preferred for off-road vehicles since they are not cost-effective. To overcome this problem “MR-Process” Combustion Chamber (CC) was proposed by Mehdiyev. The shape of MR – Process CC also enables it to be used with Diesel fuel as well as with LPG and NG. The achievements of using gaseous fuels in high compression ratio diesel-like conditions without detonation in previous studies forced us to search and optimize Diesel fuel injection conditions of MR-Process CC by using CFD techniques.

Unlike conventional Diesel engines which have single swirl, MR Process Combustion Chamber (CC) proposed by Mehdiyev realizes two stage combustion mechanisms in twin swirl turbulent flow conditions in which twin swirl promotes fuel air mixture formation and enables ideal vaporization of fuel spray directed towards tangentially to piston walls. With the help of two hole injector, approximately %95 of fuel is injected in low pressure (150 - 250 bar) tangentially to the air swirls on the CC wall thus forming a wall film and evaporating the fuel by means of wall temperature. Because the remaining smallest amount of fuel takes part in autoignition, the need of high cetane numbered fuel is decreased and lower cetane numbered petroleum based liquid fuels can be used. Pyrolysis (thermal cracking) of the fuel is prevented due to the lower temperature and unburned combustion products such as C or PM, CO and HC are significantly decreased. Besides, the pressure rise gradient decreases, due to the fact that combustion speed is limited by evaporation induced by wall temperature. Hence the additional temperature rise of the burnt gases due to Mach effect is prevented. Thus, NOx and noise emissions decreased and a combustion process with optimum speed is attained.

Design of a MR Process CC which can satisfy the ideal twin swirl conditions at the moment of Start of Injection is a challenging task. Because twin swirl concept requires a 4 –valve engine head with two intake manifolds, design of these two separate independent intake manifolds which create symmetrical swirls inside the CC is important. This optimum CC and intake manifold shape design phase will be an expensive and time consuming task if only utilized from experimental studies. Because this proposed unique MR Process CC is not known before and there is no available experimental data for the optimum values of injection characteristics, air movement and swirl conditions.

Corresponding Author:

Alper Tolga CALIK

Mechanical Engineering Faculty

Inonu Cad. No: 65 Gumussuyu, 34437 Beyoglu Istanbul

alper.calik@itu.edu.tr

CFD analysis of MR-Process CC were performed to overcome these drawbacks and investigate the feasibility of twin swirl initiation and the results are presented. The paper aims to reveal effectiveness of twin swirl application on Diesel engines with closed cycle simulations. Open sourced KIVA 3V-R2 code was used for CFD simulations. KIVA 3V-R2 code uses RANS (Reynolds Averaged Navier Stokes) and ALE (Arbitrary Lagrangian-Eulerian) method for spatial discretization. The turbulent combustion was modeled by using partially stirred reactor (PaSR) method. The spray model and ignition delay characteristics of the code is tuned and validated before this study so that temporal and spatial spray evolution under diesel-like conditions are observed and autoignition process of sprays which are injected from different nozzle geometries are investigated.

Using different angular velocities of the initial swirls and injection directions of fuel sprays, twin swirl conditions at the SOI and simulated combustion results were analyzed to determine the optimum injection settings and swirl ratios to improve fuel – air mixing process and reduce emissions. For this purpose, the existing swirl model in KIVA3V-R2 code was modified to create virtual twin swirl profiles at the beginning of the compression stroke which represents the twin swirls that will be generated with two separate intake manifolds in real engine. The initial swirl velocity profile is given by Bessel function in KIVA code. In this study 3.83 swirl profile was used and the KIVA code was modified to obtain twin swirl at the beginning of the simulation. The resulted application of this swirl motion to MR CC is shown in Figure 1.

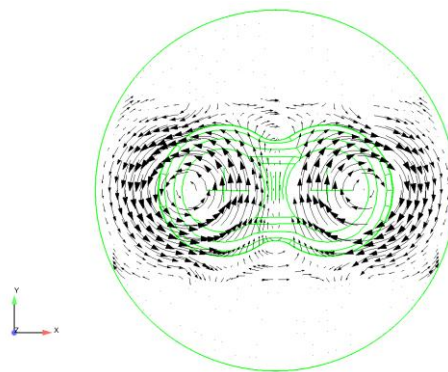


Figure 1. Applied initial swirl motion for MR CC

The numerical results including distributions of pressure, temperature, velocity and streamlines are presented to develop insight into the effective parameters of mixture formation. Due to the lack of data presented in the literature, this study presents a basis for further investigations of intake port generated twin swirls and their effect on air flow in the MR-Process CC. It is seen that although perfect virtual twin swirl are generated with the help of CFD at the beginning of compression stroke, these swirls can weaken or disappear at the end of compression stroke when piston reaches close to TDC. Only intake manifold generated swirls will not be enough to get optimum swirl profile at SOI moment, additionally piston bowl and cylinder head geometry design should be taken into account.

Keywords: MR Process, CFD, twin swirl, Diesel engine

Tek silindirli buji ateşlemeli bir motor için hava akış parametrelerinin modellenmesi

Usame Demir^{1,*}, Gökhan Coşkun¹, Hakan S. Soyhan^{1,2},

¹ Department of Mechanical Engineering, Sakarya University, Sakarya, Turkey

² Team-SAN Co, Technocity at Sakarya University, Sakarya, Turkey

Özet: Bu çalışmada buji ateşlemeli tek silindirli bir motorun hava akış parametreleri üç boyutlu Hesaplamalı Akışkanlar Dinamiği (HAD) yazılımı ile incelenmiştir. Deneysel çalışmada silindir içi basınç, emme ve egzoz havası sıcaklıkları ve emme manifoldundan silindire giren havanın debisi ölçülmüştür. Ölçülen bu değerler analiz başlangıç koşulları olarak kullanılmıştır. ANSYS yazılımının alt modülü olan ve içten yanmalı motor simülasyonu yapabilen IC Engine yazılımı kullanılarak silindir içi akış simülasyonları gerçekleştirilmiştir. Silindir içi basınç ve emme havası kütleli debisinin analiz sonuçları ile deneysel sonuçlar kıyaslanmıştır. Analiz çalışmasının deneysel çalışma ile neredeyse birebir örtüştüğü görülmüştür. Deneysel olarak ölçülemeyen ve yanma verimliliğine etkisi olan yatay girdap, dikey girdap gibi değerler analiz sonuçları ile ortaya konmuştur.

Anahtar Kelimeler: Hesaplamalı Akışkanlar Dinamiği, Silindir İçi Akış Modellenmesi, Buji Ateşlemeli Motor

Investigation of air flow simulation for a single cylinder spark ignition engine

Usame Demir^{1,*}, Gökhan Coşkun¹, Hakan S. Soyhan^{1,2}

¹ Department of Mechanical Engineering, Sakarya University, Sakarya, Turkey

² Team-SAN Co, Techno city at Sakarya University, Sakarya, Turkey

Abstract: In this study, air flow parameters for a single-cylinder spark ignition engine were investigated by three-dimensional Computational Fluid Dynamics (CFD) software. In-cylinder pressure, intake and exhaust air temperatures and air flow rate from the intake manifold were measured in the experimental study. These measured values were used as



initial conditions for analysis. In-cylinder flow simulations were performed using IC Engine sub-module of ANSYS software and can simulate internal combustion engine. The experimental results are compared with the simulation results of cylinder pressure and intake air mass flow rate. Simulation results almost agree with the experimental results. The results such as swirl and tumble which are not experimentally measured and have an effect on combustion efficiency are shown by the analysis results.

Keywords: Computational Fluid Dynamics, In-Cylinder Flow Modeling, Spark-ignition Engine

Yangin esnasında kullanılacak acil kaçış senaryolarının simülasyon destekli oluşturulması

*Mak.Müh.Recai AKSOY', Dr. Gökhan COŞKUN' ve Prof.Dr. Hakan Serhad SOYHAN'**

' Sakarya Üniversitesi, Fen Bilimleri Enstitüsü, Yangın Güvenliği ve Yanma EABD, Esentepe Kampüsü, Serdivan, 54150, SAKARYA

** TEAM-SAN Ltd.Şti., Teknokent, Sakarya Üniversitesi Esentepe Kampüsü, Serdivan, 54150, SAKARYA*

Özet: Son yıllarda nüfusun artışı ve ekonomik gelişmeler sonucunda ülkemizde Yüksek Katlı Şehir Hastanelerinin sayısında önemli artış görülmektedir. İnşa edilen bu binalar oldukça büyük ve büyüklüklerine ve yapılarına göre komplekstirler. Dolayısıyla, yangın durumunda hastanede bulunanların tahliye senaryoları ve yangın tesisatı binaların proje aşamasında planlanmalıdır. Tahliyenin anında ve önceden planlanmış senaryolara bağlı olarak başlamaması halinde, boğulma ve zehirlenme sonucu ölümlerle karşılaşılabilir. Bu çalışmada hem insani hem de yapısal tahliye unsurları ile ilgili olarak ajan temelli modeli ile analizler yapılmış ve senaryolar geliştirilmiştir.

Anahtar Kelimeler: Yangın, Tahliye, Tahliye Planları, Senaryo

Developing emergency escape scenarios by using fire simulation softwares

Abstract: In recent years, with the growth in the population and the economies, high-rise city hospitals are being built in Turkey. However, these buildings are quite large and complex because of their size and structure. Therefore, in case of fire, agents (people) will face evacuation problems. If they do not act immediately and according to a pre-defined scenarios, they may face death after suffocating and poisoning. In this study, an analysis was made with an agent-based model of both human and structural evacuation elements.

Keywords: Fire, Evacuation, Agents, Scenarios.

Spherical Flame Front Propagation Model and its Validation in Simplified Pent-Roof Combustion Chamber

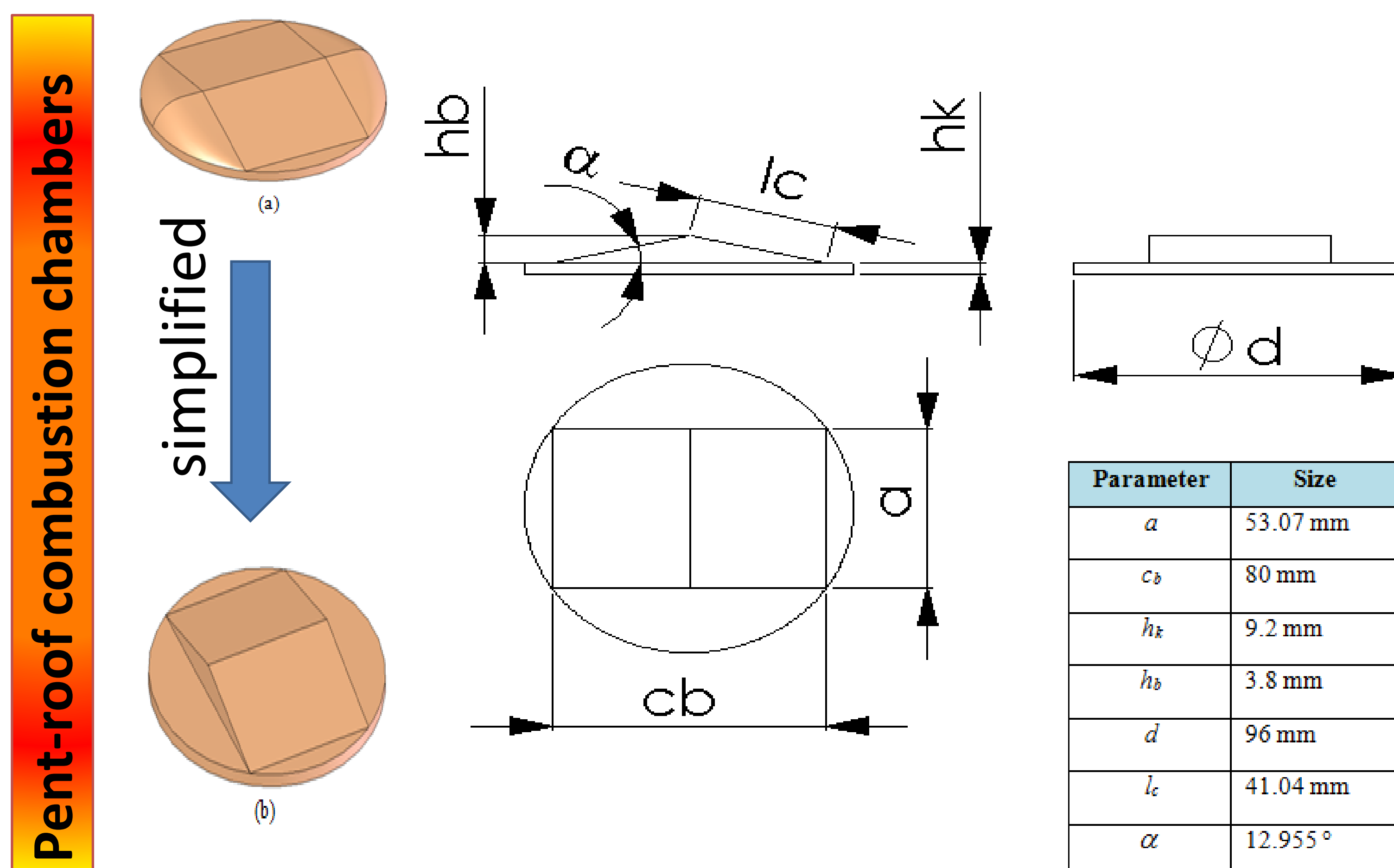
İsmail ALTIN¹, Atilla BİLGİN²^{1,2}Karadeniz Technical University, Trabzon, TURKEY

E-mail: isaltin@ktu.edu.tr (İ. ALTIN)

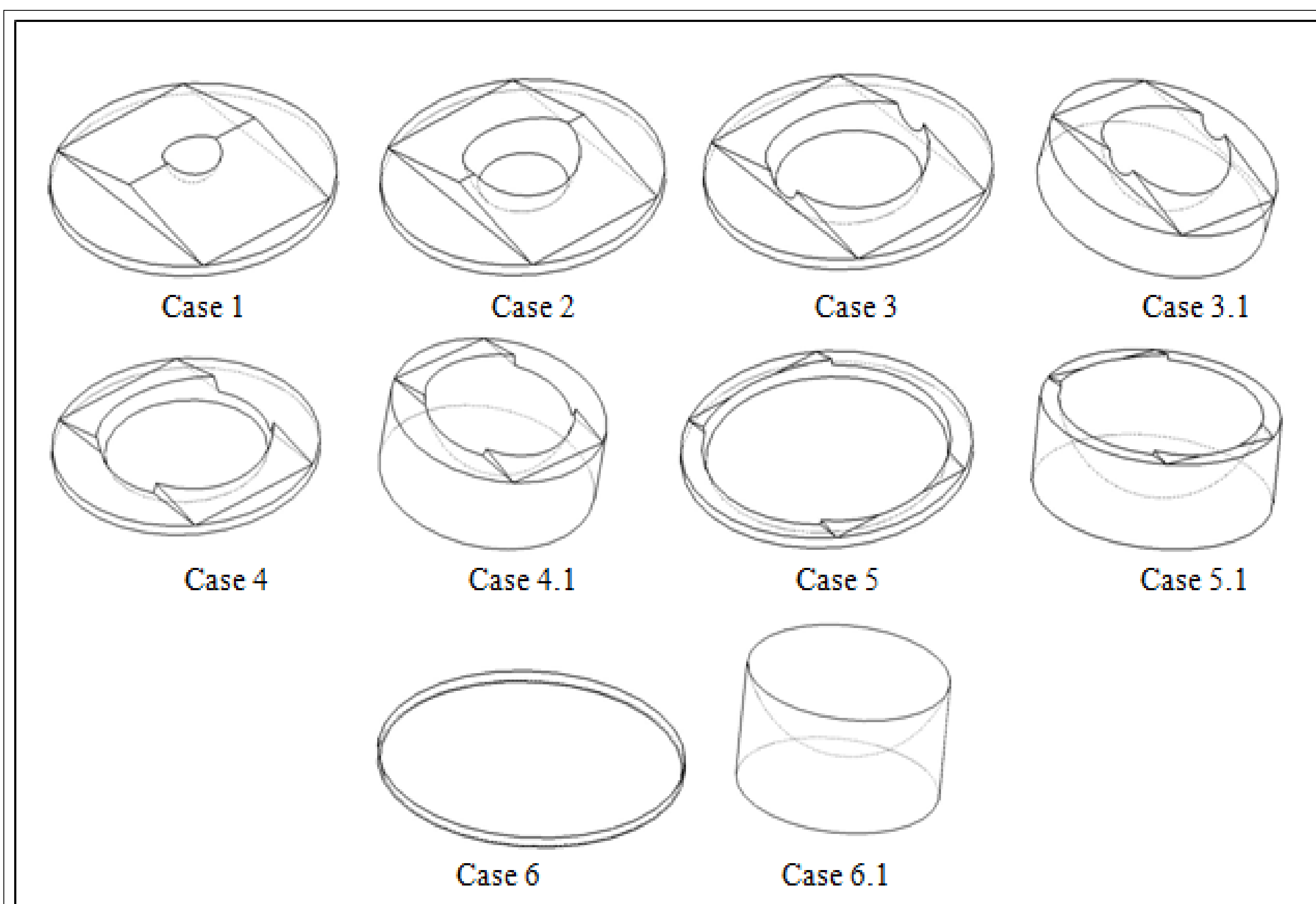
ABSTRACT

Flame propagation is one of the most important parts in quasi-dimensional (QD) models of SI. Combustion stages and heat transfer rate is determined by the flame propagation model in the QD models. There are numerous flame propagation models including analytical, statistical, CAD software and CFD software approach with variable spark plug number and position on cylinder head based on spherical, cylindrical and elliptical. Of these, analytical method gives fast response in the computational studies. Flame propagation features, i.e. flame front area, flame wetted area and enflamed volume, can be easily obtained in disc-shaped combustion chamber. In the complex combustion chamber geometries, however, analytical methods have big difficulties. Therefore, some simplifications can give modest results. In the presented study, spherical flame propagation model was analytically introduced and validated for simplified pent-roof combustion chamber

COMBUSTION CHAMBER LAYOUT

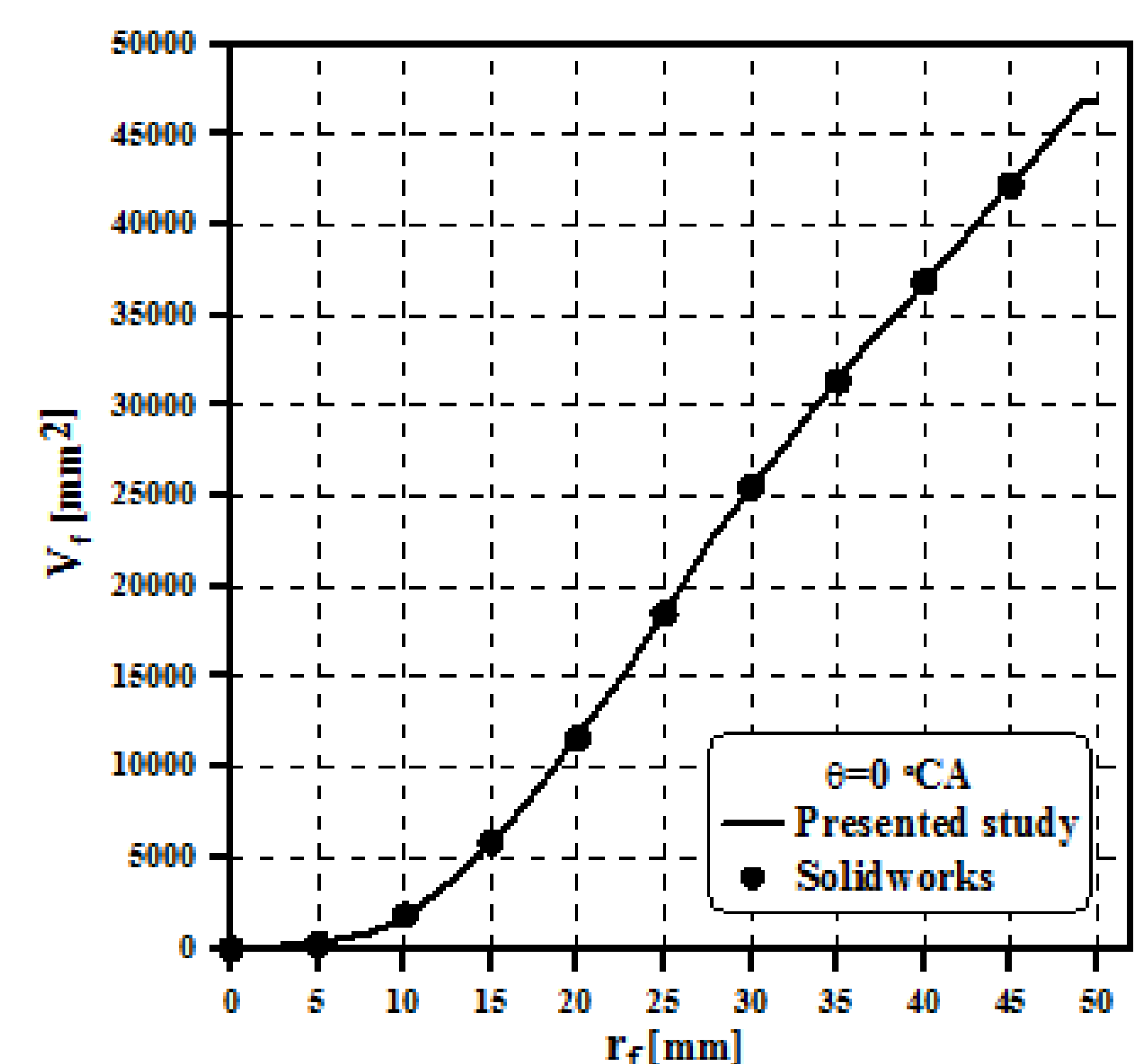
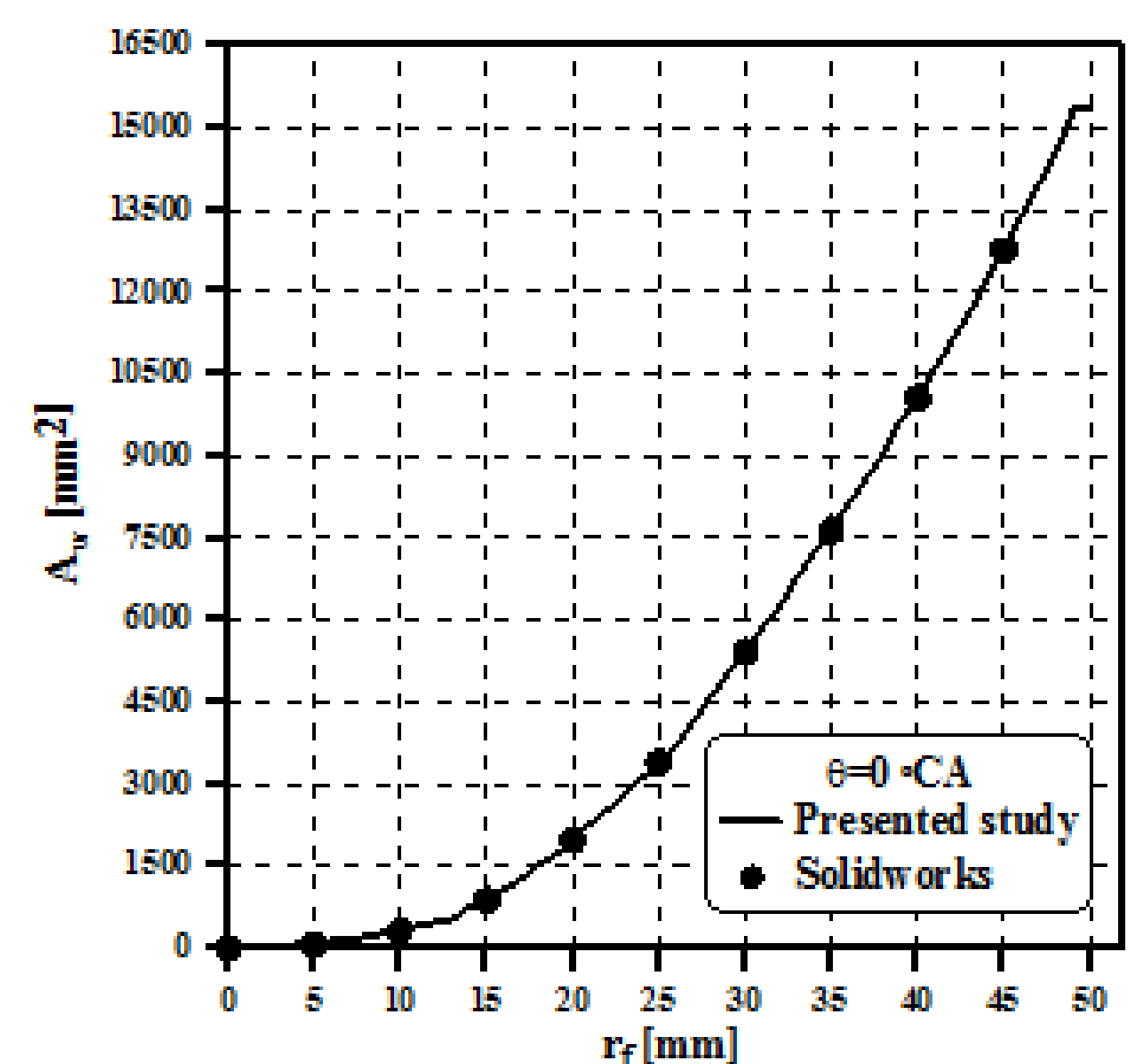
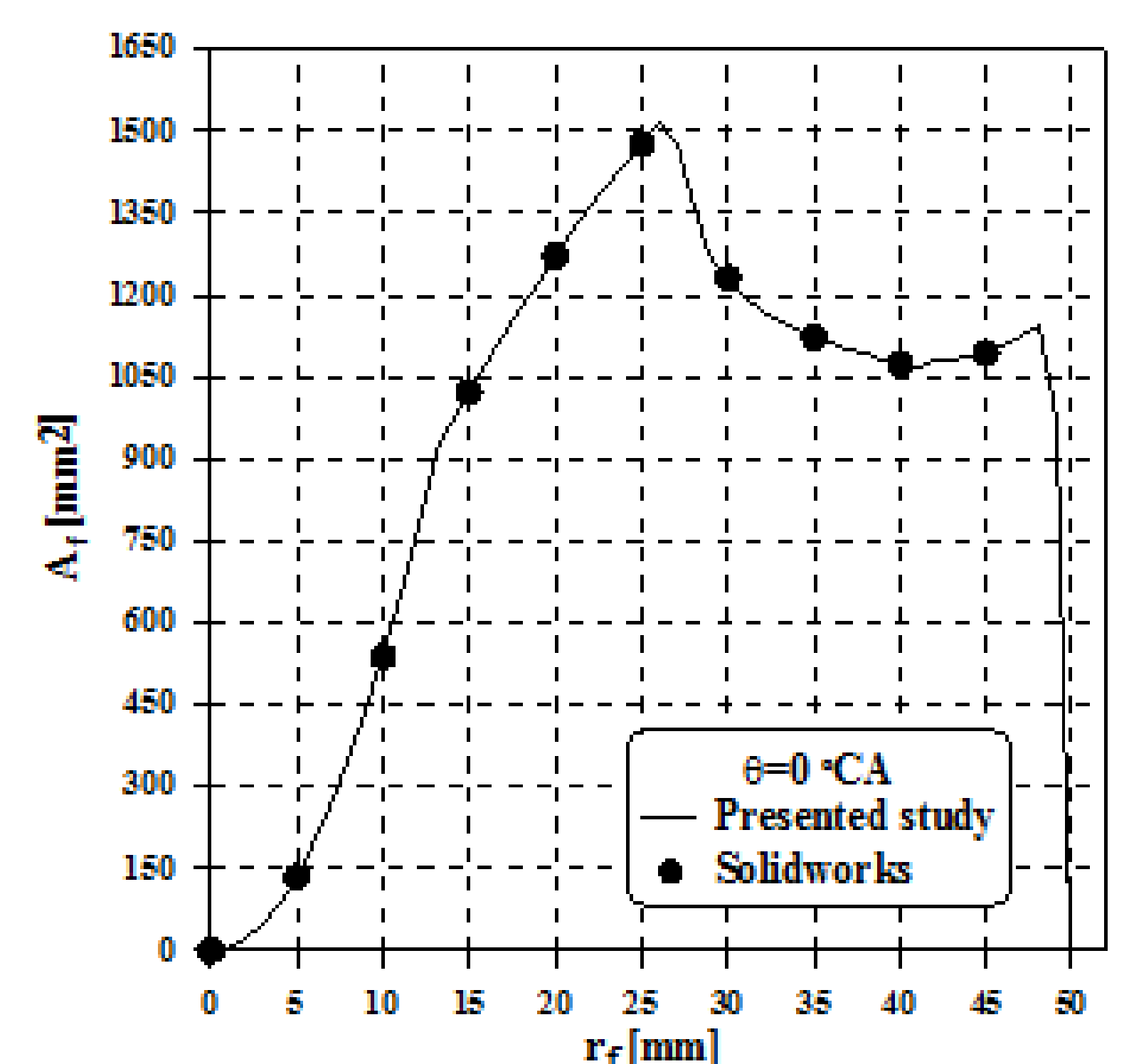


FLAME FRONT CASES IN COMBUSTION CHAMBER



Illustrations of flame front during propagation processes in the combustion chamber

RESULTS (MODEL VALIDATON)



$$\mathbf{A}_f, \mathbf{A}_w \text{ and } \mathbf{V}_f = \mathbf{f}(\mathbf{r}_f)$$



MÜHENDİSLİKTE YANICI VE PATLAYICI GAZLARIN İŞ SAĞLIĞI VE GÜVENLİĞİ AÇISINDAN YARATTIĞI SORUNLAR

Öğr. Gör. Mehmet Akif Erkan¹, Öğr. Gör. Hatice Özdemir¹,
¹Erciyes Üniversitesi, Mustafa Çıkrıkçioğlu MYO, İş Sağ.ve Güv. Pr., Kayseri



ÖZET

Mühendislikte gazlar enerji temini ve diğer üretim süreçlerinde oldukça sıklıkla kullanılmaktadır. Gazlar, uygulamada kolaylık, kolay temin edilebilirlik ve verimlilik açısından önemli avantajlar getirmekte ve özellikle yanıcı ve patlayıcı gazlar hem endüstride hem de bireysel olarak oldukça yaygın olarak kullanılmaktadır. Yanıcı ve patlayıcı gazların kullanım avantajları ile birlikte, bu gazların çalışanlar, maruz kalanlar ve çevre yönünden oldukça önemli tehlikeleri de bulunmaktadır. Bu tehlikelerden dolayı her yıl yüzlerce iş kazası olmakta, bir çok insan maddi ve manevi olarak zarar görmektedir. Bu çalışmada, yanıcı ve patlayıcı gazlar, iş sağlığı ve güvenliği açısından değerlendirilerek, bu gazların fiziksel, kimyasal, biyolojik ve mekanik tehlikeleri belirtilmiştir. Çalışmamızda bu tehlikelerin bertaraf edilmesi için gazların güvenli kullanım koşulları ve depolanma şartları konusu incelenmiştir. Özellikle patlayıcı gazların yol açabileceği patlama tehlikesinin sebepleri ve bu konuda alınması gerekli önlemler hakkında bilgi verilmiş, “Çalışanların Patlayıcı Ortamların Tehlikelerinden Korunması Hakkında Yönetmelik” hükümleri, bu çerçevede ele alınmıştır. Son olarak, yanma ve patlama konusunda mevzuatımız incelenerek, özellikle gazlar konusunda alınması zorunlu tedbirlere yer verilmiştir.

ABSTRACT

In engineering, gasses are used quite often in energy production and other production processes. Gases have significant advantages in terms of ease of application, ease of availability and efficiency, and in particular, flammable and explosive gases are widely used both industrial and individually. Along with the advantages of use of flammable and explosive gases, these gases also present significant hazards to workers, exposures and the environment. Because of these hazards, there are hundreds of occupational accidents every year, and many people suffer materially and spiritually. In this work, flammable and explosive gases are evaluated in terms of occupational health and safety and the physical, chemical, biological and mechanical hazards of these gases are indicated. In our work, the safe use conditions of the gases and the storage conditions have been examined in order to eliminate these hazards. Particularly, information on the reasons for the danger of explosion, which may be caused by explosive gases, and the precautions to be taken in this regard, were given and the provisions of "Regulation on the Protection of Employees from the Hazards of Explosive Atmospheres" were addressed in this frame. Finally, our legislation on combustion and explosion has been examined and mandatory measures have been taken in particular concerning gases.

YANICI VE PATLAYICI GAZLAR

Endüstride kullanılan gazlar çok farklı şekillerde sınıflandırılabilir. İş sağlığı ve güvenliği açısından gazlar genel olarak 6 grupta incelenir. Bu gruplar gazların tehlikeleri hakkında değerlendirme yapmamıza imkan verirler. Bu kapsamda gazları, aşındırıcı, parlayıcı, inert, oksitleyici, kriyojenik ve toksik veya zehirli gazlar olarak sınıflandırılır. Bir gaz, bu gruplardan biri yada bir kaçına aynı anda girebilir.

Çalışma ve Sosyal Güvenlik Bakanlığı tarafından 12/08/2013 tarihinde yayınlanan, *Kimyasal Maddelerle Çalışmalarda Sağlık Ve Güvenlik Önlemleri Hakkında Yönetmeliğinin* 4 maddesinde ,

- **Alevlenir madde:** Parlama noktası 21°C - 55°C arasında olan sıvı haldeki maddeler, ,
- **Kolay alevlenir madde:** Enerji uygulaması olmadan, ortam sıcaklığında hava ile temasında ısınabilen ve sonuç olarak alevlenen maddeyi veya ateş kaynağı ile kısa süreli temasta kendiliğinden yanabilen ve ateş kaynağının uzaklaştırılmasından sonra da yanmaya devam eden katı haldeki maddeyi veya parlama noktası 21°C'nin altında olan sıvı haldeki maddeyi veya su veya nemli hava ile temasında, tehlikeli miktarda, çok kolay alevlenir gaz yayan maddeler,
- **Çok kolay alevlenir madde:** 0°C'den düşük parlama noktası ve 35°C'den düşük kaynama noktasına sahip sıvı haldeki maddeler ile oda sıcaklığında ve basıncı altında hava ile temasında yanabilen, gaz haldeki maddeler,
- **Patlayıcı madde:** Atmosferik oksijen olmadan da ani gaz yayılımı ile ekzotermik reaksiyon verebilen ve/veya kısmen kapatıldığında ısınma ile kendiliğinden patlayan veya belirlenmiş test koşullarında patlayan, çabucak parlayan katı, sıvı, macunumsu, jelatinimsi haldeki maddeler,

Olarak tanımlanmıştır.

Yanıcı ve patlayıcı gazlar; Atmosferik sıcaklık ve basınçta hava ile etkileşimi, hacim olarak %13 veya daha az parlayıcı karışım oluşturan veya asgari parlama sınırı dikkate alınmaksızın havada hacim olarak %12 veya daha fazla parlama alanına sahip gazlar parlayıcı gazlar sınıfında yer alır.

Bütan (C₄H₁₀), Propan (C₃H₈), Amonyak (NH₃), Metan (CH₄), Etan (C₂H₆), Hidrojen (H), Asetilen (C₂H₂) gibi gazlar patlayıcı özelliktedir.

YANICI ve PATLAYICI GAZLARIN TEHLİKELERİ

Yanıcı ve Patlayıcı gazlarda temel tehlike patlama ve yengin tehlikesidir. Ancak bu gazlar, patlama tehlikesinin yanı sıra, zehirli, mutajenik, kanserojenik, korozif etkiler de gösterebilmektedirler.

Bir yanıcı maddenin hava içinde patlayabileceği en alt sınıra APS(Alt Patlama Sınırı) (LEL-Lower Explosion Limit) ve hacim içinde patlama özelliğini sürdürebileceği en üst sınıra ise ÜPS(Üst Patlama Sınırı) (UEL- Upper Explosion Limit) adı verilir.

Yanıcı ve patlayıcı gazlar, mühendislik uygulamalarında en çok gaz formunda ve yüksek basınç altında kullanıldıkları için, oldukça önemli patlama riski taşımaktadırlar. Gaz tüpünün içinde bulunan gaza, tüpün doluluk durumuna ve tüp boyutlarına bağlı olarak patlamanın şiddeti değişmekle birlikte, her durumda yıkıcı sonuçlar doğabilmektedir. Kontrolsüz olarak ortama yayılan yanıcı ve patlayıcı gazlar da patlama riski taşırlar. Bu gazların ortamda kabul edilebilir sınırların üzerinde birikmesi, madenler, fabrika ve atölyeler gibi kapalı ortamlarda patlama riski oluşturur.

Bu gazların ortama kontrolsüz bir şekilde yayılması / sızması, bir patlamanın ardından yangın tehlikesi oluşturabilir. Yanıcı ve patlayıcı gazlar aynı zamanda çok kolay alevlenebilir maddelerdir. Bu maddeler, depolandığı, kullanıldığı yerlerde birikebilir. Oksijenle temas, alev, kıvılcım, elektrik kontağı gibi sebeplerle yanma başlayabilir.

Yanma ve patlama içeren süreçlerde kullanılan gazlar, çalışanlarda çeşitli yanık vakalarına sebep olabilir. Gerek gazların oluşturduğu açık alevler ve gerekse gaz tüpleri ve çevre ekipmanlarının yüksek ısılara ulaşması neticesinde, gerekli önlemlerin alınmaması neticesinde çeşitli derecelerde yanıklar oluşabilir.

Yüksek basınç altında sıvı formda iken, kontrollü yada kontrolsüz şekilde düşük basınç seviyelerine gelen gazlar, hal değişimi için gerekli ısıyı çevrelerinden temin edecekleri için, basıncın azaldığı hal değişimi noktasında çok düşük sıcaklık oluştururlar. Düşük sıcaklık, bu ekipmanları kullanan çalışanlar açısından soğuk yanıklarına neden olabileceği gibi, ekipmanların kırılgan hale gelmesine sebep olabilir.

Endüstriyel amaçlı kullanılan bir çok patlayıcı gaz türü, aynı zamanda çalışanlar üzerinde zehirleyici özelliğe sahiptir. Zehirlenme, sindirim, soluma yada deri emilimi yoluyla olabilir. Bu tür gazların çalışma ortamında bulundukları seviye sürekli kontrol edilmeli ve belirli seviyelerin üzerine çıkmamalıdır.

Bazı yanıcı ve patlayıcı gazlara maruziyet, boğulma tehlikesini de beraberinde getirmektedir. Çalışma ortamındaki oksijen konsantrasyonunu %20'nin altına çekerek, insanların yeterli oksijeni alamamasına sebep olan gazlar “basit boğucu gazlar”, akciğerlere alınan hava ile, hemoglobine oksijenden daha önce tutunarak, vücut dokularına oksijen gitmemesine sebep olan gazlara da “kimyasal boğucu gazlar” denilmektedir.

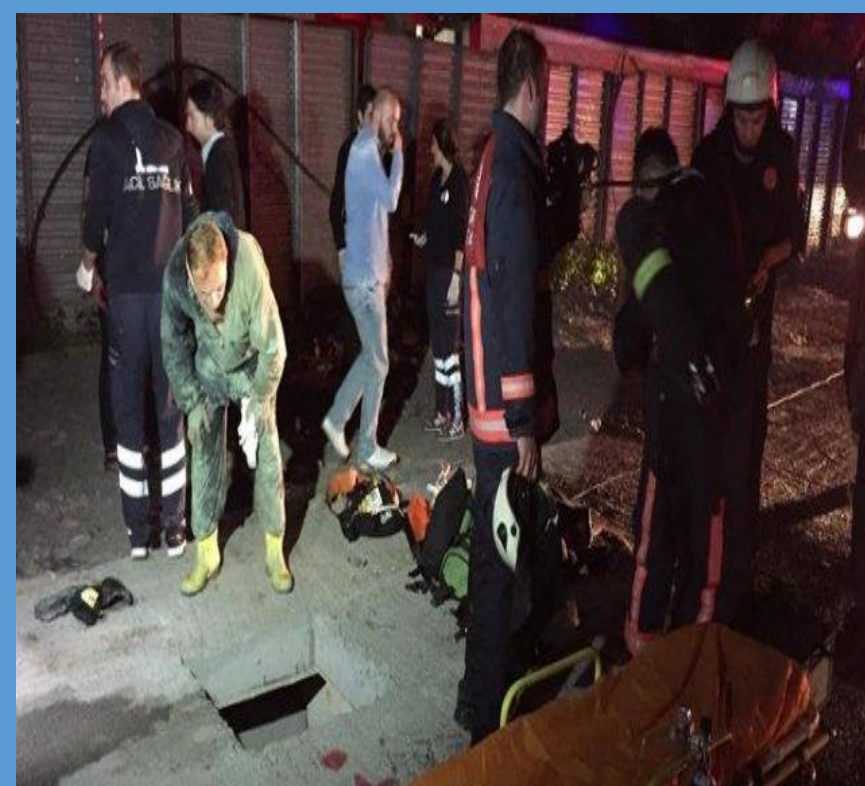
Mühendislik amacı ile, üretimde doğrudan kullanılan yada yan ürün olarak ortaya çıkan bazı yanıcı ve patlayıcı gazların bazıları da çalışanların dokularında tahriş edici özelliğe sahiptir. Bu tür gazların maruziyet şekline göre vereceği zarar değişiktir. Solunum yolu ile alınan gazlar, akciğerler ve diğer solunum organlarında, cilde temas şeklinde maruz kalınan gazlar öncelikle ciltte, özellikle tahriş edici gazların kontamine olduğu yiyecek ve içeceklerin sindirimi ile mide ve diğer sindirim organlarında tahriş oluşturabilir.

Yanıcı ve patlayıcı gazlar, yüksek basınç altında kullanılırlar ve taşınırlar. Yüksek basınca dayanıklılık amacıyla bu gazların taşındığı kaplar silindirik geometride ve metal maddelerden imal edilirler. Bu durum, basınçlı kapların çok kolay düşme ve devrilmelerine sebep olur. Düşme ve devrilme neticesinde ciddi yaralanmalar, tüplerin başka ekipmanlara zarar vermesi gibi tehlikeli durumlar ortaya çıkabilir.

Gaz tüplerinin taşıma ve nakliye işlemlerinde de ciddi tehlikeler bulunmaktadır. Bu tüplerin sabitlenmemiş olması, kapalı araçlarda taşınması, kimi durumlarda elle yükleme boşaltma yapılması gibi durumlar ciddi tehlikeler barındırmaktadır.



Ankara Ostim Organize Sanayi Bölgesinde 03 Şubat 2011 tarihinde, bir gaz firmasından alınan tüpler aynı gün içinde iki ayrı patlamaya sebep olmuş 20 kişi yaşamını yitirmiş, 45 kişi de yaralanmıştı. Patlamaya oksijen yerine doğalgaz doldurulmuş tüpler neden olmuştu



Kadıköyde dere ıslahı çalışmaları sırasında metan gazından etkilenmiş ve tedavi altına alınmıştır

GÜVENLİK TEDBİRLERİ

Genel Tedbirler

- Çalışan sayısını en aza indirmek

Yanıcı ve patlayıcı gazların bulunduğu yada bu bu ortamlardaki tehlikelerin etkilerinin yakından hissedileceği diğer ortamlarda, çalışan sayıları işin gerekliliklerini karşılayacak minimum düzeyde tutularak, oluşacak bir tehlikeden etkilenecek kişi sayısı en aza indirilir.

- Maruziyet süresini en aza indirmek

Yanıcı ve patlayıcı gazların narkotik, boğucu, zehirleyici etkilerinden en az etkilenmek için, tehlikeli gazlar altında çalışanları, kısmi zamanlı olarak çalıştırmak, iş rotasyonu ile çalışmasının bir kısmında bu gazlara maruz kalmayacağı işlere yönlendirmek, uygun bir çözüm olabilir.

- Uygun hijyen önlemleri

Çalışanların temel hijyen kurallarından başlayarak, kullanılan gaz türlerine göre özel önlemleri de içerecek şekilde hijyen kurallarına uyması, hem patlama riskine karşı, hem de diğer tehlikelere karşı etkili bir önlemdir. Çalışanlara bu kuralların öğretilmesi ve hijyen kurallarına uyulmasının sağlanması işverenlerin sorumluluğundadır.

- Ortamdaki kimyasal madde miktarını azaltmak

Çalışan ortamda, kullanılan patlayıcı ve yanıcı gaz miktarını sadece ihtiyaç olunan kadar bulundurmak, tüm riskleri azaltıcı bir düzenlemedir. Özellikle gaz tüplerinin depolanması ayrı bir tehlike kaynağı olduğundan, işyerinde ihtiyaç olandan fazla gaz tüpü bulundurulmaması gerekmektedir.

- Uygun iş ekipmanları sağlamak ve bakım yaptırmak

Gazlarla çalışırken uygun ekipman kullanılması, basınçlı gaz tüplerinin periyodik kontrol ve bakımlarının uygun yöntemlerle yapılması, tüpler ve şaloma, regülatör, kontrol vanası, alev tutucu, hortum ve rekor gibi diğer ekipmanların uygunluğunun kontrol edilmesi gereklidir.

- İş organizasyonu

Yanıcı ve patlayıcı maddelerle yapılan çalışmalarda, iş ve görev tanımları, iş emirleri, etiketleme ve diğer organizasyona ilişkin uygulamalar, güvenlik konusunda kritik öneme sahiptir. Bu uygulamalar iş sağlığı ve güvenliği önceliklerine göre düzenlenmelidir.

- Uygun çalışma prosedürleri

Tehlikeli gazlar ile yapılan çalışmalarda, çalışanların işi ve işin tehlikelerini yeterince kavrayamamış olması, dalgınlık, dikkatsizlik, şakalaşma gibi güvensiz davranışları sonucu ciddi kazalar yaşanabileceği düşünülerek, çalışma prosedürleri hazırlanmalıdır. Bu prosedürler uygun şekilde hazırlanması ve uygulanmasına önem verilmesi neticesinde, çalışanların güvensiz davranışları ciddi oranda azalacaktır.

- İş İzin Sistemleri

Patlayıcı ortamlarda yürütülen işlerde, iş izin sistemi kurulmalı, tüm yetki ve sorumluluklar belirlenmeli, işe başlamadan önce iş izni oluşturulma aşamaları belirlenmeli iş izni oluşturulmadan faaliyete başlanmamalıdır.

Bazı Yanıcı ve Patlayıcı Gazların Alt ve Üst Patlama Limit Değerleri¹¹

Yanıcı Madde	LEL (%)	UEL (%)
Asetilen	2,5	100
Bütan	1,8	8,4
Propan	2,1	9,5
Metan	5	15
Karbon Monoksit	12,5	74

MEVZUAT

Endüstriyel ve diğer amaçlarla kullanılan tüm yanıcı ve patlayıcı gazlar ile yapılacak çalışmalarda zorunlu olarak uyulması gereken yasal kuralları bulunmaktadır. Kullanılan maddelerin özelliklerine göre alt ve üst limitlerin geçilmemesi, geçildiği durumlarda mutlaka önlem alınması gerekmektedir.

1. 6331 sayılı İş Sağlığı ve Güvenliği Kanunu
2. Kimyasal Maddelerle Çalışmalarda Sağlık ve Güvenlik Önlemleri Hakkında Yönetmelik
3. Kimyasalların Envanteri Ve Kontrolü Hakkında Yönetmelik
4. Zararlı Maddeler Ve Karışımlara İlişkin Güvenlik Bilgi Formları Hakkında Yönetmelik
5. Çalışanların Patlayıcı Ortamların Tehlikelerinden Korunması Hakkında Yönetmelik
6. Muhtemel Patlayıcı Ortamda Kullanılan Teçhizat Ve Korumaya Sistemler İle İlgili Yönetmelik
7. Kontrolle Tabi Kimyasal Maddeler Hakkında Yönetmelik
8. İş Sağlığı Ve Güvenliği Risk Değerlendirmesi Yönetmeliği

KAYNAKÇA

- www.mevzuat.gov.tr.
- Durşen M. ve Yasun B. Yeraltı Madenlerinde Bulunan Gazlar ve Metan Drenajı, İSGÜM yay. 2012
- Eğri N. «Patlayıcı Ortamlarda İş Güvenliği», İSGÜM yay.
- COŞKUNSES F. Tehlikeli Kimyasal Maddelerin Oluşturduğu Riskler İSGGM yay.
- KÖSE A. «Ticari Patlayıcı Maddeler ve Patlayıcı Madde Seçimi» Basılmamış Y.Lisans Tezi, 2015 İstanbul

Baca Gazı Atık Isı Geri Kazanımı İçin Endüstriyel Pişirme Fırınında Enerji Verimliliği Sağlayan İnovatif Sistem Geliştirilmesi

M. HACI*, Z. KAHRAMAN*, K. İÇİBAL*, H.S.SOYHAN**

* Öztiryakiler Madeni Eşya San. Ve Tic. A.Ş / Ar-Ge ve Teknoloji Merkezi

** Sakarya Üniversitesi – Makine Müh. Bölümü
e-mail: mhaci@oztiryakiler.com.tr; hsoyhan@sakarya.edu.tr



AMAÇ: Mevcut gazlı endüstriyel pişirme fırın ürünlerinden farklı olarak tasarıma özgü geliştirilen sistemde, ilk kez kirlletici emisyonların azaltılması ile hem çevreci özelliğin öne çıkması hem de baca atık ısısından yararlanılarak enerji verimliliğine ilişkin Ar-Ge kazanımlarının elde edilmesi.

1. ÖZET

Gazlı endüstriyel pişirme fırınları, birçok yemek çeşidinin toplu pişirilmesi için yaygın olarak kullanıldığından endüstriyel mutfaklarda tercih edilen ürünlerin başında gelmektedir. Uluslararası alanda da gazlı endüstriyel pişirme fırınları içerdikleri teknolojilerle kendi alanında en yüksek katma değeri olan ürün kategorisinde ön plana çıkmaktadır. Ar-Ge sistematiğine dayalı geliştirilen yenilikçi prototip ile mevcut gazlı endüstriyel pişirme fırın ürünlerinden farklı olarak ilk kez kirlletici emisyonların azaltılması ile hem çevreci özelliğin öne çıkması hem de baca atık ısısından tasarıma özgü geliştirilen sistemde buhar jeneratörü suyunun ısıtılmasında yararlanarak enerji performansının artırılması ile farklı pişirim koşulları altında (çeşitli yemek türlerine özgü doldurma kapasitesi, hassas pişirim süresi, sıcaklık, nem vb.) etki eden birçok parametrelerin değerlendirilerek çeşitli sensörlerle en üst düzeyde kontrol edilmesi ve pişirim sürecindeki veriler doğrultusunda etkin pişirim sağlanması Ar-Ge projesi ile incelenmiştir.

Akıllı yenilikçi gazlı endüstriyel pişirme fırını prototipinin Ar-Ge sistematiğine dayalı çalışmalar ile mevcut ürünlerimize kıyasla hem kirlletici emisyonların azaltılması hem de baca atık ısısından yararlanarak enerji performansının artırılması ile bu alanda katma değeri en yüksek yerli yenilikçi ürünün ilk kez elde edilmesi ve benzer ithal ürünlerin önüne geçilmesi projemizin en önemli yenilikçi (inovatif) yönünü oluşturmaktadır. Tasarım doğrulamasındaki simülasyon verileri, yenilikçi prototipin farklı ebatlı modelleri geliştirilmesi ve ticari alana sunulması için de yeni Ar-Ge projelerinin başlatılmasına öncülük sağlayacaktır.

Anahtar Kelimeler: Gazlı endüstriyel pişirme fırınları, kirlletici emisyon, baca atık ısı, enerji performansı, yanma ve enerji verimliliği.

2. GİRİŞ

Baca gazı atık enerji kazanımı ile kirlletici emisyonların azaltılması ve enerji performansının artırılması için akıllı yenilikçi gazlı endüstriyel pişirme fırını tasarımı ve prototip imalatı ilk kez bu alanda Ar-Ge yeteneklerimizin geliştirilerek teknoloji geliştirme yönünde üstünlük elde ederek, proje çıktısının ticarileşebilen yenilikçi ürüne dönüşmesi ile benzer ithal endüstriyel pişirme fırınlarının yerini alması temel amacımızı oluşturmaktadır.

Yenilikçi prototip ile kirlletici emisyonların azaltılmasında atık ısıdan yararlanılması ile çevreci boyutunun öne çıkartılması ve enerji performansının da artırılması ile yenilikçi ürünün etkin çalışması yönünde ivme kazandırıcı ve yönlendirici yenilikçi çalışmaların yapılması, bu çalışmaların da simülasyon verileri ile doğrulanması ve bilimsel çalışmalarda değerlendirilmesi hedeflenmiştir. Ar-Ge projesinin başarı ile tamamlanması bu alanda yeni Ar-Ge projelerinin yapılmasına temel oluşturarak uluslararası alanda rakipler karşısında rekabet edebilirliğimize katkı sağlaması hedeflenmektedir.

Ayrıca yenilikçi gazlı endüstriyel fırını prototipinin tasarıma özgü pişirim grubu elemanlarının da (yanma odası, ısıtıcı boruların geometrisi, pervane vb.) özgün tasarımı ve kritik ısıtma grubu parçalarının (brülör, valf, fan motoru, buhar jeneratörü vb.) yerleşimi, simülasyon çalışmaları ardından etkin olarak belirlenerek pişirim işlemlerinde enerji performansının artırılmasına katkı sağlanacaktır.

3. YAKLAŞIM & DENEYSEL METOTLAR

Ar-Ge sistematiğine dayanan çalışmalar ile öncelikle yenilikçi prototipin yanma sistemi, ısıtıcı boruları ve baca kısmının özgün tasarım çalışmaları yapılmıştır. Tasarımı gerçekleştirilen yanma sistemi ile ısıtıcı borularının doğalgaza göre en verimli yanma koşulların sağlanması için simülasyon çalışmaları tasarım doğrulama aşamasında etkin olarak kullanılmıştır.

Farklı çalışma koşulları için parametrik çalışma ile yanma analizleri yapılmıştır. Kirlletici emisyonların azaltılması ve enerji performansının artırılması için yenilikçi endüstriyel pişirme fırının prototipinde özgün tasarımı yanma sistemi, ısıtıcı borular ile baca atık gazı ısısının geri kazanımı için en uygun tasarım elde edilmiştir. Yapılan denemeler sonucunda sistemin en etkin çalışma aralığı belirlenmiştir. Ayrıca simülasyon analizlerinden elde edilen çeşitli görsel sonuçlar Şekil 1-5'de gösterilmiştir.

Yenilikçi prototipin özgün tasarımı yanma sisteminin modeli üç ayrı parçadan oluşmaktadır.

- birincisi yanma odası,
- ikincisi ısıtıcı borular,
- üçüncüsü ise baca kısmı.

Ar-Ge çalışmaları öncesi mevcut endüstriyel gazlı pişirme fırını görüntüleri Şekil 1'de verilmiştir.

4. ÇALIŞMALAR & DEĞERLENDİRMELER

Baca gazı atık enerji kazanımı ile kirlletici emisyonların azaltılması ve enerji performansının artırılması için akıllı yenilikçi gazlı endüstriyel pişirme fırını prototipinin özgün tasarımı yanma sistemi duvar bölgelerine sınır tabaka atılmıştır. Akışın belirli bölgesine sweep mesh atılarak çalışmalar yürütülmüştür. Ar-Ge çalışması öncesi mevcut endüstriyel gazlı pişirme fırının çeşitli görünüşleri Şekil 1'de verilmiştir.



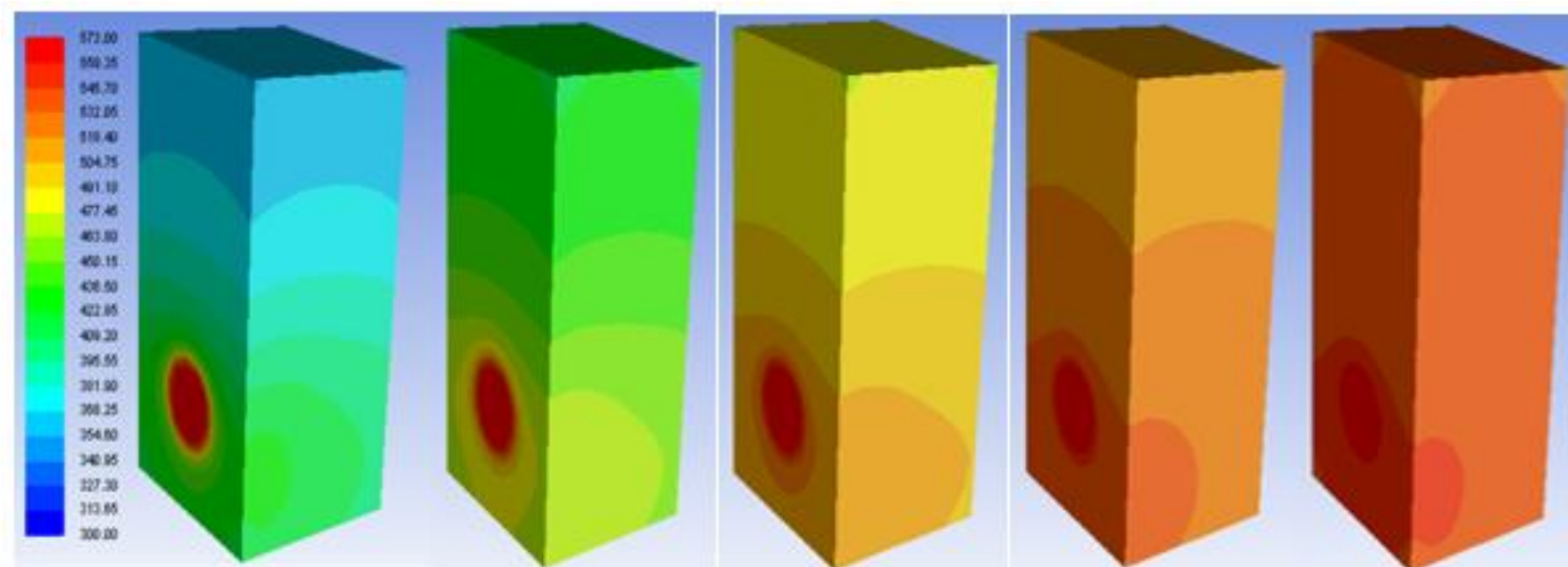
Şekil 1. Mevcut endüstriyel gazlı pişirme fırının çeşitli görünüşleri.

Simülasyon çalışmaları ile yanma sistemini oluşturan brülörlerden üretilen ısı 300 mm çapında iki fan ile içeri üflenmektedir. İçeri sürüklenen hava hızı 0.15 m/s olarak alınmış ve iki durum ile 4 farklı ısı transferi değeri incelenmiştir. Ortam havasına taşınım ile geçen ısı aktarılıp, prototip fırın iç ünitesinin sıcaklığı irdelenmiştir.

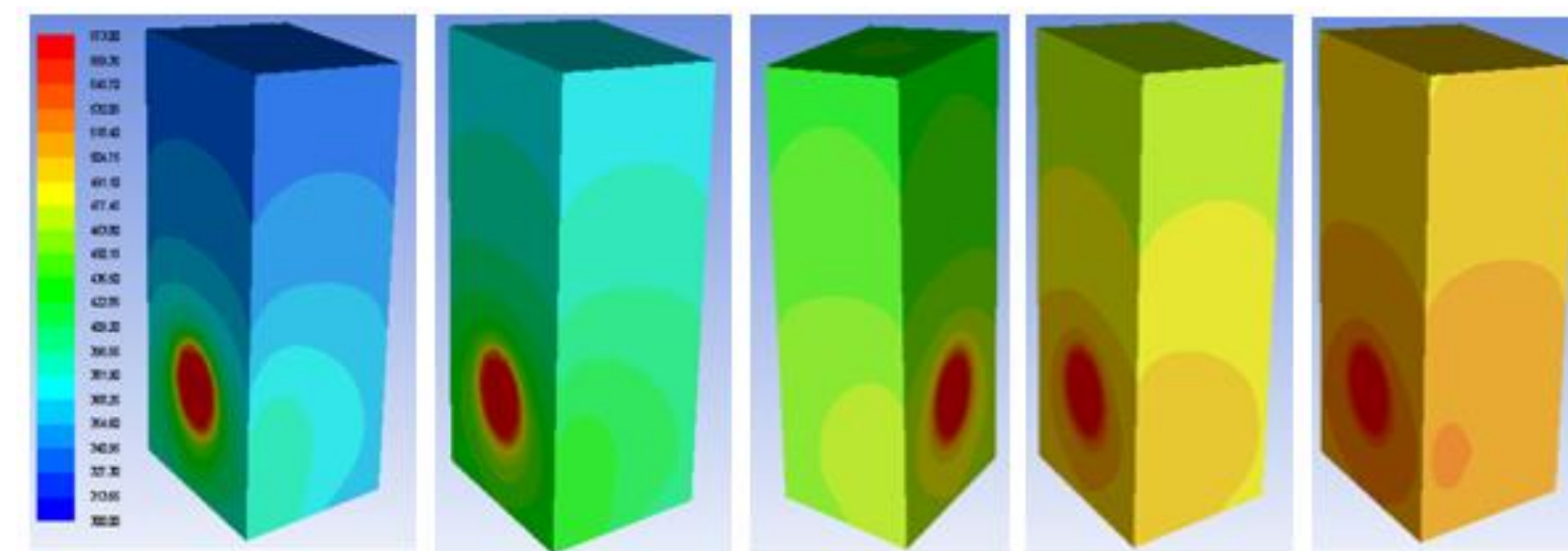
Özgün tasarımı yanma sisteminde simülasyon çalışmalarına örnekler Şekil 2-5'de verilmiştir.

1. Analiz: Tek brülörlü, taşınım katsayıları $\left[\frac{W}{m^2K} \right]$ a) adyabatik b) 0.1 c) 0.2 d) 0.4
2. Analiz: Çift brülörlü, taşınım katsayıları $\left[\frac{W}{m^2K} \right]$ a) adyabatik b) 0.1 c) 0.2 d) 0.4

A. Tek Brülörlü Pişirme Fırın Prototipi Analizleri

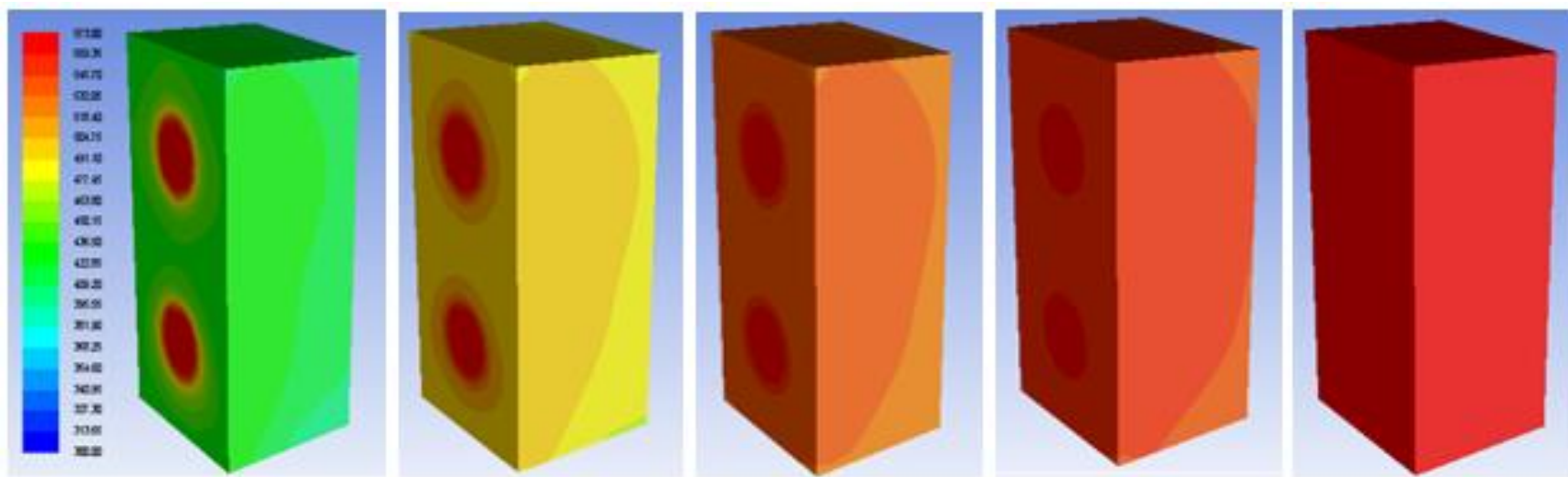


Şekil 2. Adyabatik fırın prototipinin ilk 5., 10., 20., 30. ve 40. saniye çalışma sürecinde sıcaklık değişimi simülasyonu (tek brülörlü).

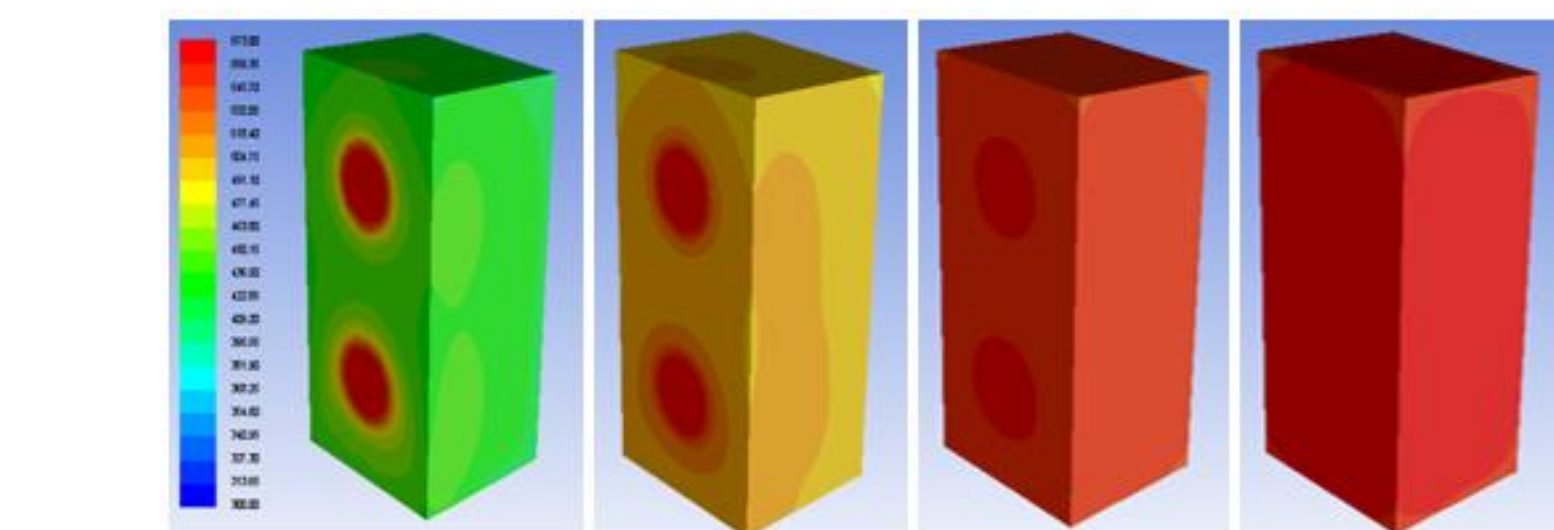


Şekil 3. Taşınım katsayısı 0.1 $\left[\frac{W}{m^2K} \right]$ ile 5., 10., 20., 30 ve 40. saniye sıcaklık değişimi simülasyon analizi (tek brülörlü).

B. Çift Brülörlü Pişirme Fırın Prototipi Analizleri

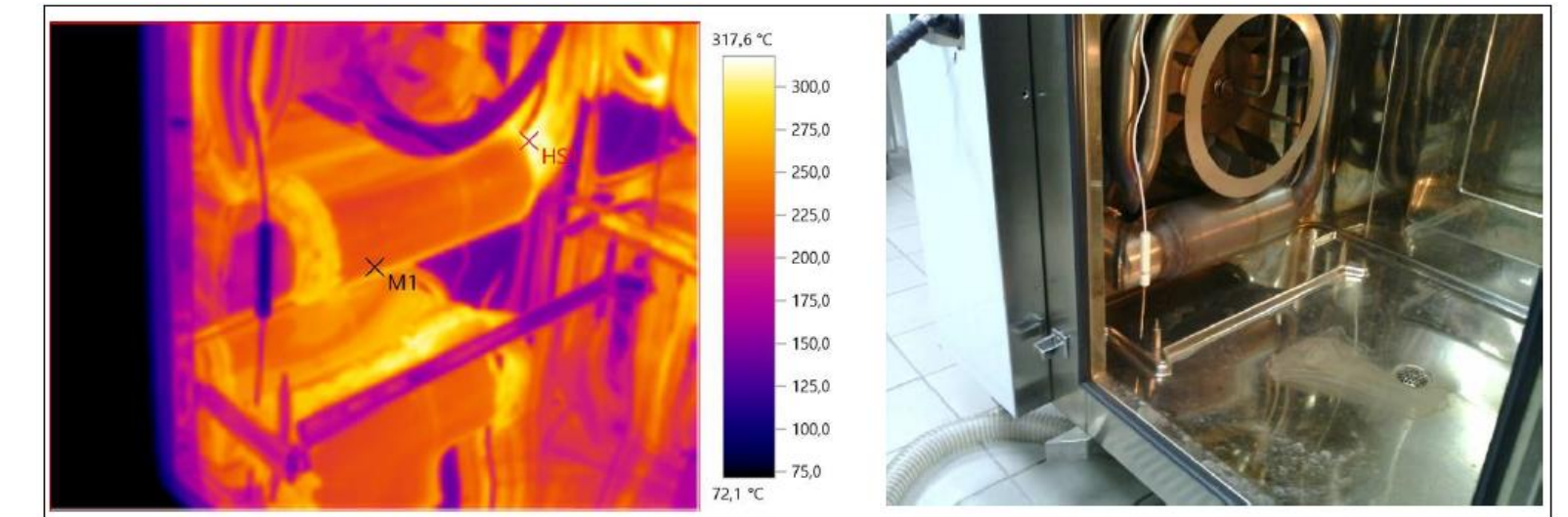
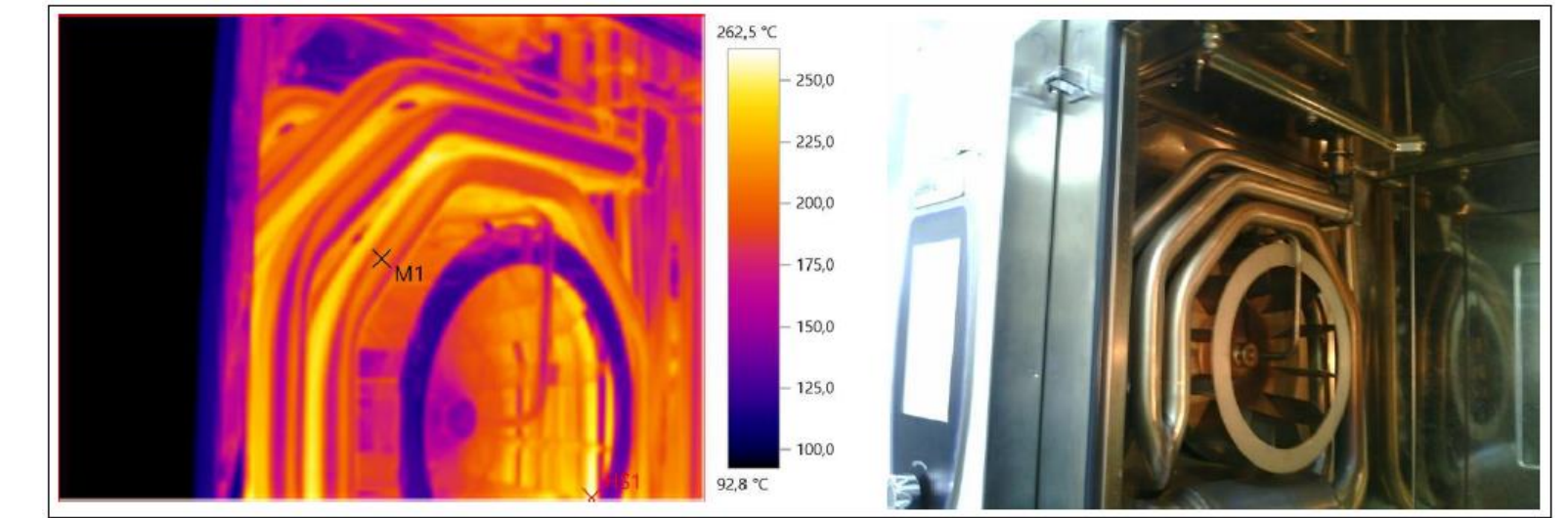


Şekil 4. Adyabatik fırın prototipinin ilk 5., 10., 16., 20. ve 30. saniye çalışma sürecinde sıcaklık değişimi simülasyonu (çift brülörlü).



Şekil 5. Taşınım katsayısı 0.1 $\left[\frac{W}{m^2K} \right]$ ile 5., 10., 20. ve 30. saniye sıcaklık değişimi simülasyon analizi (çift brülörlü).

C. Termal Kamera ile Sıcaklık Değişimi Analizleri



Şekil 6. Özgün tasarımı yanma sisteminde termal kamera ile sıcaklık ölçümleri.

Yenilikçi endüstriyel pişirme fırını prototipinde enerji verimliliğinin artırılmasına yönelik çalışmalar ile Şekil 6'da gösterilen yenilikçi prototip üzerinde termal kamera ile sıcaklık ölçümleri yapılmıştır.

5. SONUÇLAR

■Tasarım doğrulama çalışmaları ile doğalgazla çalışan endüstriyel pişirme fırın prototipinde çift brülör için etkin bir yerleşim yapılarak, sistemde dolaşan baca gazı yolu özgün bir tasarımı da artırılması başarılmıştır.

■Mevcut pişirme fırını koşullarında sağlanan standart pişirim sıcaklığına erişme süresi, özgün tasarımı yenilikçi prototipte azaltılması sağlanarak verimli çalışmasına katkı sağlanmıştır. Böylece yeni tasarımı prototipin yakıt sarfiyatında tasarruf sağlamasına katkı sağlamıştır. Bu yakıt sarfiyatındaki azalma aynı zamanda kirlletici toplam emisyonlarda da iyileşmeler elde edilmiştir.

■Yenilikçi prototip ile test ve değerlendirme aşamasındaki analiz sonuçlarına göre kirlletici emisyon değerlerinde ve yakıt sarfiyatında %30 azalma sağlanması yönünde etkin veriler elde edilmiştir.

■Özgün tasarımı gazlı endüstriyel pişirme fırını prototipinde, mevcut sisteme kıyasla baca gazı sıcaklığının %50 oranında azaltılması sağlanmıştır.

■Test ve değerlendirme çalışmaları ile baca gazı atık ısı geri kazanımı sağlayan endüstriyel pişirme fırını prototipi başarı ile elde edilmiştir. Böylece ülkemizde ilk kez kirlletici emisyonların azaltılması ve enerji performansının azaltılması yönünde yenilikçi endüstriyel gazlı pişirme fırını prototipi Ar-Ge sistematiği ile elde edilmiştir.

6. KAYNAKLAR

1. Sarah Brückner, Selina Liu, Laia Miró, Michael Radspieler, Luisa F. Cabeza, Eberhard Lävemann, Industrial waste heat recovery technologies: An economic analysis of heat transformation Technologies, Applied Energy, Volume 151, 1 August 2015, Pages 157-167.
2. Clemens Forman, Ibrahim Kolawole Muritala, Robert Pardemann, Bernd Meyer, Estimating the global waste heat potential, Renewable and Sustainable Energy Reviews, Volume 57, May 2016, Pages 1568-1579.
3. T.M. Alkhamis, M.A. Alhusein, M.M. Kablan. Utilization of waste heat from the kitchen furnace of an enclosed campus, Energy Conversion and Management, Volume 39, Issue 10, July 1998, Pages 1113-1119.
4. Anna Alberini, Andrea Bigano, How effective are energy-efficiency incentive programs? Evidence from Italian homeowners, Energy Economics, Volume 52, Supplement 1, December 2015, Pages S76-S85.
5. Bastien Girod, Tobias Stucki, Martin Woerter, How do policies for efficient energy use in the household sector induce energy-efficiency innovation? An evaluation of European countries, Energy Policy, Volume 103, April 2017, Pages 223-23.

7. TEŞEKKÜR

Bu çalışma, TÜBİTAK-TEYDEB 1501 kodlu Sanayi Araştırma Teknoloji Geliştirme ve Yenilik Projeleri Destekleme Programı kapsamında "Kirlletici Emisyonların Azaltılması ve Enerji Performansının Artırılması İçin Akıllı Yenilikçi Gazlı Endüstriyel Pişirme Fırını Tasarımı ve Prototip İmalatı" başlıklı ve 3160092 numaralı proje çalışmasından hazırlanmıştır. TÜBİTAK-TEYDEB Ulaştırma, Savunma, Enerji ve Tekstil Teknolojileri Grubu'na (USETEG) proje çalışmalarına sonsuz katkılarından dolayı teşekkür ederiz.